UNIVERSITY OF MICHIGAN MAY 26 1958
MAY 2[illegible] 1958
PHYSICS LIBRARY

Journal of Research

of the

National Bureau of Standards

APRIL 1958

VOLUME 60 NUMBER 4

U. S. DEPARTMENT OF COMMERCE
Sinclair Weeks, Secretary
NATIONAL BUREAU OF STANDARDS
A. V. Astin, Director

APRIL • 1958
VOLUME • 60
NUMBER • 4

JOURNAL OF RESEARCH
of the
NATIONAL BUREAU OF STANDARDS

The National Bureau of Standards

Functions and Activities

The functions of the National Bureau of Standards are set forth in the Act of Congress, March 3, 1901, as amended by Congress in Public Law 619, 1950. These include the development and maintenance of the national standards of measurement and the provision of means and methods for making measurements consistent with these standards; the determination of physical constants and properties of materials; the development of methods and instruments for testing materials, devices, and structures; advisory services to Government Agencies on scientific and technical problems; invention and development of devices to serve special needs of the Government; and the development of standard practices, codes, and specifications. The work includes basic and applied research, development, engineering, instrumentation, testing, evaluation, calibration services, and various consultation and information services. Research projects are also performed for other Government agencies when the work relates to and supplements the basic program of the Bureau or when the Bureau's unique competence is required. The scope of activities is suggested by the listing of divisions and sections on the inside of the back cover.

Publications

The results of the Bureau's work take the form of either actual equipment and devices or published papers. These papers appear either in the Bureau's own series of publications or in the journals of professional and scientific societies. The Bureau itself publishes three monthly periodicals, available from the Government Printing Office: The Journal of Research, which presents complete papers reporting technical investigations; the Technical News Bulletin, which presents summary and preliminary reports on work in progress; and Basic Radio Propagation Predictions, which provides data for determining the best frequencies to use for radio communications throughout the world. There are also five series of nonperiodical publications: The Applied Mathematics Series, Circulars, Handbooks, Building Materials and Structures Reports, and Miscellaneous Publications.

Information on the Bureau's publications can be found in NBS Circular 460, Publications of the National Bureau of Standards ($1.25) and its Supplement ($0.75), available from the Superintendent of Documents, Government Printing Office, Washington 25, D. C.

Order all publications from the Superintendent of Documents
U. S. Government Printing Office, Washington 25, D. C.

Use of funds for printing this publication approved by the Director of the Bureau of the Budget (May 14, 1956)

Journal of Research of the National Bureau of Standards Vol. 60, No. 4, April 1958 Research Paper 2844

Transient Radio-frequency Ground Waves Over the Surface of a Finitely Conducting Plane Earth

J. R. Johler

The complete transient signal is reconstructed after propagation via the ground-wave mode over a finitely conducting plane earth in which the displacement currents are neglected. The theory is illustrated by computations that have been made on formulas derived by the method of the inverse Laplace transformation. The results of this analysis indicate that current sources with sinusoidal form in the time domain could be used to simulate spherics. The methods employed in this analysis can be also used to reconstruct propagated signals of pulsed radio-navigation systems.

1. Introduction

In recent years considerable interest has developed in various types of electromagnetic ground-wave transients that propagate over the surface of the earth. This interest has in large measure been stimulated by the use of pulse techniques for precision radio-navigation systems and the ever presence of spherics that are propagated around the earth from various thunderstorms originating principally in the vicinity of the tropical land masses of the earth. In a previous paper by the author [1][1] and in papers by Wait [2, 3], a theory of propagation of the ground-wave transient was developed as an inverse Laplace transformation. The basic mathematical problem is the evaluation of the Fourier integral, which describes the transient signal, $E(t', d)$, in space and time as follows:

$$E(t',d)=\frac{1}{2\pi}\int_{-\infty}^{+\infty}\exp\,(i\omega t)f_s(\omega)E(\omega,d)d\omega, \qquad (1)$$

where $f_s(\omega)$ is the source current transform, and $E(\omega,d)$ is the transfer characteristic of the propagation medium. The theory was illustrated [1] by an evaluation of the sinusoidal part of the signal. Such examples describe the complete signal at the larger values of time, at low frequencies, and over highly conducting earth. It was shown that a signal generated by a sinusoidal current source, which commences abruptly at some time, $t=0$, and which is allowed to continue oscillating indefinitely, reaches a steady state condition, the amplitude and phase of which correspond precisely to the continuous-wave type of signal, i. e., the signal not interrupted in time. It is the purpose of this paper to extend the theory and reconstruct the complete signal by the addition of certain nonsinusoidal terms, which appear as a result of the inverse Laplace transformation and which describe the early time behavior of the signal.

2. Theory

The transient signal, $E(t', d)$, may be represented over a finitely conducting plane earth in which the displacement currents are negligible, for a vertically polarized source of the form, $\exp(-c_1t)\cos\omega_c t(0<t<\infty)$, at the local time, t', as follows [1]:

$$E(t,'d)=\nu C\exp(-\nu t')\left\{-1-\nu\sqrt{\pi\alpha}\exp(\nu^2\alpha)\left[\operatorname{erfc}(-\nu\sqrt{\alpha})-\operatorname{erfc}\left(\frac{t'}{2\sqrt{\alpha}}-\nu\sqrt{\alpha}\right)\right]+\frac{1}{a\nu}-\frac{1}{a^2\nu^2}\right\}$$
$$+\nu' C\exp\left[\frac{-t'^2}{4\alpha}\right]+\nu C\left[\frac{1}{a^2\nu^2}\right], \qquad (2)$$

where

$$\nu=c_1+i\omega_c \qquad (2a)$$

$$\nu'=\frac{t'}{2\alpha}+\nu \qquad (2b)$$

$$C=2\frac{I_0la^2}{4\pi\kappa d^3} \qquad (2c)$$

$$\alpha=\frac{\eta_1^3 d}{2\sigma\mu_0 c^3}, \qquad (3)$$

and where

d = the distance along the surface of the earth, in meters,
$C=2(10^{-7})/d$, where $I_0l=1$ ampere-meter [4],
η_1 = the index of refraction of air at the surface. $\eta_1\sim1.000338$,
σ = the conductivity of the ground, in mhos/meter,
μ_0 = the permeability of space, $\mu_0=4\pi\ (10^{-7})$ henry/meter,
c = the speed of light. $c\sim2.997925\ (10^8)$ meters/second,
$a=(\eta_1 d)/c$; $t-a=t'$, the local time, and
ρ_1 = the numerical distance. $\rho_1\sim\alpha\omega^2$, neglecting displacement currents in the earth.

Also, the transient signal, $E''(t', d)$, for a source, $\exp(-c_1t)\cos\omega_c t(0<t<T_2)$, i. e., a source interrupted at a time, T_2, may be represented as follows:

$$E''\,(t',d)=E(t',d)-\exp\,(-\nu T_2)\,E(t'',d), \qquad (4)$$

[1] Figures in brackets indicate the literature references at the end of this paper.

$$t''=t'-T_2 \qquad (t'>T_2). \tag{5}$$

The continuous wave or the wave not interrupted in time is the special case: $t'>>0$, $c_1=0$, $T_2=\infty$. The early values of time, $t'>0$, in this case describe the development of the steady state.

The source function, $F_s(t)$, may be brought into existence less abruptly as follows:

$$F_s(t)=\exp(-\nu t)-\exp(-\xi t) \tag{6}$$

$$\xi=c_2+i\omega_c. \tag{7}$$

ν has been previously described (2a), and c_2 is assigned a large positive value ($c_2>>c_1$). The transform, $f(\omega)$, (1) may be written

$$f(\omega)=f_s(\omega)\ E\ (\omega), \tag{8}$$

or more generally

$$f(\omega)=E(\omega)[f_{s,1}(\omega)+f_{s,2}(\omega)+\ \ldots\ .], \tag{9}$$

where $f_{s,1}(\omega)$, $f_{s,2}(\omega)$, . . . are source functions that have been superposed to determine some complicated waveform. The solution of the space-time function, $E'(t',d)$, for this source (6) then merely requires the sum of two waves calculated as previously described (2),

$$E'=E'(t',d)=E_\nu(t',d)-E_\xi(t',d). \tag{10}$$

Figures 4, 5, and 6 illustrate this signal.

It is interesting to note the space-time function, $E(t',d)$, for the special case, $\omega_c=0$, or the case of a step function source, $u(t)$, exponentially damped, exp $(-c_1t)\ u(t)$,[2]

$$E(t',d)=c_1C\exp(-c_1t')\left\{-1-c_1\sqrt{\pi\alpha}\exp(c_1^2\alpha)\left[\operatorname{erfc}(-c_1\sqrt{\alpha})-\operatorname{erfc}\left(\frac{t'}{2\alpha}-c_1\sqrt{\alpha}\right)\right]+\frac{1}{ac_1}-\frac{1}{a^2c_1^2}\right\}+\left[\frac{t'}{2\alpha}+c_1\right]C\exp\left[\frac{-t'^2}{4\alpha}\right]+c_1C\left[\frac{1}{a^2c_1^2}\right]. \tag{11}$$

In this case, the imaginary part of the function, $E(t',d)$, vanished.

The source has been assigned the form $\exp(-c_1t)$ cos ω_ct or without damping ($c_1=0$), cos ω_ct. The sine source, exp $(-c_1t)$ sin ω_ct merely involves the formation of the product $-i\ E(t',d)$ or the real part becomes the positive imaginary $+Im\ E(t',d)$. The sine source at zero frequency (11) therefore vanishes. It can be further concluded that the step function response of the ground-wave propagation medium for a step function current source, $u(t)$, is the particular case, $c_1=0$, or $\nu=0$ (2), which is simply,

$$E(t',d)=\frac{t'}{2\alpha}\,C\exp\left[\frac{-t'^2}{4\alpha}\right]. \tag{12}$$

[2] The step function, u(t), is defined as follows: $u(t)=1$ for $t>0$; $u(t)=0$ for $t<0$.

3. Computation

The detailed reconstruction of the complete transient signal over a finitely conducting plane earth, neglecting displacement currents in the earth, is shown in figs. 1 to 6. The complete signal, $E=E(t',d)$ (2), is presented as three terms,

$$E=E(t',d)=E_0(t',\mathrm{d})+E_1(t',d)+E_2(t',d). \tag{13}$$

The first term, $E_0=E_0(t',d)$, is called the sinusoid because it is multiplied by the time harmonic function $\exp(-\nu t')$ (2). The remaining terms are

$$E_1=E_1(t',d)=\nu C\left\{\exp\left[\frac{-t'^2}{4\alpha}\right]+\frac{1}{a^2\nu^2}\right\} \tag{14}$$

$$E_2=E_2(t',d)=\frac{t'}{2\alpha}\,C\exp\left[\frac{-t'^2}{4\alpha}\right] \tag{15}$$

$E'=E'(t',d)$, (figs. 4, 5, 6) describe a signal the source of which has been brought into existance less abruptly (6).

Since the complete signal is very complicated, this presentation (13) illustrates the influence of the various parts of the signal as space-time and frequency parameters are varied. Thus, for example, the term E_2 degenerates into a "spike" close to the origin of time, t', as the frequency is decreased (fig. 6), and vanishes for the less abrupt source (6) such that the terms E_0+E_1 suffice to describe the complete signal. This is consistent with the limiting condition of very small numerical distance ($\sigma=\infty$) or an attenuation factor of unity. Thus, the transform of the Norton surface wave at considerable distance from the source may be written

$$E(s)=1 \qquad (\nu=0,\ \alpha=0), \tag{16}$$

and the space-time function, $E(t',d)$, is

$$E(t',d)=\mathcal{L}^{-1}E(s)=\delta(t'), \tag{17}$$

where $\delta(t')$ is the unit impulse function at the origin of time. Therefore, the transition to infinite conductivity illustrates the development of the Dirac impulse function, $\delta(t')$.

The reconstruction of a radio-navigation type of pulse is illustrated (fig. 7) with the "classical" sine-squared current source. The transient is allowed to reach the steady state because the "leading edge" of the pulse is of primary interest. It is common practice to interrupt radio-navigation pulses at a time, T_2, (4, 5) or apply exponential damping after some time, T_2, has elapsed. The source is redefined as follows:

$$\mathrm{Re}\ F_s(t)=\sin^2\omega_pt\ \sin\omega_ct \qquad (0<t<\infty), \tag{18}$$

$$F_s(t)=\frac{i}{2}\exp(-\nu t)-\frac{i}{4}\exp(-\nu_1t)-\frac{i}{4}\exp(-\nu_2t), \tag{19}$$

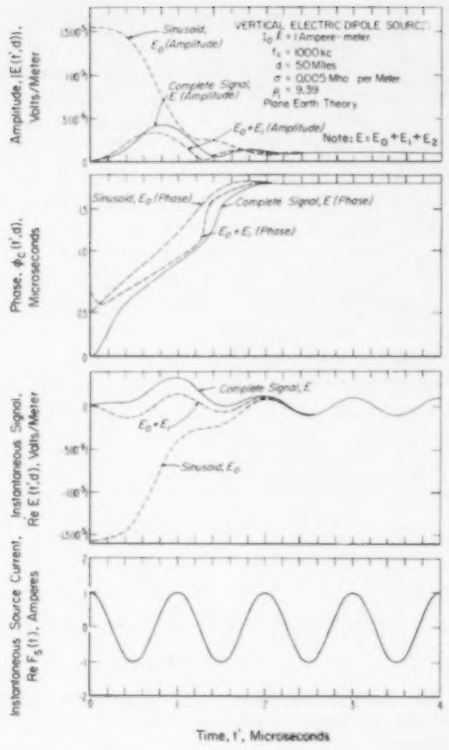

FIGURE 1. *Amplitude, phase, instantaneous signal, and corresponding source current for propagated surface-wave transient.*

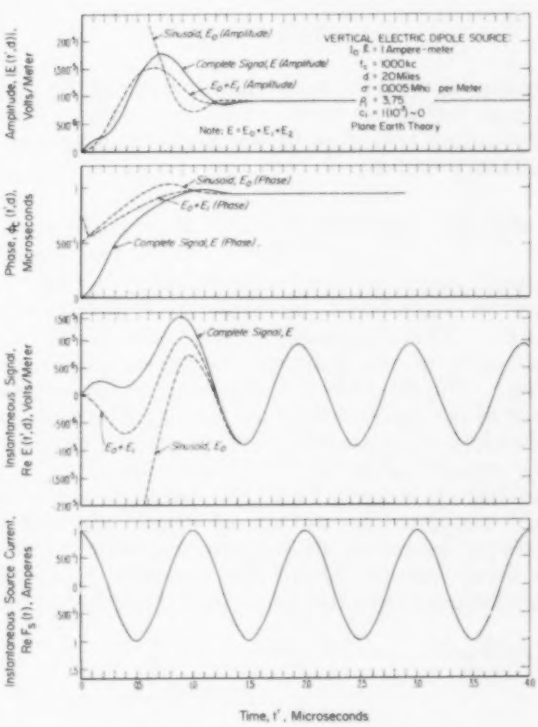

FIGURE 2. *Amplitude, phase, instantaneous signal, and corresponding source current for propagated surface-wave transient.*

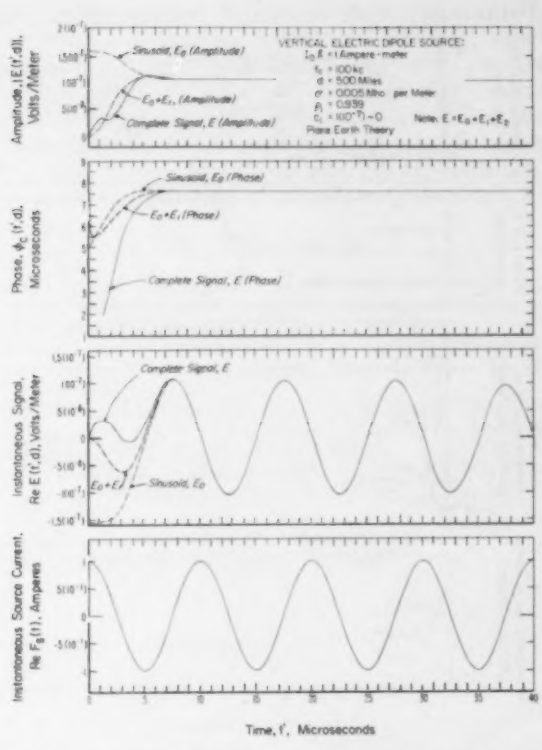

FIGURE 3. *Amplitude, phase, instantaneous signal, and corresponding source current for propagated surface-wave transient.*

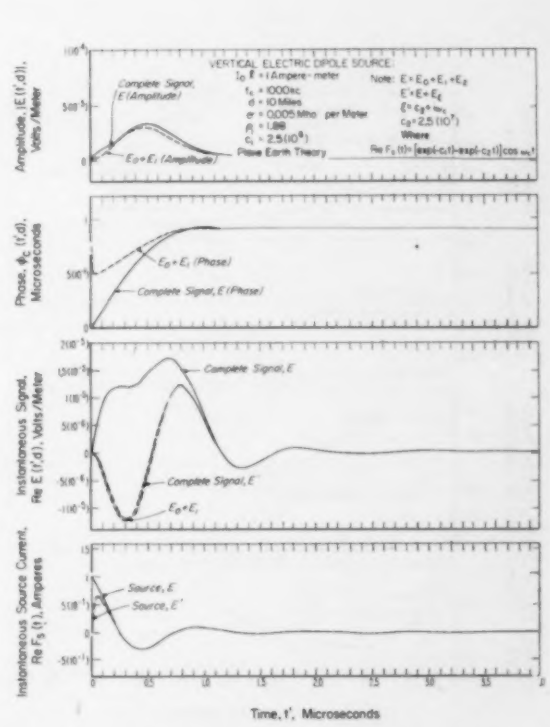

FIGURE 4. *Amplitude, phase, instantaneous signal, and corresponding source current for propagated surface-wave transient.*

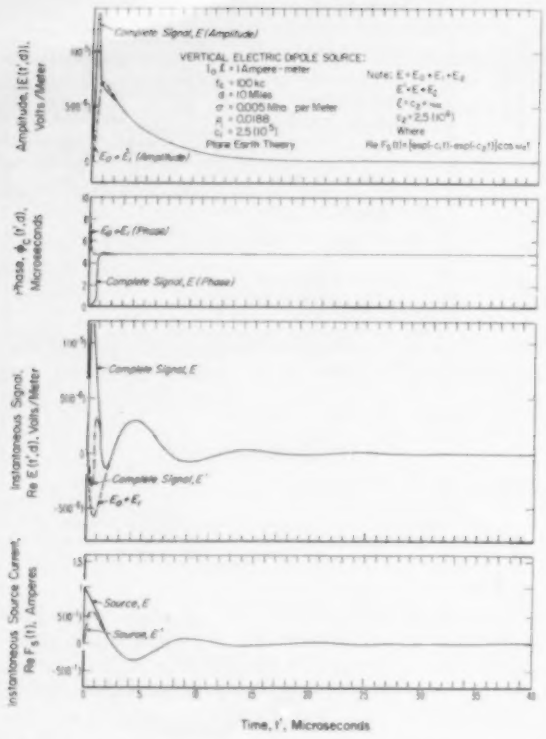

FIGURE 5. *Amplitude, phase, instantaneous signal, and corresponding source current for propagated surface-wave transient.*

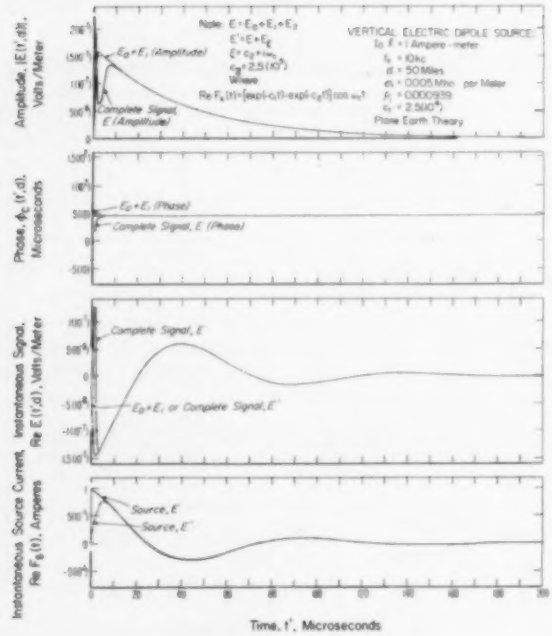

FIGURE 6. *Amplitude, phase, instantaneous signal, and corresponding source current for propagated surface-wave transient.*

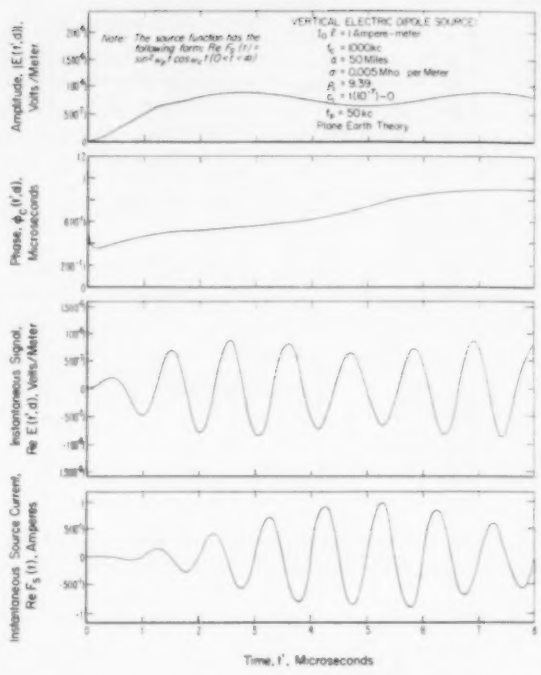

FIGURE 7. *Amplitude, phase, instantaneous signal, and corresponding sine squared source current for propagated surface-wave transient.*

where

$$\nu = c_1 + i\omega_c \text{ (as before)}, \tag{19a}$$

$$\nu_1 = c_1 + i(\omega_c + 2\omega_p), \tag{19b}$$

$$\nu_2 = c_1 + i(\omega_c - 2\omega_p). \tag{19c}$$

The exponential damping factor, c_1, may be assigned a finite value or zero. The space-time function, $E(t',d)$, may therefore be written as the sum of three oscillatory waves;

$$E(t',d) = \frac{i}{2}E_\nu(t',d) - \frac{i}{4}E_{\nu_1}(t',d) - \frac{i}{4}E_{\nu_2}(t',d). \tag{20}$$

Figure 7 describes the propagated wave (20). Each term is calculated as described previously (2) ($c_1 = 0$). The dispersion of the pulse at early times is a result of the transient behavior of the ground wave. The dispersion of the pulse at later times is a result of the operation of the propagation medium on the widely separated frequency spectra that develop after considerable time, t', has elapsed. It is interesting to suggest that the amplitude and phase could simulate the output of amplitude and phase envelope detectors of a radio receiver. However, the finite bandwidth of the receiver, $f_r(\omega)$, should be introduced into the transform, $f(\omega)$, (9) as follows:

$$f(\omega) = E(\omega)[f_{s,1}(\omega) + f_{s,2}(\omega) + \ \ldots\ ] \\ [f_{r,1}(\omega) f_{r,2}(\omega)\ \ldots\ ], \tag{21}$$

where $f_{r,1}(\omega)$, $f_{r,2}(\omega)$, . . . are the transfer characteristics of the frequency selective networks in the receiver circuit.

4. Conclusion

The propagated transient signal over a finitely conducting plane earth can be reconstructed in detail, for current sources of complicated form, for all values of local time, by application of the inverse Laplace transformation. The most important merit of this analysis is the insight gained into the details of the propagation mechanism. It should be emphasized that the reconstruction of the complete signals at times less than approximately 0.1 microsecond requires the introduction of displacement currents and earth curvature, which have been neglected in this paper [3]. The method does however serve as a check on the tedious numerical methods of integration of the Fourier integral, the direct evaluation of which seems to be the obvious method of introducing into the transient solution of the ground wave the effect of the earth curvature and the effect of the displacement currents in the earth.

The mathematical formulas were programed for the electronic computer by L. C. Walters, and the computations were performed on the electronic computer by C. M. Lilley, both of the National Bureau of Standards staff. The work was sponsored by the Air Force Cambridge Research Center, Cambridge, Mass., and the Radio Navigation project of the National Bureau of Standards, Boulder, Colo.

5. References

[1] J. R. Johler, Propagation of the radiofrequency ground wave transient over a finitely conducting plane earth, Geofis. pura e appl. **37** (May–August 1957).

[2] J. R. Wait, Transient fields of a vertical dipole over a homogeneous curved ground, Can. J. Phys. **34**, 27–35 (Jan. 1956).

[3] J. R. Wait, The transient behavior of the electromagnetic ground wave over a spherical earth, Trans. Inst. Radio Engrs. AP-**5**, No. 2 (April 1957).

[4] J. R. Johler, W. J. Kellar, and L. C. Walters, Phase of the low radiofrequency ground wave, NBS Circ. 573 (June 27, 1956).

Boulder, Colo., August 30, 1957.

Journal of Research of the National Bureau of Standards Vol. 60, No. 4, April 1958 Research Paper 2845

Measurement of Current with a Pellat-Type Electrodynamometer

R. L. Driscoll

The value of an electric current has been determined in absolute measure by means of an electrodynamometer, and simultaneously by standard cells and standard resistors as currently maintained. The electrodynamometer used was of the Pellat type, and featured a fused silica balance beam and single layer helical coils.

The relation of the NBS ampere to the absolute ampere, from this determination, may be expressed as

1 NBS ampere = 1.000013 absolute amperes.

The uncertainty in this result from all known sources is estimated to be eight parts per million.

1. Introduction

The important units in electrical measurements are the ampere, the ohm, and the volt. Since these units are connected by Ohm's law, any one of the three is fixed when the values of the other two are settled upon. These units are all defined in terms of the mechanical units, but the accuracy of their physical realization depends upon experimental approximations to unattainable ideal conditions. In the electromagnetic system, the ampere is defined as 10^{-1} cgs units, the ohm 10^{9} cgs units and the volt 10^{8} cgs units. The two units so far found susceptible of accurate independent evaluation in terms of the mechanical units are the ohm and ampere. On account of the transitory nature of electric current the ohm and the volt are the two units maintained in the form of concrete standards. It is necessary therefore to assign a value to the standard of electromotive force obtained from a combination of the results of primary standardization of the ohm and ampere. On account of the implicit relation of the electrical units to other physical constants, it is desirable that these units be close to their defined values. In order to detect drifts in the standards, repetition of absolute measurements from time to time has been the accepted practice. Experiments now being conducted at this Bureau on the precession frequency of protons in the magnetic field of a coil carrying a current, show promise of providing a precise method for determining the constancy of the current over long periods of time. An account of the last work on the ampere at this Bureau was published in 1942 [1].[1] In that investigation a current balance [2] was employed; in an effort to avoid possible systematic errors in the current balance, a Pellat-type electrodynamometer [4] (sometimes referred to as a Pellat balance) has been used in this work. In the current balance the force measured is one of translation and in the electrodynamometer it is one of rotation. This paper describes the important physical measurements that were made and assesses the accuracy of the determination of a current by the latter absolute method.

[1] Figures in brackets indicate the literature references at the end of this paper.

[2] A companion paper to follow in this Journal will present values from recent measurements.

2. Value of a Current in Terms of Mechanical Effects

The torque between two coils in which the currents i_1 and i_2 are held constant has been worked out in a general way by Maxwell [2]. In the particular case of the Pellat electrodynamometer, the two coils are adjusted to be concentric and to have an angle, θ, of 90° between their axes. With this adjustment the torque, $\mathcal{T}$, is a maximum and is given by

$$\mathcal{T} = i_1 i_2 \left[\frac{\partial M}{\partial \theta}\right]_{\theta=\frac{\pi}{2}} \tag{1}$$

where M is the mutual inductance of the coils. In absolute measurements the geometrical factor, $\partial M/\partial\theta$, is computed from measured values of the linear dimension of the coils. The mathematical contributions of Snow [3] make possible a second order calculation of this factor for the electrodynamometer that includes several small corrections made necessary by the fact that the coils are helical wires having small measurable irregularities and are not uniform current sheets.

Another factor affecting the absolute measurement of current is the accuracy realized in the evaluation of the torque produced. When single layer helical windings are employed, the torque produced is relatively small and more effort is required for its accurate evaluation than that demanded in the case where multilayer windings are used. The advantage gained in the accuracy of the geometrical factor, $\partial M/\partial\theta$ when single layer helical windings are employed more than offsets the disadvantage of the smaller torque.

3. Electrodynamometer

This instrument has a long stationary solenoid (fig. 1) with its axis horizontal; the centered inner coil, mounted on the beam of a balance (fig. 2), is a short solenoid with its axis vertical. The balance beam (fig. 7) is equipped with conventional knife edges and supports the inner coil which thus becomes rotatable about the central knife edge.

With a steady current in both coils in series, the balance is put into equilibrium by means of a suitable

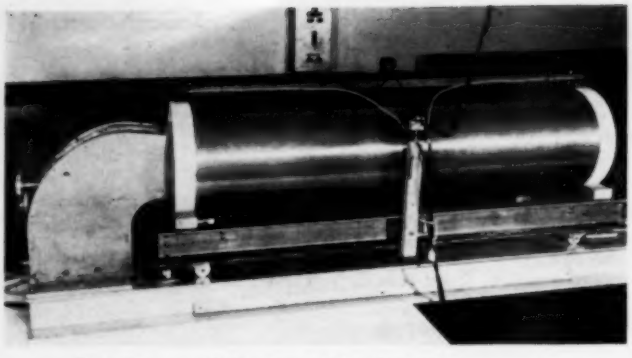

FIGURE 1. *Side view of the electrodynamometer.*

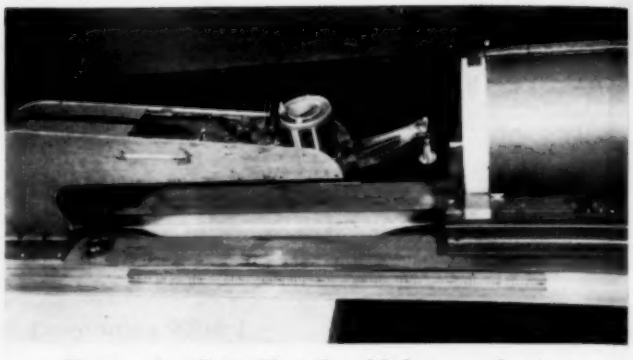

FIGURE 2. *Rotatable coil and balance mechanism.*

counterweight; on reversing the current in the stationary coil, the equilibrium of the balance is restored by placing a weight on the arm of the balance. From the known value of the balancing weight, the length of the balance arm, and the geometry of the windings, the value of the current can be calculated by eq 1.

The version of the Pellat electrodynamometer used in this work employs single-layer helical windings of bare wire the dimensions of which can be checked at any time. In his instrument Pellat employed multilayer windings. These windings produced a large torque with permissible currents but the large uncertainty in their linear dimensions would be intolerable according to present requirements. The other important modification in the present instrument is the use of a fused silica balance beam instead of the brass beam of Pellat. The construction of this type of current measuring device was proposed by Harvey L. Curtis as long ago as 1927. Materials for the beam and stationary coil were purchased around 1930. Through the efforts of Roger W. Curtis much of the support for this balance was completed by 1940. At the end of World War II a project was set up for the continuation of the primary standardization of current and it has been pursued without much interruption since 1950. Much encouragement and help on the finishing of the balance beam and the coils was obtained from Charles Moon before his death in 1953.

An over-all view of the electrodynamometer with the stationary coil in place is shown in figure 1; in figure 2 the stationary coil has been moved to the side to expose the interior of the instrument. The supports of the balance are mostly of aluminum alloy. A small amount of brass and phosphor bronze was used in the arrestment mechanism. Each piece was tested before finishing to assure that it had low magnetic susceptibility. The agate planes and knife edges of the balance were finished by the Optical Shop of this Bureau, the material for these being donated from the collection of Earl F. Webb. Electrical connections to the rotatable coil are effected by means of two sets of flexible wires. Each set consists of ten 1-mil bare copper wires, in parallel, having a length of about 3 inches. Slack in the wires was adjusted to make their restraint on the balance tolerable.

4. Construction of the Coils

Both the stationary and rotatable coils were constructed by the method of Moon that has been described in some detail by Curtis, Moon, and Sparks [5]. Following Moon's method the wire was wound in a helical groove that was produced in the coil form by the process of lapping. The stationary coil form is of fused silica and the rotatable coil form is of Pyrex glass. Oxygen-free copper wire is used in the windings of both coils. Sapphire dies were used to reduce the wire to the desired diameter. After each of the preliminary drawing operations, the wire was spooled on smooth drums in a single layer to avoid kinking. After final drawing, the wire on leaving the die was wound directly in the groove on the coil form.

5. Measurement of the Dimensions of the Coils

As far as the stationary coil is concerned, the pitch is the parameter of primary importance, the diameter is of less importance as it appears only in a correction term to take account of the finite length of this coil. On the other hand, the diameter of the rotatable coil is extremely important but the value of its pitch is needed with relatively little accuracy.

5.1. Pitch Measurement

The pitch of the rotatable coil was taken as the nominal value of the pitch of the lapped groove which was 2/3 mm.

The pitch of the stationary coil was measured by the micrometer method described by Curtis, Moon, and Sparks [5]. Longitudinal readings for the measurement of pitch were taken at several places along the coil in each of six angular positions around the winding. Measurements were made with the coil supported at its ends. It was demonstrated that the bending of the tube when supported in the manner did not affect the measured pitch by as much as 1 ppm. The results are summarized in table 1.

5.2. Diameter of Coils

The importance of the diameter of the rotatable

coil has already been mentioned. Although the diameter of the stationary coil was not needed with the highest accuracy, considerable pains were taken on account of its potential use as a standard of self inductance, and the values obtained will be recorded here. The method used in measuring both coils was similar to that described by Curtis, Moon, and Sparks [6]. The experimental arrangement of apparatus used in the measurement of the rotatable coil is shown in figure 3 and that used in the case of the stationary coil is given in figure 4. The results are given in tables 2 and 3 and in figures 5 and 6. The correction given in table 2 to the diameter of the

TABLE 1. *Axial length and pitch of stationary coil*

Date, 1952	Azimuth position	End std.	Interval measured	Intervals examined	Pitch at 25° C
	Degrees	*NBS No.*	*Turns*	*Number*	*mm/turn*
21 Mar	0	6, 827	454	8	1. 000087
24 Mar	90	6, 827	454	8	1. 000086
25 Mar	180	6, 827	454	8	1. 000085
25 Mar	270	6, 827	454	8	1. 000088
26 Mar	300	6, 827	454	8	1. 000088
27 Mar	120	6, 827	454	8	1. 000084
4 Apr	300	1, 993	281	7	1. 000093
4 Apr	300	1, 992	274	6	1. 000090
9 Apr	300	6, 827	454	8	1. 000087
9 Apr	120	6, 827	454	8	1. 000085
10 Apr	30	6, 827	454	8	1. 000086
10 Apr	210	6, 827	454	8	1. 000087
				Average	1. 000087

Axial length of coil (1,000 turns) at 25° C ..... 100.0087 cm.
Axial temperature coefficient of expansion ..... 0.2 ppm/° C.

TABLE 2. *Diameter and temperature coefficient of rotatable coil*

Position	Diameter, over-all		Temperature coefficient
Degrees	*mm at 25.0° C*	*mm at 35.7° C*	*ppm/° C*
0	116. 4014	----------	----------
45	116. 4009	116. 4068	4. 7
90	116. 4011	----------	----------
135	116. 4012	----------	----------
Average	116. 4011	----------	4. 7

Diameter of wire

Sample No.	Origin of sample	
	Beginning of winding	End of winding
	mm	*mm*
1	0. 5613	0. 5620
2	. 5619	. 5619
3	. 5617	. 5620
Average	0. 5618	

Average over-all diameter at 25.0° C ..... 116.4011 mm
Wire diameter ..... 0.5618 mm
Mean diameter of winding, $2\bar{a}_2$, at 25.0° C ..... 115.8393 mm
Force on wire during winding ..... 12 lb
Initial strain in wire, K_2 ..... 21.4×10^{-4}
Correction for current distribution, $\frac{\Delta\bar{a}_2}{\bar{a}_2}$, (see section 7) ..... -7.6 ppm
Effective radius, $a_2=\bar{a}_2+\Delta\bar{a}_2$ ..... 57.9192 mm
Resistance of winding at 25° C ..... 3.6570 ohm
Change of resistance with temperature ..... 0.01358 ohm/° C
Thickness of Pyrex glass form ..... 0.8 cm
Magnetic susceptibility of form ..... -1×10^{-6}

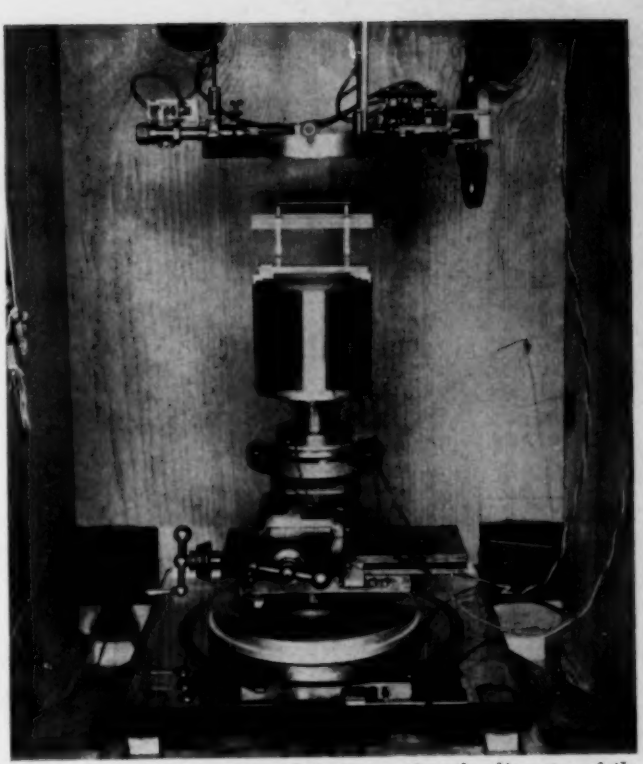

FIGURE 3. *Equipment used in measuring the diameter of the rotatable coil.*

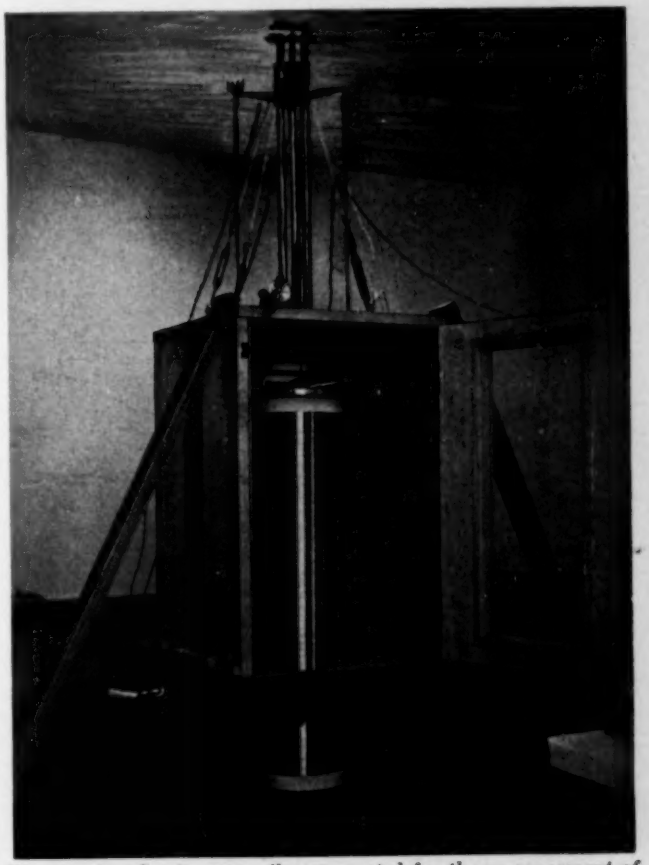

FIGURE 4. *Stationary coil as mounted for the measurement of diameter.*

rotatable coil to take account of the current distribution is based upon the theory of Chester Snow and the experiments of Thomas Wells [7] on the resistivity-strain coefficient of the wire used in this coil as discussed in section 7.

TABLE 3. *Diameter and temperature coefficient of stationary coil*

Position	Diameter, over-all				Temperature coefficient
	Top half	Bottom half	Bottom half	Bottom half	
Degrees	*mm at 25° C*	*mm at 25° C*	*mm at 28.9° C*	*mm at 34.4° C*	*ppm/° C*
0	280.3236	280.3235	.....	.....	.....
45	280.3243	280.3231	.....	.....	.....
90	280.3242	280.3246	.....	.....	.....
135	280.3235	280.3241	280.3253	280.3266	+1.0
Average	280.3239	280.3238	.....	.....	.....

Diameter of wire

Sample No.	Origin of sample	
	Beginning of winding	End of winding
	mm	*mm*
1	0.6995	0.6990
2	.6992	.6989
3	.6992	.6990
Average	.6993	.6990

Average over-all diameter at 25.0° C	280.3239 mm
Wire diameter	0.6991 mm
Mean diameter of winding, $2a_1$, at 25° C	279.6248 mm
Force on wire during winding	15 lb
Initial strain in wire, K_1	16.8×10^{-4}
Correction for current distribution, $\frac{\Delta a_1}{a_1}$ (see section 7)	−2.1 ppm
Effective radius, $a_1=a_1+\Delta a_1$	139.8121 mm
Thickness of fused silica form	2.5 cm
Magnetic susceptibility of form	-0.8×10^{-4}
Resistance of winding at 25° C	40.40 ohms
Change in winding resistance with temperature	0.15 ohm/° C

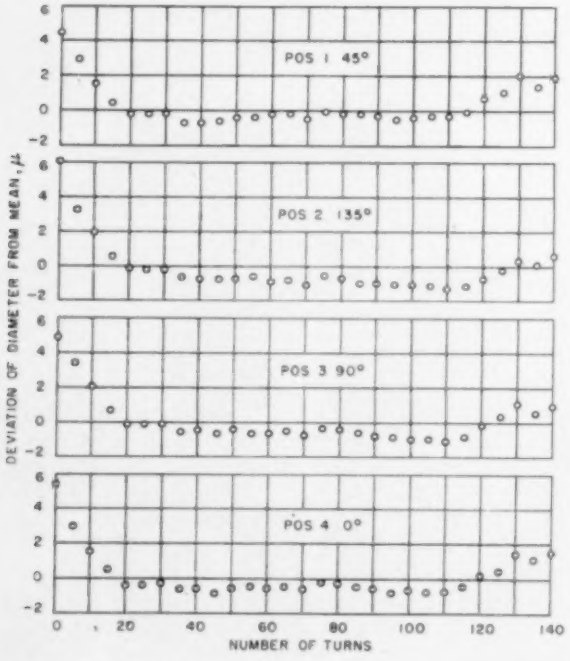

FIGURE 5. *Variation in the diameter of the rotatable coil.*

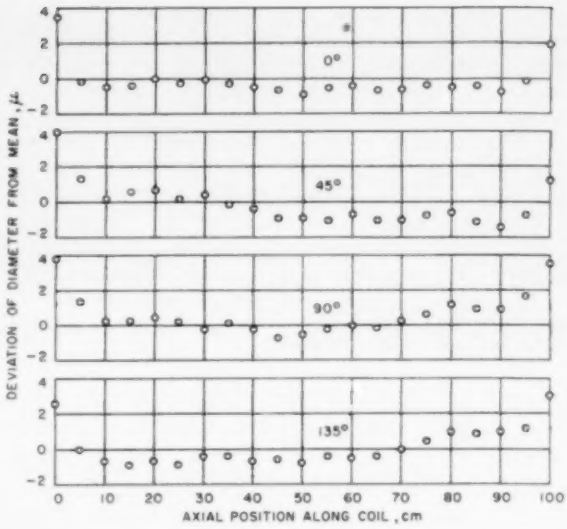

FIGURE 6. *Variation in the diameter of the stationary coil.*

6. Length of the Balance Arm

The distance between the outer knife edges of the beam, figure 7, was evaluated by comparison with a calibrated interval on a line standard. The balance beam was mounted on a comparator intended originally for the purpose of comparing line standards. In this instrument the unknown and standard are placed side by side on separately adjustable mountings. These mountings were attached to a carriage that could be moved to bring either the standard or unknown into the field of two rigidly supported microscopes. It was found possible to set the cross hairs of the microscopes over the apexes of the knife edges on the beam in the same manner as on a graduation of a line standard. The difference between the spacing of the outer knife edges and a known interval on the line standard was obtained from the readings of the filar micrometer eyepieces of the microscopes. Through the cooperation of L. V. Judson and B. L. Page of the Metrology Section, facilities were provided for making this measurement.

The ratio of the arm lengths was determined by weighing known masses. As indicated in table 4 no significant difference was found in this ratio over a period of 3 years whether 20-gram or 3-gram masses were used. The masses were transposed as far as possible but since the arm lengths differed by 1.5 percent a number of small masses had to be left on one pan. Dividing the unloaded length (l_1+l_2) by $(1+l_2/l_1)$, where l_2/l_1 is the ratio of the arms when symmetrically loaded, gives a first approximation to the length, l_1, of the arm chosen to receive the balancing mass. As pointed out by R. D. Cutkosky a further correction must be applied to allow for the increase in the length of the arm when the pan and balancing mass are applied. To measure this distortion, the beam was mounted on a surface plate, the four bosses under the central part of the beam (fig. 7) being secured to the plate with beeswax.

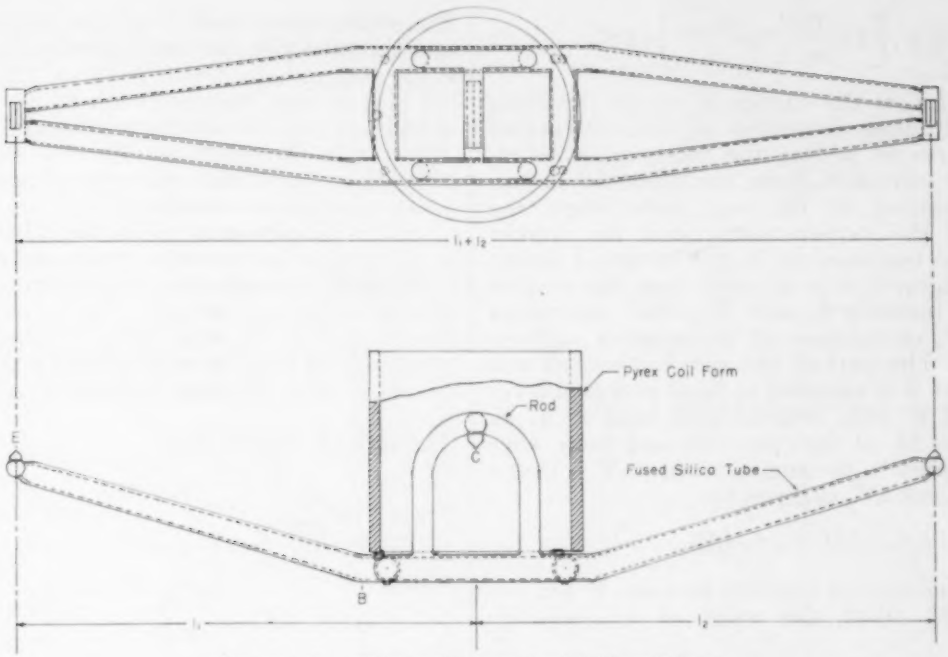

FIGURE 7. *Balance beam and rotatable coil form.*

TABLE 4. *Length of balance arm*

Distance between end knife edges, (l_1+l_2)

Date, 1951	Temperature		(l_1+l_2) Corr. to 25° C
	Beam	Standard	
	°C	°C	cm
28 June	29.0	29.0	50.59226
29 June	27.0	27.1	.59238
29 June	27.4	27.2	.59234
29 June	28.0	28.1	.59236
2 July	26.2	26.2	.59248
6 July	26.0	26.0	.59251
Average			50.59239

Above values based upon calibrated interval 390 to 896 mm on meter bar 153–R.

Ratio of balance arms, l_2/l_1

Date	l_2/l_1	Condition of weighing
19–20 Aug. 1952	0.984546	20-gram masses
15 Dec. 1953	.984548	3-gram masses transposed
22 July 1955	.984550	3-*g* masses transposed
23 July 1955	.984547	3-*g* masses transposed
Mean	0.984548	

Unloaded length l_1 of balance arm	25.49316 cm
Correction (37.1 ppm) for distortion under load	0.00095 cm
Effective length at 25° C	25.49411 cm

(It was on these bosses that the beam rested during the measurement of the distance between the end knife edges.) By means of a microscope equipped with a filar micrometer eyepiece the endwise movement of the knife edge at E figure 7 was measured when a load equal to the scale pan was applied to that end of the beam. A further complication arises when the standard mass is added to the scale pan and the current in the stationary coil is reversed, that is, there is then an additional increase in the length of the balance arm. Both distortions affect the position of all the load on the end knife edge including, though to a lesser extent, the distributed mass of the balance arm.

In order to discuss these effects, let the following notation be used:

P = Mass of scale pan,
m = standard balancing mass,
g = acceleration of gravity,
l_1 = unloaded length of balance arm,
δl_P = change in l_1 on adding load P,
$\delta.\mathscr{T}_P$ = change in torque to allow for distortion of the distributed mass of beam on adding load P,
$\mathscr{T}_1$ = torque on rotatable coil with mass m removed and stationary coil current in forward direction,
$\mathscr{T}_2$ = torque on rotatable coil with mass m on scale pan and stationary coil current reversed.

If the standard mass m is adjusted so that the balance is in equilibrium for both directions of the stationary coil current, the change in torque on the rotatable coil is given by $\mathscr{T}_2-\mathscr{T}_1$,

where

$$\mathscr{T}_1=Pg\ (l_1+\delta l_P)+\delta.\mathscr{T}_P$$

and

$$\mathscr{T}_2=(P+m)g(l_1+\delta l_{P+m})+\delta.\mathscr{T}_{P+m}.$$

Subtracting the above expressions

$$\mathscr{T}_2-\mathscr{T}_1=mgl_1\left[1+\frac{P}{m}\frac{\delta l_m}{l_1}+\frac{\delta l_{P+m}}{l_1}\right]+\delta\mathscr{T}_m. \quad (2)$$

The quantity $\delta\mathscr{T}_m$ is the change in torque resulting from the additional distortion of the distributed mass of the arm on adding the balancing mass m. Its value was estimated from the observed distortion, δl_m, measured at the end knife edge, the dimensions of the various parts, and the density of the material (assumed to be 2.2 for fused silica). Referring to figure 7 it is assumed that the portion of the beam between C and B would contribute nothing to $\delta\mathscr{T}_m$ on account of the relative stiffness of that part. The part of the arm between B and the cross rod at E is assumed to bend as a cantilever beam fixed at B with concentrated load m at E. The total mass M_r of the cross rod and knife edge at E is considered to be concentrated at E. Under these assumptions $\delta\mathscr{T}_m$ is given by

$$\delta\mathscr{T}_m=[M_r+3/8M_t]\delta l_m,$$

where M_t is the mass of the arm between B and the cross rod at E. With this value of $\delta\mathscr{T}_m$ eq. (2) becomes

$$\mathscr{T}_2-\mathscr{T}_1=mgl_1\left[1+\frac{(P+M_r+3/8M_t)}{m}\frac{\delta l_m}{l_1}+\frac{\delta l_{P+m}}{l_1}\right]. \quad (2')$$

Numerical values obtained for the quantities in the brackets of eq (2′) are as follows:

$m=1.481$ grams	$M_t=31.5$ g
$P=18.3$ grams	$\delta l_m/l_1=1.0\times10^{-6}$
$M_r=4.4$ grams	$\delta l_{P+m}/l_1=13.8\times10^{-6}$

When these numerical values are applied in eq (2′) the corrected torque is

$$\mathscr{T}_2-\mathscr{T}_1=mgl_1[1+37.1\times10^{-6}].$$

In effect the unloaded length l_1 of the balance arm is increased by 37.1 ppm as a result of the distortion under load. The correction for this is applied in table 4.

7. Geometrical Factor of the Electrodynamometer

The maximum torque, T, produced by unit currents in concentric helical wires is given by Snow [3] as follows:

$$T=\left[\frac{\partial M}{\partial\theta}\right]_{\theta=\pi/2}$$
$$=4\pi^2\frac{N_1}{L_1}a_2^2N_2\mu_1\left\{1+S+S_1+\frac{2}{L_2a_2}\int_{-L_2/2}^{L_2/2}U_a(x_2)dx_2\right.$$
$$\left.+\frac{a_1}{2\mu_1}\int_{-L_1/2}^{L_1/2}\left[\frac{(2x_1^2-a_1^2)}{(x_1^2+a_1^2)^{5/2}}U_a(x_1)-\frac{3a_1x_1}{(x_1^2+a_1^2)^{5/2}}U_x(x_1)\right]dx_1\right\}. \quad (3)$$

The subscripts 1 and 2 refer to the stationary coil and the rotatable coil respectively, and

a = radius of coil,
L = length of winding,
N = total number of turns in a winding,
x = axial distance from center of a winding,
μ = cosine of the angle between the diagonal of a coil and its axis,
$U_x(x)$, $U_a(x)$ = observed displacement of any part of a winding in an axial or radial sense respectively from the position it would have if the winding were uniform.

The series S is given by:

$$S=(1-\mu_1^2)\sum_{n=1}^{\infty}(-1)^{n+1}\left(\frac{r_2}{r_1}\right)^{2n}C_n(\mu_1)C_{n+1}(\mu_2)\left(n+\frac{1}{2}\right)A_n,$$

where

$$A_n=\frac{1\cdot3\cdot5\cdot\cdots\cdot(2n-1)}{2\cdot4\cdot6\cdot\cdots\cdot2n}$$

$$C_n(\mu)=\frac{P'_{2n}(\mu)}{n(2n+1)\mu},$$

$$r=\sqrt{a^2+L^2/4}$$

$P_n(\mu)$ is Legendre's polynomial of degree n, and $P'_n(\mu)$ is $(d/d\mu)\ P_n(\mu)$.

Also

$$S_1=\frac{(1-\mu_1^2)(1-\mu_2^2)}{6a_2^2}\sum_{n=1}^{\infty}(-1)^{n+1}\left(\frac{r_2}{r_1}\right)^{2n}$$
$$\cdot C_n(\mu_1)C_n(\mu_2)n\left(n+\frac{1}{2}\right)A_n\left[n\frac{L_1^2}{N_1^2}-\left(n+\frac{1}{2}\right)\frac{L_2^2}{N_2^2}\right]$$

The radius of the rotatable coil, a_2, in eq (3) is the effective radius rather than the mean radius, $\bar{a}_2$, of the winding, determined by mechanical measurement. The difference between the effective and mean radii depends on the variation of current density over the cross section of the wire. The "natural" distribution of current density (inversely proportional to distance from the axis of the coil) would certainly apply if the resistivity were constant everywhere in the wire. Some measurements by Wells [7] indicate that for a wire in simple tension, the resistivity-strain coefficient can be represented empirically by

$$\frac{\Delta\sigma}{\sigma_0}\Big/\frac{\Delta l}{l_0}=\beta+\gamma\left(\frac{\Delta l}{l}\right)^2, \quad (4)$$

where, σ_0, is the resistivity and l_0 is the length of the unstrained specimen. The constants β and γ were determined by Wells on oxygen-free copper wire to have the values $\beta=1.13$ and $\gamma=-2.5\times10^4$. To the extent that the strain at any point in the wire can be

determined from the initial tension and bending, the resistivity-strain relation can be incorporated in an expression for the current density as a function of the distance from the axis of the coil. A section in the wire cut by a plane through the axis of the coil is shown in figure 8. The coordinates of a point, $P(x, y')$, are shown as functions of r and θ in the wire. The current density, $i(y')$, is assumed to be inversely proportional to $(\bar{a}_2+y')$ and the resistivity, $\sigma(y')$, and is independent of x. The initial strain, K_2, is known from the winding tension and is taken to be independent of x and y'. The strain due to bending around the form is assumed to be equal to $y'/\bar{a}_2$ and independent of x. On the basis of these assumptions, the current in a filament of area $r\,d\theta\,dr$ is given by

$$i(y')rd\theta dr=\frac{Crd\theta dr}{2\pi(\bar{a}_2+y')\sigma(y')}. \tag{5}$$

On setting the strain $\Delta l/l_0=\left(K_2+\frac{y'}{\bar{a}_2}\right)$ in eq 4, the resistivity at any y' can be written

$$\sigma(y')=\sigma_0(1+\beta K_2+\gamma K_2^3)\left[1+B_1\frac{y'}{\bar{a}_2}+B_2\left(\frac{y'}{\bar{a}_2}\right)^2+B_3\left(\frac{y'}{\bar{a}_2}\right)^3\right] \tag{6}$$

where

$$B_1=\frac{\beta+3\gamma K_2^2}{1+\beta K_2+\gamma K_2^3},$$

$$B_2=\frac{3\gamma K_2^2}{1+\beta K_2+\gamma K_2^3},$$

$$B_3=\frac{\gamma}{1+\beta K_2+\gamma K_2^3}.$$

On combining eqs (5) and (6) and neglecting terms of higher order than the third in $(y'/\bar{a}_2)$, the current density is given by:

$$i(y')=\frac{C}{2\pi\bar{a}_2\sigma_0(1+\beta K_2+\gamma K_2^3)}\,[1-C_1y'/\bar{a}_2+C_2(y'/\bar{a}_2)^2-C_3(y'/\bar{a}_2)^3], \tag{7}$$

where

$C_1=B_1+1$,

$C_2=-(B_2-B_1-B_1^2-1)$, and

$C_3=(B_3-B_2+B_1+B_1^2+B_1^3-2B_1B_2+1)$.

The constant $C/2\pi\bar{a}_2\sigma_0(1+\beta K_2+\gamma K_2^3)$ must be $i(o)$ and its value, by the integral $\int_0^{\rho_2}\int_0^{2\pi} i(y')\,rd\theta dr$ that

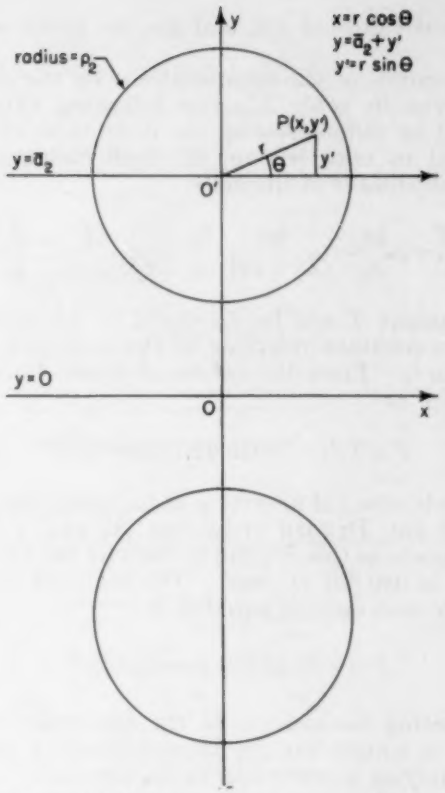

FIGURE 8. *Section through one turn of rotatable coil cut by an axial plane.*

makes unit current in the wire is

$$\frac{1}{\pi\rho_2^2}\left[1-\frac{C_2}{4}\left(\frac{\rho_2}{\bar{a}_2}\right)^2\right].$$

If this value be placed in eq 7 one gets

$$i(y')=\frac{1}{\pi\rho_2^2}\left[1-C_1\left(\frac{y'}{\bar{a}_2}\right)+C_2\left\{\left(\frac{y'}{\bar{a}_2}\right)^2-\frac{1}{4}\left(\frac{\rho_2}{\bar{a}_2}\right)^2\right\}-C_3\left(\frac{y'}{\bar{a}_2}\right)^3\right]. \tag{8}$$

The current function, eq (8), is of the same form as that considered by Snow [3] who found that in effect this current distribution in the wire changes its radius from $\bar{a}_2$ to $(\bar{a}_2+\Delta\bar{a}_2)$ where $\Delta\bar{a}_2=\frac{1}{8}(\rho_2^2/\bar{a}_2)(1-2C_1)$, terms in $(\rho_2/\bar{a}_2)^4$ and higher being neglected. Accordingly one can write to a good approximation, since the constants β, γ, and K_2 are not known with an accuracy better than a few percent.

$$\Delta\bar{a}_2=-\frac{1}{8}\frac{\rho_2^2}{\bar{a}_2}(1+2\beta+6\gamma K_2^3)$$

Likewise it is found that

$$\Delta\bar{a}_1=-\frac{1}{8}\frac{\rho_1^2}{\bar{a}_1}(1+2\beta+6\gamma K_1^3).$$

Numerical values of $\Delta\bar{a}_2$ and $\Delta\bar{a}_1$ are given in tables 2 and 3.

A summary of the computations on the constant T is given in table 5. The following expression, obtained by differentiating the main term of eq (3), was used to take account of small changes in the linear dimensions of the coils:

$$\frac{\delta T}{T}=2\frac{\delta a_2}{a_2}-\frac{4a_1^2}{(L_1^2+4a_1^2)}\frac{\delta a_1}{a_1}-\frac{L_1^2}{(L_1^2+4a_1^2)}\frac{\delta L_1}{L_1}.$$

The constant T can be set equal to Fl_1 where F is the force constant referring to the scale pan on balance arm l_1. From the results of tables 4 and 5 the value of F is

$$F=\mathrm{T}/l_1=70029.91 \text{ dynes}/\overline{\text{cgsu}^2}.$$

The acceleration of gravity g at the scale pan, on the basis of the Dryden reduction [8] and a gravity survey made at this Bureau in 1948 by the Geological Survey, is 980.081 cm/sec^2. The required balancing mass per unit current squared is

$$F/g=71.45318 \text{ grams}/\overline{\text{cgsu}^2}.$$

On reversing the current in the stationary coil the change in torque on the rotatable coil is doubled. After applying a correction to the torque of -3 ppm on account of the magnetic susceptibility of the coil forms and changing to the practical unit of current, the calculated balancing mass per ampere squared is

$$2F(1-3.0\times10^{-6})/100g=1.429059 \text{ grams}/\overline{\text{amp}^2}.$$

The correction applied above to the electrodynamometer constant on account of the magnetic susceptibility of the coil forms was estimated in the following manner. From the known susceptibility, k, of each coil form, the area A of its cross section, and the mean axial component of field H existing in the form, the quantity, q, of free magnetism existing on its ends was calculated by the expression $q=kAH$.

TABLE 5. *Computation of balance constant*

[Value used for the independent variables:

$a_1=13.98121$ cm. $L_1=100.0087$ cm. $N_1=1000$.

$a_2=5.79192$ cm. $L_2=9.3333$ cm. $N_2=140$.]

Quantity	Numerical value
μ_1	0.963064
μ_2	.6274
$4\pi^2\frac{N_1}{L_1}a_2^2N_2\mu_1$	1.785461×10^6
$C_1(\mu_1)$	1.0
$C_2(\mu_1)$	0.873111
$C_2(\mu_2)$	$-.0612$
$C_3(\mu_2)$	$-.212$
S	-63.0×10^{-6}
S_0	1.0×10^{-6}
$\frac{a_1}{2\mu_1}\int_{-L_1/2}^{L_1/2}\frac{(2z_1^2-a_1^2)}{(z_1^2+a_1^2)^{5/2}}U_a(z_1)dz_1$	$+1.0\times10^{-6}$
$T=[\partial M/\partial\theta]_{\theta=\frac{\pi}{2}}$	1.785350×10^6 dyne-cm

The magnetic charge distributed over each end of the stationary coil with one ampere flowing was thus estimated to be 1.5×10^{-3} pole. The contribution of the field of these charges to the field at the center of the stationary coil is found to be positive and of the order of one part in 10^7 even if the charges are regarded as point charges on the axis of the coil.

The magnetic charges on the ends of the rotatable coil induced by its own magnetic field are estimated to be 0.56 pole when one ampere is flowing. These charges contribute to the magnetic moment of the coil in the amount of -5×10^{-3} dyne cm/gauss. The magnetic moment of the rotatable coil in the absence of the form is 1,400 dyne cm/gauss. The correction to the torque on account of the rotatable coil form is thus estimated to be -3.0 ppm. An attempt was made to ascertain experimentally the effect of the aluminum alloy used in the balance support by placing more of this material in the opposite end of the stationary coil. No significant change in the measured torque was observed when approximately twice the original amount of aluminum alloy was added. It must be admitted that it would be difficult by this kind of test to guarantee that the effect was not as large as 1 ppm.

8. Measurement of the Torque

The electrical connections of the balance are shown in figure 9. During the measurement of the torque, the current was held constant at about 1.02 amp as determined by the standard cell and standard resistor. These standards were maintained at a constant temperature and compared from time to time with this Bureau's primary standards. When the current in the stationary coil was reversed, the change in torque was compensated by placing a mass on the balance arm. The mass (a platinum-iridium rod) was adjusted by trial and later evaluated by comparison with known standards. Small corrections to the balancing mass were made from readings on the calibrated scale of the balance. The sensitivity of the balance was 1.8 cm/mg and the corresponding half period was about 10 sec. The contribution of the current in the leads to the torque was determined separately and subtracted from the total torque. A series of runs, table 6, shows the fluctuations in the experimental result after all known corrections have been applied. The result of each run is derived from ten resting points of the balance each of which is calculated from nine observed turning points. Resting points were obtained at intervals of about 4 min with the current in the stationary coil alternately in the forward and reversed direction.

9. Results

On combining the results of the absolute current measurement with the value of the same current as derived from the NBS electrical standards, the final result of table 7 is obtained.

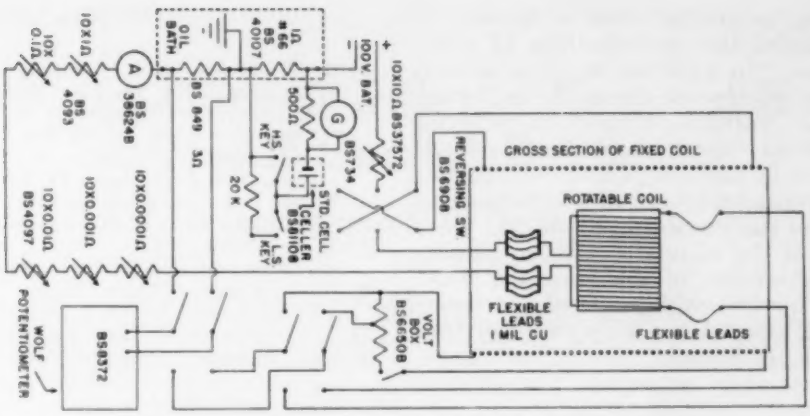

FIGURE 9. *Electrical connections of the electrodynamometer.*

TABLE 6. *Determination of balancing mass*

[Standard mass (Pt-Ir cylinder)—1481.146 mg. Buoyancy correction (air density 0.001164 gram/cm³)—0.080 mg. Standard mass corrected—1481.066 mg.

Date, 1954	Difference in rest points of balance		Corrections to individual trials for departures from 25° C						Add to standard mass
			Rot. coil		Stat. coil		Beam		
	cm	*mg*	*° C*	*mg*	*° C*	*mg*	*° C*	*mg*	*mg*
23 Apr.	0.002	0.001	36.9	−0.166	30.8	0.002	29.0	0.002	−0.161
24 Apr.	.012	.005	36.9	−.166	30.8	.002	29.0	.002	−.156
25 Apr.	.011	.006	36.8	−.164	30.7	.002	29.0	.002	−.154
26 Apr.	.016	.009	36.7	−.163	30.6	.002	29.0	.002	−.150
27 Apr.	.013	.007	36.9	−.166	30.7	.002	29.0	.002	−.155
28 Apr.	.002	.001	37.0	−.167	30.9	.002	29.0	.002	−.162
28 Apr.	.002	.001	37.1	−.168	31.0	.002	29.0	.002	−.163
29 Apr.	.007	.004	36.7	−.163	30.6	.002	29.0	.002	−.155
30 Apr.	.010	.005	36.9	−.166	30.8	.002	29.0	.002	−.157
1 May	.006	.003	37.0	−.167	30.9	.002	29.0	.002	−.160
2 May	.004	.002	37.3	−.171	31.1	.002	29.0	.002	−.165
10 May	.002	.001	36.6	−.161	30.5	.002	29.0	.002	−.156
26 May	.002	.001	36.8	−.164	30.7	.002	29.0	.002	−.159
Average									−0.158
Rotatable coil lead effect									−.111
Stationary coil lead effect									Negligible
Net balancing mass									1.480797 grams

TABLE 7. *Summary of results*

Calculated balance constant (section 7)	1.429059 grams/ampere²
Observed net balancing mass (table 6)	1.480797 grams
Current in absolute measure	1.017940 amperes
Emf of standard cell NBS 739	1.017935 volts
Resistance of standard resistor No. 66	1.000008 ohms
Current in NBS measure	1.017927 amperes
1 NBS ampere = 1.000013 ± 0.000008 absolute amperes	

TABLE 8. *Error in the final result*

Quantity	Error
	ppm
Diameter of rotatable coil	6
Length of balance arm	4
Determination of balancing mass	3
Acceleration of gravity	3
Pitch of stationary coil	1
Diameter of stationary coil	1
Pitch of rotatable coil	1
Standard resistor No. 66	1
Standard cell NBS 739	1
Adjustment of coils	1
Temperature of coils	1
I_{NBS}/I_{abs}	8

Known sources of error affecting the final result in table 7 are enumerated in table 8. The values given are intended to represent a 50-percent confidence interval in the measured current caused by the estimated uncertainty in the mean values of the quantities listed. The limiting factor in the accuracy of this electrodynamometer at present is the uncertainty in the radius of the rotatable coil. After increasing the radius by a factor of 1.5 and making use of a fused silica coil form it is estimated that the uncertainty in the radius of the rotatable coil could ultimately be cut in half. The relatively large uncertainty in the length of the balance arm is not inherent in this method but reflects the need of a more rigid balance beam.

This undertaking extending over a number of years has accumulated the contributions of many other staff members. In addition to those already named, the author wishes to thank the following: R. D. Cutkosky for valuable support in verifying the results by careful experimental checks; L. P. Slivka for assistance in the design and construction of the balance arrestment mechanism; Catherine Law for the calibration of the standard cell; W. H. Wood for the calibration of the standard resistor; Eleanor Clinton for the calibration of the standard mass; and A. G. Strang for the calibration of the length standards. Helpful suggestions were received from J. L. Thomas and F. B. Silsbee.

10. References

[1] R. W. Curtis, R. L. Driscoll, and C. L. Critchfield, J. Research NBS, **28,** 133 (1942) RP1449.
[2] J. C. Maxwell, Treatise on Electricity and Magnetism, Clarendon Press, Oxford, Vol. II, Third Ed., Section 583.
[3] Chester Snow, Torque between concentric single layer coils, NBS J. Research **22,** 607 (1939) RP1208.
[4] M. H. Pellat, J. Phys. **6,** 175 (1887); Bull. Soc. Intern. des Electriciens 2d Series **8,** 573 (1908).
[5] H. L. Curtis, Charles Moon, and C. Matilda Sparks, J. Research NBS **21,** 375 (1938) RP1137.
[6] H. L. Curtis, Charles Moon, and C. Matilda Sparks, J. Research NBS **16,** 1 (1936) RP875.
[7] T. E. Wells, Proc. Instr. Soc. of Am., Vol. II, (1956).
[8] H. L. Dryden, J. Research NBS **29,** 303 (1942) RP1502.

Washington, May 13, 1957.

Journal of Research of the National Bureau of Standards Vol. 60, No. 4, April 1958 Research Paper 2846

Measurement of Current with the National Bureau of Standards Current Balance

R. L. Driscoll and R. D. Cutkosky

Prior to the adjustment of the electrical units in 1948, the value of a current had been determined in absolute units by means of a current balance and simultaneously measured in NBS amperes by comparison with standard resistors and standard cells. This work was reported in RP1449. Similar measurements made recently with an electrodynamometer indicate a possible change in the values of the standards. The present paper reports a repetition of the work described in RP1449. The purpose of this remeasurement was to determine whether or not the standards had changed. Only minor changes were made in the equipment in order that factors which might have introduced small systematic errors in the results would remain unchanged.

According to the work described in this paper, 1 NBS ampere=1.000008 absolute amperes. Recent work with the Pellat electrodynamometer gave the result 1 NBS ampere = 1.000013 absolute amperes. The weighted mean of these two values is

1 NBS ampere-1.000010 ± 0.000005 absolute amperes

The results given above for the current balance differ by 6 ppm from those obtained in 1942. This indicates, in view of the uncertainties of measurement, that any change in the ampere as maintained by standard resistors and standard cells does not exceed a few parts in a million.

1. Introduction

The accuracy to which the electrical units as maintained at the National Bureau of Standards are known is under a continual process of improvement. A history of the development of the electrical units up to the adoption of the absolute units in 1948 [1] [1] has been presented by Silsbee [2]. Since the 1948 revision, two absolute determinations of electric current have been made at the Bureau.

The recent determination of current with a Pellat-type electrodynamometer [3] led to the result that the NBS unit of current was larger than the absolute ampere by 13 ppm (parts per million). The difference was not much more than the estimated uncertainty of the absolute measurement; but, since the values assigned to the NBS primary standard cells depend largely upon an earlier determination of current with the NBS current balance [4], it was thought necessary to repeat the earlier work in order to determine whether an appreciable drift in the electrical standards had taken place. This work was done as soon as possible after the completion of the measurement using the electrodynamometer, to assure as far as possible that both sets of absolute measurements were referred to the same electrical standards.

Photographs of the current balance used in 1942 and again in this determination appear in figures 1, 2, and 3. Briefly, the equipment consists of a helical fixed coil designated H_1 (fig. 6) in which current flows into the coil through a lead in the center of the helix, and out through leads on each end. A smaller helical coil designated P_1 hangs from an arm of a

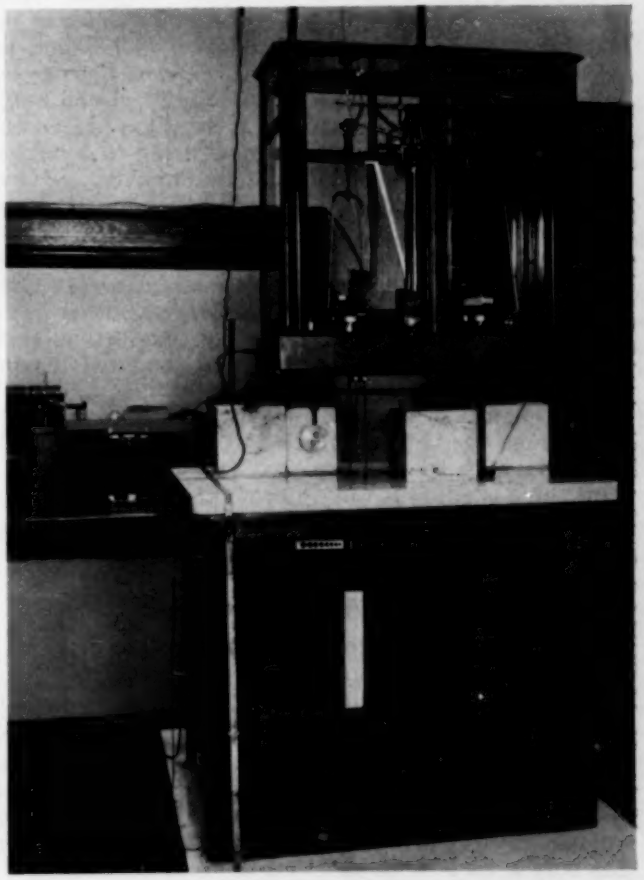

FIGURE 1. *Rear view of current balance showing fixed coil in operating position and operating room in background.*

[1] Figures in brackets indicate the literature references at the end of this paper.

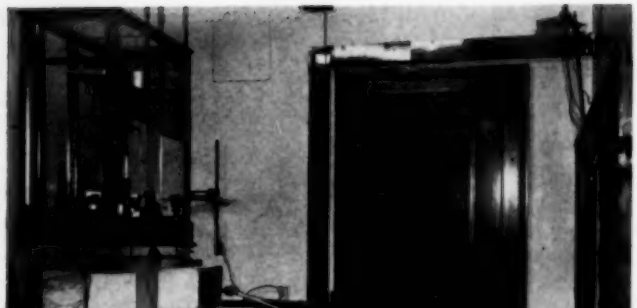

FIGURE 2. *Side view of current balance showing reversing switches and operating rod.*

sensitive balance so as to be concentric and coaxial with the fixed coil. A current flowing in the movable coil produces a force between the two coils, and tends to deflect the beam.

In practice, the current is held constant and evaluated in NBS units by comparing the potential drop it produces across a known resistance with the emf of a standard cell which is known with reference to the NBS primary standard cells. The balance is adjusted to equilibrium with this current flowing in both coils. Then, the current in the fixed coil only is reversed, and simultaneously a weight is placed on the balance pan. The weight is adjusted to equal as closely as possible the change in force caused by reversing the current. The small difference between the forces is observed as a change in the rest point of the balance. A switch for reversing the current is mounted on the coil case. A rod extends from this switch to the operating room; a cam and other connecting linkages enable the observer by turning this rod to raise and lower the weight on the balance pan and reverse the current at the same time.

The change in force caused by reversing the current is measured by comparison with the force exerted by gravity on the mass placed on the balance pan. This force is equal to the square of the current times a calculable function of the physical dimensions of the coils. From these equivalent expressions for the force, the current flowing can be determined in the mechanical units of length, mass, and time.

2. Changes in Equipment

Inasmuch as the redetermination of the ampere by means of the current balance was intended primarily as a check on the stability of the NBS standards, the principal features of the equipment were kept intact. The only geometrical change in the arrangement of the coils was a change in α, the angle between the movable and fixed coil leads, which has only a very small effect on the mutual force.

The standard cells were moved from the underground compartment to a "standard celler" [5] where

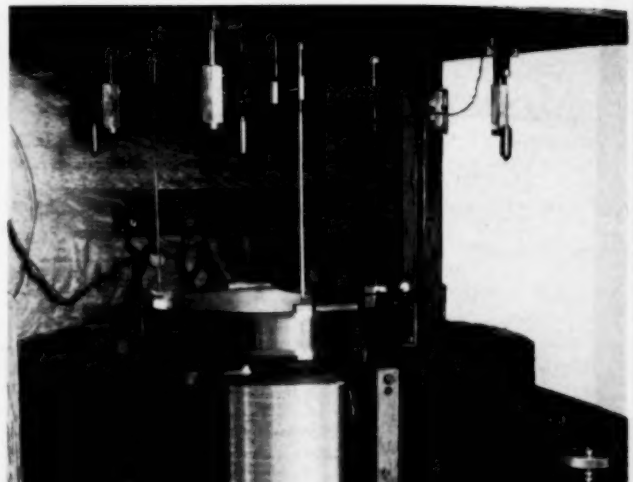

FIGURE 3. *Coil case with fixed coil lowered to show movable coil.*

their temperatures were thermostatically controlled near 34° C. This arrangement was used also for the Pellat electrodynamometer, and made it possible to regulate the cell temperatures and hence the cell voltages more precisely than had been possible before.

Changing the temperatures of the cells also changed their voltages, and made it necessary to decrease the size of the platinum weight that had been used with the balance in the earlier work.

The turning points of the balance are observed on the scale in the operating room by a beam of light reflected to the scale from a mirror mounted on the balance beam. A scheme in which the beam of light was reflected twice from a moving prism had been used before, in order to increase the balance sensitivity. We preferred to use a singly reflecting mirror instead of the doubly reflecting prism, because the hair line at the light source could be focused more sharply at the balance scale. The sensitivity of the balance dropped from 1.21 mg/cm to 2.33 mg/cm, but the reliability of the readings was improved.

During the preliminary measurements it was noticed that throwing the reversing switch mounted on the coil case gave the case a push that changed the apparent rest point of the balance as observed on the scale in the operating room. It was decided that the coil case was too shaky to be reliable, so copper straps were bound around it to make it more

rigid. These can be seen in the photographs. Also, a sliding joint was put into the switch rod. The performance of the balance was then checked with no current in the coils, and it was found that the position of the reversing switch had no effect on the rest point of the balance.

The turning points of the current balance have always been subject to random fluctuations. These are attributed to fluctuations in the air flow around the movable coil. Much experimentation has been done with ventilation of the coil case in an effort to steady the swings of the balance. The most satisfactory arrangement found was used for the final runs. This consisted of a honeycomb baffle under the movable coil and a fan to draw air from the top of the coil case. The fan was located about 20 feet from the coils and was connected with the coil case by means of a tube.

Reversing the current and changing the weight sometimes gives the balance an impulse which, if unchecked, would make the balance amplitude unsatisfactory. Previously the balance had been steadied after reversing the current by injecting short blasts of air under the balance pans. It was found that the turning points of the balance were more regular if the adjustments in balance amplitude were made by changing briefly the current through the coils. Two switches were installed in the operating room, one to increase, and one to decrease the current. All of the runs reported in this paper were obtained without the use of air jets.

3. Mechanical Dimensions

The mechanical dimensions of the coils were remeasured, using for the most part the methods that had been used in 1942. The end standards used to measure the diameters of the coils were re-evaluated by the NBS Gage Section. Summaries of the coil dimensions appear in table 1.

3.1. Diameter

Figures 4 and 5 illustrate the coherence between the earlier and recent measurements of the diameters

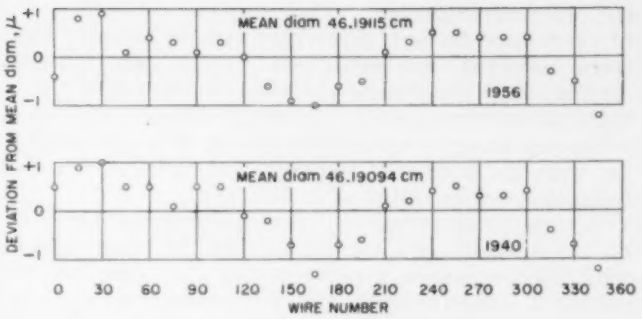

FIGURE 4. *Coherence between 1942 and 1956 measurements of fixed coil wire diameters.*

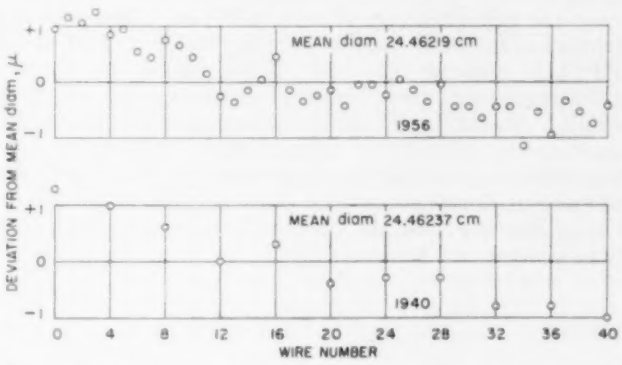

FIGURE 5. *Coherence between 1942 and 1956 measurements of movable coil wire diameters.*

of the two coils at 30° C. It can be seen that apparently the fixed coil became larger and the movable coil smaller. Some changes in dimensions are to be expected, and could be caused by a gradual relaxation of the strains in the wires or forms.

The diameter and electrical resistance of each coil were measured at three temperatures: near 25°, 30°, and 35° C. From these measurements it was possible to estimate, from measurements of the resistances of the wires, the diameters of the coils when they were in the balance case under different ambient conditions.

The newly determined temperature coefficients of expansion agree very well with the values found in

TABLE 1. *Constants of the fixed helix H_1 and the movable helix P_1*

[All values reduced to 30° C]

	H_1		P_1	
	1942	1956	1942	1956
Average outside diameter of coil ..... cm	46.20090	46.26111	24.51360	24.51342
Diameter of wire ..... cm	0.06996	0.06996	0.05123	0.05123
Mean diameter of coil ..... cm	46.19094	46.19115	24.46237	24.46219
Current distribution correction ..... cm	−0.00003	−0.00003	−0.00003	−0.00003
Weighting correction ..... cm	+.00002	+.00002	.0	.0
Effective mean diameter ..... cm	46.19093	46.19114	24.46234	24.46216
Axial length of coil ..... cm	27.51654	27.51642	2.6650	2.6649
Number of turns	344	.....	41	.....
Mean pitch ..... cm	0.0799899	0.0799896	0.065000	0.064998
Resistance of winding {Upper} ..... ohms	11.8016	11.7806	2.8220	2.8169
Resistance of winding {Lower} ..... ohms	11.7974	11.7808		
Resistance-temperature relationship {Upper} ..... ohms/°C	0.0443	0.0436	0.01079	0.01034
Resistance-temperature relationship {Lower} ..... ohms/°C	.0443	.0442		
Temperature coefficient of expansion ..... ppm/°C	3.6	3.5	3.9	3.7
Winding tension ..... kg	10	.....	3	.....

the old measurements. The temperature coefficients of resistance do not agree, but this is because they were assumed, not measured, in the earlier work. At that time the temperature coefficients were taken from tables of copper-wire characteristics. Since the wires are under considerable strain, it is not surprising that the measured temperature coefficients differ from the values assumed in RP1449.

A new measurement of the diameter of the wire on the movable coil was made, and the result agreed with the previous measurement. In view of the excellent agreement it was felt unnecessary to remeasure the fixed coil wire diameter.

The current distribution corrections contained in table 1 correct for the variation of current density over the cross section of each wire; no corresponding corrections were made in the work reported in RP1449 because the net effect based on Snow's assumption of the "natural" distribution [6] was small. Recently Wells [7] has measured the resistance-strain relation in copper wire, making it now possible to give further expression to the variation of current density over the cross section of the wires. Using Snow's formula for the helix equivalent to a helical wire, we have

$$\bar{r}_1 = r_1 + \frac{\rho_1^2}{8}\left(\frac{1}{r_1} + 2A_1\right),$$

where $\bar{r}_1$ = the effective coil radius,

r_1 = the mean coil radius,

ρ_1 = the wire radius,

$$A_1 = \frac{\left[\dfrac{du(r_1')}{dr_1'}\right]_{r_1'=r_1}}{u(r_1)},$$

and $u_1(r_1')$ is the volume density of current in the wire as a function of the distance r_1' from the x axis. A relationship similar to the above holds for the movable coil, whose coefficients will be denoted in what follows by the subscript "2." Snow has shown that the radius corrections do not depend upon the second derivative of $u(r)$. This means that a first order expansion of $u(r)$ will lead to a radius correction which is correct to second order.

The current density at a given point in the fixed coil is given by $u_1(r_1') = G/\sigma r_1' = (G/\sigma r_1)[1-(y_1/r_1)]$ to first order in y_1/r_1, where σ is the resistivity of the copper, $y_1 = r_1' - r_1$, and G is a constant. The analysis to follow is carried out for the fixed coil only, wire 1, but it is to be understood that the equations are valid for the movable coil, wire 2, also.

The resistivity of the copper has been measured in terms of the strain by Wells [7]. He finds that

$$\frac{\dfrac{\Delta\sigma}{\sigma_0}}{\dfrac{\Delta l}{l_0}} = \beta + \gamma\left(\frac{\Delta l}{l_0}\right)^2,$$

where $\beta = 1.13$ and $\gamma = -2.5\times10^4$;

or

$$\sigma = \sigma_0\left[1 + \beta\frac{\Delta l}{l_0} + \gamma\left(\frac{\Delta l}{l_0}\right)^3\right].$$

$\dfrac{\Delta l}{l_0}$ at a point in wire 1 is related to the initial strain in the wire, K_1, and the position of the point, y_1, by $\Delta l/l_0 = (y_1/r_1) + K_1$, where $K_1 = 2.5\times10^{-3}$ (and $K_2 = 1.4\times10^{-3}$). We then have to first order in y_1/r_1

$$\sigma = \sigma_0(1+\beta K_1+\gamma K_1^3)\left[1 + \frac{y_1}{r_1}\frac{(\beta+3\gamma K_1^2)}{(1+\beta K_1+\gamma K_1^3)}\right],$$

and

$$\frac{1}{\sigma} = \frac{1}{\sigma_0(1+\beta K_1+\gamma K_1^3)}\left[1 + \frac{y_1}{r_1}\frac{(\beta+3\gamma K_1^3)}{(1+\beta K_1+\gamma K_1^2)}\right]$$

leading to the result

$$u_1(r_1') = \frac{G}{r_1\sigma_0(1+\beta K_1+\gamma K_1^3)}\left[1 - \frac{y_1}{r_1}\frac{(1+\beta K_1+\gamma K_1^3+\beta+3\gamma K_1^2)}{(1+\beta K_1+\gamma K_1^3)}\right].$$

We then have

$$A_1 = -\frac{1+\beta+3\gamma K_1^2+\beta K_1+\gamma K_1^3}{1+\beta K_1+\gamma K_1^3},$$

and similarly for A_2. For the fixed coil, we have $A_1 = -0.07$, $\Delta r_1 = -1.7\times10^{-5}$ cm; and for the movable coil, $A_2 = -0.13$, $\Delta r_2 = -1.5\times10^{-5}$ cm. Δr_1 and Δr_2 are doubled and applied in table 1 as diameter corrections.

An attempt has been made to determine higher order corrections to the effective diameter based on Wells' resistivity determinations, but for the coils used here such corrections are negligible.

3.2. Pitch

The pitch of H_1 was measured as described in RP1449, and found to be insignificantly different from the earlier value. The pitch of P_1 was last measured in 1934, and was not remeasured for the 1942 work. A new determination was felt to be in order for the completeness of this determination, even though the force constant is not strongly dependent upon the pitch of the movable coil.

For the measurement of the movable-coil pitch a meter bar was set up vertically, parallel to the coil axis. A telescope was clamped to a vertical bar which was free to pivot in such a way as to swing the telescope from the meter bar to horizontal graduations ruled on the wires of the coil. The telescope was equipped with a filar micrometer eyepiece. A reading was made of the distance between a graduation ruled on a wire and a graduation on the meter bar. Then, the telescope was raised to measure the position of another wire. The distance between the

two wires is given by the distance between the two meter bar graduations plus the difference between the readings of the filar micrometer eyepiece.

The accuracy of the measurement depended upon how well the coil and meter bar remained fixed with respect to each other, and upon the repeatability of the pivot of the vertical bar. The measurement is not as good as that used to measure the fixed-coil pitch, which used two telescopes, both of which were mounted on the vertical bar. It is felt, though, that the method is better than that used in 1934, which used a single telescope mounted on a carriage with a calibrated screw movement. The two-telescope method is better than either method used, but the movable coil was too short to be viewed by both telescopes at the same time. The result of the pitch measurements is that the changes found were too small to make any change in the balance constant as large as 1 ppm.

4. Calculation of the Force Constant

The force between the two helices is computed from the formula given by Snow [6]. With the notation of RP1449,

r_1 = mean radius of fixed helix.
r_2 = mean radius of movable helix.
l_1 = axial length of fixed helix (pitch × number of turns).
l_2 = axial length of movable helix (pitch × number of turns).
N_1 = number of turns on fixed coil.
N_2 = number of turns on movable coil.
α = angle between movable coil and fixed coil leads.

$$X_1=\frac{l_2}{2}.$$

$$X_2=\frac{l_1-l_2}{2}.$$

$$X_3=\frac{l_1+l_2}{2}.$$

The force in dynes between the movable coil and the upper half of the fixed coil with unit cgs current flowing in each of them is given by

$$f=2\omega'(X_1)+\omega'(X_2)-\omega'(X_3),$$

where

$$\omega'(X)=\omega'_\theta(X)+\omega'_a(X;\alpha)+\overline{\omega}'_X(X,\alpha).$$

Also,

$$\omega'_\theta(X)=\frac{2\pi N_1N_2}{l_1l_2}\left\{X\sqrt{X^2+(r_1+r_2)^2}\,[\mathrm{K}-\mathrm{E}]+\frac{X(r_1-r_2)^2}{\sqrt{X^2+(r_1+r_2)^2}}\left[\mathrm{K}-\Pi\right]\right\};$$

$$\omega'_a(X,\alpha)=\frac{\pi X}{6\sqrt{X^2+(r_1+r_2)^2}}\left[\frac{2-k^2}{1-k^2}\mathrm{E}-2\mathrm{K}\right]+\frac{\pi X}{4\sqrt{r_1r_2}}\left(\cos\frac{\alpha}{2}\right)\sin^{-1}\left(k\cos\frac{\alpha}{2}\right)-\frac{k(2-k^2)}{2(1-k^2)}\sqrt{1-k^2\cos^2\frac{\alpha}{2}}+\left(\sin\frac{\alpha}{2}\right)\log_e\left[\frac{k\sin\frac{\alpha}{2}+\sqrt{1-k^2\cos^2\frac{\alpha}{2}}}{\sqrt{1-k^2}}\right];$$

$$\overline{w}'_X(X,\alpha)=\frac{X}{\sqrt{X^2+(r_1+r_2)^2}}\log_e\frac{r_1}{\sqrt{r_1^2+r_2^2-2r_1r_2\cos\alpha}};$$

$$k^2=\frac{4r_1r_2}{X^2+(r_1+r_2)^2};\text{ and }k_0^2=\frac{4r_1r_2}{(r_1+r_2)^2}.$$

K, E, and Π are the complete elliptic integrals of the first, second, and third kind, respectively, to the modulus k and parameter k_0.

As in RP1449, the force in dynes between the helices with one ampere in the wires, F_{HH}, taking account of both halves of the fixed helix and of reversal of the current, is $F_{HH}=4f/100$.

The formula for the calculation of the force constant assumes that the diameter of each coil is uniform throughout its length. Clearly some turns affect the force constant more strongly than others. Use of the mean diameter in the calculations attaches undue importance to certain turns of wire, such as those near the center of the fixed coil, which have little effect upon the force constant. A plot was made of the calculated force, $f(x)$, between the movable coil and a turn of the fixed coil, as a function of the distance x between the center of the moving coil and the turn. It was decided to weight the radius of the turn at position x with the factor $f(x)$.

Let $r(x)$ = the radius of a wire as a function of its axial position, $\bar{r}$ = the average radius of the coil, and r_{eff} = the weighted mean radius. Then, summing over all the turns,

$$r_{eff}=\frac{\sum_n f(x)r(x)}{\sum_n f(x)};$$

and,

$$\Delta r=r_{eff}-\bar{r}=\frac{\sum_n f(x)r(x)-\sum_n f(x)\bar{r}}{\sum_n f(x)}=\frac{\sum_n f(x)[r(x)-\bar{r}]}{\sum_n f(x)}$$

$r(x)-\bar{r}$ for the fixed coil is plotted in figure 4. Δr is found by simple summation to be +0.1 micron, and the effect is entered in table 1 as a diameter correction. A similar correction for the movable coil would be much smaller, and was not considered worth calculating.

Table 2 summarizes the calculations of the force constant F_{HH}. Comparison with table 7 of RP1449 shows the difference in F_{HH} to be close to that calculated with the variation coefficients $\partial F/\partial r_1$, $\partial F/\partial r_2$, etc.

TABLE 2.—*Summary of computations on force due to unit currents*

The following values of the independent variables were used in the computation:

$r_1 = 23.09556$. $l_1 = 27.51642$. $N_1 = 344$. $\alpha = \frac{\pi}{4}$.

$r_2 = 12.23109$. $l_2 = 2.6649$. $N_2 = 41$.

Quantities used in computing functions	Values of terms for—		
	$X_1 = 1.33245$	$X_2 = 12.42576$	$X_3 = 15.09066$
X^2	1.775 423	154.399 512	227.782 019
$X^2+(r_1+r_2)^2$	1 249.747 623	1 402.371 71	1 475.700 22
k^2	0.904 130 939	0.805 731 806	0.765 694 466
k	.950 858 001	.897 625 649	.875 039 694
$1-k^2$	.095 869 061	.194 268 194	.234 305 534
$\sqrt{1-k^2}$	.309 627 294	.440 758 658	.484 051 168
$X\sqrt{X^2+(r_1+r_2)^2}$	47.104 465 6	465.323 014	579.705 346
K	2.597 969 64	2.270 429 96	2.185 621 83
K−E	1.496 584 83	1.095 820 99	0.984 555 860
$X(r_1-r_2)^2/\sqrt{X^2+(r_1+r_2)^2}$	4.448 943 10	39.165 933 3	46.368 842 4
K−Π	−8.986 743 63	−6.951 426 49	−6.469 109 60
$X\sqrt{X^2+(r_1+r_2)^2}(\mathrm{K}-\Pi)$	70.495 828 7	509.910 727	570.752 295
$\frac{X(r_1-r_2)^2}{\sqrt{X^2+(r_1+r_2)^2}}(\mathrm{K}-\Pi)$	−39.981 511 1	−272.259 106	−299.965 123
Sum of the two preceding terms	30.514 317 6	237.651 621	270.787 172
$\omega'_s(X)$	36 876.779	287 203.747	327 248.307
$\omega'_a(X, \alpha)$	0.069 6	0.254 2	0.233 5
$\overline{\omega}'_x(X, \alpha)$	.119 1	.104 8	.124 1

Principal term: $[2\omega'_s(X_1)+\omega'_s(X_2)-\omega'_s(X_3)] = 33{,}708.998$ dynes.

Azimuthal correction term: $[2\omega'_a(X_1,\alpha)+\omega'_a(X_2,\alpha)-\omega'_a(X_3,\alpha)] = +0.1600$.

Axial correction term: $[2\overline{\omega}'_x(X_1,\alpha)+\overline{\omega}'_x(X_2,\alpha)-\overline{\omega}'_x(X_3,\alpha)] = +0.0045$.

$f = 33{,}709.163$ dynes.

$F_{HH} = 1348.3665$ dynes.

The computation of the coefficients in the variation formula for these two helices gave the equation:

$$\frac{\delta F_{HH}}{F_{HH}} = 2.73\frac{\delta r_2}{r_2} - 2.81\frac{\delta r_1}{r_1} + 0.091\frac{\delta l_1}{l_1} - 0.015\frac{\delta l_2}{l_2}.$$

The following adjustments were made for differences between the values of dimensions used in the above computation and the dimensions given in table 1:

Fixed coil diameter $\Delta r_1 = +0.1$ micron; $\Delta F = -0.0016$ dynes.

Movable coil diameter $\Delta r_2 = -0.1$ micron; $\Delta F = -0.0030$ dynes.

Total force adjustment $= -0.0046$ dynes.

Hence for H_1 and P_1 at the dimensions of the coil corresponding to 30° C,

$F_{HH} = 1348.3619$ dynes.

5. Experimental Determination of the Force Between the Coils

The experimental determination of the force between the coils was made as described in RP1449. The wiring diagram is shown in figure 6 for more convenient reference.

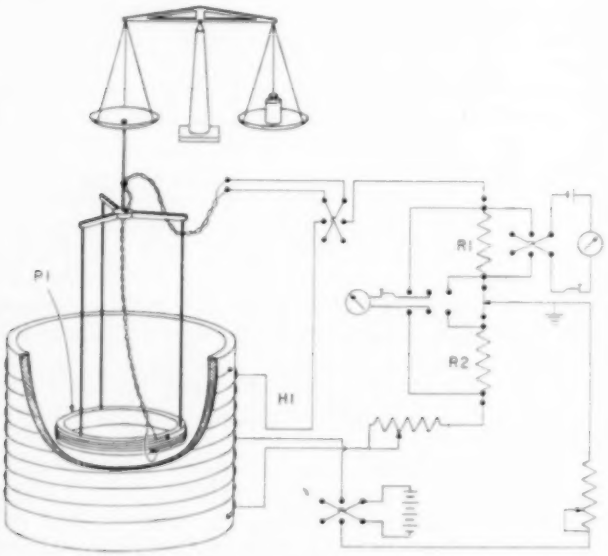

FIGURE 6. *Wiring diagram of current balance.*

Readings were made of nine turning points of the balance with the current in one direction, then the current in the fixed coil was reversed and the measurement of turning points repeated. A set of ten measurements involving nine reversals of current was averaged and entered in table 3 as one determination.

The force between the fixed-coil leads and the movable coil was measured by removing the fixed coil from the circuit without changing the lead-wire configuration. The movable-coil lead effect was measured in a similar way. These forces must be subtracted from the total force between the coils, and appear in table 4.

It was found that the mechanical dimensions of the coil supports were not as stable as had been hoped. Even with the straps around the case as described earlier, the vertical position of the movable coil with respect to the fixed coil changed about 0.2 mm in one month. The change was ascribed to dimensional changes in the wooden case due to a change in humidity, and the observed balancing mass was corrected for this change under the assumption that the shift was proportional to time. The numbers given in table 3 are corrected for the effect, which was never more than 4 ppm in the current.

The temperatures listed in table 3 are the temperatures of the wires, computed from their resistances and measured temperature coefficients. Because of temperature gradients in the coil forms, the mean

TABLE 3. *Results of measurememts of force*

Observed difference in rest points equals average difference in scale reading of rest points of the balance, δ, corresponding to "on" and "off" positions of weight, multiplied by the sensitivity of the balance (2.33 mg/cm). Mass of weight (a platinum cylinder): 1.425 569 g.

Date (May 1956)	Temperature °C			Observed difference in rest points	Difference in rest points corrected to 30° C
	P_1	H_1			
		Upper	Lower		
				mg	*mg*
18	24.79	29.84	28.60	−0.041	−0.049
21	29.45	29.45	28.26	−.001	−.009
21	29.55	29.56	28.37	−.002	−.010
22	29.54	29.56	28.37	+.004	−.004
22	29.59	29.64	28.42	−.029	−.037
23	29.88	29.93	28.71	−.049	−.057
23	29.92	29.95	28.73	+.014	+.006
23	29.96	30.00	28.78	−.063	−.071
23	29.99	30.05	28.80	−.063	−.071
24	29.95	30.05	28.82	−.046	−.053
24	29.95	30.05	28.82	−.019	−.026
24	29.96	30.06	28.82	−.002	−.009
24	29.97	30.07	28.82	−.007	−.014
Average δ times sensitivity of the balance					−0.031

TABLE 4. *Calculation of final results*

[Value of acceleration of gravity 980.081 cm/sec²]

	1942	1956
Standard mass (a platinum cylinder) grams	1.427 655	1.425 569
Buoyance correction grams	−0.000 077	−0.000 079
Lead corrections {Moving coil grams	−.000 068	−.000 044
Lead corrections {Fixed coil grams	−.000 018	−.000 022
δ times sensivity of balance grams	+.000 222	−.000 031
Correction for temperature gradients in coil forms grams	−.000 014	−.000 014
Net compensating mass = M grams	1.427 700	1.425 379
Measured force (M times gravity) = Fm dynes	1399.262	1396.987
Calculated force for unit current at 30° C = Fc dynes	1348.394	1348.361 9
Equivalent current, $I_{abs}=\sqrt{\frac{Fm}{Fc}}$ absolute amperes	1.018 688	1.017 871 4
Emf. of standard cell volts	1.018 702	1.017 870 3
Resistance of standard resistor, R_1 ohms	1.000 015	1.000 007 6
Resistance of standard resistor, R_2 ohms	1.000 019	1.000 005 6
Equivalent current . . NBS amperes	1.018 686	1.017 863 0
$\frac{I_{abs}}{I_{NBS}}$	1.000 002	1.000 008

temperatures of the coils are slightly different from the wire temperatures. A measure of this effect was made and applied to the work reported in RP1449. The 1942 temperature gradient measurements were corrected by the better resistance measurements made recently; and it was found that under equilibrium conditions with one ampere through the coils, the mean fixed coil form temperature was 1.1° C below the fixed coil wire temperature, and the mean movable coil form temperature was 0.1° C below the movable coil wire temperature. Application of the computed force-diameter variation coefficient from table 2 and the temperature coefficients of expansion from table 1 leads to −0.014 mg as the required correction. This will be found applied in table 4.

For the comparison of the present work with the work of 1942 in table 4, both of these determinations have been referred to the same electrical standards and to the same value of the acceleration of gravity. This makes it possible to interpret the results directly as an apparent change in the electrical standards. The measured values of the currents are expressed in "NBS amperes," which is taken in this paper to mean the current with reference to the present NBS standards of resistance and electromotive force, which went into effect in 1948 [1]. The value of the acceleration of gravity is based on the Dryden reduction [8] and a gravity survey made at the National Bureau of Standards by the Geological Survey. To make the comparison complete, the new diameter weighting, current distributions, and temperature gradient corrections are applied in this paper to both the 1942 and 1956 work. It may be pointed out here that these last three corrrections tend to cancel, and do not change the 1942 result by more than 1 ppm.

6. Permeability of the Forms

It was assumed in the earlier work on the current balance that the permeability of the coil forms had a negligible effect on the force constant. Inasmuch as the susceptibility of each form was only -1×10^{-6}, the correction would certainly be small; but an order of magnitude calculation was felt desirable.

In the following computation, the permeabilities of the movable coil and of the fixed coil are treated separately. Unit current (1 amp) is assumed flowing in each of the coils. It is necessary with the method used to compute the magnetic fields of the solenoids at various points. This can be done in all cases by means of formulas given in a paper by Snow [9].

The field of the movable coil serves to induce magnetic poles on the ends of the movable coil form, whose magnitude can be computed through the relation $m=(\overline{H}\chi V)/l$, where $\overline{H}=3.5$ oersteds is the mean field intensity in the form, $\chi=-1\times10^{-6}$ is the susceptibility, V is the volume of the coil form, and l is its length. m is from this approximately -3.0×10^{-4} pole. The axial component of the fixed coil field intensity, H_X, at the end of the movable coil form is computed to be $H_X=0.65$ oersted. The force on each end of the coil form is then $F'=-0.65\times3.0\times10^{-4}$ dyne. Since the total force between the coils is $F=1348/2=674$ dynes without reversal of the current, the permeability of the movable coil has an effect of $-[(2\times2.0\times10^{-4})/674]=-0.6$ ppm in the force, considering both ends of the form.

Because of the complicated field distribution inside the fixed coil form due to current in the fixed coil, a rather elaborate calculation was made of the fixed coil permeability effect. A rough estimate indicated that the form, although diamagnetic, would cause an increase in the radial component of field at the movable coil, which is not what one would at first expect.

The magnetic charge distributed over the surface of the form was calculated using the normal component of field given by Snow's formulas, and the

form susceptibility. The distribution was broken up into a series of rings of charge one centimeter wide extending around the form, and the total charge per ring was determined. This charge was then assumed concentrated on a circle located at the center of the ring. A formula for the potential of a circle of charge has been given by Smythe [10], in terms of Legendre polynomials, but this did not converge satisfactorily for our purposes. A solution was found in terms of elliptic integrals, which leads to an easier numerical calculation.

It can be shown that the potential of a circle of charge at a point a distance r from the axis of the circle and a distance d from the plane of the circle is given by $V=[2QK(k)]/(\pi\mathscr{R})$, $k^2=(4rR)/\mathscr{R}^2$, $\mathscr{R}^2=(r+R)^2+d^2$, Q is the total charge on the circle, R is the radius of the circle, and K is the complete elliptic integral of the first kind. From this the radial component of field at the point is given by

$$H_r=-\frac{2Q}{\pi\mathscr{R}^3}\left\{\left[2R-\frac{4rR(r+R)}{\mathscr{R}^2}\right]\frac{B}{1-k^2}-K(r+R)\right\}$$

where $B=K[1-(1/k^2)]+(E/k^2)$ and E is the complete elliptic integral of the second kind.

This expression allows one to sum the contributions of the separate circles of charge to the field at the movable coil. One finds the total contribution to be $H_r^{(1)}=1.25\times10^{-6}$ oersted.

The radial field at the movable coil due to the fixed coil itself can be calculated from the force F between the two coils, using the relation $F=I\int ds\times B^{(o)}$, where $B^{(o)}$ is the radial component of magnetic induction at the movable coil due to the fixed coil and I is the current in the movable coil, with the path of integration going around the movable coil. We then have, since the current is not reversed, $F=1348/2=674=(0.1\times41)\times(2\times12.2)B^{(o)}$, or $B^{(o)}=2.2$ gauss. The effect of the permeability of the fixed coil is thus $(1.25\times10^{-6})/2.2=+0.6$ ppm in the force.

A detailed calculation shows that because of the way in which the radial field of a circle of charge drops off at points away from the plane of the circle, those charges near the center of the form have the greatest effect on the field. Since the charges on the outside of the form are concentrated at the center of the coil and the charges on the inside are spread out, the charges on the outside have a slightly larger influence on the radial field at the movable coil. For this reason the fixed coil susceptibility causes an increase in the force.

The effects of the fixed and movable coil forms are in the opposite direction, and are seen to cancel. The calculations were made to a degree of precision which could cause an error of only a fraction of a part per million in the current.

7. Uncertainties

Table 5 contains estimates of known uncertainties in the current. The numbers given are probable errors for those measurements which can be treated statistically, and "50-percent-error estimates" for those cases in which no statistical information is available. Both of these measures of precision will be referred to as 50-percent errors. The estimated total uncertainty in the measurement can be determined by the usual procedure of taking the square root of the sum of the squares of the individual 50-percent errors.

TABLE 5. *Sources of error causing an uncertainty, ϵ, in ratio I_{abs}/I_{NBS} as large as 1 ppm*

	ϵ (50% error)
	ppm
Measurement of the force	2
Lead corrections	2
Radius of fixed coil	2
Radius of movable coil	3
Current distribution over wires	1
Calibration of length standards	1
Calibration of standard mass	1
Calibration of electrical standards	1
Adjustment of coils	1
Temperature of coils	1
Permeability of forms	<1
Acceleration of gravity	3
50-percent error in final result, $\sqrt{\Sigma\epsilon^2}$	6

Huntoon and McNish [11] have estimated in an as yet unpublished paper that the probable error of the mean of three gravity determinations, those of Kühnen and Furtwängler (revised), Heyl and Cook, and of Clark is about 2 ppm.

They also estimate that systematic errors could be as great as 15 ppm. We have estimated the total 50-percent error in these gravity determinations to be 6 ppm, which is equivalent to 3 ppm in the current.

Several laboratories have recently completed or are now working on new determinations of the acceleration of gravity. If the presently accepted value for the acceleration of gravity is revised as a result of such work, this paper should be revised accordingly.

8. Comparison with the Pellat Balance

According to the work described in this paper, the ratio of the absolute ampere to the ampere as presently maintained at the Bureau is, as given in table 4,

1 NBS ampere = 1.000008 ±0.000006 absolute amperes.

According to the work done on the Pellat electrodynamometer,

1 NBS ampere = 1.000013 ±0.000008 absolute amperes.

Since the acceleration of gravity is a common factor in these two determinations, it must be taken out before averaging, and reentered after averaging. Doing this and using the appropriate weighting factors, we have

1 NBS ampere = 1.000010 ±0.000005 absolute amperes.

The observed difference between the absolute and NBS units of current could be ascribed to a change in the electrical standards, to inaccuracies in the measurements which were used to define the present standards, or to the uncertainty in the present measurements. The present standards were defined by rounding off the average of several ampere determinations made in various countries to the nearest 10 ppm. The rounding off process combined with the uncertainties of the individual measurements could have caused an error large enough to explain our difference within the estimated 50-percent error. The 6-ppm difference between the results of the present work and the work using the same coils reported in RP1449 is also small enough to be interpreted as a combination of random errors.

It cannot be stated with certainty whether or not the standards have drifted. Our results indicate only that they have not drifted more than a few parts per million and that the NBS unit of current is greater than the absolute ampere by (10 ± 5) ppm.

WASHINGTON, May 13, 1957.

9. References

[1] Announcement of changes in electrical and photometric units, NBS Circ. 459 (1947).

[2] F. B. Silsbee, Establishment and maintenance of the electrical units, NBS Circ. 475 (1949).

[3] R. L. Driscoll, Measurement of current with the Pellat electrodynamometer, J. Research NBS 60, 287 (1958) RP2845.

[4] R. W. Curtis, R. L. Driscoll, and C. L. Critchfield, An absolute determination of the ampere, using helical and spiral coils, J. Research NBS 28, 133 (1942) RP1449.

[5] A. W. Spinks and F. L. Hermach, Portable potentiometer and thermostatted container for standard cells, Rev. Sci. Instr. 26, 770 (1955).

[6] Chester Snow, Mutual inductance and force between two coaxial helical wires, J. Research NBS 22, 239 (1939) RP1178.

[7] T. E. Wells, Measurement of the resistance-strain relation and Poisson's ratio for copper wires, Proc. Instr. Soc. Am. 11, Paper 56–8–3 (1956).

[8] H. L. Dryden, A reexamination of the Potsdam absolute determination of gravity, J. Research NBS 29, (1942) RP1502.

[9] Chester Snow, Magnetic fields of cylindrical coils and annular coils, NBS Applied Math. Series 38 (1953).

[10] W. R. Smythe, Static and dynamic electricity, 2d Ed. (McGraw-Hill Publishing Co., New York, N. Y. (1950).

[11] R. D. Huntoon and A. G. McNish, Present status of research on the physical constants at the (United States) National Bureau of Standards, Paper presented before the Avogadro Festival in Italy (1956). To be published in Nuovo Cimento.

Radial Distribution of the Center of Gravity of Random Points on a Unit Circle[1]

F. Scheid[2]

This paper describes some Monte Carlo computations carried out on the Standards Electronic Automatic Computer (SEAC) which are related to the problem of random walks.

In 1905 Pearson [1][3] suggested the problem of a random walk involving n steps of equal length and arbitrary direction in the plane. In 1906 Kluyver [2] obtained the solution

$$P(r,n)=r\int_0^\infty [J_0(x)]^n J_1(rx)dx$$

giving the probability of being no farther than r from the starting point after n steps of unit length. This integral has been calculated by Greenwood and Durand [3] for $n=6(1)24$, and $r=0.5(.5)n$, using punched-card tables of the Bessel functions. These tables were not extensive enough to handle the values $n=3,4$, and 5. For $n=2$ one finds by a simple argument, $P(r,2)=(2/\pi)$ arcsin $(r/2)$.

The problem described in the title is essentially the same as Pearson's. Its solution for $n=3,4$, and 5 has been obtained to roughly three decimal places by a direct sampling procedure, using SEAC. A set of n pseudorandom numbers is generated by using the multiplication method of Taussky and Todd [4]. A linear transformation converts these into a sample from the uniform distribution over $(-\pi,\pi)$. The center of gravity is found and classified in one of the intervals $j/32\leq R<(j+1)/32$, $j=0, \ldots ,31$. A new sample is then taken. Both frequency table and cumulative distribution are printed. Computation of Kluyver's integral for these values of n is possible but lengthy. If the integrand is machine computed as needed, many hours of computer time are consumed because of the two independent parameters r and n. For limited accuracy the sampling approach seems better. The distributions for $n=2$ and 6 have also been obtained for accuracy checks. Using a theorem of Kolmogoroff [5], a brief calculation indicates that, for $n=2$, the probability of a maximum error less than or equal to 0.01 after 6,000 samples have been taken is approximately one-half. A glance at table 1 shows that in fact the

[1] Preparation of this paper was initiated while the author was a member of the Numerical Analysis Training Program held at the National Bureau of Standards and sponsored by the National Science Foundation, 1957.

[2] Present address: Boston University, Boston, Mass.

[3] Figures in brackets indicate the literature references at the end of this paper.

TABLE I.

$32R$	$n=2$			$n=3$		$n=4$		$n=5$		$n=6$	
	Freq	Cum	Exact	Freq	Cum	Freq	Cum	Freq	Cum	Cum	G-D
1	121	.0197	.0199	7	.001	36	.005	28	.004	.0000	.0000
2	133	.0413	.0398	37	.007	87	.018	80	.016		
3	126	.0618	.0598	58	.017	128	.038	158	.040		
4	124	.0820	.0798	67	.028	169	.063	185	.068		
5	129	.1030	.0999	95	.043	209	.094	210	.099		
6	111	.1211	.1201	113	.061	192	.123	308	.146		
7	123	.1411	.1404	141	.084	266	.163	381	.203		
8	115	.1598	.1609	172	.112	289	.207	361	.257	.2910	.2932
9	129	.1808	.1816	224	.149	238	.242	382	.314		
10	142	.2039	.2023	336	.203	316	.290	350	.367		
11	123	.2240	.2234	466	.279	335	.340	361	.421		
12	138	.2464	.2447	344	.335	360	.394	384	.479		
13	126	.2669	.2663	291	.383	357	.448	358	.533		
14	157	.2925	.2883	285	.429	365	.503	384	.590		
15	126	.3130	.3106	269	.473	365	.558	374	.647		
16	125	.3333	.3333	255	.514	405	.618	330	.696	.7665	.7672
17	150	.3577	.3565	223	.551	353	.672	317	.744		
18	158	.3835	.3803	189	.581	255	.710	324	.802		
19	135	.4054	.4047	208	.615	275	.751	273	.834		
20	148	.4295	.4298	185	.645	262	.790	224	.867		
21	157	.4551	.4558	215	.680	182	.818	179	.894		
22	158	.4808	.4826	197	.712	159	.842	143	.916		
23	173	.5080	.5106	183	.742	163	.866	131	.935		
24	190	.5389	.5399	201	.775	168	.892	109	.952	.9749	.9732
25	191	.5710	.5708	188	.805	167	.917	93	.966		
26	211	.6053	.6038	183	.835	131	.936	70	.967		
27	197	.6374	.6393	163	.862	102	.952	45	.983		
28	247	.6776	.6783	176	.890	87	.965	39	.989		
29	262	.7202	.7221	170	.918	87	.978	36	.994		
30	308	.7703	.7737	162	.944	76	.989	24	.998		
31	424	.8394	.8407	163	.971	45	.996	12	.999		
32	987	1.0000	1.0000	178	1.000	27	1.000	3	1.000	1.0000	1.0000
Number of samples	6144			6144		6656		6656		6656	

TABLE 2.

32R	n=3 Freq	n=3 Cum	n=4 Freq	n=4 Cum	n=5 Freq	n=5 Cum
1	4	.001	9	.002	7	.002
2	10	.003	29	.007	17	.006
3	17	.006	50	.017	21	.011
4	19	.010	59	.029	40	.021
5	48	.019	71	.043	61	.036
6	45	.028	88	.060	72	.053
7	76	.043	69	.073	99	.077
8	92	.061	109	.095	113	.105
9	107	.082	133	.121	106	.131
10	160	.113	126	.145	120	.160
11	289	.169	151	.175	142	.195
12	203	.209	191	.212	149	.231
13	203	.249	221	.255	177	.274
14	176	.283	231	.300	167	.315
15	177	.318	232	.346	227	.371
16	185	.354	287	.402	217	.424
17	170	.387	248	.450	242	.483
18	172	.421	237	.496	234	.540
19	176	.455	235	.542	237	.598
20	196	.493	235	.588	207	.648
21	185	.529	215	.630	208	.699
22	196	.568	191	.667	178	.742
23	196	.606	229	.712	179	.786
24	172	.639	210	.753	168	.827
25	184	.675	205	.793	148	.863
26	224	.719	183	.829	156	.901
27	220	.762	188	.866	117	.930
28	236	.808	183	.901	97	.954
29	225	.852	167	.934	77	.972
30	239	.899	152	.964	65	.988
31	239	.946	120	.987	34	.997
32	279	1.000	66	1.000	14	1.000
Number of samples	5120		5120		4096	

WASHINGTON, September 16, 1957.

maximum error is 0.004 for this distribution. Since the inverse square root law is operative, to obtain four decimal-place accuracy would require perhaps two-thousand times as many samples, or a year of SEAC time.

Parallel results are given in table 2 for samples drawn from a triangular distribution over $(-\pi,\pi)$. The pseudorandom numbers are modified by a direct method [6] to produce the required sample.

The question how best to compute a distribution function is not, of course, answered in this paper. It is suggested, however, that even in cases where the solution can be written explicitly, circumstances may make computation by direct sampling preferable.

References

[1] K. Pearson, The problem of the random walk, Nature (1905).

[2] J. C. Kluyver, A local probability problem, Nederl. Akad. Wetensch., Proc. (1906).

[3] Greenwood and Durand, The distribution of length and components of the sum of n random unit vectors, Ann. Math. Statistics (1955).

[4] O. Taussky and J. Todd, Generation and testing of pseudo-random numbers, Symposium on Monte Carlo Methods (Univ. of Florida, 1954).

[5] W. Feller, On the Kolmogorov-Smirnov limit theorems for empirical distributions, Ann. Math. Statistics (1948).

[6] J. von Neumann, Various techniques used in connection with random digits, NBS AMS 12 (1951).

Journal of Research of the National Bureau of Standards Vol. 60, No. 4, April 1958 Research Paper 2848

An Adiabatic Calorimeter for the Range 30° to 500°C[1, 2]

E. D. West and D. C. Ginnings

An adiabatic calorimeter accurate to 0.1 percent and suitable for heat capacity measurements of solids and liquids over the the temperature range 30° to 500° C is described. Factors affecting the design and accuracy are discussed. Automatic controls permit one-man operation of the apparatus. Measurements of the heat capacity of Al_2O_3 agree to 0.1 percent with earlier measurements made with other calorimeters at the National Bureau of Standards.

1. Introduction

An ideal adiabatic calorimeter may be defined as one which has no heat transfer to its environment. As commonly used for the measurement of heat capacities, an adiabatic calorimeter is one which is heated over a small temperature interval, keeping the temperature of the environment as near as possible to the temperature of the calorimeter. This type of calorimeter has been used extensively at moderate and low temperatures. However, at high temperatures, the large coefficient for heat transfer by radiation increases the difficulty of avoiding heat transfer between the calorimeter and its environment. Only a few adiabatic calorimeters have been used above 500° C and even at this temperature, an accuracy as high as 1 percent is unusual [1, 2, 3, 4].[3] Consequently, at the high temperatures, the "drop" method has been more commonly used for the determination of heat capacities [5]. Although the drop method can reduce uncertainties due to increased heat transfer by radiation, it has one basic limitation which prevents its universal application. This limitation is that the method can be used only for materials which reach a thermodynamically reproducible state at the temperature of the calorimeter. With certain materials having slow transitions, this reproducible state may not be reached. The element sulfur is such a material, because it has slow transitions which make accurate measurements impossible by the drop method. The calorimeter described in this report was developed for the temperature range 30° to 500° C with the intention that it would be used first to measure the heat capacity of sulfur.

2. Principles of Design

This adiabatic calorimeter was designed primarily to be accurate to 0.1 percent in measuring heat capacity up to 500° C. In order to attain this accuracy, a number of factors were considered. The evaluation of electric energy input to 0.01 percent is relatively easy with modern techniques. The use of a platinum resistance thermometer for measurement of the temperature change in the calorimeter makes possible an accuracy comparable with that of the electric energy. The largest uncertainty in measuring heat capacity with adiabatic calorimeters in this temperature range is believed to be the uncertainty in "heat leak" (heat transfer between the calorimeter and its environment) which results from experimental departures from the ideal adiabatic condition. Two steps are taken to approach the ideal condition. First, the heat transfer coefficient between the calorimeter and its environment is made small. Second, the temperature of the environment is kept as close as possible to the temperature of the calorimeter. This second step is much more difficult because the surfaces of the calorimeter and its environment are not isothermal, especially during a heating period. Consequently, in many calorimeters thermocouple junctions are distributed over the surfaces to "integrate" the temperature gradients and obtain mean surface temperatures. This procedure introduces difficulties because the mechanism for heat transfer may be different over the various parts of the surface. For example, a part of the calorimeter having a metallic connection to the environment may lose heat mostly by metallic conduction. Another part may loose heat primarily by radiation or conduction through gas. The amount and proportion of heat transferred by various means change with temperature or other circumstances, so that the ideal distribution of thermocouples for proper integration is difficult to achieve.

In adiabatic calorimetry, one of the best procedures is to make two types of heat capacity experiments, one with an empty calorimeter (or with a small amount of sample) and one with the calorimeter filled with the sample. The purpose of the experiments with the empty calorimeter is twofold. The first purpose is to account for the heat capacity of the empty calorimeter by taking the difference in the results of the two experiments. A second purpose, which is sometimes overlooked, is to eliminate heat leak errors and certain other errors which have the same absolute value in the two types of experiments. This procedure can be extremely useful in the elimination of the effect of some unknown heat leaks. However, the procedure does not eliminate heat leak errors which are different in the two types of experiments. Unfortunately, the very existence of the sample in the calorimeter during the heating interval makes the temperature distribution in the full calorimeter different from that in the empty calorimeter. It is therefore vital, for high accuracy, to design a calorimeter having essentially the same temperature dis-

[1] This work was supported in part by the Allied Chemical and Dye Corporation and American Petroleum Institute Project 48A on the "Production, Isolation, and Purification of Sulfur Compounds and Measurement of Their Properties."

[2] This paper includes material from a thesis submitted by E. D. West to the University of Maryland in partial fulfillment of the requirements for the degree of Master of Science.

[3] Figures in brackets indicate the literature references at the end of this paper.

tribution over its outer surface in the two types of experiments. This has been accomplished in the present calorimeter by using a series of thin silver shields as described later.

In addition to high accuracy, the calorimeter was designed to require only one person for its operation. Adiabatic calorimeters capable of 0.1 percent accuracy over a moderate temperature range usually have required at least two operators. One of these operators has had to devote most of his time to controlling and recording the various temperatures pertinent to heat leak evaluation. The present calorimeter has been designed to use automatic equipment to make it possible for one person to operate the calorimeter without difficulty. The calorimeter was also designed to incorporate a sample container which could be removed from the calorimeter with a minimum of disturbance to the electrical system. To accomplish this, the calorimeter was designed in two parts, a sample container and a shield system surrounding and attached to the sample container.

3. Calorimetric Apparatus

Figure 1 is a schematic diagram of a vertical section of the apparatus. The calorimeter, defined as that part of the apparatus where energy changes are measured, is made in two main parts: (1) a sample container C surrounded by (2) a shield system consisting of the silver ring R_1 to which are attached two sets of silver shields S_1 and L_1. Surrounding the calorimeter is the adiabatic jacket which consists of the silver ring R_2 to which silver shields S_2 and L_2 are attached. Between the jacket ring R_2 and the calorimeter ring R_1 are two ten-junction thermopiles T_1 which indicate the vital temperature difference between the calorimeter and its jacket. Figure 2 is a photograph of the top of the calorimeter and jacket with lids L_1 and L_2 removed.

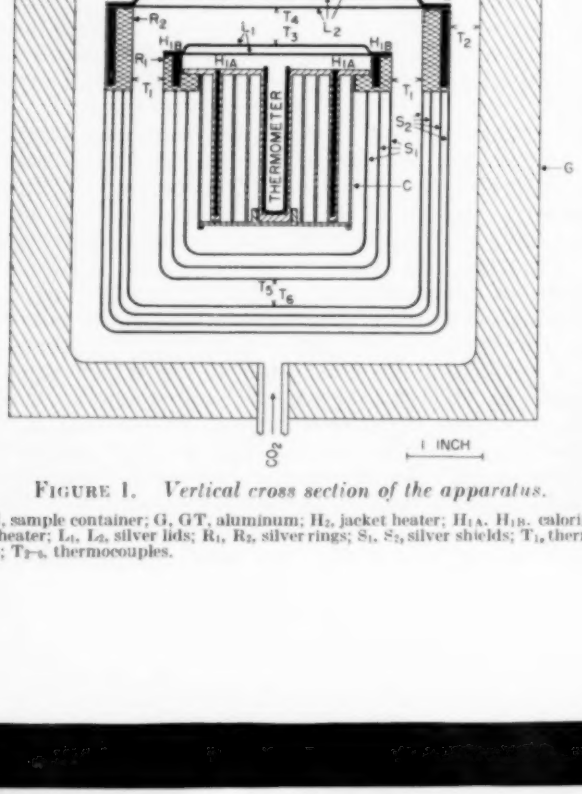

FIGURE 1. *Vertical cross section of the apparatus.*

C, sample container; G, GT, aluminum; H_2, jacket heater; H_{1A}, H_{1B}, calorimeter heater; L_1, L_2, silver lids; R_1, R_2, silver rings; S_1, S_2, silver shields; T_1, thermopile; T_{2-6}, thermocouples.

Surrounding the jacket is a "guard" G whose temperature is controlled a few tenths of a degree below that of the jacket to reduce the power required in the jacket and the consequent temperature gradients. It also guards the jacket from effects of changes in ambient conditions and in the temperature gradients in the glass fiber which is used for thermal insulation of the apparatus.

3.1. The Calorimeter

An essential requirement underlying the design of the calorimeter is that the temperature distribution on its outer silver surface must be independent of the amount of material in the sample container so that the empty calorimeter experiments will properly account for the exchange of small amounts of heat with the jacket. As a practical matter, it is important that the container be easily removed for filling. Consequently, the additional requirement must then be imposed on the design that the temperature distribution on the outer surface also be independent of variations in thermal contact due to differences in the way the sample container is installed. It is apparent that success in meeting these requirements will depend to a great extent on minimizing changes in temperature gradients on the container itself and between the container and ring R_1. It is desirable that these gradients be small so that their changes will be small. For control purposes, the design must meet the further requirement that the calorimeter must reach thermal equilibrium quickly.

The sample container C, figure 1, is a cylinder 2 in. high and 2 in. in diameter made from aluminum alloy 1100 (99+ percent pure) with a stainless steel cover screwed on the bottom. Aluminum was used here so that the container could later be adapted to the measurements on sulfur. In order to distribute heat quickly to the sample and keep gradients small, the

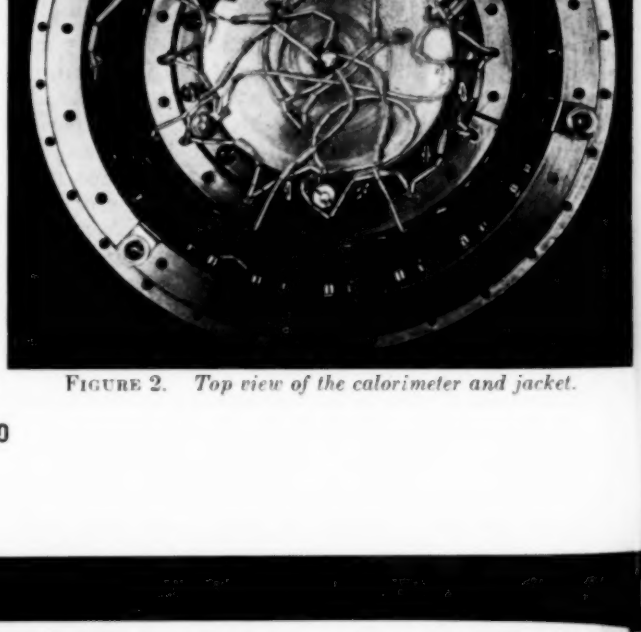

FIGURE 2. *Top view of the calorimeter and jacket.*

container is made from a solid cylinder of aluminum by boring many holes 2 to 5 mm in diameter and leaving a web of metal between holes so that no part of the sample is more than 2.5 mm from a good thermal conductor. The container has an internal volume of 70 cm^3 and a mass of about 112 g. In a central well in the container is a platinum resistance thermometer enclosed (but not sealed) in a Vycor tube which is ground cylindrical to permit a good fit in the well. Also inserted in the top of the sample container are three coils (H_{1A}, fig. 1) of the calorimeter heater. This placement of the heaters permits observation of the calorimeter temperature within a few hundredths of a degree while heating.

The sample container is held against the silver ring by a thin stainless steel ring and twelve stainless steel screws. To avoid contact of aluminum with silver, another thin stainless ring is silver-soldered to the ring where it is in contact with the sample container. This second stainless ring also provides a strong material for attaching the screws.

The ring R_1 is made of pure silver 0.8 cm^2 in cross section to reduce temperature gradients due to circumferential heat flow. It provides space for 12 short heater coils and 20 junctions of the thermopiles which measure the effective temperature difference between the calorimeter and its jacket. Silver-soldered to the ring are three silver shields each 0.25 mm thick. The function of the shields is to provide an external surface on which the effect of the gradients on the sample container and between the sample container and the ring is greatly attenuated. It is calculated that the attenuation by one shield is a factor of about 8, so that the attenuation by three shields should be about 500. The temperature differences on the surface of the sample container are significant only during the heating interval. They are calculated to be not greater than 0.02° C when empty and 0.04° C when full. The temperature difference between the sample container and the ring is made small by distributing the calorimeter heater between them approximately in proportion to their heat capacities. By various combinations of the heating coils allowance is made for the full or empty sample container. During heating, the temperature difference between the sample container and the ring is calculated to be about 0.05° C, which is less than 10 percent of what it would be if the heater were all in the ring. Assuming the uncertainty in the reproducibility of this gradient is as much as the calculated gradient, the variation in the average temperature of the outer surface of the calorimeter due to variations on the sample container is estimated to be only about 0.0001° C.

More critical than the thermal contact between the container and the ring is the contact between the lid L_1 and the ring R_1, because variations in this contact are not attenuated and directly affect the temperature over almost one-sixth of the outer surface of the calorimeter. This contact is made between the soft silver lid screwed down against a stainless steel ring. Although the heat capacity of the lid is small, all the heat required to raise its temperature during the heating interval must come from the heaters in the ring through this mechanical contact. In disassembling the calorimeter, this contact is usually found to be so good that the lid and ring must be forced apart, indicating that some heat is transferred by direct metal-to-metal conduction. However, to arrive at an estimate of how large the temperature difference between the ring and the lid may be, it is assumed that heat transfer is only by gaseous conduction through an effective spacing of 0.0002 in. With these assumptions, the temperature difference between lid and ring is calculated to be 0.001° C. The single-junction thermocouple T_3 is not sensitive enough to determine variations in this thermal contact, but it does set an upper limit of a few thousandths of a degree.

The calorimeter heater was designed to have large electrical resistance and small heat capacity. The coils for this heater (and also for the jacket heater) are made by winding helices of oxidized 38 Nichrome V wire to fit inside porcelain tubes 1 mm i. d. The lead from the lower end of each coil is brought up through a smaller porcelain tube inside the helix. To reduce the heat developed in the leads between coils, the helices are arc welded in helium to larger nickel leads. The total resistance of all calorimeter heaters in series would be 640 ohms, but the sections are connected in two series-parallel combinations to give 77 ohms for the empty calorimeter and 60 ohms for the full calorimeter. The heat capacity of the heater is about 1 j deg^{-1} C, which is less than 0.3 percent of the heat capacity of the full calorimeter.

3.2. The Adiabatic Jacket

The main purpose of the adiabatic jacket is to minimize heat transfer from the calorimeter. To accomplish this purpose, both the heat transfer coefficient and the temperature difference between the jacket and the calorimeter are made small. The jacket is adiabatic if its effective temperature is equal to that of the calorimeter. At equilibrium, this equality can be checked by following the calorimeter temperature. However, during the heating interval, no such check on the heat transfer is available. In place of effective temperature equality, the more feasible requirement has been substituted that temperature inequalities and the corresponding small heat losses be the same in the two experiments—one with the calorimeter full and one with it empty. If this substitute requirement is satisfied, then, when the empty heat capacity is subtracted from the full heat capacity, allowance is automatically made for those small heat losses which are the same in the two types of experiments. The uncertainty in the equality of these small heat losses is frequently the chief limitation on the accuracy of the heat capacity measurements.

In order that heat losses compensate, any errors in measuring the temperature difference between the calorimeter and its jacket must be the same in the two types of experiments. These errors are greatest during the heating interval. To make them the same in the empty and full experiments, the thermopile junctions must have the same thermal lags and the gradients on the outer surface of the calorimeter

and the inner surface of the jacket must be the same. The temperature difference between the jacket ring and the calorimeter ring is measured by means of two ten-junction Chromel-Alumel thermopiles (T_1, fig. 1) connected so that their emf's are additive. These two thermopiles are compared frequently by opposing their emf's to detect circumferential gradients on the silver rings. The junctions are made at "thermal tiedowns" which consist of small gold tabs sandwiched between mica washers for electric insulation and squeezed against the silver rings by stainless steel nuts. These thermal tiedowns are similar to, but larger than, those used previously in this laboratory [6]. At the usual heating rate of 0.5° C min^{-1}, tests indicate the junctions of the thermopile lag about 0.02° C below the rings. The lag in junctions on the calorimeter is compensated for by the lag in those on the jacket, so that the error in the observed temperature difference will be considerably less than 0.02° C. However, it is necessary to have this temperature difference reproducible to better than 0.001° C between the full and empty measurements. To insure maximum reproducibility, the thermopile junctions are not disturbed when the sample container is removed for filling. To prevent cooling of the thermopile junctions by conduction along the leads an extra thermal tiedown was installed in each of the four leads to bring them to the jacket temperature.

In addition to making the thermal lags the same, the gradients on the inner shield of the jacket must be reproducible, just as the gradients on the outer surface of the calorimeter must be reproducible. However, the variations to be attenuated by the jacket are due to disturbances on the outside and are considerably larger. The attenuation at 400° C has been determined by altering the guard temperature 0.75° C and observing the effect on the calorimeter. The change in the rate of heat transfer corresponds to an offset of the jacket temperature of 0.0056° C, an attenuation of 130. The attenuation is much greater at lower temperatures. The uncertainty in the guard temperature, estimated from observations of time and circumferential variations of thermocouples is less than 0.3° C. From this estimate the uncertainty in reproducing the temperature distribution inside the jacket is calculated to be about 0.002° to 400° C.

During the heating period, there are gradients on the shields S_1 and S_2 due to heat flowing from the rings R_1 and R_2 to raise the temperature of the shields. When the calorimeter is being heated at 0.5° C min^{-1}, the temperature difference between the ring and the center of the bottom of the corresponding shield is about 0.1° C. The maximum temperature difference between the outer shield of the calorimeter and the inner shield of the jacket occurs between the centers of the shield bottoms and is about 0.05° C. The gradients in these two shields and therefore the effective temperature difference between them are very nearly proportional to the rate of heating. Consequently, the rate at which heat is lost from the calorimeter by transfer between these shields is directly proportional to the rate of heating. On first thought, it may appear that the rate of heating in the empty experiment would have to be made the same as in the full experiment. That this is not the case may be seen from the following considerations: In any given experiment, the heating rate is virtually constant, so that energy lost from the calorimeter is directly proportional to the product of the heating rate and the time of heating. Since this product is equal to the change in the calorimeter temperature, the energy lost is the same in the empty and full experiments if they have the same initial and final temperatures. The rate of heating in both full and empty experiments was adjusted to 0.5° C min^{-1} within 3 percent, but, to establish the validity of the above conclusion, two experiments in which the heating rate was one-half the usual rate were carried out at 660.05 and 669.75° K. The data for these two experiments are given in table 1 (see note b). At these temperatures the large heat transfer coefficient would result in the largest effect on the heat capacity values, but no such effect is apparent.

In addition to reproducing the errors in measuring the temperature difference, it is necessary to avoid changes in the heat transfer coefficient between the empty and full experiments. During the heating interval, the gradient on the inner jacket shield is different from that on the outer calorimeter shield, resulting in a net temperature difference even when the ring temperatures are matched. If the heat transfer coefficient were to change between the empty and full measurements, there would be a systematic error equal to the product of this change and the average temperature difference between the shields, which is calculated to be about 0.026° C at the normal heating rate.

To avoid large absolute changes in the heat transfer coefficient, it has been made small by using silver for the outer surfaces of the calorimeter and the inner surfaces of the jacket. The silver surfaces were clean, but not polished. Silver loses its polish when heated, but the heat transfer by radiation is not changed much because the orientations of the new crystallite faces are at small angles with the average plane of the surface. The coefficient for heat transfer by radiation is calculated to be 0.10 w deg^{-1} C at 400° C. The coefficient for heat transfer by CO_2 gas conduction across the 1-cm space is calculated to be 0.07 w deg^{-1} C at 400° C. Although the heat transfer coefficient could be reduced by the amount of the gas conduction if the system were evacuated, the gain would be more than offset by the adverse effects where good thermal contact is desired, i. e., at the lids, heaters, thermocouple junctions and the thermometer.

Heat conduction along leads and supports is minimized by using small wires and poor conductors whenever possible. The thermopile is made of No. 36 AWG Chromel P and Alumel wires. The seven heater and thermometer leads are No. 32 AWG gold between the calorimeter and the jacket. The three supports for the calorimeter are Nichrome V, 6 mm wide and 0.1 mm thick. The total metallic conductance is about 0.006 w deg^{-1} C. The leads

TABLE 1. *Heat capacity of aluminum oxide* [a]

Temperature	Empty Calorimeter		Calorimeter+Al_2O_3		C_p° of Al_2O_3 This work	Standard deviation	C_p° of Al_2O_3 Ref. 5	Difference This work—Ref. 5
	Date	Heat capacity	Date	Heat capacity				
°K (*Int. 1948*)		*abs j deg*$^{-1}$		*abs j deg*$^{-1}$	*abs j deg*$^{-1}$ *mole*$^{-1}$	*abs j deg*$^{-1}$ *mole*$^{-1}$	*abs j deg*$^{-1}$	%
311.92	9-9-55	221.64	10-27-55	318.82	81.91	±0.019	81.90	+0.01
	9-13-55	221.59	10-28-55	318.79				
			11-3-55	318.79				
321.65	9-9-55	222.83	10-27-55	322.23	83.80	.019	83.82	−.02
	9-13-55	222.78	10-28-55	322.23				
			11-3-55	322.25				
331.35	9-6-55	224.17	10-27-55	325.81	85.66	.017	85.64	+.02
	9-9-55	224.17	10-28-55	325.79				
	9-13-55	224.15	11-3-55	325.82				
341.05	9-6-55	225.35	10-28-55	329.04	87.38	.019	87.36	+.02
	9-9-55	225.38	11-3-55	329.05				
	9-13-55	225.31						
350.65	9-6-55	226.47	10-28-55	332.06	89.01	.019	88.99	+.01
	9-9-55	226.48	11-3-55	332.09				
	9-13-55							
360.35	9-6-55	227.54	10-28-55	335.05	90.58	.019	90.58	.00
	9-9-55	227.57	11-3-55	335.06				
	9-13-55	227.57						
515.15	9-15-55	241.94	11-16-55	369.35	107.36	.022	107.19	+.16
	9-16-55	241.90	11-17-55	369.34				
	1-27-56	241.92	1-11-56	369.34				
524.95	9-15-55	242.66	11-16-55	370.92	108.05	.020	107.89	+.15
	9-16-55	242.66	11-17-55	370.91				
	1-27-56	242.69	1-11-56	370.90				
	2-7-56	242.67						
534.55	9-15-55	243.49	11-16-55	372.52	108.72	.020	108.57	+.14
	9-16-55	243.47	11-17-55	372.52				
	1-27-56	243.52	1-11-56	372.55				
	2-7-56	243.46						
544.15	9-15-55	244.28	11-16-55	374.05	109.34	.020	109.20	+.13
	9-16-55	244.25	11-17-55	374.04				
	1-27-56	244.30	1-11-56	374.04				
	2-7-56	244.21						
553.85	9-15-55	245.08	11-16-55	375.55	109.96	.020	109.83	+.12
	9-16-55	245.02	11-17-55	375.53				
	1-27-56	245.10	1-11-56	375.55				
	2-7-56	244.98						
563.55	9-15-55	245.82	11-16-55	377.04	110.56	.022	110.42	+.13
	9-16-55	245.80	11-17-55	377.02				
	1-27-56	245.80	1-11-56	377.03				
660.05	1-30-56	253.75	12-30-55	390.56	115.29	.053	115.39	−.09
	1-31-56	253.79	1-4-56	390.59				
	2-2-56	253.73	1-6-56	390.66				
	2-3-56	[b] 253.76						
669.75	1-30-56	254.62	12-30-55	391.90	115.68	.053	115.81	−.11
	1-31-56	254.55	1-4-56	391.80				
	2-2-56	254.58	1-6-56	391.97				
	2-3-56	[b] 254.58						
679.35	1-31-56	255.31	1-4-56	393.11	116.09	.065	116.20	−.09
	2-2-56	255.41	1-6-56	393.21				
689.05	1-30-56	256.27	12-30-55	394.58	116.52	.053	116.59	−.06
	1-31-56	256.19	1-4-56	394.48				
	2-2-56	256.32	1-6-56	394.65				

[a] Molecular weight 101.96. [b] Values obtained at one-half normal heating rate not included in heat capacity calculations.

are brought to the temperature of the rings by the same tiedown technique used for the thermopile junctions. The leads and supports are not disturbed when the container is removed. Calculations indicate that heat transfer by convection is wholly negligible, so that the over-all heat transfer coefficient for flow from the calorimeter is calculated to be about 0.18 w deg^{-1} C at 400° C.

By controlling the jacket temperature about 0.01° C hot or cold, the change in heat flow from the calorimeter leads to an experimental evaluation of the heat transfer coefficient. At 400° C, the mean value of this coefficient is 0.23 w deg^{-1} C, with a standard deviation of ±0.02 which is in reasonable agreement with the calculated value above. Estimating the average uncertainty in the temperature difference from all causes to be 0.001° C at 400 and considering a typical 40-min experiment, the heat loss due to this uncertainty is equivalent to 0.08 percent of the heat capacity of the Al_2O_3. This 0.08-percent uncertainty is comparable to the scatter of the heat capacity results around 670° K (table 1). This considerable heat effect from such a small temperature difference is indicative of the difficulties of adiabatic calorimetry at elevated temperatures.

3.3. Guard System

The guard G is made from aluminum 2 cm thick. The heaters are in three sections distributed over the surface. The guard temperature is automatically controlled about 0.3° C below the jacket temperature using a single junction Chromel-Alumel thermocouple between the jacket ring and the cylindrical section of the guard. This temperature difference permits

sufficient cooling to maintain automatic control of the jacket. The temperature of the top and bottom sections are controlled to the temperature of the cylindrical section by means of differential thermocouples. After temperature gradients in the guard were found to cause appreciable gradients in the jacket ring R_2, a series of thermocouples was installed to measure circumferential gradients in the guard. These gradients amounted to several degrees and were highly dependent on the variations in packing the glass fiber insulation around the guard. To reduce these gradients, which caused significant circumferential gradients on the jacket ring R_2, a heated aluminum cylinder was placed around the guard.

At the bottom of the guard is a connection to the CO_2 supply. Carbon dioxide is kept flowing into the calorimeter at all times at a rate of about 1 cm^3 sec^{-1}. A fraction diffuses through small holes in the various silver shields and lids to insure a uniform atmosphere throughout. Changing the CO_2 flow by tenfold does not affect the heat transfer from the calorimeter.

4. Energy and Temperature Measurements

The power to the calorimeter is obtained from large capacity storage batteries. It is evaluated in the conventional way by determining the current through the calorimeter heater and the potential drop across it. The current is determined by the potential drop across a 1-ohm series resistor (certified to 0.005%). The potential drop across the calorimeter heater is divided by a 20,000-ohm volt box which has a 100:1 ratio certified to 0.01 percent. The current through the volt box is accounted for in evaluating the true calorimeter current. The potential across the 1-ohm resistor and across 1 percent of the volt box is determined by means of a Wenner potentiometer certified to 0.01 percent and standardized against a saturated standard cell which is accurate to 0.002 percent.

To allow for the small amount of heat generated in the current leads between the calorimeter and its jacket, one potential lead is brought from a terminal on the calorimeter, the other from a terminal on the jacket. If the current leads are alike, this procedure accounts for that part of the heat generated in them which flows to the calorimeter. All leads are brought to the temperature of the jacket and the calorimeter by means of thermal tiedowns like those used for the thermopile. The resistance of the leads is approximately 0.03 ohm, so that only about 0.02 percent of the heat to the calorimeter is generated in the leads. A very small correction is applied for heat generated in the resistance thermometer.

The heating interval (about 1,200 sec) is measured to about 0.02 sec with an electric timer synchronized with an accurate crystal oscillator. The interval is held to integral seconds by synchronizing the heater switch with a relay which closes once each second. The coincidence of these second signals is checked daily against standard time signals from WWV.

The 25-ohm platinum resistance thermometer was calibrated at the Bureau. The resistance at the ice point is checked each time the sample container is removed. A thermometer current of 2 ma was used. The resistance is measured with a Mueller bridge calibrated in this laboratory. Temperatures are reported in degrees Celsius as obtained by use of the International Temperature Scale (1948). Temperatures on the Kelvin scale were obtained by adding 273.15°.

5. Jacket Control System

Precise control of the temperature difference between the jacket and the calorimeter is essential for accurate measurements. The apparatus has been designed with low thermal lags in the thermopiles and heaters to facilitate precise control. A commercially available servo system, used in conjunction with the thermopiles, controls the jacket temperature more precisely and for longer periods than is possible for a human operator. The servo system consists of an amplifier, a recorder and a control unit. A few refinements have been added to permit closer control at the beginning and end of the heating period. The details of the control system are described elsewhere [7].

The control system holds the temperature difference within $\pm 0.001°$ C on the average. This control is much better than that obtained by manual operation, which was attempted in some preliminary experiments. Deviations from ideal control are integrated electronically over the time of an experiment and a small correction is applied. Frequent checks of the amplifier and recorder indicate that the indicated zero is stable to ± 0.2 μv, which corresponds to 0.0002° C. Random variations of the control zero will appear in the data; long-term changes will be taken into account by the operating procedure.

6. Experimental Procedure

In a normal day's work one operator can obtain the data for six to nine experiments, depending on how much time is required to adjust the apparatus to the desired initial conditions. So that the apparatus will not be too far from these conditions, its temperature is held overnight about 10 deg below the desired initial temperature by automatic control of the guard heaters. Prior to starting a series of experiments, the temperatures of the jacket and guard are brought under automatic control. The calorimeter is then heated to the initial temperature, adjusting the number of cells in the storage battery and a resistance in series with the calorimeter heater to give a heating rate of 0.5° min^{-1}. This series resistance is kept about equal to the resistance of the calorimeter heater so that the change in heater resistance with temperature will produce only a very small change in the power level [8]. Whenever current is not desired in the calorimeter heater, it is switched to a "dummy" resistor which has about the same resistance as the calorimeter heater. This procedure keeps the external circuit at operating temperature and avoids most of the change in

external resistance which would otherwise occur when the current is turned on. From 7 to 10 minutes after the power is shut off, the temperature of the calorimeter (with the Al_2O_3 sample) can be determined. The temperature is obtained from four readings on a Mueller bridge taken at 30-sec intervals. After another 10-min period, the temperature is again observed to determine the initial temperature "drift", i. e., the rate of change of the calorimeter temperature with time. At 300° K this drift is only 0.005° hr^{-1}, but at 700° K it amounts to 0.03° hr^{-1}.

About 30 sec after the last temperature reading, the current from the storage batteries is switched from the dummy resistor to the calorimeter heater on an integral second. The emf's corresponding to the heater current and voltage are each read on the potentiometer at 3-minute intervals. The operator also has time during the heating period to check the operation of the automatic control equipment and read the various auxiliary thermocouples. About a minute before the end of the heating period, the resistance thermometer current is turned on and the temperature is observed continuously until it is a few hundredths of a degree below the desired final temperature. The power is then switched back to the dummy resistor on the nearest integral second.

The temperature is observed after the calorimeter reaches equilibrium and again after a 10-min interval to obtain the final temperature and its drift. Based on the final and initial drift experiments a correction for drift during an experiment is applied to the apparent heat capacity. This correction makes an allowance for a number of factors which change from one experiment to the next, such as changes in the control point of the jacket control system or changes in spurious emf's of the thermopile. In the time between heating periods, the apparent heat capacity is calculated, so that comparison with previous results can be made before the next experiment is begun.

To obtain the small correction for deviations of the jacket temperature from that of the calorimeter, the electronic integrator is read each time the calorimeter temperature is observed. Each day, the factor for converting the integrator readings to energy correction is evaluated by changing the jacket control point 0.01° C for 10 min and observing the corresponding integrator readings and temperature changes on the calorimeter.

After completion of a series of experiments with the empty container it is removed, filled with a sample, and replaced. When it is not necessary to seal the sample container (as with Al_2O_3) the time required for this operation is about 2 days. After filling the calorimeter, a second series of measurements is made.

7. Heat Capacity of Aluminum Oxide

The heat capacity of the Calorimetry Conference sample of Al_2O_3 [5] has been measured in this calorimeter from 305° to 365°, from 510° to 570°, and from 655° to 695° K, using a 120-g sample. The data are summarized in table 1. The data shown for the empty and full calorimeter have been corrected to the average temperature shown in the first column. The heat capacities calculated from these data have been corrected for the curvature of the heat capacity-temperature function, for buoyancy in weighing, and for the heat capacity of CO_2 displaced by the Al_2O_3. The experiments were carried out at a constant pressure of 1 atm so that C_p is determined directly. Included for comparison are smoothed data taken from earlier work in this laboratory with two different calorimeters [5]. In the last column are shown the percentage differences between the new data and the earlier work. The estimated uncertainty in the earlier data obtained in an adiabatic calorimeter is ±0.1 percent from 90 to 373° K; the uncertainty in the data obtained by the drop method increases from ±0.2 percent at 373 to ±0.4 percent at 1073° K. The agreement with the earlier data is well within these estimated uncertainties.

8. Analysis of Errors

The random errors associated with the results in table 1 have been estimated by ordinary statistical methods, using all the data in each temperature range to estimate the standard deviation of individual measurements in that range. This "pooled estimate" of the standard deviation is then used to compute the standard deviations of the heat capacity of Al_2O_3 at each temperature. These standard deviations are given in table 1. Confidence limits (99% level) for the heat capacity of Al_2O_3 are ±0.05 percent for the two lower ranges and ±0.14 percent for the highest range. These limits would include the average of an infinite number of observations 99 percent of the time, but they do not include an estimate of systematic errors.

It is believed that the variations in the data in table 1 are mainly due to heat transfer from the calorimeter which is not accounted for by the correction for the calorimeter drift experiments. This correction averages 0.05 j deg^{-1} in the lowest range, 0.12 j deg^{-1} in the middle range, and 0.50 j deg^{-1} in the highest range. The magnitude of the drift decreased with time after the heating interval in a manner which is nearly exponential with a time constant of 2 or 3 hr and probably results from thermal lags in the glass fiber insulation. The magnitude of the correction will accordingly depend on when the drift is determined. In general, the drift has been determined as described in section 6. The validity of corrections based on these drift experiments can be judged by the sets of data taken in the middle temperature range on November 16 and 17, 1955, and January 11, 1956 (table 1). These sets of data had very different drift corrections averaging respectively −0.15, +0.13 and +0.09 j deg^{-1}, yet the apparent heat capacities in the three sets agree on the average to 0.01 j deg^{-1}. By contrast, the sets of data taken in the highest range on December 30, 1955, January 4, 1956, and January 6, 1956, had corrections averaging respectively 0.55, 0.39 and 0.49 j deg^{-1}, and the average difference between the heat capacity data of January 4 and those of

January 6 is 0.14 j deg^{-1}. It is obvious that not only are the drift corrections larger at high temperatures, but they are also relatively more uncertain.

The variations in drift seem to be random in nature, not differing significantly between the empty and full calorimeter experiments. Therefore no allowance for errors in drift corrections has been made other than that for the random errors which appear as scatter in the data.

The systematic errors discussed below are estimated to be on about the same probability basis as the confidence limits given above for random variations.

An estimate of the over-all systematic error from the measuring instruments of ± 0.02 percent is obtained by taking the square root of the sum of the squares of the individual estimates in section 4. There is also a possibility of systematic errors in accounting for heat lost from the calorimeter. These errors might arise either from changes between empty and full experiments in the heat transfer coefficient or in the temperature distribution on the outer surface of the calorimeter or the inner surface of the jacket.

An estimate can be made of the systematic error which may be due to a change in the heat transfer coefficient. The error is possible because, during the heating interval, the gradient on the inner jacket shield is different from that on the outer calorimeter shield, resulting in a net temperatue difference even though the thermopiles indicate zero. If the heat transfer coefficient changes between the full and empty measurements, the empty measurement will not make the proper allowance for the small heat loss. It is therefore necessary to consider possible changes in the heat transfer coefficient.

The reproducibility of heat transfer by gas conduction depends only on the composition of the gas. The CO_2 is kept flowing through the system at all times so that a significant change in composition due to diffusion of air is unlikely. It has already been pointed out that conduction along leads and supports is the same in the full and empty experiments. It is therefore unlikely that the heat transfer coefficient might change because of changes in metallic or gas conduction.

There remains the possibility of a change in heat transfer by radiation due to a change in the emittance of the silver surfaces. This change might come about, for example, by the formation of a sulfide layer, although no such corrosion was discernible on the several occasions when the calorimeter was opened. The uncertainty in the observed heat transfer coefficient is too large to permit a significant statement about any systematic change between empty and full experiments. However, in the middle temperature range, empty experiments were made both before and after the full experiments. If there is a significant change in the heat transfer coefficient between the two series of empty measurements, it should result in a constant difference between the averages of the heat capacity values. It is apparent from table 1 that there is no evidence of such a difference.

Apart from the variation in the heat transfer coefficient, systematic error can be introduced if there is a change (between empty and full experiments) in the temperature distribution on either the outer surface of the calorimeter or the inner surface of the jacket. In section 3.1, the effect on the outer shield of the calorimeter due to loading the sample container and changing the gradient between the container and the ring is estimated to be about 0.0001° C. Taking the heat transfer coefficient at 400° C to be about 0.23 w deg^{-1}, the error in a 20-min heating period on a sample of 130 j deg^{-1} heat capacity is 0.002 percent. Also in section 3.1, the temperature drop from the ring R_1 to the lid L_1 is estimated to be 0.001° C. If the irreproducibility in squeezing the silver against the stainless steel is 50 percent, the systematic error may be 0.005 percent. A similar estimate applies to the jacket lid L_2. Both lids were removed several times during the measurements to allow work on the electrical system so that the error due to the lids appears to a considerable extent as a random error in the data.

One further possibility of error is in the reproducibility of a circumferential gradient in the silver rings which might arise from a large change in contact between the sample container and the ring, or from a change in the technique of packing the insulation around the guard. If this gradient is properly averaged around the ring by evenly spacing the thermopile junctions, no error results even if it is not reproducible; however, the thermopiles are distributed around only three-fourths of the circumference, so that one-fourth of the circumference is not included in the average. At equilibrium the thermopiles indicate a difference of less than 1 μv, and there is no apparent variation between the full and empty experiments. If a possible change in this gradient between the full and empty measurements is no greater than the limit of sensitivity of the temperature difference measurement, the resulting error is about 0.005 percent of the heat capacity of the Al_2O_3.

Taking into consideration the random and systematic errors, the error in the heat capacity of Al_2O_3 is estimated to be less than 0.1 percent in the lower ranges and less than 0.2 percent in the upper range.

The interest and cooperation of Professor William J. Svirbely is gratefully acknowledged.

9. References

[1] L. D. Armstrong, Can. J. Research [A] **28,** 44 (1950).
[2] J. H. Awberry and E. Griffiths, Proc. Roy. Soc. (London) [A] **174,** 1 (1940).
[3] H. Moser, Physik. Z. **37,** 737 (1936).
[4] J. M. North, Atomic Energy Research Establ. (G. Brit.) M/R 1016 (1952).
[5] G. T. Furukawa, T. B. Douglas, R. E. McCoskey, and D. C. Ginnings, J. Research NBS **57,** 67 (1956) RP 2694.
[6] N. S. Osborne, H. F. Stimson, and D. C. Ginnings, J. Research NBS **18,** 400 (1937) RP 983.
[7] E. D. West and D. C. Ginnings, Rev. Sci. Inst. **28,** 1070 (1957).
[8] H. J. Hoge, Rev. Sci. Instr. **20,** 59 (1949).

Washington, May 16, 1957.

Journal of Research of the National Bureau of Standards Vol. 60, No. 4, April 1958 Research Paper 2849

An Evaluation of the Luminous-Transmittance Requirements for Railroad-Signal Glassware in Terms of Standard Source A of the International Commission on Illumination

Francis C. Breckenridge

As an extension of Research Paper 1688, an estimate has been made of the transmittance for illuminant A of signal glassware having the minimum transmittance acceptable under the specifications of the Signal Section of the Association of American Railroads, which are formulated in terms of tests at 2,360° K.

In connection with the preparation of the last Secretariat Report on Colors of Signal Lights [1][1] for the International Commission on Illumination, it was desired to include values for the minimum transmittance for railroad-signal glassware used in this country and to show these values for light sources of color temperature 2,850° K since the other countries had reported transmittance values for their glassware for lamps of that color temperature. The revision of the specifications for railroad-signal glassware, which is now being considered by the Signal Section of the Association of American Railroads (AAR), suggests that this information may now have a wider interest. A method for computing minimum transmittance at 2,850° K from the currently specified minimum-transmittance values is accordingly described below.

AAR Specifications 59–39 and 69–48 control the transmittance of railroad-signal glasses by limits assigned on a scale known as the T_{AAR} scale. This scale (actually six scales, one for each of six signal colors) was established by a procedure described in RP1209 [2]. It is defined in terms of six luminous-transmittance values for a source of 2,360° K, each of these values being applicable to glasses having chromaticity characteristics similar to the filters used for one of the railroad-signal colors. The transmittance values for the six signal colors corresponding to $T_{AAR}=100$ are listed in table 6 RP1209 [2], and in table 1 in RP1688 [3]. In practice, the T_{AAR} values of glasses submitted for inspection are determined by finding the ratio of the transmittance of the glass being tested to the transmittance of one of the "limit" filters and multiplying this ratio by the T_{AAR} value of the limit filter. The transmittance values for the primary-standard "limit" filters for sources of color temperature 1,900° K, 2,360° K, and 2,848° K[2] have been published, together with their T_{AAR} values at 2,360° K, in table 4 of RP1688 [3].

The inspection of signal glassware is carried out at color temperature 2,360° K,[3] but the glassware is used in service with sources ranging from 1,900° K to 2,850° K. For a source of color temperature 2,360° K, the minimum acceptable transmittance is readily computed from the simple proportion:

$$(T)_{min}/(T)_{std}=(T_{AAR})_{min}/(T_{AAR})_{std}, \quad (1)$$

in which:

$(T)_{min}$ = transmittance of glass of minimum acceptable T_{AAR},
$(T)_{std}$ = transmittance of standard filter at 2,360° K,
$(T_{AAR})_{min}=T_{AAR}$ stated in specification as minimum acceptable,
$(T_{AAR})_{std}=T_{AAR}$ value of standard filter.

This simple proportion does not give correct values of transmittance for sources of other temperatures since the ratio of the transmittance at one color temperature to that at another varies with the value of T itself. This variation, however, is systematic and with respect to each type of glassware, it may, to a first degree of approximation, be considered as linear.

[1] Figures in brackets indicate the literature references at the end of this paper.

[2] The numerical designations of color temperature used in RP1688 [3] were based upon $C_2=14{,}350$ micron degrees in Planck's formula. We here use the same designations in order to avoid confusion. The presently-accepted value of C_2 is 14,380 micron degrees, and the corresponding values of color temperature are:

$C_2=14{,}350$ micron degrees	$C_2=14{,}380$ micron degrees
° K	° K
1,900	1,904
2,360	2,365
2,848	2,854

In service there is considerable variation in color temperature for each type of source so that the approximate values 1,900° K, 2,350° K, and 2,850° K may be used when the reference is to service conditions.

[3] The latest draft for the revision of specification AAR 69–48 provides that inspection will be made at 2,854° K.

The desired transmittance values for 2,854° K were computed in accordance with the following assumptions:

(1) That for each type and color, the glassware in service has the same characteristics as the pale limit and transmission standard filters which should be true if it contains the same colorants in about the same proportions as the filters which control it;

(2) That the ratio $T_{2,848}/T_{2,360}$ is approximately a linear function of the transmittance.

Using the vaues of transmittance listed in table 4 RP1688 [3], the ratio $T_{2,848}/T_{2,360}$ was computed for each filter and these ratios were plotted as functions of the corresponding T_{AAR} values at 2,360° K (see fig. 1). The value of minimum acceptable transmittance for a source at 2,848° K was then computed from the formula:

$$(T_{2,848})_{min}=0.01\ (T_{AAR})_{min}\times(T_{2,360})_{100}\times(T_{2,848}/T_{2,360})_{min} \quad (2)$$

in which:

$(T_{2,848})_{min}$ = transmittance of glass of minimum acceptable transmittance for light of color temperature 2,848° K,

$(T_{AAR})_{min}$ = T_{AAR} stated in specification as minimum acceptable,

$(T_{2,360})_{100}$ = transmittance corresponding to 100 on T_{AAR} scale for light of color temperature 2,360° K,

$(T_{2,848}/T_{2,360})_{min}$ = ratio of transmittances at minimum acceptable T_{AAR} value, read from graph.

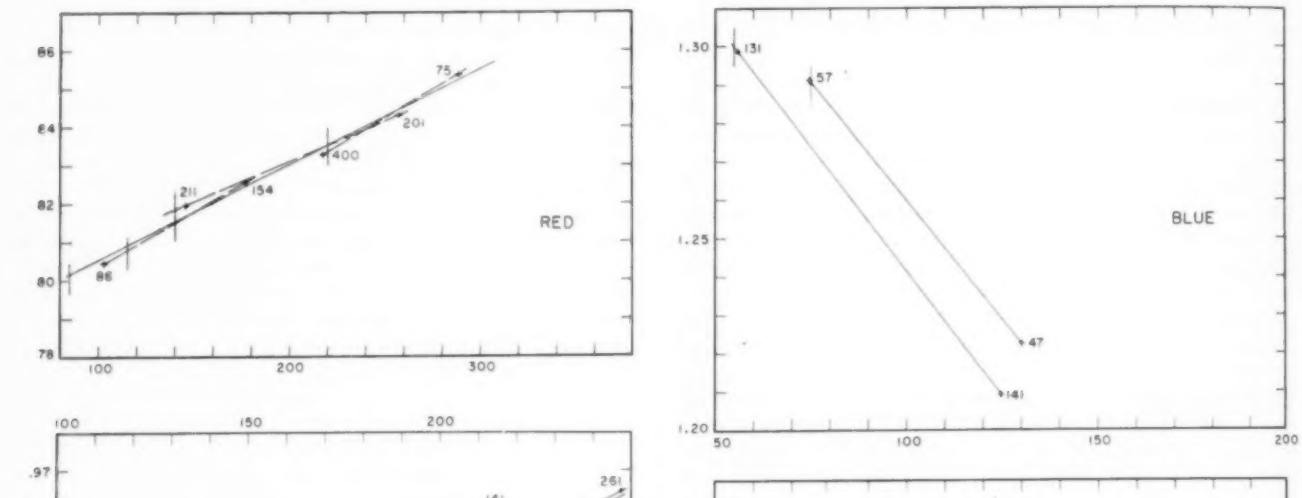

FIGURE 1. *Each of the above figures shows the relation between the ratio $T_{2,848}/T_{2,360}$ and the T_{AAR} value for the primary standard filters of one color.*

Each filter is indicated by a cross and identified by the filter number. The vertical lines mark the minimum acceptable T_{AAR} values for different classes of ware. Filters applying to the same type of ware are joined by lines and the lines representing the least-square equations have also been drawn. In each case the line used for the interpolation is shown as a full line.

TABLE 1. *Minimum acceptable transmittance for light of 2,848° K for railroad signal glassware*

Kind of ware	AAR filter numbers		At minimum acceptable transmittance			
	Pale limit[a]	Transmission Standard[a]	T_{AAR}	$T_{2,848}/T_{2,360}$		$T_{2,848}$
				By graph	By L. S. Eq.	
Red glasses (for $T_{AAR}=100$, $T_{2,360}=0.0690$)						
Pressed ware, general	154	86	85	0.7993	[b]0.8018	0.0469
Thin disks	154	86	115	.8079	[b].8092	.0641
Electric lanterns	154	86	140	.8152	[b].8155	.0788
Kerosene lanterns	201	211	140	.8185	[b].8155	.0788
Highway Crossing	75	400	220	.8336	[b].8353	.1268
Yellow glasses (for $T_{AAR}=100$, $T_{2,360}=0.2474$)						
Nonheat resisting	141	142	130	[b]0.9378	.....	0.301[6]
Thin disks	199	200	.....	.....	.....	.....
Kerosene lanterns	261	271	200	[b].9147	.9124	.452[6]
Green glasses (for $T_{AAR}=100$, $T_{2,360}=0.1186$)						
Nonheat resisting	134	87	150	1.1287	[b]1.1289	0.2008
Thin disks	139	140	138	[b]1.1157	.....	.1826
Kerosene lanterns	137	322	125	1.1404	[b]1.1400	.1690
Blue glasses (for $T_{AAR}=100$, $T_{2,360}=0.0223$)						
Nonheat resisting	47	57	75	[b]1.2907	.....	0.0216
Kerosene lanterns	141	131	55	[b]1.2987	.....	.0159
Purple glasses (for $T_{AAR}=100$, $T_{2,360}=0.0129$)						
Kerosene illuminant	56	47	73	[b]1.2698	.....	0.0120
Electric illuminant	80	108	30	[b]1.2438	.....	.0048
Lunar glasses (for $T_{AAR}=100$, $T_{2,360}=0.1895$)						
Kerosene illuminant	45	74	80	[b]1.0680	1.0651	0.162
Pressed ware electric illuminant	124	73	147	[b]1.0416	1.0445	.290
Thin disks	124	73	.....	.....	.....	.....

[a] In RP1688 [3], these filters are called "light limit" and "dark limit" because these designations are used in the railroad specifications. "Light" refers to chromaticity, however, and the true dark limit is the T_{AAR} value, which makes the designations used above seem preferable.
[b] Used for computing $T_{2,848}$.

Table 1 summarizes the computations. All the basic numerical values were taken from tables 2 and 4 of RP1688 [3] and table 6 of RP1209 [2]. The values of the ratio $T_{2,848}/T_{2,360}$ were obtained by graphical interpolation, supplemented by least-square solutions in the case of the red glassware and two types of green glassware that appeared to have similar chromaticity characteristics. The graphs used for these interpolations are presented in figure 1.

In the belief that the least-square differences may be an indication of the reliability of our basic assumption that $T_{2,848}/T_{2,360}$ is a linear function of the transmittance, these differences have been computed, not only for the red and green cases just mentioned, but also for four of the yellow filters and the four lunar white filters. These differences are listed in table 2. In no case is the difference greater than 0.3 percent of the ratio. While this value is large in comparison with the probable errors for the transmittances of the standard filters, it is not significant from the standpoint of the signal glassware in service.

The values given in column 5 of table 2 may also be used to compute the approximate transmittance for light of color temperature 2,854° K of replica filters which have been certified for light of color temperature 2,365° K (2,360° K for older certifications). It is only necessary to multiply the value given for $T_{2,848}/T_{2,360}$ corresponding to the primary standard by the certified transmittance of the replica at color temperature 2,365° K to obtain a value of transmittance for the replica at color temperature 2,854° K with an uncertainty which may be estimated from the values given in column 6 of the table.

TABLE 2. *Least-square solutions for groups of four or more related filters*

$T_{2,848}/T_{2,360}=K+k\ T_{AAR}/100$					
AAR filter number	Equation constants		$T_{2,848}/T_{2,360}$		Δ Column 5 minus column 4
	K	k	From measurements [1]	From equation	
1	2	3	4	5	6
Red	+0.78071	+0.02482			
75	.....	.....	0.8537	0.8522	−0.0015
86	.....	.....	.8045	.8062	+.0017
154	.....	.....	.8257	.8246	−.0011
201	.....	.....	.8430	.8444	+.0014
211	.....	.....	.8197	.8168	−.0029
400	.....	.....	.8329	.8347	+.0018
Yellow	+.80878	+.05180			
199	.....	.....	.9465	.9489	−.0024
200	.....	.....	.9377	.9388	−.0011
261	.....	.....	.9643	.9628	+.0015
271	.....	.....	.9358	.9337	+.0021
Green	+1.19562	−.04446			
87	.....	.....	1.1284	1.1287	−.0003
134	.....	.....	1.1048	1.1041	+.0007
137	.....	.....	1.1126	1.1134	−.0008
322	.....	.....	1.1398	1.1393	+.0005
Lunar	+1.08967	−.03071			
45	.....	.....	1.0499	1.0523	−.0024
73	.....	.....	1.0417	1.0447	−.0030
74	.....	.....	1.0682	1.0652	+.0030
124	.....	.....	1.0290	1.0266	+.0024

[1] For example, values in RP1688 [3].

References

[1] Proc. Intern. Comm. Illumination, Zurich, 13th Session, **1,** sec. 1.3.3, p. 28 (1955).

[2] Kasson S. Gibson and Geraldine Walker Haupt, Standardization of the luminous-transmission scale used in the specification of railroad signal glasses, J. Research, NBS **22,** 627 (1939) RP1209.

[3] Kasson S. Gibson, Geraldine Walker Haupt, and Harry J. Keegan, Specification of railroad signal colors and glasses, J. Research, NBS **36,** 1 (1946) RP1688.

WASHINGTON, August 12, 1957.

Journal of Research of the National Bureau of Standards Vol. 60, No. 4, April 1958 Research Paper 2850

Random Notes on Matrices

K. Goldberg

Three matrix problems are considered in this paper: Bessel functions as limits of determinants, finding all optimal strategies of a matrix game with nonzero value, and conditions for matrices to have equal principal minors.

The three sections of this paper have little relation except that they each concern matrices and each was suggested by the work of a colleague at the National Bureau of Standards.

In the first section we prove that the limit of a certain sequence of determinants is the modified Bessel function $\Lambda_s(x)$.

In the second section we show that a method for computing a pair of optimal strategies for certain square matrix games yields the unique optimal strategy for one player if the optimal strategy for the other player is totally positive. This can result in an appreciable saving in the work of computing all the optimal strategies of an arbitrary matrix game with nonzero value.

The third section contains an amplification of a result which appeared in this journal as well as a necessary and sufficient condition that two matrices have equal corresponding principal minors.

1. *Bessel functions as limits of determinants.* Let (a_{ij}) be an infinite, triple diagonal, symmetric matrix with

$$a_{i,i-1}^2=a_{11}-a_{ii}=1-(2s+1)i^{-1}+i^{-2}p(i^{-1}) \tag{1.1}$$

for some polynomial $p(t)$ and some real number s which is not a negative integer. Let $D_n(t)$ be the characteristic polynomial of the first n rows and columns of (a_{ij}). We shall prove

THEOREM 1. $$\lim_{n\to\infty} D_n(a_{11}+1-n^{-2}z^2)=\Lambda_s(z), \qquad |z|<\infty,$$

where $\Lambda_s(z)$ is the Jahnke-Emde modified Bessel function with expansion

$$\Lambda_s(z)=\sum_{k=0}^{\infty}\frac{(-1)^k z^{2k}}{4^k k!(s+k)(s+k-1)\ldots(s+1)}, \qquad |z|<\infty.$$

The theorem was suggested in considering a conjecture of J. Todd.

Since (a_{ij}) is triple diagonal and symmetric we can use the first equation in (1.1) to obtain a simple recursion for $D_n(t)$. We have $D_0(t)=1$, $D_1(t)=t-a_{11}$ and

$$D_n(t)=(t-a_{nn})D_{n-1}(t)-(a_{11}-a_{nn})D_{n-2}(t) \qquad n=2, 3, \ldots. \tag{1.2}$$

Thus

$$D_n(a_{11}+1)=1.$$

We shall expand $D_n(a_{11}+1-n^{-2}z^2)$ around $a_{11}+1$, and to this end we define

$$D_n^{(k)}=D_n^{(k)}(a_{11}+1).$$

By repeated differentiation of equation (1.2) we get the following recursion for $D_n^{(k)}$: $D_n^{(0)}=D_1^{(1)}=1$, $D_n^{(k)}=0$ if $k>n$ and

$$D_n^{(k)}-2D_{n-1}^{(k)}+D_{n-2}^{(k)}+n^{-1}(2s+1)(D_{n-1}^{(k)}-D_{n-2}^{(k)})-n^{-2}p(n^{-1})(D_{n-1}^{(k)}-D_{n-2}^{(k)})=kD_{n-1}^{(k-1)}$$

for $k=1,2\ldots,n$ and $n=2,3,\ldots$. This recursion can be solved for $D_n^{(k)}$ yielding

$$D_n^{(k)}=n^{2k}4^{-k}\prod_{j=1}^{k}(j+s)^{-1}+n^{2k-1}d_k+n^{2k-2}q_k(n^{-1})$$

for all n and $k \leq n$, some polynomial $q_k(t)$ of degree $2k-2$, and

$$d_k = 4^k \binom{2k}{k} \frac{\Gamma(k+s+1)\Gamma(s+1)}{\Gamma(2k+2s+1)} \sum_{j=1}^{k} 4^{-2j} \binom{2j}{j} \frac{\Gamma(2j+2s-1)}{\Gamma(j+s)\Gamma(j+s+1)} \frac{(2j+1)(2s+1)+2p(0)}{2j-1}$$

for all k. All that we need to know about d_k is that it is bounded and this is clear from the most crude inequalities. Let d be the bound:

$$|d_k| \leq d, \qquad k = 1,2, \ldots .$$

Denote the partial sums of $\Lambda_s(z)$ by

$$\Lambda_{sn}(x) = \sum_{k=0}^{n} \frac{(-1)^k z^{2k}}{4^k \cdot k!(s+k)(s+k-1) \ldots (s+1)}.$$

Then we have

$$D_n(a_{11}+1-n^{-2}z^2) - \Lambda_{sn}(z) = \sum_{k=0}^{n} \frac{(-1)^k z^{2k}}{k!} \left\{ \frac{D_n^{(k)}}{n^{2k}} - \frac{1}{4^k(s+k)(s+k-1) \ldots (s+1)} \right\}$$
$$= \sum_{k=1}^{n} \frac{(-1)^k z^{2k}}{k!} \left(\frac{d_k}{n} + o(n^{-1}) \right),$$

so that

$$D_n(a_{11}+1-n^{-2}z^2) - \Lambda_{sn}(z) \leq n^{-1} d e^{|z|^2} + o(1), \qquad |z| < \infty .$$

Since $\Lambda_{sn}(z)$ tends to $\Lambda_s(z)$ for all $|z| < \infty$ as n gets large the theorem is proved.

Note that

$$\Lambda_{-1/2}(z) = \cos z,$$

$$\Lambda_{1/2}(z) = z^{-1} \sin z,$$

and in general

$$\Lambda_s(z) = \Gamma(s+1)(z/2)^{-s} J_s(z),$$

where $J_s(z)$ is the Bessel function of order s. Thus our theorem can be interpreted as meaning that if $z_1, z_2, \ldots, z_n$ are the n smallest roots of $J_s(z)$ then the roots of $D_n(t)$ are approximated by

$$a_{11}+1-n^{-2}z_i^2 \qquad i = 1,2, \ldots, n,$$

with the best approximations being for the smaller z_i.

2. *On finding all optimal strategies of a matrix game with nonzero value.* Let B be a payoff matrix with nonzero value. Let K_1 and K_2 be the extremal sets of the optimal strategy spaces of the row player and the column player, respectively.

A result due to L. S. Shapley and R. N. Snow [1] states

THEOREM. Let x and y be optimal strategies for the row player and the column player respectively. A necessary and sufficient condition that $x \epsilon K_1$ and $y \epsilon K_2$ is that there exist a nonsingular submatrix A of B of order n such that, if $\bar{e}$ is the 1 by n vector of all ones,

$$\begin{aligned} v &= [\bar{e} A^{-1} \bar{e}^T]^{-1} \\ \bar{x} &= v \bar{e} A^{-1} \\ \bar{y} &= v \bar{e} (A^T)^{-1} \end{aligned} \tag{2.1}$$

where v is the value of the game, $\bar{x}$ is the vector obtained from x by deleting the elements corresponding to the rows deleted to obtain A from B, and $\bar{y}$ is the vector obtained from y by deleting the elements corresponding to the columns deleted to obtain A from B.

We shall prove that if either $\bar{x} > 0$ (that is every element in $\bar{x}$ is positive) or $\bar{y} > 0$ then the other represents the unique optimal strategy for A for the corresponding player. In other

words if, say, $\bar{x}>0$ then no element of K_2 other than y can be obtained from any submatrix of A.

This result can be used to reduce the number of submatrices of B that have to be inspected to exhaust K_1 or K_2.

Our result takes the following form:

THEOREM 2. Let A be a nonsingular payoff matrix of order n such that the nonzero row and column sums of A^{-1} are all of the same sign. If none of the row (column) sums of A^{-1} are zero then the row (column) player has a unique optimal strategy.

We shall say that 1 by n vectors $\bar{x}_0$ and $\bar{y}_0$ represent optimal strategies for the row player and the column player of A respectively if

$$\bar{x}_0 \geq 0, \qquad \bar{y}_0 \geq 0, \qquad \bar{x}_0 \bar{e}^T = \bar{y}_0 \bar{e}^T = 1$$

and for some number v_0, the value of the game,

$$\bar{x}_0 A \geq v_0 \bar{e} \geq \bar{y}_0 A^T.$$

Let v, $\bar{x}$ and $\bar{y}$ be as in (2.1). Then $\bar{x}\bar{e}^T = \bar{y}\bar{e}^T = 1$ and

$$\bar{x}A = v\bar{e} = \bar{y}A^T.$$

By hypothesis $\bar{x} \geq 0$ and $\bar{y} \geq 0$ so that $\bar{x}$ and $\bar{y}$ represent optimal strategies and v is the value of the game.

We shall assume that $\bar{x}>0$ and prove that $\bar{y}$ represents the unique optimal strategy for the column player. The proof for the other case follows in exactly the same way so this will prove Theorem 2.

Suppose $\bar{y}_0$ is a non-negative 1 by n vector such that $\bar{y}_0 \bar{e}^T = 1$ and

$$v\bar{e} \geq \bar{y}_0 A^T. \tag{2.2}$$

Since $\bar{x}>0$ we can find a 1 by n vector $\bar{u}$ such that the matrix

$$X = \bar{x}^T \bar{u} - (A^T)^{-1}$$

is non-negative. Then (2.2) implies

$$v\bar{e}X \geq \bar{y}_0 A^T X.$$

Computing these two vectors we get

$$v\bar{e}X = v\bar{e}\bar{x}^T\bar{u} - v\bar{e}(A^T)^{-1} = v\bar{u} - \bar{y}$$

and

$$\bar{y}_0 A^T X = \bar{y}_0 A^T \bar{x}^T \bar{u} - \bar{y}_0 A^T (A^T)^{-1} = v\bar{y}_0 \bar{e}^T \bar{u} - \bar{y}_0 = v\bar{u} - \bar{y}_0.$$

Therefore we have $\bar{y}_0 \geq \bar{y}$. Since the sum of the elements of these two vectors are equal we must have $\bar{y}_0 = \bar{y}$, as desired.

3. *Matrices with equal principal minors.* In a previous paper in this journal [2] we stated a result which is a special case of the following

THEOREM 3. Let (a_{ij}) be a matrix of order n with complex elements and the properties

$$a_{ij}a_{ji} \text{ is real and non-negative}, \qquad i, j = 1,2, \ldots, n, \tag{3.1}$$

$$a_{i_1 i_2} a_{i_2 i_3} \cdots a_{i_k i_1} = \overline{a_{i_2 i_1} a_{i_3 i_2} \cdots a_{i_1 i_k}}, \tag{3.2}$$

for all $k = 1,2, \ldots, n$ and $i_j = 1,2, \ldots, n$. Then (a_{ij}) has the same principle minors as the Hermitian matrix (b_{ij}) with

$$b_{ij} = (\operatorname{sgn} a_{ij})(a_{ij}\bar{a}_{ji})^{1/2} \tag{3.3}$$

and so has only real characteristic roots.

The symbol $\bar{x}$ means the complex conjugate of x, and the symbol $x^{1/2}$ means that square root of x with non-negative real part.

We shall prove this theorem by showing that

$$b_{i_1i_2}b_{i_2i_3}\cdots b_{i_ki_1}=a_{i_1i_2}a_{i_2i_3}\cdots a_{i_ki_1} \tag{3.4}$$

for all $k=1,2,\ldots,n$ and $i_j=1,2,\ldots,n$ and the result will follow as in the previous paper.

From (3.1) we see that either $a_{ij}a_{ji}=0$ or .

$$a_{ji}=c_{ij}\overline{a_{ij}}$$

for some positive real c_{ij}. These c_{ij} satisfy

$$c_{ij}=c_{ji}^{-1}$$

and, from equation (3.2),

$$c_{i_1i_2}c_{i_2i_3}\cdots c_{i_ki_1}=1 \tag{3.5}$$

whenever $a_{i_1i_2}a_{i_2i_3}\cdots a_{i_ki_1}$ does not vanish.

Therefore, either $b_{ij}=b_{ji}=0$ or,

$$b_{ij}=c_{ij}^{1/2}a_{ij}, \tag{3.6}$$

so that

$$\overline{b_{ij}}=c_{ij}^{1/2}\bar{a}_{ij}=c_{ij}^{-1/2}a_{ji}=c_{ji}^{1/2}a_{ji}=b_{ji}$$

as desired to prove that (b_{ij}) is Hermitian.

Choose an arbitrary ordered subset $i_1,i_2,\ldots,i_k$ of $\{1,2,\ldots,n\}$. Let $b=b_{i_1i_2}b_{i_2i_3}\cdots b_{i_ki_1}$, $a=a_{i_1i_2}a_{i_2i_3}\cdots a_{i_ki_1}$, $a'=a_{i_2i_1}a_{i_3i_2}\cdots a_{i_1i_k}$.

If b vanishes then, by (3.3), either a or a' vanishes. By (3.2) this means that a vanishes, so $b=a$.

If b does not vanish we have

$$b=c_{i_1i_2}^{1/2}c_{i_2i_3}^{1/2}\cdots c_{i_ki_1}^{1/2}a_{i_1i_2}a_{i_2i_3}\cdots a_{i_ki_1}=a$$

by combining equations (3.5) and (3.6).

Therefore $b=a$ in general and we have proved equation (3.3) and so the theorem.

We are naturally led from this theorem to ask for a necessary and sufficient condition that two matrices have the same principal minors. We shall find such a condition based on a little known expansion of the determinant of a matrix.

Let $A=(a_{ij})$ be a matrix of order n. Choose any set of k distinct indices $\{i_1,i_2,\ldots,i_k\}$ with $1\leq i_j\leq n$. Then define the symbols

$$\{i_1\}_A=a_{i_1i_1}$$

if $k=1$, and (3.7)

$$\{i_1,i_2,\ldots,i_k\}_A=\sum_\sigma a_{i_1i_{\sigma(1)}}a_{i_{\sigma(1)}i_{\sigma^2(1)}}\cdots a_{i_{\sigma^{k-1}(1)}i_1}$$

if $k=2,3,\ldots,n$, where the sum is taken over all full cycles σ on $\{1,2,\ldots,k\}$.

Given an arbitrary partition of $\{1,2,\ldots,n\}$

$$\tau=\{i_{11},i_{12},\ldots,i_{1k_1}\}\{i_{21},i_{22},\ldots,i_{2k_2}\}\cdots\{i_{m1},i_{m2},\ldots,i_{mk_m}\}$$

define the symbol

$$\tau_A=(-1)^m\{i_{11},i_{12},\ldots,i_{1k_1}\}_A\{i_{21},i_{22},\ldots,i_{2k_2}\}_A\cdots\{i_{m1},i_{m2},\ldots,i_{mk_m}\}_A. \tag{3.8}$$

Then the determinant of A may be expanded in

$$\det A=(-1)^n\sum\tau_A \tag{3.9}$$

where the sum is taken over all partitions τ of $\{1, 2, \ldots, n\}$.

To prove that this expansion is valid we need only show that the generic term in the usual expansion of the determinant appears in this expansion, that whenever it does appear it does so with the proper sign, and that there are exactly $n!$ such terms.

The generic term in the expansion of the determinant can be denoted by

$$a=(-1)^\rho a_{1\rho(1)}a_{2\rho(2)}\ldots a_{n\rho(n)}$$

where ρ is a permutation of degree n and $(-1)^\rho$ is $+1$ or -1 as ρ is even or odd respectively.

Write ρ in its unique decomposition into cycles

$$\rho=(i_{11}i_{12}\ldots i_{1k_1})(i_{21}i_{22}\ldots i_{2k_2})\ldots(i_{m1}i_{m2}\ldots i_{mk_m}).$$

Then the only τ_A in which a can appear is the one described in (3.8). Since $(-1)^\rho=(-1)^{n-m}$ the sign is always right. Finally it is clear that a appears at least once in τ_A.

Now, consider the partition $k_1+k_2+\ldots+k_m$ of n. Let s_i be the number of k_j equal to i. Then there are

$$\frac{n!}{s_1!s_2!\ldots s_n!k_1!k_2!\ldots k_m!}$$

partitions τ of $\{1,2, \ldots ,n\}$ with subsets of order $k_1,k_2, \ldots, k_m$. By (3.7) a subset with k_i elements contributes $(k_i-1)!$ summands to τ_A. Thus the total number of summands on the r.h.s. of equation (3.9) is

$$\sum\frac{n!}{s_1!s_2!\ldots s_n!}\frac{(k_1-1)!(k_2-1)!\ldots(k_m-1)!}{k_1!k_2!\ldots k_m!}=\sum\frac{n!}{s_1!s_2!\ldots s_n!1^{s_1}2^{s_2}\ldots n^{s_n}}=n!$$

as desired, the sums being taken over all partitions of n.

Suppose $B=(b_{ij})$ is a matrix of order n and

$$\{i_1,i_2, \ldots, i_k\}_A=\{i_1,i_2, \ldots, i_k\}_B \tag{3.10}$$

for all subsets $\{i_1,i_2, \ldots, i_k\}$ of $\{1,2, \ldots, n\}$. By (3.8) and the expansion (3.9) this implies that the corresponding principle minors of A and B are equal. We shall prove the converse.

Suppose A and B have equal corresponding principal minors. Then (3.10) holds for $k=1$. Suppose it holds for $k=1,2, \ldots, m-1$. Consider the expansion as in (3.9) of the minor with row and column indices $i_1, i_2, \ldots, i_m$. For every τ except $\tau'=\{i_1,i_2, \ldots, i_m\}$ we are summing products of equal sums $\{i'_1, i'_2, \ldots, i'_k\}_A=\{i'_1,i'_2, \ldots, i'_k\}_B$ with $k\leq m-1$. Therefore the equality of the minors implies $\tau'_A=\tau'_B$ which completes the proof by induction. We have proved

Theorem 4. Let A and B be matrices of order n. They have equal corresponding principal minors if and only if equation (3.10) holds for all subsets $\{i_1,i_2, \ldots, i_k\}$ of $\{1,2, \ldots, n\}$.

We remark that theorem 4 (and thus theorem 3 as well) also follows from a result noted by A. Ostrowski (footnote 13 in [3]), which is closely related to the expansion (3.8).

References

[1] L. S. Shapley and R. N. Snow, Basic solutions of discrete games, Contributions to the Theory of Games, vol. I, Annals of Mathematics Study No. 24 (Princeton University Press, 1954).

[2] K. Goldberg, A matrix with real characteristic roots, J. Research NBS **56**, 87 (1956) RP2652.

[3] A. Ostrowski, Determinanten mit überwiegender Hauptdiagonale und die absolute Konvergenz von linearen Iterationsprozessen, Commentarii Mathematici Helvetici **30**, 175 (1956).

Washington, October 18, 1957.

Journal of Research of the National Bureau of Standards Vol. 60, No. 4, April 1958 Research Paper 2851

Range Finders Using Projected Images

Robert E. Stephens

Two optical range finders of six-inch base length have been designed and constructed for making measurements to arbitrary points on a model. One measures distances from 2.5 feet to 10 feet, the other from 9.7 feet to 25 feet. The accuracy of all distances is plus or minus one-quarter inch or better. Because of unusual requirements of use these range finders operate by projecting two images of a bright cross upon the target, which may be fused into a single image by adjustment of the range knob.

1. Introduction

Two optical range finders of 6-in. base length have been designed and constructed for making measurements to arbitrary points on a model. One measures distances from 2.5 to 10 ft, the other from 9.7 to 25 ft. The accuracy of all distances is $\pm\frac{1}{4}$ in. or better. Because of the unusual requirements of the application in which they are used these range finders operate by projecting two images of a bright cross upon the target, which may be fused into a single image by adjustment of the range knob.

The problems involved in the choice of the type and base length of the instruments, types of compensators, synchronization of compensation and focusing, adjustment, and calibration are discussed in considerable detail in the following sections.

2. Base and Magnification

The ability of a base-type range finder to discriminate between a distance R_1 and another distance R_2 depends upon the size of angle $\Delta\alpha$, the difference between the two parallax angles α_1 and α_2 subtended by the base of length B at the points P_1 and P_2 whose distances are R_1 and R_2 (see fig. 1). Since B is small compared to R, take

$$\alpha=\frac{B}{R}, \tag{1}$$

and

$$\Delta\alpha=B\frac{R_1-R_2}{R_1R_2}$$

or, for small differences ΔR,

$$\Delta\alpha=-\frac{B}{R^2}\Delta R. \tag{2}$$

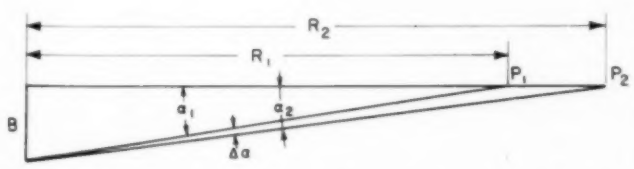

FIGURE 1. *Base B, range R, and parallax angle α of a base-type range finder.*

Range finders are almost invariably telescopic and the angle of disparity presented to the eye of the observer is consequently

$$\Delta A=M\Delta\alpha=\frac{MB}{R^2}\Delta R, \tag{3}$$

where M is the magnification of the telescope. The negative sign has been dropped because in the following argument only the magnitude is of importance.

The present application requires ability to measure ranges up to 25 ft with an accuracy of ± 0.25 in. The quantity $\Delta R/R^2$ is smallest at the greatest distance; at 25 ft it is $0.25\div\overline{300}^2=2.78\times10^{-6}$ radian per inch of base. This is equivalent to 0.573 sec/in.

An average observer can match the two parts of the image in a split-field-type range finder to within approximately ± 12 sec. His precision of matching for the two parts in the superimposed-image type is a little poorer, about ± 20 sec. Because of the greater complexity and cost of the split-field type it was decided that the superimposed image would be used if practicable. By eq (2), with $\Delta R/R^2=0.573$ sec/in. and $\Delta A=20$ sec it is found that $MB=34.9$ in. We chose to make $M=6$ and $B=6$ in.; this makes $MB=36$ and $\Delta A=20.6$ sec. At all shorter distances ΔA will be greater, and the precision of matching well within the required 0.25 in.

3. Compensators

A compensator in a range finder is a device that produces a variable angular deviation of the line of sight by way of one window to bring the two images, one by one window and one by the other window, into coincidence. The position of this device when coincidence exists indicates the range. There are several types of compensator each of which has characteristics that make it advantageous for some special application. It is beyond the scope of this report to give a complete discussion of the characteristics of all the types. It will suffice to describe the characteristics necessary and desirable for our specific application and to show that the chosen type has these, or most of them.

The first characteristic to be considered is the sensitivity. This may be defined as the increment of

displacement of the compensator corresponding to the smallest increment of range that is to be measurable. The sensitivity is not constant but increases from a minimum at the long-range end of the scale to a maximum at the short-range end. This feature definitely limits the spread between the maximum and minimum distances measurable by one range finder. Adequate sensitivity must be provided at the long-range end of the scale; at shorter ranges the sensitivity increases until such a large movement is necessary for a small change in distance that making a match becomes intolerably slow.

The second consideration in the choice of the compensator is the law relating the displacement of the compensator to the resulting deviation of the line of sight. For our purpose a compensator whose deviation angle is proportional to the displacement is desirable. Important reasons for this are that adjustment and calibration are simplified, and that it facilitates coupling to a focusing mechanism, which will be discussed in detail later.

Another consideration is simplicity of construction. If the other conditions are satisfied the compensator of the simplest construction is the obvious choice.

The sliding-lens compensator seemed to fit these requirements better than any other type. This consists of a low-power lens that is larger than the window and may be moved across the window along a line parallel to the base. A schematic drawing of this is shown in figure 2. In (a) the lens is shown centered on the line of sight, giving no deviation. In (b) the lens is displaced so that the line of sight goes through it eccentrically and suffers a deviation D. The magnitude of the deviation is proportional to the eccentricity (this is an approximation of sufficient accuracy for the purpose). Let D be the deviation, x the eccentricity of the lens, and Φ the power of the lens, then

$$D=x\Phi, \tag{4}$$

and

$$\Delta D=\Phi\Delta x. \tag{5}$$

In section 2 it was determined that the change in parallax angle represented by 0.25 in. at a distance of 25 ft was 2.78×10^{-6} radian per in. of base length. Also it was decided that a base length of 6 in. would be used. The minimum increment in parallax angle that is to be perceived and measured is then 16.67×10^{-6} radian. It is convenient to first compute the eccentricity of a 1-diopter lens for a deviation of 16.67×10^{-6} radian. This is, of course, 16.67×10^{-6} m or 0.01667 mm. This can be measured with sufficient accuracy by a micrometer screw with spring preloading to take up the play. A 1-diopter lens is therefore the choice for the compensator.

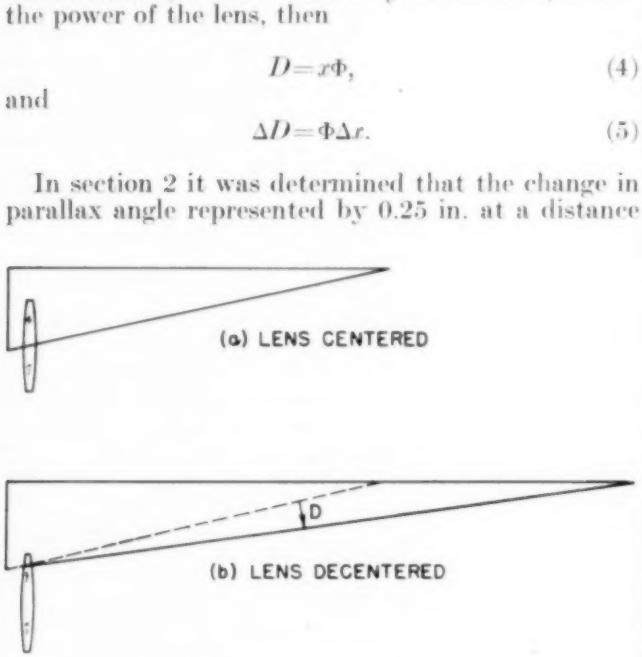

FIGURE 2. *The action of a sliding-lens compensator.*

For the experimental model it would be impracticable to rule a special scale indicating distance directly, and it was decided to use a commercially available linear scale indicating in hundredths of a turn up to ten turns. Consequently it was decided that the compensator would be decentered by a precision screw whose position would be indicated by one of these dials. This makes the scale 1,000 divisions long. These divisions are of such a size and quality that estimation to one-half division is easy and of sufficient accuracy. It was therefore decided to let one scale division represent approximately 0.5 in. at a distance of 25 ft.

We have computed the decentration corresponding to 0.25 in. at 25 ft to be 0.01667 mm. Our entire scale is to be 2,000 times this long, approximately; this is 33.33 mm. The desired lead for the screw then is one-tenth of this or 3.333 mm per turn. One-eighth in. is 3.175 mm, and because screws of this lead can be made on easily available machines this was adopted for the construction of the instrument. The total available range of displacement for the compensator is 1.25 in. or 31.75 mm with this screw. The total change of deviation is then, by eq (5), 0.03175 radian. At 25 ft the parallax is 0.02 radian. If the instrument is built with a bias of approximately 0.035 radian it can be made to work from a parallax angle of 0.02 to 0.05175 radian. This latter parallax corresponds to a distance of 9.66 ft, where one division of the scale represents 0.071 in. The total distance range of the instrument then is from 9.66 to 25 ft. It would be rather impracticable to try to increase this total range by increasing the length of the scale because, at the short-distance end of the scale the instrument is already much too sensitive. Even if the length of the scale were doubled it would only extend the range down to 6.2 ft. It is therefore obvious that another instrument with a less sensitive compensator is necessary for distances shorter than about 10 ft.

To measure distances under 10 ft, a sliding lens compensator of sufficient power and low sensitivity for a range finder of 6-in. base would have to be corrected for spherical and chromatic aberrations, and coma. This would make it so complex that another type of compensator was chosen for the second instrument. A rotating mirror has the desired characteristics—it has no aberrations regardless of the magnitude of the deviation produced; and its sensitivity is inherently low because the angle of rotation of the mirror is only half the resulting deviation. The

sensitivity can be made adequate by the use of a long lever arm for producing the rotation of the mirror.

At a distance of 10 ft the parallax angle for a 6-in. base is 0.050 radian. For an increment of distance of 0.25 in. the change in parallax is 0.0001042 radian. If as before we let this be the change corresponding to one-half scale division the entire scale of 1,000 divisions will cover a range of 0.2084 radian. The minimum distance will then correspond to 0.05+ 0.2084, or 0.2584 radian. This distance is 1.935 ft, or 23.2 in.

The increment of parallax corresponding to 0.25 in. at a distance of 10 ft is 0.0001042 radian or 21.5 sec. This is large enough for satisfactory matching to within ± 0.25 in. without magnification. At any shorter distance it is still larger and thus more than adequate for matching with the required precision without telescopic magnification.

4. Projection

These range finders are to be used for measuring the slant distance to a particular point on a scale model. Because various points on the model are to be chosen for observation at various times the models are painted a uniform white and there is no permanent mark whose two images could be bought to coincidence in a range finder. It is necessary to provide a temporary mark and desirable that this be done without disfiguring the model. This can be done by working in a darkened room and projecting a tiny spot of light on the desired part of the model.

If an optical range finder of the usual type were used the location of the projector would be unimportant, so long as a small bright spot could be projected to the proper place on the model. The observer would look into the eyepiece of the range finder, turn the knob to achieve coincidence, then obtain the distance by reading the scale. Because of the diverse locations of the model the observer would have to be prepared to follow the eyepiece, and take whatever position would be necessary to sight in the direction of the model. Complex construction might be resorted to, to bring the image from any direction into a fixed eyepiece. However, in this application such construction was impractical, partly because of the space it would require and partly because of rather considerable extra cost.

An alternative is to construct the range finder so that it projects two bright images of a cross, one through one window and another through the other window, that are to be brought into coincidence at the desired point on the model by means of the compensator. A telescope of suitable magnifying power, located in any convenient place, could be used for viewing the images while adjusting them into coincidence. This arrangement, although still requiring some variation in the position of the observer and direction of view, allows viewing without impracticable contortions. This is the plan that was adopted and the range finders accordingly were designed to contain the means for projecting two bright images upon the model.

5. Focusing

In order that coincidence may be established with sufficient precision to assure the requisite precision of the distance measurement, the projected images must be focused sharply on the model at the point to which the distance is to be measured. Adjustment of the focus and adjustment of parallax to achieve coincidence could very well be independent. However, this would necessitate two separate adjustments for each measurement and would consequently be somewhat inconvenient and necessarily slower. Fortunately the laws governing the motion of the compensator and the focusing of a lens are so similar that it is easy to provide mechanical coupling of the two functions to achieve simultaneously both coincidence and sharp focus.

Both the sliding lens and the rotating mirror produce angular deviations of the line of sight that are proportional to the displacement of the compensator, thus:

$$D = Kx \tag{6}$$

where D is the deviation, x the displacement of the compensator (a length for the sliding lens and an angle for the rotating mirror), and K is a constant. For the purpose of this discussion the displacement of the compensator, x, is measured from the position it would have to make the parallax angle, α, of the two lines of sight equal to zero, that is, when the two lines of sight are parallel. Then D of eq (6) equals α of eq (a) and consequently

$$x = \frac{B}{KR} \tag{7}$$

The law relating the object distance l and the image distance l' for image formation by a lens is expressible in several forms. The one that is convenient for this discussion is the Newtonian form,

$$ll' = f^2, \tag{8}$$

where l and l' are the object and image distances measured from their respective principal foci, and f is the equivalent focal length of the lens. If the range finder and projection lens were so positioned that the front focal point of the lens coincided with the point from which the distance was measured (a condition that exists nearly enough in practice), R and l' would be equal. Since $R = B/Kx$, $l' = f^2/l$, and $B/Kx = f^2/l$,

thus
$$l = \frac{Kf^2}{B}x. \tag{9}$$

Since K, f^2, and B are constants, l is proportional to x. Consequently the two movements may be coupled by a simple mechanical device such as a lever or gears having the ratio Kf^2/B.

6. Design

The superimposed-image type of range finder makes use of what is known as a "beam-splitter,"

FIGURE 3. *The elements of a superimposed-image range finder.*

a surface made either of a very thin layer of metal or a multiple layer system of dielectric films. This is so made that at the desired angle of incidence the reflectance is approximately equal to the transmittance. The schematic diagram of a range finder of this type is shown in figure 3. The beam splitter is in the cube at 1, which is made by fastening together with optical cement the equal hypotenuse faces of two right angle prisms, one of which has the beam-splitting layer on it. The resulting cube is a beam splitter that has the same length of glass in both paths, transmitted and reflected. Thus light entering along the solid line of figure 3 is split into two parts approximately at right angles to one another and, except for a minor difference in intensity, these are both alike.

The optical system of the long-range instrument is shown in figure 4. The reticle, r, is illuminated by lamp, l, through condensing lens, c. The projection lens, L_3, projects an image of r to the appropriate distance. The projected beam passes through the beam-splitting cube behind window 1 where it is split into two parts of approximately equal intensity, one transmitted and emerging at 1, the other reflected and finally emerging at 2. The position of the beam splitter is such that the two parts of the beam emerge from it approximately at right angles. The pentaprism, P, is used to fold the projector beam so as to reduce the bulk of the instrument.

The large, low-powered lens, L_1, is the compensator. It is movable along a line approximately parallel to the base line of the instrument. The fixed concave lens, L_2, has diverging power equal to the converging power of the compensator; its function is to nullify the converging effect of the compensator. The two lenses together form, in effect, a prism of variable angle with no power of convergence or divergence.

The right-angled prism behind window 2 is oriented so that in the absence of deviation by the compensator the beam emerging from window 2 intersects that from window 1 at a distance whose parallax angle is the mean of those for the maximum and minimum ranges of the instrument. This bias allows the compensator lens to function over a range that is centered on the lens thus minimizing the effects of aberrations and permitting a simple uncorrected lens to be used.

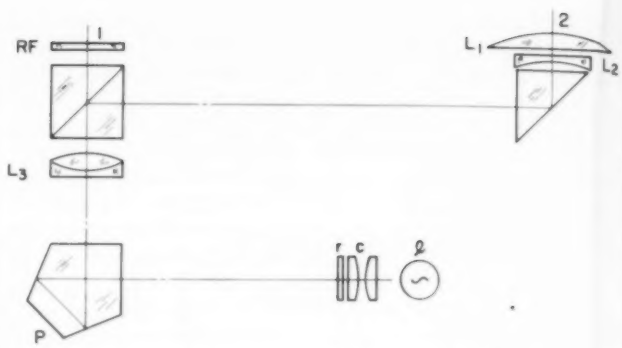

FIGURE 4. *Schematic diagram of long-range instrument.*

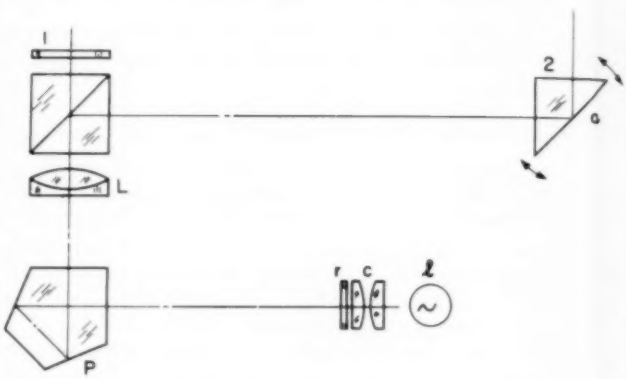

FIGURE 5. *Schematic diagram of short-range instrument.*

The direction-determining image, from window 1, is colored red by a filter designated *RF*. It was originally intended that the other image would be colored blue because of the improved precision of setting in coincidence that is usually achieved when the images are in complementary colors. However, the inclusion of a blue filter so reduced the brightness of the image that the hue became almost inappreciable. The precision of setting was reduced rather than increased because of the low brightness. The blue filter was consequently omitted.

The assembly consisting of reticle, condensing lens, and lamp is mechanically linked to the compensator so that the image of the reticle is focused at the same distance at which the two beams emerging from 1 and 2 intersect.

The short-range instrument is shown schematically in figure 5; it differs only in the compensator. The right-angled prism at 2 in this case instead of being fixed in position is mounted so that it may be rotated through several degrees on an axis normal to the plane of the diagram at point a. The beam from the window at 2 may thus be varied in direction so as to intersect the other beam at distances from approximately 2 to 10 ft. The reticle-condenser-lamp assembly is linked to the compensator prism so that as the prism is rotated this assembly is displaced along the line of projection thus maintaining the focus at the same distance at which the beams from 1 and 2 intersect.

In the long-range instrument the movement of the compensator is several times that of the reticle. To minimize the effect of mechanical play between the scale and the compensator and to make the mechanical advantage favorable, the precision screw, to which the scale is attached, drives the compensator directly. In the short-range instrument the movement of the reticle is large compared to the displacement of the lever that rotates the prism compensator. In this case the screw drives the reticle assembly directly. The mechanical play is reduced to inconsequential magnitude by preloading at all points of contact in the linkage.

The beam of light projected through window 2 will travel farther than that through window 1 in reaching the point where they intersect and the images are supposed to be coincident. Because of this the two images cannot both be in sharp focus. The best compromise is to have them focused so that the sharp focus of the beam from 1 is beyond the point of intersection and that from 2 is ahead of it. Then both will be sufficiently sharp for the purpose. Since the two images will be the same size only at their respective positions of sharp focus, one will be smaller and the other larger at their position of coincidence. This reduces the precision of setting but not enough to be serious in this application.

The positions of the points, F_1 and F_2, from which l'_1 and l'_2, the two image distances, are measured are illustrated in figure 6. Here F_1 is the front principal focus of the projection lens, L, for the transmitted beam emerging from window 1, and F_2 is the front principal focus for the beam reflected by the beam splitter and emerging from window 2. These are the points from which l'_1 and l'_2, respectively, are measured. However, the distance R to the observed point is measured from the base line.

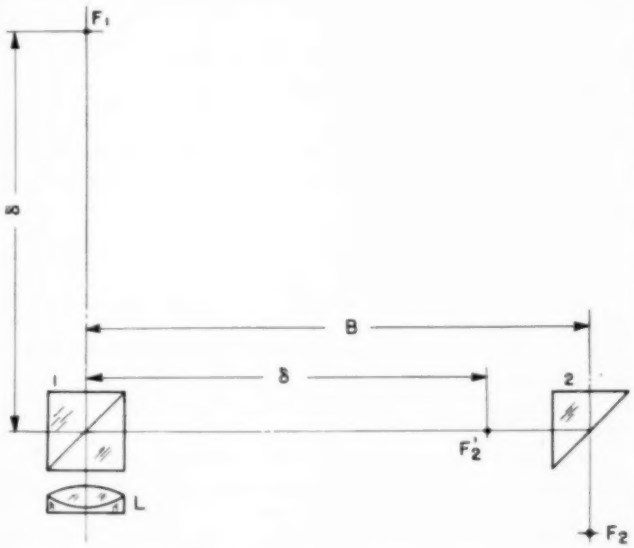

FIGURE 6. *Positions of front focal points for beams transmitted and reflected at beam splitter.*

If the images were focused so that $l'_1=l'_2=R$, then the point of coincidence would not be exactly half way between the two sharp images, because in our range finders $\delta=110$ mm, approximately, and the base length is 150 mm. The coincidence point would be much closer to the image from window 2, and also the distances of the sharp images from the point of coincidence would remain constant at all ranges if the motion of the reticle were coupled to that of the compensator with the ratio kf^2/B, in accordance with eq 9. Although this condition is not optimum it might be satisfactory because of the depth of focus.

It is possible, however, to maintain a more nearly optimum condition. If the ratio of the linkage is made slightly different from that of eq 9, and the reticle position changed slightly, it is possible for two different ranges to locate the sharp images equidistant from the point of coincidence. If these ranges are chosen properly, somewhere near but not at the ends of the scale, the condition of focus will change only slightly from one end of the scale to the other.

For the short-range instrument the linkage ratio was computed so that the two images would be equidistant from the point of coincidence when the distance of coincidence was 1.0 m and 2.7 m. At these distances $l_1=R+.075-0.110$ or 0.965 m and 2.665 m. The conjugate values of l are 0.018056 and 0.006538 m for $f=0.132$ m). The difference, $\Delta l=0.011518$. The corresponding values of the parallax angle are 0.15000 and 0.05556 radian; $\Delta\alpha=0.094444$. Consequently $\Delta l/\Delta\alpha=0.1219$ m per radian. Because the rotation of the mirror-type compensator is only half the resulting change in the parallax angle the linkage ratio is $2\times\Delta l/\Delta\alpha=0.2438$ m per radian. This, converted to more appropriate units, is 4.255 mm per degree. For comparison the value of Kf^2/B is 4.055 mm per degree. For other ranges the distances from the point of coincidence to the sharp images are not equal, but the discrepancy is small. It is shown graphically in figure 7. The two ranges of optimum focus were chosen as a result of a previous trial.

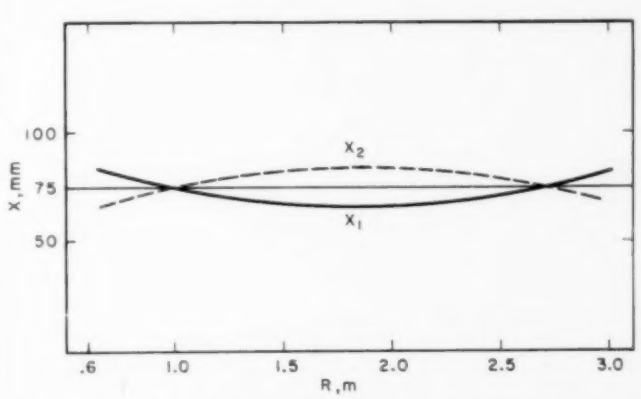

FIGURE 7. *The distances, x_1 and x_2, from the point of coincidence at distance R to the sharp images of the reticle projected through windows 1 and 2 (both plotted as positive).*

Similar analysis for the long-range instrument gives an optimum linkage ratio of 0.118. This is dimensionless and means that the displacement of the reticle is 0.118 times the displacement of the sliding-lens compensator. In this case the tracking errors are completely negligible.

It is not possible to realize this accuracy of synchronization by construction in which practicable optical and mechanical tolerances are allowed. Consequently the linkages were made adjustable, and the correct ratio achieved by experiment.

7. Telescope

A telescope is necessary for ± 0.25-in. accuracy with the long-range instrument. A 90-degree elbow type was adopted so that the position of the eyepiece and direction of viewing would permit comfortable use regardless of the direction to the object. It is constructed of components from a 6×30 binocular except that a pentaprism has been substituted for one of the customary Porro prisms to give the 90-degree bend to the line of sight. Also the spacings of the components have been changed slightly so that the range of focusing encompasses the working range of the range finder, 9.7 to 25 ft. The optical layout of the telescope is shown in figure 8.

8. Adjustment

No attempt will be made to describe in detail the tedious procedures found necessary to adjust the instruments as received from the shop. An outline of these adjustments and the means for making them will suffice. The necessity for adjustments arises from the fact that the requisite accuracy of the finished instrument can not be achieved by the application of tolerances to the separate parts. The following characteristics must be adjusted after assembly:

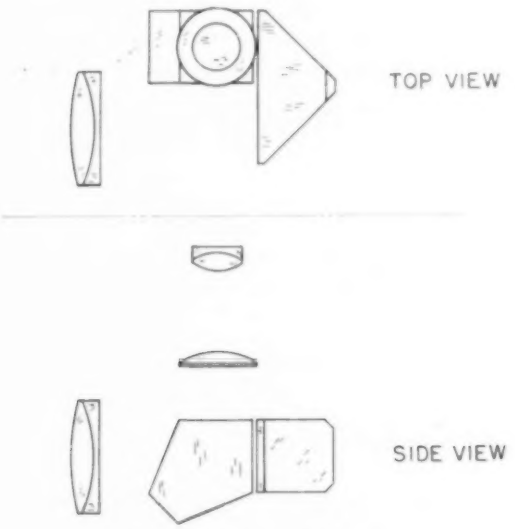

FIGURE 8. *Elbow telescope.*

8.1. The Bias

This is the adjustment that makes the range between zero and maximum displacement of the compensator correspond to the desired maximum and minimum ranges for the instrument. The bias of either instrument is adjusted by slight turning of the right-angle prism around an axis parallel to its axis. Simultaneous with this adjustment any existing dip-vergence [1] is corrected by the use of shims to tilt this prism. When the prism has been correctly placed it is clamped, and locating retainers are screwed down so as to hold it permanently in this position.

8.2. Focus

The focus is adjusted for maximum sharpness of both images by sliding the reticle longitudinally in its carriage. Because of the construction the transverse adjustment of the reticle is likely to be disturbed by the focusing adjustment. Because of this the alinement of axes is left until last.

8.3. Focusing Linkage Ratio

This must be adjusted to achieve optimum tracking between focusing and compensation to produce simultaneous coincidence and focus over the entire distance range of the instrument. The ratio of the levers between the compensator and the reticle carriage is adjusted so that at two positions, approximately one-eighth of the total distance range from each end of the range, the two sharp images are equidistant from the position of coincidence. Provision for adjusting either the length of one arm or the position of the fulcrum has been made in the construction of the instruments. The focusing will require adjustment again after each change in the lever. Once the correct ratio and focus have been obtained at these two distances the departure from optimum focus at other distances will be negligible.

8.4. Pointing Accuracy

The image from window 1, or both images when in coincidence, is used for determining the azimuth and elevation of the line of sight. The direction of the line of sight, therefore, must not change with change in focus.

8.5. Alinement of Optical and Mechanical Axes

One of the three axes of the mounting approximately coincides with the base line of the range finder. When the circular scale that indicates rotation around this axis is set at zero, the line of sight must coincide with one of the other two mechanical axes.

Adjustment to aline the optical axis with the mechanical one and to allow focusing without changing the direction of the optical axis is a tedious one. It is accomplished by achieving simultaneously the

[1] The projected beam from window 2 must, of course, intersect that from window 1 at any setting of the compensator. If it does not it is not possible to bring the images into coincidence. Such disparity is called dip-vergence.

proper position and tilt of the pentaprism and proper transverse position of the reticle.

9. Calibration

The parallax angle, α, of a range finder is given by eq (1). This angle is a linear function of the displacement of the compensator, thus

$$\alpha = Ks + \alpha_o, \tag{10}$$

where s is scale reading and α_o is a constant. This, substituted into eq (1), gives

$$Ks + \alpha_o = \frac{E}{R}. \tag{11}$$

However, none of the constants K, α_o, or E is known precisely; consequently the relation between the distance of coincidence and the scale reading must be determined experimentally. It is neither necessary nor desirable to evaluate these constants explicitly.

If eq (11) is divided by E, the result is

$$\frac{K}{E}s + \frac{\alpha_o}{E} = \frac{1}{R}$$

or, since K/E and α_o/E are instrumental constants, let us rewrite the relation as

$$Ps + Q = \frac{1}{R}. \tag{12}$$

Theoretically P and Q could be evaluated from the data obtained by setting for coincidence and reading the two scale readings corresponding to any two known distances. However, the accuracy of that method is insufficient. Settings should be made for perhaps five different known distances, the average of the scale reading for ten successive settings being used as the value of s for each distance. The constants may then be evaluated by the least-squares method or the method of averages. A method that should give sufficient accuracy for the purpose is to plot points on a large-scale graph corresponding to each of the known distances using as abscissae the values of s and as ordinates the values of $1/R$. It is then a matter of judgment to draw the straight line that best fits the data. The constants may then be evaluated from two widely spaced arbitrary points on the line. The line itself may be used as the calibration but is inconvenient because it is plotted with respect to the reciprocal of R instead of R directly. It is more convenient to have a table giving R as a function of s. This may be computed from eq (12) once accurate values of the constants have been obtained.

In subsequent use of the instrument an occasional check of the correctness of the scale should be made by making several settings at a known distance. If there is any discrepancy it can be corrected by repositioning the pointer. This procedure is theoretically exact because of the nature of the law governing the compensator.

Washington, August 22, 1957.

Journal of Research of the National Bureau of Standards Vol. 60, No. 4, April 1958 Research Paper 2852

Effect of Rib Flexibility on the Vibration Modes of a Delta-Wing Aircraft

Wilhelmina D. Kroll

A systematic study was made to determine whether decreasing the number of ribs or making the ribs more flexible would have any appreciable effect on the vibration modes and frequencies of a delta-wing aircraft. The modes and frequencies were computed for the basic wing and for the following modifications of the basic wing: (1) One rib outboard of the fuselage removed, (2) two ribs removed, (3) stiffness of ribs outboard of fuselage reduced one-half, and (4) rib stiffness reduced nine-tenths. The results indicated that the frequencies and mode shapes of the modified wings differed little from those of the basic wing and, therefore, that changes similar to these modifications would not appreciably affect the vibration characteristics of delta wings.

1. Introduction

The designer of an airplane might eliminate some of the wing ribs or reduce their stiffnesses if he were faced with the problem of providing room for fuel tanks or other stores in the airplane wing or of making the wing thinner for flight at higher speeds. As a result of these structural modifications, the airplane wings during flight might be subject to chordwise bending with attendant changes in the modes and frequencies of the wing vibration.

An experimental investigation on model wings was carried out at the Southwest Research Institute to determine the effect of chordwise bending on the flutter characteristics of several shapes of wings [1].[1] The models were low-aspect ratio cantilever wings having wing-bending, wing-torsion, and rib-bending degrees of freedom. The bending and torsion stiffnesses of the wings were kept fixed but the rib stiffnesses were reduced by cutting the main ribs at three chordwise stations and then reconnecting adjacent sections of the ribs with steel beam-type springs of specified stiffnesses. The critical flutter speeds of the wings for four different values of rib stiffness were obtained in a wind tunnel at subsonic speeds. One of the conclusions from this study was that decreasing the rib-bending stiffness of an airplane wing consistently decreases its critical flutter speed. The reduction in critical flutter speed was 13 percent of the rigid rib condition for the delta wing, 22 percent for the 45 degree sweptback wing, and 40 percent for the straight wing.

This experimental work led to the present investigation in which the purpose was to determine if the computed natural modes and frequencies of airplanes which differ in chordwise stiffness would indicate that one might expect a reduction of critical flutter speed for full-scale airplanes similar to the reduction found in the model experiments. No flutter analyses were made.

As the trend for high-speed, low-aspect ratio, thin wings is toward the delta shape, a delta-wing airplane was used for this study. The vibration modes and frequencies of the airplane were computed. The wing structure was then modified so as to differ from the original in having lower chordwise stiffnesses. These modifications were: (1) One rib outboard of fuselage removed, (2) two ribs outboard of fuselage removed, (3) stiffnesses of ribs outboard of fuselage reduced one-half, and (4) rib stiffness reduced nine-tenths. The frequencies and modes of vibration of these modified wings were also computed.

This work was done at the National Bureau of Standards under the sponsorship and with the financial assistance of the Bureau of Aeronautics, Department of the Navy.

2. Structure

The airplane chosen for this study had a delta wing with 6 spars and 12 ribs, figure 1. The actual structure was simplified, for ease of computation, into the structure of figure 2 which had the same number of spars but only 5 ribs. The moments of inertia of the 5 composite ribs were equal to those of the 12 ribs in the actual structure. The simplified structure had, therefore, the same torsional and bending properties as the original one. Rib 5 was on the centerline of the airplane, rib 4 was at the junction of the wing and the fuselage and ribs 1, 2, and 3 were all outboard of the fuselage. The locations of the spars and composite ribs are shown in figure 2.

The following four modifications of the wing which would result in the wing having less chordwise stiffness were considered:

Case A.1	Rib 2 removed from wing.
Case A.2	Ribs 1 and 3 removed from wing.
Case B.1	Stiffnesses of ribs 1, 2, and 3 reduced to half their original values.
Case B.2	Stiffnesses of ribs 1, 2, and 3 reduced to one-tenth their original values.

These modified wings are shown in figure 3.

3. Influence Coefficients

The method of obtaining the influence coefficient matrix of the wing is described in reference [2]. It is a method of consistent deformations. The total load carried by the wing is considered to be the sum

[1] Figures in brackets indicate the literature references at the end of this paper.

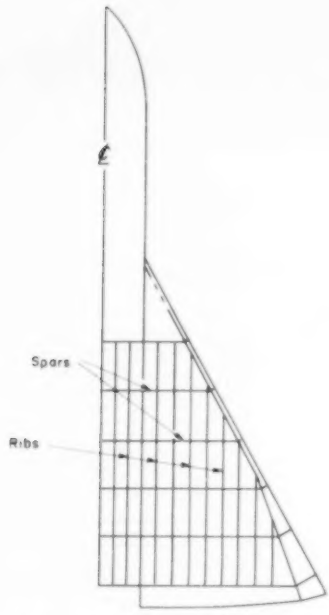

FIGURE 1. *Structure of delta-wing airplane.*

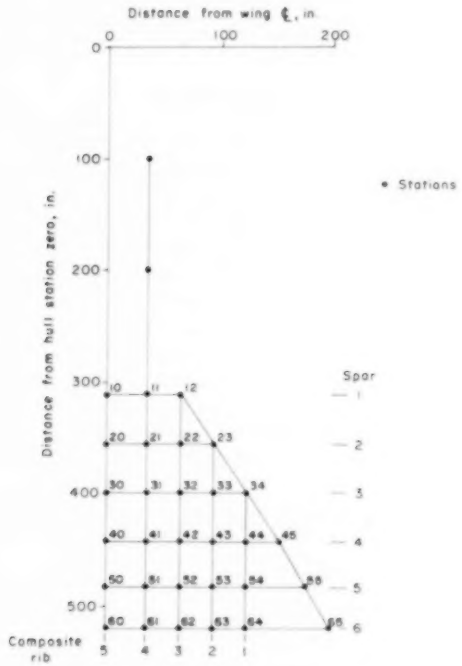

FIGURE 2. *Location of stations on the wing and fuselage of simplified structure.*

of the loads carried (1) by the spars in bending, (2) by the ribs in bending, and (3) by the cover sheet in torsion.

In computing the influence coefficients, the following conditions were used:

(1) The station at the junction of rib 5 and spar 6, station 60, was clamped.

(2) The leading edge of the wing had no bending stiffness.

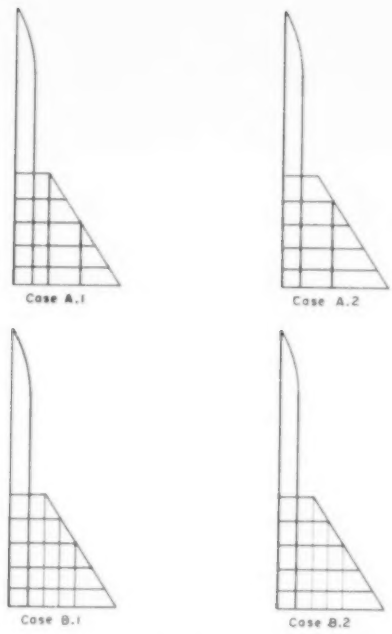

FIGURE 3. *Modifications of basic wing.*

Case A.1, Rib 2 removed from wing; Case A.2, ribs 1 and 3 removed from wing; Case B.1, bending stiffness of ribs 1, 2, and 3 reduced to one-half their original stiffness; Case B.2, bending stiffness of ribs 1, 2, and 3 reduced to one-tenth their original stiffness.

(3) The spars extended to the leading edge. The moment of inertia of a spar at the leading edge was zero, condition (2), but was taken arbitrarily as 3.5 in.^{4} so that influence coefficients for stations on the leading edge could be computed. This value of 3.5 in.^{4} is small compared to moments of inertia at other stations along the spar.

(4) Half of the fuselage stiffness was added to the stiffness of rib 4 in computing the influence coefficient matrix for symmetric modes.

(5) One-tenth of the fuselage stiffness was added to the stiffness of rib 4, and the torsional stiffnesses of the torque boxes between ribs 4 and 5 were increased by a factor of 10 in computing the matrix for the antisymmetric modes.

(6) For the torsion boxes, the triangular segments of the wing form part of the adjacent rectangular boxes.

3.1. Influence Coefficients for Unmodified Wing

The influence coefficient matrix for the symmetric case gives the deflection at point n due to a unit up-load at point m on both sides of the wing when station 60 is clamped. The influence coefficient matrix for the antisymmetric case gives the deflection at point n due to a unit up-load at point m on the left half of the wing and a unit down-load at point m on the right half of the wing with station 60 clamped. Therefore, the deflections of the wing as given by the influence coefficient matrix are those obtained by subtracting from the wing deflection at the various stations the deflection of a plane tangent to the wing at station 60.

a. Influence Coefficients for Symmetric Modes

For the symmetric modes, the reference plane for the deflections has displacement and pitch but no roll. The slope of the reference plane normal to the fuselage axis must be zero along the fuselage axis.

The influence coefficients were computed by SEAC, Standards Eastern Automatic Computer, for each of the spars and ribs considering the root stations clamped. The method used is explained in [3]. The root stations for the spars were along the fuselage axis and those for the ribs along spar 6, figure 2. For spars 1 to 5, the root stations can be displaced but the slopes at those stations are zero due to the symmetrical loads on the other half of the wing. In matrix notation, for spars 1 to 5, the computation above yields

$$\{y-y_t\}=[\delta]\{L\} \tag{1}$$

where

$\{y-y_t\}$ is the matrix of deflections at all stations but the root station t,

$[\delta]$ is the matrix of influence coefficients considering the root station clamped,

$\{L\}$ is the load matrix for all stations but the root station t.

For spar 1, for example, the following matrix using the data of table 1 was obtained

$$\begin{Bmatrix} y_{11}-y_{10} \\ y_{12}-y_{10} \end{Bmatrix} = \begin{bmatrix} 0.0000198943 & 0.0000444295 \\ .0000444295 & .0001295786 \end{bmatrix} \begin{Bmatrix} L_{11} \\ L_{12} \end{Bmatrix} \tag{1a}$$

To obtain the loads in terms of the deflections, from (1),

$$\{L\}=[\delta]^{-1}\{y-y_t\} \tag{2}$$

where $[\delta]^{-1}$ is the inverse of $[\delta]$. This is eq (11a), [2]

TABLE 1.—*Data needed to determine influence coefficients of spar 1*

Station	Distance from rib 5	Moment of inertia
	in.	*in.*^{4}
10	0	124.55
a	7	112.00
b	14	100.80
c	21	90.20
d	28	79.80
11	35	69.04
e	42	59.40
f	49	49.50
g	56	39.40
h	63	29.70
12	65	25.00

For spar 1, from (1a),

$$\begin{Bmatrix} L_{11} \\ L_{12} \end{Bmatrix} = \begin{bmatrix} 251275 & -145955.4 \\ -145955.4 & 175689.7 \end{bmatrix} \begin{Bmatrix} y_{11}-y_{10} \\ y_{12}-y_{10} \end{Bmatrix}$$

$$= \begin{bmatrix} 251275 & -145955.4 & -105320 \\ 145955.4 & 175689.7 & -29734.3 \end{bmatrix} \begin{Bmatrix} y_{11} \\ y_{12} \\ y_{10} \end{Bmatrix}. \tag{2a}$$

However, in symmetric motion, the sum of the vertical forces is equal to zero, or

$$L_t=-L_r-L_s-\ldots-L_j\ldots-L_n \tag{3}$$

where the subscript t refers to the root station and other subscripts to the other stations along the spars. Applying this to eq (2a) for spar 1, the loads at all the stations on spar 1 in terms of the deflections at those stations for a root condition of free displacement, zero root slope, are

$$\begin{Bmatrix} L_{11} \\ L_{12} \\ L_{10} \end{Bmatrix} = \begin{bmatrix} 251275 & -145955.4 & -105320 \\ -145955.4 & 175689.7 & -29734.3 \\ -105320 & -29734.3 & 135054 \end{bmatrix} \begin{Bmatrix} y_{11} \\ y_{12} \\ y_{10} \end{Bmatrix}. \tag{3a}$$

The loads for spars 2, 3, 4, and 5 were obtained in a similar manner. The loads in spar 6 and in rib 5 were obtained by using eq (2b), reference [2], which is applicable for a clamped root condition. Equations (11) and (12), reference [2], were used to determine the loads in ribs 1 to 4 with free root conditions.

The loads carried by the individual torsion boxes were computed according to the method outlined in reference [2].

The deflections equivalent to the loads carried by the spars, ribs and torsion boxes were summed to give the external load carried by the composite wing. The matrix relating the external loads to the deflections, or the composite stiffness matrix, was then inverted to give the symmetric influence coefficient matrix for the wing.

b. Influence Coefficients for Antisymmetric Modes

For the wing in antisymmetric vibration, the airplane will have roll but no pitch or displacement relative to a plane tangent to the airplane wing at station 60. This would mean that the fuselage axis could rotate but not deflect, and, therefore, the deflections at stations along the fuselage axis would be zero.

As in the case for symmetric modes, the influence coefficients, considering the root clamped, were computed for the ribs and spars by the method of reference [3]. The loads carried by spars 1 to 5 were obtained by use of eq (10), reference [2], for a simply-supported root condition; the loads carried by spar

6 were given by eq (2b), reference [2], for a clamped root condition; and the loads carried by ribs 1 to 4 were given by eqs (11) and (12), reference [2], for a free root condition. No computations were made for rib 5 because rib 5 is along the fuselage axis and, as stated above, the deflections would be zero.

The loads carried by the individual torsion boxes were computed as outlined in reference [2].

The composite stiffness matrix for antisymmetrical vibration, obtained by summing the deflections equivalent to the loads carried by the spars, ribs, and torsion boxes at the various wing stations, was inverted to give the antisymmetric influence coefficient matrix.

3.2. Influence Coefficients for Wings With Ribs Removed

Two different configurations of the wing with fewer ribs than the basic wing were investigated. In case A.1, rib 2 was removed and in case A.2, ribs 1 and 3 were removed. It was assumed, in computing the influence coefficients, that shear webs were present to transmit shear at the locations of the removed ribs but that these shear webs contributed nothing to the bending stiffness of the wing. It is believed that this assumption would not cause large errors in the results.

The composite stiffness matrix for case A.1 was obtained by summing the deflections equivalent to the loads carried by the spars, by ribs 1, 3, 4, and 5, and by the torsion boxes.

The composite stiffness matrix for case A.2 was obtained by summing the deflections equivalent to the loads carried by the spars, by ribs 2, 4, and 5, and by the torsion boxes.

The composite stiffness matrices were inverted to give the influence coefficient matrices.

3.3. Influence Coefficients for Wings With Reduced Flexibility

In order to study the effect of reduced rib flexibility of the entire wing outboard of the fuselage on the vibration characteristics of the airplane, the ribs in that region were considered to have one-half of their original stiffness in case B.1 and one-tenth of their original stiffness in case B.2. The composite stiffness matrices differed from those for the basic wing by having the deflections equivalent to the loads carried by ribs 1, 2, and 3 reduced by 50 percent in case B.1 and by 90 percent in case B.2. The influence coefficient matrices were obtained by inverting these stiffness matrices.

4. Modes of Vibration

The modes and frequencies of the airplanes were computed by SEAC. The method of computation and the codes written to do this work on SEAC are described in reference [4]. The masses at stations along the fuselage axis were considered lumped with those on rib 4 which is at the junction of the wing and fuselage. The locations of the stations and the masses at the stations are given in table 2. These, together with the composite influence coefficient matrices, were used in the computation.

TABLE 2. *Masses at stations and location of stations.*

Station	Mass	Spanwise location x	Chordwise location z
	lb sec²/in.	*in.*	*in.*
61	3.79593	35	0
62	0.14034	65	↓
63	.14195	95	↓
64	.32369	125	↓
65	.18343	198.6	↓
50	0	0	37
51	3.71553	35	↓
52	0.12099	65	↓
53	.12093	95	↓
54	.12707	125	↓
55	.16938	177.1	↓
40	0	0	77
41	2.82958	35	↓
42	0.31897	65	↓
43	.29490	95	↓
44	.15024	125	↓
45	.05325	154.1	↓
30	0	0	121
31	1.38148	35	↓
32	0.50266	65	↓
33	.37260	95	↓
34	.08068	125	↓
20	0	0	165
21	1.61046	35	↓
22	0.48945	65	↓
23	.15619	95	↓
10	0	0	209
11	4.55061	35	↓
12	0.26255	65	↓
02	2.34865	35	320
01	3.29669	35	420

The frequencies of the symmetric and antisymmetric modes of vibration of the basic wing and of the four modified wings are given in table 3. The nodal lines and relative displacements of parts of the airplane wing and fuselage are shown in figure 4 for the symmetric modes of vibration and in figure 5 for the antisymmetric ones. In a particular mode of vibration, the cross-hatched parts of the airplane would be deflected downward and the other parts upward, or vice versa.

The normalized deflections of the wing in the symmetric and antisymmetric modes for case B.1, wing-rib stiffness 50 percent of original stiffness, are plotted in figure 6. The dotted lines indicate negative deflections of the wing and the solid lines, positive deflections. These are typical of the results obtained in the other cases. The values of the deflections for the symmetric case are given in table 4.

5. Results and Discussion

The ratios of the frequencies for the modified wings to those of the basic wing were computed and are given in table 5. It is seen from the values of the ratios that, for the first three modes of symmetric and antisymmetric vibration, the frequencies of the modified wings are within 2 percent of the frequencies for the unmodified wing. In the fourth symmetric mode, however, the frequency for case A.2, two ribs

TABLE 3. *Natural frequencies of wings*

Mode	1		2		3		4		5	
Frequency / Case	rad/sec	cps	rad/sec	cps	rad/sec	cps	rad/sec	cps	rad/sec	cps
SYMMETRIC										
Basic	48.78	7.76	69.14	11.00	133.90	21.31	168.68	26.85	.....	.....
A.1	48.29	7.69	68.71	10.94	133.24	21.21	159.51	25.39	185.34	29.50
A.2	48.28	7.68	68.59	10.92	133.01	21.17	142.42	22.67	181.07	28.82
B.1	48.34	7.69	68.65	10.93	133.41	21.23	152.95	24.34	183.37	29.18
B.2	47.86	7.62	68.56	10.91	131.89	20.99	135.72	21.60	179.88	28.63
ANTISYMMETRIC										
Basic	19.36	3.08	58.08	9.24	97.67	15.54	120.41	19.16	151.33	24.08
A.1	19.36	3.08	57.77	9.19	97.59	15.53	119.44	19.01	150.85	24.01
A.2	19.34	3.08	57.43	9.14	97.40	15.50	117.84	18.75	144.91	23.06
B.1	19.35	3.08	57.66	9.18	97.50	15.52	118.86	18.92	149.54	23.80
B.2	19.34	3.08	57.12	9.09	97.30	15.49	116.53	18.55	141.44	22.51

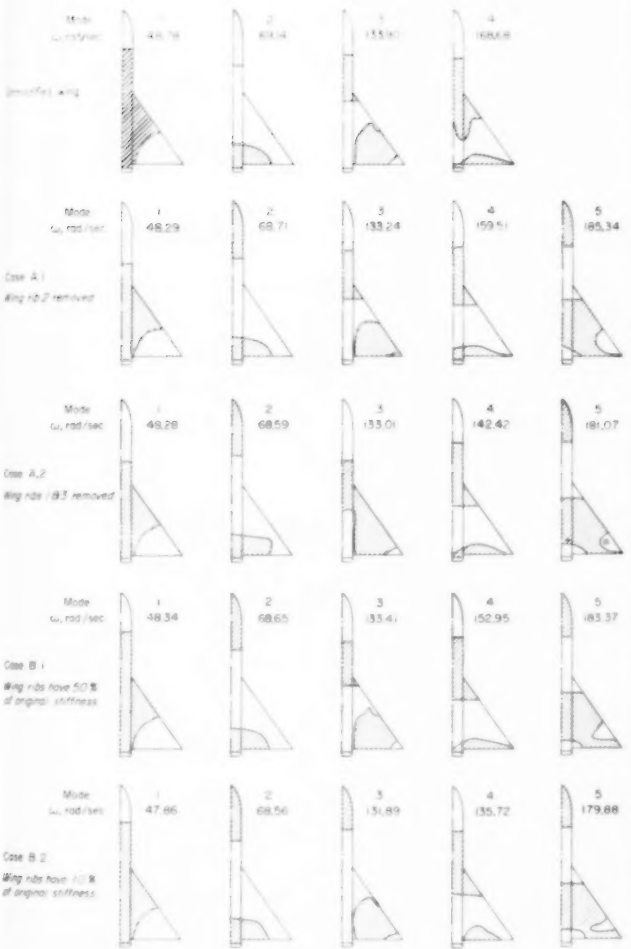

FIGURE 4. *Nodal lines for symmetric modes of vibration.*

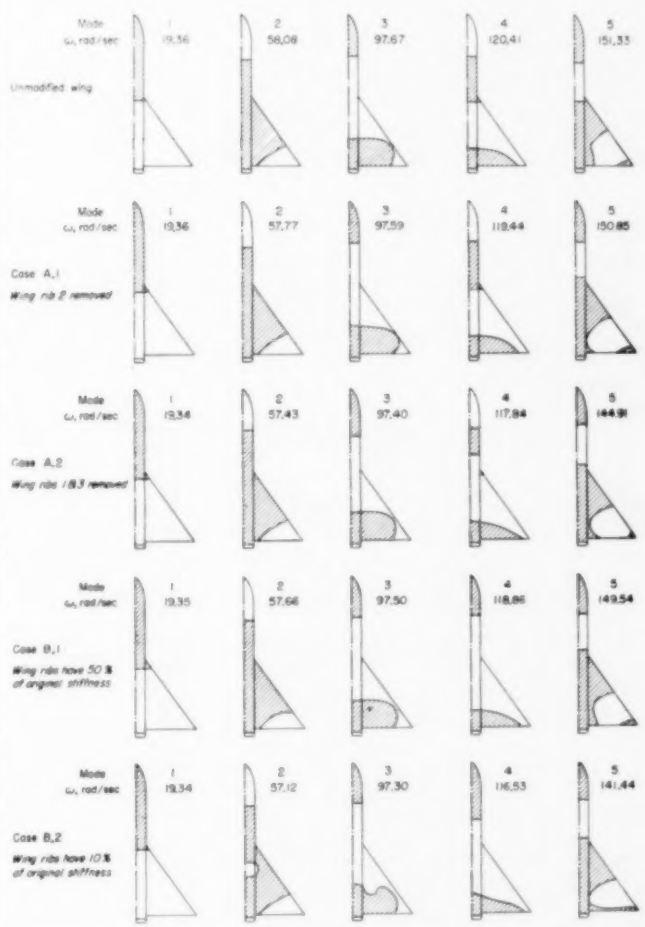

FIGURE 5. *Nodal lines for antisymmetric modes of vibration.*

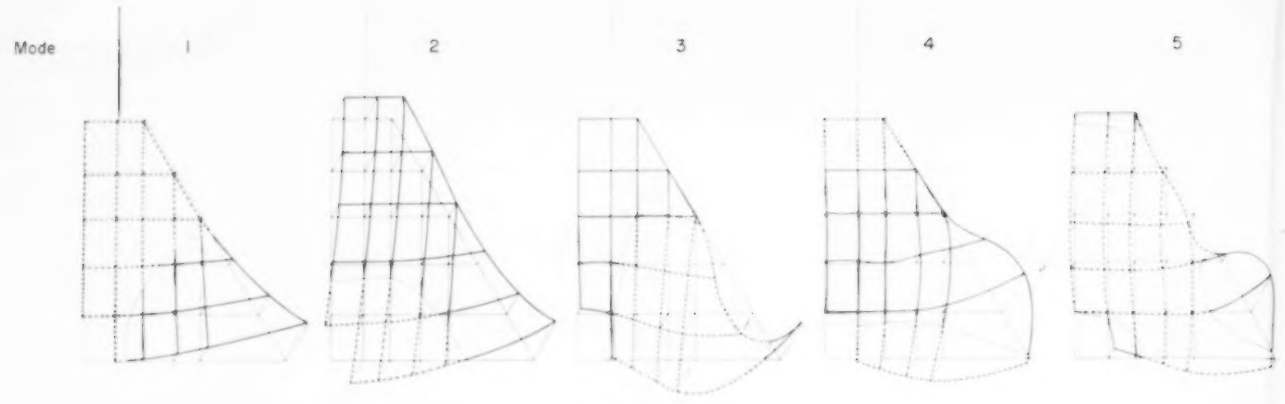

(a) Symmetric modes

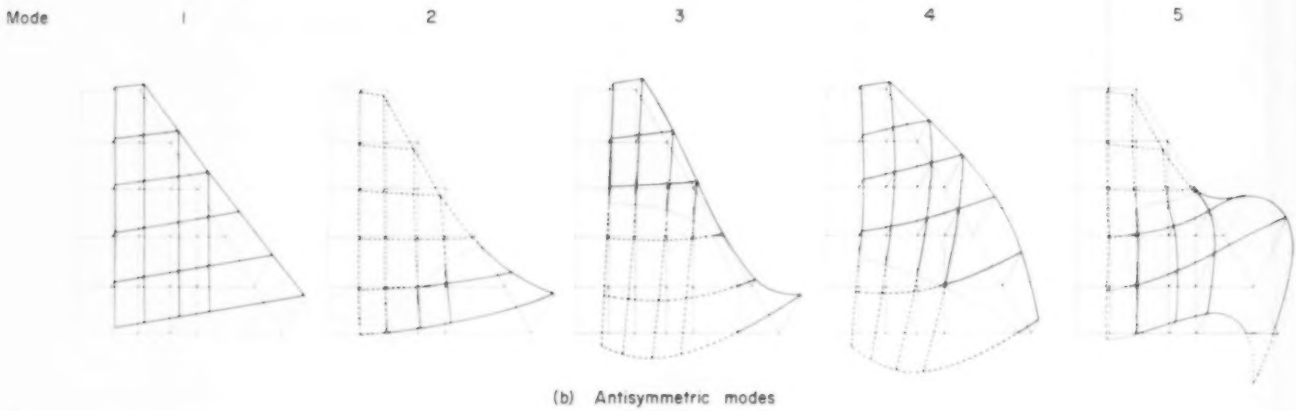

(b) Antisymmetric modes

FIGURE 6. *Normalized deflections for case F.1.*

TABLE 4. *Frequencies and normalized deflections of airplane in symmetric modes of vibration for case B.1*

Station \ ω	y_1	y_2	y_3	y_4	y_5
	48.338	68.646	133.406	152.951	183.370
61	−0.023366	−0.597532	0.064970	−0.039576	0.244639
62	.055915	−.522353	−.221243	−.223265	.070761
63	.181575	−.373947	−.554459	−.441755	−.166899
64	.353876	−.135694	−.710980	−.585403	−.359846
65	1.000000	1.000000	1.000000	−.127819	−.214930
50	−0.048380	−0.273765	0.119176	0.024826	−0.007621
51	−.029058	−.256161	.044341	.018315	−.028416
52	.017086	−.203917	−.137259	.016923	−.067289
53	.094203	−.106702	−.372036	.055241	−.086634
54	.203519	.049471	−.570739	.198112	−.063063
55	.490470	.533566	−.539838	1.000000	1.000000
40	−0.041609	0.056758	0.059669	0.035455	−0.192319
41	−.035294	.066205	.027762	.050300	−.207610
42	−.016061	.092546	−.061488	.000034	−.225663
43	.019798	.142327	−.192616	.205203	−.197289
44	.076395	.224714	−.329663	.372557	−.067638
45	.150926	.343674	−.402425	.606766	.177174
30	−0.036457	0.332393	0.018014	0.043027	−0.217790
31	−.037428	.332424	.015574	.042329	−.231232
32	−.037508	.338331	.002902	.034431	−.275082
33	−.036011	.343156	−.009667	.035737	−.297386
34	−.035739	.335534	.011301	.049961	−.232237
20	−0.035268	0.498628	0.006089	0.008233	−0.117637
21	−.035779	.500058	.007170	.007191	−.121968
22	−.036003	.504975	.007660	.007018	−.139345
23	−.036025	.502543	.007948	.007373	−.129656
10	−0.031148	0.582293	0.000760	−0.036406	0.050795
11	−.030888	.576310	.000625	−.036367	.053813
12	−.031025	.581933	.000666	−.037373	.054991
02	−0.003892	0.314251	−0.007880	−0.103372	0.425884
01	.046376	−.793464	.005584	.045834	−.147923

TABLE 5. *Ratios of frequencies of modified wings to those of basic wing*

Case \ Mode	1	2	3	4	5
SYMMETRIC					
A.1	0.980	0.994	0.995	0.946	
A.2	.990	.992	.993	.844	
B.1	.991	.993	.996	.967	
B.2	.981	.992	.985	.805	
ANTISYMMETRIC					
A.1	1.000	0.995	0.999	0.992	0.997
A.2	0.999	.989	.997	.979	.958
B.1	.999	.993	.998	.987	.988
B.2	.999	.983	.996	.968	.935

removed, was about 16 percent lower than the frequency for the basic wing. For this same mode, case B.2, wing-rib stiffness 10 percent of basic wing-rib stiffness, showed a reduction of about 20 percent. Although the fifth symmetric mode was not computed for the basic wing, the frequencies of the modified wing differ little from each other, table 3, so it is reasonable to assume that the reduction in frequency is small for this mode also.

The airplane whose ribs outboard of the fuselage had a stiffness of only 10 percent of the original stiffness, case B.2, showed the greatest reduction in all frequencies, table 5. The airplane with only one of its ribs outboard of the fuselage removed, case A.1, showed the least reduction.

While the modes of vibration differ somewhat, there seems to be little change in the general shape of the vibrations for a particular mode even though the chordwise stiffness of the wing outboard of the fuselage was reduced drastically. This is indicated by the positions of the nodal lines in figures 4 and 5. However, these graphs do show some regions of local vibration, as for example, in case B.2 antisymmetric where there is a local vibration extending from the fuselage axis a short distance into the wing at station 21. The deflections in these local regions are very small.

Figure 6 shows how the surface of the airplane looks when vibrating in a particular mode. It should be remembered, however, that these are normalized deflections and that the magnitude of the deflections in mode 5, for example, would be much smaller actually than the deflections in mode 1.

6. Conclusions

Based on the results obtained in this study, rib stiffness apparently has little effect on the modes or frequencies of vibration of the delta wing. Modifications of a delta wing similar to those investigated in this paper would not appreciably affect the airplane's vibration characteristics.

No reduction in critical flutter speed as a result of decreased rib stiffness would be indicated from the results.

7. References

[1] Leo E. Wilson and Guido E. Ransleben, Jr., The effect of rib flexibility upon flutter characteristics of low aspect ratio wings, Report No. 206c–1 (Southwest Research Inst., Dec. 30, 1952).

[2] Samuel Levy, Structural analysis and influence coefficients for delta wings, J. Aeronaut. Sci. **20,** 449 (July 1953).

[3] Samuel Levy, Influence coefficients of tapered cantilever beams computed on SEAC, J. Appl. Mechanics **20,** 131 (March 1953).

[4] William F. Cahill and Samuel Levy, Computation of vibration modes and frequencies on SEAC, J. Aeronaut. Sci. **22,** 837 (Dec. 1955).

WASHINGTON, November 15, 1957.

Journal of Research of the National Bureau of Standards Vol. 60, No. 4, April 1958 Research Paper 2853

Thermal Degradation of Cellulosic Materials [1,2]

S. L. Madorsky, V. E. Hart,[3] and S. Straus

Fortisan, cellulose triacetate, and NO_2-oxidized cellulose were pyrolyzed in a vacuum in the temperature range 180° to 465° C. Cotton cellulose and cellulose triacetate were also pyrolyzed in nitrogen at atmospheric pressure. The tar yields were in the decreasing order from: Cotton, Fortisan, cellulose triacetate, and oxidized cellulose. The other volatiles consisted mainly of acetic acid, carbon dioxide, and carbon monoxide, from the triacetate; and water, carbon dioxide, and carbon monoxide from the other celluloses. In all cases there was a carbonaceous residue (volatilization end point), the amount depending on the nature of the cellulose and the temperature of pyrolysis. When pyrolyzed in nitrogen at atmospheric pressure, cotton cellulose and cellulose triacetate yielded less tar than when pyrolyzed in a vacuum. The tar from cellulose triacetate consisted of a compound whose infrared spectrum resembled that of the original triacetate. Cotton cellulose, Fortisan, and cellulose triacetate do not differ much in their initial rates and activation energies of thermal degradation. Oxidized cellulose has very high initial rates of thermal degradation.

1. Introduction

It was shown in an earlier publication [1] [4] by the present authors that cotton cellulose, cotton hydrocellulose, and viscose rayon, when pyrolyzed in a vacuum, yield volatile products consisting mainly of tar, H_2O, CO_2, and CO, and also a nonvolatile carbonaceous residue. It was also shown that the main constituent of the tar from cotton cellulose was levoglucosan, which is isomeric with the structural cellulose unit, but has an oxygen linkage between the 1 and 6 carbons, in addition to the 1 to 5 oxygen linkage.

The present paper describes results of a further study of the thermal degradation of cellulosic materials, including cotton cellulose, Fortisan, cellulose triacetate, and NO_2-oxidized cellulose. This study consisted in:

(1) Pyrolyzing the celluloses at various temperatures, fractionating the volatile products, and analyzing the volatile and nonvolatile fractions [5] by mass-spectrometric, infrared, and microcryoscopic methods;

(2) Determining the rates of thermal degradation at various temperatures, and calculating from these rates the over-all activation energies involved in the reactions. All the experiments, except where indicated otherwise, were carried out in a vacuum of about 10^{-4} mm of Hg. The experimental procedure and the apparatus used in this study are the same as those described previously [1].

2. Materials Used

The cotton used in this investigation was an Empire cotton obtained from the Southern Utilization Research Branch of the U. S. Department of Agriculture. Details of its purification have been described previously [1]. The purified cotton had a moisture content of 3.7 percent, based on the dry weight.

Fortisan,[6] a regenerated cellulose, was purified by scouring for 1 hr in an aqueous solution containing d percent Na_2CO_3 and 0.5 percent Castile soap, a1 70° C. This was followed by washing with distillet water and drying in air. The purified material had a moisture content of 5.24 percent, based on the dry weight.

A commercial cellulose triacetate, Arnel,[6] was extracted with cold ethanol, dried in air, washed with hot distilled water, and again dried in air. The purified material was dried at 50° C for 30 min. It lost 1.4 percent based on the dry weight.

The NO_2-oxidized cellulose was a pure product intended for surgical use. The moisture content was determined by heating a sample in a vacuum at 50° C for 30 min, and also by evacuating another sample at room temperature for 16 hr. The loss in both cases was about the same, 10.1 percent based on dry weight. Analysis for carboxyl content by the calcium acetate method showed 92.3 percent oxidation of the primary alcohol. The dried NO_2-oxidized cellulose analyzed 40.73 C, 4.43 H_2, 54.62 O_2, and 0.22 N_2, as compared with a theoretical content of 41.19 C, 4.71 H_2, and 54.10 O_2, calculated on the basis of 92.3 percent oxidation of the primary alcohol to carboxyl.

High-purity 2,3,4-levoglucosan-triacetate, melting point 110° C, was obtained from the Northern Utilization Research Branch of the U. S. Department of Agriculture.

3. Pyrolysis Experiments

3.1. Fortisan

Two pyrolysis experiments were carried out on Fortisan. The results are shown in table 1 in comparison with those previously obtained for viscose rayon and cotton cellulose [1].

[1] This work was performed as part of a research project sponsored by the Office of the Quartermaster General, Department of the Army, Natick, Mass.

[2] This paper was presented at the 131st National Meeting of the American Chemical Society in Miami, Fla., April 7–12, 1957.

[3] Present address National Institutes of Health, Bethesda, Md.

[4] Figures in brackets indicate the literature references at the end of this paper.

[5] The following fractions were collected: (1) Residue; (2) V_{pyr}, volatile at the temperature of pyrolysis but not at room temperature; (3) V_{25}, volatile at room temperature, but not at −80° C; (4) V_{-80}, volatile at −80° C, but not at −190° C; (5) V_{-196}, volatile at −190° C.

[6] Fortisan and Arnel are trademarked names for the completely deacetylated acetate and for cellulose triacetate fibers, respectively, of the Celanese Corporation of America.

No mass spectrometer analysis was made of the various volatile fractions from pyrolysis of Fortisan. Since Fortisan closely resembles viscose rayon in its structure and thermal behavior it was assumed that the analyses of the fractions from Fortisan would be similar to those obtained previously for viscose rayon.

The average molecular weight of the tar from Fortisan as determined by a freezing-point lowering method in phenol was 167, which is about the same as that found for the tar from cotton, 166. As compared with these values, the molecular weight of a structural unit of cellulose is 162.

Fortisan and viscose rayon behave similarly during vacuum pyrolysis (see table 1), but in comparison with cotton cellulose and cotton hydrocellulose [1] they yield, in general, less tar and more water. As was pointed out previously [1], such a difference could not be due to a difference in type and extent of crystallinity, nor to a difference in the degree of polymerization. However, it is possible that the difference in the thermal behavior of Fortisan and viscose rayon, as compared with cotton cellulose and cotton hydrocellulose, is caused by the greater ash content in the first two polymers. Analysis showed that cotton cellulose and hydrocellulose contained 0.06 percent ash, based on dry samples, while Fortisan contained 0.11 percent and viscose rayon 0.14 percent, on the same basis. In order to check on this point cotton was impregnated with 0.14 percent Na_2CO_3, a compound which is known to suppress the yield of tar, and pyrolyzed at 280° C for 149 min. Total loss by volatilization was 15 percent, and the volatiles consisted, in weight percent, of 21 V_{pyr}, 54 V_{25}, 13 V_{-87}, and 12 V_{-193}. This distribution of volatiles is intermediate between that obtained from cotton cellulose alone and that from cotton impregnated with 7 percent NA_2CO_3 [1].

Venn [2] found that by washing raw cotton with water he could increase the yield of levoglucosan from 0 to 28 percent during pyrolysis at reduced pressure. Further treatment of the cotton with 1.5 percent solution of NaOH, followed by 1 percent solution of HCl and a thorough washing, increased the yield to 38 percent.

TABLE 1. *Volatile fractions from pyrolysis of Fortisan, viscose rayon, and cotton cellulose*

Material	Weight of sample	Temp.	Duration	Volatilization, based on dry sample	Volatile fractions, based on total volatilized			
					V_{pyr} (tar)	V_{25} (H_2O)	V_{-80} (CO_2)	V_{-190} (CO)
	mg	*°C*	*min*	*wt %*	*wt %*	*wt %*	*wt %*	*wt %*
1. Fortisan	30.2	295	39	20	38.2	45.2	9.6	7.0
2. Fortisan	54.6	310	57	68	49.1	41.0	6.7	3.2
1. Viscose rayon *	85.6	280	169	41	53.0	37.0	8.0	2.0
2. Viscose rayon	12.5	295	57	45	48.2	40.8	7.8	3.2
1. Cotton cellulose *	83.3	280	249	35	51.2	31.2	5.8	1.8
2. Cotton cellulose	39.5	321	9	22	65.2	28.2	4.3	2.3

* Data for viscose rayon and cotton cellulose were taken from table 1 of reference [1]. Results for viscose rayon at 280° and for cotton cellulose at 280° are cumulative for experiments carried out in several consecutive steps.

3.2. Cellulose Triacetate

Results of pyrolysis of cellulose triacetate, alone and mixed with NaCl or Na_2CO_3, are shown in table 2. In experiment No. 1 the sample was pyrolyzed

TABLE 2. *Volatile fractions from pyrolysis of cellulose triacetate*

Expt. No.	Temperature	Weight of sample	Duration		Volatilization		Volatile fractions, based on total volatilized			
			For step	Cumulative	For step	Cumulative	V_{pyr}	V_{25}	V_{-80}	V_{-190}
CELLULOSE TRIACETATE										
	°C	*mg*	*min*	*min*	*wt %*	*wt %*	*wt %*	*wt %*	*wt %*	*wt %*
1	25 to 465	10.5	325	325	89.6	89.6	44.5	44.6	6.0	4.9
2-a	250	43.2	30	30	1.8	1.8				
2-b	310		56	86	33.1	34.9	44.8	47.5	4.4	3.3
2-c	310		58	144	27.2	62.1	48.0	45.9	4.0	2.1
2-d	310		90	234	14.3	76.4	35.7	55.5	5.7	3.1
CELLULOSE TRIACETATE IMPREGNATED WITH 9.1% NACL										
3-a	250	47.8	30	30	1.6	1.6				
3-b	310		22	52	46.9	48.5	51.1	45.1	2.5	1.3
4-a	250	20.0	30	30	1.7	1.7				
4-b	300		25	55	38.9	38.9	51.0	44.7	3.7	0.6
4-c	300		60	115	79.1	79.1	44.7	48.7	5.9	0.7
CELLULOSE TRIACETATE IMPREGNATED WITH 9.0% Na_2CO_3										
5-a	250	47.0	22	22	8.2	8.2	13.0	64.6	21.0	1.4
5-b	250		157	179	14.8	23.0	5.1	75.3	16.9	2.7
5-c	310		43	222	44.3	67.3	4.8	80.5	11.5	3.2
6	310	44.8	60	60	69.5	69.5	5.1	76.9	14.8	3.2
7	310	20.0	60	60	69.3	69.3	5.5	78.3	13.1	3.1

in one step from room temperature to 465° C. In experiments of group 2 pyrolysis was performed on the same sample in 4 consecutive steps and the products were weighed after each step. Similarly, groups of experiments 3, 4, and 5 were performed in steps. Experiments 6 and 7 were each performed in single steps.

In all experiments in which additives were used, except experiment 6, the sample was mixed with the powdered salt and the mixture was moistened with a small drop of water in order to obtain a better distribution of the salt through the cellulose triacetate. The sample was heated in air at 80° to 90° C to a constant weight, prior to pyrolysis. In experiment 6 the sample was intimately mixed with powdered Na_2CO_3 and the mixture used dry. The object of performing experiment 6 was to ascertain whether the heating of the wet mixture of cellulose triacetate and Na_2CO_3 at 80° to 90° C in the other experiments had caused any deacetylation of the acetate. In experiments 6 and 7 pyrolysis was carried out under similar conditions. The results, as seen from table 3, are quite similar.

TABLE 3. *Mass-spectrometer analysis of volatile fractions from pyrolysis of cellulose triacetate*

Experiment number [a]	Fraction	Composition in mole percent
1	V_{25}	100 CH_3COOH
	V_{-80}	96.6 CO_2, 2.2 CH_3CHO, 1.2 CH_3COCH_3
	V_{-196}	72.7 CO, 22.6 CH_4, 4.7 H_2
6	V_{25}	98.6 CH_3COOH, 1.4 CH_3COCH_3
	V_{-80}	100 CO_2
	V_{-196}	89.2 CO, 7.4 CH_4, 3.4 H_2
7	V_{25}	96.2 CH_3COOH, 2 CH_3CHO, 1.8 CH_3OH

[a] Experiment numbers are the same as those given in table 2.

Mass-spectrometer analyses of the more volatile fractions are shown in table 3 for experiments 1, 6, and 7. In each case fraction V_{25} consists primarily of CH_3COOH. If the moist alkali used in experiment 7 had resulted in deacetylation, H_2O would have appeared in this fraction. The absence of H_2O is further proof that no appreciable deacetylation took place under the conditions employed in the preparation of samples for pyrolysis.

The tar fraction had an average molecular weight of 236, as determined by a microcryoscopic method in phenol. This is less than the molecular weight of a structural unit of cellulose triacetate, 288.

An infrared spectrum [7] of the tar obtained in the pyrolysis of cellulose triacetate is shown in figure 1 in comparison with similar spectra of the original cellulose triacetate and of 2,3,4-levoglucosan triacetate. As can be seen from this figure, the spectrum of tar (III), obtained in the pyrolysis of cellulose triacetate, resembles that of the original cellulose triacetate (II), particularly in the region below 9 microns, but is entirely unlike the spectrum of 2,3,4-levoglucosan triacetate (V). That the tar from cellulose triacetate does not consist of levoglucosan triacetate is

[7] The authors are indebted to Florence H. Forziati and M. Kathryn Wharton for obtaining the infrared spectra reported in this paper and for aiding in their interpretation.

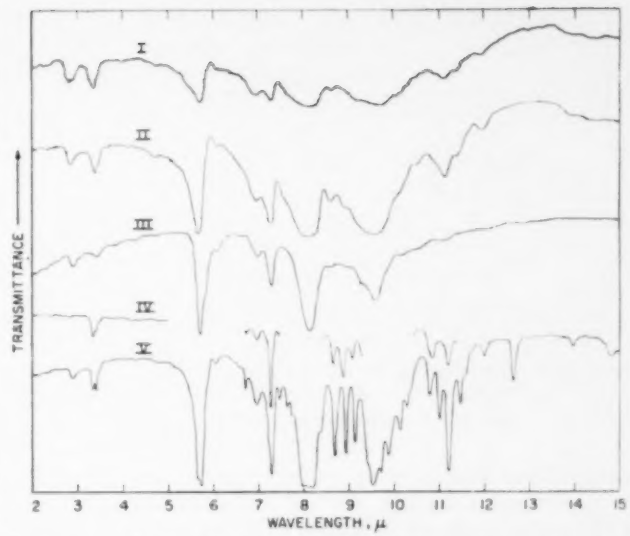

FIGURE 1. *Infrared spectra of: I, Cellulose triacetate residue, after a loss of 23% by volatilization, finely dispersed in a KBr pellet; II, cellulose triacetate finely dispersed in a KBr pellet; III, a thin film prepared by evaporation of a methanolic solution of tar from pyrolysis of cellulose triacetate, on a AgCl plate; IV, a CCl_4 solution of 2,3,4-levoglucosan triacetate; V, pure 2,3,4-levoglucosan triacetate finely dispersed in a KBr pellet.*

shown also by the fact that it is insoluble in CCl_4 whereas levoglucosan triacetate is soluble. With the thought that the tar might be a mixture of levoglucosan triacetate with a component that was insoluble in CCl_4, it was extracted with a small amount of CCl_4 and the infrared absorption spectrum of the extract recorded. The spectrum was found to be identical with that of CCl_4. Spectrum IV was obtained from a carbon tetrachloride solution of levoglucosan triacetate. Those regions of spectrum IV in which CCl_4 does not absorb are shown in comparison with spectrum V.

An infrared spectrum of a residue from cellulose triacetate, after 23 percent loss due to pyrolysis, is shown in figure 1 as spectrum I. This spectrum resembles closely that of the original cellulose triacetate (II).

In figure 2 spectra of cotton cellulose (I) and of the residue of cotton cellulose (II) remaining after 16 percent loss due to pyrolysis are shown. Here, too, there is a close resemblance between the two spectra. However, spectrum II differs from spectrum I in that it has an absorption band at approximately 5.7 microns. This band is probably attributable to one of the various types of carbonyl groups which absorb in this region.

3.3. NO_2-Oxidized Cellulose

When heated in a vacuum, oxidized cellulose begins to lose weight at a very high rate even at low temperatures. However, this rate falls off rapidly so that it becomes necessary to raise the temperature in order to continue pyrolysis. Results of pyrolysis are shown in table 4. Experiments 1, 2, and 3 were carried out in steps, while in experiment 4 the

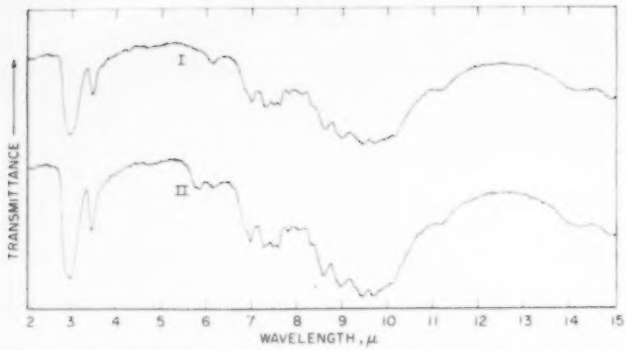

FIGURE 2. *Infrared spectra of: I, Cotton cellulose; II, residue from cotton cellulose after a loss of 16% by volatilization.*

The test samples, in a finely ground state, were dispersed in KBr pellets.

sample was heated from room temperature to 407° C in one step. Unlike cotton cellulose and cellulose triacetate, oxidized cellulose yields on pyrolysis very little tar.

Mass spectrometer analysis of the more volatile fractions is shown in table 5. The average molecular weight of the tar by a microcryoscopic determination in phenol was 157 as compared with 176 for a structural unit.

In figure 3 the infrared spectrum of a residue from NO_2-oxidized cellulose after a loss of 20 percent due to pyrolysis (II) is compared with that of the original NO_2-oxidized cellulose (I). Here, as in the case of cotton cellulose and cellulose triacetate there is a close resemblance between the two spectra. However, the spectrum of the residue from oxidized cellulose differs in some respects from that of the original material. In spectrum II the band at 5.7 microns is broader and the band at 6.1 microns is more intensive, relative to that at 5.7 microns, than in spectrum I. Groups that might be responsible for the increased absorption include $\diagdown C{=}C \diagup$ and $\diagdown C{=}O \diagup$ groups.

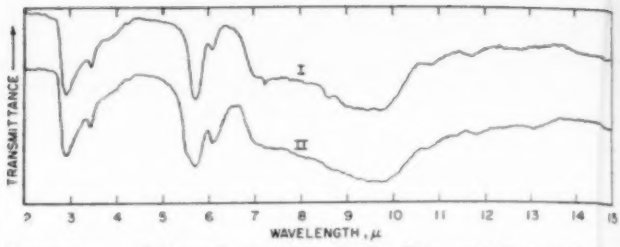

FIGURE 3. *Infrared spectra of: I, NO_2-oxidized cellulose; II, residue from NO_2-oxidized cellulose after a loss of 20% by volatilization.*

The test samples, in a finely ground state, were dispersed in KBr pellets.

3.4. Cotton and Cellulose Triacetate in Nitrogen

Pyrolyses of cotton and cellulose triacetate were carried out in nitrogen at atmospheric pressure. The same apparatus was used as in the vacuum pyrolysis. A pure grade of nitrogen, analyzing 99.8 percent N_2 and 0.2 percent O_2, was used. The apparatus was evacuated for about 20 hr. prior to filling it with nitrogen at atmospheric pressure. Fractions V_{pyr} (tar), V_{25} (H_2O or CH_3COOH), and V_{-80} (CO_2) were first condensed together in a liquid nitrogen trap. After evacuating the N_2 from the apparatus, the fractions were separated by the same method that was used in experiments with pyrolysis in a vacuum, and then weighed. The noncondensable fraction V_{-190} (mostly CO) was mixed with the N_2 and was not collected. Weight of this fraction was calculated on

TABLE 5. *Mass-spectrometer analysis of volatile fractions from pyrolysis of No_2-oxidized cellulose*

Experiment number [a]	Fraction	Composition in mole percent
1-a	V_{25}	98.4 H_2O, 1.2 CH_2O, 0.4 CH_3OH
	V_{-80}	100 CO_2
	V_{-190}	Fraction too small for analysis
4	V_{25}	91.7 H_2O, 3.8 CH_3COOH, 1.9 CH_3CHO, 1.2 CH_3OH, 1.2 C_2H_5OH, trace HCOOH
	V_{-80}	100 CO_2
	V_{-190}	99.3 CO, 0.7 H_2

[a] Experiment numbers are the same as shown in table 4.

TABLE 4. *Volatile fractions from pyrolysis of oxidized cellulose*

Experiment number	Temperature	Weight of sample	Duration		Volatilization		Volatile fractions, based on total volatilized			
			For step	Cumulative	For step	Cumulative	V_{pyr}	V_{25}	V_{-80}	V_{-190}
	°C	*mg*	*min*	*min*	%	%	%	%	%	%
1-a	180	55.3	5	5	4.7	4.7	6.6	67.2	25.1	1.1
1-b	180		19	24	7.8	12.5	3.9	54.3	40.5	1.3
1-c	180		51	75	6.2	18.7	4.8	57.4	35.7	2.1
2-a	180	48.5	120	120	20.3	20.3				
2-b	211		11	131	6.8	27.1	4.6	55.3	37.7	2.4
2-c	211		93	224	6.6	33.7	6.4	49.3	40.4	3.9
2-d	240		45	269	6.9	40.6	8.0	41.3	44.2	6.5
2-e	270		35	304	7.2	47.8	8.4	36.2	46.1	9.3
2-f	300		36	340	5.9	53.7	7.5	30.2	46.1	16.2
2-g	331		57	397	5.0	58.7	9.9	25.3	40.0	24.8
3-a	200	4.5	44	44	29.8	29.8	8.3	53.0	35.6	3.1
3-b	280		98	142	26.2	56.0	13.0	29.2	51.3	6.5
4	25 to 407	6.1	132	132	66.1	66.1	4.0	38.5	51.5	6.0

TABLE 6. *Volatile fractions from pyrolysis of cotton cellulose and cellulose triacetate in a vacuum and in nitrogen*

Weight of sample	Temp.	Duration		Volatilization		Volatile fractions, based on total volatilized			
		For step	Cumulative	For step	Cumulative	V_{pyr}	V_{25}	V_{-80}	V_{-190}
COTTON CELLULOSE IN A VACUUM [a]									
mg	°*C*	*min*	*min*	*%*	*%*	*%*	*%*	*%*	*%*
83.3	280	96	96	10.3	10.3	49.0	40.7	7.4	2.9
83.3	280	153	249	25.0	35.3	60.3	32.0	5.9	1.8
83.3	280	77	326	9.8	45.1	62.5	30.2	5.6	1.7
COTTON CELLULOSE IN NITROGEN									
48.2	280	96	96	10.7	10.7	20.4	63.3	11.8	4.5
48.2	280	153	249	23.6	34.3	17.6	65.5	13.0	3.9
48.2	280	77	326	9.3	43.6	6.1	71.0	17.6	5.3
CELLULOSE TRIACETATE IN A VACUUM [b]									
43.2	310	56	.....	33.1	.....	44.8	47.5	4.4	3.3
CELLULOSE TRIACETATE IN NITROGEN									
93.5	310	56	56	35.8	35.8	7.9	79.4	6.5	6.2

[a] Data are given in cumulative values, based on experiments 2a, 2b, 2c, 2d, and 2e, in table 1 of reference [1].
[b] These data are the same as for experiment 2b in table 2 above, and are not cumulative.

the assumption that the ratio of V_{-80} to V_{-190} was the same here as in vacuum pyrolysis. This assumption appears reasonable in view of the fact that the fractions added up to give a good material balance of the sample.

When pyrolysis is carried out in a vacuum, the conditions for the escape of the volatile products from the hot zone are similar to those obtained in molecular distillation where the condenser is located near the hot zone. Under these conditions even the larger fragments, in this case the tar molecules, escape without undergoing appreciable further decomposition. However, when pyrolysis is carried out in nitrogen at atmospheric pressure, the tar molecules, due to collisions with the nitrogen molecules, will remain long enough in the hot zone so that an appreciable part of them will undergo secondary decomposition.

Results of pyrolysis of cotton cellulose and cellulose triacetate in nitrogen are shown in table 6 compared with results of pyrolysis of the same materials in a vacuum. As shown in this table pyrolysis in nitrogen gave a greater yield of the lighter fractions: V_{25}, V_{-80}, and V_{-190}, at the expense of the tar. However, the rates of volatilization and the ratio of V_{25} to V_{-80} remained about the same.

4. Rates of Thermal Degradation

4.1. Fortisan and Cellulose Triacetate

The rates of thermal degradation of Fortisan and cellulose triacetate were determined in a vacuum apparatus provided with a tungsten spring balance. The apparatus and the experimental procedure have been described previously [3]. Results for Fortisan and cellulose triacetate are shown in figures 4, 5, 6, and 7. In figures 4 and 5 percentage volatilization, referred to the dry sample, is shown plotted versus time (solid lines) for Fortisan and cellulose triacetate, respectively. The interrupted lines in these figures represent plots of logarithm of percentage residue versus time.[8] The log-time plots deviate from straight lines, indicating that the over-all degradation reaction is complex and not entirely of first order. In figures 6 and 7 the rates of volatilization

[8] In figure 3 of our previous paper on thermal degradation of cellulose [1] the scale for the logarithm of percentage residue should read from 1 to 2 instead of from 0 to 2.

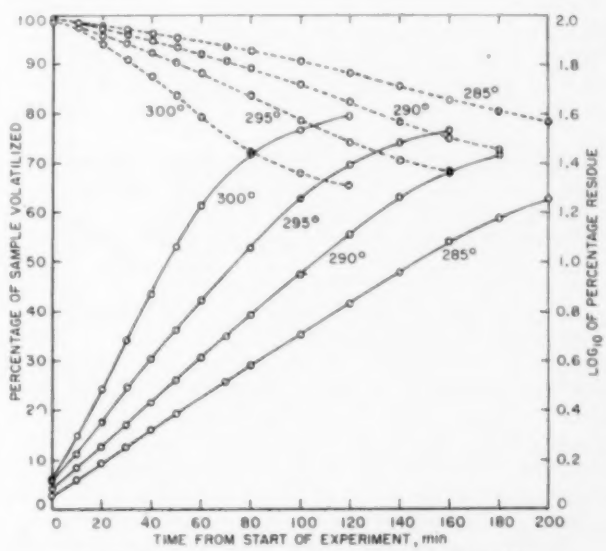

FIGURE 4. *Thermal degradation of Fortisan.*
———, Percentage of sample volatilized versus time; ------, $\log_{10}$ of percentage residue versus time.

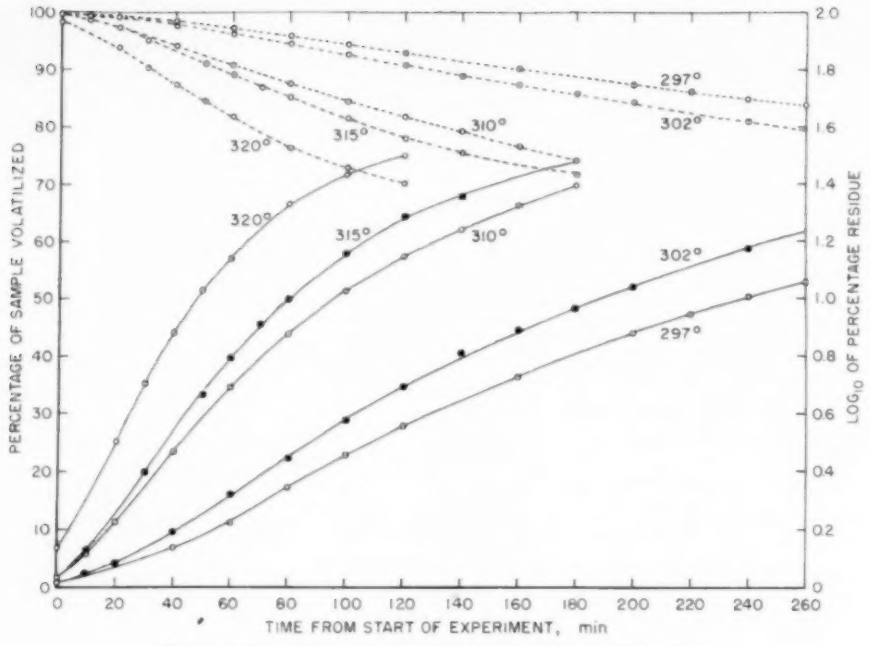

FIGURE 5. *Thermal degradation of cellulose triacetate.*
———, Percentage of sample volatilized versus time; . . . , log 10 of percentage residue versus time.

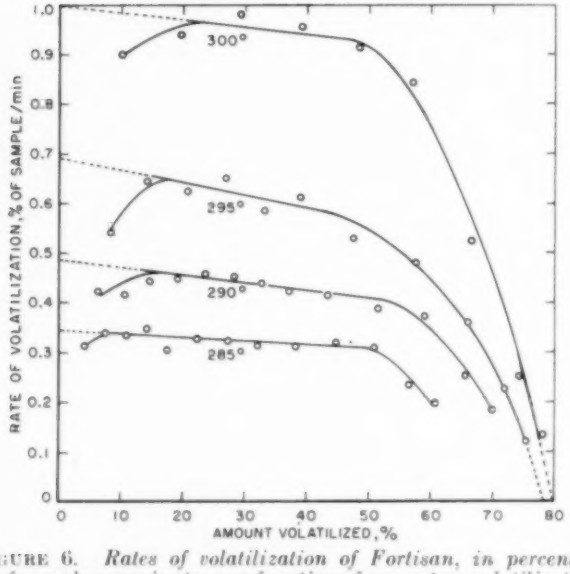

FIGURE 6. *Rates of volatilization of Fortisan, in percentage of sample per minute, as a function of percentage volatilization.*

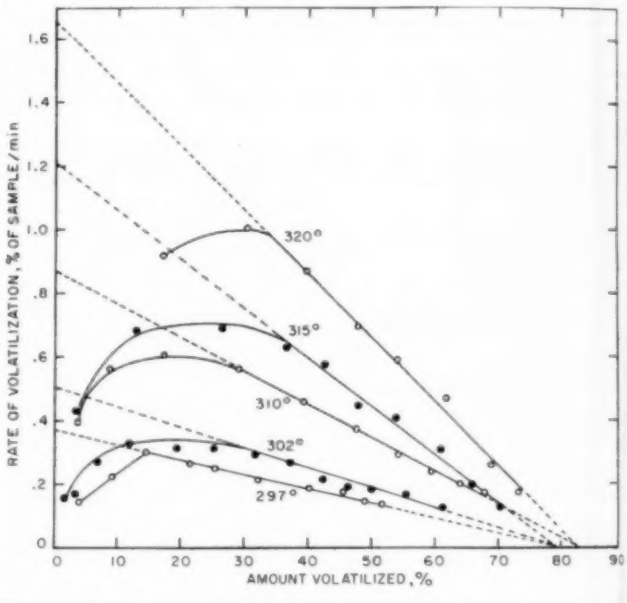

FIGURE 7. *Rates of volatilization of cellulose triacetate, in percentage of sample per minute, as a function of percentage volatilization.*

in percentage of sample per minute, are plotted versus percentage volatilization. The intercepts of the extrapolated straight parts of the plots with the ordinate are defined as the apparent initial rates for the corresponding temperatures. The intercepts of the rate curves with the abscissa are defined as the carbonization end points. A carbonization end point indicates that for a given temperature volatilization approaches zero at a given percentage volatilization. However, the residue at this point is not completely carbonized. As was pointed out previously [1], in the case of cotton these residues, when heated further to about 1,000° C, lost half of their weight. The carbonization end points for the lower temperatures for Fortisan (fig. 6) could not be obtained by extrapolation of the rate curves. However, it is apparent that these end points do not differ much from those at the higher temperatures.

By plotting the logarithm of the apparent initial rates versus the reciprocal of the absolute temperature straight lines were obtained whose slopes represent the activation energies of thermal degradation of Fortisan and cellulose triacetate.

Numerical data for rates, carbonization end points, and activation energies for Fortisan and cellulose triacetate, are shown in table 7. On the whole, the data do not differ much from those obtained previously for cotton cellulose, cotton hydrocellulose, and viscose rayon, without additives [1].

TABLE 7. *Results of rate studies of thermal degradation of Fortisan and cellulose triacetate*

Temperature	Apparent initial rate	Carbonization end point	Activation energy
FORTISAN			
°C	%/min	%	kcal/mole
285	0.35	------	46
290	.49	------	
295	.69	78	
300	1.00	80	
CELLULOSE TRIACETATE			
297	0.37	80	45
302	.51	80	
310	.87	82	
315	1.21	80	
320	1.66	82	

4.2. NO_2-Oxidized Cellulose

Because of the very rapid initial loss of weight during pyrolysis it was not possible to obtain rate curves for oxidized cellulose by the loss of weight method in the tungsten spring apparatus. Instead, the rates were determined during the pyrolysis experiments (see table 4) by reading at intervals the total pressure developed in the apparatus by means of a multiplying manometer. The distribution of volatiles at the times when pressures were read are interpolated from the values given under "volatile fractions . . ." in table 4. In this way loss of weight for any interval between pressure readings can be calculated, and the loss divided by the time interval gives the rate for that interval. The rates are shown plotted in figure 8. The apparent initial rate cannot be extrapolated from these curves.

5. Discussion

In discussing the formation of levoglucosan in the vacuum distillation of cotton cellulose [I] it was assumed that the mechanism involves a thermal scission of a C—O link between rings, which is accompanied by a transfer of hydrogen from the primary alcohol to the oxygen of the broken C—O link and the formation of an oxygen linkage between carbons 1 and 6. When a similar scission takes place at a point one structural unit removed from either end formed by the first scission, the resulting fragments are levoglucosan molecules. When scissions occur further along the chain the multiple unit fragments are not volatilized.

If the mechanism of thermal degradation of cellulose triacetate were similar to that of cotton cellulose, the tar would have consisted mostly of 2,3,4-

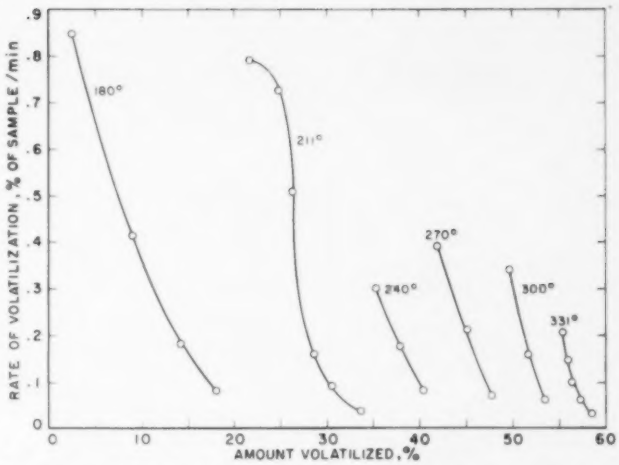

FIGURE 8. *Rates of volatilization of NO_2-oxidized cellulose, in percentage of sample per minute, as a function of percentage volatilization.*

levoglucosan triacetate. Infrared analysis shows that the tar consists mainly of a molecular species which is more related to that of the original cellulose triacetate than to that of 2,3,4-levoglucosan triacetate. Further experimental work will be required to determine the chemical nature of this tar.

NO_2-oxidized cellulose pyrolyzes very rapidly even at low temperatures. It seems that the whole ring structure is weakened by the oxidation of the primary alcohol so that the products consist mainly of H_2O, CO_2, and CO, and very little tar.

In general, it can be said that by converting the primary alcohol to an ester, formation of levoglucosan is blocked due to steric hinderance between carbons 6 and 1, while oxidation of the primary alcohol to an acid not only introduces a steric hinderance to the formation of levoglucosan but also introduces a weakness in the cellulose ring.

Addition of Na_2CO_3 to cellulose triacetate probably acts as a catalyst affecting differently the rates of formation of the various fragments so as to favor formation of CH_3COOH at the expense of the tar and to speed up the over-all reaction rate. This effect of Na_2CO_3 on the pyrolysis of cellulose triacetate is similar to that on cotton cellulose [1]. However, NaCl, while effective in reducing the tar in pyrolysis of cotton cellulose [1], had little effect on cellulose tracetate.

6. References

[1] S. L. Madorsky, V. E. Hart, and S. Straus, J. Research NBS **56,** 343 (1956) RP 2685.
[2] H. J. P. Venn, J. Textile Inst. **15,** 414 (1924).
[3] S. L. Madorsky, J. Polymer Sci. **9,** 133 (1952); **11,** 491 (1953).

WASHINGTON, October 21, 1957.

Journal of Research of the National Bureau of Standards Vol. 60, No. 4, April 1958 Research Paper 2854

Role of Vitrons in Alkali Silicate Binary Glasses[1]

Leroy W. Tilton

Applications of vitron theory to analyses of properties of R_2O silicate binary glasses indicate that changes in slope on the property-composition curves may occur where there are integral numbers of cations per dodecahedral cavity or cage of the network. From geometrical considerations it is found that 1 or 2 oxygens and 6 sodiums can be accommodated inside a cage, and similarly not more than 1 oxygen and 4 potassiums can be inclosed in a cage.

Data on chemical attack and on solubility losses in water suggest for alkali silicate glasses a maximal average inclosure of oxygen inside the cavities at 16.7-mole percent for K_2O, 23.1 percent for Na_2O, and probably 28.6 percent for Li_2O. These compositions correspond to 1, 1.5, and 2 oxygens per cage. These compositions mark the beginning deterioration of the net, possibly because of nonbridging oxygen. Changes in rate of volatilization occur at 28.6-, 37.5-, and 50.0-percent R_2O for potash, soda, and lithia silicate glasses, respectively. These critical compositions are considered those for which the cavities in the glasses are completely saturated with the modifier oxides, R_2O, and with additional cations, R.

Detailed analyses of curves of molar volume versus composition show that the critical points for oxide saturation are evident and that changes in slope may occur at other critical compositions corresponding to integral numbers of cations per cage. It is found that the percentage of 16.7-percent Na_2O at high temperatures and the saturation point of 37.5 percent at low temperatures are critical in curves for specific (electrical) resistance. The "deep-well" point at 16.7-percent Na_2O critically separates soda silicate glasses that are very readily devitrified from those that contain more oxide modifier and are more stable.

1. Introduction

A noncrystal ionic model for silica glass was constructed by the writer and described at the annual meeting of the Optical Society of America in October 1956. He simultaneously announced a new concept applicable to studies of glasses, namely a small, stressed microstructure having near crystal symmetries and almost capable of forming macrocrystals. The particular structure found to accord with many data on fused silica glass consists of clusters of distorted pentagonal dodecahedra, called vitrons, having as subunits the well-known silicon-oxygen tetrahedra. A four element vitron is represented in figure 1.

The most important characteristic of the proposed vitrons is the fivefold symmetry which is incompatible with the formation of macrocrystals. See figure 2. A second important feature is a balanced distribution of stresses and bond strengths. Within each vitron (clusters of dodecahedral cages) the bonds are very strong at the center but weak at the peripheries where high-tangential tensions and lowered force constants are automatically limiting the growth potential.

In a previous paper [1] the author shows how the properties of silica glass, including density, differential diffusion of gases, interatomic distances, low tensile strengths, unusual (reversible) temperature and pressure effects on volume, irreversible heat effects, and internal friction at low temperatures can be better understood according to the vitron theory which can be considered as a modification of existing theories in such manner as to reconcile and amplify them.

It is suggested that vitrons grow simultaneously throughout a melt of glass at very high temperatures and become more or less imperfectly united through common pentagonal faces or occasional oxygen bridges between unsatisfied silicon atoms in adjacent vitrons. Smaller vitrons could grow in the inter-

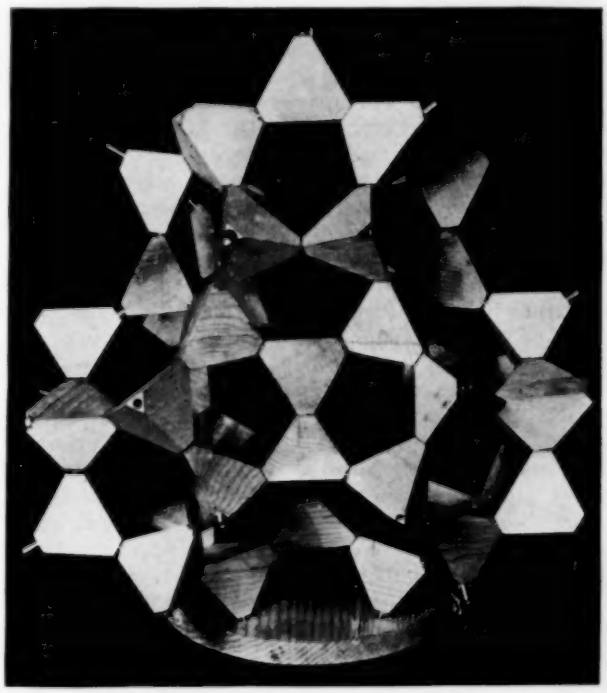

FIGURE 1. *Off-axis view of model of completed 4-element vitron (type 4, tetrahedral).*

Coiled wire springs indicate extra O^- charges and vacant tetrahedral corners indicate Si^+ charges available for attachments to other vitrons by oxygen bridges. At center foreground is a reentrant three-face that can unite with another vitron presenting a similar three-face.

[1] Reported in part at the Annual Meeting of the Optical Society of America, Abstract F4, J. Opt. Soc. Am. **47**, 115 (1957).

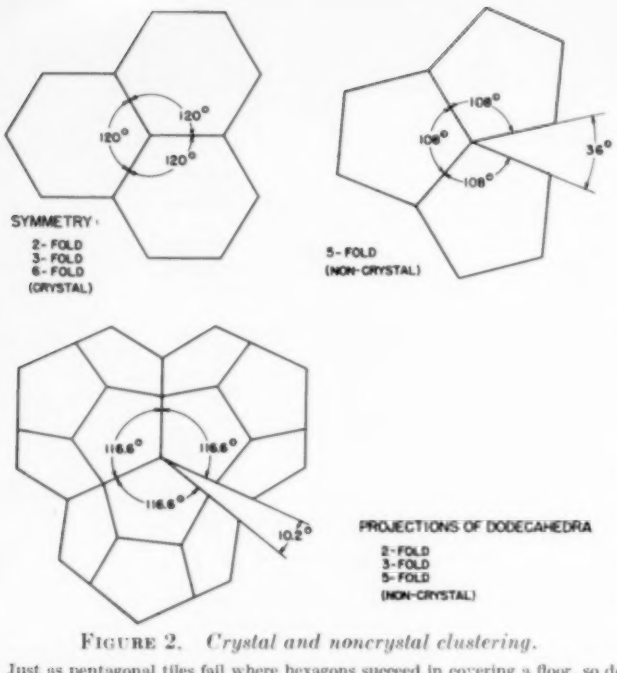

FIGURE 2. *Crystal and noncrystal clustering.*

Just as pentagonal tiles fail where hexagons succeed in covering a floor, so do regular pentradodecahedra fail to fill space completely and extensively. By radial compression, the neighboring dodecahedra may be distorted and meet each other and thus a limited degree of growth in space is possible.

stices between larger vitrons. A single-element vitron is only 8 A in diameter (on centers) and an upper limit for vitron dimensions may be approximately 30 A.

The next step in testing the vitron theory is an application to binary glasses, and of these the simplest and best known are the alkali silicates. This paper is a reconnaissance study of simple potash, soda, and lithia silicate binary glasses by analyses of such limited and imperfect data as may now exist on the properties of such glasses as functions of the concentration of the respective modifiers.

The stepwise nature of changes in the properties of some binary glasses has been noticed and discussed by several investigators. In general, in such studies, there has been unfortunate emphasis on the possibility of the existence of chemical compounds that might cause discontinuities or sharp breaks in properties such as would be evidenced by the intersection of straight-line segments. A more comprehensive view would give weight also to points of inflection, maxima and minima of ordinates or slopes, intersections of tangents, or other especially noticeable features not technically discontinuities. Sometimes, also, there are tacit assumptions that a special feature at a given composition on the curve of one property should, in general, be found on the curves of other properties. Actually, of course, it must be recognized that a circumstance which definitely affects sensitive measures of volatility, for example, may leave no noticeable imprint on rate of change of density. Special points on a property curve for a given temperature range may necessarily be entirely absent at very different temperatures.

Vitron theory suggests causes other than compound formation for the existence of special points on property-composition curves. For example, some oxygen may enter the cages (cavities) together with its cation and there should be critical compositions at which, approximately, this oxide saturation is completed and the process of net deterioration by "unshared oxygen" begins. Then at other compositions the cavities should become completely saturated with additional cations. Also to be considered, although perhaps of less importance, are the compositions at which there are integral numbers of cations per cavity.

Among properties that have been found useful in this study are solubility, chemical attack, volatilization, molar volume, electrical resistance, and fluidity.

2. Structural Characteristics of R_2O Silicate Glasses

Vitron theory has interesting quantitative aspects that may be used in applications to existing data.

2.1. Numerical Distribution of Cations

From the compositions expressed in mole proportions, it is easy to compute for the vitron model the numbers of cations per cavity. For the simple case of binary glasses with oxides R_2O and SiO_2 in the proportions r and s (where $r+s=1$), the number of cavities (or cages) is proportional to $s/5$ and the silicon to oxygen ratio is $s/(2s+r)$. It would seem that integral numbers of cations per cavity, R_b, may be significant for some purposes and the corresponding proportions of R_2O are readily computed as $r=R_b/(R_b+10)$. Also, a maximum upper limiting value of the coordination number, N_c, is necessarily twice the ratio of oxygen to cation, R, and therefore $N_c=1+2s/r$.

The stability of the network is estimated by computing for the average tetrahedron the number of corners that are securely tied into the net by the sharing of oxygens. On the conventional basis, the "shared oxygens" (half oxygens) per tetrahedron are computed as $O_s=4-2r/s$. This assumes that all oxygen added by the modifier oxide becomes attached to only one silicon and therefore is effective in weakening the network. If it be assumed that some oxygen as well as cation can be enclosed in the cages, insofar as their capacity and other conditions may permit, then the computation of shared oxygen is a multiple process, depending on the number, O_i, of oxygens that may be inclosed as oxide inside the cages, and $O_s=4+0.40\ O_i-2r/s$. On this basis, the network will not start deteriorating until certain threshold values of added oxygen are reached. As compared with the conventional basis, $O_i=0$, it then becomes easier to realize why some glasses with relatively high modifier content do not show marked instability even at compositions near those for which the glasses are commonly said to have sheet and chain structures of their tertahedra rather than veritable networks.

Table 1 gives useful data for applying the vitron theory to simple binary glasses having modifier oxides of the type R_2O. It is suggested that above the horizontal dotted line in table 1, devitrification may develop rapidly at relatively high temperatures because there is insufficient nonsilica inside the cages to effectively resist or impede the crystallization or contractural potential. In general, other glasses above the upper stepwise line should be stable, because the three-dimensional connections remain intact. Between the stepwise lines the network persists but is weakened. Below that region marked weaknesses may be manifest because spacial coherence of the network is not assured.

One of the most convincing proponents of the use of straight-line segments in representing the volume of glass as a function of composition is Huggins [2] who discussed details of possible structures in soda silicate glass and numerically designated 6 or 7 compositions where the property-composition curves showed, or might be expected to show, more or less abrupt changes in slope. As shown in the last columns of table 1, the points designated by Huggins are in close agreement with the compositions at which vitron theory finds for R_2O silicate glasses that the numbers of cations per hole in the net are 3, 5, 6, 8, 9, and 10. At these degrees of saturation or supersaturation for alkali silicate binary glasses, it will be shown below that changes in slope of certain property-composition curves may occur.

2.2. Geometrical Evidence

It has long been assumed that most cations introduced in silicate glasses in small proportions are located within the cavities of the network. In a glass of 16.7 mole percent Na_2O, there are 2 atoms of sodium per cavity or cage according to the vitron theory (see table 1). It is logical to expect that each cation will be found in closest possible contact with 3 oxygens of a single silicon-oxygen tetrahedron and this basic assumption underlies this analysis. It is further assumed here that the first oxygen introduced into the melt by each pair of cations will also be found in a cage with its 2 cations. If 2 sodiums are on opposite sides of their oxygen, that is, if the 3 centers lie on a straight line (as might be expected in a high-temperature state of Na_2O), then their center line can coincide with any one of the 10 threefold axes of a cage. Further, if the effective radius of sodium is 0.93 A, there is just sufficient space inside a cage to permit such an alinement (see fig. 13). Each Na will then be in contact with 4 oxygens and not far from 6 other oxygens. This unique arrangement is the "deep-potential-well" condition for soda in silica that is discussed in section 6.

If the concentration of soda is higher than 16.7-mole percent, sodium atoms can occupy some of the 6 other positions which they could take and each be in contact with 4 oxygens and not far from 6 others. There will be only 8 (not 10) such positions available for Na. That is, because of mutual interpenetration at nearest neighbor positions, the geometrical saturation of a symmetrical cage would be reached when only 4 of the 10 axes of threefold symmetry are simultaneously occupied by pairs of Na ions. If such geometrical saturation could be reached there would be 12 (Na–2dNa) distances of 2.58 A and 12 of 3.66 A within each cavity. The distribution would be symmetrical with the 8 sodium ions at the corners of an inscribed cube. However, because of distortional flattening of the cages along a diameter directed radially with respect to the whole vitron of which it is a component, only 6 Na per cage instead of 8 can be inclosed. Thus there will be only 6 internal distances of 2.58 A and 6 of 3.66 A, and this degree of saturation will be reached at 37.5-mole percent Na_2O as read from table 1.

There is unique space inside the cages for only 1 oxygen but possibly 2 oxygens and their cations can be inclosed in some of the more oblate cages. The oxygen added, as modifier increases, need not necessarily begin to weaken the network immediately after the cages are saturated with 1 central oxygen because some of the added oxygen can locate partly in one cage and partly in another and still be in such close contact with its cation that it does not break

TABLE 1. *Constitutional characteristics of* R_2O *silicate binary glasses*

Molar composition		Formula		Cages $s/5$	Cations per cavity P_A	Upper limiting coordination with oxygen	Shared oxygens, O_s (connected tetrahedral corners)					Special ratios of silicon to oxygen		
							Values of O_i					Computed from vitron model	Found by Huggins [2]	
R_2O	SiO_2	R_2O	SiO_2				0	1	2	3	4		1940	1954
0.000	1.00	0	5	0.200	0		4.0	4.0	4.0	4.0	4.0	0.50	0.50	0.50
.091	0.909	0.5	5	.182	1	21.0	3.8	4.0	4.0	4.0	4.0	.476		
.167	.833	1	5	.167	2	11.0	3.6	4.0	4.0	4.0	4.0	.454		
.231	.769	1.5	5	.154	3	7.7	3.4	3.8	4.0	4.0	4.0	.435	.435	.437
.286	.714	2	5	.143	4	6.0	3.2	3.6	4.0	4.0	4.0	.417		
.333	.667	2.5	5	.133	5	5.0	3.0	3.4	3.8	4.0	4.0	.409	.40	.40
.375	.625	3	5	.125	6	4.3	2.8	3.2	3.6	4.0	4.0	.385		(0.375)
.411	.589	3.5	5	.118	7	3.9	2.6	3.0	3.4	3.8	4.0	.371		
.444	.556	4	5	.111	8	3.5	2.4	2.8	3.2	3.6	4.0	.357	[a](0.364)	(0.357)
.474	.526	4.5	5	.105	9	3.2	2.2	2.6	3.0	3.4	3.8	.345	0.345	
.500	.500	5	5	.100	10	3.0	2.0	2.4	2.8	3.2	3.6	.333	(0.333)	0.333
...	...	...	...	...	...	...	...	...	...	...	...	...	...	...
...	...	...	...	...	...	...	...	...	...	...	...	...	...	...
...	...	...	...	...	...	...	...	...	...	...	...	...	...	...
.630	.370	8.5	5	.074	17	2.2	0.6	1.0	1.4	1.8	2.2	.270	0.27	...

[a] Ratios in parentheses were less prominent or seem to be given less weight by Huggins.

Si—O bonds. Whenever bonds are broken the unshared oxygen can probably be located near the cations and maintain electrical neutrality within satisfactorily small volumes.

For potash silicate glasses the conditions are somewhat similar, especially for low-cation content, but the K ion is so much larger than Na that the unique alinement of atoms in contact, with the oxygen center on one of the threefold axes, is impossible. The maximum angle, K–O–K, for K_2O inside a cavity would be about 80° instead of 180°, as can occur for Na–O–Na. The space inside a symmetrical cavity can accommodate 1 oxygen with 2 or with 3 K. Geometrically, the maximum K content is 4 per cage, even with no fully inclosed oxygen. In that case (28.6% K_2O), the 4 K atoms can form a tetrahedron within each cage and give 6 uniform K–K distances of 2.8 A. An interesting question is: Can distortion of cages proceed to such extent that an oxygen can be included somewhere near the center and 4 K also be inclosed with a slightly reduced K–K distance?

2.3. Differential Diffraction Patterns

Diffraction studies have been the principal direct and quantitative means of investigating the structure in glasses. Warren and his associates [3] pioneered in the construction of radial-distribution curves by means of Fourier transforms of the scattering curve for vitreous silica. Such curves give directly the distances from a silicon, or from an oxygen, to the near-neighbor atoms. This method has been applied to several soda-silicate glasses [4], to potash silicate glasses [5], and to some soda silicate glasses containing lime [6]. Such work has been done, also, on some simple borate glasses [7], and phosphate glasses [8].

The combined curves, however, become too crowded for resolution of pertinent peaks. Hartlief [5] seems first to have analyzed the radial-distribution curves by differential treatment in order to get resolution in the residual curves. He subtracted ordinates for a SiO_2 curve from those for each of several potash silicate glasses and thus obtained separately, as residuals, the average radial distributions from a potassium atom in each of the potash silicate glasses. Lukesh [9] independently applied the differential process to existing data on soda silicate glasses, and Dietzel [10] also did this work.

As pointed out by Hartlief and by Dietzel, the peaks on the residual radial distribution curves do not shift with change in composition as much as should be expected if they are evidences of an *average* equitable distribution of cations throughout the melts. It is reasonable to conclude that the ions free to migrate randomly can contribute little or nothing to noticeable peaks on such curves, whereas those that are more or less fixed may give peaks that should be interpretable.

Even the relatively constant residual curves characteristic of a given type of cation in fixed locations, are not unambiguously interpretable because there are multiple cation-silicon and cation-oxygen distances as well as the cation-cation distances in which (for this analysis) the chief interest lies. Without some definite three-dimensional model to test, little progress can be made. With a model, however, it is not too difficult to decide whether the model is or is not in accord with the radial-distribution curves. In order to fairly compare proposed models with the results deduced from X-ray data, it is necessary to compute the distances (between centers) from any modifier cation to each position that a neighbor atom might logically be expected to occupy. See figure 3. Then some consideration must be given to the extent of probable shielding that might prevent detection of the various neighbors. This has been done for both soda silicate and potash silicate glasses, in *undeformed* cages of vitron, and the results are expressed in tables 2 and 3, respectively (after elimination of some numerical results obviously impossible because of interpenetrations or gross shielding).

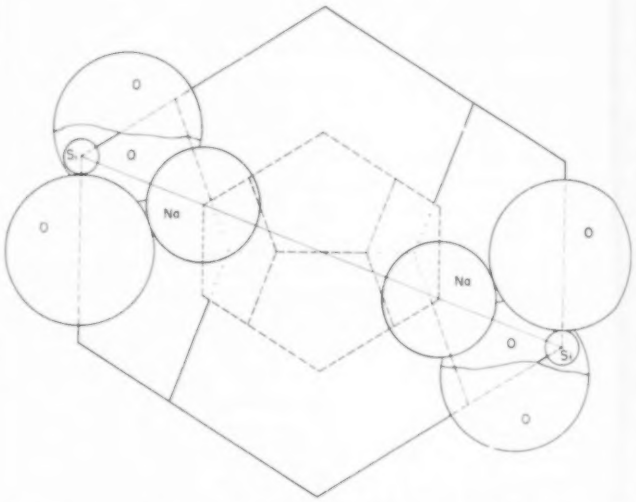

FIGURE 3. *Loci of cations in dodecahedral cages of SiO_2.*

There are 10 axes through opposite Si centers, and cation centers can lie on these axes and be in direct contact with 4 oxygens and not far from 6 other oxygens.

In both types of glass it is indicated that the residual peaks on the curves deduced from X-ray diffraction are caused principally by nearest and next-nearest neighbors. Second, it was noticed that the modifier cation can be distributed uniformly not only within each cavity but also similarly distributed in adjacent cavities on threefold axes so oriented that many of the cations are distributed at approximately equal distances from each other over longer ranges than are attainable within a single cage. Such equal longer-range separations computed for the Na ions and the K ions in binary R_2O silicate glasses approximate 6.2 and 6.5 A, respectively, for low concentrations of the modifier cations. Similar equal separations approximating 4.9 and 4.8 A also can occur in increased numbers at high concentrations.

TABLE 2. *Radial distribution of ions around sodium in soda silicate glasses (angstroms)*

Computed possibilities			Vitron model	Remarks and estimates of shielding (s)	Estimated peaks	X-ray evidence	
To silicon	To oxygen	To sodium				Lukesh [9] (Warren) peaks	Dietzel [10] peaks
1 Si_{1st}			2.24	Nearest Si	2.2	[a](2.2)	
	4 O_{1st}		2.25	Contact O	2.3	2.4	2.4
		6 Na_{2d}	2.58	Nearest Na	2.6	(2.9)	
3 Si_{2d}			3.19	Much s		(3.2)	
	6 O_{2d}		3.43	Very little s	3.4	(3.4)	
		6 Na_{3d}	3.66	Very little s	3.7	3.7	3.6
		3 Na_{ext}	3.77	Very little s but few paths			
	3 O_{3d}		3.99	Very little s	4.0		
		6 Na_{ext}	4.12	Appreciable s			
6 Si_{3d}		3 Na_{4th}	4.19	Appreciable s			
		1 Na_{3th}	4.49	Much s	4.3	(4.5)	
		6 Na_{ext}	4.6	Appreciable s			
	6 O_{4th}		4.76	Very little s	4.9	4.8	4.7
		3 Na_{ext}	5.1	Appreciable s			
	3 O_{5th}		5.42	Very little s	5.4	(5.5)	(5.5)
		12 Na_{ext}	5.5	Appreciable s but numerous paths.			
	6 O_{6th}		5.84	Very little s	5.8	(5.8)	
		12 Na_{ext}	6.0	Appreciable s but numerous paths.	6.0	(6.1)	5.9
		12 Na_{ext}	6.3	Appreciable s but numerous paths.	6.3	(6.3)	

[a] Distances in parentheses were read from very small peaks.

TABLE 3. *Radial distribution of ions around potassium in potash silicate glasses (angstroms)*

Computed possibilities				Remarks and estimates of shielding (s)	Estimated peaks	X-ray evidence	
To silicon	To oxygen	To potassium	Vitron model			Hartlief [5]	Tilton (Warren)
	4 O_{1st}		2.65	Contact O	2.6	2.3	2.3
1 Si_{1st}			2.76	Nearest Si	2.7		2.7
		6 K_{2d}	2.81	Nearest K			
	6 O_{2d}		3.49	Little s	3.5	3.5	
	3 O_{3d}		3.93	Little s	3.9		3.7
	6 O_{4th}		4.54	Little s	4.5		
		K_{ext}	4.5	Little s but few paths			
		K_{ext}	4.7	Little s	4.8	4.7	4.8
		K_{ext}	5.0	Little s			
		K_{ext}	5.7	Appreciable s	5.8	5.8	
		K_{ext}	5.9	Appreciable s			
		K_{ext}	6.5 ±2	Appreciable s but numerous paths.	6.5		6.2

3. Effective Cage Saturation

One of the most interesting questions about the structure of simple silicate glasses concerns the rate of deterioration of the silica network as oxygens are added, and another concerns the extent to which cations can be effectively inclosed in the cages.

3.1. Chemical Attack and Water Solubility

If the silica network begins to deteriorate immediately upon the addition of modifiers, one would expect an increased vulnerability of unshared oxygen to be immediately evidenced by rate of swelling in acids or solution in alkali. In fact, however, Hubbard [11] et al. have found such effects to be small or negligible below about 10-, 20-, and 30-mole percent of K_2O, Na_2O, and Li_2O, respectively, in R_2O silicate binary glasses (see fig. 4). Tentatively, then, and in accord with geometrical conditions as discussed above, it may be suggested that at least 1 and sometimes 2 oxygens may go into each cage, together with the cations simultaneously introduced, because 1 such oxygen is provided for each cage at 16.7-mole percent of R_2O, and at 28.6 percent there are available 2 (R_2O) for every cage.

Some data on water solubility of these glasses were published by Dietzel and Sheybany [12]. From their curves (see fig. 5) it is seen that 16.7 percent of K_2O, 23.1 percent of Na_2O, and 28.6 percent of Li_2O are reasonable estimates for maximal inclosure of oxygen and beginning deterioration of the network because of unshared oxygen. It will be noticed that the actual damages at the suggested critical percentages are greatest for K_2O and smallest for Li_2O in accord with the relative sizes of the respective cations. Hence it is suggested that mere size of cation is not negligible in expanding the volume of the network, and perhaps damaging it, even if all modifiers are inclosed in cages.

The same data by Hubbard [11] et al. on rate of chemical attack indicate that very serious damage to potash silicate glass can occur at mole percentages of modifier near 25 and to soda silicate glass near 35. This accords with the idea that maximum inclosure of K ion is reached at not more than 28.6-percent K_2O or 4 K per cage, and maximum inclosure of Na at 37.5-percent Na_2O or 6 Na per cage. The ater-

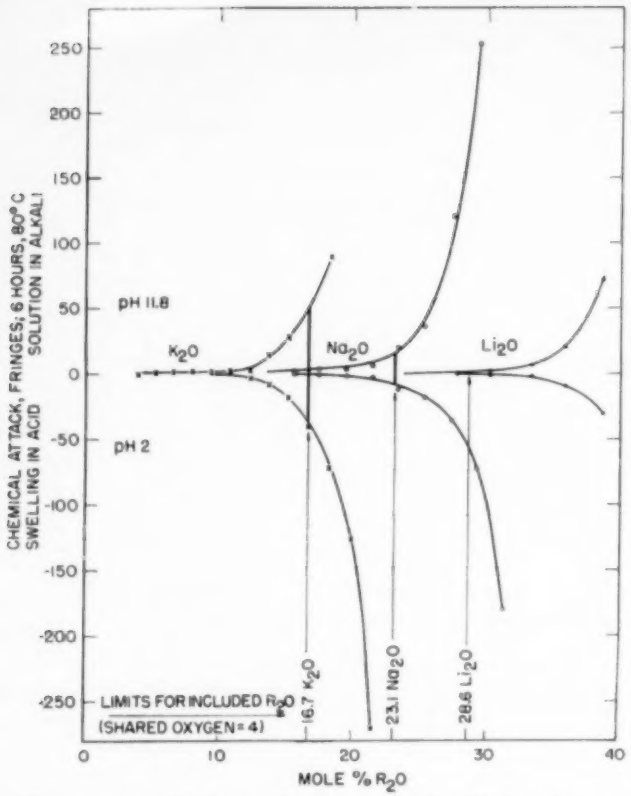

FIGURE 4. *Chemical attack on alkali silicate glasses.*

Data of Hubbard [11] et al. Noticeable rates of attack begin near the critical percentages for maximal inclosure of oxygen and beginning decrease in shared oxygen.

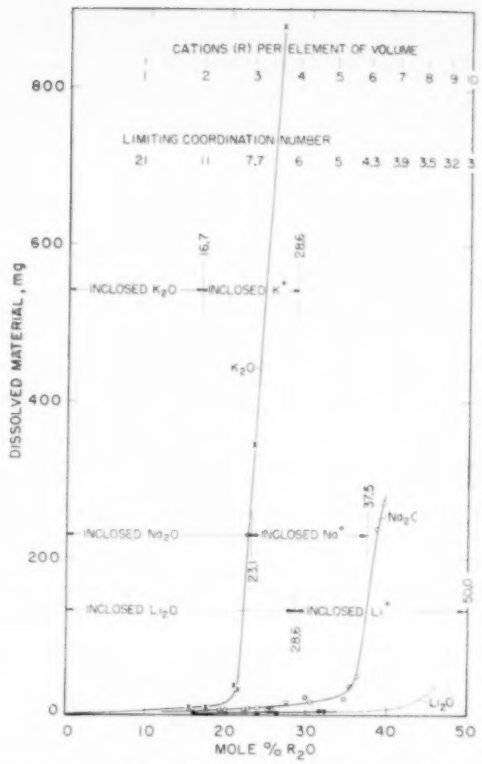

FIGURE 5. *Water solubility of al)ali silicate glasses (1 hr, room temperature).*

Data of Dietzel and Sheybany [12]. Near critical percentages of 16.7, 23.1, and 28.6, where maximal oxygen is inclosed in the cages and the shared oxygen begins to decrease, there is beginning appreciable water solubility. The full saturation points of 28.6 and 37.5 occur near extremely high rates of solubility, and 50 percent for Li_2O is not unreasonable.

solubility curves indicate that these estimates of effective saturation are reasonable, and the estimates accord with the geometrical evidence deduced from the model.

3.2. Volatilization

Fortunately, it is possible to get more precise confirmations of the critical percentages of modifiers that will give saturation of the silica cages with cations. This is possible because of an extensive and remarkably significant series of experiments made at Sheffield, England, some 20 years ago by E. Preston and W. E. S. Turner [13] on the volatilization losses at high temperatures from simple binary melts including potash, soda, and lithia silicate glasses. Rate of volatilization of alkali from such melts would seem to be a property that might be especially sensitive to any alkali content over and above that necessary to saturate the cages of a network of silica, and also sensitive to temperature increases that are sufficiently high to damage a network and expose alkali that had previously been protectively inclosed. The results obtained by Preston and Turner, when plotted against compositions, did indeed show regions of particular interest but, unfortunately, the curves were analyzed primarily for evidence of the existence of chemical compounds in the glasses. The adverse criticism that followed has diverted attention from the data; and although the peculiarities have not been acceptably explained, other possible uses of these data for interpretations concerning glass structure seem to have been overlooked.

Concerning these experiments Weyl [14] says, "The results were startling, and caused considerable controversial comment. * * * For constant time the rate of volatilization changed abruptly with a continuous change of composition. * * * aside from * * * terminology and * * * structural interpretation, the fact remains that the findings of W. E. S. Turner and his associates contradict the assumption of a continuous and completely random network."

For structural purposes it is not material whether the loss-composition curves are really straight lines or somewhat curved. The important matter is localization of the composition ranges within which a *decided* change in slope occurs. Their data do permit quantitative estimates of chemical compositions at or near which some important changes in structural conditions occur. For soda silicate glasses the critical region is certainly included between 32- and 38-mole percent of soda, as shown in figure 6. For glasses richer in soda, the rate of loss increases much more rapidly as soda content increases. This, essentially, must be the conclusion whether one looks at the original graph by Preston and Turner,[2] or at

[2] Figure 4, p. 338 of 1st citation in literature reference [13].

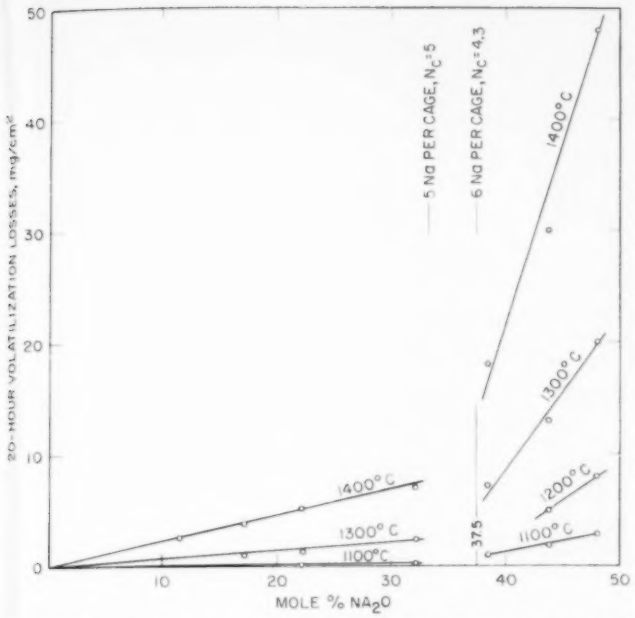

FIGURE 6. *Losses in weight while soda silicate glasses are held at high temperature.*

Data of Preston and Turner [13]. A concentration of 37.5 percent of Na_2O is indicated as critical. Each cage of the net then contains 6 Na and above this percentage of soda the silica is supersaturated with modifier.

the graph as redrawn by Morey [15]; and the estimate would not be materially changed (although its locale might be accentuated) by consideration of the progressive changes in composition that are occurring during an experiment, especially for the minimum periods of 20 hrs, which alone will be considered here.

According to vitron theory there are two possible critical compositions within the region 32- to 38-mole percent Na_2O, namely 33.3 or 37.5 percent. These compositions are those at which there are available, respectively, 5 or 6 sodium atoms per cage. Six seems the more likely number for a critical condition because it is geometrically the maximum of Na ions that can be rationally accommodated within any deformed component cage of a vitron (except a veritable center cage—which alone can escape distortional deformation).

The interpretation from a similar exhibit of the corresponding evidence from potash silicate glasses heated at 1,400° C is less definite because, as will be shown presently, 1,400° causes so much deterioration of the network of potash silica glasses that differences in losses above and below saturation are minimized. A corresponding exhibit that can be drawn for 1,300° C[3] would show some important change in conditions between glasses 34.74 and 39.60 percent (weight) of potash. The only possible critical composition that vitron theory offers is 28.6-mole percent (38.6 weight), where 4 potassium atoms per cavity are available and, as already mentioned, 4 constitute geometrical saturation with rationally distributed potassium atoms.

The same result for the same potash silica series of glasses is obtained in a striking manner by plotting ratios of 20-hour losses, 1,400° C/1,300° C, as in figure 7 where the rapid change in slope, and an inflection,[4] show definitely the critical mole percentage 28.6 at which saturation of the cavities occurs. The high values on the left side of figure 7 are caused by much greater temperature deterioration of the net from 1,300° to 1,400° as compared with 1,200° to 1,300° C.

From similar data for lithia silicate glasses it will be seen in figure 8 that 50 percent, which corresponds to 10 inclosed Li per cavity, is the critical composition of effective saturation with Li cations. Here it

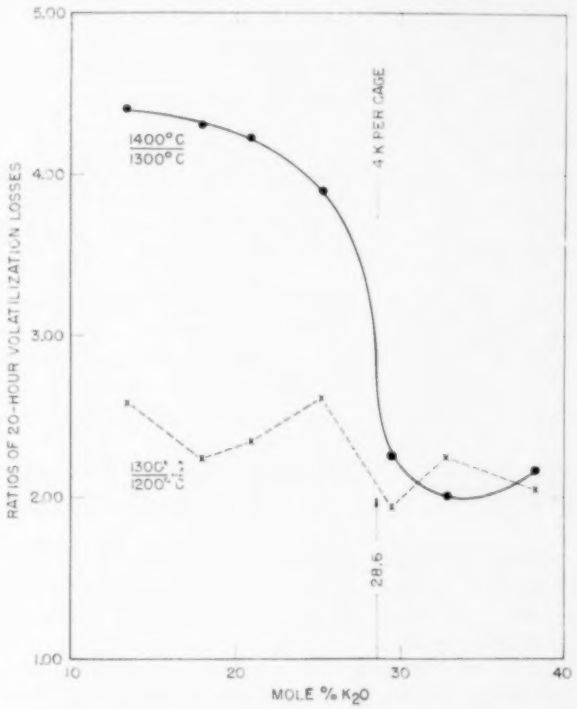

FIGURE 7. *Ratios of losses in weight while potash silicate glasses are held at high temperatures.*

A concentration of 28.6 percent of K_2O is indicated as critical. Each cage of the net then contains 4 K and above this percentage of potash the silica is supersaturated with modifier. From the left side it can be inferred that at some temperature between 1,300° and 1,400° C the unsaturated network suffers very appreciable deterioration. From the right, where supersaturation has already damaged the network, it appears that a Δt from 1,200° to 1,300° C is relatively as effective as a t from 1,300° to 1,400° C.

can be inferred that even a temperature increase from 1,200° to 1,300° C causes appreciable deterioration of the net (such as occurred from 1,300° to 1,400° C for potash silica glasses) and that between 1,300° and 1,400° the deterioration in Li_2O glasses is still progressing. In contrast with the varying effects of progressively higher heat levels as evidenced in the left-hand portions of figures 6, 7, and 8, it appears on the right that an increase of 100° C in holding temperature has a more nearly constant effect and approximately doubles the loss from supersaturated glasses, whether of soda, potash, or lithia, and regardless of the temperature level at least between 1,200° and 1,400° C.

Having selected tentative critical compositions for effective saturation it is now possible to compare

[3] See table VIII, p. 133 of 2d citation in literature reference [13].

[4] This remarkable curve was published as figure 4, p. 134 of 2d citation in literature reference [13] and seems never to have been explained.

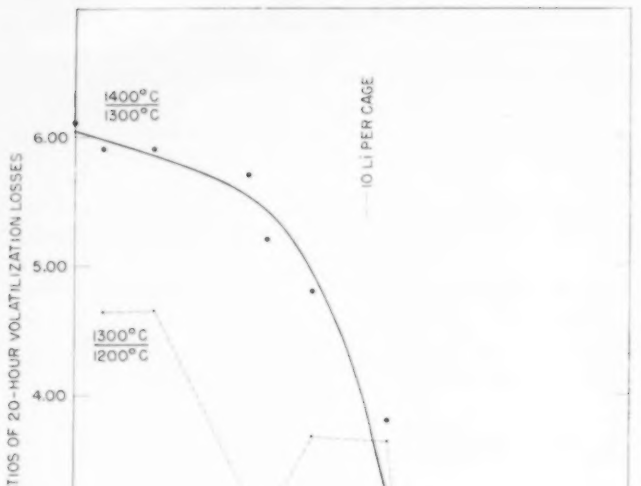

FIGURE 8. *Ratios of losses in weight while lithia silicate glasses are held at high temperatures.*

Above a critical concentration of 50-percent lithia, where 10 Li are available for each cage of the network, the silica is supersaturated. A critical temperature for some deterioration of the unsaturated net of lithia silicate glasses seems to lie below 1,300° C.

equitably the losses by volatilization of the different alkalis after conversions from weights to moles of loss per unit concentration of modifier oxide. This is exhibited in figure 9 for 1,300° C and figure 10 for 1,400° C where positive abscissae represent supersaturation. In the writer's opinion the relative volatilities as they appear in figures 9 and 10 are more logical than is the case when the abscissae are plotted without regard to degree of saturation.

At 1,400° C lithia is found to be somewhat more volatile than potash, molecularly, but soda a little less so. At 1,300° C the differences between lithia and potash and soda seem negligible at low concentrations well below cation saturation, but at concentrations near and above saturation the soda is definitely less volatile than the other alkalis. In other words, a temperature of 1,400° C, which damages the network, does not volatilize soda as easily as it does lithia and potash. Further, this effect is marked at moderate degrees of supersaturation even at 1,300° where one would expect soda to be intermediate between the other alkalis. This seems to indicate that some of the soda is more firmly bound or inclosed in the silica net than either lithia or potash. The facts suggest that in general by mere inclosure of R_2O it is very effectively protected, but that some "deep potential well" condition of some of the soda is so important that it continues to give protection to soda even when the net is somewhat deteriorated either by heat or damage because of reduction in shared oxygen.

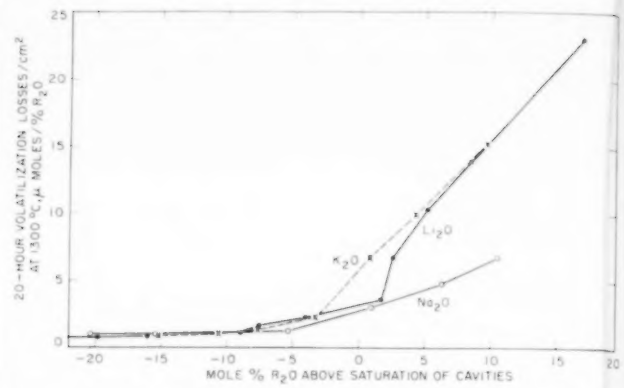

FIGURE 9. *Volatilization losses at 1,300° C in micromoles per unit concentration at comparable degrees of saturation of network.*

Lithia and potash are about equally volatile but soda somewhat less so at 1,300° C and above saturation.

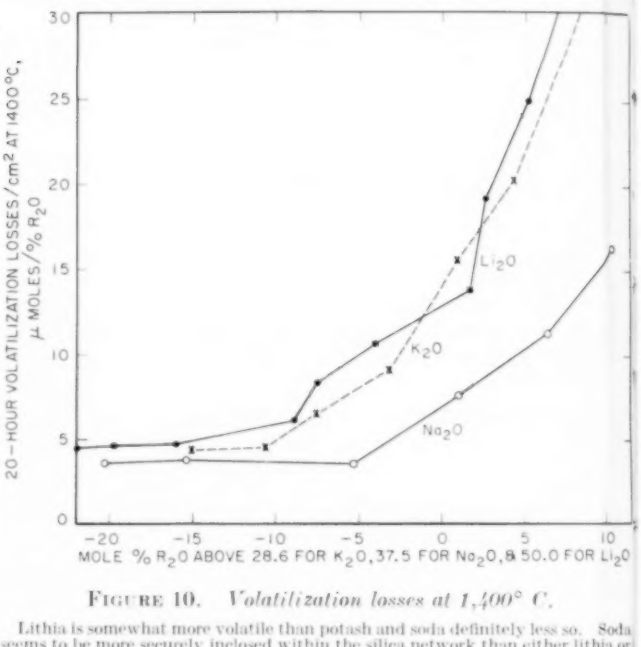

FIGURE 10. *Volatilization losses at 1,400° C.*

Lithia is somewhat more volatile than potash and soda definitely less so. Soda seems to be more securely inclosed within the silica network than either lithia or potash and the increased stability is evidenced even at moderate degrees of supersaturation.

4. Molar Volume and Degree of Saturation

An interesting feature of glass is the openness of its structure. In fused silica the volume of the voids is much greater than the volume of the ions, comprising about 62 percent of the total volume, whereas for the "most open" packing of equal spheres the voids are only 48 percent of the total. It has been said [16] that regular pentagonal dodecahedra have the largest possible cavities for a structure of interlaced tetrahedra. This openness in glass would seem to be particularly useful in studies of the structure of glasses containing known molecular proportions of nonsilica, especially if the idea of predominant randomness is supplanted by that of predominant order.

A difficulty is the volume sensitivity of glasses to the temperatures employed in their annealing [27]. Permanent volume changes of as much as 1 percent are possible in annealed glasses and thus comparisons may have errors as large as 2 percent unless the annealings are "comparable." Just what constitutes comparability in annealings is not entirely clear but one can at least see that glasses are annealed at temperatures that are all comparably high or all low in their respective annealing ranges.

For a series of many simple soda silicate glasses, it is found that those with low-soda content have densities, d, or specific volumes, V, that, as functions of their composition, can be represented better by intersecting straight lines than by continuous curves. Some differences of opinion have been expressed about this, particularly when it was found that the intersections sometimes occurred where the constituent oxides were related approximately in simple proportions such as 1:1, 1:2, 1:3, etc. and no such compounds were known to exist. The use of segmented straight lines has persisted, however, and one outstanding example of their use was published by Huggins [2] who found intersections at several of the compositions to which vitron theory now (table 1) calls attention because integral numbers of sodium ions should at those points be expected in the dodecahedral cages of the network. The coefficients that Huggins gives for the computation of densities from his "structon" analysis may, therefore, to some extent, be regarded as analagous to coefficients that could be given for computing densities according to the number of cations per cage as deduced from a vitron analysis.

From the agreement between vitron and structon theories as set forth in table 1, it may be inferred that curves of specific volume versus composition for soda silicate glasses will show changes in slope near the points for integral numbers of sodium atoms per cage of the silica network. Presumably the same may be true for potash and lithia glasses.

In previous sections of this paper it has been suggested that conditions are somewhat more complicated and that some oxygen as well as cation can be inclosed in the cages of the silica network. From data on water solubility, swelling in acids, and solution in alkali, it was estimated that oxygen is inclosable up to mole percentages of 16.7 for K_2O, 23.1 for Na_2O and 28.6 for Li_2O, and that added oxygens begin to produce unshared oxygen at some of the tetrahedral corners at about the compositions named. To test these estimates further and to show the results graphically on an open scale, it is desirable to plot only differences in volume between some function of composition and the volumes as computed from observed densities.

With such ideas and tentative structural data in mind, one can proceed to analyze data on the specific volumes computed from the measured densities of a series of simple binary silicate glasses provided all of them have been carefully and consistently annealed for comparison purposes. Data on such a series have been published by Young, Glaze, Faick, and Finn [17], particularly for soda and potash silicate glasses but including some lithia silicates, and these data will be used here. It is proposed to express all observations as gram molecular volumes of glass, $V_g = w/d$, where w is the molecular weight (linearly interpolated according to composition) and d is observed density at room temperatures; and from these volumes to subtract a computed volume

$$V_c = (1-p)V_S + xpV_S \qquad (1)$$

where p is the mole fraction of the modifier oxide, $V_S = w/d = 27.263$ cm^3 is the gram molecular volume attributable to the silica network (density 2.203), and x is a *volume replacement* or expansion factor to be so determined that V_c from eq (1) shall equal V_g as observed when R_2O replaces silica in very small amounts. In other words eq (1) is written to apply to the initial straight-line segments of curves when volume is plotted against modifier oxide beginning with 100-percent silica. This means that x could be computed from the equation $xpV_S = pV_R$, if V_S and V_R are true partial molar volumes of silica [5] and of oxide, and if V_R be known.

It will be evident that if all R_2O enters the cavities without distending the volume of the net, then V_R must be zero and x be zero. Or, if the rate of change in net expansion should be proportional to added R_2O, then eq (1) would continue to represent the observations and $V_c = V_g$ with an initially determined constant value of x, identical for K_2O, Na_2O, or Li_2O.

However, the actual values of x, computed from glasses with various small values of p, are 1.114, 0.644, and 0.339 for K_2O, Na_2O, and Li_2O silicate glasses, respectively. These replacement factors contrast decidedly with the values $x=0$ which are to be expected for small proportions of any R_2O added to silica if all atoms of the oxides are inclosed in the cages *without distending the volume of the net*.

The diversity among these replacement factors, x, accords with the suggestion now being made that not only cations but some oxygens are inclosable in the cages of the network. This follows because if only cations are inclosed, and all oxygen added to the net, then the replacement factors, x, would for these R_2O glasses depend chiefly on the rate of addition of oxygen, which does not differ among R_2O oxides, and thus the values of x would be nearly identical for each of the oxides.

It seems necessary, then, to conclude that even small proportions of modifier oxides, which presumably can be maximally inclosed in holes of the network, are distending the silica component, that is the network, whose volume is $(1-p)\ V_S$ to the extent $\Delta V_g = xpV_S$. Specifically (see fig. 11a), the replacement of silica by K_2O to the extent of 10 percent causes 12 percent increase in volume of the *residual* (or 90% silica) net, but corresponding replacements with Na_2O and Li_2O will cause increases of only 7 and 4 percent, respectively. Otherwise stated, but perhaps less pertinently, replacements to the extent

[5] Tentatively, 27 cm^3 may be used as the partial molar volume of silica in both soda and potash silicate glasses at low-modifier content and room temperatures, as shown by Callow [18], and the same is true at 1,400° C as reported by White[19].

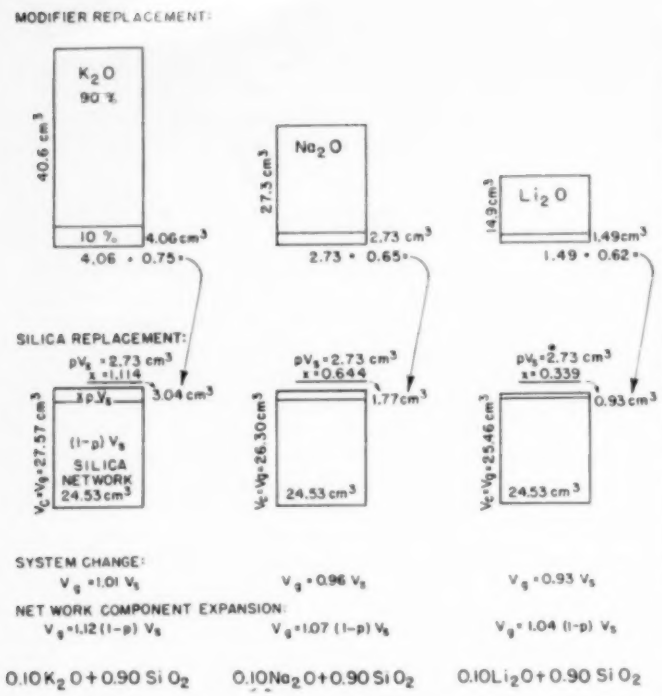

FIGURE 11a. *Changes in molar volume by additions of 10-percent R_2O.*

The most important facts are (1) apparent shrinkage of added modifier and (2) expansion of the silica network component, even for the small lithium atoms. Since the silica-replacement factors, x, differ from zero and from each other, it is inferred (1) that modifiers do penetrate the network and (2) that the network expansion (even for small additions of modifier) cannot be due solely to the added oxygens which are identical in number for each modifier.

of 10 percent cause an increase in *total* volume of the initial system (100% silica) of 1.1 percent with K_2O but decreases of 3.5 and 6.6 percent with Na_2O and Li_2O. Then the interpretation sometimes given is that the relatively stronger ionic potentials of sodium and lithium result in contractions of the networks. In view of prevailing ideas concerning the great strength and relative invariance of silica nets, the appropriateness of such an interpretation may be questioned.

As first stated, however, and if all additions go inside the silica net that is simultaneously formed, no contractual effect of the *network* is evident, even in the case of lithia silicate glass. In all three glasses the over-all effects on the net are expansional and the interpretation here suggested, on a vitron basis, is that all of the added oxides *at these small proportions of nonsilica* are inclosed in the cavities and that the content of oxides either strengthens the elemental dodecahedral volumes or by its mere presence restricts their deformability. This would result in reduced size limits for the growth of vitrons (clusters of elemental volumes), and increase the number and widths of the intersticial channels between vitrons. The three oxides, K_2O, Na_2O, Li_2O, are found to have this expansive effect in the ratios 44:26:14 which correspond roughly to ratios of their gram molecular volumes, namely, 41:27:15, which can be estimated from the densities of these oxides at room temperatures.

The linear eq (1) yields good values for the volumes of only a few of these two-component glasses at the lower concentrations of nonsilica, and it is found that additional terms or a series of values for x would be required in order to extend its application beyond values of p larger than about 17 percent for K_2O, 23 percent for Na_2O, and 29 percent for Li_2O. These are the critical percentages near which it was concluded from solubility and chemical-attack data that maximal oxygen is inclosed.

The extent, ΔV, of the failure of eq (1) has been evaluated as $\Delta V = V_g - V_c$ for the three glass types mentioned, using the data on densities and compositions as published by Young, Glaze, Faick, and Finn. [17] These increases in volume are plotted in figure 11b to show that the stepwise nature of the increases is consistent with a thesis that changes in slope can occur at each composition corresponding to an integral number of cations per hole; also to show how nearly identical are the rates of increase in volume upon the addition of very diverse oxides.

For the intervals considered here, the points where slopes may change are at the percentages 16.7, 23.1, 28.6, 33.3, 37.5, and 41.1 corresponding to 2, 3, 4, 5, 6, and 7 cations per elemental cage of volume.

Noticeable features of the curves in figure 11b are the points at which the linear eq (1) becomes inadequate for computing volumes. Mention has already been made of these points near 17, 23, and 29 percent of R_2O where the maximum inclosure of *oxygen* is reached. After that, the addition of modifier oxygen increases the oxygen of the network, unconnected tetrahedral corners can occur, and the effective volume of the network can be further expanded. In further accord with estimates of cation saturation in preceding sections of this paper, it is suggested (see fig. 11b) that 2 additional cations of potassium are inclosable (at 28.6% K_2O) with coordination lowered to 6; also that as many as 3 additional cations of sodium per cage can be inclosed (at 37.5% Na_2O) with coordination lowered to 4.3; and for Li_2O possibly 6 additional cations are inclosable (at 50%) to give a coordination number of 3. These percentages of 29, 38, and 50 are to be considered as estimates of the compositions for which the cavities in these silicate binary glasses are effectively filled, and as limits beyond which the cations become much less firmly anchored within or protected by the silica framework. It will be noticed that the ranges from maximum inclosure of oxygen to maximum effective inclosure of cation are such that the upper limits for coordination extend on both sides of currently accepted estimates of normal coordination at 8 to 10 for K, 6 for Na, and 4 for Li.

A noteworthy feature of figure 11b is the near parallelism of these curves. This is interpreted as evidence that any progressive disruption of the network is largely independent of the size and nature of the modifier cations. This, of course, should be the case if the controlling factor is the rate at which oxygen is being added to cause progress in the disconnection of the tetrahedra. If, as suggested in this analysis, the numbers of inclosed oxygens average 1, 1.5, and 2 per element of volume, for K_2O,

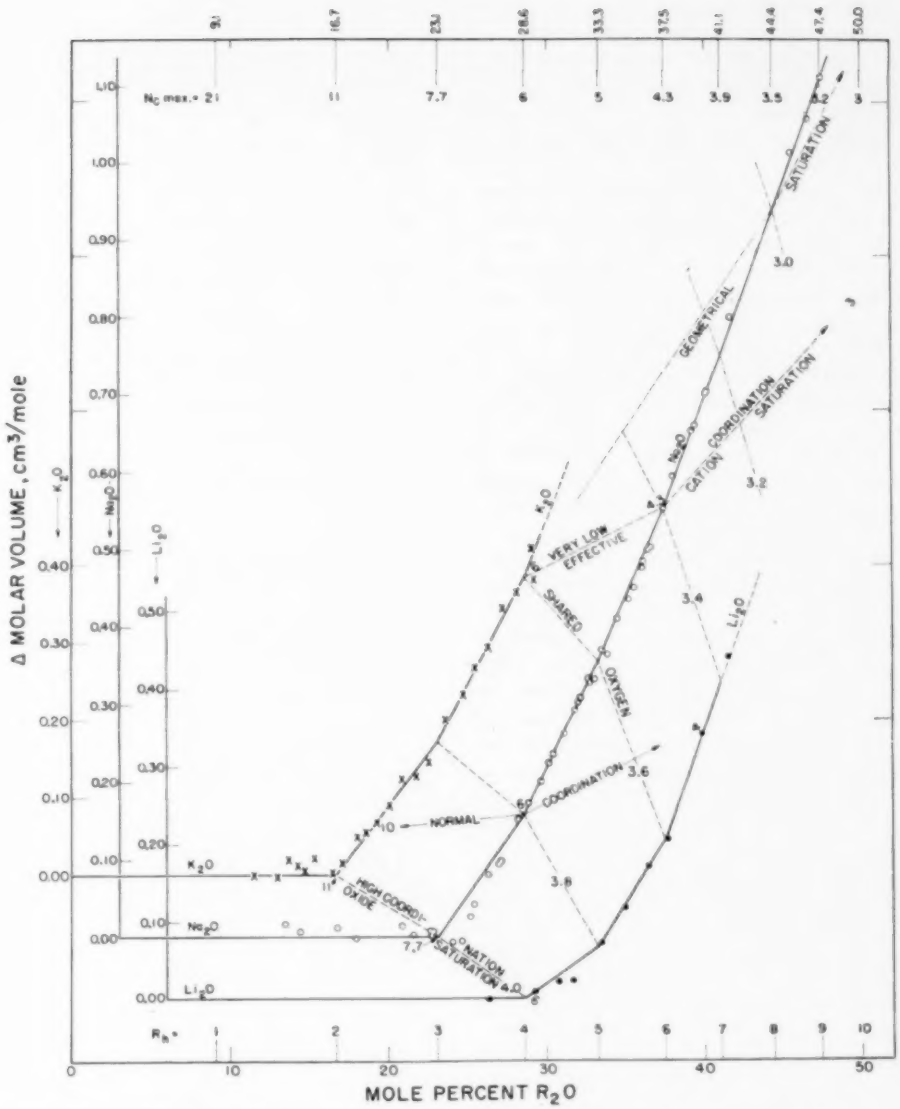

FIGURE 11b. *Changes in volume of alkali silicate binary glasses with increased* R_2O *content.*

Data of Young, Glaze, Faick, and Finn [17]; displaced ordinates, common abscissae. At the critical percentages 16.7, 23.1, and 28.6 there is maximal inclosure of oxide modifier in the cages of the glass and the coordination numbers are large. At the critical percentages 28.6, 37.5, and 50.0 the cages are completely filled with oxide plus cations and the coordination is below normal. The rates of volume increase tend to become independent of the nature of the R_2O, probably because they depend mainly on the constant rate of addition of oxygen that is not inclosed and therefore weakens the network.

Na_2O, and Li_2O, respectively, then at percentages of 28.6, 33.3, and 37.5 the respective nets are only slightly, and about equally, disrupted to an average of 3.6 connected corners per tetrahedron. This is indicated in figure 11b where dotted lateral lines 4.0, 3.8, 3.6, etc. unite points of comparable degree of shared oxygen ,that is degree of connection of the tetrahedra in the network.

5. Electrical Resistance

The sodium ion with a radius of 0.98 A is appreciably smaller than neon, radius 1.2 A, which is the largest of the noble gases that readily passes through silica glass at any considerable rate. In general, other common network modifiers are larger than sodium and it is not surprising that the conductivity of glass at temperatures below annealing is commonly ascribed to migrations of the sodium ions. Question is sometimes raised concerning the potassium ion but its radius of 1.38 A approaches that of argon, 1.6 A, which does not pass through silica except with great difficulty. Consequently it is not surprising that experiments have shown [20] that at temperatures below 600° C conduction by K ions is either negligible or excluded.

An extensive investigation of the electrical resistivity of soda silica glasses as a function of composition and temperature was made by Seddon, Tippett, and Turner [21]. Their results for logarithm of

specific resistance at several temperatures between 250° and 500° C have been replotted in figure 12 after conversions from weight to mole percentages of Na_2O. Data for 1,300° C from work by Endell and Hellbrügge [22] have been added. Similar work was done by Babcock [23] with good agreement in the regions of overlapping.

These curves show decreases in the resistances as soda is added, and this accords with a general deterioration of the network. Further, the curves show a possibility that the progressive deterioration may be nearly linear between certain definite percentages of Na_2O. The particular changes in slope explicitly noticed by Seddon, Tippett, and Turner near 37.5 percent Na_2O at temperatures of 250° to 400° C were confirmed by Babcock at 394° to 727° C or higher; but at much higher temperatures, near 1,200° and 1,300° C, he definitely found no change in slope (in agreement with Endell and Hellbrügge). This is in general accord with the conclusions reached above in section 3.2 concerning high-temperature deterioration of the networks that can gradually obliterate the structural effects that can be observed at lower temperatures.

In addition to changes in slope of the low-temperature resistivity curves near the "saturation point" at 37.5 percent Na_2O, there is a definite change near 16.7 percent for the high temperatures. Possibly further work might confirm a less noticeable change at 28.6 percent. These special compositions of soda silicate glasses correspond to averages of 2, 4, and 6 sodium cations per dodecahedral element. Below 2 Na per element of volume, soda silica glasses are not stable and devitrification readily occurs. At 6 Na per element or 37.5 percent, it has already been suggested that the cages of the net are filled. At higher soda contents there is uninclosed soda and the disruption of the network begins to be a cause of instability. At the intermediate composition of 28.6 there are 4 Na per element and the maximum coordination number becomes exactly 6, which is probably nearly an optimum condition for soda silicate glasses. It is interesting to note that at the high temperature of 1,300° C the network is so much disrupted that resistance is low long before the cages in the network are filled at 37.5 percent soda, and only one special point, at 16.7 percent soda, remains in evidence. This is the point at which there may be a "deep potential well" distribution of the Na_2O within the cages as suggested in figure 13, of this paper.

6. Deep Potential Wells in Soda Silicate Glasses

A soda content of 16.7-mole percent of modifier in R_2O glasses gives 2 cations per dodecahedral element of volume of glass according to the vitron model, as shown by table 1. If the cation is sodium, with radius 0.93 Å, the logical arrangement is that shown in figure 13 and it is apparent that a strengthened cage structure may result and the sodium atoms so placed may be more integrally related to the network structure than additional sodium or any other cation. References have been made to this unique geometrical arrangement in section 2.2 above; also in section 3.2 in discussing differential volatilization of soda and potash, and in section 5 regarding electrical resistivity of soda silicate glasses.

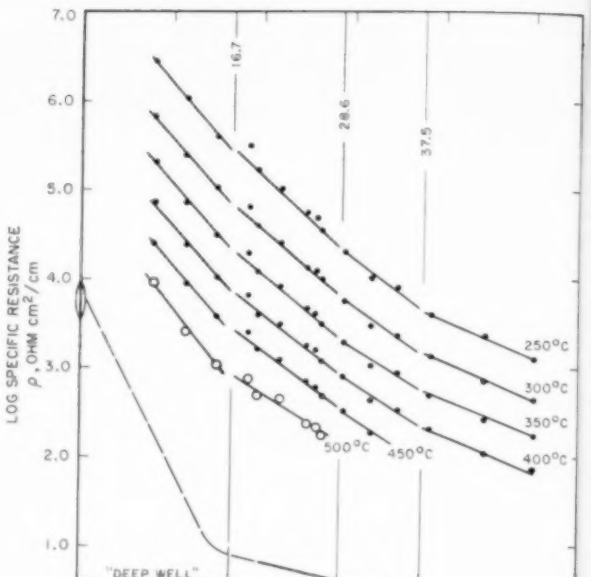

FIGURE 12. *Effect of composition on specific resistance of soda silicate glasses.*

Data of Seddon, Tippett, and Turner [21], after conversion to mole percent; also curve from Endell u. Hellbrügge [10, 22] for 1,300° C. At 16.7-percent Na_2O each element of the vitrons has its complement of inclosed or "deep well" cations and at 28.6 percent the normal complement of 4 Na with coordination number of 6. At 37.5 percent there are 6 Na ions per element, the cages in the net are probably completely filled, and the average number of connected corners of the tetrahedra has fallen to 3.4 so that some disruption of the network has occurred. At 1,300° C, only the "deep well" effect at 16.7 percent is noticeable. Even slightly increased disruption of the net by high temperatures seriously impairs resistance.

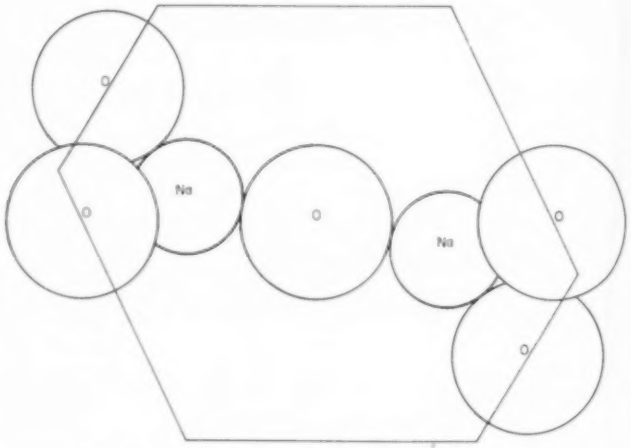

FIGURE 13. *A uniquely metastable arrangement for a glass of 16.7-mole percent soda and 83.3-percent silica.*

See also figure 3. The Na ions are each in closest possible contact (2.25 A between centers) with four oxygen halves and not far (3.4 A) from 6 others. The Na ions are as far from each other as possible (4.55 A) within the interior of a dodecahedral element of a vitron. These distances accord with the differential analyses of radial distribution curves deduced by Lukesh and by Dietzel from X-ray diffraction patterns.

In discussing electrical conductivity and dielectric losses, Stevels [24] distinguishes between Na ions that are "free" and others that are "enclosed". He considers that the enclosed ions lie in "deep potential holes", that annealing provides opportunity for a more thorough occupation of such positions (there is sometimes a factor of 3 between the conductivity of strained glass and the lower values for well-annealed glass), and that "the first Na ions added to a network are taken up in the deepest potential holes in which they stay with preference for energy reasons".

The idea that sodium ions situated as shown in figure 13 should resist migration may be related to the peculiarity found by Jenckel and Schwittman [25] near 17 percent Na_2O when they determined temperatures of equifluidity of soda silicate glasses. Their curves of equifluidity have extremely well marked abrupt changes in slope as shown in figure 14 which is plotted from their data. Very rapid increases in viscosity as silica content increases are well known. Dietzel and Sheybany [12] in their discussions concerning the filling of voids with cations, have cited the work of Endell and Hellbrügge [22] on the viscosities of potash, soda, and lithia silicate glasses. Unfortunately, the viscosity seems

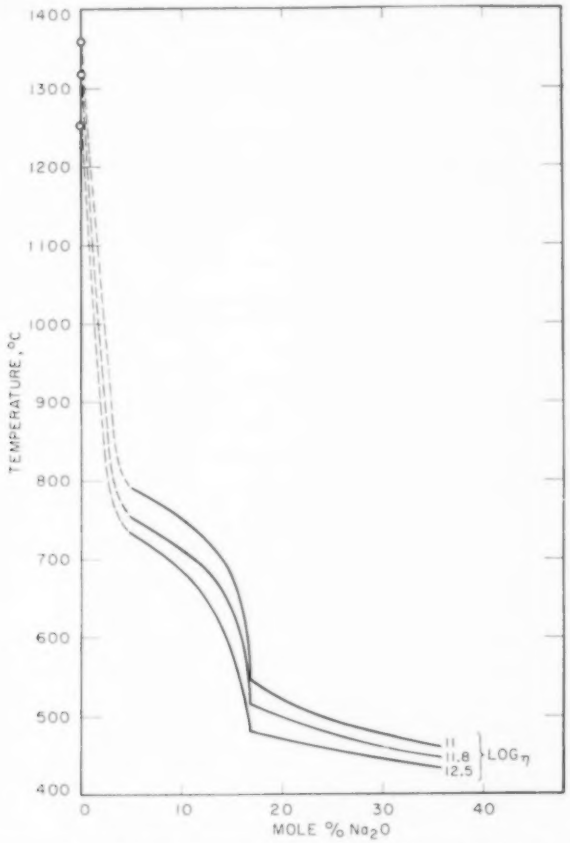

FIGURE 14. *Temperatures for equiviscosity of soda silicate glasses.*

Data by Jenckel and Schwittman [25] have been averaged, and points at 0 percent Na_2O are averages for two specimens measured by Volarovich and Leontieva [26]. At 16.7 percent Na_2O a critical demarkation may exist between stable glasses and those that crystallize so easily that viscosities are greatly increased.

very sensitive to small degrees of crystallization and, aside from temperature difficulties, it has not seemed particularly useful to work with binary R_2O glasses having large concentrations of SiO_2. Jenckel and Schwittman, however, extended their fluidity measurements well into the conentrations that tend to crystallize and also to temperatures fairly low in the annealing ranges. The lower the temperatures at which they measured fluidity, the sharper was the cutoff point in Na_2O content below which the fluidity decreased more or less abruptly, possibly on account of devitrification. Supposing it is incipient crystallization that caused sudden changes in the viscosity, it is interesting to ask, why this crystallization effect is so critical at approximately the composition of 16.7-percent Na_2O. Does the deep-well condition so strengthen the cages and resist migrations as to prevent collapse in structure incident to and necessarily prerequisite to devitrification? If crystallization is not active why is there a sudden change in fluidity at this definite composition? Can it be that at low concentrations Na_2O enters the cages only as a unit so that at all soda contents below 16.7 percent there will be some cages in which there are no cations? Such empty cages might deform more easily and thus be compatible with narrower intervitron channels and conducive to lower fluidities at temperatures in and above the annealing ranges.

7. Conclusion

In this paper it has been found geometrically possible that the beginning of deterioration of the silica network by addition of modifier oxides can be deferred up to 16.7-mole percent even for K_2O and possibly 23.1 or 28.6 percent for Na_2O. Also from such considerations it is found that the maximum content of completely inclosed cation per cage is 4 of K or 6 of Na. The probable loci of these ions in the dodecahedral cages lead to radial distances between ions that agree well with data from differential analyses of diffraction pattern data.

From data on chemical attack and water solubility it appears that 16.7 percent of K_2O, 23.1 percent of Na_2O, and 28.6 percent of Li_2O are reasonable estimates for maximal inclosure of oxygen and simultaneous beginning deterioration of the network because of unshared oxygen. From data on volatilization at high temperatures it is found that percentages of 28.6, 37.5, and 50, corresponding to inclosures of 4, 6, and 10 ions of K, Na, and Li, respectively, are fairly definitely indicated for full saturation of the cages.

Changes in the molar volumes of these alkali glasses as a function of R_2O content are in accord with the idea that there may be structural-change points corresponding to some of the percentage compositions of 16.7, 23.1, 28.6, 33.3, 37.5, and 41.1 where there are 2, 3, 4, 5, 6, and 7 cations per cage or cavity of the network.

For sodium silicate glasses, the change in slope indicating cage saturation at 37.5-percent Na_2O is detectable on curves of resitivity at low temperatures

but not for temperatures near 1,300° C where temperature deterioration of the network may mask the saturation point. The deep-potential-well point at 16.7-percent Na_2O probably becomes prominent above 400° C on curves of resistivity but is definitely less so at lower temperatures. This point at 16.7-percent Na_2O is very prominent on curves of equifluidity near annealing temperatures. Glasses richer in SiO_2 devitrify very readily.

Thus it is apparent that considerable qualitative and some semiquantitative and intercorrelated evidence in support of the vitron theory of glass structure is given by analyses of existing data on property-composition curves of solubility, chemical attack, volatilization, molar volume, electrical resistance, and fluidity of alkali silicate binary glasses. It is concluded that further studies of this nature should be made when more varied, more extensive, and more accurate data are available.

8. References

[1] L. W. Tilton, J. Research NBS **59,** 139 (1957) RP2782.
[2] M. L. Huggins, J. Opt. Soc. Am. **30,** 421 (1940); J. Phys. Chem. **58,** 1145 (1954).
[3] B. E. Warren and A. D. Loring, J. Am. Ceram. Soc. **18,** 269 (1935); B. E. Warren, H. Krutter, and O. Morningstar, J. Am. Ceram. Soc. **19,** 202 (1936).
[4] B. E. Warren and J. Biscoe, J. Am. Ceram. Soc. **21,** 259 (1938).
[5] G. Hartlief, Z. anorg. u. allgem. Chem. **238,** 379 (1938); J. Biscoe, M. A. A. Druesne, and B. E. Warren, J. Am. Ceram. Soc. **24,** 100 (1941).
[6] J. Biscoe, J. Am. Ceram. Soc. **24,** 262 (1941).
[7] J. Biscoe and B. E. Warren, J. Am. Ceram. Soc. **21,** 287 (1938); R. L. Green, J. Am. Ceram. Soc. **25,** 83 (1942).
[8] J. Biscoe, A. G. Pincus, C. S. Smith, and B. E. Warren, J. Am. Ceram. Soc. **24,** 116 (1941).
[9] J. S. Lukesh, Proc. Natl. Acad. Sci. **28,** 278 (1942).
[10] A. Dietzel, Glastech. Ber. **22,** 214 (1949).
[11] D. Hubbard, M. H. Black, S. F. Holley, and G. F. Rynders, J. Research NBS **46,** 168 (1951) RP2189; D. Hubbard and G. W. Cleek, J. Research NBS **49,** 267 (1952) RP2363.
[12] A. Dietzel and H. A. Sheybany, Verres et réfractaires **2,** 63 (1948).
[13] E. Preston and W. E. S. Turner, J. Soc. Glass Technol. **16,** 331 (1932); **17,** 122 (1933); **18,** 143 (1934).
[14] W. A. Weyl, J. Soc. Glass Technol. **35,** 442 (1951).
[15] G. E. Morey, J. Am. Ceram. Soc. **17,** 320 (1934).
[16] Eugène Poncelet, Verres et réfractaires **2,** 208 (1948).
[17] J. C. Young, F. W. Glaze, C. A. Faick, and A. N. Finn; J. Research NBS **22,** 453 (1939) RP1197.
[18] R. J. Callow, J. Soc. Glass Technol. **36,** 137 (1952).
[19] Jack L. White, Ph. D. Dissertation, U. of Calif., p. 101 (1955); J. O'M. Bockris, J. W. Tomlinson, and J. L. White, Trans. Faraday Soc. **52,** 306 (1956).
[20] R. Schwarz and J. Halberstadt, Z. anorg. u. allgem. Chem. **203,** 365 (1932); **210,** 286 (1933).
[21] E. Seddon, E. J. Tippett, and W. E. S. Turner, J. Soc. Glass Technol. **16,** 474 (1932).
[22] K. Endell and H. Hellbrügge, Beiheft Nr. 38 zu der Z. VDGh. 1940; Z. angew. Chem. **53,** 271 (1940).
[23] C. L. Babcock, J. Am. Ceram. Soc. **17,** 329 (1934).
[24] J. M. Stevels, Progress in theory of physical properties of glass, p. 59, 67, 75, 79 (Elsevier, New York, N. Y., 1948).
[25] E. Jenckel and A. Schwittmann, Glastech. Ber. **16,** 168 (1938).
[26] M. P. Volarovich and A. A. Leontieva, J. Soc. Glass Technol. **20,** 139, 1036.
[27] L. W. Tilton, J. Soc. Glass Technol. **40,** T338 (1956).

WASHINGTON, July 12, 1957.

Journal of Research of the National Bureau of Standards Vol. 60, No. 4, April 1958 Research Paper 2855

Elastic Problem for a Ring of Uniform Force in an Infinite Body [1]

William H. Pell

Kelvin has given an integral representation for the displacements in an infinite elastic body produced by a body force acting in an arbitrary portion of this body. By a limit procedure, solutions have been found for point and line singularities acting in the interior of such a body. A similar method is used in this paper to obtain the displacements produced by a uniform force applied along, and normal to, a circle lying in the interior of an infinite elastic body.

1. Introduction

One of the important results of the classicial theory of elasticity is the solution of Kelvin [1, 3] for the displacements in an infinite elastic solid due to a body force distribution throughout all, or a part of the body. From this, one obtains by a limiting procedure the displacements for the case in which the body force reduces to a concentrated force at some point in the infinite solid. This solution is singular at the point of application of the concentrated force, and plays a role for the Navier equations of elasticity analogous to that which the potential of a point charge plays for Laplace's equation. By the process of superposition, the displacements, due to any finite number of concentrated forces with different directions and at different points, can be obtained. The principle of superposition and a limiting process such as is used in mechanics to obtain a concentrated moment can be employed to obtain solutions for higher-order singularities. For example, one may superpose the solutions for point forces P, a distance h apart, and with opposite senses. By allowing $h \to 0$ while Ph remains constant, the solution corresponding to a "double force" is obtained. Superposition of three of these with mutually perpendicular lines of action gives the "center of compression". In this way, a catalogue of singular solutions can be built up. A number of such solutions has been given by Boussinesq [4] and Dougall [5], and, more recently, using other methods, Mindlin [6] has given an extensive list of such "nuclei of strain", as they have been called by Love.

By superposition of these nuclei of strain in our infinite solid, one may hope to be able to solve problems for domains with boundaries, and this has been done in a number of important cases, e. g., the half space under concentrated normal load on its boundary, or concentrated load on a line, or over an area such as a circle or rectangle [7].

The Kelvin integrals will be used here to obtain the displacements due to a concentrated force applied along, and normal to a circle in an infinite solid. While no mathematical features of particular novelty arise in the analysis, the solution does exhibit an interesting use of elliptic integrals. The problem has been undertaken as a first step in the application of such methods to problems dealing with bodies having axial symmetry; in particular, it is hoped to use the result obtained here as a first step in obtaining the solution due to a ring of pressure applied to the surface of an elastic cone. It is therefore natural to carry out the work in spherical, rather than the somewhat simpler cylindrical, coordinates, and this has been done.

2. Kelvin's Integral of the Navier Equations

Consider an elastic solid of infinite extent, and let its material points be referred to rectangular cartesian coordinates x_i, $i=1,2,3$. If a body force with components $F_j(x_1,x_2,x_3)$,

[1] This research was supported by the United States Air Force, through the Office of Scientific Research of the Air Research and Development Command.

$j=1,2,3$, per unit volume acts within a region V of the solid, and $u_j(x_1,x_2,x_3), j=1,2,3$ represent the displacement components in the solid, then the Navier equations in V are

$$\mu\nabla^2 u_i+(\lambda+\mu)\frac{\partial}{\partial x_i}\Delta=-F_i, \qquad i=1,2,3, \tag{2.1}$$

where λ and μ are Lame's elastic constants, and Δ is the sum of the extensional strains. The right side of (2.1) vanishes outside of V.

Lord Kelvin [1,3] has given a solution of these equations, valid throughout the solid, which represents the effects of the body force, viz.,

$$u_i(x)=A\int_V\left[B\frac{F_i(\xi)}{R}-\frac{\partial}{\partial x_i}\left(\frac{1}{R}\right)\sum_{j=1}^{3}(x_j-\xi_j)F_j(\xi)\right]dV, \qquad i=1,2,3 \tag{2.2}$$

where ξ_j, $j=1,2,3$ are variables of integration, x and ξ have been used to indicate the three variables x_j and ξ_j, and

$$R^2=\sum_{j=1}^{3}(x_j-\xi_j)^2, \tag{2.3}$$

$$A=\frac{\lambda+\mu}{8\mu\pi(\lambda+2\mu)}, \qquad B=\frac{\lambda+3\mu}{\lambda+\mu}. \tag{2.4}$$

3. The Kelvin Integrals in Spherical Coordinates

It will be convenient for our purposes to obtain the spherical coordinate equivalents of (2.2), i. e., to obtain displacement components in the spherical coordinate directions expressed in terms of spherical coordinates.

Let r,θ, and ϕ be spherical coordinates related to the x_i coordinates by

$$\begin{aligned} x_1&=r\sin\theta\cos\phi,\\ x_2&=r\sin\theta\sin\phi,\\ x_3&=r\cos\theta, \end{aligned} \tag{3.1}$$

as indicated in figure 1. If $V_i(x)$ denote the components of a vector in the x_i coordinate system

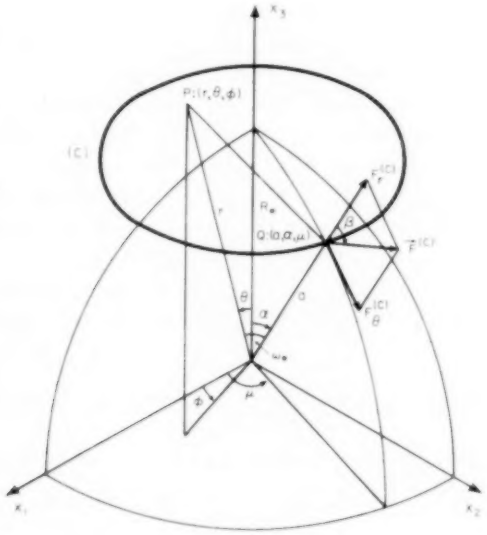

FIGURE 1. *Concentrated force applied to a ring.*

and $V_r(r,\theta,\phi)$, $V_\theta(r,\theta,\phi)$, $V_\phi(r,\theta,\phi)$ its components in spherical coordinates, then it is easily shown either by tensor methods or by elementary geometry that

$$\begin{aligned} V_r &= (V_1 \cos\phi + V_2 \sin\phi)\sin\theta + V_3\cos\theta, \\ V_\theta &= (V_1\cos\phi + V_2\sin\phi)\cos\theta - V_3\sin\theta, \\ V_\phi &= -V_1\sin\phi + V_2\cos\phi. \end{aligned} \tag{3.2}$$

Inversion of this system gives

$$\begin{aligned} V_1 &= (V_r\sin\theta + V_\theta\cos\theta)\cos\phi - V_\phi\sin\phi, \\ V_2 &= (V_r\sin\theta + V_\theta\cos\theta)\sin\phi + V_\phi\cos\phi, \\ V_3 &= V_r\cos\theta - V_\theta\sin\theta. \end{aligned} \tag{3.3}$$

If we let u_r, u_θ, u_ϕ be the components of the elastic displacement in spherical coordinates, then they are connected with the cartesian components u_i through (3.2) with V_r, etc., replaced by u_r, etc., and V_i replaced by u_i. If we suppose this done, and the expressions (2.2) for u_i inserted in the result, then we obtain, after some simplification,

$$\begin{aligned} v_r(r,\theta,\phi) &= A\int_V \left\{ B\frac{\overline{F}_r}{R} + \frac{1}{R^3}[r\overline{F}_r - \rho F_r][r-\rho\cos\omega] \right\} dV, \\ v_\theta(r,\theta,\phi) &= A\int_V \left\{ B\frac{\overline{F}_\theta}{R} + \frac{\rho}{R^3}[r\overline{F}_r - \rho F_r][\sin\theta\cos\lambda - \cos\theta\sin\lambda\cos(\phi-\mu)] \right\} dV, \\ v_\phi(r,\theta,\phi) &= A\int_V \left\{ B\frac{\overline{F}_\phi}{R} + \frac{\rho}{R^3}[r\overline{F}_r - \rho F_r]\sin\lambda\sin(\phi-\mu) \right\} dV, \end{aligned} \tag{3.4}$$

where ρ, λ, μ are the values of r, θ, ϕ, respectively, associated with the integration variables ξ_i. It is easy to verify that

$$R^2 = r^2 + \rho^2 - 2r\rho\cos\omega, \tag{3.5}$$

$$\cos\omega = \cos\theta\cos\lambda + \sin\theta\sin\lambda\cos(\phi-\mu), \tag{3.6}$$

i. e., R is the distance between the fixed point (r, θ, ϕ) at which the displacements are to be calculated and the variable point of integration (ρ, λ, μ), while ω is the angle between the radii vectors r and ρ. We let F_r, etc., be the components of the body force in spherical coordinates. The arguments of F_r in (3.4) are ρ, λ, μ, but $\overline{F}_r$ etc., are used to designate certain terms which are as yet incompletely expressed in spherical coordinates, viz,

$$\begin{aligned} \overline{F}_r &= [F_1(\xi)\cos\phi + F_2(\xi)\sin\phi]\sin\theta + F_3(\xi)\cos\theta, \\ \overline{F}_\theta &= [F_1(\xi)\cos\phi + F_2(\xi)\sin\phi]\cos\theta - F_3(\xi)\sin\theta, \\ \overline{F}_\phi &= -F_1(\xi)\sin\phi + F_2(\xi)\cos\phi. \end{aligned}$$

But the $F_i(\xi)$ are given in terms of $F_r(\rho, \lambda, \mu)$, etc., by (3.3) with the obvious replacements, and hence we find that

$$\begin{aligned} \overline{F}_r &= F_r\cos\omega - F_\theta\Omega + F_\phi\sin\theta\sin(\phi-\mu), \\ \overline{F}_\theta &= -F_r\Lambda + F_\theta\Xi + F_\phi\cos\theta\sin(\phi-\mu), \\ \overline{F}_\phi &= -(F_r\sin\lambda + F_\theta\cos\lambda)\sin(\phi-\mu) + F_\phi\cos(\phi-\mu), \end{aligned} \tag{3.7}$$

where the arguments of F_r, etc., are ρ, λ, μ, and

$$\Xi=\sin\theta\sin\lambda+\cos\theta\cos\lambda\cos(\mu-\phi),$$
$$\Lambda=\sin\theta\cos\lambda-\cos\theta\sin\lambda\cos(\mu-\phi), \tag{3.8}$$
$$\Omega=\cos\theta\sin\lambda-\sin\theta\cos\lambda\cos(\mu-\phi).$$

With the insertion of (3.7) in (3.4), we obtain the displacements in spherical coordinates obtained from the Kelvin integrals:

$$v_r=A\int_V\left\{\frac{B}{R}\left[(F_r\cos\omega-F_\theta\Omega+F_\phi\sin\theta\sin(\phi-\mu)\right]\right.$$
$$\left.+\frac{r-\rho\cos\omega}{R^3}\left[F_r(r\cos\omega-\rho)-F_\theta r\Omega+rF_\phi\sin\theta\sin(\phi-\mu)\right]\right\}dV,$$

$$v_\theta=A\int_V\left\{\frac{B}{R}\left[-\Lambda F_r+\Xi F_\theta+F_\phi\cos\theta\sin(\phi-\mu)\right]+\frac{\rho\Lambda}{R^3}\left[F_r(r\cos\omega-\rho)\right.\right.$$
$$\left.\left.-F_\theta r\Omega+rF_\phi\sin\theta\sin(\phi-\mu)\right]\right\}dV, \tag{3.9}$$

$$v_\phi=A\int_V\left\{\frac{B}{R}\left[-(F_r\sin\lambda+F_\theta\cos\lambda)\sin(\phi-\mu)+F_\phi\cos(\phi-\mu)\right]\right.$$
$$\left.-\frac{\rho}{R^3}\sin\lambda\sin(\phi-\mu)\left[F_r(r\cos\omega-\rho)-F_\theta r\Omega+rF_\phi\sin\theta\sin(\phi-\mu)\right]\right\}dV.$$

4. The Displacement Integrals for a Ring of Concentrated Force

The concept of a concentrated force $\vec{F}^{(c)}$ acting at a point P of an infinite body may be arrived at in the following way. We first define a distributed body force which vanishes outside some volume ΔV containing P in its interior, and inside ΔV is some continuous $\vec{F}$ which has the property that

$$\vec{F}^{(c)}=\int_{\Delta V}\vec{F}dV.$$

Now ΔV is let tend to zero, always with P in its interior, and $\vec{F}$ allowed to increase in such a way that the value of the integral maintains the constant value $\vec{F}^{(c)}$. Thus

$$\vec{F}^{(c)}(P)=\lim_{\Delta V\to 0}\int_{\Delta V}\vec{F}dV. \tag{4.1}$$

We wish to consider a continuous distribution of concentrated force along a circle (C) whose center lies on the x_3 axis, and whose plane is parallel to that of the x_1 and x_2 axes. (See fig. 1.) In spherical coordinates we take the equation of the circle to be

$$r=a,\ \theta=\alpha,$$

where $0<a<\infty$, $0<\alpha<\pi$. Suppose $\vec{F}(\phi)=(F_r(\phi),\ F_\theta(\phi),0)$ is a continuous distribution of force defined in the region $a-\Delta r<r<a+\Delta r$, $\alpha-\Delta\theta<\theta<\alpha+\Delta\theta$ $\mu-\Delta\phi<\phi<\mu+\Delta\phi$ enclosing the point P: (a,α,μ). For simplicity, let us consider only the component F_θ. In general, because the θ-direction varies from point to point in ΔV, this distribution of force will have a nonzero resultant force and moment with respect to the coordinate directions at (a,α,μ). It is easy to show, however, that if the resultant $F_\theta^{(c)}$ in the θ-direction is held fixed as we let Δr, $\Delta\theta$, $\Delta\phi$ tend

to zero, then we obtain in the limit only a force $F_\theta^{(c)}$ acting in the θ-direction. The same remark holds for the component $F_r(\phi)$. In this way we obtain a concentrated force $\vec{F}^{(c)}(\mu)=(F_r^{(c)}(\mu), F_\theta^{(c)}(\mu), 0)$, acting at $\phi=\mu$ on the circle $r=a$, $\theta=\alpha$. This force lies in the plane $\phi=\mu$, and is therefore normal to the ring.

The displacements corresponding to the distribution $\vec{F}=(F_r,F_\theta,0)$ in ΔV are seen from (3.9) to be

$$\begin{aligned}
v_r&=A\int_{\Delta V}\left\{\frac{B}{R}[F_r\cos\omega-F_\theta\Omega]+\frac{1}{R^3}[r-\rho\cos\omega][F_r(r\cos\omega-\rho)-r\Omega F_\theta]\right\}dV,\\
v_\theta&=A\int_{\Delta V}\left\{\frac{B}{R}[-\Lambda F_r+\Xi F_\theta]+\frac{\rho\Lambda}{R^3}F_r(r\cos\omega-\rho)-r\Omega F_\theta]\right\}dV,\\
v_\phi&=A\int_{\Delta V}\left\{-\frac{B}{R}[F_r\sin\lambda+F_\theta\cos\lambda]+\frac{\rho}{R^3}\sin\lambda[F_r(r\cos\omega-\rho)-r\Omega F_\theta]\right\}\sin(\phi-\mu)\,dV,
\end{aligned}\tag{4.2}$$

where $dV=\rho^2\sin\lambda\,d\rho\,d\lambda\,d\mu$. Each of these expressions consists of a sum of terms of the form

$$\int_{\Delta V}f(r,\theta,\phi;\rho,\lambda,\mu)F(\phi)\,dV,$$

where $F(\phi)$ is either $F_r(\phi)$ or $F_\theta(\phi)$, and f represents its coefficient. It is not difficult to show that if $(r,\theta,\phi)\neq(a,\alpha,\mu)$, then under the assumed behavior of $\vec{F}$ in (4.1),

$$\lim_{\Delta V\to 0}\int_{\Delta V}f(r,\theta,\phi;\rho,\lambda,\mu)F(\phi)\,dV=f(r,\theta,\phi;a,\alpha,\mu)F^{(c)}(\mu).\tag{4.3}$$

Accordingly, if we now consider a distribution of force of strength $\vec{F}^{(c)}$ per unit of arc length along the circle (C), we obtain for the displacements at (r,θ,ϕ) the expressions

$$\begin{aligned}
v_r&=A\int_0^{2\pi}\frac{1}{R_*}\Big\{B[F_r^{(c)}(\mu)\cos\omega_*-\Omega_*F_\theta^{(c)}(\mu)]+\\
&\qquad\frac{1}{R_*^2}[r-a\cos\omega_*][F_r^{(c)}(\mu)(r\cos\omega_*-a)-r\Omega_*F_\theta^{(c)}(\mu)]\Big\}\,d\mu,\\
v_\theta&=A\int_0^{2\pi}\frac{1}{R_*}\Big\{B[-F_r^{(c)}(\mu)\Lambda_*+F_\theta^{(c)}(\mu)\Xi_*]+\\
&\qquad\frac{a\Lambda_*}{R_*^2}[F_r^{(c)}(\mu)(r\cos\omega_*-a)-r\Omega_*F_\theta^{(c)}(\mu)]\Big\}\,d\mu,\\
v_\phi&=A\int_0^{2\pi}\frac{1}{R_*}\Big\{-B[F_r^{(c)}(\mu)\sin\alpha+F_\theta^{(c)}(\mu)\cos\alpha]+\\
&\qquad\frac{a\sin\alpha}{R_*^2}[F_r^{(c)}(\mu)(r\cos\omega_*-a)-r\Omega_*F_\theta^{(c)}(\mu)]\Big\}\sin(\phi-\mu)\,d\mu,
\end{aligned}\tag{4.4}$$

where * indicates evaluation of the quantity to which it is attached at $\rho=a$, $\lambda=\alpha$, i. e.,

$$\begin{aligned}
R_*^2&=r^2+a^2-2ar\cos\omega_*,\\
\cos\omega_*&=\cos\theta\cos\alpha+\sin\theta\sin\alpha\cos(\mu-\phi),\\
\Xi_*&=\sin\theta\sin\alpha+\cos\theta\cos\alpha\cos(\mu-\phi),\\
\Lambda_*&=\sin\theta\cos\alpha-\cos\theta\sin\alpha\cos(\mu-\phi),\text{ and}\\
\Omega_*&=\cos\theta\sin\alpha-\sin\theta\cos\alpha\cos(\mu-\phi).
\end{aligned}\tag{4.5}$$

The evaluation of the integrals occurring in (4.4) will be difficult, or impossible, in finite

terms, unless F_r and F_θ have the form of trigonometric polynomials. More general functions F_r and F_θ may be replaced by their Fourier series expansions. This leads to an infinite series for each displacement component, the terms of which contain integrals evaluable in terms of complete elliptic integrals of the first and second kinds. The process of such evaluation involves the use of recursion formulas which lead to extremely long and cumbersome expressions. We shall therefore restrict our consideration to the case in which the components $F_r^{(c)}$ and $F_\theta^{(c}$ are constant. This does not mean that the direction of the force is the same at every point of the ring, but that at every point it lies in the plane of the point and the x_3 axis, and has the same orientation in this plane. (See fig. 1.) If we denote the magnitude of this force by P and its angle with the r-direction by β, where the positive sense of β is the same as that of θ, then $F_r=P\cos\beta$ and $F_\theta=P\sin\beta$, and (4.4) may be written as

$$\begin{aligned} v_r&=AP\int_0^{2\pi}\frac{1}{R_*}\left\{Bg_1+\frac{1}{R_*^2}(r-a\cos\omega_*)(rg_1-a\cos\omega_*)\right\}d\mu,\\ v_\theta&=AP\int_0^{2\pi}\frac{1}{R_*}\left\{Bg_2+\frac{a}{R_*^2}\Lambda_*(rg_1-a\cos\omega_*)\right\}d\mu, \end{aligned} \tag{4.6}$$

where

$$\begin{aligned} g_1(\theta,\phi,\alpha,\beta,\mu)&=\cos(\alpha+\beta)\cos\theta+\sin(\alpha+\beta)\sin\theta\cos(\mu-\phi),\\ g_2(\theta,\phi,\alpha,\beta,\mu)&=-\cos(\alpha+\beta)\sin\theta+\sin(\alpha+\beta)\cos\theta\cos(\mu-\phi). \end{aligned} \tag{4.7}$$

The third integral of (4.4) vanishes, since the integrand is an odd function with respect to $\mu=\pi$. It is now convenient to introduce nondimensional quantities η and h defined by

$$r=\eta a, \qquad R_*=ah. \tag{4.8}$$

Thus

$$h^2=1+\eta^2-2\eta\cos\omega_*, \tag{4.9}$$

and (4.6) become

$$\begin{aligned} v_r&=\frac{AP}{a}\int_0^{2\pi}\frac{1}{h}\left\{Bg_1+\frac{1}{h^2}(\eta-\cos\omega_*)(\eta g_1-\cos\omega_*)\right\}d\mu,\\ v_\theta&=\frac{AP}{a}\int_0^{2\pi}\frac{1}{h}\left\{Bg_2+\frac{1}{h^2}a\Lambda_*(\eta g_1-\cos\omega_*)\right\}d\mu. \end{aligned} \tag{4.10}$$

5. Evaluation of the Integrals

When the expressions (4.5) and (4.7) are inserted for Λ_*, g_1 and g_2, it will be seen that v_r and v_θ consist of sums of terms of the form

$$I_n^m(\eta,\theta,\phi,\alpha)=\int_0^{2\pi}\frac{\cos^m(\mu-\phi)d\mu}{[1+\eta^2-2\eta\cos\omega_*]^{\frac{n}{2}}}, \qquad m=0,1,2; \quad n=1,3, \tag{5.1}$$

with coefficients which are functions of α, β, θ, and η. If we let

$$p^2=h^2_{\max}=1+\eta^2-2\eta\cos(\alpha+\theta), \quad q^2=h^2_{\min}=1+\eta^2-2\eta\cos(\alpha-\theta), \tag{5.2}$$

then

$$h^2=p^2\sin^2\frac{\mu-\phi}{2}+q^2\cos^2\frac{\mu-\phi}{2},$$

and it is easy to show that

$$I_n^m=2\int_0^{2\pi}\frac{\cos^m\xi d\xi}{\left[p^2\sin^2\frac{\xi}{2}+q^2\cos^2\frac{\xi}{2}\right]^{\frac{n}{2}}}. \tag{5.3}$$

These integrals are evaluable in terms of complete elliptic integrals of the first and second kinds [8]; specifically,

$$\begin{aligned}
I_1^0&=\frac{4}{p}F\left(\frac{\pi}{2},k\right),\\
I_3^0&=\frac{4}{p^3k'^2}E\left(\frac{\pi}{2},k\right),\\
I_1^1&=\frac{4}{p}\left[\frac{1+k'^2}{k^2}F\left(\frac{\pi}{2},k\right)-\frac{2}{k^2}E\left(\frac{\pi}{2},k\right)\right],\\
I_3^1&=\frac{4}{p^3}\left[\frac{1+k'^2}{k^2k'^2}E\left(\frac{\pi}{2},k\right)-\frac{2}{k^2}F\left(\frac{\pi}{2},k\right)\right],\\
I_3^2&=\frac{4}{p^3}\left[\frac{(1+k'^2)^2+4k'^2}{k^4k'^2}E\left(\frac{\pi}{2},k\right)-4\frac{1+k'^2}{k^4}F\left(\frac{\pi}{2},k\right)\right].
\end{aligned} \tag{5.4}$$

where $k=[(p^2-q^2)/p^2]^{\frac{1}{2}}$ is the modulus of the functions E and F, and $k^2+k'^2=1$. Using these quantities, the final form of the displacements is found to be

$$\begin{aligned}
u_r=\frac{4AP}{ap}\Bigg\{&B(K_1F-2\sin\theta\sin(\alpha+\beta))\frac{E}{k^2}\\
&+\frac{1}{p^2}\left[\frac{E}{k'^2}\left(K_1\eta^2+[\cos\beta-\eta K_1]K_2-\frac{4k'^2\eta}{k^4}\sin^2\theta\sin\alpha\sin(\alpha+\beta)\right)\right.\\
&\left.\left.-\frac{2F}{k^2}\left(\sin\theta[\sin\alpha\cos\beta+\eta^2\sin(\alpha+\beta)]-\eta\sin\theta[K_1\sin\alpha+K_2\sin(\alpha+\beta)]\right)\right]\right\},
\end{aligned}$$

$$\begin{aligned}
u_\theta=\frac{4AP}{ap}\Bigg\{&B\left(K_3F-2\cos\theta\sin(\alpha+\beta)\frac{E}{k^2}\right)+\frac{1}{p^2}\left[\frac{E}{k'^2}\left([\cos\beta-\eta K_1]K_4-\frac{4k'^2\eta}{k^4}\sin\theta\cos\theta\sin(\alpha+\beta)\right)\right.\\
&\left.+\frac{2F}{k^2}(-\cos\theta\sin\alpha\cos\beta+\eta[K_1\cos\theta\sin\alpha+K_4\sin\theta\sin(\alpha+\beta)])\right]\Bigg\}
\end{aligned}$$

where we have introduced the abbreviations

$$\begin{aligned}
K_1&=\cos\theta\cos(\alpha+\beta)+\frac{1+k'^2}{2}\sin\theta\sin(\alpha+\beta),\\
K_2&=\cos\theta\cos\alpha+\frac{1+k'^2}{k^2}\sin\theta\sin\alpha,\\
K_3&=-\sin\theta\cos(\alpha+\beta)+\frac{1+k'^2}{k^2}\cos\theta\sin(\alpha+\beta),\\
K_4&=-\sin\theta\cos\alpha+\frac{1+k'^2}{k^2}\cos\theta\sin\alpha.
\end{aligned} \tag{5.6}$$

In obtaining the results (5.5) the ring has been taken in the most general position in which the force specified acting on it can be written in terms of one coordinate. If we place the ring in a more special position, viz, in the $x_1\,x_2$ plane, center at the origin, then (5.5) and (5.6) become somewhat simpler. Thus

$$v_r=\frac{4Ai'}{ap}\left\{B\left(K_1'F-2\sin\theta\cos\beta\frac{E}{k^2}\right)+\frac{1}{p^2}\left[\frac{E}{k'^2}\left(K_1'\eta^2+[\cos\beta-\eta K_1']K_2'-\frac{4k'^2\eta}{k^4}\sin^2\theta\cos\beta\right)\right.\right.$$
$$\left.\left.-\frac{2F}{k^2}(\sin\theta\cos\beta[1+\eta^2]-\eta\sin\theta[K_1'+K_2'\cos\beta])\right]\right\},$$
$$v_\theta=\frac{4AP}{ap}\left\{B\left(K_3'F-2\cos\theta\cos\beta\frac{E}{k^2}\right)+\frac{1}{p^2}\left[\frac{E}{k'^2}\left([\cos\beta-\eta K_1']K_4'-\frac{4k'^2}{k^4}\eta\sin\theta\cos\theta\cos\beta\right)\right.\right.$$
$$\left.\left.+\frac{2F}{k^2}(-\cos\theta\cos\beta+\eta[K_1'\cos\theta+K_4'\sin\theta\cos\beta])\right]\right\}$$

where

$$K_1'=-\cos\theta\sin\beta+\frac{1+k'^2}{k^2}\sin\theta\cos\beta,$$
$$K_2'=\frac{1+k'^2}{k^2}\sin\theta,\tag{5.8}$$
$$K_3'=\sin\theta\sin\beta+\frac{1+k'^2}{k^2}\cos\theta\cos\beta,$$
$$K_4'=\frac{1+k'^2}{k^2}\cos\theta.$$

6. A Limiting Form of the Displacements

Let the ring be located as above, and let $\beta=\pi/2$. The force P at each point of the ring is now normal to the $x_1\,x_2$ plane and has the sense of decreasing x_3. The distribution thus has a resultant force $2\pi aP=\overline{P}$. At distances far removed from the ring, it may be expected that the distribution on the ring will have essentially the same effect as a concentrated force $\overline{P}$ located at the origin. We show that this is the case.

If we let the point (r,θ,ϕ) recede to infinity, then $\lim_{r\to\infty}1/\eta=0$, and we see from (5.2) that for $r\gg a$

$$p=\eta+\epsilon_1,\quad q=\eta+\epsilon_2\tag{6.1}$$

where $\lim_{r\to\infty}\epsilon_1=\lim_{r\to\infty}\epsilon_2=0$. Moreover,

$$k^2=\frac{p^2-q^2}{p^2}=\frac{4\sin\theta}{\eta}\tag{6.2}$$

from which we see that $\lim_{r\to\infty}k=0$, and hence that for $r\gg a$

$$E\left(\frac{\pi}{2},k\right)=\frac{\pi}{2}+\epsilon_3,\quad F\left(\frac{\pi}{2},k\right)=\frac{\pi}{2}+\epsilon_4,\tag{6.3}$$

$$pk^2=4\sin\theta+\epsilon_5\tag{6.4}$$

where $\lim_{r\to\infty}\epsilon_i=0$, $i=3,4,5$.

Using these results, it can be shown that for $r\gg a$

$$v_r\simeq-A(B+1)\overline{P}\frac{\cos\theta}{r},\quad v_\theta\simeq AB\overline{P}\frac{\sin\theta}{r}.\tag{6.5}$$

If these are converted to cartesian coordinates, we find that for $r \gg a$

$$v_1 \simeq -A\bar{P}\frac{x_1 x_3}{r^3}, \quad v_2 \simeq -A\bar{P}\frac{x_2 x_3}{r^3}, \quad v_3 \simeq -A\bar{P}\left(B\frac{1}{r}+\frac{x^2}{r^3}\right). \tag{6.6}$$

The right-hand members are the displacements produced in an infinite elastic medium by a concentrated force $\bar{P}$ at the origin directed along the negative x_3 axis [3].

7. References

[1] Sir William Thomson, Cambridge & Dublin Mathematical Journal, 1848; Mathematical & Physical Papers, vol. 1, p. 97.

[2] A. E. H. Love, Mathematical theory of elasticity, 4th ed. (Cambridge Press, 1927).

[3] I. S. Sokolnikoff, Mathematical theory of elasticity, 2d ed. (McGraw-Hill, 1956).

[4] J. Boussinesq, Applications des potentiel à l'étude de l'équilibre et du mouvement des solides élastiques (Paris, 1885).

[5] J. Dougall, A general method of solving the equations of elasticity, Proc. Edinburgh Mathematical Soc. 16, 82 (1898).

[6] R. Mindlin, Force at a point in the interior of a semi-infinite solid, Physics, 7, 195 (1936).

[7] A. E. H. Love, A treatise on the mathematical theory of elasticity, 4th ed. (reprinted by Dover Publications, New York, N. Y., 1944).

[8] P. F. Byrd and M. D. Friedman, Handbook of Elliptic Integrals for Engineers and Physicists (Springer, Berlin, Germany, 1954).

Washington, June 19, 1957.

Journal of Research of the National Bureau of Standards Vol. 60, No. 4, April 1958 Research Paper 2856

Description and Analysis of the Second Spectrum of Molybdenum, Mo II

C. C. Kiess

Wavelengths and estimated intensities are presented for 3,800 lines of Mo II in the spectral range from 6100 A in the red to 1550 A in the ultraviolet. For approximately 970 of these lines, Zeeman patterns have been measured. Analysis of these spectral data shows that about 70 percent of the lines can be accounted for as transitions between levels of the even terms in the electron configurations $4d^5$ and $4d^4\ 5s$, and levels of the odd terms in the configuration $4d^4\ 5p$. No series have been found from which an ionization potential can be derived.

1. Introduction

The description and analysis of the second spectrum of molybdenum presented in this paper are the results of investigations that for more than three decades have been in progress at the National Bureau of Standards. Work on the analysis of the molybdenum spectra was begun here shortly after similar work on the chromium spectra had been initiated, when it was realized that spectral structures like those of chromium should occur also in the spectra of its homologue molybdenum. A brief search through the spectroscopic data available at that time for molybdenum readily brought to light the expected structures. Subsequently these were published [1][1] in illustration of the operation of the spectroscopic displacement and alternation laws among the elements of the second long period of Mendeléeff's table.

This earlier phase of the work demonstrated the need for better descriptions of the molybdenum spectra than existed at that time. Many of the weaker lines, which are essential to the thorough analysis of a rich-lined spectrum, were missing from the published wavelength lists; and the intensities of the lines, estimated on a compressed scale, were inadequate for the finer discrimination of apparently related spectral regularities. Such Zeeman-effect observations as were available extended over only a limited range of wavelengths and, with a few exceptions, gave unresolved patterns for many of the lines. In view of these circumstances, it was decided to make a new description of the molybdenum spectra throughout the range accessible to photographic recording with the spectrographs at the Bureau.

2. Experimental Procedure

The spectrographic equipment of the Bureau has been described in detail in earlier papers [2]. The three concave gratings, of 21-ft radius of curvature, used in this work, were the ones ruled with 7,500, 20,000, and 30,000 lines/in. by J. A. Anderson, H. A. Rowland, and R. W. Wood, respectively. They were mounted according to the Wadsworth style, and recorded the spectra from 1975 A in the ultraviolet to 12000 A in the infrared. First-order spectra were obtained with each of the gratings, but, wherever possible, second- and, in a few cases, third-order spectra also were obtained with the Rowland and Wood gratings. The first-order dispersions of these gratings are 10, 3.5, and 2 A/mm, respectively. A set of spectrograms covering the region shortward of 3000 A was obtained with the quartz-prism spectrographs. Hilger's E 1 instrument was used for the range 2150 to 1975 A, with an average dispersion of 1 A/mm; the E 185 instrument was used for wavelengths from 3000 to 2100 A, with dispersion ranging from 1 A/mm to 0.3 A/mm.

The plates for recording the spectra were selected from the varieties offered in the Eastman Kodak Co. (EK) catalog. For the earlier observations, the EK 33 emulsions were used, sensitized in dye solutions, when necessary, for the longer wavelength regions beyond the reach of ordinary plates. For the later observations, the EK sensitizings appropriate to the various spectral regions were used. For the ultraviolet shorter than 2300 A, Schumann plates supplied by Hilger were used.

The electrodes for both the arc and spark exposures were cut from rods of very pure molybdenum metal about 5 mm in diameter. To the Research Laboratory of the General Electric Co., we are indebted for the electrode material used in the earlier observations; and to the Climax Molybdenum Co. for the material used in the later series of observations. The only impurities detected were traces of iron, and possibly silicon.

For the arc spectra, the exposures were made to arcs-in-air, and to arcs in an enclosed chamber, of the type described by Curtis [3], in which the pressure could be reduced or in which an atmosphere of inert gases could be maintained. The arcs were operated at 5 or 6 amp from 220-v d-c mains. For the spark spectra, the exposures were made to sparks-in-air, or in the enclosed chamber used in the work on chromium. The spark discharges were supplied by a battery of condensers of 0.006 μf capacitance that was charged up to 30,000 v from the secondary coil of a transformer of which the primary coil carried 110-v ac. In the case of the arc spectrum, the object of enclosing the arc was to reduce the intensity of the molybdenum oxide bands that black out a considerable portion of the spectrum when the arc is operated in air. In the case of the spark

[1] Figures in brackets indicate the literature references at the end of this paper.

spectrum, enclosure of the spark in an inert gas or in air at lowered pressure reduced the intensity and diffuseness of the atmospheric lines that are always present in spectrograms of a spark in air. In both cases, enclosure of the light source at reduced pressure sharpens the spectral lines, which enhances the accuracy of measurement of lines that are diffuse or asymmetrical. All exposures to the molybdenum sources were made in juxtaposition to exposures of the iron arc as the source of the standards for wavelength determinations. In the extreme ultraviolet, where the lines of iron are weak or insufficient in number, electrodes of copper-silver alloy were used for the comparison spectrum. The wavelengths of the standard copper lines were those published by Burns and Walters [4].

Measurements of the plates, on which this investigation is based, were made by the author in cooperation with C. L. Zimmerman [5]. In addition to the spectrograms made at the Bureau, there were available for measurement several spectrograms of the region shortward of 2000 A made with vacuum spectrographs, by A. G. Shenstone at Princeton, University, and J. C. Boyce at the Massachusetts Institute of Technology (MIT). The scale of the plates obtained with these spectrographs is practically the same, about 4.2 A/mm.

In addition to an accurate and homogeneous set of wavelengths and reliable estimates of intensities, an analysis of a complex spectrum requires also a knowledge of the patterns of the lines in magnetic fields. Two sets of observations of the Zeeman effect of molybdenum have been made for this investigation. One set of plates covering the spectral range from 2250 A to 7500 A was made with the water-cooled Weiss magnet of the Bureau. In a pole gap of 6 mm, a field of 35,000 oersteds was attained with a current of 180 amp in the coils under a potential of 90 v. The other set of Zeeman-effect plates was obtained with the Bitter magnet and the spectrographs of MIT. This equipment has been adequately described by G. R. Harrison [6,7] who kindly sent us the molybdenum plates for this investigation. These plates, taken with fields of 86,000 oersteds, cover the range from 2180 A to 8180 A. All the plates of both sets were measured by the author.

3. Results

3.1. Wavelengths and Intensities

The new wavelengths and estimated intensities for lines characteristic of Mo II are recorded in the first two columns of tables 1 and 2. The values adopted for the wavelengths of table 1 are the means of two or more measurements and, in general, are given to the nearest 0.01 A. In many cases, however, for which more than two highly accordant measurements were made, the third decimal place of the mean value has been retained. All the wavelengths in table 1 are their values in air. All the lines listed in table 2 were measured on the spectrograms made with the vacuum spectrographs; but the wavelengths assigned to them are the values calculated from combinations between the terms derived from the analysis of the lines in table 1.

The numbers and letters in the second column of the tables indicate the relative strengths and characteristics of the lines. There are no photometrically-determined intensities known for lines of Mo II, so that it is not possible to compare the visual estimates with measured values. However, there are available at the Bureau, some unpublished estimated intensities made by Meggers for lines emitted by molybdenum arcs relative to lines of calibrated intensity in the copper arc. The lines of Mo II included in his list show a good correlation with the estimated intensities reported in this work, if due allowance is made for differences in mode of excitation.

The letters following the intensities have the following meanings: d=double; e=enhanced at the electrode; h=hazy; H=very hazy; l=shaded longward; s=shaded shortward; w=wide; W=very wide. Lines designated w are probably unresolved pairs, and lack the appearance of diffuseness that is characteristic of those marked h. The letter Z means that a Zeeman pattern, measured on NBS or MIT spectrograms, is recorded for the line in table 3.

3.2. Zeeman Effects

The Zeeman patterns for about 970 lines of Mo II are given in table 3. A dagger (†) indicates that the pattern was measured only on NBS spectrograms; the letters A, B, C, and D indicate the type of shading displayed by unresolved patterns, thus: A=⩘; B=|⩘|; C=∧; D=⊓. The only Zeeman patterns published heretofore for lines of molybdenum are those by Jack [8] and by Wilhelmy [9]. Of the 150 lines measured by Jack, in a field of approximately 25,000 oersteds, about one-third belong to Mo II. His fully resolved patterns are in good agreement with corresponding ones in table 3. Wilhelmy, using a higher field of approximately 35,000 oersteds, likewise got magnetic patterns for about 55 lines of Mo II and thereby established the identity of the low ^6D term of the ion. His results also are in very good agreement with those of table 3.

3.3. Term Structures of Mo II

The first multiplets of Mo II were announced in 1926, by Meggers and Kiess [1], as part of the evidence for the operation of the spectroscopic displacement law in the second long period of the periodic table. Although the unraveling of the spectrum has continued steadily since that time, no other results have been reported from the Bureau. In the meantime, additional terms and classified lines have been announced by Schauls and Sawyer [10] and by V. R. Rao [11]. Some erroneous designations of levels occur, in each of these earlier investigations, which, it is believed, the present analysis corrects.

Theoretically, the singly ionized atom of molybdenum is isoelectronic with the neutral atom of niobium and, therefore, in accordance with the displacement law, the spectra of the two atoms should be similar. Although the term structures of these spectra arise in electron configurations of the same type yet,

owing to differences in the relative importance of these configurations, the spectra Nb I and Mo II have the appearance of being strikingly dissimilar. In atoms with 41 external electrons, 36 are in closed shells. The 5 outermost electrons, which determine the optical properties of the atoms, may assume, on excitation, the various configurational groupings that govern the distribution of radiant energy in the spectrum. The low, even states of the atom are given by the configurations $4d^5$, $4d^4\,5s$, and $4d^3\,5s^2$, whereas the higher, excited, odd states arise in the configurations $4d^4\,5p$ and $4d^3\,5s\,5p$. In Nb I the group $4d^5$ is the least important of the low, even configurations, but in Mo II it is first in importance and $4d^3\,5s^2$ is least. Of the odd configurations, only $4d^4\,5p$ contributes to Mo II, whereas both share prominently in Nb I.

The even and odd terms of Mo II, and the electron configurations in which they arise, are recorded in tables 4 and 5. All but the two highest terms of the configuration $4d^5$ have been found. In the configuration $4d^4\,5s$, all the quartets except the high ^4P, and most of the doublets have been found. None of the terms of the configuration $4d^3\,5s^2$, which is so prominent in Nb I, have been located. The only odd terms that have been established belong to the configuration $4d^4\,5p$. Table 6 lists the terms that are theoretically possible for Mo II, those actually found being designated in bold-faced type. The g values assigned to each level are, in general, the means of several determinations.

The assignment of the various terms to the electron configurations to which they belong presents no difficulty for the lower members of a configurational group. In general, the intervals between the levels of the $4d^5$ terms are smaller than those of the $4d^4\,5s$ terms, and exhibit partial inversions. But in the higher members of a family of terms, these characteristics are not so evident, and reliance has been placed on theoretical calculations of the origin and energy of the expected terms. Such calculations have been made for this investigation by Goldgraber [12] for the low, even terms of the configurations $4d^5$ and $4d^4\,5s$, and by Trees [13] for the odd $4d^4\,5p$ terms.

3.4. Series and Ionization Potential

No series of two or more members have been found in Mo II, and therefore it is not yet possible to calculate an ionization potential for the singly ionized molybdenum atom from experimental data derived from the atom itself. But from similarities that exist in the term structure of neighboring atoms for which good spectral series have been worked out, it is possible to derive closely approximate values for series limits and ionization potentials for atoms for which these values are not directly available. This has been done by Catalán and Rico [14] for some of the neutral and singly ionized atoms of the second long period of elements. In a subsequent revision of this work they [15] give 130,300 cm^{-1} for the separation of the ground states of Mo II and Mo III, which corresponds to an ionization potential of 16.15 ev.

Over the long period during which this work has been in progress, it has been aided in various ways by several individuals. A. G. Shenstone and J. C. Boyce have sent their spectrograms of the extreme ultraviolet spectra of molybdenum, and G. R. Harrison has sent his spectrograms of the Zeeman patterns. C. L. Zimmerman measured and reduced most of the spectrograms of the ultraviolet region. In the reductions of many of the other spectrograms, Miss M. M. Harvey and W. Lyle took part. Finally, H. D. Goldgraber and R. E. Trees contributed greatly to the theoretical interpretation and configurational assignment of the energy states. To each of them it is a pleasure to express appreciation for contributions to this work.

4. References

[1] W. F. Meggers and C. C. Kiess, J. Opt. Soc. Am. **12,** 417 (1926).
[2] W. F. Meggers and K. Burns, BS Sci. Pap. **18,** 191 (1922) S441.
[3] H. D. Curtis, J. Opt. Soc. Am. **8,** 697 (1924).
[4] K. Burns and F. M. Walters, Jr., Publ. Allegheny Observatory, Univ. Pittsburgh **8,** 27 (1930).
[5] C. L. Zimmerman, Dissertation (Duke Univ., Durham, N. C., 1937).
[6] G. R. Harrison and F. Bitter, Phys. Rev. **57,** 15 (1940).
[7] G. R. Harrison and J. R. McNally, Jr., Phys. Rev. **58,** 703 (1940).
[8] R. Jack, Ann. Physik **IV 28,** 1032 (1909).
[9] E. Wilhelmy, Ann. Physik **IV 80,** 305 (1926).
[10] R. Schauls and R. A. Sawyer, Phys. Rev. **58,** 781 (1940).
[11] V. R. Rao, Indian J. Phys. **23,** 387 (1949).
[12] H. D. Goldgraber, University of Pennsylvania dissertation (1953).
[13] R. E. Trees (private communication).
[14] M. A. Catalán and F. R. Rico, An. Españ. Soc. Fis. Quim. [**A**] **48,** 328 (1952).
[15] F. R. Rico (letter, dated Dec. 12, 1956).

TABLE 1. *Wavelengths and term combinations of* Mo II

Wavelength λ_{air}	Intensity	Wave No.	Term combination	Wavelength λ_{air}	Intensity	Wave No.	Term combination
6083. 68	1	16432. 88	$c\ ^4D_{2\frac{1}{2}}$—$z\ ^6D^0_{3\frac{1}{2}}$	5835. 525	5	17131. 67	
5914. 066	8	16904. 17	$c\ ^4F_{4\frac{1}{2}}$—$z\ ^4G^0_{5\frac{1}{2}}$	5831. 593	2	17143. 22	$d\ ^2F_{3\frac{1}{2}}$—$z\ ^2G^0_{3\frac{1}{2}}$
5905. 348	20	16929. 12					
5885. 121	10	16987. 31		5827. 136	7	17156. 33	$b\ ^2G_{3\frac{1}{2}}$—$z\ ^6D^0_{3\frac{1}{2}}$ $c\ ^4D_{3\frac{1}{2}}$—$z\ ^6D^0_{4\frac{1}{2}}$
5871. 014	1	17028. 12	$c\ ^4D_{3\frac{1}{2}}$—$z\ ^6D^0_{3\frac{1}{2}}$	5788. 455	3	17270. 98	$b\ ^4F_{2\frac{1}{2}}$—$z\ ^6F^0_{1\frac{1}{2}}$
5862. 68	1	17052. 33	$c\ ^4D_{1\frac{1}{2}}$—$z\ ^6D^0_{2\frac{1}{2}}$	5775. 674	3	17309. 20	$d\ ^2G_{3\frac{1}{2}}$—$z\ ^4G^0_{3\frac{1}{2}}$
5862. 22	1	17053. 67		5774. 314	2	17313. 27	$a\ ^2P_{1\frac{1}{2}}$—$z\ ^4F^0_{2\frac{1}{2}}$
5851. 76	3	17084. 15		5754. 46	2	17373. 01	$d\ ^2G_{4\frac{1}{2}}$—$z\ ^4I^0_{5\frac{1}{2}}$

Wavelength λ_{air}	Intensity	Wave No.	Term combination
5719.93	7	17477.88	$c\ ^4D_{0\frac{1}{2}}-z\ ^4F^\circ_{1\frac{1}{2}}$
5693.56	1	17558.83	$b\ ^2G_{3\frac{1}{2}}-z\ ^6D^\circ_{4\frac{1}{2}}$
5644.956	2	17710.01	$d\ ^2F_{3\frac{1}{2}}-y\ ^4D^\circ_{3\frac{1}{2}}$
5601.400	3	17847.72	$c\ ^4D_{1\frac{1}{2}}-z\ ^4F^\circ_{1\frac{1}{2}}$
5596.98	1	17861.82	
5596.723	4	17862.64	$c\ ^4D_{2\frac{1}{2}}-z\ ^4F^\circ_{2\frac{1}{2}}$
5559.88	1	17981.01	$d\ ^2F_{3\frac{1}{2}}-z\ ^2G^\circ_{4\frac{1}{2}}$
5490.785	8*Z*	18207.27	$c\ ^4D_{1\frac{1}{2}}-z\ ^4F^\circ_{2\frac{1}{2}}$
5469.04	1	18279.67	$c\ ^4F_{4\frac{1}{2}}-x\ ^4D^\circ_{3\frac{1}{2}}$
5448.797	15*Z*	18347.57	$c\ ^4D_{2\frac{1}{2}}-z\ ^4F^\circ_{3\frac{1}{2}}$
5389.72	1	18548.68	
5342.098	4	18714.03	$d\ ^2D_{2\frac{1}{2}}-z\ ^2G^\circ_{3\frac{1}{2}}$
5334.28	7	18741.46	$c\ ^4F_{4\frac{1}{2}}-y\ ^4G^\circ_{4\frac{1}{2}}$
5318.665	2	18796.48	
5317.62	1	18800.18	
5291.62	2	18892.55	$c\ ^4F_{4\frac{1}{2}}-y\ ^4F^\circ_{3\frac{1}{2}}$
5290.29	1	18897.30	$c\ ^2D_{1\frac{1}{2}}-y\ ^4D^\circ_{1\frac{1}{2}}$
5268.58	5	18975.17	$d\ ^2F_{2\frac{1}{2}}-x\ ^4D^\circ_{2\frac{1}{2}}$
5265.38	1	18986.70	$b\ ^4P_{1\frac{1}{2}}-z\ ^6F^\circ_{2\frac{1}{2}}$
5263.02	2	18995.21	$c\ ^4F_{4\frac{1}{2}}-y\ ^4G^\circ_{5\frac{1}{2}}$
5221.678	2	19145.60	$b\ ^4F_{2\frac{1}{2}}-z\ ^4P^\circ_{1\frac{1}{2}}$
5214.805	4	19170.84	
5181.543	40*Z*	19293.90	$c\ ^4D_{3\frac{1}{2}}-z\ ^4F^\circ_{4\frac{1}{2}}$
5113.41	5	19550.97	$d\ ^2F_{2\frac{1}{2}}-y\ ^4G^\circ_{3\frac{1}{2}}$
5108.13	6	19571.18	$c\ ^4F_{4\frac{1}{2}}-y\ ^4F^\circ_{4\frac{1}{2}}$; $d\ ^2D_{2\frac{1}{2}}-z\ ^2D^\circ_{2\frac{1}{2}}$
5105.58	7	19580.96	$b\ ^4P_{1\frac{1}{2}}-z\ ^4P^\circ_{0\frac{1}{2}}$
5103.57	1	19588.67	$b\ ^2G_{4\frac{1}{2}}-z\ ^4F^\circ_{4\frac{1}{2}}$
5082.63	3	19669.37	
5039.35	12	19838.30	$c\ ^2G_{4\frac{1}{2}}-z\ ^4H^\circ_{3\frac{1}{2}}$; $b\ ^4P_{2\frac{1}{2}}-z\ ^4P^\circ_{2\frac{1}{2}}$
5030.53	3	19873.09	$b\ ^2S_{0\frac{1}{2}}-z\ ^2P^\circ_{1\frac{1}{2}}$
5029.89	4	19875.61	
4970.25	10	20114.10	$c\ ^4F_{4\frac{1}{2}}-x\ ^4F^\circ_{4\frac{1}{2}}$
4954.15	7	20179.46	
4943.62	2	20222.46	$b\ ^2S_{0\frac{1}{2}}-z\ ^2P^\circ_{0\frac{1}{2}}$; $c\ ^2D_{2\frac{1}{2}}-z\ ^2G^\circ_{3\frac{1}{2}}$
4927.43	2	20288.89	
4921.66	2	20312.68	
4921.24	2	20314.41	$b\ ^4G_{5\frac{1}{2}}-z\ ^6D^\circ_{4\frac{1}{2}}$
4919.27	2	20322.55	$d\ ^2G_{3\frac{1}{2}}-x\ ^4D^\circ_{3\frac{1}{2}}$
4918.60	4	20325.31	$d\ ^2D_{2\frac{1}{2}}-z\ ^2P^\circ_{1\frac{1}{2}}$
4909.80	6	20361.74	
4903.55	5	20387.69	
4901.79	7	20395.02	$b\ ^4P_{1\frac{1}{2}}-z\ ^4P^\circ_{1\frac{1}{2}}$
4878.62	2	20491.88	$b\ ^4F_{3\frac{1}{2}}-z\ ^6P^\circ_{3\frac{1}{2}}$; $b\ ^4G_{4\frac{1}{2}}-z\ ^6D^\circ_{4\frac{1}{2}}$
4856.14	5	20586.74	$b\ ^4P_{2\frac{1}{2}}-z\ ^6P^\circ_{2\frac{1}{2}}$
4853.63	50*Z*	20597.38	$c\ ^2D_{1\frac{1}{2}}-z\ ^2D^\circ_{1\frac{1}{2}}$
4841.96	5	20647.02	$d\ ^2G_{4\frac{1}{2}}-y\ ^4G^\circ_{4\frac{1}{2}}$
4754.34	7*w*	21027.53	$d\ ^2F_{2\frac{1}{2}}-z\ ^2F^\circ_{2\frac{1}{2}}$
4748.71	3	21052.46	$d\ ^2D_{1\frac{1}{2}}-(1)^\circ_{2\frac{1}{2}}$
4744.64	4	21070.52	$c\ ^4F_{4\frac{1}{2}}-y\ ^2H^\circ_{4\frac{1}{2}}$; $d\ ^2D_{2\frac{1}{2}}-x\ ^4D^\circ_{3\frac{1}{2}}$
4742.61	50*Z*	21079.54	$c\ ^2D_{2\frac{1}{2}}-z\ ^2D^\circ_{2\frac{1}{2}}$
4722.38	3	21169.84	$b\ ^4P_{2\frac{1}{2}}-z\ ^6D^\circ_{1\frac{1}{2}}$
4721.61	3*s*	21173.29	$d\ ^2D_{2\frac{1}{2}}-(1)^\circ_{2\frac{1}{2}}$
4721.09	3	21175.62	$d\ ^2F_{3\frac{1}{2}}-x\ ^4F^\circ_{2\frac{1}{2}}$
4717.01	2	21193.94	$b\ ^4D_{1\frac{1}{2}}-z\ ^6F^\circ_{0\frac{1}{2}}$
4715.86	2	21199.11	
4712.86	5	21212.60	$c\ ^4F_{4\frac{1}{2}}-y\ ^2H^\circ_{5\frac{1}{2}}$
4667.40	15*Z*	21419.23	$b\ ^4P_{0\frac{1}{2}}-z\ ^4P^\circ_{1\frac{1}{2}}$
4656.32	8	21470.17	
4653.94	1*h*	21481.18	$b\ ^4D_{0\frac{1}{2}}-z\ ^6F^\circ_{0\frac{1}{2}}$
4637.95	8*Z*	21555.22	$b\ ^4P_{2\frac{1}{2}}-z\ ^6D^\circ_{2\frac{1}{2}}$
4635.89	5*w*	21564.79	
4622.80	12	21625.85	$c\ ^2G_{4\frac{1}{2}}-z\ ^4I^\circ_{4\frac{1}{2}}$
4613.08	3	21671.44	$b\ ^4F_{4\frac{1}{2}}-z\ ^6D^\circ_{4\frac{1}{2}}$
4612.59	1	21673.74	$b\ ^4G_{2\frac{1}{2}}-z\ ^4F^\circ_{1\frac{1}{2}}$
4610.56	7	21683.26	$d\ ^2D_{2\frac{1}{2}}-y\ ^4F^\circ_{3\frac{1}{2}}$
4604.20	10*w*, *Z*	21713.24	$b\ ^4G_{3\frac{1}{2}}-z\ ^4F^\circ_{2\frac{1}{2}}$
4590.96	5*h*	21775.84	$b\ ^4D_{0\frac{1}{2}}-z\ ^6F^\circ_{1\frac{1}{2}}$
4580.92	7	21823.56	$d\ ^2G_{4\frac{1}{2}}-z\ ^2H^\circ_{4\frac{1}{2}}$
4578.80	7	21833.66	$c\ ^2D_{2\frac{1}{2}}-z\ ^2P^\circ_{1\frac{1}{2}}$; $d\ ^2G_{4\frac{1}{2}}-y\ ^4H^\circ_{5\frac{1}{2}}$
4575.24	5	21850.65	$d\ ^2D_{1\frac{1}{2}}-y\ ^4F^\circ_{2\frac{1}{2}}$
4566.19	2	21893.96	$d\ ^2F_{2\frac{1}{2}}-y\ ^2F^\circ_{3\frac{1}{2}}$
4565.69	8*Z*	21896.38	$d\ ^2G_{4\frac{1}{2}}-x\ ^4F^\circ_{3\frac{1}{2}}$
4559.32	3	21926.97	
4553.501	10*Z*	21954.99	$b\ ^4D_{1\frac{1}{2}}-z\ ^6F^\circ_{2\frac{1}{2}}$
4543.40	8*Z*	22003.80	$b\ ^4G_{4\frac{1}{2}}-z\ ^4F^\circ_{3\frac{1}{2}}$
4519.599	15*Z*	22119.67	$b\ ^4D_{2\frac{1}{2}}-z\ ^6F^\circ_{3\frac{1}{2}}$
4508.696	5	22173.16	$c\ ^2G_{4\frac{1}{2}}-z\ ^4G^\circ_{4\frac{1}{2}}$
4503.56	4	22198.45	$b\ ^4G_{3\frac{1}{2}}-z\ ^4F^\circ_{3\frac{1}{2}}$; $b\ ^2F_{3\frac{1}{2}}-z\ ^6P^\circ_{2\frac{1}{2}}$
4500.47	8	22213.69	$c\ ^2D_{1\frac{1}{2}}-y\ ^4P^\circ_{1\frac{1}{2}}$; $a\ ^4F_{2\frac{1}{2}}-z\ ^6F^\circ_{1\frac{1}{2}}$
4498.12	4*s*	22225.30	$d\ ^2G_{3\frac{1}{2}}-z\ ^2F^\circ_{2\frac{1}{2}}$
4493.49	10	22248.20	$c\ ^2G_{3\frac{1}{2}}-z\ ^4I^\circ_{4\frac{1}{2}}$
4489.30	5	22268.96	$d\ ^2F_{3\frac{1}{2}}-y\ ^2F^\circ_{3\frac{1}{2}}$
4482.58	2	22302.34	
4463.85	8	22395.92	$a\ ^2F_{2\frac{1}{2}}-z\ ^6F^\circ_{3\frac{1}{2}}$
4452.76	8	22451.68	$b\ ^2G_{4\frac{1}{2}}-z\ ^4D^\circ_{3\frac{1}{2}}$; $b\ ^4G_{3\frac{1}{2}}-z\ ^4F^\circ_{3\frac{1}{2}}$
4452.02	20*Z*	22455.41	$d\ ^2D_{2\frac{1}{2}}-z\ ^2F^\circ_{3\frac{1}{2}}$; $a\ ^2G_{3\frac{1}{2}}-z\ ^4P^\circ_{2\frac{1}{2}}$
4445.33	2	22489.20	$b\ ^4F_{1\frac{1}{2}}-z\ ^4F^\circ_{1\frac{1}{2}}$
4439.50	3	22518.74	
4433.49	100*Z*	22549.26	$b\ ^4D_{1\frac{1}{2}}-z\ ^4P^\circ_{0\frac{1}{2}}$
4430.50	2	22564.50	$b\ ^4P_{1\frac{1}{2}}-z\ ^6D^\circ_{1\frac{1}{2}}$
4417.83	1	22629.21	$b\ ^4G_{4\frac{1}{2}}-z\ ^4F^\circ_{4\frac{1}{2}}$
4412.22	2	22657.96	$b\ ^4D_{3\frac{1}{2}}-z\ ^6F^\circ_{4\frac{1}{2}}$
4407.377	10*Z*	22682.86	$d\ ^2G_{3\frac{1}{2}}-y\ ^2G^\circ_{3\frac{1}{2}}$
4404.188	5	22699.28	$b\ ^2F_{2\frac{1}{2}}-z\ ^6D^\circ_{2\frac{1}{2}}$
4403.287	8*Z*	22703.93	$c\ ^2G_{3\frac{1}{2}}-z\ ^2G^\circ_{3\frac{1}{2}}$
4390.912	5	22767.92	$d\ ^2G_{4\frac{1}{2}}-z\ ^2H^\circ_{5\frac{1}{2}}$
4388.265	8*Z*	22781.65	$d\ ^2D_{2\frac{1}{2}}-x\ ^4F^\circ_{3\frac{1}{2}}$
4385.578	8	22795.61	$c\ ^2G_{3\frac{1}{2}}-z\ ^4G^\circ_{4\frac{1}{2}}$
4377.752	100*Z*	22836.36	$b\ ^4D_{0\frac{1}{2}}-z\ ^4P^\circ_{0\frac{1}{2}}$
4374.66	1	22852.50	$c\ ^2D_{1\frac{1}{2}}-z\ ^2P^\circ_{0\frac{1}{2}}$; $d\ ^2D_{1\frac{1}{2}}-z\ ^2F^\circ_{2\frac{1}{2}}$
4374.099	5	22855.42	$b\ ^4F_{2\frac{1}{2}}-z\ ^4F^\circ_{2\frac{1}{2}}$
4363.638	100*Z*	22910.22	$b\ ^4D_{2\frac{1}{2}}-z\ ^4P^\circ_{1\frac{1}{2}}$
4361.914	30*Z*	22919.27	$c\ ^2G_{4\frac{1}{2}}-z\ ^2G^\circ_{4\frac{1}{2}}$
4358.272	50*Z*	22938.43	$c\ ^2F_{3\frac{1}{2}}-z\ ^4I^\circ_{4\frac{1}{2}}$
4356.100	10*Z*	22949.86	$b\ ^4P_{1\frac{1}{2}}-z\ ^6D^\circ_{2\frac{1}{2}}$
4355.26	4	22954.29	$d\ ^2G_{4\frac{1}{2}}-y\ ^2F^\circ_{3\frac{1}{2}}$
4328.009	20*Z*	23098.82	$c\ ^2D_{1\frac{1}{2}}-x\ ^4D^\circ_{2\frac{1}{2}}$
4325.27	2	23113.44	$d\ ^2G_{3\frac{1}{2}}-y\ ^2H^\circ_{4\frac{1}{2}}$
4315.230	10*Z*	23167.22	$b\ ^2F_{1\frac{1}{2}}-z\ ^6D^\circ_{2\frac{1}{2}}$

Wavelength λ_{air}	Intensity	Wave No.	Term combination	Wavelength λ_{air}	Intensity	Wave No.	Term combination
4312. 46	3	23182. 10	$c\ ^2D_{1\frac{1}{2}}$—$y\ ^4P^o_{2\frac{1}{2}}$	4108. 657	2	24332. 01	
4312. 38	1	23182. 53	$b\ ^4F_{4\frac{1}{2}}$—$z\ ^4F^o_{3\frac{1}{2}}$	4106. 60	1	24344. 20	$a\ ^2D_{1\frac{1}{2}}$—$z\ ^4P^o_{0\frac{1}{2}}$
4311. 649	40Z	23186. 46	$a\ ^2F_{2\frac{1}{2}}$—$z\ ^4P^o_{1\frac{1}{2}}$	4105. 44	3	24351. 08	$a\ ^2F_{3\frac{1}{2}}$—$z\ ^4P^o_{2\frac{1}{2}}$
4311. 041	40Z	23189. 73	$c\ ^2F_{2\frac{1}{2}}$—$z\ ^4G^o_{3\frac{1}{2}}$	4100. 303	5Z	24381. 58	$b\ ^4D_{1\frac{1}{2}}$—$z\ ^6P^o_{1\frac{1}{2}}$
4310. 63	2	23191. 94	$c\ ^2D_{2\frac{1}{2}}$—$y\ ^4F^o_{3\frac{1}{2}}$	4098. 46	1	24392. 55	$b\ ^2I_{6\frac{1}{2}}$—$z\ ^4H^o_{7\frac{1}{2}}$
4303. 87	4	23228. 37	$b\ ^4F_{3\frac{1}{2}}$—$z\ ^4F^o_{3\frac{1}{2}}$	4095. 55	2	24409. 88	$d\ ^2D_{2\frac{1}{2}}$—(3)$^o_{3\frac{1}{2}}$ $d\ ^2G_{4\frac{1}{2}}$—$w\ ^4D^o_{3\frac{1}{2}}$
4291. 53	2l	23295. 16	$b\ ^2F_{3\frac{1}{2}}$—$z\ ^6D^o_{3\frac{1}{2}}$	4094. 965	10Z	24413. 37	$c\ ^2F_{2\frac{1}{2}}$—$y\ ^4D^o_{3\frac{1}{2}}$
4283. 28	4	23340. 05	$b\ ^4F_{2\frac{1}{2}}$—$z\ ^4F^o_{3\frac{1}{2}}$	4090. 994	3	24437. 06	$d\ ^2G_{4\frac{1}{2}}$—$x\ ^4G^o_{5\frac{1}{2}}$
4281. 22	10	23351. 26	$c\ ^2D_{1\frac{1}{2}}$— (1)$^o_{2\frac{1}{2}}$	4084. 00	2h	24478. 89	
4280. 57	2	23354. 80	$b\ ^2I_{5\frac{1}{2}}$—$z\ ^4H^o_{5\frac{1}{2}}$	4082. 035	2	24490. 67	
4279. 02	50Z	23363. 26	$b\ ^4D_{1\frac{1}{2}}$—$z\ ^4P^o_{1\frac{1}{2}}$	4081. 070	10Z	24496. 46	$b\ ^4D_{2\frac{1}{2}}$—$z\ ^6P^o_{2\frac{1}{2}}$
4274. 441	20Z	23388. 29	$d\ ^2G_{4\frac{1}{2}}$—$y\ ^2G^o_{4\frac{1}{2}}$	4077. 68	10Z	24516. 85	
4267. 83	1	23424. 52	$c\ ^4D_{0\frac{1}{2}}$—$y\ ^4D^o_{0\frac{1}{2}}$	4074. 437	3	24536. 34	$a\ ^4H_{3\frac{1}{2}}$—$z\ ^6D^o_{2\frac{1}{2}}$
4266. 67	5	23430. 89	$d\ ^2D_{2\frac{1}{2}}$—$y\ ^2G^o_{3\frac{1}{2}}$	4067. 835	3	24576. 16	
4256. 67	10	23485. 93	$c\ ^2F_{3\frac{1}{2}}$—$z\ ^4G^o_{4\frac{1}{2}}$	4058. 61	2Z	24632. 02	$c\ ^4D_{0\frac{1}{2}}$—$z\ ^2S^o_{0\frac{1}{2}}$
4253. 38	4	23504. 10		4057. 70	3	24637. 54	$b\ ^2G_{4\frac{1}{2}}$—$z\ ^4H^o_{3\frac{1}{2}}$
4250. 687	30Z	23519. 01	$b\ ^4D_{3\frac{1}{2}}$—$z\ ^4P^o_{2\frac{1}{2}}$	4055. 60	1	24650. 30	
4248. 57	2	23530. 71		4053. 28	1h	24664. 41	$a\ ^4H_{3\frac{1}{2}}$—$z\ ^6D^o_{3\frac{1}{2}}$
4246. 58	10Z	23541. 73	$c\ ^2G_{3\frac{1}{2}}$—$z\ ^2G^o_{4\frac{1}{2}}$	4053. 03	1h	24665. 93	$d\ ^2D_{2\frac{1}{2}}$—$x\ ^4G^o_{3\frac{1}{2}}$ $d\ ^2F_{3\frac{1}{2}}$—$x\ ^2F^o_{2\frac{1}{2}}$
4244. 725	50Z	23552. 02	$c\ ^2F_{2\frac{1}{2}}$—$z\ ^2D^o_{1\frac{1}{2}}$	4049. 75	1	24685. 91	
4243. 099	10	23561. 05	$c\ ^2G_{3\frac{1}{2}}$—$z\ ^2D^o_{2\frac{1}{2}}$	4048. 98	2h	24690. 60	
4238. 15	3	23588. 56	$b\ ^4P_{0\frac{1}{2}}$—$z\ ^6D^o_{1\frac{1}{2}}$	4046. 84	2	24703. 66	$c\ ^2F_{2\frac{1}{2}}$—$z\ ^2D^o_{2\frac{1}{2}}$
4227. 073	12Z	23650. 37	$b\ ^4D_{0\frac{1}{2}}$—$z\ ^4P^o_{1\frac{1}{2}}$	4036. 32	1	24768. 07	$d\ ^2F_{3\frac{1}{2}}$—$x\ ^2G^o_{3\frac{1}{2}}$
4209. 648	60Z	23748. 27	$b\ ^4D_{2\frac{1}{2}}$—$z\ ^4P^o_{2\frac{1}{2}}$	4036. 12	2	24769. 27	$b\ ^4P_{0\frac{1}{2}}$—$z\ ^4F^o_{1\frac{1}{2}}$
4198. 935	10	23808. 85	$b\ ^4F_{4\frac{1}{2}}$—$z\ ^4F^o_{4\frac{1}{2}}$	4035. 566	5	24772. 67	$a\ ^2F_{2\frac{1}{2}}$—$z\ ^6P^o_{2\frac{1}{2}}$
4192. 272	12Z	23846. 69	$c\ ^2F_{2\frac{1}{2}}$—$z\ ^2G^o_{3\frac{1}{2}}$	4029. 966	10lZ	24807. 09	$b\ ^2F_{3\frac{1}{2}}$—$z\ ^4F^o_{3\frac{1}{2}}$
4191. 03	5Z	23853. 78	$b\ ^2F_{2\frac{1}{2}}$—$z\ ^4F^o_{2\frac{1}{2}}$ $b\ ^4F_{3\frac{1}{2}}$—$z\ ^4F^o_{3\frac{1}{2}}$	4027. 700	2	24821. 05	$b\ ^2I_{5\frac{1}{2}}$—$z\ ^4G^o_{4\frac{1}{2}}$
4177. 939	5	23928. 50	$b\ ^4D_{2\frac{1}{2}}$—$z\ ^6P^o_{3\frac{1}{2}}$	4025. 01	1	24837. 64	$c\ ^2D_{2\frac{1}{2}}$—$z\ ^4S^o_{1\frac{1}{2}}$
4172. 280	4l	23960. 96	$c\ ^2F_{3\frac{1}{2}}$—$y\ ^4D^o_{3\frac{1}{2}}$	4023. 535	10Z	24846. 74	$b\ ^2H_{4\frac{1}{2}}$—$z\ ^4H^o_{3\frac{1}{2}}$
4171. 790	10Z	23963. 77	$c\ ^2D_{2\frac{1}{2}}$—$z\ ^2F^o_{3\frac{1}{2}}$	4016. 095	3h	24892. 77	
4171. 19	3	23967. 22	$c\ ^4F_{4\frac{1}{2}}$—$w^4F^o_{3\frac{1}{2}}$	4013. 200	12Z	24910. 73	$c\ ^2G_{3\frac{1}{2}}$—$x\ ^4D^o_{3\frac{1}{2}}$
4161. 247	7Z	24024. 48	$a\ ^2F_{2\frac{1}{2}}$—$z\ ^4P^o_{2\frac{1}{2}}$ $d\ ^2F_{2\frac{1}{2}}$—$x\ ^2F^o_{3\frac{1}{2}}$	4010. 309	3Z	24928. 69	$a\ ^2P_{1\frac{1}{2}}$—$y\ ^4D^o_{2\frac{1}{2}}$
4161. 02	3s	24025. 80		4008. 615	5	24939. 22	$c\ ^2D_{2\frac{1}{2}}$—$y\ ^2G^o_{3\frac{1}{2}}$
4154. 272	3	24064. 82		4006. 968	2	24949. 47	$b\ ^4D_{1\frac{1}{2}}$—$z\ ^6P^o_{2\frac{1}{2}}$
4152. 22	1	24076. 71		4005. 120	5Z	24960. 98	$b\ ^4D_{3\frac{1}{2}}$—$z\ ^6D^o_{3\frac{1}{2}}$
4150. 82	5l, Z	24084. 83	$d\ ^2G_{4\frac{1}{2}}$—$x\ ^4G^o_{4\frac{1}{2}}$	4002. 965	4Z	24974. 42	
4150. 627	2	24085. 95	$b\ ^2I_{5\frac{1}{2}}$—$z\ ^4H^o_{5\frac{1}{2}}$	4002. 38	1	24978. 07	$d\ ^2D_{2\frac{1}{2}}$—$w\ ^4D^o_{1\frac{1}{2}}$
4147. 37	1	24104. 87	$b\ ^4P_{1\frac{1}{2}}$—$z\ ^4F^o_{2\frac{1}{2}}$	4000. 717	3	24988. 45	$b\ ^4G_{2\frac{1}{2}}$—$z\ ^4D^o_{1\frac{1}{2}}$
4146. 874	8Z	24107. 75	$a\ ^2P_{1\frac{1}{2}}$—$z\ ^2S^o_{0\frac{1}{2}}$	3999. 840	10Z	24993. 93	$c\ ^2G_{3\frac{1}{2}}$—$y\ ^4P^o_{2\frac{1}{2}}$
4141. 454	10Z	24139. 30	$b\ ^4D_{3\frac{1}{2}}$—$z\ ^6P^o_{3\frac{1}{2}}$	3998. 565	10Z	25001. 90	$c\ ^4D_{1\frac{1}{2}}$—$z\ ^2S^o_{0\frac{1}{2}}$
4139. 780	8Z	24149. 06	$c\ ^2D_{1\frac{1}{2}}$—$y\ ^4F^o_{2\frac{1}{2}}$	3996. 64	2	25013. 94	
4138. 733	2	24155. 17		3992. 54	1	25039. 63	
4136. 761	3	24166. 68	$a\ ^4F_{4\frac{1}{2}}$—$z\ ^6F^o_{4\frac{1}{2}}$	3990. 79	15l, Z	25050. 61	$c\ ^2G_{4\frac{1}{2}}$—$y\ ^4F^o_{3\frac{1}{2}}$ $b\ ^2G_{3\frac{1}{2}}$—$z\ ^4H^o_{4\frac{1}{2}}$
4136. 49	2s	24168. 27		3989. 45	5H	25059. 02	
4130. 85	3	24201. 26	$b\ ^4D_{1\frac{1}{2}}$—$z\ ^4P^o_{2\frac{1}{2}}$	3986. 155	50Z	25079. 74	$b\ ^4D_{2\frac{1}{2}}$—$z\ ^6D^o_{1\frac{1}{2}}$
4130. 28	2	24204. 61	$a\ ^2F_{2\frac{1}{2}}$—$z\ ^6P^o_{1\frac{1}{2}}$	3980. 03	5H	25118. 33	$a\ ^2H_{4\frac{1}{2}}$—$z\ ^4F^o_{4\frac{1}{2}}$
4127. 296	2	24222. 10	$d\ ^2G_{3\frac{1}{2}}$—$x\ ^4G^o_{4\frac{1}{2}}$	3974. 84	4h	25151. 13	$c\ ^2D_{1\frac{1}{2}}$—$z\ ^2F^o_{2\frac{1}{2}}$ $b\ ^2H_{4\frac{1}{2}}$—$z\ ^4H^o_{3\frac{1}{2}}$
4126. 31	2s	24227. 89		3974. 46	1	25153. 53	$c\ ^2G_{4\frac{1}{2}}$—$y\ ^4G^o_{3\frac{1}{2}}$
4125. 628	15Z	24231. 90	$c\ ^2F_{3\frac{1}{2}}$—$z\ ^2G^o_{4\frac{1}{2}}$	3972. 950	7Z	25163. 10	$c\ ^2G_{3\frac{1}{2}}$—(1)$^o_{2\frac{1}{2}}$
4123. 26	1	24245. 81	$c\ ^4D_{0\frac{1}{2}}$—$y\ ^4D^o_{1\frac{1}{2}}$	3972. 17	2h	25168. 04	$c\ ^2F_{2\frac{1}{2}}$—$y\ ^4P^o_{1\frac{1}{2}}$
4122. 350	50Z	24251. 19	$c\ ^2F_{3\frac{1}{2}}$—$z\ ^2D^o_{2\frac{1}{2}}$	3968. 667	20Z	25190. 25	$b\ ^4D_{2\frac{1}{2}}$—$z\ ^6D^o_{3\frac{1}{2}}$
4119. 634	40Z	24267. 18	$b\ ^4D_{3\frac{1}{2}}$—$z\ ^6P^o_{2\frac{1}{2}}$	3967. 80	8Z	25195. 75	$a\ ^2P_{0\frac{1}{2}}$—$y\ ^4D^o_{1\frac{1}{2}}$
4118. 53	5Z	24273. 68	$b\ ^2I_{5\frac{1}{2}}$—$z\ ^4I^o$	3967. 686	3	25196. 48	$b\ ^4G_{3\frac{1}{2}}$—$z\ ^4D^o_{2\frac{1}{2}}$
4117. 58	3	24279. 28		3965. 45	1	25210. 68	
4115. 76	2Z	24290. 02	$c\ ^2D_{2\frac{1}{2}}$—$x\ ^4F^o_{3\frac{1}{2}}$	3961. 520	200Z	25235. 70	$b\ ^4D_{3\frac{1}{2}}$—$z\ ^6D^o_{2\frac{1}{2}}$

TABLE 1. *Wavelengths and term combinations of* Mo II—Continued

Wavelength λ_{air}	Intensity	Wave No.	Term combination	Wavelength λ_{air}	Intensity	Wave No.	Term combination
3960. 17	3	25244. 30	$c\ ^2G_{4\frac{1}{2}}—y\ ^4H^o_{3\frac{1}{2}}$	3887. 59	2	25715. 59	$b\ ^2H_{4\frac{1}{2}}—z\ ^4H^o_{3\frac{1}{2}}$
3952. 985	20*Z*	25290. 18	$b\ ^4D_{1\frac{1}{2}}—z\ ^6D^o_{0\frac{1}{2}}$	3887. 38	1	25716. 98	
3948. 79	1	25317. 05		3886. 06	1	25725. 71	
3943. 96	4	25348. 08	$c\ ^2D_{2\frac{1}{2}}—y\ ^2F^o_{3\frac{1}{2}}$	3885. 96	1	25726. 38	
3942. 734	10*Z*	25355. 93	$a\ ^2F_{2\frac{1}{2}}—z\ ^6D^o_{1\frac{1}{2}}$	3884. 19	1*hl*	25738. 10	
3941. 485	200*Z*	25363. 97	$b\ ^4D_{3\frac{1}{2}}—z\ ^6D^o_{4\frac{1}{2}}$	3883. 71	5*l*	25741. 28	$a\ ^2F_{2\frac{1}{2}}—z\ ^6D^o_{2\frac{1}{2}}$
3932. 86	1	25419. 59		3882. 96	4*s*	25746. 25	$d\ ^2G_{4\frac{1}{2}}—x\ ^2G^o_{4\frac{1}{2}}$
3931. 694	7	25427. 13		3882. 319	10*Z*	25750. 50	$c\ ^2F_{3\frac{1}{2}}—x\ ^4D^o_{3\frac{1}{2}}$
3930. 829	15*Z*	25432. 72	$b\ ^2F_{3\frac{1}{2}}—z\ ^4F^o_{4\frac{1}{2}}$	3881. 58	2	25755. 40	$a\ ^4F_{3\frac{1}{2}}—z\ ^6P^o_{2\frac{1}{2}}$
3929. 595	12*Z*	25440. 71	$b\ ^2D_{2\frac{1}{2}}—z\ ^2S^o_{1\frac{1}{2}}$	3880. 792	2*h*	25760. 64	
3927. 60	3*hl*	25453. 61	$d\ ^2G_{4\frac{1}{2}}—x\ ^2G^o_{3\frac{1}{2}}$	3879. 32	1	25770. 41	
3926. 945	5*h*	25457. 88	$c\ ^2F_{2\frac{1}{2}}—z\ ^2P^o_{1\frac{1}{2}}$	3879. 20	1	25771. 21	
3925. 828	30*Z*	25465. 12	$b\ ^4D_{2\frac{1}{2}}—z\ ^6D^o_{2\frac{1}{2}}$	3877. 55	1	25782. 17	
3925. 62	10	25466. 50	$a\ ^2F_{2\frac{1}{2}}—z\ ^6D^o_{3\frac{1}{2}}$	3877. 41	1	25783. 10	
3921. 530	5*Z*	25493. 03	$b\ ^4G_{4\frac{1}{2}}—z\ ^4D^o_{3\frac{1}{2}}$	3877. 26	2*h*	25784. 10	
3919. 459	15*Z*	25506. 50	$b\ ^2G_{4\frac{1}{2}}—z\ ^4H^o_{3\frac{1}{2}}$	3877. 21	1	25784. 43	
3917. 90	2	25516. 65	$b\ ^4G_{2\frac{1}{2}}—z\ ^4D^o_{2\frac{1}{2}}$	3875. 07	1	25798. 67	$c\ ^4D_{3\frac{1}{2}}—y\ ^4D^o_{2\frac{1}{2}}$
3917. 54	5*Z*	25519. 00	$b\ ^2I_{5\frac{1}{2}}—z\ ^4I^o_{5\frac{1}{2}}$	3874. 29	5	25803. 87	$b\ ^4F_{1\frac{1}{2}}—z\ ^4D^o_{1\frac{1}{2}}$
3917. 07	2	25522. 06	$c\ ^2G_{3\frac{1}{2}}—y\ ^4G^o_{4\frac{1}{2}}$	3873. 85	1	25806. 80	
3915. 434	40*Z*	25532. 72	$b\ ^4D_{1\frac{1}{2}}—z\ ^6D^o_{1\frac{1}{2}}$	3873. 55	1	25808. 79	
3914. 310	3*s*	25540. 05		3873. 27	4*l*	25810. 66	$b\ ^4F_{2\frac{1}{2}}—z\ ^4D^o_{1\frac{1}{2}}$
3914. 12	2	25541. 29		3872. 78	2	25813. 93	
3913. 97	1	25542. 27		3871. 90	15*Z*	25819. 79	$b\ ^4D_{0\frac{1}{2}}—z\ ^6D^o_{1\frac{1}{2}}$
3913. 75	2	25543. 71	$d\ ^2G_{3\frac{1}{2}}—x\ ^4P^o_{2\frac{1}{2}}$	3871. 451	50*Z*	25822. 79	$\begin{cases} c\ ^2G_{4\frac{1}{2}}—z\ ^2F^o_{3\frac{1}{2}} \\ c\ ^4D_{1\frac{1}{2}}—y\ ^4D^o_{2\frac{1}{2}} \end{cases}$
3913. 20	2	25547. 30		3869. 90	2*h*	25833. 14	
3910. 78	1*h*	25563. 11		3869. 62	2*h*	25835. 01	
3910. 43	2*h*	25565. 39		3867. 87	1	25846. 70	$d\ ^2G_{3\frac{1}{2}}—w\ ^4F^o_{2\frac{1}{2}}$
3910. 16	5	25567. 16	$b\ ^2I_{5\frac{1}{2}}—z\ ^2G^o_{4\frac{1}{2}}$	3867. 78	1	25847. 30	
3909. 13	2	25573. 90		3866. 884	6*Z*	25853. 29	$c\ ^2F_{3\frac{1}{2}}—\ (1)^o_{2\frac{1}{2}}$
3908. 79	2	25576. 12		3863. 63	3	25875. 06	
3908. 608	20*Z*	25577. 31	$b\ ^4D_{0\frac{1}{2}}—z\ ^6D^o_{0\frac{1}{2}}$	3862. 42	1*w*	25883. 16	$d\ ^2G_{3\frac{1}{2}}—x\ ^2G^o_{4\frac{1}{2}}$
3908. 09	4	25580. 73	$c\ ^2G_{3\frac{1}{2}}—\ (2)^o_{3\frac{1}{2}}$	3862. 17	1*w*	25884. 84	
3906. 54	2*Z*	25590. 88	$d\ ^2G_{3\frac{1}{2}}—x\ ^2G^o_{3\frac{1}{2}}$	3861. 294	30*Z*	25890. 71	$b\ ^2H_{5\frac{1}{2}}—z\ ^4H^o_{6\frac{1}{2}}$
3905. 96	2*d*?	25594. 68		3860. 25	2	25897. 71	
3904. 965	15*Z*	25601. 20	$c\ ^2F_{3\frac{1}{2}}—x\ ^4D^o_{2\frac{1}{2}}$	3859. 35	2*l*	25903. 75	
3904. 16	5*h*	25606. 45		3858. 84	3*Z*	25907. 18	$b\ ^2G_{3\frac{1}{2}}—z\ ^4G^o_{2\frac{1}{2}}$
3903. 81	2	25608. 75	$c\ ^4D_{2\frac{1}{2}}—z\ ^4G^o_{3\frac{1}{2}}$	3857. 197	50*Z*	25918. 21	$\begin{cases} c\ ^2D_{2\frac{1}{2}}—\ (3)^o_{3\frac{1}{2}} \\ b\ ^4D_{1\frac{1}{2}}—z\ ^6D^o_{2\frac{1}{2}} \end{cases}$
3903. 61	3	25610. 06	$c\ ^2G_{3\frac{1}{2}}—y\ ^4G^o_{2\frac{1}{2}}$	3855. 29	2	25931. 03	
3903. 42	1	25611. 30		3854. 88	2	25933. 79	
3902. 49	2	25617. 41		3854. 71	2	25934. 93	
3901. 13	2	25626. 34		3853. 15	2	25945. 44	$c\ ^4D_{0\frac{1}{2}}—z\ ^2D^o_{1\frac{1}{2}}$
3901. 04	1	25626. 93		3852. 59	2	25949. 21	
3900. 95	1	25627. 52	$a\ ^4F_{3\frac{1}{2}}—z\ ^6P^o_{3\frac{1}{2}}$	3850. 838	5	25961. 01	$c\ ^2G_{3\frac{1}{2}}—y\ ^4F^o_{2\frac{1}{2}}$
3900. 81	1	25628. 44		3850. 51	2	25963. 22	
3899. 94	2	25634. 16		3845. 31	2	25998. 33	
3899. 06	2*h*	25639. 94		3845. 11	1	25999. 68	
3898. 49	2	25643. 69					
3897. 819	4*h*	25648. 11	$a\ ^4F_{4\frac{1}{2}}—z\ ^6P^o_{3\frac{1}{2}}$	3842. 59	10*Z*	26016. 73	$\begin{cases} b\ \ ^2I_{6\frac{1}{2}}—z\ ^4G^o_{5\frac{1}{2}} \\ a\ ^2P_{0\frac{1}{2}}—y\ ^4D^o_{1\frac{1}{2}} \\ d\ ^2G_{4\frac{1}{2}}—w\ ^4F^o_{3\frac{1}{2}} \end{cases}$
3897. 23	1	25651. 98					
3897. 06	1	25653. 10		3838. 99	4*H*	26041. 16	
3896. 01	3*h*	25660. 91		3837. 62	1	26050. 43	
3895. 17	2*h*	25665. 55	$b\ ^4P_{2\frac{1}{2}}—z\ ^4D^o_{1\frac{1}{2}}$	3837. 49	1	26051. 31	
3894. 81	1*h*	25667. 92		3837. 195	10*Z*	26053. 31	$c\ ^2F_{2\frac{1}{2}}—x\ ^4D^o_{2\frac{1}{2}}$
3894. 74	2	25668. 38		3835. 332	25*Z*	26065. 97	$c\ ^2G_{3\frac{1}{2}}—y\ ^4H^o_{4\frac{1}{2}}$
3894. 00	2	25673. 26	$c\ ^2G_{3\frac{1}{2}}—y\ ^4F^o_{3\frac{1}{2}}$	3833. 486	75*Z*	26078. 52	$b\ ^2H_{5\frac{1}{2}}—z\ ^4I^o_{4\frac{1}{2}}$
3893. 50	1	25676. 56		3832. 363	15*Z*	26086. 16	$c\ ^2G_{4\frac{1}{2}}—y\ ^4H^o_{5\frac{1}{2}}$
3892. 33	2	25684. 27	$c\ ^2F_{3\frac{1}{2}}—y\ ^4P^o_{2\frac{1}{2}}$	3823. 125	5*l*	26149. 19	$\begin{cases} a\ ^2G_{4\frac{1}{2}}—z\ ^4F^o_{3\frac{1}{2}} \\ c\ ^2G_{4\frac{1}{2}}—x\ ^4F^o_{3\frac{1}{2}} \end{cases}$
3892. 10	1	25685. 79		3821. 55	1	26159. 97	
3891. 87	4	25687. 31	$b\ ^4G_{3\frac{1}{2}}—z\ ^4D^o_{3\frac{1}{2}}$	3821. 07	7*H*	26163. 25	
3891. 28	2	25691. 20	$a\ ^4H_{3\frac{1}{2}}—z\ ^4F^o_{2\frac{1}{2}}$	3820. 16	2	26169. 49	$c\ ^2D_{2\frac{1}{2}}—y\ ^2D^o_{2\frac{1}{2}}$

TABLE 1. *Wavelengths and term combinations of* Mo II—Continued

Wavelength λ_{air}	Intensity	Wave No.	Term combination
3819. 185	5*h*	26176. 17	$\begin{cases} a\ ^2D_{1\frac{1}{2}}—z\ ^6P^\circ_{1\frac{1}{2}} \\ c\ ^2F_{3\frac{1}{2}}—y\ ^4G^\circ_{3\frac{1}{2}} \\ a\ ^4H_{3\frac{1}{2}}—z\ ^4F^\circ_{3\frac{1}{2}} \end{cases}$
3816. 64	5*h*	26193. 65	$b\ ^4P_{2\frac{1}{2}}—z\ ^4D^\circ_{2\frac{1}{2}}$
3815. 78	1	26199. 55	
3815. 267	5*Z*	26203. 07	$c\ ^2F_{2\frac{1}{2}}—x\ ^4D^\circ_{3\frac{1}{2}}$
3813. 909	10*Z*	26212. 40	$c\ ^2F_{3\frac{1}{2}}—y\ ^4G^\circ_{4\frac{1}{2}}$
3812. 208	25*Z*	26224. 10	$b\ ^2G_{4\frac{1}{2}}—z\ ^4G^\circ_{3\frac{1}{2}}$
3811. 792	12*Z*	26226. 96	$b\ ^4F_{3\frac{1}{2}}—z\ ^4D^\circ_{2\frac{1}{2}}$
3809. 96	1	26239. 57	
3807. 70	1*H*	26255. 15	
3807. 36	3	26257. 49	$a\ ^4F_{2\frac{1}{2}}—z\ ^6D^\circ_{1\frac{1}{2}}$
3806. 92	4*l*	26260. 53	$b\ ^4D_{2\frac{1}{2}}—z\ ^4F^\circ_{1\frac{1}{2}}$
3806. 68	4*l*	26262. 18	$\begin{cases} b\ ^2D_{1\frac{1}{2}}—y\ ^4D^\circ_{2\frac{1}{2}} \\ c\ \ ^2F_{2\frac{1}{2}}—x\ ^4D^\circ_{1\frac{1}{2}} \end{cases}$
3806. 17	1	26265. 70	$c\ ^4D_{2\frac{1}{2}}—z\ ^2G^\circ_{3\frac{1}{2}}$
3805. 40	3	26271. 02	$c\ ^2F_{3\frac{1}{2}}—(2)^\circ_{2\frac{1}{2}}$
3804. 11	1	26279. 92	$d\ ^2D_{1\frac{1}{2}}—w\ ^4F^\circ_{1\frac{1}{2}}$
3804. 02	1	26280. 55	
3803. 38	5	26284. 97	
3802. 42	1	26291. 60	$d\ ^2D_{2\frac{1}{2}}—x\ ^4P^\circ_{2\frac{1}{2}}$
3801. 17	4*h*	26300. 25	$c\ ^2F_{3\frac{1}{2}}—y\ ^4G^\circ_{2\frac{1}{2}}$
3800. 79	1	26302. 88	
3799. 30	2*h*	26313. 17	
3796. 555	6	26332. 19	$\begin{cases} b\ ^2G_{3\frac{1}{2}}—z\ ^4G^\circ_{3\frac{1}{2}} \\ b\ ^4F_{1\frac{1}{2}}—z\ ^4D^\circ_{2\frac{1}{2}} \end{cases}$
3795. 588	10	26338. 90	$\begin{cases} d\ ^2D_{2\frac{1}{2}}—x\ ^2G^\circ_{3\frac{1}{2}} \\ b\ ^4F_{2\frac{1}{2}}—z\ ^4D^\circ_{2\frac{1}{2}} \end{cases}$
3793. 29	1	26354. 86	$a\ ^4H_{4\frac{1}{2}}—z\ ^4F^\circ_{4\frac{1}{2}}$
3792. 07	5	26363. 34	$\begin{cases} d\ ^2F_{2\frac{1}{2}}—w\ ^2F^\circ_{2\frac{1}{2}} \\ c\ \ ^2F_{3\frac{1}{2}}—y\ ^4F^\circ_{3\frac{1}{2}} \end{cases}$
3791. 376	5	26368. 16	$a\ ^4F_{2\frac{1}{2}}—z\ ^6D^\circ_{3\frac{1}{2}}$
3788. 72	1*H*	26386. 64	
3786. 374	50*Z*	26402. 99	$a\ ^2P_{0\frac{1}{2}}—z\ ^2S^\circ_{0\frac{1}{2}}$
3783. 173	35*Z*	26425. 33	$b\ ^2G_{4\frac{1}{2}}—z\ ^4I^\circ_{4\frac{1}{2}}$
3782. 058	60*Z*	26433. 12	$b\ ^2H_{4\frac{1}{2}}—z\ ^4G^\circ_{3\frac{1}{2}}$
3781. 09	1	26439. 89	$a\ ^4F_{1\frac{1}{2}}—z\ ^6D^\circ_{2\frac{1}{2}}$
3780. 16	2	26446. 39	
3780. 06	1	26447. 09	
3779. 12	1*h*	26453. 67	
3779. 02	1	26454. 37	
3777. 88	1*h*	26462. 36	
3776. 81	2	26469. 85	$a\ ^4F_{4\frac{1}{2}}—z\ ^6D^\circ_{3\frac{1}{2}}$
3767. 766	20*Z*	26533. 39	$b\ ^2G_{3\frac{1}{2}}—z\ ^4I^\circ_{4\frac{1}{2}}$
3765. 64	1	26548. 37	$b\ ^2I_{6\frac{1}{2}}—z\ ^4I^\circ_{5\frac{1}{2}}$
3762. 106	15*Z*	26573. 30	$a\ ^2P_{1\frac{1}{2}}—z\ ^2D^\circ_{2\frac{1}{2}}$
3760. 29	1	26586. 14	$c\ ^4D_{3\frac{1}{2}}—z\ ^2G^\circ_{3\frac{1}{2}}$
3757. 37	5*h*	26606. 80	
3756. 76	1	26611. 12	$b\ ^4P_{1\frac{1}{2}}—z\ ^4D^\circ_{0\frac{1}{2}}$
3755. 500	50*Z*	26620. 05	$b\ ^4D_{2\frac{1}{2}}—z\ ^4F^\circ_{2\frac{1}{2}}$
3754. 669	15*Z*	26625. 94	$b\ ^2H_{3\frac{1}{2}}—z\ ^4G^\circ_{4\frac{1}{2}}$
3753. 93	2	26631. 18	
3753. 773	4	26632. 29	
3753. 480	15*Z*	26634. 37	$b\ ^2H_{4\frac{1}{2}}—z\ ^4I^\circ_{4\frac{1}{2}}$
3752. 80	1	26639. 20	
3752. 260	3	26643. 03	$a\ ^4F_{2\frac{1}{2}}—z\ ^6D^\circ_{2\frac{1}{2}}$
3751. 60	1	26647. 72	
3751. 110	5	26651. 20	$c\ ^2F_{3\frac{1}{2}}—y\ ^4F^\circ_{2\frac{1}{2}}$
3748. 117	30*Z*	26672. 48	$b\ ^4F_{4\frac{1}{2}}—z\ ^4D^\circ_{3\frac{1}{2}}$
3747. 010	5*h*	26680. 36	
3746. 435	25*Z*	26684. 46	$b\ ^4P_{2\frac{1}{2}}—z\ ^4D^\circ_{3\frac{1}{2}}$
3744. 420	35*Z*	26698. 82	$c\ ^2G_{3\frac{1}{2}}—z\ ^2H^\circ_{4\frac{1}{2}}$
3742. 335	60*Z*	26713. 69	$\begin{cases} c\ ^2F_{2\frac{1}{2}}—y\ ^4F^\circ_{1\frac{1}{2}} \\ b\ ^4D_{1\frac{1}{2}}—z\ ^4F^\circ_{1\frac{1}{2}} \end{cases}$
3741. 778	15*Z*	26717. 67	$b\ ^4F_{3\frac{1}{2}}—z\ ^4D^\circ_{3\frac{1}{2}}$
3741. 36	1*h*	26720. 65	
3740. 43	3*h*	26727. 29	
3738. 973	5*h*	26737. 71	$d\ ^2F_{3\frac{1}{2}}—w\ ^2F^\circ_{2\frac{1}{2}}$
3738. 84	10*Z*	26738. 69	
3736. 399	12*Z*	26756. 13	$c\ ^2F_{3\frac{1}{2}}—y\ ^4H^\circ_{4\frac{1}{2}}$
3734. 21	1	26771. 81	$\begin{cases} b\ ^2S_{0\frac{1}{2}}—y\ ^2P^\circ_{0\frac{1}{2}} \\ c\ ^2G_{3\frac{1}{2}}—x\ ^4F^\circ_{3\frac{1}{2}} \end{cases}$
3733. 839	8*h*	26774. 47	$a\ ^2G_{4\frac{1}{2}}—z\ ^4F^\circ_{4\frac{1}{2}}$
3730. 539	10*Z*	26798. 16	$c\ ^2G_{4\frac{1}{2}}—y\ ^2G^\circ_{3\frac{1}{2}}$
3730. 024	3	26801. 86	$a\ ^4H_{3\frac{1}{2}}—z\ ^4F^\circ_{4\frac{1}{2}}$
3728. 50	10*Z*	26812. 84	
3728. 07	1*h*	26815. 90	$c\ ^2F_{2\frac{1}{2}}—y\ ^4F^\circ_{3\frac{1}{2}}$
3727. 41	1*h*	26820. 65	
3725. 80	2*h*	26832. 24	$c\ ^4D_{2\frac{1}{2}}—y\ ^4D^\circ_{3\frac{1}{2}}$
3723. 018	4	26852. 29	$a\ ^4F_{3\frac{1}{2}}—z\ ^6D^\circ_{4\frac{1}{2}}$
3720. 200	30*Z*	26872. 66	$a\ ^4F_{4\frac{1}{2}}—z\ ^6D^\circ_{3\frac{1}{2}}$
3719. 777	35*Z*	26875. 69	$b\ ^4D_{3\frac{1}{2}}—z\ ^4F^\circ_{3\frac{1}{2}}$
3719. 18	4	26880. 00	
3719. 05	10*Z*	26880. 94	$b\ ^2G_{4\frac{1}{2}}—z\ ^2G^\circ_{3\frac{1}{2}}$
3717. 130	5	26894. 83	$c\ ^2G_{3\frac{1}{2}}—x\ ^4F^\circ_{4\frac{1}{2}}$
3716. 920	22*Z*	26896. 34	$a\ ^2F_{2\frac{1}{2}}—z\ ^4F^\circ_{2\frac{1}{2}}$
3713. 920	25*Z*	26918. 07	
3708. 04	1*H*	26960. 75	
3707. 98	2	26961. 19	$b\ ^2D_{2\frac{1}{2}}—z\ ^2D^\circ_{1\frac{1}{2}}$
3707. 705	2	26963. 19	$c\ ^2G_{3\frac{1}{2}}—z\ ^2F^\circ_{2\frac{1}{2}}$
3704. 150	10*Z*	26989. 07	$b\ ^2G_{3\frac{1}{2}}—z\ ^2G^\circ_{3\frac{1}{2}}$
3702. 550	250*Z*	27000. 73	$b\ ^4D_{0\frac{1}{2}}—z\ ^4F^\circ_{1\frac{1}{2}}$
3701. 360	3	27009. 41	$c\ ^2F_{2\frac{1}{2}}—y\ ^4H^\circ_{3\frac{1}{2}}$
3701. 068	4	27011. 54	$d\ ^2F_{3\frac{1}{2}}—x\ ^2H^\circ_{4\frac{1}{2}}$
3700. 72	15	27014. 08	
3699. 845	20*Z*	27020. 47	$d\ ^2D_{2\frac{1}{2}}—x\ ^4P^\circ_{1\frac{1}{2}}$
3699. 76	5	27021. 09	$c\ ^2G_{4\frac{1}{2}}—z\ ^2H^\circ_{5\frac{1}{2}}$
3698. 67	2	27029. 05	$b\ ^2S_{0\frac{1}{2}}—y\ ^2P^\circ_{1\frac{1}{2}}$
3697. 025	7*Z*	27041. 08	
3696. 32	1	27046. 26	
3695. 11	2	27055. 12	
3694. 43	20	27060. 10	$b\ ^4P_{1\frac{1}{2}}—z\ ^4D^\circ_{1\frac{1}{2}}$
3693. 11	2	27069. 77	
3692. 647	250*Z*	27073. 17	$b\ ^4D_{1\frac{1}{2}}—z\ ^4F^\circ_{2\frac{1}{2}}$
3691. 59	2	27080. 92	$b\ ^2G_{3\frac{1}{2}}—z\ ^4G^\circ_{4\frac{1}{2}}$
3690. 35	20*Z*	27090. 02	$b\ ^2H_{4\frac{1}{2}}—z\ ^2G^\circ_{3\frac{1}{2}}$
3689. 91	2	27093. 25	
3688. 310	300*Z*	27105. 00	$b\ ^4D_{2\frac{1}{2}}—z\ ^4F^\circ_{3\frac{1}{2}}$
3687. 705	3	27109. 42	$d\ ^2F_{3\frac{1}{2}}—w^2F^\circ_{3\frac{1}{2}}$
3685. 27	1	27127. 33	
3684. 875	1	27130. 24	$c\ ^2D_{1\frac{1}{2}}—w^4D^\circ_{0\frac{1}{2}}$
3684. 61	1	27132. 19	
3684. 18	25*Z*	27135. 36	$c\ ^2F_{3\frac{1}{2}}—z\ ^2F^\circ_{3\frac{1}{2}}$
3681. 78	5	27153. 04	$c\ ^4D_{3\frac{1}{2}}—y\ ^4D^\circ_{3\frac{1}{2}}$
3678. 64	3	27176. 22	$b\ ^2S_{0\frac{1}{2}}—x\ ^4P^\circ_{0\frac{1}{2}}$
3677. 894	4	27181. 73	$b\ ^2H_{4\frac{1}{2}}—z\ ^4G^\circ_{4\frac{1}{2}}$
3677. 63	1	27183. 68	
3674. 65	3	27205. 73	
3670. 673	50*Z*	27235. 20	$a\ ^4F_{1\frac{1}{2}}—z\ ^4F^\circ_{1\frac{1}{2}}$
3669. 850	3	27241. 31	
3667. 51	3*H*	27258. 69	
3658. 970	25*Z*	27322. 31	$b\ ^2I_{5\frac{1}{2}}—z\ ^2I^\circ_{5\frac{1}{2}}$
3658. 840	8	27323. 28	$b\ ^2H_{5\frac{1}{2}}—z\ ^4I^\circ_{5\frac{1}{2}}$
3658. 32	25*Z*	27327. 15	

TABLE 1. *Wavelengths and term combinations of* Mo II—Continued

Wavelength λ_{air}	Intensity	Wave No.	Term combination
3658. 29	20*Z*	27327. 39	$\begin{cases} a\ ^2P_{1\frac{1}{2}}-z\ ^2P^\circ_{1\frac{1}{2}} \\ a\ ^2D_{1\frac{1}{2}}-z\ ^6D^\circ_{1\frac{1}{2}} \end{cases}$
3656. 15	1	27343. 38	
3655. 788	8*Z*	27346. 09	$d\ ^2F_{2\frac{1}{2}}-x\ ^2D^\circ_{2\frac{1}{2}}$
3653. 96	2	27359. 77	
3652. 450	60*Z*	27371. 08	$\begin{cases} d\ ^2F_{2\frac{1}{2}}-x\ ^2D^\circ_{1\frac{1}{2}} \\ c\ ^2G_{4\frac{1}{2}}-y\ ^2H^\circ_{5\frac{1}{2}} \end{cases}$
3652. 315	60*Z*	27372. 10	$b\ ^2H_{5\frac{1}{2}}-z\ ^2G^\circ_{4\frac{1}{2}}$
3651. 100	150*Z*	27381. 20	$a\ ^2F_{2\frac{1}{2}}-z\ ^4F^\circ_{3\frac{1}{2}}$
3650. 075	5	27388. 89	$c\ ^2F_{3\frac{1}{2}}-z\ ^2H^\circ_{4\frac{1}{2}}$
3646. 74	2	27413. 94	
3643. 473	20*Z*	27438. 52	$a\ ^4F_{2\frac{1}{2}}-z\ ^4F^\circ_{1\frac{1}{2}}$
3642. 85	1	27443. 21	$c\ ^4D_{3\frac{1}{2}}-z\ ^2D^\circ_{2\frac{1}{2}}$
3642. 22	5	27447. 96	$b\ ^2G_{4\frac{1}{2}}-y\ ^4D^\circ_{3\frac{1}{2}}$
3640. 384	1	27461. 80	$c\ ^2F_{3\frac{1}{2}}-x\ ^4F^\circ_{3\frac{1}{2}}$
3639. 641	20*Z*	27467. 41	$c\ ^4D_{1\frac{1}{2}}-z\ ^2D^\circ_{2\frac{1}{2}}$
3638. 775	2	27473. 95	
3637. 772	22*Z*	27481. 52	$d\ ^2D_{2\frac{1}{2}}-y\ ^2P^\circ_{1\frac{1}{2}}$
3636. 570	4	27490. 60	
3635. 142	500*Z*	27501. 40	$b\ ^4D_{3\frac{1}{2}}-z\ ^4F^\circ_{4\frac{1}{2}}$
3634. 31	1	27507. 70	$d\ ^2D_{1\frac{1}{2}}-x\ ^4P^\circ_{0\frac{1}{2}}$
3633. 311	30*Z*	27515. 26	$b\ ^2H_{5\frac{1}{2}}-z\ ^4G^\circ_{5\frac{1}{2}}$
3631. 52	1	27528. 83	
3627. 96	3	27555. 84	$b\ ^2G_{3\frac{1}{2}}-y\ ^4D^\circ_{3\frac{1}{2}}$
3627. 348	60*d*?*Z*	27560. 49	$d\ ^2G_{3\frac{1}{2}}-w^2F^\circ_{2\frac{1}{2}}$
3625. 535	30*Z*	27574. 27	$b\ ^2I_{5\frac{1}{2}}-z\ ^2I^\circ_{6\frac{1}{2}}$
3623. 74	20	27587. 93	$c\ ^2F_{2\frac{1}{2}}-z\ ^2F^\circ_{3\frac{1}{2}}$
3623. 68	30*Z*	27588. 39	$b\ ^4P_{1\frac{1}{2}}-z\ ^4D^\circ_{2\frac{1}{2}}$
3622. 845	8*Z*	27594. 75	$a\ ^4F_{1\frac{1}{2}}-z\ ^4F^\circ_{2\frac{1}{2}}$
3620. 178	3*Z*	27615. 08	$c\ ^2F_{2\frac{1}{2}}-x\ ^4F^\circ_{1\frac{1}{2}}$
3618. 359	8*Z*	27628. 96	$b\ ^2I_{6\frac{1}{2}}-z\ ^2I^\circ_{5\frac{1}{2}}$
3617. 555	15*Z*	27635. 10	$b\ ^4P_{0\frac{1}{2}}-z\ ^4D^\circ_{0\frac{1}{2}}$
3616. 81	1	27640. 82	$c\ ^2G_{4\frac{1}{2}}-y\ ^2G^\circ_{4\frac{1}{2}}$
3615. 16	4	27653. 40	$c\ ^2F_{3\frac{1}{2}}-z\ ^2F^\circ_{2\frac{1}{2}}$
3614. 705	15	27656. 89	$b\ ^2H_{4\frac{1}{2}}-y\ ^4D^\circ_{3\frac{1}{2}}$
3612. 125	30*Z*	27676. 64	$a\ ^2P_{1\frac{1}{2}}-z\ ^2P^\circ_{0\frac{1}{2}}$
3606. 905	60*Z*	27716. 69	$a\ ^2P_{0\frac{1}{2}}-z\ ^2D^\circ_{1\frac{1}{2}}$
3606. 642	8*Z*	27718. 71	$b\ ^2G_{4\frac{1}{2}}-z\ ^2G^\circ_{4\frac{1}{2}}$
3606. 36	4	27720. 88	$d\ ^2F_{3\frac{1}{2}}-x\ ^2D^\circ_{2\frac{1}{2}}$
3604. 73	1*h*	27733. 42	
3602. 28	2	27752. 28	
3600. 60	1	27765. 23	
3599. 025	4	27777. 38	$c\ ^2G_{4\frac{1}{2}}-$ (3)$^\circ_{3\frac{1}{2}}$
3597. 851	3	27786. 44	
3597. 685	4*Z*	27787. 72	
3597. 48	1	27789. 31	
3597. 37	2	27790. 16	
3596. 746	7*Z*	27794. 98	$d\ ^2G_{4\frac{1}{2}}-w^2F^\circ_{3\frac{1}{2}}$
3596. 355	150*Z*	27798. 00	$a\ ^4F_{2\frac{1}{2}}-z\ ^4F^\circ_{2\frac{1}{2}}$
3596. 100	3	27799. 97	$c\ ^2D_{2\frac{1}{2}}-x\ ^4P^\circ_{2\frac{1}{2}}$
3595. 375	8	27805. 57	$\begin{cases} b\ ^2F_{3\frac{1}{2}}-z\ ^4D^\circ_{2\frac{1}{2}} \\ b\ ^4G_{5\frac{1}{2}}-z\ ^4H^\circ_{4\frac{1}{2}} \end{cases}$
3594. 43	3*l*	27812. 89	
3593. 18	1	27822. 56	$b\ ^2D_{2\frac{1}{2}}-y\ ^4D^\circ_{3\frac{1}{2}}$
3592. 614	12*Z*	27826. 94	$b\ ^2G_{3\frac{1}{2}}-z\ ^2G^\circ_{4\frac{1}{2}}$
3592. 266	10*Z*	27829. 64	$c\ ^2G_{3\frac{1}{2}}-y\ ^2F^\circ_{3\frac{1}{2}}$
3591. 645	60*Z*	27834. 45	$d\ ^2G_{3\frac{1}{2}}-x\ ^2H^\circ_{4\frac{1}{2}}$
3590. 129	20*Z*	27846. 20	$b\ ^2G_{3\frac{1}{2}}-z\ ^2D^\circ_{2\frac{1}{2}}$
3589. 483	30*Z*	27851. 22	$\begin{cases} c\ ^2G_{3\frac{1}{2}}-y\ ^2H^\circ_{4\frac{1}{2}} \\ c\ ^4D_{0\frac{1}{2}}-z\ ^2P^\circ_{1\frac{1}{2}} \end{cases}$
3588. 50	1*h*	27858. 85	
3588. 098	4	27861. 97	$b\ ^2G_{4\frac{1}{2}}-z\ ^4G^\circ_{3\frac{1}{2}}$
3586. 720	5	27872. 67	$b\ ^4G_{3\frac{1}{2}}-z\ ^4H^\circ_{3\frac{1}{2}}$
3585. 898	20*Z*	27879. 06	$\begin{cases} a\ ^4F_{3\frac{1}{2}}-z\ ^4F^\circ_{2\frac{1}{2}} \\ c\ ^2F_{2\frac{1}{2}}-x\ ^4F^\circ_{2\frac{1}{2}} \\ b\ ^2H_{4\frac{1}{2}}-z\ ^4I^\circ_{5\frac{1}{2}} \end{cases}$
3585. 674	50*Z*	27880. 80	$b\ ^2I_{6\frac{1}{2}}-z\ ^2I^\circ_{6\frac{1}{2}}$
3582. 677	15	27904. 12	
3582. 411	10	27906. 20	$b\ ^2D_{1\frac{1}{2}}-z\ ^2D^\circ_{2\frac{1}{2}}$
3581. 383	2	27914. 21	$c\ ^2F_{2\frac{1}{2}}-x\ ^4F^\circ_{3\frac{1}{2}}$
3580. 275	5	27922. 84	$a\ ^2P_{1\frac{1}{2}}-x\ ^4D^\circ_{2\frac{1}{2}}$
3579. 061	20*l*, *Z*	27932. 32	$d\ ^2G_{3\frac{1}{2}}-w^2F^\circ_{3\frac{1}{2}}$
3572. 556	10*Z*	27983. 17	$b\ ^4G_{4\frac{1}{2}}-z\ ^4H^\circ_{4\frac{1}{2}}$
3567. 98	2	28019. 06	$d\ ^2F_{3\frac{1}{2}}-w^2G^\circ_{4\frac{1}{2}}$
3566. 26	4*s*	28032. 58	
3564. 490	4	28046. 49	$b\ ^2H_{5\frac{1}{2}}-z\ ^4I^\circ_{6\frac{1}{2}}$
3563. 93	2	28050. 90	
3562. 935	1	28058. 73	
3562. 49	1	28062. 24	
3561. 38	15*Z*	28070. 98	$b\ ^2H_{4\frac{1}{2}}-z\ ^4G^\circ_{5\frac{1}{2}}$
3559. 725	20*Z*	28084. 03	$b\ ^4P_{0\frac{1}{2}}-z\ ^4D^\circ_{1\frac{1}{2}}$
3558. 99	2	28089. 84	
3558. 784	7	28091. 46	$b\ ^2I_{5\frac{1}{2}}-y\ ^4H^\circ_{4\frac{1}{2}}$
3557. 40	5	28102. 39	
3556. 961	35*Z*	28105. 86	$c\ ^2F_{2\frac{1}{2}}-z\ ^2F^\circ_{2\frac{1}{2}}$
3556. 696	2	28107. 95	$b\ ^2I_{6\frac{1}{2}}-y\ ^4G^\circ_{5\frac{1}{2}}$
3556. 327	20*Z*	28110. 87	$c\ ^2F_{2\frac{1}{2}}-y\ ^2G^\circ_{3\frac{1}{2}}$
3555. 14	4	28120. 25	
3553. 690	5*Z*	28131. 73	$a\ ^2P_{1\frac{1}{2}}-x\ ^4D^\circ_{1\frac{1}{2}}$
3549. 720	3	28163. 19	
3549. 03	1	28168. 67	
3547. 937	35*Z*	28177. 34	$b\ ^4G_{3\frac{1}{2}}-z\ ^4H^\circ_{4\frac{1}{2}}$
3545. 983	40*Z*	28192. 87	$b\ ^4G_{2\frac{1}{2}}-z\ ^4H^\circ_{3\frac{1}{2}}$
3542. 386	45*Z*	28221. 50	$c\ ^4D_{1\frac{1}{2}}-z\ ^2P^\circ_{1\frac{1}{2}}$
3541. 19	1	28231. 03	
3537. 71	1	28258. 80	
3537. 123	25*Z*	28263. 49	$c\ ^2G_{2\frac{1}{2}}-y\ ^2G^\circ_{4\frac{1}{2}}$
3536. 84	2	28265. 75	
3536. 53	2	28268. 23	
3534. 695	40*Z*	28282. 90	$a\ ^4F_{2\frac{1}{2}}-z\ ^4F^\circ_{3\frac{1}{2}}$
3532. 998	30*Z*	28296. 48	$b\ ^2F_{3\frac{1}{2}}-z\ ^4D^\circ_{3\frac{1}{2}}$
3532. 466	5	28300. 75	$c\ ^2G_{3\frac{1}{2}}-x\ ^4G^\circ_{2\frac{1}{2}}$
3527. 877	15*Z*	28337. 56	$c\ ^2G_{4\frac{1}{2}}-x\ ^4G^\circ_{4\frac{1}{2}}$
3526. 17	2	28351. 27	
3525. 28	2	28358. 43	
3524. 64	40*Z*	28363. 61	$a\ ^4F_{3\frac{1}{2}}-z\ ^4F^\circ_{3\frac{1}{2}}$
3524. 59	40*Z*	28364. 01	$d\ ^2G_{4\frac{1}{2}}-x\ ^2H^\circ_{5\frac{1}{2}}$
3523. 889	7	28369. 63	$\begin{cases} a\ ^2S_{0\frac{1}{2}}-y\ ^4D^\circ_{0\frac{1}{2}} \\ b\ ^4G_{5\frac{1}{2}}-z\ ^4H^\circ_{5\frac{1}{2}} \end{cases}$
3522. 060	15*Z*	28384. 36	$a\ ^4F_{4\frac{1}{2}}-z\ ^4F^\circ_{3\frac{1}{2}}$
3520. 161	20*Z*	28399. 67	$c\ ^2G_{3\frac{1}{2}}-$ (3)$^\circ_{3\frac{1}{2}}$
3515. 681	22*Z*	28435. 86	$b\ ^4F_{1\frac{1}{2}}-y\ ^4D^\circ_{0\frac{1}{2}}$
3514. 974	8	28441. 58	$b\ ^4G_{2\frac{1}{2}}-y\ ^4D^\circ_{1\frac{1}{2}}$
3513. 927	2	28450. 05	
3513. 41	2	28454. 24	
3512. 51	3	28461. 53	$c\ ^2F_{2\frac{1}{2}}-z\ ^4S^\circ_{1\frac{1}{2}}$
3511. 76	2	28467. 61	
3511. 10	2*Hl*	28472. 96	$c\ ^4D_{2\frac{1}{2}}-x\ ^4D^\circ_{2\frac{1}{2}}$
3510. 14	2	28480. 75	
3509. 250	4	28487. 97	
3509. 03	2	28489. 75	
3506. 699	15*Z*	28508. 69	$a\ ^2D_{1\frac{1}{2}}-z\ ^4F^\circ_{1\frac{1}{2}}$

TABLE 1. *Wavelengths and term combinations of* Mo II—Continued

Wavelength λ_{air}	Intensity	Wave No.	Term combination
3506. 35	2	28511. 53	
3506. 16	2	28513. 07	
3505. 33	20	28519. 86	$c\ ^2F_{3\frac{1}{2}}$—$y\ ^2F^{\circ}_{3\frac{1}{2}}$
3503. 36	2	28535. 86	
3502. 690	12*Z*	28541. 32	$c\ ^2F_{3\frac{1}{2}}$—$y\ ^2H^{\circ}_{4\frac{1}{2}}$
3501. 942	200*Z*	28547. 42	$b\ ^4G_{4\frac{1}{2}}$—$z\ ^4H^{\circ}_{5\frac{1}{2}}$
3501. 53	3*l*	28550. 78	
3500. 92	4	28555. 75	$c\ ^4D_{2\frac{1}{2}}$—$y\ ^4P^{\circ}_{2\frac{1}{2}}$
3499. 972	100*Z*	28563. 49	$c\ ^2F_{2\frac{1}{2}}$—$y\ ^2G^{\circ}_{3\frac{1}{2}}$
3499. 075	100*Z*	28570. 81	$c\ ^4D_{1\frac{1}{2}}$—$z\ ^2P^{\circ}_{0\frac{1}{2}}$
3498. 29	4*l*	28577. 22	$b\ ^2D_{2\frac{1}{2}}$—$y\ ^4P^{\circ}_{1\frac{1}{2}}$
3492. 05	2*l*	28628. 28	
3491. 92	1	28629. 35	
3490. 93	1	28637. 47	
3488. 77	1	28655. 20	
3488. 150	30*Z*	28660. 29	$b\ ^2D_{1\frac{1}{2}}$—$z\ ^2P^{\circ}_{1\frac{1}{2}}$
3487. 890	6	28662. 43	$c\ ^2G_{4\frac{1}{2}}$—$w\ ^4D^{\circ}_{3\frac{1}{2}}$
3487. 02	2	28669. 58	
3486. 89	3	28670. 65	
3486. 73	1	28671. 76	$d\ ^2F_{2\frac{1}{2}}$—$w\ ^2D^{\circ}_{1\frac{1}{2}}$
3485. 722	50*Z*	28680. 25	$d\ ^2D_{2\frac{1}{2}}$—$w\ ^2F^{\circ}_{3\frac{1}{2}}$
3484. 561	100*Z*	28689. 81	$c\ ^2G_{4\frac{1}{2}}$—$x\ ^4G^{\circ}_{5\frac{1}{2}}$
3482. 769	10*Z*	28704. 57	$d\ ^2G_{4\frac{1}{2}}$—$w\ ^2G^{\circ}_{4\frac{1}{2}}$
3481. 10	1	28718. 33	$b\ ^2G_{4\frac{1}{2}}$—$z\ ^2G^{\circ}_{4\frac{1}{2}}$
3479. 90	1*d*?	28728. 23	
3479. 20	2	28734. 01	$b\ ^2I_{5\frac{1}{2}}$—$y\ ^4H^{\circ}_{5\frac{1}{2}}$
3472. 87	1	28786. 39	
3468. 29	2*e*	28824. 40	
3466. 12	3*hl*	28842. 44	
3464. 86	3*e*	28852. 93	
3464. 73	1*e*	28854. 01	
3463. 55	5	28863. 84	$b\ ^2S_{0\frac{1}{2}}$—$x\ ^2D^{\circ}_{1\frac{1}{2}}$
3463. 179	8	28866. 93	$b\ ^2D_{2\frac{1}{2}}$—$z\ ^2P^{\circ}_{1\frac{1}{2}}$
3463. 033	20*Z*	28868. 15	$a\ ^2D_{1\frac{1}{2}}$—$z\ ^4F^{\circ}_{2\frac{1}{2}}$
3462. 07	18*Z*	28876. 21	$c\ ^4D_{3\frac{1}{2}}$—$y\ ^4P^{\circ}_{2\frac{1}{2}}$
3461. 47	1*l*	28881. 19	
3459. 19	1*w*	28900. 22	$c\ ^4D_{1\frac{1}{2}}$—$y\ ^4P^{\circ}_{2\frac{1}{2}}$
3458. 850	12	28903. 06	$b\ ^4F_{3\frac{1}{2}}$—$z\ ^4H^{\circ}_{3\frac{1}{2}}$
3458. 49	3	28906. 07	
3456. 77	2	28920. 45	$b\ ^2I_{5\frac{1}{2}}$—$x\ ^4F^{\circ}_{4\frac{1}{2}}$
3455. 874	8	28927. 95	$d\ ^2F_{3\frac{1}{2}}$—$w^2H^{\circ}_{4\frac{1}{2}}$
3455. 02	2*hl*	28935. 10	
3454. 12	2*w*	28942. 64	$c\ ^4D_{3\frac{1}{2}}$—$x\ ^4D^{\circ}_{3\frac{1}{2}}$
3453. 73	1	28945. 91	
3452. 822	40*Z*	28953. 52	$c\ ^2F_{3\frac{1}{2}}$—$y\ ^2G^{\circ}_{4\frac{1}{2}}$
3452. 33	1	28957. 65	
3452. 05	3	28960. 00	$c\ ^2G_{3\frac{1}{2}}$—$x\ ^4G^{\circ}_{4\frac{1}{2}}$
3451. 29	1	28966. 37	
3450. 591	30*Z*	28972. 24	$c\ ^2F_{2\frac{1}{2}}$—$y\ ^2F^{\circ}_{3\frac{1}{2}}$
3449. 56	1	28980. 90	
3448. 76	3	28987. 62	
3448. 531	20*Z*	28989. 55	$c\ ^2D_{2\frac{1}{2}}$—$y\ ^2P^{\circ}_{1\frac{1}{2}}$ $a\ ^4F_{3\frac{1}{2}}$—$z\ ^4F^{\circ}_{4\frac{1}{2}}$
3447. 54	1	28997. 88	
3446. 98	3	29002. 59	
3446. 72	1	29004. 78	
3446. 092	200*Z*	29010. 06	$a\ ^2P_{0\frac{1}{2}}$—$y\ ^4P^{\circ}_{0\frac{1}{2}}$ $b\ ^2D_{1\frac{1}{2}}$—$z\ ^2P^{\circ}_{0\frac{1}{2}}$ $a\ ^4F_{4\frac{1}{2}}$—$z\ ^4F^{\circ}_{4\frac{1}{2}}$
3445. 500	75	29015. 05	$b\ ^4F_{2\frac{1}{2}}$—$z\ ^4H^{\circ}_{3\frac{1}{2}}$
3444. 40	5	29024. 31	$d\ ^2G_{3\frac{1}{2}}$—$w^2G^{\circ}_{3\frac{1}{2}}$
3444. 21	3	29025. 91	$c\ ^4D_{1\frac{1}{2}}$—$x\ ^4D^{\circ}_{1\frac{1}{2}}$
3443. 68	1	29030. 38	
3443. 11	3	29035. 19	
3442. 48	10*w*	29040. 53	$b\ ^2I_{6\frac{1}{2}}$—$y\ ^4H^{\circ}_{5\frac{1}{2}}$
3441. 892	7	29045. 46	$c\ ^4D_{3\frac{1}{2}}$—(1)$^{\circ}_{2\frac{1}{2}}$
3440. 55	4	29056. 79	$a\ ^4D_{0\frac{1}{2}}$—$z\ ^6F^{\circ}_{0\frac{1}{2}}$
3439. 01	3	29069. 80	$c\ ^4D_{1\frac{1}{2}}$— (1)$^{\circ}_{2\frac{1}{2}}$
3438. 43	1	29074. 70	
3437. 970	2	29078. 60	
3436. 60	1*w*	29090. 22	$c\ ^2F^{\circ}_{3\frac{1}{2}}$— (3)$^{\circ}_{3\frac{1}{2}}$
3436. 30	1*l*	29092. 73	
3435. 38	60*Z*	29100. 52	$b\ ^4G_{5\frac{1}{2}}$—$z\ ^4H^{\circ}_{6\frac{1}{2}}$
3433. 256	7*l*	29118. 52	$d\ ^2F_{2\frac{1}{2}}$—$v\ ^2F^{\circ}_{2\frac{1}{2}}$ $b\ ^4P_{2\frac{1}{2}}$—$y\ D^{\circ}_{1\frac{1}{2}}$
3432. 228	65*Z*	29127. 24	$b\ ^2H_{5\frac{1}{2}}$—$z\ ^2I^{\circ}_{5\frac{1}{2}}$
3431. 50	1*hl*	29133. 42	
3430. 53	2*d*?	29141. 66	
3429. 64	1	29149. 22	
3428. 88	25*Z*	29155. 68	$c\ ^2F_{2\frac{1}{2}}$—$y\ ^2D^{\circ}_{1\frac{1}{2}}$
3428. 082	8	29162. 47	$b\ ^4F_{4\frac{1}{2}}$—$z\ ^4H^{\circ}_{4\frac{1}{2}}$
3427. 74	1	29165. 38	
3427. 07	15*Z*	29171. 08	$d\ ^2D_{1\frac{1}{2}}$—$x\ ^2D^{\circ}_{2\frac{1}{2}}$
3426. 14	1	29179. 00	
3424. 79	5	29190. 50	$a\ ^2S_{0\frac{1}{2}}$—$y\ ^4D^{\circ}_{1\frac{1}{2}}$
3424. 172	8	29195. 77	$b\ ^2G_{3\frac{1}{2}}$—$x\ ^4D^{\circ}_{2\frac{1}{2}}$ $d\ ^2D_{1\frac{1}{2}}$—$x\ ^2D^{\circ}_{1\frac{1}{2}}$
3423. 876	2	29198. 29	$c\ ^2D_{1\frac{1}{2}}$—$x\ ^4P^{\circ}_{1\frac{1}{2}}$
3422. 765	200*Z*	29207. 77	$b\ ^4F_{3\frac{1}{2}}$—$z\ ^4H^{\circ}_{4\frac{1}{2}}$
3419. 59	4	29234. 89	$c\ ^4D_{2\frac{1}{2}}$—$y\ ^4F^{\circ}_{3\frac{1}{2}}$
3419. 38	2	29236. 68	$c\ ^2G_{3\frac{1}{2}}$—$w^4D^{\circ}_{2\frac{1}{2}}$
3419. 283	2	29237. 51	$b\ ^2G_{4\frac{1}{2}}$—$x\ ^4D^{\circ}_{3\frac{1}{2}}$
3419. 020	8	29239. 76	$d\ ^2G_{4\frac{1}{2}}$—$w^2H^{\circ}_{5\frac{1}{2}}$
3417. 007	7	29256. 99	$b\ ^4F_{1\frac{1}{2}}$—$y\ ^4D^{\circ}_{1\frac{1}{2}}$
3416. 21	55	29263. 81	$b\ ^4F_{2\frac{1}{2}}$—$y\ ^4D^{\circ}_{1\frac{1}{2}}$
3416. 08	45	29264. 92	$b\ ^4G_{4\frac{1}{2}}$—$z\ ^4G^{\circ}_{3\frac{1}{2}}$
3414. 430	10*Z*	29279. 07	$b\ ^2G_{3\frac{1}{2}}$—$y\ ^4P^{\circ}_{2\frac{1}{2}}$
3413. 77	2	29284. 73	$c\ ^2G_{3\frac{1}{2}}$—$w^4D^{\circ}_{3\frac{1}{2}}$
3412. 956	8*Z*	29291. 71	$d\ ^2D_{2\frac{1}{2}}$—$x\ ^2D^{\circ}_{2\frac{1}{2}}$
3412. 366	8*Z*	29296. 77	
3410. 618	15*Z*	29311. 79	
3410. 049	2	29316. 68	$d\ ^2\Gamma_{2\frac{1}{2}}$—$x\ ^2D^{\circ}_{1\frac{1}{2}}$
3409. 82	2	29318. 65	
3409. 36	1	29322. 64	
3408. 666	15*Z*	29328. 57	$b\ ^4G_{3\frac{1}{2}}$—$y\ ^4D^{\circ}_{2\frac{1}{2}}$
3408. 20	3*H*	29332. 58	$a\ ^2P^{\circ}_{0\frac{1}{2}}$—$y\ ^4P^{\circ}_{1\frac{1}{2}}$
3407. 63	10*Z*	29337. 49	$c\ ^2G_{4\frac{1}{2}}$—$x\ ^2F^{\circ}_{3\frac{1}{2}}$
3407. 203	12*Z*	29341. 17	$c\ ^2F_{3\frac{1}{2}}$—$y\ ^2D^{\circ}_{2\frac{1}{2}}$
3405. 70	6	29354. 12	$b\ ^4G_{2\frac{1}{2}}$—$z\ ^4G^{\circ}_{2\frac{1}{2}}$
3404. 02	2	29368. 60	$c\ ^4D_{3\frac{1}{2}}$—$y\ ^4G^{\circ}_{3\frac{1}{2}}$
3402. 810	200*Z*	29379. 05	$b\ ^2H_{5\frac{1}{2}}$—$z\ ^2I^{\circ}_{6\frac{1}{2}}$
3401. 665	3	29388. 93	
3401. 530	1	29390. 10	
3400. 80	1	29396. 41	
3400. 15	4*Z*	29402. 03	$c\ ^2D_{1\frac{1}{2}}$—$y\ ^2P^{\circ}_{0\frac{1}{2}}$
3399. 574	4	29407. 01	
3399. 396	2	29408. 55	
3399. 100	3	29411. 11	
3398. 970	4	29412. 23	$c\ ^4D_{1\frac{1}{2}}$—$x\ ^4D^{\circ}_{0\frac{1}{2}}$
3397. 105	2	29428. 38	$c\ ^4D_{2\frac{1}{2}}$—$y\ ^4H^{\circ}_{3\frac{1}{2}}$

TABLE 1. *Wavelengths and term combinations of* Mo II—Continued

Wavelength λ_{air}	Intensity	Wave No.	Term combination	Wavelength λ_{air}	Intensity	Wave No.	Term combination
3395. 75	4Z	29440. 12	$a\ ^4D_{1\frac{1}{2}}$—$z\ ^6F^o_{2\frac{1}{2}}$	3348. 99	20	29851. 17	$b\ ^2D_{1\frac{1}{2}}$—$x\ ^4D^o_{0\frac{1}{2}}$
3395. 360	35Z	29443. 51	$c\ ^2F_{2\frac{1}{2}}$—$x\ ^4G^o_{2\frac{1}{2}}$	3348. 92	45Z	29851. 79	$a\ ^2F_{2\frac{1}{2}}$—$z\ ^4D^o_{1\frac{1}{2}}$
3394. 810	7Z	29448. 28	$b\ ^2G_{3\frac{1}{2}}$— $(1)^o_{2\frac{1}{2}}$	3347. 91	2	29860. 80	
3394. 335	1h	29452. 40		3347. 254	75Z	29866. 65	$b\ ^4D_{0\frac{1}{2}}$—$z\ ^4D^o_{0\frac{1}{2}}$
3393. 557	7	29459. 15	$b\ ^4G_{3\frac{1}{2}}$—$z\ ^4G^o_{3\frac{1}{2}}$	3346. 386	100Z	29874. 40	$b\ ^4D_{3\frac{1}{2}}$—$z\ ^4D^o_{2\frac{1}{2}}$
3393. 122	10	29462. 93	$b\ ^2D_{2\frac{1}{2}}$—$x\ ^4D^o_{2\frac{1}{2}}$ $c\ ^4D_{3\frac{1}{2}}$—$(2)^o_{4\frac{1}{2}}$	3346. 120	20Z	29876. 77	$b\ ^2I_{5\frac{1}{2}}$—$y\ ^2H^o_{5\frac{1}{2}}$
3392. 92	4	29464. 68	$b\ ^2D_{1\frac{1}{2}}$—$x\ ^4D^?$	3344. 87	2	29887. 93	$a\ ^4D_{2\frac{1}{2}}$—$z\ ^6F^o_{3\frac{1}{2}}$
3392. 755	4	29466. 11	$b\ ^4G_{4\frac{1}{2}}$—$z\ ^4I^o_{4\frac{1}{2}}$	3344. 55	3	29890. 80	
3391. 843	100Z	29474. 04	$b\ ^2G_{4\frac{1}{2}}$—$z\ ^2I^o_{5\frac{1}{2}}$	3344. 025	1	29895. 49	$b\ ^2G_{3\frac{1}{2}}$—$y\ ^4G^o_{2\frac{1}{2}}$
3391. 442	5	29477. 52	$c\ ^4D_{1\frac{1}{2}}$—$y\ ^4F^o_{1\frac{1}{2}}$	3343. 896	1	29896. 64	$b\ ^2H_{5\frac{1}{2}}$—$y\ ^4H^o_{4\frac{1}{2}}$
				3343. 02	3	29904. 47	
			$d\ ^2F_{3\frac{1}{2}}$—$v\ ^2F^o_{2\frac{1}{2}}$	3342. 588	5	29908. 34	$b\ ^2H_{4\frac{1}{2}}$—$y\ ^4G^o_{4\frac{1}{2}}$
3389. 76	3	29492. 15	$c\ ^4D_{3\frac{1}{2}}$—$y\ ^4G^o_{2\frac{1}{2}}$	3341. 36	2	29919. 33	
3388. 33	1	29504. 59		3341. 072	3	29921. 91	$b\ ^4G_{4\frac{1}{2}}$—$z\ ^2G^o_{3\frac{1}{2}}$
3387. 88	4	29508. 51	$b\ ^2D_{1\frac{1}{2}}$—$(1)^o_{2\frac{1}{2}}$	3340. 74	3	29924. 88	
3386. 98	7Z	29516. 38	$c\ ^4D_{1\frac{1}{2}}$—$y\ ^4G^o_{2\frac{1}{2}}$				
3386. 27	8	29522. 54	$c\ ^4D_{2\frac{1}{2}}$—$y\ F^o_{2\frac{1}{2}}$	3340. 525	5	29926. 81	$c\ ^2F_{3\frac{1}{2}}$—$w\ ^4D^o_{2\frac{1}{2}}$
3383. 982	60Z	29542. 50	$c\ ^2F_{2\frac{1}{2}}$— $(3)^o_{3\frac{1}{2}}$	3339. 48	2	29936. 17	
3380. 218	150Z	29575. 40	$b\ ^4D_{2\frac{1}{2}}$—$z\ ^4D^o_{1\frac{1}{2}}$	3339. 14	4	29939. 22	
3380. 08	5	29576. 60	$a\ ^2S_{0\frac{1}{2}}$—$z\ ^2S^o_{0\frac{1}{2}}$	3338. 88	4	29941. 55	
3379. 753	125Z	29579. 47	$b\ ^4D_{1\frac{1}{2}}$—$z\ ^4D^o_{0\frac{1}{2}}$	3338. 67	3d?	29943. 44	
3376. 710	40Z	29606. 12	$b\ ^2H_{5\frac{1}{2}}$—$y\ ^4G^o_{5\frac{1}{2}}$	3338. 152	5	29948. 08	$c\ ^4D_{3\frac{1}{2}}$—$y\ ^4H^o_{4\frac{1}{2}}$
3376. 02	1	29612. 17	$b\ ^2D_{2\frac{1}{2}}$—$x\ ^4D^o_{3\frac{1}{2}}$	3337. 82	2	29951. 06	
3375. 872	3	29613. 47	$d\ ^2G_{4\frac{1}{2}}$—$w\ ^2H^o_{4\frac{1}{2}}$	3337. 66	1	29952. 50	$b\ ^2G_{4\frac{1}{2}}$—$y\ ^4G^o_{5\frac{1}{2}}$
3375. 54	2	29616. 38		3337. 01	4w	29958. 35	$b\ ^2G_{3\frac{1}{2}}$—$y\ ^4F^o_{3\frac{1}{2}}$
3374. 839	20Z	29622. 53	$a\ ^2P_{0\frac{1}{2}}$—$z\ ^2P^o_{1\frac{1}{2}}$	3336. 06	6w	29966. 89	$b\ ^2H_{4\frac{1}{2}}$— $(2)^o_{3\frac{1}{2}}$
3373. 98	2l	29630. 08		3335. 55	3	29971. 44	
3373. 10	20Z	29637. 80	$a\ ^2G_{4\frac{1}{2}}$—$z\ ^4D^o_{3\frac{1}{2}}$	3335. 497	10Z	29971. 92	$a\ ^2P_{0\frac{1}{2}}$—$z\ ^2P^o_{0\frac{1}{2}}$
3372. 47	1	29643. 34	$b\ ^4F_{1\frac{1}{2}}$—$z\ ^2S^o_{0\frac{1}{2}}$	3335. 36	2	29973. 15	
3371. 690	100Z	29650. 20	$c\ ^2F_{3\frac{1}{2}}$—$x\ ^4G^o_{4\frac{1}{2}}$				$c\ ^2F_{3\frac{1}{2}}$—$w\ ^4D^o_{3\frac{1}{2}}$
3371. 54	7	29651. 52		3335. 106	10Z	29975. 43	$a\ ^2P_{1\frac{1}{2}}$—$z\ ^2F^o_{2\frac{1}{2}}$
3370. 541	50Z	29660. 31	$b\ ^4G_{3\frac{1}{2}}$—$z\ ^4I^o_{4\frac{1}{2}}$				$b\ ^2I_{6\frac{1}{2}}$—$z\ ^2H^o_{5\frac{1}{2}}$
				3334. 398	1	29981. 80	
3369. 932	15Z	29665. 67	$a\ ^4H_{3\frac{1}{2}}$—$z\ ^4D^o_{3\frac{1}{2}}$				
3369. 59	8	29668. 71	$b\ ^2I_{5\frac{1}{2}}$—$z\ ^2H^o_{5\frac{1}{2}}$	3334. 24	1	29983. 22	
3367. 960	300Z	29683. 04	$b\ ^2H_{4\frac{1}{2}}$—$z\ ^2I^o_{5\frac{1}{2}}$	3334. 07	2	29984. 75	
3366. 930	10Z	29692. 12	$b\ ^4P_{1\frac{1}{2}}$—$y\ ^4D^o_{0\frac{1}{2}}$	3333. 84	3	29986. 82	
3366. 14	3	29699. 08	$b\ ^2G_{4\frac{1}{2}}$—$y\ ^4G^o_{4\frac{1}{2}}$	3333. 64	3d?	29988. 62	
				3332. 524	75Z	29998. 66	$c\ ^2G_{4\frac{1}{2}}$—$x\ ^2G^o_{4\frac{1}{2}}$
3365. 314	2	29706. 37	$c\ ^2G_{4\frac{1}{2}}$—$x\ ^2G^o_{3\frac{1}{2}}$	3332. 320	2	30000. 49	
3365. 041	2	29708. 78	$b\ ^2I_{5\frac{1}{2}}$—$y\ ^4H^o_{6\frac{1}{2}}$	3332. 07	2	30002. 74	
3364. 38	2	29714. 62	$b\ ^2D_{2\frac{1}{2}}$— $(1)^o_{2\frac{1}{2}}$	3331. 914	2	30004. 15	
3363. 012	75Z	29726. 71	$b\ ^4F_{4\frac{1}{2}}$—$z\ ^4H^o_{3\frac{1}{2}}$	3331. 610	5	30006. 89	$c\ ^4D_{2\frac{1}{2}}$—$z\ ^2F^o_{3\frac{1}{2}}$
3360. 54	6	29748. 57	$a\ ^2P_{1\frac{1}{2}}$—$x\ ^4F^o_{2\frac{1}{2}}$ $c\ ^4D_{3\frac{1}{2}}$—$y\ ^4H^o_{3\frac{1}{2}}$	3331. 40	15Z	30008. 81	$c\ ^4D_{0\frac{1}{2}}$—$x\ ^4F^o_{1\frac{1}{2}}$
3360. 285	35Z	29750. 83	$d\ ^2G_{3\frac{1}{2}}$—$w\ ^2H^o_{3\frac{1}{2}}$	3330. 882	35	30013. 44	$b\ ^2F_{2\frac{1}{2}}$—$z\ ^4H^o_{3\frac{1}{2}}$ $b\ ^4G_{4\frac{1}{2}}$—$z\ ^4G^o_{4\frac{1}{2}}$
3360. 104	7	29752. 43		3330. 669	10	30015. 36	$b\ ^2I_{6\frac{1}{2}}$—$y\ ^4H^o_{5\frac{1}{2}}$
3357. 96	2	29771. 43	$b\ ^2G_{3\frac{1}{2}}$—$y\ ^4G^o_{3\frac{1}{2}}$	3330. 288	18	30018. 80	$b\ ^2I_{5\frac{1}{2}}$—$y\ ^2H^o_{5\frac{1}{2}}$
3357. 785	10	29772. 98	$a\ ^2D_{2\frac{1}{2}}$—$z\ ^4F^o_{3\frac{1}{2}}$	3329. 208	100Z	30028. 54	$b\ ^4D_{1\frac{1}{2}}$—$z\ ^4D^o_{1\frac{1}{2}}$
3357. 074	50Z	29779. 29	$b\ ^4G_{2\frac{1}{2}}$—$z\ ^4G^o_{3\frac{1}{2}}$	3328. 564	10Z	30034. 34	$a\ ^4D_{1\frac{1}{2}}$—$z\ ^4P^o_{0\frac{1}{2}}$ $c\ ^4D_{2\frac{1}{2}}$—$x\ ^4F^o_{1\frac{1}{2}}$
3356. 40	3	29785. 27		3328. 13	1	30038. 26	$b\ ^2D_{2\frac{1}{2}}$—$y\ ^4G^o_{3\frac{1}{2}}$
3355. 50	2	29793. 26		3327. 91	1	0040. 25	$d\ ^2F_{3\frac{1}{2}}$—$v\ ^2F^o_{3\frac{1}{2}}$
3355. 46	2	29793. 61	$c\ ^2F_{2\frac{1}{2}}$—$y\ ^2D^o_{2\frac{1}{2}}$	3327. 522	5	30043. 75	$b\ ^2G_{4\frac{1}{2}}$—$y\ ^4H^o_{3\frac{1}{2}}$
3353. 92	2h	29807. 29	$b\ ^2G_{3\frac{1}{2}}$—$y\ ^4G^o_{4\frac{1}{2}}$	3326. 900	2s	30049. 37	
3353. 700	4	29809. 25		3326. 76	2	30050. 63	
						3	
3352. 834	15d?Z	29816. 94	$c\ ^2D_{2\frac{1}{2}}$—$w\ ^2F^o_{2\frac{1}{2}}$	3326. 56	2	0052. 44	
3352. 16	2h	29822. 94		3326. 39	2	30053. 97	
3350. 715	2	29835. 80	$b\ ^4G_{5\frac{1}{2}}$—$z\ ^4G^o_{4\frac{1}{2}}$	3325. 85	1h	30058. 85	$b\ ^2H_{4\frac{1}{2}}$—$y\ ^4F^o_{3\frac{1}{2}}$
3350. 57	2	29837. 09	$d\ ^2F_{3\frac{1}{2}}$—$w\ ^2D^o_{2\frac{1}{2}}$	3325. 222	50Z	30064. 53	$b\ ^4F_{3\frac{1}{2}}$—$z\ ^4G^o_{2\frac{1}{2}}$
3349. 70	2	29844. 84		3324. 93	2h	330067. 20	

TABLE 1. *Wavelengths and term combinations of* Mo II—Continued

Wavelength λ_{air}	Intensity	Wave No.	Term combination	Wavelength λ_{air}	Intensity	Wave No.	Term combination
3324. 85	2	30067. 90		3295. 759	12Z	30333. 29	$c\ ^4D_{2\frac{1}{2}}$—$x\ ^4F^o_{3\frac{1}{2}}$
3324. 63	2	30069. 88		3295. 61	1	30334. 66	
3324. 47	2	30071. 33		3294. 39	1	30345. 89	
3324. 22	1	30073. 59		3294. 04	1	30349. 12	
3322. 68	2	30087. 53		3293. 956	2	30349. 89	
3322. 552	10	30088. 69		3292. 964	12Z	30359. 03	$b\ ^4F_{3\frac{1}{2}}$—$y\ ^4D^o_{3\frac{1}{2}}$
3322. 126	15Z	30092. 58	$b\ ^2S_{0\frac{1}{2}}$—$x\ ^2P^o_{0\frac{1}{2}}$	3292. 310	350Z	30365. 06	$b\ ^4D_{3\frac{1}{2}}$—$z\ ^4D^o_{3\frac{1}{2}}$
3321. 204	20Z	30100. 90	$a\ ^4F_{1\frac{1}{2}}$—$z\ ^4D^o_{0\frac{1}{2}}$	3292. 21	3	30365. 99	
3320. 897	300Z	30103. 68	$b\ ^4D_{2\frac{1}{2}}$—$z\ ^4D^o_{2\frac{1}{2}}$	3290. 82	20	30378. 84	$c\ ^2F_{2\frac{1}{2}}$—$w\ ^4D^o_{2\frac{1}{2}}$ $c\ ^4D_{1\frac{1}{2}}$—$x\ ^4F^o_{1\frac{1}{2}}$
3320. 53	2	30107. 01		3290. 70	40Z	30379. 92	$a\ ^2F_{2\frac{1}{2}}$—$z\ ^4D^o_{2\frac{1}{2}}$
3319. 249	10	30118. 63					
3318. 85	2	30122. 25		3288. 86	1	30396. 91	
3318. 77	1	30122. 98	$b\ ^2D_{2\frac{1}{2}}$—$y\ ^4F^o_{1\frac{1}{2}}$	3287. 90	2*hl*	30405. 79	
3318. 65	2	30124. 06		3287. 20	25Z	30412. 27	$a\ ^4D_{0\frac{1}{2}}$—$z\ ^4P^o_{0\frac{1}{2}}$
3318. 53	2	30125. 15		3286. 48	3	30418. 93	$b\ ^2D_{2\frac{1}{2}}$—$y\ ^4H^o_{3\frac{1}{2}}$ $c\ ^2G_{4\frac{1}{2}}$—$y\ ^2I^o_{3\frac{1}{2}}$
3317. 574	2*l*	30133. 84		3286. 265	10	30420. 92	
3317. 046	10	30138. 63					
3316. 76	2	30141. 23	$b\ ^4G_{2\frac{1}{2}}$—$z\ ^2D^o_{1\frac{1}{2}}$	3286. 13	5	30422. 17	
3316. 72	5	30141. 59		3285. 89	5	30424. 39	$d\ ^2D_{1\frac{1}{2}}$—$x\ ^2P^o_{0\frac{1}{2}}$
3316. 58	2	30142. 87		3285. 595	6	30427. 12	$a\ ^2P_{0\frac{1}{2}}$—$x\ ^4D^o_{1\frac{1}{2}}$ $c\ ^2F_{2\frac{1}{2}}$—$w\ ^4D^o_{3\frac{1}{2}}$
3316. 44	2	30144. 14		3284. 595	75Z	30436. 38	$b\ ^4G_{2\frac{1}{2}}$—$z\ ^2G^o_{3\frac{1}{2}}$
3315. 573	2	30152. 02	$b\ ^2G_{3\frac{1}{2}}$—$y\ ^4H^o_{3\frac{1}{2}}$	3284. 087	1	30441. 09	
3315. 37	2	30153. 87	$a\ ^4P_{1\frac{1}{2}}$—$z\ ^6F^o_{0\frac{1}{2}}$				
3315. 30	10*h*	30154. 50		3283. 73	3*dl*?	30444. 40	$b\ ^4F_{4\frac{1}{2}}$—$z\ ^4G^o_{3\frac{1}{2}}$
3314. 48	10	30161. 96	$b\ ^2D_{2\frac{1}{2}}$—$y\ ^4G^o_{2\frac{1}{2}}$ $b\ ^2H_{4\frac{1}{2}}$—$y\ ^4G^o_{3\frac{1}{2}}$	3283. 240	4	30448. 94	$a\ ^4P_{1\frac{1}{2}}$—$z\ ^6F^o_{1\frac{1}{2}}$
3314. 117	5	30165. 27	$b\ ^2S_{0\frac{1}{2}}$—$w\ ^2D^o_{1\frac{1}{2}}$	3282. 892	60Z	30452. 17	$b\ ^2H_{4\frac{1}{2}}$—$y\ ^4H^o_{3\frac{1}{2}}$
3313. 629	200	30169. 71	$b\ ^4F_{1\frac{1}{2}}$—$z\ ^4G^o_{2\frac{1}{2}}$	3282. 454	6	30456. 24	$b\ ^4P_{2\frac{1}{2}}$—$z\ ^4G^o_{3\frac{1}{2}}$
3312. 885	75	30176. 49	$b\ ^4F_{2\frac{1}{2}}$—$z\ ^4G^o_{2\frac{1}{2}}$	3281. 84	1	30461. 93	
3312. 53	1	30179. 72		3281. 596	12	30464. 20	$b\ ^4F_{1\frac{1}{2}}$—$y\ ^4D^o_{2\frac{1}{2}}$
3312. 20	1	30182. 73		3280. 862	12	30471. 01	$b\ ^4F_{2\frac{1}{2}}$—$y\ ^4D^o_{2\frac{1}{2}}$
				3279. 690	7	30481. 90	$b\ ^2F_{3\frac{1}{2}}$—$z\ ^4H^o_{3\frac{1}{2}}$
3311. 54	2	30188. 77	$c\ ^2D_{2\frac{1}{2}}$—$w\ ^2F^o_{3\frac{1}{2}}$	3279. 196	20	30486. 49	$c\ ^2D_{1\frac{1}{2}}$—$w\ ^2F^o_{2\frac{1}{2}}$
3310. 35	2	30199. 59		3278. 95	15	30488. 78	$b\ ^4G_{4\frac{1}{2}}$—$y\ ^4D^o_{3\frac{1}{2}}$
3310. 16	2	30201. 33					
3309. 458	5Z	30207. 73	$b\ ^4G_{2\frac{1}{2}}$—$z\ ^4G^o_{4\frac{1}{2}}$	3278. 86	50Z	30489. 62	$b\ ^4F_{3\frac{1}{2}}$—$z\ ^4G^o_{3\frac{1}{2}}$
3309. 115	2*h*	30210. 86		3278. 05	8Z	30497. 13	$d\ ^2D_{1\frac{1}{2}}$—$w^2D^o_{1\frac{1}{2}}$
				3277. 87	1	30498. 83	
3308. 315	1	30218. 17		3277. 58	1	30501. 52	
3308. 138	2*l*	30219. 79		3276. 322	125Z	30513. 24	$b\ ^2D_{2\frac{1}{2}}$—$y\ ^4F^o_{2\frac{1}{2}}$ $b\ ^4P_{1\frac{1}{2}}$—$y\ ^4D^o_{1\frac{1}{2}}$
3307. 91	2	30221. 87					
3307. 81	1	30222. 78					
3307. 418	40	30226. 36	$c\ ^2G_{3\frac{1}{2}}$—$x\ ^2F^o_{2\frac{1}{2}}$	3274. 620	50	30529. 09	$b\ ^2G_{4\frac{1}{2}}$—$y\ ^4F^o_{4\frac{1}{2}}$ $b\ ^2H_{5\frac{1}{2}}$—$z\ ^2H^o_{4\frac{1}{2}}$
3305. 59	5	30243. 08	$b\ ^2G_{4\frac{1}{2}}$—$y\ ^4H^o_{4\frac{1}{2}}$	3274. 185	4	30533. 15	$b\ ^4G_{5\frac{1}{2}}$—$z\ ^4I^o_{5\frac{1}{2}}$
3305. 244	8	30246. 25	$b\ ^2G_{3\frac{1}{2}}$—$y\ ^4F^o_{2\frac{1}{2}}$	3273. 573	10Z	30538. 86	$b\ ^2H_{5\frac{1}{2}}$—$y\ ^4H^o_{5\frac{1}{2}}$
3304. 86	1	30249. 76		3272. 372	15Z	30550. 07	$a\ ^4F_{1\frac{1}{2}}$—$z\ ^4D^o_{1\frac{1}{2}}$
3304. 515	10	30252. 92	$b\ ^2H_{4\frac{1}{2}}$—$y\ ^4H^o_{3\frac{1}{2}}$	3271. 659	200Z	30556. 72	$b\ ^4D_{1\frac{1}{2}}$—$z\ ^4D^o_{2\frac{1}{2}}$
3303. 967	8	30257. 94	$a\ ^4P_{0\frac{1}{2}}$—$z\ ^6F^o_{1\frac{1}{2}}$				
				3270. 30	1*l*	30569. 42	$a\ ^2H_{5\frac{1}{2}}$—$z\ ^4H^o_{4\frac{1}{2}}$
3303. 52	7	30262. 03	$b\ ^2F_{2\frac{1}{2}}$—$y\ ^4D^o_{1\frac{1}{2}}$	3270. 14	2	30570. 92	
3302. 685	18Z	30269. 67	$c\ ^2G_{4\frac{1}{2}}$—$w\ ^4F^o_{4\frac{1}{2}}$	3268. 970	22Z	30581. 86	$b\ ^4G_{5\frac{1}{2}}$—$z\ ^2G^o_{4\frac{1}{2}}$
3301. 574	4	30279. 86		3267. 625	100Z	30594. 45	$b\ ^4D_{2\frac{1}{2}}$—$z\ ^4D^o_{3\frac{1}{2}}$
3301. 24	2	30282. 93		3266. 867	100Z	30601. 55	$b\ ^4F_{2\frac{1}{2}}$—$z\ ^4G^o_{3\frac{1}{2}}$
3300. 984	3	30285. 28	$a\ ^4D_{2\frac{1}{2}}$—$z\ ^6F^o_{3\frac{1}{2}}$				
3300. 570	15Z	30289. 08	$b\ ^2I_{5\frac{1}{2}}$—$y\ ^2G^o_{4\frac{1}{2}}$	3265. 14	5	30617. 76	$d\ ^2D_{2\frac{1}{2}}$—$w\ ^2D^o_{1\frac{1}{2}}$
3299. 592	10Z	30298. 05	$c\ ^4D_{2\frac{1}{2}}$—$x\ ^4F^o_{2\frac{1}{2}}$	3264. 79	7	30621. 01	$c\ ^2G_{3\frac{1}{2}}$—$x\ ^2G^o_{4\frac{1}{2}}$
3299. 347	10	30300. 30		3264. 66	7	30622. 23	$b\ ^2G_{4\frac{1}{2}}$—$z\ ^2F^o_{3\frac{1}{2}}$
3298. 834	6*l*	30305. 01		3264. 13	1	30627. 20	
3298. 693	6*s*	30306. 31	$b\ ^2D_{1\frac{1}{2}}$—$y\ ^4F^o_{2\frac{1}{2}}$	3263. 60	1	30632. 18	
3297. 677	60Z	30315. 65	$b\ ^4D_{0\frac{1}{2}}$—$z\ ^4D^o_{1\frac{1}{2}}$	3262. 482	15	30642. 67	$c\ ^4D_{1\frac{1}{2}}$—$x\ ^4F^o_{2\frac{1}{2}}$
3296. 592	40	30325. 62	$b\ ^2I_{6\frac{1}{2}}$—$y\ ^2H^o_{5\frac{1}{2}}$	3262. 164	30Z	30645. 66	$b\ ^4F_{4\frac{1}{2}}$—$z\ ^4I^o_{4\frac{1}{2}}$
3296. 57	50Z	30325. 83	$b\ ^4P_{2\frac{1}{2}}$—$y\ ^4D^o_{2\frac{1}{2}}$	3261. 69	5	30650. 11	$c\ ^2F_{3\frac{1}{2}}$—$x\ ^2F^o_{3\frac{1}{2}}$
3296. 238	12Z	30328. 88	$c\ ^2G_{3\frac{1}{2}}$—$x\ ^2G^o_{3\frac{1}{2}}$	3261. 30	2	30653. 78	$c\ ^4D_{3\frac{1}{2}}$—$x\ ^4F^o_{3\frac{1}{2}}$
3296. 10	5	30330. 15		3259. 664	4	30669. 16	

Wavelength λ_{air}	Intensity	Wave No.	Term combination
3258. 990	8	30675. 51	
3258. 676	50*Z*	30678. 46	$a\ ^4D_{2\frac{1}{2}}$—$z\ ^4P^o_{1\frac{1}{2}}$
3257. 370	10*Z*	30690. 76	$b\ ^4F_{3\frac{1}{2}}$—$z\ ^4I^o_{4\frac{1}{2}}$
3256. 81	2	30696. 04	
3255. 69	1	30706. 60	$a\ ^2F_{3\frac{1}{2}}$—$z\ ^4D^o_{2\frac{1}{2}}$
3255. 62	1	30707. 26	
3255. 236	40*Z*	30710. 88	$b\ ^4G_{4\frac{1}{2}}$—$z\ ^4I^o_{5\frac{1}{2}}$
3254. 680	75*Z*	30716. 13	$b\ ^4P_{0\frac{1}{2}}$—$y\ ^4D^o_{0\frac{1}{2}}$
3253. 733	85*Z*	30725. 07	$b\ ^2H_{5\frac{1}{2}}$—$x\ ^4F^o_{4\frac{1}{2}}$; $b\ ^4G_{5\frac{1}{2}}$—$z\ ^4G^o_{5\frac{1}{2}}$
3253. 34	1	30728. 78	
3253. 17	2	30730. 38	$b\ ^2G_{3\frac{1}{2}}$—$z\ ^2F^o_{3\frac{1}{2}}$
3253. 04	1	30731. 61	
3252. 335	20*Z*	30738. 27	$b\ ^2H_{4\frac{1}{2}}$—$y\ ^4F^o_{4\frac{1}{2}}$
3251. 25	1	30748. 53	$c\ ^2G_{3\frac{1}{2}}$—$w\ ^4F^o_{3\frac{1}{2}}$
3250. 745	100*Z*	30753. 31	$a\ ^4F_{2\frac{1}{2}}$—$z\ ^4D^o_{1\frac{1}{2}}$
3250. 075	10	30759. 65	$b\ ^4G_{4\frac{1}{2}}$—$z\ ^2G^o_{4\frac{1}{2}}$
3249. 66	1	30763. 57	
3248. 225	20	30777. 16	$c\ ^4D_{3\frac{1}{2}}$—$x\ ^4F^o_{4\frac{1}{2}}$
3247. 994	5	30779. 35	$d\ ^2F_{2\frac{1}{2}}$—$u\ ^2F^o_{3\frac{1}{2}}$
3247. 258	6	30786. 33	$b\ ^2F_{3\frac{1}{2}}$—$z\ ^4H^o_{4\frac{1}{2}}$
3246. 34	2*hl*	30795. 06	
3245. 787	12	30800. 28	$c\ ^2D_{2\frac{1}{2}}$—$x\ ^2D^o_{2\frac{1}{2}}$
3244. 82	2*h*	30809. 46	
3244. 14	1*hs*	30815. 92	
3243. 964	2	30817. 59	$b\ ^2D_{1\frac{1}{2}}$—$x\ ^4F^o_{1\frac{1}{2}}$
3243. 50	1*h*	30822. 00	
3243. 185	20*Z*	30824. 99	$c\ ^2D_{2\frac{1}{2}}$—$x\ ^2D^o_{1\frac{1}{2}}$
3242. 81	3	30828. 56	
3242. 511	5	30831. 40	$b\ ^2H_{4\frac{1}{2}}$—$z\ ^2F^o_{3\frac{1}{2}}$
3241. 962	6	30836. 62	
3241. 408	2	30841. 89	
3240. 723	100*Z*	30848. 41	$a\ ^4D_{1\frac{1}{2}}$—$z\ ^4P^o_{1\frac{1}{2}}$
3240. 169	2	30853. 68	$a\ ^2P_{1\frac{1}{2}}$—$y\ ^2F^o_{2\frac{1}{2}}$
3240. 04	1*e*	30854. 91	
3239. 19	5	30863. 01	$d\ ^2G_{3\frac{1}{2}}$—$v\ ^2F^o_{3\frac{1}{2}}$
3238. 92	4	30865. 58	
3238. 81	3	30866. 63	
3238. 504	6	30869. 54	$c\ ^4D_{1\frac{1}{2}}$—$z\ ^2F^o_{2\frac{1}{2}}$
3238. 400	20*Z*	30870. 54	$a\ ^2F_{2\frac{1}{2}}$—$z\ ^4D^o_{3\frac{1}{2}}$
3237. 840	20*Z*	30875. 88	$b\ ^2G_{4\frac{1}{2}}$—$z\ ^2H^o_{4\frac{1}{2}}$
3237. 317	1	30880. 86	$c\ ^4D_{2\frac{1}{2}}$—$z\ ^4S^o_{1\frac{1}{2}}$
3236. 824	6	30885. 57	$b\ ^2G_{4\frac{1}{2}}$—$y\ ^4H^o_{5\frac{1}{2}}$
3236. 14	4	30892. 09	$c\ ^2G_{3\frac{1}{2}}$—$w\ ^4F^o_{4\frac{1}{2}}$
3235. 38	20*Z*	30899. 35	$b\ ^4P_{1\frac{1}{2}}$—$z\ ^2S^o_{0\frac{1}{2}}$
3235. 015	25*Z*	30902. 84	$b\ ^4G_{4\frac{1}{2}}$—$z\ ^4G^o_{5\frac{1}{2}}$
3234. 51	2*h*	30907. 66	
3234. 48	6	30907. 95	
3233. 75	10	30914. 92	$a\ ^4P_{1\frac{1}{2}}$—$z\ ^6F^o_{2\frac{1}{2}}$
3232. 924	5	30922. 82	$a\ ^4P_{2\frac{1}{2}}$—$z\ ^6F^o_{3\frac{1}{2}}$
3231. 79	1	30933. 67	
3230. 898	8*Z*	30942. 21	$d\ ^2D_{1\frac{1}{2}}$—$v\ ^2F^o_{2\frac{1}{2}}$
3230. 222	5	30948. 72	$b\ ^2G_{4\frac{1}{2}}$—$x\ ^4F^o_{3\frac{1}{2}}$; $a\ ^4G_{2\frac{1}{2}}$—$z\ ^6F^o_{1\frac{1}{2}}$
3229. 940	12	30951. 39	
3229. 681	35*Z*	30953. 87	$b\ ^4G_{3\frac{1}{2}}$—$z\ ^2G^o_{4\frac{1}{2}}$
3229. 360	6	30956. 95	$b\ ^4F_{1\frac{1}{2}}$—$z\ ^2D^o_{1\frac{1}{2}}$
3228. 07	1	30969. 32	
3227. 82	4	30971. 72	$c\ ^2F_{3\frac{1}{2}}$—$x\ ^4P^o_{2\frac{1}{2}}$
3227. 68	3	30973. 06	$b\ ^4G_{3\frac{1}{2}}$—$z\ ^2D^o_{2\frac{1}{2}}$
3227. 455	6	30975. 22	
3227. 19	5	30977. 77	
3226. 702	4	30982. 45	$c\ ^4D_{2\frac{1}{2}}$—$y\ ^2G^o_{3\frac{1}{2}}$
3226. 560	20*Z*	30983. 81	$b\ ^2G_{3\frac{1}{2}}$—$z\ ^2H^o_{4\frac{1}{2}}$
3226. 39	2	30985. 45	$b\ ^2I_{5\frac{1}{2}}$—$x\ ^4G^o_{4\frac{1}{2}}$
3225. 75	6*w*, *Z*	30991. 62	
3225. 21	1	30996. 78	$b\ ^2D_{2\frac{1}{2}}$—$z\ ^2F^o_{3\frac{1}{2}}$
3224. 557	20*Z*	31003. 06	$b\ ^4G_{2\frac{1}{2}}$—$y\ ^4D^o_{3\frac{1}{2}}$
3222. 907	45*Z*	31018. 93	$c\ ^2F_{3\frac{1}{2}}$—$x\ ^2G^o_{3\frac{1}{2}}$
3222. 272	8	31025. 04	$a\ ^2P_{1\frac{1}{2}}$—$y\ ^2D^o_{1\frac{1}{2}}$
3219. 407	10*Z*	31052. 65	$a\ ^4D_{3\frac{1}{2}}$—$z\ ^6F^o_{4\frac{1}{2}}$
3218. 96	2*e*	31056. 96	$b\ ^2G_{3\frac{1}{2}}$—$x\ ^4F^o_{3\frac{1}{2}}$
3218. 350	15*Z*	31062. 85	$d\ ^2D_{2\frac{1}{2}}$—$v\ ^2F^o_{2\frac{1}{2}}$
3217. 67	5*wh*	31068. 87	
3217. 42	3	31071. 83	$b\ ^2G_{4\frac{1}{2}}$—$x\ ^4F^o_{4\frac{1}{2}}$
3216. 067	100*Z*	31084. 90	$b\ ^2H_{4\frac{1}{2}}$—$z\ ^2H^o_{4\frac{1}{2}}$
3215. 68	1	31088. 64	
3214. 39	90*Z*	31101. 12	$b\ ^4F_{4\frac{1}{2}}$—$z\ ^2G^o_{3\frac{1}{2}}$
3213. 134	25*Z*	31113. 27	$b\ ^4P_{2\frac{1}{2}}$—$z\ ^2G^o_{3\frac{1}{2}}$
3211. 967	20*Z*	31124. 58	$d\ ^2F_{2\frac{1}{2}}$—$u\ ^2F^o_{3\frac{1}{2}}$
3210. 96	15*Z*	31134. 37	$a\ ^2H_{5\frac{1}{2}}$—$z\ ^4H^o_{5\frac{1}{2}}$
3209. 717	20*Z*	31146. 40	$b\ ^4F_{3\frac{1}{2}}$—$z\ ^2G^o_{3\frac{1}{2}}$
3209. 22	1	31151. 22	
3208. 68	2	31156. 46	
3208. 556	4	31157. 67	$b\ ^2H_{4\frac{1}{2}}$—$x\ ^4F^o_{3\frac{1}{2}}$
3207. 31	3*l*	31169. 77	
3207. 19	8*Z*	31170. 96	
3206. 818	8*Z*	31174. 55	$b\ ^2F_{2\frac{1}{2}}$—$z\ ^4G^o_{2\frac{1}{2}}$
3206. 26	7	31179. 98	$b\ ^2G_{3\frac{1}{2}}$—$x\ ^4F^o_{4\frac{1}{2}}$
3204. 930	50*Z*	31192. 92	$b\ ^4F_{4\frac{1}{2}}$—$z\ ^4G^o_{4\frac{1}{2}}$
3204. 47	1*d*?	31197. 39	$a\ ^2F_{3\frac{1}{2}}$—$z\ ^4D^o_{3\frac{1}{2}}$
3202. 13	2	31220. 19	
3202. 04	6	31221. 07	
3201. 94	4*hl*	31222. 04	
3201. 503	40*Z*	31226. 30	$a\ ^4D_{0\frac{1}{2}}$—$z\ ^4P^o_{1\frac{1}{2}}$
3200. 295	45*Z*	31238. 09	$b\ ^4F_{3\frac{1}{2}}$—$z\ ^4G^o_{4\frac{1}{2}}$
3199. 244	15*Z*	31248. 35	$b\ ^2G_{3\frac{1}{2}}$—$z\ ^2F^o_{2\frac{1}{2}}$
3198. 409	20*Z*	31256. 51	$b\ ^4G_{3\frac{1}{2}}$—$z\ ^4I^o_{4\frac{1}{2}}$
3198. 22	3	31258. 36	$b\ ^4F_{2\frac{1}{2}}$—$z\ ^2G^o_{3\frac{1}{2}}$
3197. 82	1	31262. 27	
3196. 85	3*h*	31271. 75	
3196. 56	1*l*	31274. 59	$c\ ^2F_{3\frac{1}{2}}$—$w\ ^4F^o_{2\frac{1}{2}}$
3196. 32	2	31276. 94	
3195. 86	15*Z*	31281. 44	$b\ ^2H_{4\frac{1}{2}}$—$x\ ^4F^o_{4\frac{1}{2}}$; $a\ ^4F_{2\frac{1}{2}}$—$z\ ^4D^o_{2\frac{1}{2}}$
3195. 64	2	31283. 59	$a\ ^4G_{3\frac{1}{2}}$—$z\ ^6F^o_{2\frac{1}{2}}$
3195. 234	10*Z*	31287. 57	$d\ ^2D_{1\frac{1}{2}}$—$w\ ^2D^o_{2\frac{1}{2}}$
3194. 655	3	31293. 24	$b\ ^4G_{2\frac{1}{2}}$—$z\ ^2D^o_{2\frac{1}{2}}$
3194. 35	2	31296. 23	
3193. 83	3	31301. 32	
3193. 690	4	31302. 69	$c\ ^4D_{3\frac{1}{2}}$—$y\ ^2G^o_{3\frac{1}{2}}$
3193. 113	8*Z*	31308. 35	$b\ ^2D_{1\frac{1}{2}}$—$z\ ^2F^o_{2\frac{1}{2}}$
3192. 642	3	31312. 97	$a\ ^2P_{1\frac{1}{2}}$—$x\ ^4G^o_{2\frac{1}{2}}$
3192. 103	45*Z*	31318. 26	$a\ ^4P_{0\frac{1}{2}}$—$z\ ^4P^o_{0\frac{1}{2}}$
3189. 364	12*Z*	31345. 15	$b\ ^2S_{0\frac{1}{2}}$—$x\ ^2P^o_{1\frac{1}{2}}$
3188. 85	2*hlZ*	31350. 20	
3187. 592	75*Z*	31362. 57	$a\ ^4F_{3\frac{1}{2}}$—$z\ ^4D^o_{2\frac{1}{2}}$
3187. 22	1	31366. 23	
3186. 388	30*Z*	31374. 42	$a\ ^2D_{1\frac{1}{2}}$—$z\ ^4D^o_{0\frac{1}{2}}$
3185. 561	18*Z*	31382. 57	$d\ ^2F_{2\frac{1}{2}}$—$t\ ^2F^o_{3\frac{1}{2}}$
3185. 28	3	31385. 34	
3184. 69	2	31391. 15	$c\ ^4D_{2\frac{1}{2}}$—$y\ ^2F^o_{3\frac{1}{2}}$
3183. 41	15*Z*	31403. 77	$a\ ^4H_{4\frac{1}{2}}$—$z\ ^4H^o_{3\frac{1}{2}}$

TABLE 1. *Wavelengths and term combinations of* Mo II—Continued

Wavelength λ_{air}	Intensity	Wave No.	Term combination
3182.960	30	31408.21	$d\,^2D_{2\frac{1}{2}}$—$w^2D^\circ_{2\frac{1}{2}}$
3181.170	18Z	31425.89	$b\,^4P_{1\frac{1}{2}}$—$z\,^4G^\circ_{2\frac{1}{2}}$
3180.60	5*hl*	31431.52	
3178.89	5	31448.42	
3177.997	30Z	31457.26	$a\,^4H_{3\frac{1}{2}}$—$z\,^4H^\circ_{4\frac{1}{2}}$
3176.74	7	31469.71	$c\,^2D_{1\frac{1}{2}}$—$x\,^2D^\circ_{2\frac{1}{2}}$
3176.33	90Z	31473.77	$b\,^2H_{5\frac{1}{2}}$—$z\,^2H^\circ_{5\frac{1}{2}}$
3175.050	90Z	31486.46	$a\,^2G_{3\frac{1}{2}}$—$z\,^4H^\circ_{3\frac{1}{2}}$
3174.53	2	31491.61	$d\,^2F_{2\frac{1}{2}}$—$w^4G^\circ_{2\frac{1}{2}}$
3174.233	20Z	31494.56	$c\,^2D_{1\frac{1}{2}}$—$x\,^2D^\circ_{1\frac{1}{2}}$
3173.760	18*w*Z	31499.25	$d\,^2F_{3\frac{1}{2}}$—$u\,^2F^\circ_{3\frac{1}{2}}$
3172.85	10*w*	31508.29	
3172.745	90	31509.33	$a\,^4P_{1\frac{1}{2}}$—$z\,^4P^\circ_{0\frac{1}{2}}$
3172.300	35	31513.75	$b\,^2H_{5\frac{1}{2}}$—$y\,^4H^\circ_{4\frac{1}{2}}$
3172.030	75	31516.43	$a\,^4D_{2\frac{1}{2}}$—$z\,^4P^\circ_{2\frac{1}{2}}$
3169.934	30	31537.27	$b\,^4P_{0\frac{1}{2}}$—$y\,^4D^\circ_{1\frac{1}{2}}$
3169.580	10	31540.79	$a\,^4P_{2\frac{1}{2}}$—$z\,^6F^\circ_{3\frac{1}{2}}$
3169.44	2*w*	31542.19	
3169.02	2*w*	31546.37	
3168.730	10Z	31549.25	$c\,^4D_{0\frac{1}{2}}$—$y\,^2D^\circ_{1\frac{1}{2}}$
3167.727	20Z	31559.24	$d\,^2F_{2\frac{1}{2}}$—$t\,^2F^\circ_{2\frac{1}{2}}$
3167.17	2*w*	31564.79	
3167.017	20Z	31566.32	
3166.31	2*hl*	31573.37	
3166.19	3*w*	31574.56	$c\,^4D_{2\frac{1}{2}}$—$y\,^2D^\circ_{1\frac{1}{2}}$
3165.58	1	31580.65	
3165.42	3*w*	31582.24	$c\,^2F_{3\frac{1}{2}}$—$w^4F^\circ_{4\frac{1}{2}}$
3163.89	8Z	31597.51	
3163.87	7	31597.71	$b\,^2G_{4\frac{1}{2}}$—$y\,^2G^\circ_{3\frac{1}{2}}$
3162.56	8	31610.80	$d\,^2D_{2\frac{1}{2}}$—$v\,^2F^\circ_{3\frac{1}{2}}$
3161.32	2*w*	31623.20	
3161.12	8*wlZ*	31625.20	
3160.106	10*w*	31635.35	
3159.34	10Z	31643.05	$b\,^2F_{3\frac{1}{2}}$—$z\,^4G^\circ_{2\frac{1}{2}}$
3159.205	25	31644.37	$b\,^2I_{6\frac{1}{2}}$—$x\,^4G^\circ_{5\frac{1}{2}}$
3158.950	18	31646.93	$a\,^4H_{6\frac{1}{2}}$—$z\,^4H^\circ_{5\frac{1}{2}}$
3157.66	3	31659.85	
3157.327	20Z	31663.19	$a\,^2P_{1\frac{1}{2}}$—$y\,^2D^\circ_{2\frac{1}{2}}$
3156.848	40Z	31668.00	$b\,^4F_{4\frac{1}{2}}$—$y\,^4D^\circ_{3\frac{1}{2}}$
3156.34	4	31673.09	$b\,^2S_{0\frac{1}{2}}$—$w^2P^\circ_{0\frac{1}{2}}$
3155.951	12	31677.00	$d\,^2D_{1\frac{1}{2}}$—$x\,^2P^\circ_{1\frac{1}{2}}$
3155.655	50Z	31679.97	$b\,^4P_{2\frac{1}{2}}$—$y\,^4D^\circ_{3\frac{1}{2}}$
3155.50	7*w*	31681.52	$b\,^2H_{5\frac{1}{2}}$—$y\,^2H^\circ_{4\frac{1}{2}}$
3155.008	12*d*Z	31686.46	$a\,^4D_{1\frac{1}{2}}$—$z\,^4P^\circ_{2\frac{1}{2}}$
3154.52	3	31691.37	
3154.00	2*w*	31696.59	$a\,^4D_{2\frac{1}{2}}$—$z\,^6P^\circ_{1\frac{1}{2}}$
3153.06	3	31706.07	$b\,^2G_{3\frac{1}{2}}$—$y\,^2G^\circ_{3\frac{1}{2}}$
3152.825	150Z	31708.40	$a\,^4H_{4\frac{1}{2}}$—$z\,^4H^\circ_{4\frac{1}{2}}$
3152.344	8	31713.24	$b\,^4F_{3\frac{1}{2}}$—$y\,^4D^\circ_{3\frac{1}{2}}$
3151.637	100Z	31720.35	$b\,^4P_{1\frac{1}{2}}$—$y\,^4D^\circ_{2\frac{1}{2}}$
3150.354	8Z	31733.27	$c\,^4D_{3\frac{1}{2}}$—$y\,^2H^\circ_{4\frac{1}{2}}$
3148.920	2*w*	31747.73	$c\,^4D_{1\frac{1}{2}}$—$y\,^2F^\circ_{2\frac{1}{2}}$
3148.69	5	31750.04	
3148.36	6	31753.37	$a\,^2H_{4\frac{1}{2}}$—$z\,^4G^\circ_{3\frac{1}{2}}$
3148.303	8Z	31753.95	
3147.975	25	31757.26	$d\,^2F_{3\frac{1}{2}}$—$t\,^2F^\circ_{3\frac{1}{2}}$ $b\,^4G_{2\frac{1}{2}}$—$y\,^4P^\circ_{1\frac{1}{2}}$
3146.47	2*wl*	31772.44	$a\,^4F_{2\frac{1}{2}}$—$z\,^4D^\circ_{3\frac{1}{2}}$
3145.743	20Z	31779.79	$a\,^2P_{0\frac{1}{2}}$—$x\,^4F^\circ_{1\frac{1}{2}}$
3144.616	22Z	31791.18	$a\,^2G_{3\frac{1}{2}}$—$z\,^4H^\circ_{4\frac{1}{2}}$
3143.313	4Z	31804.35	$a\,^4G_{4\frac{1}{2}}$—$z\,^6F^\circ_{3\frac{1}{2}}$
3143.058	70Z	31806.93	$b\,^2H_{4\frac{1}{2}}$—$y\,^2G^\circ_{3\frac{1}{2}}$
3141.729	95Z	31820.39	$b\,^2G_{4\frac{1}{2}}$—$z\,^2H^\circ_{5\frac{1}{2}}$
3141.405	75Z	31823.67	$a\,^2D_{1\frac{1}{2}}$—$z\,^4D^\circ_{1\frac{1}{2}}$ $a\,^2G_{4\frac{1}{2}}$—$z\,^4H^\circ_{3\frac{1}{2}}$ $b\,^2H_{3\frac{1}{2}}$—$y\,^2H^\circ_{3\frac{1}{2}}$
3139.403	6Z	31843.96	
3138.727	100Z	31850.82	$a\,^4H_{3\frac{1}{2}}$—$z\,^4H^\circ_{3\frac{1}{2}}$
3138.48	10Z	31853.33	$a\,^4F_{3\frac{1}{2}}$—$z\,^4D^\circ_{3\frac{1}{2}}$
3138.22	2	31855.97	
3137.57	3	31862.57	$c\,^4D_{2\frac{1}{2}}$—$x\,^4G^\circ_{2\frac{1}{2}}$
3137.313	6*w*	31865.18	$a\,^2H_{5\frac{1}{2}}$—$z\,^4H^\circ_{6\frac{1}{2}}$
3137.17	5	31866.63	$a\,^4D_{1\frac{1}{2}}$—$z\,^6P^\circ_{1\frac{1}{2}}$ $d\,^2F_{3\frac{1}{2}}$—$w^4G^\circ_{2\frac{1}{2}}$
3136.466	100Z	31873.78	$a\,^4F_{4\frac{1}{2}}$—$z\,^4D^\circ_{3\frac{1}{2}}$
3135.56	2*w*	31882.99	
3134.86	5	31890.11	$b\,^4F_{4\frac{1}{2}}$—$z\,^4I^\circ_{5\frac{1}{2}}$
3133.74	4*w*	31901.51	$a\,^4G_{3\frac{1}{2}}$—$z\,^6F^\circ_{3\frac{1}{2}}$
3132.54	25	31913.76	$a\,^4D_{3\frac{1}{2}}$—$z\,^4P^\circ_{2\frac{1}{2}}$
3131.22	4*w*	31927.18	
3130.180	6	31937.79	$b\,^2F_{3\frac{1}{2}}$—$y\,^4D^\circ_{2\frac{1}{2}}$
3130.057	22Z	31939.04	$b\,^4F_{4\frac{1}{2}}$—$z\,^2G^\circ_{4\frac{1}{2}}$
3129.47	2*wl*	31945.03	
3128.549	10	31954.44	$a\,^2P_{1\frac{1}{2}}$—$w^4D^\circ_{0\frac{1}{2}}$
3127.817	25Z	31961.92	$b\,^2F_{2\frac{1}{2}}$—$z\,^2D^\circ_{1\frac{1}{2}}$ $c\,^4D_{2\frac{1}{2}}$— (3)$^\circ_{3\frac{1}{2}}$
3126.99	2	31970.37	$b\,^4P_{2\frac{1}{2}}$—$z\,^2D^\circ_{2\frac{1}{2}}$
3126.780	15Z	31972.52	$b\,^2D_{2\frac{1}{2}}$—$y\,^2G^\circ_{3\frac{1}{2}}$
3126.318	7*w*Z	31977.24	$d\,^2G_{3\frac{1}{2}}$—$u\,^2F^\circ_{2\frac{1}{2}}$
3126.13	1	31979.16	
3126.025	10Z	31980.24	$a\,^2P_{1\frac{1}{2}}$—$w^4D^\circ_{1\frac{1}{2}}$
3125.64	10	31984.18	$b\,^4F_{2\frac{1}{2}}$—$z\,^2G^\circ_{4\frac{1}{2}}$
3125.10	2*w*	31989.70	
3124.893	6*w*Z	31991.82	
3124.206	20Z	31998.86	
3123.991	15*w*Z	32001.06	
3123.46	50Z	32006.50	$b\,^2G_{4\frac{1}{2}}$—$y\,^2F^\circ_{3\frac{1}{2}}$
3122.36	2*ws*	32017.77	
3122.003	250Z	32021.43	$a\,^4H_{5\frac{1}{2}}$—$z\,^4H^\circ_{5\frac{1}{2}}$
3121.61	2*ws*	32025.47	
3121.344	8	32028.19	$b\,^2G_{4\frac{1}{2}}$—$y\,^2H^\circ_{4\frac{1}{2}}$
3121.225	15Z	32029.42	$b\,^2H_{4\frac{1}{2}}$—$z\,^2H^\circ_{5\frac{1}{2}}$
3120.92	2	32032.55	$a\,^4G_{2\frac{1}{2}}$—$z\,^6F^\circ_{3\frac{1}{2}}$
3119.44	20Z	32047.74	$c\,^2G_{4\frac{1}{2}}$—$w^2F^\circ_{3\frac{1}{2}}$ $b\,^4G_{2\frac{1}{2}}$—$z\,^2P^\circ_{1\frac{1}{2}}$
3118.944	10Z	32052.84	$a\,^2H_{5\frac{1}{2}}$—$z\,^4I^\circ_{4\frac{1}{2}}$
3117.466	18Z	32068.03	$b\,^2F_{3\frac{1}{2}}$—$z\,^4G^\circ_{3\frac{1}{2}}$
3116.100	300Z	32082.09	$b\,^4F_{4\frac{1}{2}}$—$z\,^4G^\circ_{3\frac{1}{2}}$
3114.964	25Z	32093.79	$b\,^2H_{5\frac{1}{2}}$—$y\,^2G^\circ_{4\frac{1}{2}}$
3113.520	8	32108.68	$b\,^4F_{1\frac{1}{2}}$—$z\,^2D^\circ_{2\frac{1}{2}}$
3112.95	3*w*	32114.55	$b\,^2G_{3\frac{1}{2}}$—$y\,^2F^\circ_{3\frac{1}{2}}$
3112.85	3*h*	32115.59	$b\,^4F_{2\frac{1}{2}}$—$z\,^2D^\circ_{2\frac{1}{2}}$
3112.48	1	32119.40	
3112.22	4	32122.09	
3111.650	50Z	32127.97	$a\,^2G_{4\frac{1}{2}}$—$z\,^4H^\circ_{4\frac{1}{2}}$
3111.234	15Z	32132.27	$a\,^4P_{0\frac{1}{2}}$—$z\,^4P^\circ_{1\frac{1}{2}}$
3110.846	75	32136.27	$a\,^4D_{2\frac{1}{2}}$—$z\,^6P^\circ_{3\frac{1}{2}}$ $b\,^2G_{3\frac{1}{2}}$—$y\,^2H^\circ_{4\frac{1}{2}}$
3108.987	20Z	32155.49	$a\,^4H_{3\frac{1}{2}}$—$z\,^4H^\circ_{4\frac{1}{2}}$
3108.60	2*w*	32159.49	
3107.549	30Z	32170.37	$b\,^2G_{4\frac{1}{2}}$—$y\,^2H^\circ_{5\frac{1}{2}}$
3106.945	10Z	32176.62	$b\,^2S_{0\frac{1}{2}}$—$w\,^2P^\circ_{1\frac{1}{2}}$

TABLE 1. *Wavelengths and term combinations of* Mo II—Continued

Wavelength λ_{air}	Intensity	Wave No.	Term combination
3106. 246	6*Z*	32183. 86	$a\ ^2S_{0\frac{1}{2}}$—$y\ ^4P^o_{0\frac{1}{2}}$
3106. 15	2*w*	32184. 86	$d\ ^2G_{4\frac{1}{2}}$—$u\ ^2F^o_{3\frac{1}{2}}$
3105. 99	2*w*	32186. 51	$b\ ^2D_{1\frac{1}{2}}$—$y\ ^2F^o_{2\frac{1}{2}}$
3105. 67	1*w*	32189. 83	
3105. 12	2*hl*	32195. 56	
3104. 91	1	32197. 71	
3103. 468	20*Z*	32212. 67	$b\ ^4P_{1\frac{1}{2}}$—$z\ ^2D^o_{1\frac{1}{2}}$; $c\ ^4D_{2\frac{1}{2}}$—$y\ ^2D^o_{2\frac{1}{2}}$
3102. 73	1*w*	32220. 33	
3102. 49	1	32222. 82	
3102. 35	2	32224. 28	
3102. 13	4*wl*	32226. 56	
3101. 098	20*Z*	32237. 29	$b\ ^2H_{4\frac{1}{2}}$—$y\ ^2H^o_{4\frac{1}{2}}$
3100. 508	15*Z*	32243. 42	$a\ ^2D_{2\frac{1}{2}}$—$z\ ^4D^o_{1\frac{1}{2}}$
3100. 000	15*Z*	32248. 70	$a\ ^2P_{1\frac{1}{2}}$—$w\ ^4D^o_{2\frac{1}{2}}$
3099. 249	35*Z*	32256. 52	$b\ ^2F_{2\frac{1}{2}}$—$z\ ^2G^o_{3\frac{1}{2}}$
3098. 470	45*Z*	32264. 63	$a\ ^4D_{2\frac{1}{2}}$—$z\ ^6P^o_{2\frac{1}{2}}$
3098. 020	12*w*	32269. 31	$b\ ^2F_{3\frac{1}{2}}$—$z\ ^4I^o_{4\frac{1}{2}}$
3097. 694	40*Z*	32272. 71	$a\ ^4H_{4\frac{1}{2}}$—$z\ ^4H^o_{3\frac{1}{2}}$
3097. 20	2*ws*	32277. 86	$b\ ^4G_{4\frac{1}{2}}$—$x\ ^4D^o_{3\frac{1}{2}}$
3096. 86	2*w*	32281. 40	$c\ ^4D_{3\frac{1}{2}}$— $(3)^o_{3\frac{1}{2}}$
3096. 50	1	32285. 16	
3096. 14	2	32288. 91	
3095. 340	3*w*	32297. 25	
3095. 23	3*ws*	32298. 40	$c\ ^2G_{3\frac{1}{2}}$—$w\ ^2F^o_{2\frac{1}{2}}$
3094. 987	4*w*	32300. 94	
3093. 62	3*wl*	32315. 21	
3092. 950	10	32322. 21	$d\ ^2G_{3\frac{1}{2}}$—$u\ ^2F^o_{3\frac{1}{2}}$
3092. 850	7	32323. 26	$a\ ^4P_{1\frac{1}{2}}$—$z\ ^4P^o_{1\frac{1}{2}}$; $b\ ^4G_{3\frac{1}{2}}$—$x\ ^4D^o_{2\frac{1}{2}}$
3092. 092	150*Z*	32331. 18	$a\ ^4P_{2\frac{1}{2}}$—$z\ ^4P^o_{1\frac{1}{2}}$
3091. 541	5*wZ*	32336. 94	$b\ ^4G_{3\frac{1}{2}}$—$z\ ^2I^o_{3\frac{1}{2}}$
3090. 71	3*w*	32345. 63	
3090. 38	1	32349. 09	
3089. 520	10*wZ*	32358. 09	$b\ ^2D_{1\frac{1}{2}}$—$y\ ^2D^o_{1\frac{1}{2}}$
3088. 691	6*w*	32366. 78	
3088. 168	2*w*	32372. 26	
3087. 627	300*Z*	32377. 93	$a\ ^4H_{6\frac{1}{2}}$—$z\ ^4H^o_{5\frac{1}{2}}$
3087. 310	8	32381. 25	$b\ ^2D_{2\frac{1}{2}}$—$y\ ^2F^o_{3\frac{1}{2}}$
3086. 97	1*w*	32384. 82	
3086. 16	2*w*	32393. 32	$b\ ^2D_{2\frac{1}{2}}$—$y\ ^2F^o_{2\frac{1}{2}}$
3085. 35	1	32401. 82	
3085. 20	1*w*	32403. 40	
3084. 94	3	32406. 13	$b\ ^4G_{3\frac{1}{2}}$—$y\ ^4P^o_{2\frac{1}{2}}$
3084. 82	3*w*	32407. 39	
3084. 52	8*w*,*d*?*Z*	32410. 54	$a\ ^2H_{4\frac{1}{2}}$—$z\ ^2G^o_{3\frac{1}{2}}$
3083. 51	1	32421. 16	
3083. 26	1	32423. 79	
3082. 98	2	32426. 73	
3082. 224	60*Z*	32434. 68	$b\ ^4P_{2\frac{1}{2}}$—$y\ ^4P^o_{1\frac{1}{2}}$; $a\ ^4D_{1\frac{1}{2}}$—$z\ ^6P^o_{2\frac{1}{2}}$
3081. 660	20*Z*	32440. 62	$b\ ^2G_{4\frac{1}{2}}$—$y\ ^2G^o_{4\frac{1}{2}}$
3081. 08	2*wl*	32446. 73	
3078. 64	12*Z*	32472. 44	$b\ ^4G_{3\frac{1}{2}}$—$x\ ^4D^o_{3\frac{1}{2}}$
3078. 47	3	32474. 23	
3078. 051	10*Z*	32478. 65	$c\ ^4D_{0\frac{1}{2}}$—$w^4D^o_{0\frac{1}{2}}$
3077. 660	250*Z*	32482. 78	$b\ ^2I_{5\frac{1}{2}}$—$z\ ^2K^o_{5\frac{1}{2}}$
3075. 597	5*wZ*	32504. 57	$c\ ^4D_{0\frac{1}{2}}$—$w\ ^4D^o_{1\frac{1}{2}}$
3075. 40	3*w*	32506. 65	$a\ ^2S_{0\frac{1}{2}}$—$y\ ^4P^o_{1\frac{1}{2}}$
3075. 228	6*w*	32508. 47	$d\ ^2D_{1\frac{1}{2}}$—$w\ ^2P^o_{1\frac{1}{2}}$
3074. 635	15	32514. 74	$b\ ^4G_{4\frac{1}{2}}$—$z\ ^2I^o_{5\frac{1}{2}}$
3074. 37	20*Z*	32517. 57	
3073. 72	1*w*	32524. 42	
3073. 23	25	32529. 60	$c\ ^4D_{2\frac{1}{2}}$—$w\ ^4D^o_{1\frac{1}{2}}$
3072. 89	8*wZ*	32533. 20	$c\ ^4D_{3\frac{1}{2}}$—$y\ ^2D^o_{2\frac{1}{2}}$; $a\ ^4D_{3\frac{1}{2}}$—$z\ ^6P^o_{3\frac{1}{2}}$
3072. 413	3*w*	32538. 25	$c\ ^4D_{3\frac{1}{2}}$—$x\ ^4G^o_{3\frac{1}{2}}$
3071. 30	7*w*	32550. 04	$b\ ^4D_{3\frac{1}{2}}$—$z\ ^4H^o_{3\frac{1}{2}}$
3071. 05	4*w*	32552. 69	$a\ ^4G_{5\frac{1}{2}}$—$z\ ^6F^o_{4\frac{1}{2}}$
3070. 620	35*Z*	32557. 25	$c\ ^4D_{1\frac{1}{2}}$—$y\ ^2D^o_{2\frac{1}{2}}$
3069. 195	35*Z*	32572. 37	$c\ ^2D_{2\frac{1}{2}}$—$v\ ^2F^o_{2\frac{1}{2}}$; $c\ ^2G_{3\frac{1}{2}}$—$x\ ^2H^o_{4\frac{1}{2}}$
3068. 927	7*Z*	32575. 21	$b\ ^4G_{3\frac{1}{2}}$— $(1)^o_{2\frac{1}{2}}$
3068. 776	8*Z*	32576. 81	$b\ ^2G_{4\frac{1}{2}}$— $(3)^o_{3\frac{1}{2}}$
3068. 48	6*w*	32579. 96	$b\ ^4F_{2\frac{1}{2}}$—$y\ ^4P^o_{1\frac{1}{2}}$; $d\ ^2G_{3\frac{1}{2}}$—$t\ ^2F^o_{3\frac{1}{2}}$
3067. 92	2	32585. 90	$b\ ^2G_{3\frac{1}{2}}$—$x\ ^4G^o_{2\frac{1}{2}}$
3067. 642	65*Z*	32588. 86	$b\ ^4G_{5\frac{1}{2}}$—$z\ ^2I^o_{6\frac{1}{2}}$
3066. 58	4*w*	32600. 14	$a\ ^2H_{5\frac{1}{2}}$—$z\ ^4G^o_{4\frac{1}{2}}$
3066. 16	5	32604. 61	$d\ ^2D_{1\frac{1}{2}}$—$u\ ^2F^o_{2\frac{1}{2}}$
3065. 64	2*H*	32610. 14	
3065. 05	50	32616. 44	$c\ ^2G_{4\frac{1}{2}}$—$x\ ^2H^o_{5\frac{1}{2}}$
3064. 628	10	32620. 91	
3064. 11	2	32626. 42	$a\ ^2P_{0\frac{1}{2}}$—$z\ ^4S^o_{1\frac{1}{2}}$
3063. 86	4*w*	32629. 08	$d\ ^2D_{2\frac{1}{2}}$—$w\ ^2P^o_{1\frac{1}{2}}$
3063. 55	2	32632. 39	
3062. 57	2	32642. 83	$b\ ^4G_{2\frac{1}{2}}$—$x\ ^4D^o_{2\frac{1}{2}}$
3062. 29	6	32645. 81	$b\ ^2D_{1\frac{1}{2}}$—$x\ ^4G^o_{2\frac{1}{2}}$
3062. 105	8*Z*	32647. 78	$a\ ^2G_{3\frac{1}{2}}$—$z\ ^4G^o_{3\frac{1}{2}}$
3061. 936	7	32649. 58	$b\ ^2H_{4\frac{1}{2}}$—$y\ ^2G^o_{4\frac{1}{2}}$
3061. 29	5*w*	32656. 47	
3060. 93	12	32660. 31	$b\ ^4D_{1\frac{1}{2}}$—$y\ ^4D^o_{0\frac{1}{2}}$
3060. 782	30*Z*	32661. 89	$a\ ^4D_{3\frac{1}{2}}$—$z\ ^6P^o_{2\frac{1}{2}}$
3060. 026	15*Z*	32669. 96	$c\ ^2G_{3\frac{1}{2}}$—$w^2F^o_{3\frac{1}{2}}$
3059. 724	1	32673. 19	
3058. 61	7*wZ*	32685. 09	$b\ ^2G_{3\frac{1}{2}}$— $(3)^o_{3\frac{1}{2}}$
3058. 373	3*Z*	32687. 62	
3058. 16	3*w*	32689. 90	$d\ ^2G_{3\frac{1}{2}}$—$^4G^o_{2\frac{1}{2}}$
3057. 86	50*d*?*Z*	32693. 10	$a\ ^2G_{4\frac{1}{2}}$—$z\ ^4H^o_{5\frac{1}{2}}$; $d\ ^2F_{3\frac{1}{2}}$—$v\ ^2G^o_{4\frac{1}{2}}$
3056. 815	10*wZ*	32704. 28	$b\ ^4G_{4\frac{1}{2}}$—$y\ ^4G^o_{3\frac{1}{2}}$
3055. 64	5*w*	32716. 85	
3054. 94	10*wZ*	32724. 35	$b\ ^4P_{2\frac{1}{2}}$—$z\ ^2P^o_{1\frac{1}{2}}$
3054. 761	10*Z*	32726. 27	$b\ ^4G_{2\frac{1}{2}}$—$y\ ^4P^o_{2\frac{1}{2}}$
3053. 474	50*Z*	32740. 06	$b\ ^4G_{4\frac{1}{2}}$—$y\ ^4G^o_{4\frac{1}{2}}$
3052. 32	50*Z*	32752. 44	$a\ ^4H_{5\frac{1}{2}}$—$z\ ^4H^o_{6\frac{1}{2}}$
3050. 85	5*w*	32768. 22	
3050. 53	1	32771. 66	$a\ ^2D_{2\frac{1}{2}}$—$z\ ^4D^o_{2\frac{1}{2}}$
3050. 37	6*wZ*	32773. 37	
3050. 204	3*w*	32775. 16	$a\ ^4D_{1\frac{1}{2}}$—$z\ ^6D^o_{0\frac{1}{2}}$
3050. 04	2*w*	32776. 92	
3049. 56	2*H*	32782. 08	
3049. 20	8	32785. 95	$b\ ^2H_{4\frac{1}{2}}$— $(3)^o_{3\frac{1}{2}}$
3048. 888	50*Z*	32789. 31	$b\ ^2I_{6\frac{1}{2}}$—$z\ ^2K^o_{5\frac{1}{2}}$
3048. 80	12*Z*	32790. 25	$b\ ^2H_{5\frac{1}{2}}$—$x\ ^4G^o_{4\frac{1}{2}}$
3048. 308	10*Z*	32795. 54	$c\ ^2D_{1\frac{1}{2}}$—$w^2D^o_{1\frac{1}{2}}$
3048. 054	40*Z*	32798. 28	$c\ ^4D_{2\frac{1}{2}}$—$w^4D^o_{2\frac{1}{2}}$
3047. 50	5*w*	32804. 24	$b\ ^4G_{4\frac{1}{2}}$—$y\ ^4G^o_{3\frac{1}{2}}$
3046. 41	8*Z*	32815. 98	$b\ ^4G_{5\frac{1}{2}}$—$y\ ^4G^o_{5\frac{1}{2}}$
3045. 730	18*Z*	32823. 30	$b\ ^2F_{2\frac{1}{2}}$—$y\ ^4D^o_{3\frac{1}{2}}$; $a\ ^4G_{2\frac{1}{2}}$—$z\ ^4P^o_{1\frac{1}{2}}$
3044. 81	4	32833. 22	$b\ ^2G_{4\frac{1}{2}}$—$x\ ^4G^o_{3\frac{1}{2}}$
3044. 60	2*wl*	32835. 48	
3044. 24	1*wl*	32839. 37	

Wavelength λ_{air}	Intensity	Wave No.	Term combination
3043. 974	10	32842. 24	$d\ {}^2F_{3\frac{5}{2}}$—$w\ {}^4G^\circ_{3\frac{5}{2}}$ / $c\ {}^4D_{3\frac{5}{2}}$—$x\ {}^4G^\circ_{3\frac{5}{2}}$
3043. 438	30Z	32848. 02	$a\ {}^4D_{2\frac{5}{2}}$—$z\ {}^6D^\circ_{1\frac{5}{2}}$
3043. 38	10	32848. 65	$c\ {}^4D_{1\frac{5}{2}}$—$w\ {}^4F^\circ_{0\frac{5}{2}}$
3043. 09	8	32851. 78	$b\ {}^4G_{2\frac{5}{2}}$—$x\ {}^4D^\circ_{1\frac{5}{2}}$
3043. 01	5	32852. 64	$b\ {}^2D_{2\frac{5}{2}}$—$x\ {}^4G^\circ_{2\frac{5}{2}}$
3042. 41	2	32859. 12	
3042. 060	10	32862. 90	$b\ {}^4F_{1\frac{5}{2}}$—$z\ {}^2P^\circ_{1\frac{1}{2}}$
3041. 010	35	32874. 24	$c\ {}^4D_{1\frac{5}{2}}$—$w\ {}^4D^\circ_{1\frac{5}{2}}$
3040. 58	2w	32878. 89	
3039. 45	2	32891. 12	$b\ {}^4G_{4\frac{1}{2}}$—$y\ {}^4F^\circ_{3\frac{1}{2}}$
3039. 064	40Z	32895. 29	$b\ {}^4G_{2\frac{5}{2}}$— (1)$^\circ_{2\frac{5}{2}}$
3038. 77	6w	32898. 48	$b\ {}^4G_{3\frac{5}{2}}$—$y\ {}^4G^\circ_{3\frac{5}{2}}$
3037. 82	4w	32908. 77	
3037. 25	2w	32914. 94	
3037. 088	6wZ	32916. 70	$c\ {}^2D_{2\frac{5}{2}}$—$w\ {}^2D^\circ_{2\frac{5}{2}}$
3036. 106	3hl	32927. 34	
3035. 473	8Z	32934. 21	$b\ {}^4G_{3\frac{5}{2}}$—$y\ {}^4G^\circ_{3\frac{5}{2}}$
3034. 922	40Z	32940. 19	$a\ {}^4H_{5\frac{5}{2}}$—$z\ {}^4I^\circ_{4\frac{5}{2}}$
3034. 73	3	32942. 27	$a\ {}^2G_{3\frac{5}{2}}$—$y\ {}^4D^\circ_{2\frac{5}{2}}$
3034. 254	10Z	32947. 44	$b\ {}^4D_{0\frac{5}{2}}$—$y\ {}^4D^\circ_{0\frac{5}{2}}$
3033. 880	8	32951. 50	$b\ {}^2D_{2\frac{5}{2}}$— (3)$^\circ_{3\frac{5}{2}}$
3033. 333	200Z	32957. 44	$c\ {}^2G_{4\frac{1}{2}}$—$w\ {}^2G^\circ_{3\frac{1}{2}}$
3033. 24	20Z	32958. 45	$a\ {}^4D_{2\frac{5}{2}}$—$z\ {}^6D^\circ_{3\frac{5}{2}}$
3031. 50	1	32977. 37	$a\ {}^2H_{4\frac{1}{2}}$—$y\ {}^4D^\circ_{3\frac{5}{2}}$
3030. 812	4w	32984. 86	
3030. 65	1hl	32986. 62	
3030. 315	18Z	32990. 25	$a\ {}^4H_{4\frac{1}{2}}$—$z\ {}^4G^\circ_{3\frac{5}{2}}$
3029. 991	8Z	32993. 79	$b\ {}^4G_{3\frac{5}{2}}$—$y\ {}^4G^\circ_{3\frac{5}{2}}$
3029. 770	5Z	32996. 20	$b\ {}^2D_{1\frac{5}{2}}$—$y\ {}^2D^\circ_{2\frac{1}{2}}$
3028. 78	2	33006. 98	
3028. 291	6Z	33012. 31	$a\ {}^4H_{3\frac{5}{2}}$—$z\ {}^4G^\circ_{2\frac{5}{2}}$
3027. 773	60Z	33017. 96	$a\ {}^4D_{1\frac{5}{2}}$—$z\ {}^6D^\circ_{1\frac{5}{2}}$
3027. 39	3	33022. 14	$b\ {}^4G_{3\frac{5}{2}}$—$y\ {}^4G^\circ_{2\frac{5}{2}}$
3026. 801	12Z	33028. 56	$b\ {}^4D_{2\frac{5}{2}}$—$y\ {}^4D^\circ_{1\frac{5}{2}}$
3026. 33	1	33033. 70	
3026. 12	2w	33036. 00	
3025. 57	10wlZ	33042. 00	$b\ {}^2H_{4\frac{1}{2}}$—$x\ {}^4G^\circ_{3\frac{5}{2}}$
3025. 44	4	33043. 42	
3024. 793	8w	33050. 49	
3023. 303	125Z	33066. 78	$b\ {}^2I_{5\frac{1}{2}}$—$y\ {}^2I^\circ_{5\frac{1}{2}}$
3022. 748	10Z	33072. 85	$a\ {}^2G_{3\frac{5}{2}}$—$z\ {}^4G^\circ_{3\frac{5}{2}}$
3021. 605	45Z	33085. 36	$b\ {}^4G_{3\frac{5}{2}}$—$y\ {}^4F^\circ_{3\frac{5}{2}}$
3020. 682	20Z	33095. 47	
3020. 27	1	33099. 98	
3019. 72	8	33106. 01	$b\ {}^4G_{5\frac{5}{2}}$—$y\ {}^4H^\circ_{5\frac{5}{2}}$
3018. 56	45Z	33118. 73	$c\ {}^4D_{3\frac{5}{2}}$—$w\ {}^4D^\circ_{2\frac{5}{2}}$
3018. 50	55Z	33119. 42	$c\ {}^2D_{2\frac{5}{2}}$—$v\ {}^2F^\circ_{3\frac{5}{2}}$
3017. 18	1	33133. 88	
3016. 87	10Z	33137. 28	$b\ {}^2G_{4\frac{1}{2}}$—$x\ {}^4G^\circ_{4\frac{1}{2}}$
3016. 37	4w	33142. 78	$b\ {}^2H_{5\frac{1}{2}}$—$x\ {}^4G^\circ_{5\frac{1}{2}}$ / $c\ {}^4D_{1\frac{1}{2}}$—$w\ {}^4D^\circ_{2\frac{1}{2}}$
3016. 122	6	33145. 50	$a\ {}^2S_{0\frac{1}{2}}$—$z\ {}^2P^\circ_{0\frac{1}{2}}$
3015. 417	12Z	33153. 27	$a\ {}^4D_{0\frac{5}{2}}$—$z\ {}^6D^\circ_{1\frac{5}{2}}$
3014. 67	8	33161. 44	$a\ {}^4P_{1\frac{1}{2}}$—$z\ {}^4P^\circ_{2\frac{1}{2}}$
3014. 155	50Z	33167. 13	$c\ {}^4D_{3\frac{5}{2}}$—$w\ {}^4D^\circ_{3\frac{5}{2}}$
3013. 94	5	33169. 50	$a\ {}^4P_{2\frac{5}{2}}$—$z\ {}^4P^\circ_{2\frac{5}{2}}$
3012. 81	2w	33181. 94	$a\ {}^4F_{1\frac{5}{2}}$—$y\ {}^4D^\circ_{0\frac{5}{2}}$
3012. 65	5	33183. 70	
3012. 47	1	33185. 68	
3011. 948	35	33191. 43	$a\ {}^4H_{4\frac{1}{2}}$—$z\ {}^4I^\circ_{4\frac{1}{2}}$
3011. 184	5Z	33199. 85	$a\ {}^2H_{4\frac{1}{2}}$—$z\ {}^4I^\circ_{5\frac{5}{2}}$
3010. 917	35Z	33202. 80	$b\ {}^2D_{2\frac{1}{2}}$—$y\ {}^2D^\circ_{2\frac{1}{2}}$
3010. 07	1	33212. 15	$b\ {}^4F_{1\frac{5}{2}}$—$z\ {}^2P^\circ_{0\frac{1}{2}}$
3009. 79	4Z	33215. 23	
3009. 46	6Z	33218. 87	$b\ {}^4G_{2\frac{5}{2}}$—$y\ {}^4G^\circ_{3\frac{5}{2}}$
3008. 15	30Z	33233. 33	$a\ {}^4D_{2\frac{5}{2}}$—$z\ {}^6D^\circ_{2\frac{5}{2}}$
3007. 79	7	33237. 31	$b\ {}^4P_{0\frac{5}{2}}$—$z\ {}^2D^\circ_{1\frac{5}{2}}$
3007. 47	20Z	33240. 85	$c\ {}^2D_{1\frac{5}{2}}$—$v\ {}^2F^\circ_{2\frac{5}{2}}$
3007. 085	8	33245. 11	$b\ {}^2G_{3\frac{1}{2}}$—$x\ {}^4G^\circ_{4\frac{1}{2}}$
3007. 00	2	33246. 05	
3006. 766	5Z	33248. 63	$a\ {}^2H_{4\frac{1}{2}}$—$z\ {}^2G^\circ_{4\frac{1}{2}}$
3005. 50	4w	33262. 64	$c\ {}^2F_{3\frac{5}{2}}$—$x\ {}^2H^\circ_{4\frac{1}{2}}$ / $a\ {}^2D_{2\frac{1}{2}}$—$z\ {}^4D^\circ_{3\frac{5}{2}}$
3005. 44	7	33263. 30	
3005. 02	6	33267. 95	
3004. 45	60	33274. 26	$a\ {}^2G_{3\frac{5}{2}}$—$z\ {}^4I^\circ_{4\frac{1}{2}}$
3004. 03	3	33278. 91	$b\ {}^4G_{3\frac{5}{2}}$—$y\ {}^4H^\circ_{3\frac{5}{2}}$
3003. 773	10Z	33281. 76	$c\ {}^2G_{3\frac{1}{2}}$—$x\ {}^2D^\circ_{2\frac{5}{2}}$
3003. 260	8	33287. 45	$b\ {}^2D_{1\frac{5}{2}}$—$w\ {}^4D^\circ_{0\frac{5}{2}}$
3002. 850	5Z	33291. 99	$b\ {}^2F_{3\frac{5}{2}}$—$y\ {}^4D^\circ_{3\frac{5}{2}}$
3002. 12	8	33300. 09	
3001. 825	8w	33303. 36	$b\ {}^4G_{2\frac{5}{2}}$—$y\ {}^4F^\circ_{1\frac{5}{2}}$
3001. 510	10w	33306. 85	$c\ {}^2D_{2\frac{5}{2}}$—$x\ {}^2P^\circ_{1\frac{1}{2}}$ / $a\ {}^4H_{3\frac{5}{2}}$—$y\ {}^4D^\circ_{2\frac{5}{2}}$
3000. 94	6	33313. 18	$b\ {}^4G_{2\frac{5}{2}}$—(2)$^\circ_{3\frac{5}{2}}$ / $b\ {}^2D_{1\frac{5}{2}}$—$w\ {}^4D^\circ_{1\frac{5}{2}}$
3000. 290	60Z	33320. 40	$a\ {}^2P_{0\frac{1}{2}}$—$y\ {}^2D^\circ_{1\frac{1}{2}}$ / $b\ {}^4P_{2\frac{5}{2}}$—$x\ {}^4D^\circ_{2\frac{5}{2}}$
2999. 591	10Z	33328. 16	$d\ {}^2D_{2\frac{5}{2}}$—$t\ {}^2F^\circ_{3\frac{1}{2}}$
2998. 70	4	33338. 06	
2998. 37	4Z	33341. 73	$a\ {}^4P_{1\frac{1}{2}}$—$z\ {}^6P^\circ_{1\frac{1}{2}}$
2998. 29	1w	33342. 62	$b\ {}^4G_{2\frac{5}{2}}$—$y\ {}^4G^\circ_{3\frac{5}{2}}$
2997. 961	40Z	33346. 28	$a\ {}^2H_{5\frac{1}{2}}$—$z\ {}^2G^\circ_{4\frac{1}{2}}$ / $b\ {}^2H_{4\frac{1}{2}}$—$x\ {}^4G^\circ_{4\frac{1}{2}}$
2997. 661	7Z	33349. 62	$a\ {}^4P_{2\frac{5}{2}}$—$z\ {}^6P^\circ_{1\frac{5}{2}}$
2997. 326	50Z	33353. 35	$b\ {}^4F_{3\frac{5}{2}}$—$x\ {}^4D^\circ_{2\frac{5}{2}}$
2997. 101	5Z	33355. 85	$a\ {}^4D_{3\frac{5}{2}}$—$z\ {}^6D^\circ_{3\frac{5}{2}}$
2996. 695	12Z	33360. 37	$c\ {}^2F_{3\frac{5}{2}}$—$w\ {}^2F^\circ_{3\frac{1}{2}}$
2996. 275	20Z	33365. 04	$b\ {}^4P_{1\frac{1}{2}}$—$z\ {}^2D^\circ_{2\frac{1}{2}}$
2995. 528	12Z	33373. 36	$b\ {}^2I_{6\frac{1}{2}}$—$y\ {}^2I^\circ_{5\frac{1}{2}}$ / $b\ {}^4G_{3\frac{5}{2}}$—$y\ {}^4F^\circ_{2\frac{5}{2}}$
2995. 215	4	33376. 85	
2995. 04	1	33378. 80	$d\ {}^2G_{4\frac{1}{2}}$—$v\ {}^2G^\circ_{4\frac{1}{2}}$
2994. 60	4w	33383. 71	
2994. 55	4w	33384. 26	$d\ {}^2D_{1\frac{5}{2}}$—$t\ {}^2F^\circ_{2\frac{1}{2}}$
2993. 865	6	33391. 90	$a\ {}^2H_{4\frac{1}{2}}$—$z\ {}^4G^\circ_{3\frac{5}{2}}$ / $b\ {}^4G_{3\frac{5}{2}}$—$y\ {}^4F^\circ_{4\frac{1}{2}}$
2993. 501	35Z	33395. 96	$a\ {}^4D_{0\frac{5}{2}}$—$z\ {}^6D^\circ_{1\frac{5}{2}}$
2992. 840	75	33403. 34	$b\ {}^4P_{2\frac{5}{2}}$—$y\ {}^4P^\circ_{2\frac{5}{2}}$ / $a\ {}^4D_{1\frac{5}{2}}$—$z\ {}^6D^\circ_{2\frac{5}{2}}$
2992. 63	20	33405. 68	$b\ {}^4G_{2\frac{5}{2}}$—$y\ {}^4F^\circ_{3\frac{5}{2}}$
2992. 250	20Z	34409. 92	$a\ {}^2G_{4\frac{1}{2}}$—$z\ {}^4G^\circ_{3\frac{5}{2}}$
2991. 51	5hlZ	33418. 19	
2990. 08	1w	33434. 17	
2989. 855	50Z	33436. 68	$b\ {}^4F_{3\frac{5}{2}}$—$y\ {}^4P^\circ_{2\frac{5}{2}}$ / $a\ {}^4H_{3\frac{5}{2}}$—$z\ {}^4G^\circ_{3\frac{5}{2}}$
2989. 46	8	33441. 10	$c\ {}^2F_{2\frac{5}{2}}$—$w\ {}^2F^\circ_{2\frac{5}{2}}$
2989. 16	1w	33444. 46	
2987. 960	50	33457. 89	$b\ {}^4F_{4\frac{5}{2}}$—$x\ {}^4D^\circ_{3\frac{5}{2}}$
2987. 347	50Z	33464. 76	
2986. 897	50Z	33469. 80	$b\ {}^4P_{2\frac{5}{2}}$—$x\ {}^4D^\circ_{3\frac{5}{2}}$
2986. 147	100Z	33478. 20	$b\ {}^4G_{3\frac{5}{2}}$—$y\ {}^4H^\circ_{4\frac{5}{2}}$
2985. 309	8	33487. 60	$a\ {}^4H_{5\frac{5}{2}}$—$z\ {}^4G^\circ_{4\frac{5}{2}}$
2984. 862	15Z	33492. 61	$c\ {}^2G_{4\frac{5}{2}}$—$w\ {}^2H^\circ_{3\frac{5}{2}}$

TABLE 1. *Wavelengths and term combinations of* Mo II—Continued

Wavelength λ_{air}	Intensity	Wave No.	Term combination
2983. 955	75*d*	33502. 79	$\begin{cases} b\ {}^2I_{3\frac{1}{2}}—y\ {}^2I^{\circ}_{4\frac{1}{2}} \\ b\ {}^4F_{3\frac{1}{2}}—x\ {}^4D^{\circ}_{3\frac{1}{2}} \end{cases}$
2983. 590	35*Z*	33506. 89	$b\ {}^4P_{1\frac{1}{2}}—y\ {}^4P^{\circ}_{2\frac{1}{2}}$
2982. 768	10*Z*	33516. 13	$d\ {}^2G_{3\frac{1}{2}}—v\ {}^2G^{\circ}_{4\frac{1}{2}}$
2982. 446	12*Z*	33519. 75	$b\ {}^2D_{2\frac{1}{2}}—w\ {}^4D^{\circ}_{1\frac{1}{2}}$
2981. 637	3*d*	33528. 84	$b\ {}^4P_{2\frac{1}{2}}—x\ {}^4D^{\circ}_{1\frac{1}{2}}$
2980. 495	4	33541. 68	$b\ {}^4F_{1\frac{1}{2}}—y\ {}^4P^{\circ}_{2\frac{1}{2}}$
2979. 787	35*Z*	33549. 65	
2978. 607	50*Z*	33562. 95	$b\ {}^2F_{3\frac{1}{2}}—z\ {}^2G^{\circ}_{4\frac{1}{2}}$
2977. 98	3	33570. 01	$\begin{cases} b\ {}^2G_{3\frac{1}{2}}—w\ {}^4D^{\circ}_{3\frac{1}{2}} \\ b\ {}^4G_{4\frac{1}{2}}—y\ {}^4F^{\circ}_{4\frac{1}{2}} \end{cases}$
2977. 760	50*Z*	33572. 49	$b\ {}^4P_{2\frac{1}{2}}—(1)^{\circ}_{2\frac{1}{2}}$
2977. 095	7	33579. 99	$c\ {}^2G_{3\frac{1}{2}}—w\ {}^2G^{\circ}_{4\frac{1}{2}}$
2976. 898	30*Z*	33582. 21	$\begin{cases} b\ {}^2D_{1\frac{1}{2}}—w\ {}^4D^{\circ}_{2\frac{1}{2}} \\ b\ {}^2F_{3\frac{1}{2}}—z\ {}^2D^{\circ}_{2\frac{1}{2}} \end{cases}$
2976. 39	2	33587. 94	
2976. 277	2	33589. 22	
2976. 10	3	33591. 22	
2975. 625	20*Z*	33596. 58	$a\ {}^2P_{1\frac{1}{2}}—w\ {}^4F^{\circ}_{2\frac{1}{2}}$
2975. 390	75*Z*	33599. 23	$b\ {}^4G_{2\frac{1}{2}}—y\ {}^4H^{\circ}_{3\frac{1}{2}}$
2975. 06	1*s*	33602. 96	
2974. 810	4	33605. 78	$b\ {}^4F_{3\frac{1}{2}}—(1)^{\circ}_{2\frac{1}{2}}$
2974. 310	5	33611. 43	$a\ {}^2G_{4\frac{1}{2}}—z\ {}^4I^{\circ}_{4\frac{1}{2}}$
2974. 00	8	33614. 93	$b\ {}^4F_{2\frac{1}{2}}—x\ {}^4D^{\circ}_{3\frac{1}{2}}$
2972. 607	150*Z*	33630. 69	$a\ {}^4D_{3\frac{1}{2}}—z\ {}^6D^{\circ}_{2\frac{1}{2}}$
2971. 904	125*Z*	33638. 64	$a\ {}^4H_{3\frac{1}{2}}—z\ {}^4I^{\circ}_{3\frac{1}{2}}$
2971. 140	15*Z*	33647. 29	$a\ {}^4H_{4\frac{1}{2}}—z\ {}^2G^{\circ}_{3\frac{1}{2}}$
2970. 56	1	33653. 86	
2970. 46	3*w*	33654. 99	
2970. 38	4*w*	33655. 90	
2969. 742	7	33663. 13	$b\ {}^4G_{4\frac{1}{2}}—z\ {}^2F^{\circ}_{3\frac{1}{2}}$
2969. 548	4	33665. 33	$d\ {}^2G_{3\frac{1}{2}}—w\ {}^4G^{\circ}_{3\frac{1}{2}}$
2969. 365	10*Z*	33667. 40	$b\ {}^4F_{1\frac{1}{2}}—x\ {}^4D^{\circ}_{1\frac{1}{2}}$
2968. 775	40*Z*	33674. 09	$b\ {}^4F_{2\frac{1}{2}}—x\ {}^4D^{\circ}_{1\frac{1}{2}}$
2968. 25	1	33680. 05	
2968. 17	1	33680. 96	
2967. 61	1*w*	33687. 31	$a\ {}^2F_{3\frac{1}{2}}—z\ {}^4H^{\circ}_{4\frac{1}{2}}$
2967. 075	20*Z*	33693. 39	$b\ {}^4G_{2\frac{1}{2}}—y\ {}^4F^{\circ}_{2\frac{1}{2}}$
2966. 985	30	33694. 41	$b\ {}^4F_{4\frac{1}{2}}—z\ {}^2I^{\circ}_{5\frac{1}{2}}$
2966. 77	4	33696. 85	
2966. 634	8	33698. 39	$b\ {}^2H_{4\frac{1}{2}}—x\ {}^4G^{\circ}_{5\frac{1}{2}}$
2965. 538	7	33710. 85	$b\ {}^4F_{1\frac{1}{2}}—(1)^{\circ}_{2\frac{1}{2}}$
2965. 276	60*Z*	33713. 83	$a\ {}^6D_{3\frac{1}{2}}—z\ {}^6F^{\circ}_{2\frac{1}{2}}$
2964. 948	12	33717. 56	$b\ {}^4F_{2\frac{1}{2}}—(1)^{\circ}_{2\frac{1}{2}}$
2964. 77	1	33719. 58	
2964. 391	10	33723. 89	
2964. 14	1	33726. 75	
2963. 786	75	33730. 78	$a\ {}^6D_{2\frac{1}{2}}—z\ {}^6F^{\circ}_{1\frac{1}{2}}$
2963. 45	2	33734. 60	
2963. 07	2*w*	33738. 93	$\begin{cases} b\ {}^4G_{5\frac{1}{2}}—z\ {}^2H^{\circ}_{4\frac{1}{2}} \\ a\ {}^4H_{4\frac{1}{2}}—z\ {}^4G^{\circ}_{4\frac{1}{2}} \end{cases}$
2962. 212	15*Z*	33748. 70	$b\ {}^4G_{5\frac{1}{2}}—y\ {}^4H^{\circ}_{5\frac{1}{2}}$
2961. 327	65*Z*	33758. 78	$a\ {}^4D_{3\frac{1}{2}}—z\ {}^6D^{\circ}_{4\frac{1}{2}}$
2961. 036	10	33762. 10	$c\ {}^2G_{3\frac{1}{2}}—w\ {}^2G^{\circ}_{3\frac{1}{2}}$
2960. 464	8*Z*	33768. 62	$b\ {}^4D_{0\frac{1}{2}}—y\ {}^4D^{\circ}_{1\frac{1}{2}}$
2960. 228	50*Z*	33771. 32	$a\ {}^6D_{4\frac{1}{2}}—z\ {}^6F^{\circ}_{3\frac{1}{2}}$
2959. 90	2	33775. 06	
2959. 00	1*l*	33785. 33	$b\ {}^4F_{4\frac{1}{2}}—y\ {}^4G^{\circ}_{5\frac{1}{2}}$
2958. 732	10*Z*	33788. 39	$\begin{cases} b\ {}^2D_{2\frac{1}{2}}—w\ {}^4D^{\circ}_{2\frac{1}{2}} \\ c\ {}^4D_{2\frac{1}{2}}—x\ {}^2F^{\circ}_{2\frac{1}{2}} \end{cases}$
2958. 35	5*w*	33792. 76	
2958. 12	2*w*	33795. 38	
2957. 56	1*w*	33801. 78	
2956. 915	75*Z*	33809. 15	$b\ {}^2I_{6\frac{1}{2}}—y\ {}^2I^{\circ}_{6\frac{1}{2}}$
2956. 79	10*Z*	33810. 58	$a\ {}^4H_{6\frac{1}{2}}—z\ {}^4I^{\circ}_{5\frac{1}{2}}$
2956. 59	6	33812. 87	$c\ {}^2F_{2\frac{1}{2}}—w\ {}^2F^{\circ}_{3\frac{1}{2}}$
2956. 057	30*Z*	33818. 96	$a\ {}^6D_{1\frac{1}{2}}—z\ {}^6F^{\circ}_{0\frac{1}{2}}$
2955. 828	50*Z*	33821. 58	$a\ {}^2G_{3\frac{1}{2}}—z\ {}^4G^{\circ}_{4\frac{1}{2}}$
2955. 46	2*w*	33825. 79	
2955. 154	20*Z*	33829. 30	$\begin{cases} b\ {}^4F_{3\frac{1}{2}}—y\ {}^4G^{\circ}_{3\frac{1}{2}} \\ b\ {}^4P_{1\frac{1}{2}}—y\ {}^4P^{\circ}_{1\frac{1}{2}} \end{cases}$
2954. 518	5*Z*	33836. 58	$b\ {}^2D_{2\frac{1}{2}}—w\ {}^4D^{\circ}_{3\frac{1}{2}}$
2954. 36	4*w*	33838. 39	
2953. 942	15*Z*	33843. 18	$c\ {}^4D_{2\frac{1}{2}}—x\ {}^4P^{\circ}_{2\frac{1}{2}}$
2952. 765	15	33856. 67	
2952. 71	6	33857. 30	$b\ {}^4G_{3\frac{1}{2}}—z\ {}^2F^{\circ}_{3\frac{1}{2}}$
2952. 06	1*w*	33864. 75	
2951. 86	3*w*	33867. 05	$c\ {}^2G_{4\frac{1}{2}}—w\ {}^2H^{\circ}_{5\frac{1}{2}}$
2951. 817	15*lZ*	33867. 54	$\begin{cases} b\ {}^2F_{2\frac{1}{2}}—z\ {}^2P^{\circ}_{1\frac{1}{2}} \\ b\ {}^4D_{1\frac{1}{2}}—z\ {}^2S^{\circ}_{0\frac{1}{2}} \end{cases}$
2951. 28	1*w*	33873. 70	
2951. 09	1*w*	33875. 88	
2950. 25	2*l*	33885. 53	
2949. 805	2	33890. 64	$c\ {}^4D_{2\frac{1}{2}}—x\ {}^2G^{\circ}_{3\frac{1}{2}}$
2949. 66	1	33892. 31	
2949. 356	5	33895. 80	$b\ {}^4P_{2\frac{1}{2}}—y\ {}^4G^{\circ}_{3\frac{1}{2}}$
2949. 130	2	33898. 40	
2948. 90	1	33901. 04	
2948. 157	10	33909. 58	$a\ {}^4P_{1\frac{1}{2}}—z\ {}^6P^{\circ}_{2\frac{1}{2}}$
2947. 77	1*w*	33914. 04	
2947. 290	125*Z*	33919. 56	$b\ {}^4F_{4\frac{1}{2}}—y\ {}^4G^{\circ}_{4\frac{1}{2}}$
2946. 692	125*Z*	33926. 44	$\begin{cases} b\ {}^4G_{4\frac{1}{2}}—y\ {}^4H^{\circ}_{5\frac{1}{2}} \\ c\ {}^4D_{0\frac{1}{2}}—w\ {}^4F^{\circ}_{1\frac{1}{2}} \end{cases}$
2945. 946	100*Z*	33935. 03	$b\ {}^4G_{5\frac{1}{2}}—x\ {}^4F^{\circ}_{4\frac{1}{2}}$
2944. 814	150*Z*	33948. 08	$b\ {}^2I_{6\frac{1}{2}}—z\ {}^2K^{\circ}_{7\frac{1}{2}}$
2944. 48	2*w*	33951. 93	$c\ {}^4D_{2\frac{1}{2}}—w\ {}^4F^{\circ}_{1\frac{1}{2}}$
2943. 988	7	33957. 60	$a\ {}^4F_{2\frac{1}{2}}—z\ {}^4H^{\circ}_{3\frac{1}{2}}$
2943. 364	40*Z*	33964. 80	$b\ {}^4F_{3\frac{1}{2}}—y\ {}^4G^{\circ}_{4\frac{1}{2}}$
2943. 01	1*w*	33968. 88	
2942. 73	5	33972. 12	$c\ {}^2F_{3\frac{1}{2}}—x\ {}^2D^{\circ}_{2\frac{1}{2}}$
2942. 214	6	33978. 07	$b\ {}^4F_{4\frac{1}{2}}—(2)^{\circ}_{3\frac{1}{2}}$
2942. 01	2	33980. 43	$b\ {}^4P_{2\frac{1}{2}}—y\ {}^4F^{\circ}_{1\frac{1}{2}}$
2941. 88	3	33981. 93	
2941. 214	80*Z*	33989. 63	$b\ {}^4G_{4\frac{1}{2}}—x\ {}^4F^{\circ}_{3\frac{1}{2}}$
2940. 38	1*hl*	33999. 27	
2940. 090	50*Z*	34002. 62	$\begin{cases} a\ {}^4F_{1\frac{1}{2}}—y\ {}^4D^{\circ}_{1\frac{1}{2}} \\ a\ {}^4H_{6\frac{1}{2}}—z\ {}^4G^{\circ}_{5\frac{1}{2}} \end{cases}$
2939. 765	7	34006. 38	$b\ {}^4D_{3\frac{1}{2}}—y\ {}^4D^{\circ}_{2\frac{1}{2}}$
2938. 878	10	34016. 64	
2938. 65	10	34019. 28	$b\ {}^4P_{2\frac{1}{2}}—y\ {}^4G^{\circ}_{2\frac{1}{2}}$
2938. 51	12*Z*	34020. 90	$a\ {}^2H_{5\frac{1}{2}}—z\ {}^4I^{\circ}_{4\frac{1}{2}}$
2938. 292	40*Z*	34023. 43	$b\ {}^4F_{3\frac{1}{2}}—(2)^{\circ}_{3\frac{1}{2}}$
2937. 839	4	34028. 67	$a\ {}^4D_{2\frac{1}{2}}—z\ {}^4F^{\circ}_{1\frac{1}{2}}$
2937. 46	1	34033. 06	
2937. 39	1	34033. 87	
2937. 24	2	34035. 61	
2936. 98	4	34038. 62	$a\ {}^4F_{3\frac{1}{2}}—z\ {}^4H^{\circ}_{3\frac{1}{2}}$
2936. 773	40*Z*	34041. 02	$b\ {}^4F_{2\frac{1}{2}}—y\ {}^4G^{\circ}_{3\frac{1}{2}}$
2935. 698	18*Z*	34053. 49	$\begin{cases} b\ {}^4F_{1\frac{1}{2}}—x\ {}^4D^{\circ}_{0\frac{1}{2}} \\ a\ {}^4G_{4\frac{1}{2}}—z\ {}^6P^{\circ}_{3\frac{1}{2}} \end{cases}$
2935. 39	5*wl*	34057. 09	
2935. 196	15*Z*	34059. 31	$\begin{cases} a\ {}^4P_{0\frac{1}{2}}—z\ {}^6D^{\circ}_{0\frac{1}{2}} \\ a\ {}^4F_{3\frac{1}{2}}—z\ {}^4H^{\circ}_{3\frac{1}{2}} \end{cases}$
2934. 76	4	34064. 37	

TABLE 1. *Wavelengths and term combinations of* Mo II—Continued

Wavelength λ_{air}	Intensity	Wave No.	Term combination
2934. 293	100*Z*	34069. 79	$b\ {}^4F_{4\frac{1}{2}}$—$y\ {}^4F^\circ_{3\frac{1}{2}}$ $a\ {}^6D_{0\frac{1}{2}}$—$z\ {}^6F^\circ_{0\frac{1}{2}}$
2933. 98	5	34073. 43	
2933. 67	1	34077. 03	
2933. 43	3	34079. 82	
2933. 201	10*Z*	34082. 47	$b\ {}^4P_{2\frac{1}{2}}$—$y\ {}^4F^\circ_{3\frac{1}{2}}$
2932. 80	1*h*	34087. 14	
2932. 394	7	34091. 86	
2932. 185	15*Z*	34094. 28	$a\ {}^4H_{3\frac{1}{2}}$—$z\ {}^2G^\circ_{3\frac{1}{2}}$
2931. 36	2*w*	34103. 88	
2931. 11	2*w*	34106. 79	
2930. 77	20	34110. 74	$b\ {}^4G_{3\frac{1}{2}}$—$z\ {}^2H^\circ_{4\frac{1}{2}}$
2930. 478	100*Z*	34114. 14	$a\ {}^6D_{1\frac{1}{2}}$—$z\ {}^6F^\circ_{1\frac{1}{2}}$
2930. 072	25*Z*	34118. 86	$b\ {}^4P_{1\frac{1}{2}}$—$z\ {}^2P^\circ_{1\frac{1}{2}}$ $b\ {}^4F_{1\frac{1}{2}}$—$y\ {}^4F^\circ_{1\frac{1}{2}}$
2929. 493	10*Z*	34125. 61	$b\ {}^4F_{2\frac{1}{2}}$—$y\ {}^4F^\circ_{1\frac{1}{2}}$
2929. 04	1*w*	34130. 89	
2928. 494	18*Z*	34137. 25	$b\ {}^4D_{3\frac{1}{2}}$—$z\ {}^4G^\circ_{3\frac{1}{2}}$ $c\ {}^2D_{2\frac{1}{2}}$—$w\ {}^2P^\circ_{1\frac{1}{2}}$ $b\ {}^2G_{4\frac{1}{2}}$—$x\ {}^2F^\circ_{3\frac{1}{2}}$
2927. 542	50*Z*	34148. 35	$b\ {}^4G_{3\frac{1}{2}}$—$x\ {}^4F^\circ_{2\frac{1}{2}}$
2926. 96	2	34155. 15	$b\ {}^4D_{0\frac{1}{2}}$—$z\ {}^2S^\circ_{0\frac{1}{2}}$
2926. 743	20*Z*	34157. 68	$b\ {}^4F_{1\frac{1}{2}}$—$y\ {}^4G^\circ_{2\frac{1}{2}}$
2926. 22	20	34163. 78	$c\ {}^4D_{3\frac{1}{2}}$—$x\ {}^4P^\circ_{2\frac{1}{2}}$
2926. 15	20	34164. 60	$b\ {}^4F_{2\frac{1}{2}}$—$y\ {}^4G^\circ_{2\frac{1}{2}}$
2925. 416	50*Z*	34173. 17	$b\ {}^4F_{4\frac{1}{2}}$—$y\ {}^4G^\circ_{5\frac{1}{2}}$
2924. 320	65*Z*	34185. 98	$a\ {}^4H_{3\frac{1}{2}}$—$z\ {}^4G^\circ_{4\frac{1}{2}}$ $a\ {}^4H_{5\frac{1}{2}}$—$z\ {}^4I^\circ_{5\frac{1}{2}}$
2924. 17	5	34187. 73	$c\ {}^4D_{1\frac{1}{2}}$—$x\ {}^4P^\circ_{2\frac{1}{2}}$
2923. 387	100*Z*	34196. 89	$a\ {}^6D_{2\frac{1}{2}}$—$z\ {}^6F^\circ_{2\frac{1}{2}}$
2923. 215	10	34198. 90	$a\ {}^4D_{1\frac{1}{2}}$—$z\ {}^4F^\circ_{1\frac{1}{2}}$
2922. 732	22*Z*	34204. 55	$b\ {}^4G_{2\frac{1}{2}}$—$x\ {}^4F^\circ_{1\frac{1}{2}}$
2922. 183	4	34210. 98	$c\ {}^4D_{3\frac{1}{2}}$—$x\ {}^2G^\circ_{3\frac{1}{2}}$
2921. 92	8*Z*	34214. 06	$a\ {}^4H_{4\frac{1}{2}}$—$y\ {}^4D^\circ_{3\frac{1}{2}}$
2921. 40	2*wl*	34220. 15	
2920. 878	2	34226. 26	$a\ {}^2P_{1\frac{1}{2}}$—$y\ {}^2P^\circ_{0\frac{1}{2}}$
2920. 46	3	34231. 16	
2920. 250	12*Z*	34233. 62	$c\ {}^2D_{2\frac{1}{2}}$—$u\ {}^2F^\circ_{3\frac{1}{2}}$ $a\ {}^4H_{5\frac{1}{2}}$—$z\ {}^2G^\circ_{4\frac{1}{2}}$
2920. 084	5*Z*	34235. 57	$b\ {}^4D_{2\frac{1}{2}}$—$y\ {}^4D^\circ_{2\frac{1}{2}}$
2918. 94	10	34248. 99	
2918. 835	40*Z*	34250. 22	$a\ {}^4P_{1\frac{1}{2}}$—$z\ {}^6D^\circ_{0\frac{1}{2}}$
2917. 157	15*Z*	34269. 92	$c\ {}^2F_{3\frac{1}{2}}$—$w\ {}^2G^\circ_{4\frac{1}{2}}$
2916. 698	3*hl*	34275. 31	$a\ {}^2P_{0\frac{1}{2}}$—$w\ {}^4D^\circ_{1\frac{1}{2}}$
2916. 47	3*w*	34277. 99	$d\ {}^2G_{4\frac{1}{2}}$—$w\ {}^4G^\circ_{4\frac{1}{2}}$ $d\ {}^2D_{1\frac{1}{2}}$—$v\ {}^2D^\circ_{2\frac{1}{2}}$
2916. 28	1	34280. 22	
2915. 655	4	34287. 57	$b\ {}^2H_{5\frac{1}{2}}$—$z\ {}^2K^\circ_{6\frac{1}{2}}$
2914. 901	4	34296. 44	$a\ {}^2G_{3\frac{1}{2}}$—$y\ {}^4D^\circ_{3\frac{1}{2}}$ $c\ {}^4D_{1\frac{1}{2}}$—$w\ {}^4F^\circ_{1\frac{1}{2}}$
2914. 83	3	34297. 28	
2914. 70	4	34298. 80	
2914. 435	8*Z*	34301. 92	$a\ {}^4P_{0\frac{1}{2}}$—$z\ {}^6D^\circ_{1\frac{1}{2}}$
2914. 313	12*Z*	34303. 36	$c\ {}^2D_{1\frac{1}{2}}$—$w\ {}^2P^\circ_{0\frac{1}{2}}$
2914. 010	6	34306. 93	$b\ {}^4G_{3\frac{1}{2}}$—$x\ {}^4F^\circ_{4\frac{1}{2}}$
2913. 82	30*Z*	34309. 16	$b\ {}^4F_{3\frac{1}{2}}$—$y\ {}^4H^\circ_{3\frac{1}{2}}$
2913. 74	40*Z*	34310. 10	$c\ {}^4D_{2\frac{1}{2}}$—$w\ {}^4F^\circ_{3\frac{1}{2}}$
2912. 513	5	34324. 56	
2911. 915	125*Z*	34331. 61	$a\ {}^6D_{3\frac{1}{2}}$—$z\ {}^6F_{3\frac{1}{2}}$
2911. 57	3*s*	34335. 68	
2911. 30	2	34338. 86	
2910. 927	10*Z*	34343. 26	$a\ {}^4F_{3\frac{1}{2}}$—$z\ {}^4H^\circ_{4\frac{1}{2}}$
2910. 47	1	34348. 65	
2909. 913	4	34355. 23	
2909. 46	1	34360. 58	
2909. 108	75*Z*	34364. 73	$a\ {}^6D_{0\frac{1}{2}}$—$z\ {}^6F^\circ_{1\frac{1}{2}}$
2908. 642	4	34370. 24	$b\ {}^4P_{2\frac{1}{2}}$—$y\ {}^4F^\circ_{2\frac{1}{2}}$
2908. 22	8	34375. 23	
2908. 18	4	34375. 70	$b\ {}^4G_{3\frac{1}{2}}$—$z\ {}^2F^\circ_{2\frac{1}{2}}$
2907. 66	1	34381. 84	
2907. 54	1	34383. 27	
2907. 113	30*Z*	34388. 32	$a\ {}^4D_{2\frac{1}{2}}$—$z\ {}^4F^\circ_{2\frac{1}{2}}$
2906. 61	1	34394. 27	$b\ {}^4D_{1\frac{1}{2}}$—$z\ {}^4G^\circ_{2\frac{1}{2}}$
2906. 507	4	34395. 48	
2905. 833	12*Z*	34403. 46	$b\ {}^4F_{3\frac{1}{2}}$—$y\ {}^4F^\circ_{2\frac{1}{2}}$
2905. 45	3	34408. 00	
2904. 781	4	34415. 92	
2904. 334	8	34421. 22	$b\ {}^4F_{2\frac{1}{2}}$—$y\ {}^4H^\circ_{3\frac{1}{2}}$
2904. 11	6*w*	34423. 87	$c\ {}^2F_{2\frac{1}{2}}$—$x\ {}^2D^\circ_{2\frac{1}{2}}$
2903. 69	2*wl*	34428. 85	
2903. 055	125*Z*	34436. 38	$a\ {}^4H_{4\frac{1}{2}}$—$z\ {}^4I^\circ_{5\frac{1}{2}}$
2902. 72	2	34440. 35	
2902. 56	1	34442. 26	
2902. 45	1*w*	34443. 56	
2901. 98	2	34449. 14	$c\ {}^2F_{2\frac{1}{2}}$—$x\ {}^2D^\circ_{1\frac{1}{2}}$
2901. 794	12*Z*	34451. 34	$b\ {}^2H_{5\frac{1}{2}}$—$x\ {}^2G^\circ_{4\frac{1}{2}}$
2900. 780	40*Z*	34463. 39	$b\ {}^2F_{2\frac{1}{2}}$—$x\ {}^4D^\circ_{2\frac{1}{2}}$ $b\ {}^4F_{4\frac{1}{2}}$—$y\ {}^4H^\circ_{4\frac{1}{2}}$
2900. 506	6	34466. 64	$c\ {}^4D_{3\frac{1}{2}}$—$w\ {}^4F^\circ_{2\frac{1}{2}}$
2900. 363	6	34468. 34	$b\ {}^4G_{2\frac{1}{2}}$—$x\ {}^4F^\circ_{2\frac{1}{2}}$ $d\ {}^2G_{3\frac{1}{2}}$—$v\ {}^4F^\circ_{4\frac{1}{2}}$ $b\ {}^4P_{1\frac{1}{2}}$—$z\ {}^2P^\circ_{0\frac{1}{2}}$
2900. 17	2	34470. 64	
2899. 703	6	34476. 19	
2899. 079	6	34483. 61	$a\ {}^2P_{1\frac{1}{2}}$—$y\ {}^2P^\circ_{1\frac{1}{2}}$
2898. 961	4	34485. 01	$a\ {}^4H_{4\frac{1}{2}}$—$z\ {}^2G^\circ_{4\frac{1}{2}}$
2898. 646	10*Z*	34488. 78	$c\ {}^2G_{3\frac{1}{2}}$—$w\ {}^2H^\circ_{4\frac{1}{2}}$
2898. 477	15*Z*	34490. 77	$c\ {}^4D_{1\frac{1}{2}}$—$w\ {}^4F^\circ_{2\frac{1}{2}}$
2898. 30	2	34492. 88	$a\ {}^4P_{1\frac{1}{2}}$—$z\ {}^6D^\circ_{1\frac{1}{2}}$
2897. 627	35	34500. 89	$a\ {}^4P_{2\frac{1}{2}}$—$z\ {}^6D^\circ_{1\frac{1}{2}}$
2897. 42	15*s*	34503. 35	$b\ {}^4G_{2\frac{1}{2}}$—$x\ {}^4F^\circ_{3\frac{1}{2}}$ $c\ {}^4D_{3\frac{1}{2}}$—$x\ {}^2G^\circ_{4\frac{1}{2}}$
2896. 98	3	34508. 62	$b\ {}^4F_{3\frac{1}{2}}$—$y\ {}^4H^\circ_{4\frac{1}{2}}$ $b\ {}^4F_{1\frac{1}{2}}$—$y\ {}^4F^\circ_{2\frac{1}{2}}$
2896. 75	4	34511. 33	
2896. 71	5	34511. 81	$b\ {}^2D_{2\frac{1}{2}}$—$x\ {}^2F^\circ_{3\frac{1}{2}}$ $b\ {}^2G_{3\frac{1}{2}}$—$x\ {}^2F^\circ_{3\frac{1}{2}}$
2896. 417	15	34515. 30	$b\ {}^4F_{2\frac{1}{2}}$—$y\ {}^4F^\circ_{2\frac{1}{2}}$
2895. 91	2*w*	34521. 34	
2895. 82	2*h*	34522. 41	
2895. 73	2	34523. 49	
2895. 137	10	34530. 56	$b\ {}^4P_{0\frac{1}{2}}$—$y\ {}^4P^\circ_{0\frac{1}{2}}$
2894. 867	10	34533. 78	$a\ {}^4H_{6\frac{1}{2}}$—$z\ {}^4I^\circ_{5\frac{1}{2}}$
2894. 446	80*Z*	34538. 80	$a\ {}^6D_{4\frac{1}{2}}$—$z\ {}^6F^\circ_{4\frac{1}{2}}$
2894. 12	2	34542. 69	
2893. 97	3	34544. 48	$a\ {}^2F_{3\frac{1}{2}}$—$z\ {}^4G^\circ_{2\frac{1}{2}}$
2893. 795	6	34546. 57	$b\ {}^2F_{2\frac{1}{2}}$—$y\ {}^4P^\circ_{2\frac{1}{2}}$ $c\ {}^4D_{0\frac{1}{2}}$—$x\ {}^4P^\circ_{1\frac{1}{2}}$
2893. 60	1*w*	34548. 90	
2893. 46	1*w*	34550. 57	
2892. 817	60*Z*	34558. 25	$a\ {}^4D_{1\frac{1}{2}}$—$z\ {}^4F^\circ_{2\frac{1}{2}}$
2892. 47	1	34562. 39	
2892. 044	12*Z*	34567. 49	$a\ {}^2G_{3\frac{1}{2}}$—$z\ {}^2G^\circ_{4\frac{1}{2}}$
2891. 67	3*w*	34571. 96	$b\ {}^2D_{1\frac{1}{2}}$—$x\ {}^2F^\circ_{2\frac{1}{2}}$ $c\ {}^4D_{2\frac{1}{2}}$—$x\ {}^4P^\circ_{1\frac{1}{2}}$
2891. 290	25*Z*	34576. 50	$a\ {}^4D_{0\frac{1}{2}}$—$z\ {}^4F^\circ_{1\frac{1}{2}}$

TABLE 1. *Wavelengths and term combinations of* Mo II—Continued

Wavelength λ_{air}	Intensity	Wave No.	Term combination
2890. 995	100Z	34580. 03	$a\ ^6D_{1\frac{1}{2}}$—$z\ ^6F^o_{2\frac{1}{2}}$
2890. 43	4	34586. 79	$a\ ^2G_{3\frac{1}{2}}$—$z\ ^2D^o_{2\frac{1}{2}}$
2890. 38	1	34587. 39	
2890. 16	2*wl*	34590. 02	
2889. 60	5*w*	34596. 75	$b\ ^2I_{3\frac{1}{2}}$—$x\ ^2H^o_{4\frac{1}{2}}$
2888. 70	10Z	34607. 50	
2888. 38	4	34611. 33	$a\ ^4P_{2\frac{1}{2}}$—$z\ ^6D^o_{3\frac{1}{2}}$
2888. 171	50Z	34613. 84	$b\ ^2G_{3\frac{1}{2}}$—$x\ ^2G^o_{3\frac{1}{2}}$
2886. 982	15Z	34628. 09	$a\ ^4H_{4\frac{1}{2}}$—$z\ ^4G^o_{5\frac{1}{2}}$
2886. 799	5	34630. 29	$a\ ^2P_{1\frac{1}{2}}$—$x\ ^4P^o_{0\frac{1}{2}}$ $c\ ^4D_{3\frac{1}{2}}$—$w\ ^4F^o_{3\frac{1}{2}}$
2886. 53	3	34633. 52	$a\ ^2G_{4\frac{1}{2}}$—$y\ ^4D^o_{3\frac{1}{2}}$
2886. 13	7	34638. 32	$b\ ^4G_{4\frac{1}{2}}$—$y\ ^2G^o_{3\frac{1}{2}}$
2885. 789	25Z	34642. 41	$a\ ^2F_{2\frac{1}{2}}$—$z\ ^4G^o_{3\frac{1}{2}}$
2885. 73	8	34643. 12	
2884. 799	6Z	34654. 30	
2884. 224	3	34661. 20	$a\ ^4H_{3\frac{1}{2}}$—$y\ ^4D^o_{3\frac{1}{2}}$
2883. 969	8Z	34664. 27	
2883. 324	8Z	34672. 02	$b\ ^2F_{2\frac{1}{2}}$—$x\ ^4D^o_{1\frac{1}{2}}$
2882. 376	22Z	34683. 43	$b\ ^4G_{5\frac{1}{2}}$—$z\ ^2H^o_{5\frac{1}{2}}$
2882. 048	10Z	34687. 37	
2881. 932	8Z	34688. 77	$b\ ^4D_{1\frac{1}{2}}$—$y\ ^4D^o_{2\frac{1}{2}}$
2881. 386	18Z	34695. 34	$b\ ^4G_{2\frac{1}{2}}$—$z\ ^2F^o_{2\frac{1}{2}}$
2880. 19	2	34709. 75	
2879. 75	10Z	34715. 05	$b\ ^2H_{4\frac{1}{2}}$—$x\ ^2G^o_{3\frac{1}{2}}$ $b\ ^4P_{1\frac{1}{2}}$—$x\ ^4D^o_{2\frac{1}{2}}$
2879. 69	12	34715. 77	$b\ ^2F_{2\frac{1}{2}}$— $(1)^o_{2\frac{1}{2}}$
2879. 38	2	34719. 51	
2879. 046	100Z	34723. 54	$b\ ^4G_{5\frac{1}{2}}$—$y\ ^4H^o_{5\frac{1}{2}}$
2878. 70	4*ws*	34727. 71	
2878. 43	1*hl*	34730. 97	
2878. 09	1*w*	34735. 07	$b\ ^2D_{1\frac{1}{2}}$—$w\ ^4F^o_{1\frac{1}{2}}$
2876. 826	10Z	34750. 33	$c\ ^4D_{0\frac{1}{2}}$—$y\ ^2P^o_{0\frac{1}{2}}$
2876. 173	2	34758. 22	
2875. 82	2	34762. 49	
2875. 76	1	34763. 21	
2875. 43	2	34767. 20	$a\ ^2H_{4\frac{1}{2}}$—$x\ ^4D^o_{3\frac{1}{2}}$
2874. 847	10Z	34774. 25	$c\ ^4D_{3\frac{1}{2}}$—$w\ ^4F^o_{4\frac{1}{2}}$
2874. 39	3Z	34779. 78	
2873. 24	2	34793. 70	$b\ ^4D_{3\frac{1}{2}}$—$z\ ^2G^o_{3\frac{1}{2}}$ $b\ ^4F_{3\frac{1}{2}}$—$y\ ^4F^o_{4\frac{1}{2}}$
2872. 90	2Z	34797. 82	$b\ ^4P_{1\frac{1}{2}}$—$y\ ^4P^o_{2\frac{1}{2}}$
2872. 880	60Z	34798. 06	$b\ ^2G_{4\frac{1}{2}}$—$x\ ^2G^o_{4\frac{1}{2}}$
2872. 54	2*w*	34802. 18	
2872. 14	3	34807. 03	$c\ ^2D_{1\frac{1}{2}}$—$w\ ^2P^o_{1\frac{1}{2}}$
2871. 506	125Z	34814. 71	$a\ ^6D_{2\frac{1}{2}}$—$z\ ^6F^o_{3\frac{1}{2}}$
2870. 66	2	34824. 97	
2870. 08	1	34832. 01	
2869. 984	7Z	34833. 17	$b\ ^2D_{2\frac{1}{2}}$—$x\ ^4P^o_{2\frac{1}{2}}$ $b\ ^4G_{3\frac{1}{2}}$—$y\ ^2G^o_{3\frac{1}{2}}$
2869. 221	12Z	34842. 44	$b\ ^4F_{4\frac{1}{2}}$—$z\ ^2F^o_{3\frac{1}{2}}$
2868. 64	3	34849. 49	
2868. 334	25Z	34853. 21	$b\ ^4P_{0\frac{1}{2}}$—$y\ ^4P^o_{1\frac{1}{2}}$
2868. 116	25Z	34855. 86	$a\ ^2G_{4\frac{1}{2}}$—$z\ ^4I^o_{5\frac{1}{2}}$
2867. 68	3	34861. 16	$b\ ^4G_{4\frac{1}{2}}$—$z\ ^2H^o_{5\frac{1}{2}}$
2867. 20	1	34866. 99	
2866. 82	12	34871. 62	$b\ ^2H_{5\frac{1}{2}}$—$y\ ^2I^o_{5\frac{1}{2}}$
2866. 705	35Z	34873. 01	$a\ ^4D_{2\frac{1}{2}}$—$z\ ^4F^o_{3\frac{1}{2}}$
2866. 53	4	34875. 17	$a\ ^4G_{4\frac{1}{2}}$—$z\ ^6D^o_{3\frac{1}{2}}$
2866. 270	7*w*	34878. 31	$a\ ^4P_{1\frac{1}{2}}$—$z\ ^6D^o_{2\frac{1}{2}}$
2866. 086	7	34880. 55	$b\ ^2D_{2\frac{1}{2}}$—$x\ ^2G^o_{3\frac{1}{2}}$
2865. 880	4	34883. 05	
2865. 64	10	34885. 97	$a\ ^4P_{2\frac{1}{2}}$—$z\ ^6D^o_{2\frac{1}{2}}$
2865. 502	10	34887. 66	$b\ ^4F_{3\frac{1}{2}}$—$z\ ^2F^o_{3\frac{1}{2}}$
2865. 205	10	34891. 27	$b\ ^4G_{5\frac{1}{2}}$—$y\ ^2H^o_{4\frac{1}{2}}$
2864. 43	2*w*	34900. 71	
2864. 13	8	34904. 37	$c\ ^2F_{2\frac{1}{2}}$—$w\ ^2G^o_{3\frac{1}{2}}$ $a\ ^2G_{4\frac{1}{2}}$—$z\ ^2G^o_{4\frac{1}{2}}$
2863. 801	90Z	34908. 38	$a\ ^4H_{5\frac{1}{2}}$—$z\ ^4I^o_{5\frac{1}{2}}$
2863. 57	2	34911. 19	
2863. 20	18Z	34915. 70	$a\ ^4F_{1\frac{1}{2}}$—$z\ ^4G^o_{2\frac{1}{2}}$
2863. 16	15	34916. 19	$c\ ^4D_{1\frac{1}{2}}$—$x\ ^4P^o_{1\frac{1}{2}}$
2862. 97	2	34918. 51	
2862. 403	7	34925. 42	$b\ ^2G_{4\frac{1}{2}}$—$w\ ^4F^o_{3\frac{1}{2}}$
2862. 200	6	34927. 90	$a\ ^4F_{4\frac{1}{2}}$—$z\ ^4H^o_{5\frac{1}{2}}$
2862. 051	5	34929. 72	$b\ ^2D_{1\frac{1}{2}}$—$w\ ^4F^o_{2\frac{1}{2}}$
2861. 865	8	34931. 99	$b\ ^2F_{3\frac{1}{2}}$—$x\ ^4D^o_{2\frac{1}{2}}$ $a\ ^4H_{3\frac{1}{2}}$—$z\ ^2G^o_{4\frac{1}{2}}$
2861. 579	7	34935. 48	
2861. 350	4	34938. 28	
2860. 95	4	34943. 16	
2860. 750	5	34945. 60	$c\ ^2D_{2\frac{1}{2}}$—$w\ ^4G^o_{2\frac{1}{2}}$
2860. 34	1*wl*	34950. 61	
2860. 27	1	34951. 47	$a\ ^4H_{3\frac{1}{2}}$—$z\ ^2D^o_{2\frac{1}{2}}$
2860. 113	3	34953. 39	$a\ ^2S_{0\frac{1}{2}}$—$x\ ^4F^o_{1\frac{1}{2}}$
2860. 03	1	34954. 40	
2859. 62	2*w*	34959. 41	
2859. 52	2	34960. 64	
2859. 002	15Z	34966. 97	$b\ ^4P_{1\frac{1}{2}}$— $(1)^o_{2\frac{1}{2}}$
2858. 594	5	34971. 96	$a\ ^4G_{3\frac{1}{2}}$—$z\ ^6D^o_{3\frac{1}{2}}$
2858. 077	10Z	34978. 29	$c\ ^2G_{4\frac{1}{2}}$—$v\ ^2F^o_{3\frac{1}{2}}$
2857. 50	20	34985. 35	
2856. 900	10Z	34992. 70	$a\ ^4G_{2\frac{1}{2}}$—$z\ ^6D^o_{1\frac{1}{2}}$
2856. 606	2*wl*	34996. 30	
2856. 46	3	34998. 08	
2856. 009	20Z	35003. 61	$a\ ^2H_{4\frac{1}{2}}$—$z\ ^2I^o_{5\frac{1}{2}}$
2855. 707	18Z	35007. 31	$b\ ^2H_{4\frac{1}{2}}$—$x\ ^2G^o_{4\frac{1}{2}}$ $c\ ^4D_{0\frac{1}{2}}$—$y\ ^2P^o_{1\frac{1}{2}}$
2855. 37	2	35011. 45	
2855. 22	3	35013. 28	$c\ ^2D_{2\frac{1}{2}}$—$t\ ^2F^o_{2\frac{1}{2}}$
2855. 06	2	35015. 25	$b\ ^2F_{3\frac{1}{2}}$—$y\ ^4P^o_{2\frac{1}{2}}$
2854. 66	6*w*	35020. 15	$b\ ^4F_{1\frac{1}{2}}$—$x\ ^4F^o_{1\frac{1}{2}}$
2854. 428	6	35023. 00	$b\ ^4D_{2\frac{1}{2}}$—$z\ ^2G^o_{3\frac{1}{2}}$
2854. 120	12	35026. 78	$b\ ^4F_{2\frac{1}{2}}$—$x\ ^4F^o_{1\frac{1}{2}}$
2853. 84	1*w*	35030. 28	
2853. 600	20	35033. 16	$b\ ^2G_{3\frac{1}{2}}$—$w\ ^4F^o_{3\frac{1}{2}}$ $b\ ^4G_{5\frac{1}{2}}$—$y\ ^2H^o_{5\frac{1}{2}}$ $c\ ^4D_{2\frac{1}{2}}$—$y\ ^2P^o_{1\frac{1}{2}}$
2853. 220	150Z	35037. 83	$a\ ^4H_{6\frac{1}{2}}$—$z\ ^4I^o_{7\frac{1}{2}}$
2852. 89	4*s*	35041. 88	
2852. 60	2	35045. 44	
2852. 419	4*s*	35047. 67	$a\ ^2G_{4\frac{1}{2}}$—$z\ ^4G^o_{5\frac{1}{2}}$ $b\ ^4G_{4\frac{1}{2}}$—$y\ ^2F^o_{3\frac{1}{2}}$
2852. 022	2	35052. 54	$c\ ^2G_{3\frac{1}{2}}$—$v\ ^2F^o_{2\frac{1}{2}}$
2851. 80	2	35055. 27	
2851. 09	4	35064. 00	
2850. 676	35Z	35069. 09	$b\ ^2G_{4\frac{1}{2}}$—$w\ ^4F^o_{4\frac{1}{2}}$ $b\ ^4G_{4\frac{1}{2}}$—$y\ ^2H^o_{4\frac{1}{2}}$
2850. 37	3*w*	35072. 86	
2850. 15	1	35075. 57	
2849. 66	4*w*	35081. 60	$b\ ^2F_{3\frac{1}{2}}$—$x\ ^4D^o_{3\frac{1}{2}}$
2848. 85	3	35091. 57	
2848. 238	175Z	35099. 11	$a\ ^6D_{3\frac{1}{2}}$—$z\ ^6F^o_{4\frac{1}{2}}$
2847. 686	8	35105. 91	$b\ ^4F_{4\frac{1}{2}}$—$y\ ^4H^o_{5\frac{1}{2}}$
2847. 43	2	35109. 07	
2846. 632	15Z	35118. 91	$a\ ^4F_{2\frac{1}{2}}$—$z\ ^4G^o_{2\frac{1}{2}}$

TABLE 1. *Wavelengths and term combinations of* Mo II—Continued

Wavelength λ_{air}	Intensity	Wave No.	Term combination
2846.250	4Z	35123.63	$b\ ^2F_{2\frac{1}{2}}$—$y\ ^4F^\circ_{1\frac{1}{2}}$
2846.08	1	35125.72	
2845.668	10Z	35130.81	
2845.392	6	35134.21	$b\ ^2H_{4\frac{1}{2}}$—$w\ ^4F^\circ_{3\frac{1}{2}}$
2845.222	2	35136.31	$b\ ^2D_{2\frac{1}{2}}$—$w\ ^4F^\circ_{2\frac{1}{2}}$
2845.14	2	35137.33	
2844.834	18Z	35141.11	$b\ ^4F_{3\frac{1}{2}}$—$z\ ^2H^\circ_{3\frac{1}{2}}$
2844.67	1	35143.13	$b\ ^4P_{0\frac{1}{2}}$—$z\ ^2P^\circ_{1\frac{1}{2}}$
2844.507	3w	35145.15	$b\ ^4P_{2\frac{1}{2}}$—$x\ ^4F^\circ_{2\frac{1}{2}}$
2843.97	2	35151.78	
2843.734	10Z	35154.70	$c\ ^4D_{0\frac{1}{2}}$—$x\ ^4P^\circ_{0\frac{1}{2}}$
2843.09	4	35162.66	$b\ ^2F_{2\frac{1}{2}}$—$y\ ^4G^\circ_{2\frac{1}{2}}$
2842.492	35Z	35170.06	$a\ ^2F_{3\frac{1}{2}}$—$z\ ^4I^\circ_{4\frac{1}{2}}$
2842.148	40Z	35174.31	$a\ ^6D_{1\frac{1}{2}}$—$z\ ^4P^\circ_{0\frac{1}{2}}$
2841.788	12Z	35178.77	$c\ ^2F_{3\frac{1}{2}}$—$w\ ^2H^\circ_{3\frac{1}{2}}$ $b\ ^4F_{3\frac{1}{2}}$—$x\ ^4F^\circ_{2\frac{1}{2}}$
2841.60	3	35181.10	$b\ ^4P_{2\frac{1}{2}}$—$x\ ^4F^\circ_{3\frac{1}{2}}$
2841.56	1	35181.59	$b\ ^4D_{1\frac{1}{2}}$—$z\ ^2D^\circ_{1\frac{1}{2}}$
2841.34	2	35184.32	$b\ ^2F_{3\frac{1}{2}}$— $(1)^\circ_{2\frac{1}{2}}$
2841.11	2	35187.16	
2840.080	7Z	35199.93	$a\ ^4F_{3\frac{1}{2}}$—$z\ ^4G^\circ_{2\frac{1}{2}}$
2839.872	3	35202.50	
2839.25	8lZ	35210.22	$a\ ^4F_{1\frac{1}{2}}$—$y\ ^4D^\circ_{2\frac{1}{2}}$
2839.19	25Z	35210.96	$b\ ^4G_{4\frac{1}{2}}$—$y\ ^2H^\circ_{4\frac{1}{2}}$
2838.94	2	35214.06	$b\ ^4F_{3\frac{1}{2}}$—$x\ ^4F^\circ_{3\frac{1}{2}}$
2838.00	3	35225.72	$b\ ^2F_{2\frac{1}{2}}$—$y\ ^4F^\circ_{3\frac{1}{2}}$
2836.721	30Z	35241.60	$b\ ^4G_{3\frac{1}{2}}$—$y\ ^2F^\circ_{3\frac{1}{2}}$
2836.307	10Z	35246.75	$a\ ^4G_{3\frac{1}{2}}$—$z\ ^6D^\circ_{2\frac{1}{2}}$
2835.342	30Z	35258.74	$a\ ^4G_{5\frac{1}{2}}$—$z\ ^6D^\circ_{4\frac{1}{2}}$
2834.993	10	35263.08	$b\ ^4G_{3\frac{1}{2}}$—$y\ ^2H^\circ_{4\frac{1}{2}}$
2834.873	18	35264.58	$b\ ^2I_{5\frac{1}{2}}$—$x\ ^2H^\circ_{5\frac{1}{2}}$
2834.416	40Z	35270.26	$a\ ^4D_{3\frac{1}{2}}$—$z\ ^4F^\circ_{3\frac{1}{2}}$
2833.796	8	35277.98	$b\ ^2H_{4\frac{1}{2}}$—$w\ ^4F^\circ_{4\frac{1}{2}}$ $a\ ^4G_{4\frac{1}{2}}$—$z\ ^6D^\circ_{4\frac{1}{2}}$
2833.71	2w	35279.05	
2833.333	6	35283.74	$b\ ^4F_{1\frac{1}{2}}$—$x\ ^4F^\circ_{2\frac{1}{2}}$
2832.788	10	35290.53	$b\ ^4F_{2\frac{1}{2}}$—$x\ ^4F^\circ_{2\frac{1}{2}}$
2832.663	10	35292.09	$b\ ^4F_{4\frac{1}{2}}$—$x\ ^4F^\circ_{4\frac{1}{2}}$
2832.078	20Z	35299.38	$a\ ^2F_{2\frac{1}{2}}$—$z\ ^2G^\circ_{3\frac{1}{2}}$
2832.00	10Z	35300.35	$b\ ^2D_{2\frac{1}{2}}$—$w\ ^4F^\circ_{3\frac{1}{2}}$
2831.76	3	35303.34	$b\ ^4G_{5\frac{1}{2}}$—$y\ ^2G^\circ_{4\frac{1}{2}}$
2831.442	40Z	35307.31	$b\ ^2H_{5\frac{1}{2}}$—$y\ ^2I^\circ_{5\frac{1}{2}}$
2830.61	3w	35317.68	
2829.88	4	35326.79	$b\ ^4F_{2\frac{1}{2}}$—$x\ ^4F^\circ_{3\frac{1}{2}}$ $a\ ^2H_{5\frac{1}{2}}$—$y\ ^4G^\circ_{4\frac{1}{2}}$
2829.039	12Z	35337.29	$b\ ^4F_{3\frac{1}{2}}$—$x\ ^4F^\circ_{4\frac{1}{2}}$
2827.752	100Z	35353.38	$a\ ^2H_{5\frac{1}{2}}$—$z\ ^2I^\circ_{6\frac{1}{2}}$
2827.42	2	35357.53	$d\ ^2G_{4\frac{1}{2}}$—$w\ ^4G^\circ_{3\frac{1}{2}}$
2827.185	10Z	35360.47	$b\ ^4D_{3\frac{1}{2}}$—$y\ ^4D^\circ_{3\frac{1}{2}}$
2826.550	10	35368.41	
2826.017	6	35375.08	$b\ ^4P_{1\frac{1}{2}}$—$y\ ^4F^\circ_{1\frac{1}{2}}$ $a\ ^4G_{3\frac{1}{2}}$—$z\ ^6D^\circ_{4\frac{1}{2}}$
2825.95	4	35375.92	
2825.80	2	35377.80	$a\ ^4G_{2\frac{1}{2}}$—$z\ ^6D^\circ_{2\frac{1}{2}}$ $c\ ^4D_{1\frac{1}{2}}$—$y\ ^2P^\circ_{1\frac{1}{2}}$
2825.60	1	35380.30	$a\ ^2H_{4\frac{1}{2}}$—$y\ ^4F^\circ_{3\frac{1}{2}}$
2825.299	8Z	35384.07	
2824.188	8Z	35397.99	$c\ ^2G_{3\frac{1}{2}}$—$w\ ^2D^\circ_{2\frac{1}{2}}$
2822.937	10Z	35413.68	$b\ ^4P_{1\frac{1}{2}}$—$y\ ^4G^\circ_{2\frac{1}{2}}$ $a\ ^4F_{2\frac{1}{2}}$—$y\ ^4D^\circ_{2\frac{1}{2}}$
2822.416	7	35420.21	
2822.035	12Z	35424.99	$a\ ^6D_{0\frac{1}{2}}$—$z\ ^4P^\circ_{0\frac{1}{2}}$
2821.843	18Z	35427.40	$b\ ^2H_{4\frac{1}{2}}$—$y\ ^2I^\circ_{5\frac{1}{2}}$
2821.02	10wlZ	35437.74	
2820.38	3w	35445.78	
2820.22	2h	35447.79	$a\ ^2D_{2\frac{1}{2}}$—$z\ ^4H^\circ_{2\frac{1}{2}}$
2820.018	8Z	35450.33	
2819.594	8Z	35455.66	
2818.98	5	35463.38	
2818.81	2	35465.52	
2818.56	2hl	35468.67	$b\ ^4D^\circ_{0\frac{1}{2}}$—$z\ ^2D^\circ_{1\frac{1}{2}}$
2817.54	15Z	35481.51	$b\ ^4G_{4\frac{1}{2}}$—$y\ ^2G^\circ_{4\frac{1}{2}}$
2817.44	15Z	35482.77	$a\ ^2H_{4\frac{1}{2}}$—$y\ ^4G^\circ_{5\frac{1}{2}}$ $a\ ^4P_{0\frac{1}{2}}$—$z\ ^4F^\circ_{1\frac{1}{2}}$
2816.50	4	35494.61	$a\ ^4F_{3\frac{1}{2}}$—$y\ ^4D^\circ_{2\frac{1}{2}}$
2816.153	150Z	35498.98	$a\ ^6D_{4\frac{1}{2}}$—$z\ ^6F^\circ_{5\frac{1}{2}}$
2815.80	4w	35503.43	
2815.46	3	35507.72	$b\ ^2F_{3\frac{1}{2}}$—$y\ ^4G^\circ_{3\frac{1}{2}}$
2814.997	3Z	35513.56	$b\ ^2F_{2\frac{1}{2}}$—$y\ ^4F^\circ_{2\frac{1}{2}}$
2814.678	12Z	35517.58	$b\ ^4F_{2\frac{1}{2}}$—$z\ ^2F^\circ_{2\frac{1}{2}}$
2814.123	8Z	35524.59	$c\ ^4D_{1\frac{1}{2}}$—$x\ ^4P^\circ_{0\frac{1}{2}}$
2813.34	4Z	35534.47	
2813.191	5	35536.35	
2812.65	4Z	35543.21	$b\ ^2F_{3\frac{1}{2}}$—$y\ ^4G^\circ_{4\frac{1}{2}}$
2812.612	6Z	35543.67	$a\ ^4F_{2\frac{1}{2}}$—$z\ ^4G^\circ_{3\frac{1}{2}}$
2812.04	1	35550.90	
2811.90	1	35552.67	
2811.387	3Z	35559.16	$b\ ^2D_{1\frac{1}{2}}$—$y\ ^2P^\circ_{0\frac{1}{2}}$
2811.165	8Z	35561.97	$b\ ^2D_{2\frac{1}{2}}$—$x\ ^4P^\circ_{1\frac{1}{2}}$ $b\ ^4G_{2\frac{1}{2}}$—$y\ ^2F^\circ_{3\frac{1}{2}}$
2810.45	3Z	35571.01	$b\ ^2I_{6\frac{1}{2}}$—$x\ ^2H^\circ_{5\frac{1}{2}}$
2810.25	3	35573.54	$a\ ^2H_{4\frac{1}{2}}$—$y\ ^4H^\circ_{3\frac{1}{2}}$ $b\ ^4G_{2\frac{1}{2}}$—$y\ ^2F^\circ_{2\frac{1}{2}}$
2809.72	2	35580.25	$a\ ^2H_{6\frac{1}{2}}$—$y\ ^4G^\circ_{5\frac{1}{2}}$
2808.974	10Z	35589.70	$b\ ^4D_{2\frac{1}{2}}$—$y\ ^4D^\circ_{3\frac{1}{2}}$
2808.473	5Z	35596.05	
2808.09	3	35600.91	$c\ ^2G_{3\frac{1}{2}}$—$v\ ^2F^\circ_{3\frac{1}{2}}$
2807.750	100Z	35605.22	$b\ \ ^2I_{5\frac{1}{2}}$—$w\ ^2G^\circ_{4\frac{1}{2}}$ $a\ ^6D_{2\frac{1}{2}}$—$z\ ^4P^\circ_{1\frac{1}{2}}$
2807.016	15Z	35614.53	$a\ ^4H_{6\frac{1}{2}}$—$z\ ^2I^\circ_{5\frac{1}{2}}$
2806.193	8Z	35624.97	$a\ ^4F_{3\frac{1}{2}}$—$z\ ^4G^\circ_{3\frac{1}{2}}$
2805.70	1w	35631.23	$b\ \ ^2F_{3\frac{1}{2}}$—$y\ ^4G^\circ_{2\frac{1}{2}}$ $b\ ^4D_{3\frac{1}{2}}$—$z\ ^2G^\circ_{4\frac{1}{2}}$
2804.59	1	35645.33	$a\ ^4F_{4\frac{1}{2}}$—$z\ ^4G^\circ_{3\frac{1}{2}}$
2802.360	15	35673.70	$a\ ^4P_{1\frac{1}{2}}$—$z\ ^4F^\circ_{1\frac{1}{2}}$
2801.244	10	35687.91	
2800.745	10Z	35694.27	$b\ ^2F_{3\frac{1}{2}}$—$y\ ^4F^\circ_{3\frac{1}{2}}$
2800.363	10	35699.13	
2800.057	8Z	35703.03	$a\ ^4F_{1\frac{1}{2}}$—$z\ ^2D^\circ_{1\frac{1}{2}}$
2798.910	10Z	35717.67	$a\ ^2F_{3\frac{1}{2}}$—$z\ ^4G^\circ_{4\frac{1}{2}}$
2798.070	20Z	35728.39	$b\ ^4P_{2\frac{1}{2}}$—$z\ ^4S^\circ_{1\frac{1}{2}}$
2796.93	5eZ		
2796.777	8Z	35744.91	$b\ ^4G_{2\frac{1}{2}}$—$y\ ^2D^\circ_{1\frac{1}{2}}$
2796.342	5Z	35750.46	$c\ ^2F_{2\frac{1}{2}}$—$w\ ^2D^\circ_{1\frac{1}{2}}$
2794.604	5Z	35772.70	$a\ ^2H_{4\frac{1}{2}}$—$y\ ^4H^\circ_{4\frac{1}{2}}$
2794.38	1	35775.57	
2792.387	5w	35801.10	
2791.553	50Z	35811.79	$b\ ^4G_{3\frac{1}{2}}$—$(3)^\circ_{3\frac{1}{2}}$
2790.427	30Z	35826.24	$a\ ^4F_{3\frac{1}{2}}$—$z\ ^4I^\circ_{4\frac{1}{2}}$
2789.485	2	35838.34	
2789.10	1	35843.29	
2788.86	5	35846.37	$a\ ^4F_{4\frac{1}{2}}$—$z\ ^4I^\circ_{4\frac{1}{2}}$
2788.660	8	35848.94	
2787.558	1	35863.12	$b\ ^4F_{3\frac{1}{2}}$—$y^2G^\circ_{3\frac{1}{2}}$

TABLE 1. *Wavelengths and term combinations of* Mo II—Continued

Wavelength λ_{air}	Intensity	Wave No.	Term combination
2787. 321	5*Z*	35866. 16	$\begin{cases} a\ {}^2F_{2\frac{1}{2}} - y\ {}^4D^\circ_{3\frac{1}{2}} \\ a\ {}^4H_{6\frac{1}{2}} - z\ {}^2I^\circ_{6\frac{1}{2}} \end{cases}$
2786. 99	1	35870. 42	$a\ {}^2H_{5\frac{1}{2}} - y\ {}^4H^\circ_{4\frac{1}{2}}$
2786. 73	1	35873. 77	$\begin{cases} b\ {}^4F_{2\frac{1}{2}} - z\ {}^4S^\circ_{1\frac{1}{2}} \\ b\ {}^4G_{4\frac{1}{2}} - x\ {}^4G^\circ_{3\frac{1}{2}} \end{cases}$
2786. 240	5*Z*	35880. 08	$b\ {}^4D_{2\frac{1}{2}} - z\ {}^2D^\circ_{2\frac{1}{2}}$
2785. 638	8*Z*	35887. 83	$b\ {}^2F_{3\frac{1}{2}} - y\ {}^4H^\circ_{3\frac{1}{2}}$
2784. 990	50*Z*	35896. 18	$a\ {}^4D_{3\frac{1}{2}} - z\ {}^4F^\circ_{4\frac{1}{2}}$
2784. 17	2	35906. 75	$\begin{cases} a\ {}^4F_{2\frac{1}{2}} - z\ {}^2D^\circ_{1\frac{1}{2}} \\ c\ {}^2D_{2\frac{1}{2}} - v\ {}^2D^\circ_{2\frac{1}{2}} \end{cases}$
2784. 13	10*Z*	35907. 27	
2781. 967	8*wZ*	35935. 19	
2781. 265	2	35944. 25	
2781. 07	2	35946. 77	$b\ {}^4P_{0\frac{1}{2}} - x\ {}^4D^\circ_{1\frac{1}{2}}$
2780. 022	50*Z*	35960. 33	$a\ {}^6D_{3\frac{1}{2}} - z\ {}^4P^\circ_{2\frac{1}{2}}$
2779. 244	15*Z*	35970. 39	
2778. 88	1	35975. 10	$b\ {}^4F_{2\frac{1}{2}} - y\ {}^2G^\circ_{3\frac{1}{2}}$
2778. 56	1	35979. 25	
2778. 37	1	35981. 71	
2777. 86	15*Z*	35988. 31	$a\ {}^6D_{1\frac{1}{2}} - z\ {}^4P^\circ_{1\frac{1}{2}}$
2776. 94	1	36000. 23	$b\ {}^4G_{5\frac{1}{2}} - x\ {}^4G^\circ_{5\frac{1}{2}}$
2776. 685	15*Z*	36003. 54	$a\ {}^4H_{4\frac{1}{2}} - x\ {}^4D^\circ_{3\frac{1}{2}}$
2776. 48	1	36006. 20	
2775. 386	50*Z*	36020. 39	$a\ {}^6D_{4\frac{1}{2}} - z\ {}^6P^\circ_{3\frac{1}{2}}$
2774. 401	20*Z*	36033. 18	$\begin{cases} a\ {}^4P_{1\frac{1}{2}} - z\ {}^4F^\circ_{2\frac{1}{2}} \\ b\ {}^4G_{2\frac{1}{2}} - x\ {}^4G^\circ_{2\frac{1}{2}} \end{cases}$
2773. 804	12*Z*	36040. 93	$\begin{cases} a\ {}^4P_{2\frac{1}{2}} - z\ {}^4F^\circ_{3\frac{1}{2}} \\ b\ {}^4F_{4\frac{1}{2}} - z\ {}^2H^\circ_{5\frac{1}{2}} \end{cases}$
2771. 97	1	36064. 78	
2771. 710	12*Z*	36068. 16	$b\ {}^4G_{3\frac{1}{2}} - x\ {}^4G^\circ_{3\frac{1}{2}}$
2770. 934	4	36078. 26	
2770. 597	12*Z*	36082. 65	
2770. 178	5*Z*	36088. 11	$c\ {}^2F_{3\frac{1}{2}} - w\ {}^2D^\circ_{2\frac{1}{2}}$
2769. 762	25*Z*	36093. 52	$a\ {}^4H_{6\frac{1}{2}} - y\ {}^4G^\circ_{5\frac{1}{2}}$
2766. 824	8	36131. 85	$b\ {}^4G_{2\frac{1}{2}} - (3)^\circ_{3\frac{1}{2}}$
2766. 198	15	36140. 03	$b\ {}^2I_{5\frac{1}{2}} - w\ {}^2H^\circ_{5\frac{1}{2}}$
2765. 28	2	36152. 02	$a\ {}^2H_{4\frac{1}{2}} - z\ {}^2F^\circ_{3\frac{1}{2}}$
2765. 09	3	36154. 51	
2764. 954	4	36156. 29	$\begin{cases} a\ {}^2F_{2\frac{1}{2}} - z\ {}^2D^\circ_{2\frac{1}{2}} \\ a\ {}^2H_{5\frac{1}{2}} - y\ {}^4F^\circ_{4\frac{1}{2}} \end{cases}$
2764. 66	1	36160. 13	
2764. 53	2	36161. 83	
2764. 38	1	36163. 79	
2763. 626	20*Z*	36173. 66	$a\ {}^4G_{2\frac{1}{2}} - z\ {}^4F^\circ_{1\frac{1}{2}}$
2763. 305	7*Z*	36177. 86	$b\ {}^4G_{4\frac{1}{2}} - x\ {}^4G^\circ_{4\frac{1}{2}}$
2763. 185	2	36179. 43	
2762. 455	7*Z*	36188. 99	$\begin{cases} a\ {}^2D_{1\frac{1}{2}} - z\ {}^4G^\circ_{2\frac{1}{2}} \\ a\ {}^2G_{3\frac{1}{2}} - (1)^\circ_{2\frac{1}{2}} \end{cases}$
2761. 803	5	36197. 54	
2761. 39	1	36202. 95	
2760. 537	18*Z*	36214. 14	$a\ {}^4H_{5\frac{1}{2}} - y\ {}^4G^\circ_{4\frac{1}{2}}$
2760. 103	2*Z*	36219. 83	
2759. 70	2	36225. 12	
2759. 204	4*Z*	36231. 63	$c\ {}^4D_{2\frac{1}{2}} - w\ {}^2F^\circ_{3\frac{1}{2}}$
2758. 633	7*Z*	36239. 13	$\begin{cases} b\ {}^4P_{2\frac{1}{2}} - y\ {}^2F^\circ_{3\frac{1}{2}} \\ a\ {}^6D_{0\frac{1}{2}} - z\ {}^4P^\circ_{1\frac{1}{2}} \end{cases}$
2758. 51	7*Z*	36240. 75	$a\ {}^4H_{5\frac{1}{2}} - z\ {}^2I^\circ_{6\frac{1}{2}}$
2757. 93	4	36248. 37	$b\ {}^4F_{4\frac{1}{2}} - y\ {}^2H^\circ_{4\frac{1}{2}}$
2757. 54	1	36253. 49	
2757. 20	1*w*	36257. 96	
2756. 065	50*Z*	36272. 90	
2755. 88	2	36275. 33	
2755. 15	1	36284. 94	
2754. 88	2	36288. 50	$b\ {}^2F_{2\frac{1}{2}} - x\ {}^4F^\circ_{2\frac{1}{2}}$
2754. 70	3	36290. 87	$c\ {}^2F_{3\frac{1}{2}} - v\ {}^3F^\circ_{3\frac{1}{2}}$
2754. 49	10*Z*	36293. 63	$\begin{cases} a\ {}^2P_{1\frac{1}{2}} - x\ {}^2D^\circ_{2\frac{1}{2}} \\ b\ {}^4F_{3\frac{1}{2}} - y\ {}^2H^\circ_{4\frac{1}{2}} \end{cases}$
2753. 95	2	36300. 75	$a\ {}^4H_{3\frac{1}{2}} - x\ {}^4D^\circ_{2\frac{1}{2}}$
2753. 82	10*Z*	36302. 46	$a\ {}^4F_{4\frac{1}{2}} - z\ {}^2G^\circ_{3\frac{1}{2}}$
2753. 34	2	36308. 79	
2753. 03	1	36312. 88	
2752. 63	3*w*	36318. 16	$a\ {}^2P_{0\frac{1}{2}} - x\ {}^4P^\circ_{1\frac{1}{2}}$
2752. 49	3*w*	36320. 00	
2752. 26	2*s*	36323. 04	
2750. 635	1	36344. 50	$b\ {}^4D_{2\frac{1}{2}} - y\ {}^4P^\circ_{1\frac{1}{2}}$
2750. 40	3	36347. 60	
2750. 027	40*Z*	36352. 53	$b\ {}^4G_{5\frac{1}{2}} - x\ {}^4G^\circ_{5\frac{1}{2}}$
2749. 83	3	36355. 14	
2749. 18	1	36363. 73	
2748. 74	1	36369. 55	
2748. 44	7*Z*	36373. 52	$a\ {}^4F_{3\frac{1}{2}} - z\ {}^4G^\circ_{4\frac{1}{2}}$
2747. 65	4	36383. 98	$\begin{cases} b\ {}^4F_{2\frac{1}{2}} - y\ {}^2F^\circ_{3\frac{1}{2}} \\ a\ {}^4H_{3\frac{1}{2}} - y\ {}^4P^\circ_{2\frac{1}{2}} \end{cases}$
2747. 155	6*Z*	36390. 53	$b\ {}^4F_{4\frac{1}{2}} - y\ {}^2H^\circ_{5\frac{1}{2}}$
2746. 305	35*Z*	36401. 80	$a\ {}^4G_{3\frac{1}{2}} - z\ {}^4F^\circ_{2\frac{1}{2}}$
2745. 60	2	36411. 14	
2745. 293	8*Z*	36415. 21	$a\ {}^2H_{4\frac{1}{2}} - y\ {}^4H^\circ_{3\frac{1}{2}}$
2744. 478	2	36426. 03	
2744. 193	25*Z*	36429. 81	$a\ {}^4H_{4\frac{1}{2}} - y\ {}^4G^\circ_{3\frac{1}{2}}$
2743. 587	2	36437. 86	$c\ {}^2G_{4\frac{1}{2}} - u\ {}^2F^\circ_{3\frac{1}{2}}$
2743. 185	25*Z*	36443. 20	$a\ {}^6D_{2\frac{1}{2}} - z\ {}^4P^\circ_{2\frac{1}{2}}$
2742. 888	20*Z*	36447. 14	$b\ {}^2I_{6\frac{1}{2}} - w\ {}^2H^\circ_{5\frac{1}{2}}$
2741. 627	15*Z*	36463. 90	$a\ {}^2F_{3\frac{1}{2}} - z\ {}^2G^\circ_{4\frac{1}{2}}$
2741. 489	2	36465. 74	$a\ {}^4H_{4\frac{1}{2}} - y\ {}^4G^\circ_{4\frac{1}{2}}$
2741. 432	1*Z*	36466. 50	$b\ {}^2F_{3\frac{1}{2}} - z\ {}^2F^\circ_{3\frac{1}{2}}$
2741. 314	15*Z*	36468. 07	$a\ {}^4H_{5\frac{1}{2}} - y\ {}^4G^\circ_{5\frac{1}{2}}$
2740. 367	2	36480. 67	
2740. 06	3*Z*	36484. 78	
2739. 360	3	36494. 08	$a\ {}^2S_{0\frac{1}{2}} - y\ {}^2D^\circ_{1\frac{1}{2}}$
2738. 913	3	36500. 03	
2738. 637	30*Z*	36503. 71	$a\ {}^2H_{5\frac{1}{2}} - z\ {}^2H^\circ_{4\frac{1}{2}}$
2737. 99	3	36512. 34	$a\ {}^2G_{3\frac{1}{2}} - y\ {}^4G^\circ_{3\frac{1}{2}}$
2737. 868	15*Z*	36513. 97	$b\ {}^2I_{5\frac{1}{2}} - w\ {}^2H^\circ_{4\frac{1}{2}}$
2737. 727	5	36515. 85	$b\ {}^2F_{2\frac{1}{2}} - z\ {}^2F^\circ_{2\frac{1}{2}}$
2737. 107	10*Z*	36525. 45	
2736. 95	5*Z*	36526. 21	$a\ {}^4P_{2\frac{1}{2}} - z\ {}^4F^\circ_{3\frac{1}{2}}$
2736. 657	3	36530. 12	$b\ {}^4G_{4\frac{1}{2}} - x\ {}^4G^\circ_{3\frac{1}{2}}$
2736. 420	8	36533. 29	$a\ {}^4G_{2\frac{1}{2}} - z\ {}^4F^\circ_{2\frac{1}{2}}$
2735. 708	8	36542. 79	
2735. 318	10*Z*	36548. 00	$a\ {}^2G_{3\frac{1}{2}} - y\ {}^4G^\circ_{3\frac{1}{2}}$
2734. 997	5	36552. 29	$c\ {}^4D_{3\frac{1}{2}} - w\ {}^2F^\circ_{3\frac{1}{2}}$
2734. 90	1	36553. 59	
2734. 382	8	36560. 51	$b\ {}^4F_{1\frac{1}{2}} - y\ {}^2D^\circ_{1\frac{1}{2}}$
2733. 37	5	36574. 05	
2733. 126	3	36577. 31	
2732. 889	15*Z*	36580. 48	$a\ {}^6D_{3\frac{1}{2}} - z\ {}^6P^\circ_{3\frac{1}{2}}$
2732. 648	5*Z*	36583. 71	$b\ {}^2G_{3\frac{1}{2}} - w\ {}^2F^\circ_{2\frac{1}{2}}$
2730. 943	8	36606. 55	$a\ {}^2G_{3\frac{1}{2}} - (2)^\circ_{3\frac{1}{2}}$
2730. 212	25*Z*	36616. 35	$a\ {}^4H_{4\frac{1}{2}} - y\ {}^4F^\circ_{3\frac{1}{2}}$
2729. 680	20*Z*	36623. 49	$a\ {}^6D_{2\frac{1}{2}} - z\ {}^6P^\circ_{1\frac{1}{2}}$
2728. 903	3	36633. 91	$b\ {}^4D_{2\frac{1}{2}} - z\ {}^2P^\circ_{1\frac{1}{2}}$
2728. 718	10	36636. 40	

TABLE 1. *Wavelengths and term combinations of* Mo II—Continued

Wavelength λ_{air}	Intensity	Wave No.	Term combination	Wavelength λ_{air}	Intensity	Wave No.	Term combination
2728. 191	8Z	36643. 47	$b\ ^2D_{1\frac{1}{2}}$—$w\ ^2F^o_{2\frac{1}{2}}$	2700. 580	2w	37018. 10	$a\ ^4G_{2\frac{1}{2}}$—$z\ ^4F^o_{3\frac{1}{2}}$
2727. 804	8Z	36648. 67	$b\ ^4G_{3\frac{1}{2}}$—$w\ ^4D^o_{2\frac{1}{2}}$	2700. 430	1	37020. 16	
2727. 53	1	36652. 35		2699. 990	10Z	37026. 19	$a\ ^4H_{6\frac{1}{2}}$—$y\ ^4H^o_{5\frac{1}{2}}$
2726. 983	100Z	36659. 71	$a\ ^2G_{4\frac{1}{2}}$—$z\ ^2I^o_{5\frac{1}{2}}$	2699. 404	30Z	37034. 23	$a\ ^2D_{2\frac{1}{2}}$—$z\ ^4G^o_{3\frac{1}{2}}$
2724. 897	1	36687. 77		2699. 26	2	37036. 20	$a\ ^2G_{4\frac{1}{2}}$—$y\ ^4F^o_{3\frac{1}{2}}$
2724. 022	20Z	36699. 55	$a\ ^2H_{5\frac{1}{2}}$—$x\ ^4F^o_{4\frac{1}{2}}$; $a\ ^2I_{5\frac{1}{2}}$—$z\ ^4I^o_{4\frac{1}{2}}$	2698. 17	1	37051. 16	
2723. 56	2Z	36705. 78	$b\ ^4F_{3\frac{1}{2}}$—$y\ ^2G^o_{4\frac{1}{2}}$	2698. 049	2	37052. 83	$b\ ^4F_{4\frac{1}{2}}$—$x\ ^4G^o_{3\frac{1}{2}}$
2723. 366	8Z	36708. 39	$a\ ^6D_{3\frac{1}{2}}$—$z\ ^6P^o_{2\frac{1}{2}}$	2697. 68	1	37057. 89	$a\ ^4F_{2\frac{1}{2}}$—$z\ ^2D^o_{2\frac{1}{2}}$
2722. 880	3	36714. 95	$c\ ^2G_{3\frac{1}{2}}$—$u\ ^2F^o_{2\frac{1}{2}}$	2697. 51	5	37060. 23	$c\ ^2G_{3\frac{1}{2}}$—$u\ ^2F^o_{3\frac{1}{2}}$; $b\ ^4P_{2\frac{1}{2}}$—$y\ ^2D^o_{2\frac{1}{2}}$
2722. 570	10Z	36719. 12	$a\ ^4H_{4\frac{1}{2}}$—$y\ ^4G^o_{5\frac{1}{2}}$	2697. 249	8Z	37063. 81	$a\ ^4H_{3\frac{1}{2}}$—$y\ ^4F^o_{3\frac{1}{2}}$; $a\ ^6D_{2\frac{1}{2}}$—$z\ ^6P^o_{3\frac{1}{2}}$
2721. 741	10Z	36730. 31					
2721. 28	1	36736. 53		2696. 839	30Z	37069. 45	$b\ ^2H_{5\frac{1}{2}}$—$x\ ^2H^o_{5\frac{1}{2}}$
2720. 337	5	36749. 27	$b\ ^2G_{4\frac{1}{2}}$—$x\ ^2H^o_{4\frac{1}{2}}$	2695. 80	4	37083. 73	$b\ ^4D_{3\frac{1}{2}}$—$y\ ^4P^o_{2\frac{1}{2}}$
2719. 951	1	36754. 48		2695. 72	4	37084. 83	$b\ ^4D_{0\frac{1}{2}}$—$y\ ^4P^o_{1\frac{1}{2}}$
2719. 80	1	36756. 52		2695. 217	35Z	37091. 75	$a\ ^2G_{3\frac{1}{2}}$—$y\ ^4H^o_{4\frac{1}{2}}$; $a\ ^4F_{4\frac{1}{2}}$—$z\ ^4I^o_{5\frac{1}{2}}$
2719. 693	5Z	36757. 97	$b\ ^2F_{3\frac{1}{2}}$—$x\ ^4F^o_{2\frac{1}{2}}$; $a\ ^4H_{5\frac{1}{2}}$—$y\ ^4H^o_{4\frac{1}{2}}$	2694. 72	8Z	37098. 60	$b\ ^4F_{3\frac{1}{2}}$—$x\ ^4G^o_{3\frac{1}{2}}$
2719. 460	3	36761. 12		2693. 84	1w	37110. 71	
2719. 196	8	36764. 69		2693. 19	15Z	37119. 67	$a\ ^4F_{3\frac{1}{2}}$—$z\ ^2G^o_{4\frac{1}{2}}$
2718. 967	8Z	36767. 78	$a\ ^4F_{2\frac{1}{2}}$—$y\ ^4D^o_{3\frac{1}{2}}$	2692. 945	10Z	37123. 05	$b\ ^4P_{1\frac{1}{2}}$—$z\ ^4S^o_{1\frac{1}{2}}$
2718. 147	5	36778. 87	$a\ ^2P_{0\frac{1}{2}}$—$y\ ^2P^o_{1\frac{1}{2}}$	2692. 63	20Z	37127. 39	$a\ ^2H_{4\frac{1}{2}}$—$y\ ^2G^o_{3\frac{1}{2}}$
2717. 357	100Z	36789. 56	$a\ ^4G_{4\frac{1}{2}}$—$z\ ^4F^o_{3\frac{1}{2}}$	2692. 436	3	37130. 06	
2716. 766	2	36797. 56	$b\ ^4D_{1\frac{1}{2}}$—$y\ ^4P^o_{1\frac{1}{2}}$; $b\ ^4F_{4\frac{1}{2}}$—(3)$^o_{3\frac{1}{2}}$	2691. 82	1	37138. 56	$a\ ^2G_{4\frac{1}{2}}$—$y\ ^4G^o_{5\frac{1}{2}}$
2716. 43	1	36802. 12		2691. 698	10Z	37140. 24	$a\ ^4F_{4\frac{1}{2}}$—$z\ ^2G^o_{4\frac{1}{2}}$
2716. 148	3w	36805. 94		2690. 980	10Z	37150. 16	$b\ ^4D_{3\frac{1}{2}}$—$x\ ^4D^o_{3\frac{1}{2}}$
2715. 850	2	36809. 98	$a\ ^4H_{4\frac{1}{2}}$—$y\ ^4H^o_{3\frac{1}{2}}$	2690. 26	1	37160. 10	
2715. 593	2h	36813. 46		2690. 01	1	37163. 55	$c\ ^4D_{3\frac{1}{2}}$—$x\ ^2D^o_{2\frac{1}{2}}$
2713. 501	30Z	36841. 84	$b\ ^4F_{3\frac{1}{2}}$—(3)$^o_{3\frac{1}{2}}$; $a\ ^6D_{4\frac{1}{2}}$—$z\ ^6D^o_{3\frac{1}{2}}$	2689. 69	1	37167. 97	
2713. 38	1	36843. 48	$c\ ^4D_{2\frac{1}{2}}$—$x\ ^2D^o_{2\frac{1}{2}}$	2688. 24	1	37188. 02	$c\ ^4D_{1\frac{1}{2}}$—$x\ ^2D^o_{2\frac{1}{2}}$
2712. 955	3	36849. 25	$b\ ^4F_{1\frac{1}{2}}$—$x\ ^4G^o_{2\frac{1}{2}}$; $a\ ^2G_{4\frac{1}{2}}$—$y\ ^4G^o_{5\frac{1}{2}}$; $a\ ^4F_{3\frac{1}{2}}$—$y\ ^4D^o_{3\frac{1}{2}}$	2687. 994	60Z	37191. 42	$a\ ^6D_{2\frac{1}{2}}$—$z\ ^6P^o_{2\frac{1}{2}}$
2712. 53	2	36855. 03	$a\ ^4F_{1\frac{1}{2}}$—$z\ ^2D^o_{2\frac{1}{2}}$; $b\ ^4F_{2\frac{1}{2}}$—$x\ ^4G^o_{2\frac{1}{2}}$	2687. 597	5	37196. 92	
2712. 346	20Z	36857. 53	$b\ ^2G_{3\frac{1}{2}}$—$x\ ^2H^o_{4\frac{1}{2}}$	2686. 987	1	37205. 37	$b\ ^4F_{2\frac{1}{2}}$—$y\ ^2D^o_{2\frac{1}{2}}$
2711. 879	1	36863. 87		2686. 608	2	37210. 61	$b\ ^4F_{2\frac{1}{2}}$—$x\ ^4G^o_{3\frac{1}{2}}$
2711. 485	10Z	36869. 23	$a\ ^4F_{4\frac{1}{2}}$—$y\ ^4D^o_{3\frac{1}{2}}$	2685. 785	20Z	37222. 01	$b\ ^2D_{2\frac{1}{2}}$—$w\ ^2F^o_{3\frac{1}{2}}$
2710. 928	15Z	36876. 80	$a\ ^4H_{3\frac{1}{2}}$—$y\ ^4G^o_{3\frac{1}{2}}$	2685. 16	3	37230. 67	$b\ ^4D_{2\frac{1}{2}}$—$x\ ^4D^o_{2\frac{1}{2}}$
2710. 500	1	36882. 63		2684. 148	60Z	37244. 71	$a\ ^6D_{4\frac{1}{2}}$—$z\ ^6D^o_{4\frac{1}{2}}$
2710. 207	15Z	36886. 62	$a\ ^4G_{3\frac{1}{2}}$—$z\ ^4F^o_{3\frac{1}{2}}$	2683. 234	50Z	37257. 39	$a\ ^4H_{3\frac{1}{2}}$—$y\ ^4H^o_{3\frac{1}{2}}$; $a\ ^6D_{0\frac{1}{2}}$—$z\ ^6P^o_{1\frac{1}{2}}$
2709. 765	10	36892. 63	$a\ ^2G_{3\frac{1}{2}}$—$y\ ^4H^o_{3\frac{1}{2}}$				
2708. 957	3	36903. 63	$a\ ^2D_{2\frac{1}{2}}$—$y\ ^4D^o_{2\frac{1}{2}}$	2682. 430	8Z	37268. 56	
2708. 499	2	36909. 88		2681. 373	40Z	37283. 25	$a\ ^4F_{4\frac{1}{2}}$—$z\ ^4G^o_{5\frac{1}{2}}$
2708. 300	2	36912. 59	$a\ ^4H_{3\frac{1}{2}}$—$y\ ^4G^o_{4\frac{1}{2}}$	2680. 516	2	37295. 17	$a\ ^4H_{4\frac{1}{2}}$—$y\ ^4F^o_{4\frac{1}{2}}$
				2680. 134	1	37300. 49	$b\ ^4P_{0\frac{1}{2}}$—$x\ ^4F^o_{1\frac{1}{2}}$
2708. 064	2	36915. 80	$b\ ^2F_{3\frac{1}{2}}$—$x\ ^4F^o_{4\frac{1}{2}}$	2679. 86	4	37304. 30	
2707. 68	1	36921. 04					
2707. 33	1	36925. 81	$a\ ^2P_{0\frac{1}{2}}$—$x\ ^4P^o_{0\frac{1}{2}}$	2678. 811	1	37318. 91	$a\ ^4F_{1\frac{1}{2}}$—$y\ ^4P^o_{1\frac{1}{2}}$
2707. 014	8Z	36930. 12	$c\ ^2F_{2\frac{1}{2}}$—$x\ ^2P^o_{1\frac{1}{2}}$	2678. 470	5Z	37323. 66	$c\ ^4D_{2\frac{1}{2}}$—$w\ ^2G^o_{3\frac{1}{2}}$
2705. 956	3lZ	36944. 56		2677. 860	2	37332. 16	
				2677. 00	1hZ	37344. 15	$a\ ^4D_{2\frac{1}{2}}$—$z\ ^4D^o_{1\frac{1}{2}}$
2704. 928	10Z	36958. 60	$b\ ^2H_{4\frac{1}{2}}$—$x\ ^2H^o_{4\frac{1}{2}}$	2676. 90	1h	37345. 55	
2704. 274	5	36967. 54					
2703. 857	5Z	36973. 24	$b\ ^2F_{2\frac{1}{2}}$—$y\ ^2G^o_{3\frac{1}{2}}$	2676. 489	20Z	37351. 28	$a\ ^4H_{3\frac{1}{2}}$—$y\ ^4F^o_{2\frac{1}{2}}$
2703. 618	8	36976. 51	$a\ ^2D_{1\frac{1}{2}}$—$z\ ^2D^o_{1\frac{1}{2}}$	2676. 24	3	37354. 75	
2703. 08	3Z	36983. 87	$b\ ^2F_{3\frac{1}{2}}$—$z\ ^2F^o_{2\frac{1}{2}}$	2676. 06	1	37357. 27	$b\ ^4F_{4\frac{1}{2}}$—$x\ ^4G^o_{4\frac{1}{2}}$
				2674. 753	2h	37375. 52	
2702. 870	5Z	36986. 74	$a\ ^2G_{3\frac{1}{2}}$—$y\ ^4F^o_{2\frac{1}{2}}$	2674. 468	1	37379. 50	$b\ ^4D_{2\frac{1}{2}}$—$x\ ^4D^o_{3\frac{1}{2}}$
2702. 502	8	36991. 78					
2701. 875	20Z	37000. 36	$b\ ^4D_{3\frac{1}{2}}$—$x\ ^4D^o_{2\frac{1}{2}}$; $a\ ^4H_{3\frac{1}{2}}$—$y\ ^4G^o_{3\frac{1}{2}}$	2674. 30	1	37381. 85	$b\ ^2F_{2\frac{1}{2}}$—$y\ ^2F^o_{3\frac{1}{2}}$
2701. 409	50Z	37006. 74	$a\ ^6D_{1\frac{1}{2}}$—$z\ ^6P^o_{1\frac{1}{2}}$	2673. 27	40Z	37396. 25	$a\ ^2D_{2\frac{1}{2}}$—$z\ ^2D^o_{1\frac{1}{2}}$; $a\ ^4G_{3\frac{1}{2}}$—$z\ ^4F^o_{3\frac{1}{2}}$
2701. 22	2	37009. 33	$a\ ^4H_{4\frac{1}{2}}$—$y\ ^4H^o_{4\frac{1}{2}}$	2672. 84	60Z	37402. 27	$b\ ^4F_{3\frac{1}{2}}$—$x\ ^4G^o_{4\frac{1}{2}}$; $a\ ^6D_{3\frac{1}{2}}$—$z\ ^6D^o_{3\frac{1}{2}}$
				2672. 29	1	37409. 97	$b\ ^2H_{5\frac{1}{2}}$—$w\ ^2G^o_{4\frac{1}{2}}$
				2671. 86	40Z	37415. 99	$a\ ^4G_{4\frac{1}{2}}$—$z\ ^4F^o_{4\frac{1}{2}}$; $b\ ^2G_{4\frac{1}{2}}$—$x\ ^2H^o_{5\frac{1}{2}}$

TABLE 1. *Wavelengths and term combinations of* Mo II—Continued

Wavelength λ_{air}	Intensity	Wave No.	Term combination
2671.34	1	37423.27	$a\ ^2S_{0\frac{1}{2}}$—$w\ ^4D^o_{0\frac{1}{2}}$
2670.955	10Z	37428.66	$a\ ^2G_{4\frac{1}{2}}$—$y\ ^4H^o_{4\frac{1}{2}}$
2670.019	10Z	37441.78	$b\ ^2F_{3\frac{1}{2}}$—$y\ ^2G^o_{3\frac{1}{2}}$
2669.584	3Z	37447.89	$a\ ^2H_{5\frac{1}{2}}$—$z\ ^2H^o_{5\frac{1}{2}}$
2668.982	2	37456.33	$a\ ^4H_{3\frac{1}{2}}$—$y\ ^4H^o_{3\frac{1}{2}}$
2668.577	2	37462.02	$c\ ^4D_{3\frac{1}{2}}$—$w\ ^2G^o_{4\frac{1}{2}}$
2667.944	10Z	37470.90	$a\ ^2G_{3\frac{1}{2}}$—$z\ ^2F^o_{3\frac{1}{2}}$
2667.38	10	37478.83	
2667.16	1	37481.92	$b\ ^4D_{2\frac{1}{2}}$— (1)$^o_{3\frac{1}{2}}$
2666.75	3	37487.68	$a\ ^2H_{5\frac{1}{2}}$—$y\ ^4H^o_{4\frac{1}{2}}$
2666.60	1	37489.79	$b\ ^4F_{1\frac{1}{2}}$—$w\ ^4D^o_{0\frac{1}{2}}$
2666.237	8	37494.89	$c\ ^2G_{3\frac{1}{2}}$—$t\ ^2F^o_{2\frac{1}{2}}$
2665.355	3	37507.30	
2665.05	2	37511.59	
2664.914	5Z	37513.51	$a\ ^4D_{1\frac{1}{2}}$—$z\ ^4D^o_{1\frac{1}{2}}$ $a\ ^4G_{3\frac{1}{2}}$—$z\ ^4F^o_{4\frac{1}{2}}$
2664.290	5Z	37522.29	$a\ ^4F_{2\frac{1}{2}}$—$y\ ^4P^o_{1\frac{1}{2}}$ $b\ ^4F_{2\frac{1}{2}}$—$w\ ^4D^o_{1\frac{1}{2}}$
2663.780	15Z	37529.47	
2663.541	2	37532.84	
2662.53	2	37547.09	$a\ ^2P_{1\frac{1}{2}}$—$x\ ^2P^o_{0\frac{1}{2}}$ $b\ ^4G_{4\frac{1}{2}}$—$x\ ^2G^o_{3\frac{1}{2}}$
2662.27	1	37550.76	
2661.97	1	37554.99	
2661.785	2	37557.60	$a\ ^2H_{4\frac{1}{2}}$—$y\ ^2H^o_{4\frac{1}{2}}$
2661.22	2	37565.57	$b\ ^2F_{2\frac{1}{2}}$—$y\ ^2D^o_{1\frac{1}{2}}$
2661.09	2	37567.41	
2660.581	100Z	37574.60	$a\ ^6D_{1\frac{1}{2}}$—$z\ ^6P^o_{2\frac{1}{2}}$
2659.720	5Z	37586.76	$a\ ^4H_{5\frac{1}{2}}$—$x\ ^4F^o_{4\frac{1}{2}}$
2659.540	1	37589.30	$a\ ^2F_{2\frac{1}{2}}$—$y\ ^4P^o_{2\frac{1}{2}}$
2659.195	1w	37594.18	
2657.930	8	37612.07	$b\ ^4D_{3\frac{1}{2}}$—$y\ ^4G^o_{4\frac{1}{2}}$
2657.387	8Z	37620.80	
2657.005	20Z	37625.17	$b\ ^2H_{4\frac{1}{2}}$—$x\ ^2H^o_{5\frac{1}{2}}$
2656.891	1	37626.78	$b\ ^2D_{1\frac{1}{2}}$—$x\ ^2D^o_{2\frac{1}{2}}$
2656.54	1	37631.75	$c\ ^2G_{4\frac{1}{2}}$—$v\ ^2G^o_{4\frac{1}{2}}$
2656.025	2	37639.05	$b\ ^4G_{3\frac{1}{2}}$—$x\ ^2F^o_{2\frac{1}{2}}$
2655.821	10Z	37641.94	$a\ ^4H_{4\frac{1}{2}}$—$z\ ^2H^o_{4\frac{1}{2}}$
2655.547	5	37645.82	$b\ ^4P_{2\frac{1}{2}}$—$w\ ^4D^o_{2\frac{1}{2}}$
2655.138	10Z	37651.62	$b\ ^2D_{1\frac{1}{2}}$—$x\ ^2D^o_{1\frac{1}{2}}$ $a\ ^4H_{4\frac{1}{2}}$—$y\ ^4H^o_{5\frac{1}{2}}$
2654.848	5Z	37655.73	$a\ ^2F_{2\frac{1}{2}}$—$x\ ^4D^o_{3\frac{1}{2}}$ $a\ ^2H_{5\frac{1}{2}}$—$y\ ^2H^o_{4\frac{1}{2}}$
2653.799	10Z	37670.62	$b\ ^4D_{3\frac{1}{2}}$— (2)$^o_{3\frac{1}{2}}$
2653.348	60Z	37677.02	$a\ ^6D_{3\frac{1}{2}}$—$z\ ^6D^o_{2\frac{1}{2}}$
2652.998	5	37681.99	$b\ ^4F_{4\frac{1}{2}}$—$w\ ^4D^o_{3\frac{1}{2}}$
2652.51	2	37688.92	
2652.368	8Z	37690.94	$a\ ^2D_{2\frac{1}{2}}$—$z\ ^2G^o_{3\frac{1}{2}}$
2652.165	8	37693.82	$b\ ^4P_{2\frac{1}{2}}$—$w\ ^4D^o_{3\frac{1}{2}}$ $b\ ^4G_{3\frac{1}{2}}$—$x\ ^4P^o_{2\frac{1}{2}}$
2651.733	30Z	37699.96	$a\ ^2H_{4\frac{1}{2}}$—$y\ ^2H^o_{5\frac{1}{2}}$ $b\ ^4D_{3\frac{1}{2}}$—$y\ ^4G^o_{2\frac{1}{2}}$
2651.06	8	37709.53	$b\ ^4F_{4\frac{1}{2}}$—$x\ ^4G^o_{5\frac{1}{2}}$
2650.327	3	37719.96	
2650.012	20Z	37724.45	$a\ ^2G_{3\frac{1}{2}}$—$z\ ^2H^o_{4\frac{1}{2}}$
2649.811	5	37727.31	$b\ ^4F_{3\frac{1}{2}}$—$w\ ^4D^o_{3\frac{1}{2}}$
2649.330	5	37734.16	
2648.225	20Z	37749.90	$c\ ^2F_{3\frac{1}{2}}$—$u\ ^2F^o_{3\frac{1}{2}}$
2648.08	1	37752.00	
2647.751	8	37756.66	$b\ ^2G_{4\frac{1}{2}}$—$w\ ^2G^o_{4\frac{1}{2}}$
2647.62	1	37758.53	$a\ ^2F_{2\frac{1}{2}}$— (1)$^o_{2\frac{1}{2}}$
2647.080	8Z	37766.23	$b\ ^4D_{1\frac{1}{2}}$—$y\ ^4P^o_{2\frac{1}{2}}$
2646.487	60Z	37774.69	$a\ ^6D_{2\frac{1}{2}}$—$z\ ^6D^o_{1\frac{1}{2}}$
2646.20	1	37778.79	
2645.63	3	37786.93	
2645.34	3	37791.07	$b\ ^4F_{2\frac{1}{2}}$—$w\ ^4D^o_{2\frac{1}{2}}$
2644.877	3Z	37797.68	$a\ ^2G_{3\frac{1}{2}}$—$x\ ^4F^o_{3\frac{1}{2}}$ $a\ ^2H_{5\frac{1}{2}}$—$y\ ^2H^o_{5\frac{1}{2}}$
2644.343	50Z	37805.32	$b\ ^4D_{2\frac{1}{2}}$—$y\ ^4G^o_{3\frac{1}{2}}$ $a\ ^6D_{3\frac{1}{2}}$—$z\ ^6D^o_{4\frac{1}{2}}$
2644.141	5Z	37808.20	$a\ ^2G_{4\frac{1}{2}}$—$z\ ^2F^o_{3\frac{1}{2}}$
2643.858	5	37812.25	$a\ ^4F_{2\frac{1}{2}}$—$z\ ^2P^o_{1\frac{1}{2}}$
2643.538	2	37816.83	$b\ ^4P_{1\frac{1}{2}}$—$y\ ^2D^o_{1\frac{1}{2}}$
2642.86	2	37826.53	
2642.40	15Z	37833.11	$b\ ^2D_{2\frac{1}{2}}$—$x\ ^2D^o_{2\frac{1}{2}}$ $a\ ^2F_{3\frac{1}{2}}$—$x\ ^4D^o_{3\frac{1}{2}}$
2641.189	5Z	37850.46	$b\ ^2F_{3\frac{1}{2}}$—$y\ ^2F^o_{3\frac{1}{2}}$
2640.88	12Z	37854.89	
2640.678	2	37857.78	$c\ ^2F_{2\frac{1}{2}}$—$u\ ^2F^o_{2\frac{1}{2}}$
2639.96	1	37868.08	$a\ ^2I_{6\frac{1}{2}}$—$z\ ^4G^o_{5\frac{1}{2}}$
2639.685	5Z	37872.02	$b\ ^2F_{3\frac{1}{2}}$—$y\ ^2H^o_{4\frac{1}{2}}$ $a\ ^4D_{2\frac{1}{2}}$—$z\ ^4D^o_{2\frac{1}{2}}$
2639.40	4	37876.11	
2638.768	100Z	37885.18	$a\ ^6D_{2\frac{1}{2}}$—$z\ ^6D^o_{3\frac{1}{2}}$
2638.412	5	37890.29	$b\ ^4D_{2\frac{1}{2}}$—$y\ ^4F^o_{1\frac{1}{2}}$
2638.31	5	37891.76	$a\ ^4D_{0\frac{1}{2}}$—$z\ ^4D^o_{1\frac{1}{2}}$ $b\ ^4D_{1\frac{1}{2}}$—$x\ ^4D^o_{1\frac{1}{2}}$
2637.08	1	37909.43	
2636.672	50Z	37915.30	$a\ ^6D_{1\frac{1}{2}}$—$z\ ^6D^o_{0\frac{1}{2}}$
2636.30	1	37920.65	$a\ ^2G_{3\frac{1}{2}}$—$x\ ^4F^o_{4\frac{1}{2}}$
2635.512	20Z	37931.98	$b\ ^4G_{5\frac{1}{2}}$—$w\ ^4F^o_{4\frac{1}{2}}$
2635.275	10Z	37935.40	$b\ ^4D_{1\frac{1}{2}}$— (1)$^o_{2\frac{1}{2}}$
2634.91	3	37940.65	
2634.623	3	37944.78	$b\ ^2H_{5\frac{1}{2}}$—$w\ ^2H^o_{5\frac{1}{2}}$
2634.104	10Z	37952.26	$b\ ^2F_{2\frac{1}{2}}$— (3)$^o_{3\frac{1}{2}}$
2633.816	1	37956.41	$b\ ^4D_{3\frac{1}{2}}$—$y\ ^4H^o_{3\frac{1}{2}}$
2633.67	1Z	37958.51	$a\ ^4F_{1\frac{1}{2}}$—$z\ ^2P^o_{0\frac{1}{2}}$ $b\ ^4G_{2\frac{1}{2}}$—$x\ ^2F^o_{2\frac{1}{2}}$
2633.52	100Z	37960.67	$a\ ^4H_{6\frac{1}{2}}$—$z\ ^2H^o_{5\frac{1}{2}}$
2633.136	10Z	37966.21	$b\ ^2H_{4\frac{1}{2}}$—$w\ ^2G^o_{4\frac{1}{2}}$ $b\ ^4G_{4\frac{1}{2}}$—$w\ ^4F^o_{3\frac{1}{2}}$
2632.855	10Z	37970.26	$a\ ^2H_{4\frac{1}{2}}$—$y\ ^2G^o_{4\frac{1}{2}}$
2631.564	20Z	37988.89	$a\ ^2G_{3\frac{1}{2}}$—$z\ ^2F^o_{2\frac{1}{2}}$
2631.05	10	37996.32	$b\ ^4G_{3\frac{1}{2}}$—$w\ ^4F^o_{2\frac{1}{2}}$
2630.741	80Z	38000.78	$a\ ^4H_{6\frac{1}{2}}$—$y\ ^4H^o_{5\frac{1}{2}}$
2630.227	20Z	38008.20	$c\ ^2F_{3\frac{1}{2}}$—$t\ ^2F^o_{3\frac{1}{2}}$
2629.854	10	38013.59	$b\ ^4G_{2\frac{1}{2}}$—$z\ ^4P^o_{2\frac{1}{2}}$
2629.652	20	38016.51	
2629.144	20	38023.86	
2628.74	5	38029.70	
2627.915	15Z	38041.64	$a\ ^4D_{1\frac{1}{2}}$—$z\ ^4D^o_{2\frac{1}{2}}$
2627.538	30	38047.09	$b\ ^2G_{3\frac{1}{2}}$—$w\ ^2G^o_{3\frac{1}{2}}$
2627.282	3	38050.80	$b\ ^4D_{3\frac{1}{2}}$—$y\ ^4F^o_{2\frac{1}{2}}$
2626.99	1h	38055.03	
2626.548	3	38061.43	$a\ ^2G_{4\frac{1}{2}}$—$z\ ^2H^o_{4\frac{1}{2}}$ $b\ ^4G_{2\frac{1}{2}}$—$x\ ^2G^o_{3\frac{1}{2}}$
2626.099	40Z	38067.94	$a\ ^2H_{5\frac{1}{2}}$—$y\ ^2G^o_{4\frac{1}{2}}$
2625.869	10Z	38071.27	$a\ ^2G_{4\frac{1}{2}}$—$y\ ^4H^o_{5\frac{1}{2}}$ $c\ ^4D_{0\frac{1}{2}}$—$x\ ^2P^o_{0\frac{1}{2}}$
2625.151	15Z	38081.69	$a\ ^2F_{2\frac{1}{2}}$—$y\ ^4G^o_{3\frac{1}{2}}$ $b\ ^4G_{5\frac{1}{2}}$—$y\ ^2I^o_{5\frac{1}{2}}$
2624.643	30Z	38089.06	$a\ ^4H_{3\frac{1}{2}}$—$z\ ^2H^o_{4\frac{1}{2}}$
2623.408	45Z	38106.99	$a\ ^2H_{4\frac{1}{2}}$— (3)$^o_{5\frac{1}{2}}$
2623.201	5	38109.99	$b\ ^4G_{4\frac{1}{2}}$—$w\ ^4F^o_{4\frac{1}{2}}$

TABLE 1. *Wavelengths and term combinations of* Mo II—Continued

Wavelength λ_{air}	Intensity	Wave No.	Term combination
2622.305	5	38123.02	
2621.945	5	38128.25	$a\ ^2D_{1\frac{1}{2}}$—$z\ ^2D^o_{2\frac{1}{2}}$
2621.524	15	38134.37	$a\ ^2G_{4\frac{1}{2}}$—$x\ ^4F^o_{3\frac{1}{2}}$
2621.43	1	38135.74*	$a\ ^2I_{5\frac{1}{2}}$—$z\ ^4G^o_{5\frac{1}{2}}$
2621.28	1	38137.92	
2621.08	2	38140.83	
2620.656	20	38147.00	$b\ ^4P_{0\frac{1}{2}}$—$z\ ^4S^o_{1\frac{1}{2}}$
2620.053	30Z	38155.78	$b\ ^4D_{3\frac{1}{2}}$—$y\ ^4H^o_{4\frac{1}{2}}$
2619.759	15	38160.06	$d\ ^2F_{2\frac{1}{2}}$—$u\ ^2G^o_{3\frac{1}{2}}$ $b\ ^4G_{3\frac{1}{2}}$—$w\ ^4F^o_{3\frac{1}{2}}$ $a\ ^6D_{2\frac{1}{2}}$—$z\ ^6D^o_{2\frac{1}{2}}$
2619.636	10	38161.85	$a\ ^4H_{3\frac{1}{2}}$—$x\ ^4F^o_{3\frac{1}{2}}$
2619.340	30Z	38166.17	$a\ ^2F_{2\frac{1}{2}}$—$y\ ^4F^o_{1\frac{1}{2}}$ $a\ ^6D_{0\frac{1}{2}}$—$z\ ^6D^o_{0\frac{1}{2}}$
2619.13	1	38169.23	$c\ ^4D_{2\frac{1}{2}}$—$w\ ^2D^o_{1\frac{1}{2}}$
2618.97	2	38171.56	
2618.85	2	38173.31	
2617.993	10	38185.80	$b\ ^4D_{2\frac{1}{2}}$—$y\ ^4H^o_{3\frac{1}{2}}$
2616.646	3	38205.46	$a\ ^2F_{2\frac{1}{2}}$—$y\ ^4G^o_{3\frac{1}{2}}$
2616.430	2	38208.61	$b\ ^2F_{2\frac{1}{2}}$—$x\ ^4G^o_{3\frac{1}{2}}$
2615.63	1	38220.30	
2614.508	5	38236.70	
2612.28	10Z	38269.32	$a\ ^4D_{3\frac{1}{2}}$—$z\ ^4D^o_{2\frac{1}{2}}$
2611.53	1	38280.30	$b\ ^4D_{2\frac{1}{2}}$—$y\ ^4F^o_{2\frac{1}{2}}$
2611.03	1	38287.63	$a\ ^4F_{1\frac{1}{2}}$—$y\ ^4P^o_{2\frac{1}{2}}$
2609.215	50Z	38314.26	$b\ ^2D_{2\frac{1}{2}}$—$w\ ^2G^o_{3\frac{1}{2}}$
2608.88	10Z	38319.19	$b\ ^2H_{5\frac{1}{2}}$—$w\ ^2H^o_{4\frac{1}{2}}$
2607.781	10Z	38335.33	$a\ ^4H_{5\frac{1}{2}}$—$z\ ^2H^o_{5\frac{1}{2}}$
2607.24	3	38343.28	$b\ ^4D_{1\frac{1}{2}}$—$y\ ^4F^o_{1\frac{1}{2}}$
2606.88	1	38348.58	$a\ ^4P_{0\frac{1}{2}}$—$z\ ^4D^o_{0\frac{1}{2}}$
2606.60	50Z	38352.71	
2605.95	10Z	38362.26	$a\ ^4D_{2\frac{1}{2}}$—$z\ ^4D^o_{3\frac{1}{2}}$
2605.826	10Z	38364.09	$a\ ^4H_{4\frac{1}{2}}$—$y\ ^2G^o_{3\frac{1}{2}}$
2605.079	50	38375.09	$a\ ^4H_{5\frac{1}{2}}$—$y\ ^4H^o_{5\frac{1}{2}}$
2604.600	10Z	38382.14	$b\ ^4D_{1\frac{1}{2}}$—$y\ ^4G^o_{2\frac{1}{2}}$
2604.424	3	38384.74	
2603.41	2	38399.69	$a\ ^2I_{6\frac{1}{2}}$—$z\ ^4I^o_{6\frac{1}{2}}$
2602.802	80Z	38408.66	$a\ ^2F_{3\frac{1}{2}}$—$y\ ^4G^o_{3\frac{1}{2}}$ $a\ ^6D_{0\frac{1}{2}}$—$z\ ^6D^o_{1\frac{1}{2}}$
2602.497	5	38413.16	$a\ ^4F_{1\frac{1}{2}}$—$x\ ^4D^o_{1\frac{1}{2}}$
2602.241	3	38416.93	
2601.971	30Z	38420.92	$b\ ^2F_{3\frac{1}{2}}$— (3)$^o_{3\frac{1}{2}}$
2600.233	20	38446.60	$a\ ^2G_{3\frac{1}{2}}$—$y\ ^2G^o_{3\frac{1}{2}}$
2600.104	80Z	38448.51	
2599.552	10	38456.67	$a\ ^4F_{1\frac{1}{2}}$— (1)$^o_{2\frac{1}{2}}$
2599.39	15	38459.07	
2599.189	20Z	38462.04	$a\ ^2F_{2\frac{1}{2}}$—$y\ ^4H^o_{3\frac{1}{2}}$
2597.392	40Z	38488.65	$a\ ^4F_{3\frac{1}{2}}$—$x\ ^4D^o_{2\frac{1}{2}}$
2596.429	5Z	38502.92	$a\ ^2F_{3\frac{1}{2}}$— (2)$^o_{3\frac{1}{2}}$
2595.695	3	38513.81	$c\ ^4D_{1\frac{1}{2}}$—$w\ ^2D^o_{1\frac{1}{2}}$
2594.551	5	38530.79	$c\ ^2G_{4\frac{1}{2}}$—$w\ ^4G^o_{4\frac{1}{2}}$
2594.258	5	38535.15	$b\ ^4D_{3\frac{1}{2}}$—$z\ ^2F^o_{3\frac{1}{2}}$ $d\ ^2F_{3\frac{1}{2}}$—$u\ ^2G^o_{3\frac{1}{2}}$
2593.707	50Z	38543.33	$a\ ^4H_{5\frac{1}{2}}$—$y\ ^2H^o_{4\frac{1}{2}}$ $a\ ^6D_{1\frac{1}{2}}$—$z\ ^6D^o_{2\frac{1}{2}}$
2593.378	50Z	38548.22	$a\ ^2D_{2\frac{1}{2}}$—$z\ ^2D^o_{2\frac{1}{2}}$
2592.782	25Z	38557.08	$a\ ^4F_{2\frac{1}{2}}$—$x\ ^4D^o_{3\frac{1}{2}}$
2592.22	1	38565.44	$b\ ^4D_{0\frac{1}{2}}$—$x\ ^4D^o_{0\frac{1}{2}}$
2592.09	2	38567.37	
2591.776	30Z	38572.05	$a\ ^4F_{3\frac{1}{2}}$—$y\ ^4P^o_{2\frac{1}{2}}$
2590.792	2e	38586.69	$a\ ^4H_{4\frac{1}{2}}$—$z\ ^2H^o_{5\frac{1}{2}}$
2590.42	2	38592.24	$a\ ^2D_{1\frac{1}{2}}$—$y\ ^4P^o_{1\frac{1}{2}}$
2590.221	2	38595.20	$a\ ^2F_{3\frac{1}{2}}$—$y\ ^4F^o_{3\frac{1}{2}}$
2589.788	5	38601.65	
2589.54	1	38605.35	
2588.788	30Z	38616.56	$a\ ^4F_{2\frac{1}{2}}$—$x\ ^4D^o_{1\frac{1}{2}}$
2587.852	15Z	38630.53	$b\ ^4D_{0\frac{1}{2}}$—$y\ ^4F^o_{1\frac{1}{2}}$
2587.36	5	38637.88	$c\ ^2F_{2\frac{1}{2}}$—$t\ ^2F^o_{2\frac{1}{2}}$
2587.32	3	38638.47	$a\ ^4F_{3\frac{1}{2}}$—$x\ ^4D^o_{3\frac{1}{2}}$
2587.046	15Z	38642.56	
2585.966	20Z	38658.70	$a\ ^4F_{4\frac{1}{2}}$—$x\ ^4D^o_{3\frac{1}{2}}$
2585.490	8	38665.82	$b\ ^2G_{4\frac{1}{2}}$—$w\ ^2H^o_{4\frac{1}{2}}$
2585.077	10Z	38671.99	$b\ ^2F_{2\frac{1}{2}}$—$y\ ^2D^o_{2\frac{1}{2}}$
2584.94	1	38674.04	
2584.728	5Z	38677.22	$b\ ^2F_{3\frac{1}{2}}$—$x\ ^4G^o_{3\frac{1}{2}}$
2584.196	10Z	38685.18	$a\ ^4H_{5\frac{1}{2}}$—$y\ ^2H^o_{5\frac{1}{2}}$
2583.95	1Z	38688.86	
2583.821	10Z	38690.79	$b\ ^4P_{2\frac{1}{2}}$—$x\ ^4P^o_{2\frac{1}{2}}$
2582.39	2h	38712.23	
2582.38	2	38712.38	
2580.984	20Z	38733.32	$b\ ^4D_{1\frac{1}{2}}$—$y\ ^4F^o_{2\frac{1}{2}}$
2580.67	1	38738.03	$b\ ^4P_{2\frac{1}{2}}$—$x\ ^2G^o_{3\frac{1}{2}}$
2580.482	3Z	38740.85	$a\ ^4F_{3\frac{1}{2}}$— (1)$^o_{2\frac{1}{2}}$
2580.31	1	38743.44	
2580.14	1	38745.99	$b\ ^4P_{1\frac{1}{2}}$—$w\ ^4D^o_{0\frac{1}{2}}$
2579.67	5	38753.05	
2579.437	20Z	38756.55	$a\ ^6D_{4\frac{1}{2}}$—$z\ ^4F^o_{3\frac{1}{2}}$
2578.910	50	38764.47	$a\ ^2H_{5\frac{1}{2}}$—$x\ ^4G^o_{4\frac{1}{2}}$ $b\ ^4D_{2\frac{1}{2}}$—$z\ ^2F^o_{3\frac{1}{2}}$
2578.347	40Z	38772.93	$a\ ^4H_{4\frac{1}{2}}$—$y\ ^2F^o_{3\frac{1}{2}}$
2578.06	5	38777.25	
2576.913	5	38794.50	$a\ ^4H_{4\frac{1}{2}}$—$y\ ^2H^o_{4\frac{1}{2}}$
2576.70	5	38797.72	$a\ ^4P_{0\frac{1}{2}}$—$z\ ^4D^o_{1\frac{1}{2}}$
2576.565	30Z	38799.74	$a\ ^2P_{1\frac{1}{2}}$—$x\ ^2P^o_{1\frac{1}{2}}$ $b\ ^4P_{2\frac{1}{2}}$—$w\ ^4F^o_{1\frac{1}{2}}$ $a\ ^4F_{1\frac{1}{2}}$—$x\ ^4D^o_{0\frac{1}{2}}$
2575.807	10Z	38811.16	$a\ ^4H_{3\frac{1}{2}}$—$y\ ^2G^o_{3\frac{1}{2}}$
2574.425	30Z	38831.99	$a\ ^6D_{3\frac{1}{2}}$—$z\ ^4F^o_{2\frac{1}{2}}$
2574.166	1	38835.90	$b\ ^4F_{2\frac{1}{2}}$—$x\ ^4P^o_{2\frac{1}{2}}$
2573.84	1	38840.82	$b\ ^4P_{0\frac{1}{2}}$—$y\ ^2D^o_{1\frac{1}{2}}$
2573.697	15	38842.98	
2572.873	10	38855.42	$a\ ^2G_{3\frac{1}{2}}$—$y\ ^2F^o_{3\frac{1}{2}}$
2572.475	10	38861.43	$b\ ^4D_{3\frac{1}{2}}$—$x\ ^4F^o_{3\frac{1}{2}}$
2572.241	30Z	38864.96	$a\ ^4F_{1\frac{1}{2}}$—$y\ ^4F^o_{1\frac{1}{2}}$
2571.447	20Z	38876.96	$a\ ^2G_{3\frac{1}{2}}$—$y\ ^2H^o_{4\frac{1}{2}}$
2571.245	20Z	38880.02	$b\ ^2D_{1\frac{1}{2}}$—$x\ ^2P^o_{0\frac{1}{2}}$
2571.028	10	38883.30	$a\ ^2F_{3\frac{1}{2}}$—$y\ ^4F^o_{2\frac{1}{2}}$ $b\ ^4F_{2\frac{1}{2}}$—$x\ ^2G^o_{3\frac{1}{2}}$
2570.847	50w	38886.04	
2570.73	1	38887.81	$a\ ^2D_{1\frac{1}{2}}$—$z\ ^2P^o_{1\frac{1}{2}}$
2570.231	3	38895.36	$a\ ^4F_{4\frac{1}{2}}$—$z\ ^2I^o_{5\frac{1}{2}}$
2568.83	5	38916.57	
2567.67	2	38934.15	$c\ ^4D_{3\frac{1}{2}}$—$v\ ^2F^o_{2\frac{1}{2}}$
2567.507	15Z	38936.62	$a\ ^4H_{4\frac{1}{2}}$—$y\ ^2H^o_{5\frac{1}{2}}$
2567.25	3	38940.52	
2566.446	1	38952.71	$b\ ^2D_{1\frac{1}{2}}$—$w\ ^2D^o_{1\frac{1}{2}}$
2566.257	30Z	38955.58	$a\ ^4H_{5\frac{1}{2}}$—$y\ ^2G^o_{4\frac{1}{2}}$ $a\ ^6D_{2\frac{1}{2}}$—$z\ ^4F^o_{1\frac{1}{2}}$
2566.083	20Z	38958.22	$c\ ^4D_{1\frac{1}{2}}$—$v\ ^2F^o_{2\frac{1}{2}}$
2565.803	2	38962.48	
2565.58	1	38965.86	
2564.572	5Z	38981.18	$b\ ^2F_{3\frac{1}{2}}$—$x\ ^4G^o_{4\frac{1}{2}}$
2564.334	40Z	38984.79	$b\ ^4D_{3\frac{1}{2}}$—$x\ ^4F^o_{3\frac{1}{2}}$
2564.091	2	38988.49	$a\ ^2F_{3\frac{1}{2}}$—$y\ ^4H^o_{4\frac{1}{2}}$ $a\ ^4P_{1\frac{1}{2}}$—$z\ ^4D^o_{1\frac{1}{2}}$

TABLE 1. *Wavelengths and term combinations of* Mo II—Continued

Wavelength λ_{air}	Intensity	Wave No.	Term combination
2563. 876	3	38991. 76	$a\ ^2H_{4½}—w\ ^4D^o_{3½}$
2562. 941	3	39005. 98	$a\ ^2G_{4½}—z\ ^2H^o_{3½}$
2562. 078	40Z	39019. 12	$a\ ^2H_{4½}—x\ ^4G^o_{3½}$
2561. 93	5	39021. 37	
2561. 555	2	39027. 08	$b\ ^4F_{3½}—w\ ^4F^o_{2½}$
2560. 669	20Z	39040. 59	$a\ ^2F_{2½}—z\ ^2F^o_{3½}$; $b\ ^4P_{1½}—w\ ^4D^o_{2½}$
2560. 34	1h	39045. 60	
2559. 688	30Z	39055. 55	$b\ ^4D_{2½}—x\ ^4F^o_{2½}$
2559. 121	30	39064. 20	$b\ ^4F_{3½}—x\ ^2G^o_{4½}$; $a\ ^4F_{3½}—y\ ^4G^o_{3½}$
2558. 867	40	39068. 08	$a\ ^2F_{2½}—x\ ^4F^o_{1½}$; $a\ ^4F_{2½}—y\ ^4F^o_{1½}$
2558. 727	20	39070. 22	
2558. 577	5	39072. 51	
2558. 18	10	39078. 54	$c\ ^2F_{3½}—v\ ^2D^o_{2½}$
2557. 759	5	39085. 00	$a\ ^4F_{4½}—y\ ^4G^o_{3½}$
2557. 378	30Z	39090. 83	$b\ ^4D_{2½}—x\ ^4F^o_{3½}$
2556. 756	40Z	39100. 33	$a\ ^4F_{3½}—y\ ^4G^o_{4½}$
2556. 56	5	39103. 33	
2556. 309	15Z	39107. 17	$a\ ^4F_{2½}—y\ ^4G^o_{2½}$
2556. 07	5	39110. 83	
2555. 68	5	39116. 80	$a\ ^2H_{5½}—x\ ^4G^o_{5½}$
2555. 420	50Z	39120. 78	$a\ ^4F_{4½}—y\ ^4G^o_{4½}$
2554. 979	3	39127. 53	$a\ ^2P_{1½}—w\ ^2P^o_{0½}$
2554. 669	1	39132. 28	$b\ ^4F_{1½}—w\ ^4F^o_{2½}$
2554. 24	1	39138. 85	$b\ ^4F_{2½}—w\ ^4F^o_{2½}$
2552. 99	2	39158. 01	$b\ ^4P_{2½}—w\ ^4F^o_{3½}$
2552. 918	5	39159. 11	$b\ ^2D_{2½}—w\ ^2D^o_{1½}$
2552. 73	3	39162. 00	$c\ ^4D_{2½}—v\ ^2F^o_{3½}$
2552. 54	1	39164. 91	
2552. 39	1	39167. 21	
2552. 193	20Z	39170. 24	$a\ ^4F_{2½}—y\ ^4F^o_{3½}$
2551. 21	1	39185. 33	
2550. 740	40Z	39192. 55	$a\ ^2G_{4½}—y\ ^2F^o_{3½}$
2550. 03	2	39203. 46	$b\ ^4G_{2½}—y\ ^2P^o_{1½}$
2549. 892	3	39205. 58	$c\ ^2G_{3½}—v\ ^4F^o_{4½}$
2549. 73	3	39208. 07	
2549. 351	10Z	39213. 90	$a\ ^2G_{4½}—y\ ^2H^o_{4½}$
2549. 067	2	39218. 27	
2548. 95	2	39220. 07	$a\ ^4H_{3½}—y\ ^2F^o_{3½}$; $d\ ^2G_{4½}—u^2\ G^o_{3½}$
2548. 212	10Z	39231. 43	$a\ ^2D_{1½}—z\ ^2P^o_{0½}$; $a\ ^4H_{3½}—y\ ^2F^o_{2½}$
2547. 71	3h	39239. 16	
2547. 562	30Z	39241. 44	$a\ ^4H_{3½}—y\ ^2H^o_{4½}$
2547. 34	50	39244. 86	$b\ ^4D_{1½}—x\ ^4F^o_{1½}$
2546. 920	10Z	39251. 33	$a\ ^4F_{3½}—y\ ^4F^o_{3½}$
2546. 696	10	39254. 78	$a\ ^4F_{1½}—y\ ^4F^o_{2½}$
2546. 497	5	39257. 85	$b\ ^2F_{3½}—w\ ^4D^o_{2½}$
2545. 600	20	39271. 68	$a\ ^4F_{4½}—y\ ^4F^o_{3½}$
2544. 900	20	39282. 48	$b\ ^4D_{2½}—z\ ^2F^o_{2½}$
2544. 456	40Z	39289. 33	$b\ ^4F_{4½}—w\ ^4F^o_{4½}$; $a\ ^2G_{3½}—y\ ^2G^o_{4½}$
2543. 611	40Z	39302. 39	$a\ ^2D_{2½}—z\ ^2P^o_{1½}$; $b\ ^4F_{2½}—w\ ^4F^o_{3½}$
2543. 06	1	39310. 90	
2542. 783	30	39315. 18	$a\ ^6D_{2½}—z\ ^4F^o_{3½}$
2542. 668	50Z	39316. 96	$a\ ^6D_{3½}—z\ ^4F^o_{3½}$
2542. 041	20	39326. 66	$a\ ^2G_{3½}—x\ ^4G^o_{3½}$
2541. 49	2h	39335. 18	$b\ ^4F_{3½}—w\ ^4F^o_{4½}$
2541. 251	10	39338. 88	$a\ ^6D_{1½}—z\ ^4F^o_{1½}$
2540. 585	10Z	39349. 19	$c\ ^4D_{2½}—x\ ^2P^o_{2½}$
2540. 133	40	39356. 20	$a\ ^2G_{4½}—y\ ^2H^o_{5½}$
2539. 643	5	39363. 79	$a\ ^4F_{3½}—y\ ^4H^o_{3½}$
2539. 436	40Z	39367. 00	$a\ ^2F_{3½}—z\ ^2F^o_{3½}$; $a\ ^2F_{2½}—x\ ^4F^o_{3½}$
2539. 16	3	39371. 28	
2538. 996	2	39373. 82	
2538. 444	200Z	39382. 38	$a\ ^6D_{4½}—z\ ^4F^o_{4½}$
2537. 86	2	39391. 44	
2537. 445	30Z	39397. 89	$b\ ^2D_{1½}—v\ ^2F^o_{2½}$
2536. 80	5	39407. 90	
2536. 618	3	39410. 73	
2536. 044	1	39419. 65	$b\ ^4P_{2½}—x\ ^4P^o_{1½}$
2535. 856	1	39422. 57	
2535. 44	3h	39429. 04	
2534. 41	10Z	39444. 91	$a\ ^4F_{3½}—y\ ^4H^o_{3½}$
2533. 994	3	39451. 54	
2533. 580	40Z	39457. 98	$a\ ^4F_{2½}—y\ ^4F^o_{2½}$
2533. 09	3	39465. 61	$a\ ^4F_{4½}—y\ ^4H^o_{5½}$
2532. 81	3	39469. 98	
2532. 62	2Z	39472. 94	
2532. 295	50Z	39478. 00	$a\ ^2D_{1½}—x\ ^4D^o_{2½}$
2531. 437	5Z	39491. 38	$a\ ^2S_{0½}—x\ ^4P^o_{1½}$
2531. 23	1	39494. 61	
2530. 67	5	39503. 35	
2530. 327	50Z	39508. 71	$b\ ^4D_{1½}—x\ ^4F^o_{2½}$
2530. 196	5	39510. 75	$b\ ^4D_{3½}—y\ ^2G^o_{3½}$
2529. 807	40	39516. 83	$a\ ^4P_{1½}—z\ ^4D^o_{2½}$
2529. 548	5	39520. 87	
2529. 304	5	39524. 68	$a\ ^4P_{2½}—z\ ^4D^o_{3½}$
2528. 852	50Z	39531. 75	$b\ ^4D_{0½}—x\ ^4F^o_{1½}$
2528. 383	30Z	39539. 08	$a\ ^4F_{3½}—y\ ^4F^o_{2½}$
2527. 25	40	39556. 81	
2527. 135	50Z	39558. 61	$a\ ^2F_{2½}—z\ ^2F^o_{3½}$
2526. 747	4	39564. 68	$b\ ^4F_{2½}—x\ ^4P^o_{1½}$; $d\ ^2F_{3½}—u\ ^2G^o_{4½}$
2526. 555	4	39567. 69	
2524. 515	5	39599. 06	$a\ ^4H_{4½}—x\ ^4G^o_{3½}$
2523. 785	2h	39611. 11	
2523. 165	30Z	39620. 84	$a\ ^2F_{3½}—z\ ^2H^o_{4½}$
2522. 84	40	39625. 95	$a\ ^2G_{4½}—y\ ^2G^o_{4½}$
2522. 590	30Z	39629. 88	$a\ ^4H_{6½}—x\ ^4G^o_{5½}$
2522. 05	1	39638. 36	$b\ ^4D_{2½}—z\ ^4S^o_{1½}$
2521. 683	30Z	39644. 13	$a\ ^4F_{3½}—y\ ^4H^o_{4½}$
2521. 33	1	39649. 68	
2521. 187	10Z	39651. 93	$a\ ^4H_{5½}—x\ ^4G^o_{4½}$; $c\ ^4D_{0½}—w\ ^2P^o_{0½}$
2521. 059	30Z	39653. 94	$a\ ^4H_{3½}—y\ ^2G^o_{4½}$
2520. 77	2	39658. 48	$a\ ^2F_{3½}—x\ ^4F^o_{2½}$
2520. 392	20	39664. 43	$a\ ^4F_{4½}—y\ ^4H^o_{4½}$
2519. 607	20Z	39676. 79	$a\ ^2G_{3½}—y\ ^2D^o_{2½}$
2519. 19	5	39683. 36	$b\ ^2G_{3½}—w\ ^2D^o_{2½}$
2518. 978	5	39686. 70	$a\ ^2D_{1½}—x\ ^4D^o_{1½}$
2518. 700	20	39691. 08	$a\ ^4H_{3½}—x\ ^4G^o_{2½}$
2518. 53	20	39693. 76	$a\ ^2F_{3½}—x\ ^4F^o_{3½}$; $c\ ^4D_{1½}—x\ ^2P^o_{1½}$
2518. 43	30Z	39695. 33	$a\ ^2S_{0½}—y\ ^2P^o_{0½}$
2518. 24	3	39698. 33	$a\ ^6D_{1½}—z\ ^4F^o_{2½}$
2516. 092	50Z	39732. 22	$a\ ^2I_{6½}—z\ ^2I^o_{6½}$
2515. 602	30Z	39739. 95	$b\ ^4D_{2½}—y\ ^2G^o_{3½}$

TABLE 1. *Wavelengths and term combinations of* Mo II—Continued

Wavelength λ_{air}	Intensity	Wave No.	Term combination
2515. 101	50Z	39747. 87	$a\ ^2I_{5\frac{1}{2}}$—$z\ ^2I^o_{5\frac{1}{2}}$
2514. 16	30Z	39762. 75	$a\ ^2G_{4\frac{1}{2}}$— $(3)^o_{3\frac{1}{2}}$
2513. 950	20Z	39766. 07	$a\ ^4F_{1\frac{1}{2}}$—$x\ ^4F^o_{1\frac{1}{2}}$
2513. 12	30	39779. 20	$b\ ^2F_{2\frac{1}{2}}$—$x\ ^2F^o_{2\frac{1}{2}}$
2512. 39	10*b*	39790. 76	$b\ ^4G_{4\frac{1}{2}}$—$x\ ^2H^o_{5\frac{1}{2}}$
2511. 80	4Z	39800. 10	$a\ ^6D_{2\frac{1}{2}}$—$z\ ^4F^o_{3\frac{1}{2}}$
2511. 29	40	39808. 18	
2511. 24	30*e*	39808. 98	
2510. 733	2	39817. 01	$a\ ^2F_{3\frac{1}{2}}$—$x\ ^4F^o_{4\frac{1}{2}}$
2510. 343	10Z	39823. 20	
2510. 065	3	39827. 61	
2509. 790	3	39831. 97	
2509. 148	40Z	39842. 16	$a\ ^2P_{0\frac{1}{2}}$—$x\ ^2P^o_{0\frac{1}{2}}$
2506. 975	1	39876. 70	
2506. 684	40	39881. 33	$b\ ^2F_{2\frac{1}{2}}$—$x\ ^2G^o_{3\frac{1}{2}}$
2506. 432	5	39885. 33	$a\ ^2F_{3\frac{1}{2}}$—$z\ ^2F^o_{2\frac{1}{2}}$ $a\ ^4G_{3\frac{1}{2}}$—$z\ ^4D^o_{2\frac{1}{2}}$
2505. 642	15Z	39897. 91	$a\ ^2D_{2\frac{1}{2}}$—$x\ ^4D^o_{2\frac{1}{2}}$
2505. 302	10	39903. 32	$a\ ^4H_{4\frac{1}{2}}$—$x\ ^4G^o_{4\frac{1}{2}}$
2504. 623	2	39914. 14	$a\ ^2F_{2\frac{1}{2}}$—$z\ ^4S^o_{1\frac{1}{2}}$
2504. 298	10	39919. 32	$b\ ^4D_{3\frac{1}{2}}$—$y\ ^2F^o_{3\frac{1}{2}}$
2503. 594	50	39930. 55	
2502. 945	5	39940. 90	$b\ ^4D_{3\frac{1}{2}}$—$y\ ^2H^o_{4\frac{1}{2}}$
2502. 826	5Z	39942. 80	$b\ ^2F_{2\frac{1}{2}}$—$w\ ^4F^o_{1\frac{1}{2}}$ $a\ ^4F_{2\frac{1}{2}}$—$z\ ^2F^o_{3\frac{1}{2}}$ $a\ ^6D_{3\frac{1}{2}}$—$z\ ^4F^o_{4\frac{1}{2}}$
2502. 37	5	39950. 08	$b\ ^2D_{2\frac{1}{2}}$—$w\ ^2D^o_{2\frac{1}{2}}$ $a\ ^4F_{4\frac{1}{2}}$—$y\ ^4F^o_{4\frac{1}{2}}$
2502. 216	50Z	39952. 53	$a\ ^2S_{0\frac{1}{2}}$—$y\ ^2P^o_{1\frac{1}{2}}$
2501. 807	10	39959. 07	$a\ ^2I_{6\frac{1}{2}}$—$y\ ^4G^o_{5\frac{1}{2}}$
2500. 92	3	39973. 24	$a\ ^2I_{5\frac{1}{2}}$—$y\ ^4G^o_{4\frac{1}{2}}$
2500. 74	20*e*	39976. 11	
2500. 425	40Z	39981. 15	$a\ ^2D_{2\frac{1}{2}}$—$y\ ^4P^o_{2\frac{1}{2}}$ $b\ ^2F_{3\frac{1}{2}}$—$x\ ^2F^o_{3\frac{1}{2}}$
2500. 15	5	39985. 55	$a\ ^2G_{3\frac{1}{2}}$—$x\ ^4G^o_{4\frac{1}{2}}$
2499. 58	5	39994. 67	
2499. 253	20	39999. 90	$a\ ^2I_{5\frac{1}{2}}$—$z\ ^2I^o_{6\frac{1}{2}}$
2498. 969	2	40004. 44	$a\ ^4H_{5\frac{1}{2}}$—$x\ ^4G^o_{5\frac{1}{2}}$
2498. 280	40	40015. 48	$a\ ^2F_{2\frac{1}{2}}$—$y\ ^2G^o_{3\frac{1}{2}}$ $a\ ^4P_{2\frac{1}{2}}$—$z\ ^4D^o_{3\frac{1}{2}}$
2498. 088	40	40018. 55	$a\ ^2G_{4\frac{1}{2}}$—$x\ ^4G^o_{3\frac{1}{2}}$
2497. 80	50	40023. 16	$a\ ^4F_{3\frac{1}{2}}$—$z\ ^2F^o_{3\frac{1}{2}}$
2497. 371	35Z	40030. 04	$a\ ^4F_{1\frac{1}{2}}$—$x\ ^4F^o_{2\frac{1}{2}}$
2497. 240	10	40032. 14	
2497. 020	35	40035. 67	$a\ ^2H_{4\frac{1}{2}}$—$x\ ^2G^o_{3\frac{1}{2}}$
2496. 520	30	40043. 68	$a\ ^4F_{1\frac{1}{2}}$—$z\ ^2F^o_{2\frac{1}{2}}$
2496. 280	30Z	40047. 53	$a\ ^2D_{2\frac{1}{2}}$—$x\ ^4D^o_{3\frac{1}{2}}$
2495. 45	3	40060. 85	
2494. 682	20Z	40073. 18	$a\ ^2D_{1\frac{1}{2}}$—$x\ ^4D^o_{0\frac{1}{2}}$
2494. 185	20	40081. 17	
2493. 921	8	40085. 41	$b\ ^4P_{1\frac{1}{2}}$—$x\ ^4P^o_{2\frac{1}{2}}$
2493. 25	30	40096. 20	$b\ ^2S_{0\frac{1}{2}}$—$v\ ^2P^o_{1\frac{1}{2}}$
2493. 054	8	40099. 35	$a\ ^2S_{0\frac{1}{2}}$—$x\ ^4P^o_{0\frac{1}{2}}$
2492. 588	8	40106. 85	$a\ ^2D_{2\frac{1}{2}}$—$x\ ^4D^o_{1\frac{1}{2}}$
2490. 64	10Z	40138. 21	$a\ ^2D_{1\frac{1}{2}}$—$y\ ^4F^o_{1\frac{1}{2}}$
2490. 19	1	40145. 47	$a\ ^4D_{1\frac{1}{2}}$—$y\ ^4D^o_{0\frac{1}{2}}$
2490. 018	50	40148. 24	$b\ ^4D_{2\frac{1}{2}}$—$y\ ^2F^o_{3\frac{1}{2}}$
2489. 212	1	40161. 24	
2488. 365	2	40174. 91	
2487. 98	1	40181. 12	$c\ ^4D_{2\frac{1}{2}}$—$w\ ^2P^o_{1\frac{1}{2}}$
2487. 364	1	40191. 07	
2486. 531	8	40204. 54	
2486. 363	3	40207. 25	
2485. 30	1	40224. 45	
2485. 16	1	40226. 71	$a\ ^2I_{5\frac{1}{2}}$—$y\ ^4G^o_{5\frac{1}{2}}$
2484. 752	40Z	40233. 32	$a\ ^4F_{2\frac{1}{2}}$—$x\ ^4F^o_{2\frac{1}{2}}$
2484. 60	3Z	40235. 78	
2484. 48	20*e*	40237. 72	
2483. 710	10	40250. 20	$d\ ^2G_{4\frac{1}{2}}$—$u\ ^2G^o_{4\frac{1}{2}}$
2483. 383	20	40255. 50	$a\ ^4H_{4\frac{1}{2}}$—$x\ ^4G^o_{5\frac{1}{2}}$
2482. 973	30	40262. 15	$a\ ^2G_{3\frac{1}{2}}$—$w\ ^4D^o_{2\frac{1}{2}}$ $a\ ^2H_{5\frac{1}{2}}$—$z\ ^2K^o_{6\frac{1}{2}}$
2482. 566	60Z	40268. 75	$a\ ^4F_{2\frac{1}{2}}$—$x\ ^4F^o_{3\frac{1}{2}}$
2482. 075	20	40276. 71	$a\ ^4F_{3\frac{1}{2}}$—$z\ ^2H^o_{4\frac{1}{2}}$ $c\ ^4D_{2\frac{1}{2}}$—$u\ ^2F^o_{2\frac{1}{2}}$
2481. 918	10	40279. 26	$b\ ^4G_{3\frac{1}{2}}$—$x\ ^2H^o_{3\frac{1}{2}}$ $a\ ^4G_{4\frac{1}{2}}$—$z\ ^4D^o_{3\frac{1}{2}}$
2481. 795	2	40281. 26	
2480. 193	10	40307. 27	$a\ ^4F_{4\frac{1}{2}}$—$y\ ^4H^o_{5\frac{1}{2}}$
2479. 75	10	40314. 47	$a\ ^4F_{3\frac{1}{2}}$—$x\ ^4F^o_{2\frac{1}{2}}$
2479. 239	50	40322. 78	$d\ ^2F_{3\frac{1}{2}}$—$t\ ^2G^o_{4\frac{1}{2}}$ $a\ ^2G_{4\frac{1}{2}}$—$x\ ^4G^o_{4\frac{1}{2}}$
2478. 93	1	40327. 80	$a\ ^2H_{4\frac{1}{2}}$—$x\ ^2G^o_{4\frac{1}{2}}$
2478. 672	30Z	40332. 00	$b\ ^4D_{2\frac{1}{2}}$—$y\ ^2D^o_{1\frac{1}{2}}$
2478. 229	25Z	40339. 21	$b\ ^2D_{2\frac{1}{2}}$—$x\ ^2P^o_{1\frac{1}{2}}$
2478. 008	30Z	40342. 81	$a\ ^2F_{3\frac{1}{2}}$—$y\ ^2G^o_{3\frac{1}{2}}$
2477. 570	100Z	40349. 94	$b\ ^2F_{3\frac{1}{2}}$—$x\ ^2G^o_{3\frac{1}{2}}$ $a\ ^4F_{3\frac{1}{2}}$—$x\ ^4F^o_{3\frac{1}{2}}$ $a\ ^4H_{3\frac{1}{2}}$—$x\ ^4G^o_{4\frac{1}{2}}$
2475. 511	10	40383. 50	
2475. 235	15	40388. 00	$d\ ^2G_{3\frac{1}{2}}$—$u\ ^2G^o_{3\frac{1}{2}}$ $b\ ^4P_{1\frac{1}{2}}$—$w\ ^4F^o_{2\frac{1}{2}}$
2474. 24	15Z	40404. 24	
2472. 970	5	40424. 99	$a\ ^2F_{2\frac{1}{2}}$—$y\ ^2F^o_{3\frac{1}{2}}$ $a\ ^2H_{5\frac{1}{2}}$—$x\ ^2G^o_{4\frac{1}{2}}$
2472. 24	4	40436. 92	$a\ ^2F_{2\frac{1}{2}}$—$y\ ^2F^o_{2\frac{1}{2}}$
2472. 08	1	40439. 54	$a\ ^2P_{1\frac{1}{2}}$—$w\ ^4G^o_{2\frac{1}{2}}$
2471. 81	1	40443. 96	
2471. 011	10	40457. 04	$b\ ^4G_{4\frac{1}{2}}$—$x\ ^2H^o_{5\frac{1}{2}}$
2470. 803	3	40460. 44	$b\ ^2D_{1\frac{1}{2}}$—$w\ ^2P^o_{0\frac{1}{2}}$ $a\ ^4F_{2\frac{1}{2}}$—$z\ ^2F^o_{2\frac{1}{2}}$
2470. 662	1	40462. 75	
2470. 043	50Z	40472. 89	$a\ ^4F_{3\frac{1}{2}}$—$x\ ^4F^o_{4\frac{1}{2}}$
2469. 020	10	40489. 66	$b\ ^4D_{3\frac{1}{2}}$—$(3)^o_{3\frac{1}{2}}$
2468. 790	70Z	40493. 43	$a\ ^4F_{4\frac{1}{2}}$—$x\ ^4F^o_{4\frac{1}{2}}$
2468. 76	8Z	40493. 92	
2467. 944	8	40507. 31	$d\ ^2F_{2\frac{1}{2}}$—$t\ ^2G^o_{3\frac{1}{2}}$ $a\ ^2P_{1\frac{1}{2}}$—$t\ ^2F^o_{2\frac{1}{2}}$ $a\ ^4G_{2\frac{1}{2}}$—$z\ ^4D^o_{3\frac{1}{2}}$
2467. 350	50Z	40517. 06	$a\ ^2I_{5\frac{1}{2}}$—$y\ ^4H^o_{4\frac{1}{2}}$
2466. 971	40Z	40523. 29	$a\ ^4D_{0\frac{1}{2}}$—$y\ ^4D^o_{0\frac{1}{2}}$
2466. 671	50Z	40528. 22	$a\ ^2D_{1\frac{1}{2}}$—$y\ ^4F^o_{2\frac{1}{2}}$
2466. 021	30	40538. 90	
2465. 879	30	40541. 23	$a\ ^4F_{3\frac{1}{2}}$—$z\ ^2F^o_{2\frac{1}{2}}$
2464. 84	2	40558. 32	$a\ ^2D_{2\frac{1}{2}}$—$y\ ^4F^o_{1\frac{1}{2}}$
2463. 536	25	40579. 79	
2462. 482	40Z	40597. 15	$a\ ^2D_{2\frac{1}{2}}$—$y\ ^4G^o_{2\frac{1}{2}}$ $c\ ^4D_{3\frac{1}{2}}$—$u\ ^2F^o_{2\frac{1}{2}}$
2461. 805	50Z	40608. 32	$a\ ^2F_{2\frac{1}{2}}$—$y\ ^2D^o_{1\frac{1}{2}}$
2461. 48	3	40613. 68	$b\ ^4D_{1\frac{1}{2}}$—$y\ ^2F^o_{2\frac{1}{2}}$

Wavelength λ_{air}	Intensity	Wave No.	Term combination
2461. 102	15	40619. 92	$b\ ^4D_{2\frac{1}{2}}—x\ ^4G^o_{3\frac{1}{2}}$ $b\ ^4G_{3\frac{1}{2}}—w\ ^2G^o_{4\frac{1}{2}}$
2461. 010	10	40621. 43	$c\ ^4D_{2\frac{1}{2}}—u\ ^2F^o_{3\frac{1}{2}}$ $c\ ^4D_{1\frac{1}{2}}—u\ ^2F^o_{2\frac{1}{2}}$
2460. 683	10	40626. 83	$a\ ^4H_{3\frac{1}{2}}—w\ ^4D^o_{2\frac{1}{2}}$
2459. 762	70Z	40642. 04	$b\ ^2F_{3\frac{1}{2}}—x\ ^2G^o_{4\frac{1}{2}}$
2458. 655	40Z	40660. 34	$a\ ^2D_{2\frac{1}{2}}—y\ ^4F^o_{3\frac{1}{2}}$
2458. 208	8	40667. 73	
2457. 771	100Z	40674. 96	$a\ ^2G_{4\frac{1}{2}}—x\ ^4G^o_{3\frac{1}{2}}$ $a\ ^4H_{3\frac{1}{2}}—w\ ^4D^o_{3\frac{1}{2}}$
2456. 53	2	40695. 51	
2455. 92	3	40705. 62	
2455. 792	3	40707. 74	$b\ ^4P_{2\frac{1}{2}}—w\ ^2F^o_{2\frac{1}{2}}$
2455. 222	2	40717. 19	
2455. 11	1	40719. 05	$b\ ^4D_{2\frac{1}{2}}—(3)^o_{3\frac{1}{2}}$
2454. 57	1	40728. 00	
2453. 798	25	40740. 82	$b\ ^4D_{3\frac{1}{2}}—y\ ^2D^o_{2\frac{1}{2}}$ $b\ ^4F_{3\frac{1}{2}}—w\ ^2F^o_{2\frac{1}{2}}$
2453. 361	25Z	40748. 07	$a\ ^2H_{4\frac{1}{2}}—y\ ^2I^o_{5\frac{1}{2}}$
2453. 143	45Z	40751. 69	$a\ ^2F_{3\frac{1}{2}}—y\ ^2F^o_{3\frac{1}{2}}$
2452. 772	4	40757. 86	
2452. 206	30	40767. 26	
2451. 762	20	40774. 64	$a\ ^4H_{6\frac{1}{2}}—z\ ^2K^o_{5\frac{1}{2}}$
2451. 38	2	40781. 00	
2450. 79	1	40790. 82	
2450. 27	2	40799. 47	
2449. 62	3	40810. 30	
2449. 273	3	40816. 08	$a\ ^4F_{2\frac{1}{2}}—z\ ^4S^o_{1\frac{1}{2}}$
2447. 76	1	40841. 31	
2447. 484	10	40845. 91	$a\ ^2H_{5\frac{1}{2}}—y\ ^2I^o_{5\frac{1}{2}}$ $b\ ^4F_{1\frac{1}{2}}—w\ ^2F^o_{2\frac{1}{2}}$
2447. 068	25	40852. 85	$b\ ^4F_{2\frac{1}{2}}—w\ ^2F^o_{2\frac{1}{2}}$
2446. 921	1	40855. 30	
2446. 378	5	40864. 38	
2444. 735	30Z	40891. 84	$a\ ^2I_{6\frac{1}{2}}—y\ ^4H^o_{5\frac{1}{2}}$
2444. 482	45Z	40896. 07	$a\ ^2F_{2\frac{1}{2}}—x\ ^4G^o_{3\frac{1}{2}}$
2444. 077	4	40902. 85	$a\ ^4H_{4\frac{1}{2}}—x\ ^2F^o_{3\frac{1}{2}}$
2443. 463	8	40913. 13	$b\ ^2F_{3\frac{1}{2}}—w\ ^4F^o_{4\frac{1}{2}}$
2443. 188	45Z	40917. 73	$a\ ^4F_{2\frac{1}{2}}—y\ ^2G^o_{3\frac{1}{2}}$
2442. 957	2	40921. 60	
2442. 231	5	40933. 76	
2441. 36	3	40948. 36	$a\ ^2D_{2\frac{1}{2}}—y\ ^4F^o_{2\frac{1}{2}}$
2440. 415	3	40964. 22	$b\ ^2D_{1\frac{1}{2}}—w\ ^2P^o_{1\frac{1}{2}}$
2440. 265	45Z	40966. 74	$a\ ^4D_{1\frac{1}{2}}—y\ ^4D^o_{1\frac{1}{2}}$
2440. 05	40Z	40970. 35	$b\ ^4D_{2\frac{1}{2}}—y\ ^2D^o_{2\frac{1}{2}}$
2439. 466	3	40980. 15	$b\ ^4G_{4\frac{1}{2}}—w\ ^2G^o_{3\frac{1}{2}}$
2438. 95	1	40988. 82	$c\ ^4D_{2\frac{1}{2}}—w\ ^4G^o_{2\frac{1}{2}}$
2438. 574	40Z	40995. 14	$a\ ^2F_{2\frac{1}{2}}—(3)^o_{3\frac{1}{2}}$
2438. 356	15	40998. 81	$a\ ^4F_{3\frac{1}{2}}—y\ ^2G^o_{3\frac{1}{2}}$
2438. 265	10	41000. 34	$b\ ^2G_{3\frac{1}{2}}—u\ ^2F^o_{2\frac{1}{2}}$
2437. 90	3	41006. 48	
2437. 37	2	41015. 39	$b\ ^4F_{3\frac{1}{2}}—x\ ^2H^o_{4\frac{1}{2}}$
2437. 16	1	41018. 92	$a\ ^4F_{4\frac{1}{2}}—y\ ^2G^o_{3\frac{1}{2}}$
2435. 941	50Z	41039. 45	$a\ ^2D_{1\frac{1}{2}}—x\ ^4F^o_{1\frac{1}{2}}$
2435. 80	3e	41041. 82	
2435. 33	1	41049. 74	$b\ ^4D_{3\frac{1}{2}}—x\ ^4G^o_{4\frac{1}{2}}$
2434. 95	1	41056. 15	$c\ ^4D_{2\frac{1}{2}}—t\ ^2F^o_{2\frac{1}{2}}$
2434. 72	1	41060. 03	$b\ ^2D_{1\frac{1}{2}}—u\ ^2F^o_{2\frac{1}{2}}$
2433. 970	15Z	41072. 68	$b\ ^4D_{0\frac{1}{2}}—y\ ^2D^o_{1\frac{1}{2}}$ $b\ ^4D_{1\frac{1}{2}}—x\ ^4G^o_{2\frac{1}{2}}$
2432. 645	3	41095. 05	$a\ ^2P_{0\frac{1}{2}}—x\ ^2P^o_{1\frac{1}{2}}$
2431. 35	3	41116. 94	
2430. 272	25Z	41135. 17	$a\ ^4F_{1\frac{1}{2}}—y\ ^2F^o_{2\frac{1}{2}}$
2429. 390	50Z	41150. 11	$a\ ^2I_{5\frac{1}{2}}—z\ ^2H^o_{4\frac{1}{2}}$
2429. 071	10	41155. 51	$b\ ^4G_{3\frac{1}{2}}—w\ ^2H^o_{3\frac{1}{2}}$
2428. 38	1	41167. 22	
2428. 172	20Z	41170. 75	$b\ ^2D_{2\frac{1}{2}}—w\ ^2P^o_{1\frac{1}{2}}$
2427. 795	3	41177. 14	
2427. 289	25Z	41185. 72	$a\ ^2F_{3\frac{1}{2}}—y\ ^2G^o_{4\frac{1}{2}}$
2427. 097	4	41188. 98	
2426. 968	5	41191. 17	
2426. 37	2	41201. 32	
2425. 727	10	41212. 24	
2425. 085	10	41223. 15	$a\ ^2F_{3\frac{1}{2}}—x\ ^4G^o_{2\frac{1}{2}}$
2424. 99	1	41224. 77	$b\ ^4F_{2\frac{1}{2}}—w\ ^2F^o_{3\frac{1}{2}}$
2424. 77	2	41228. 51	
2424. 262	15Z	41237. 14	$b\ ^2G_{4\frac{1}{2}}—u\ ^2F^o_{3\frac{1}{2}}$
2423. 988	70Z	41241. 81	$a\ ^4F_{4\frac{1}{2}}—z\ ^2H^o_{3\frac{1}{2}}$
2423. 720	15Z	41246. 36	$a\ ^2F_{2\frac{1}{2}}—y\ ^2D^o_{2\frac{1}{2}}$
2423. 41	2	41251. 64	$a\ ^2F_{2\frac{1}{2}}—x\ ^4G^o_{3\frac{1}{2}}$
2422. 185	35	41272. 50	$a\ ^4H_{4\frac{1}{2}}—x\ ^2G^o_{3\frac{1}{2}}$
2421. 647	15Z	41281. 67	$a\ ^2H_{5\frac{1}{2}}—y\ ^2I^o_{5\frac{1}{2}}$
2421. 328	10	41287. 11	$b\ ^4D_{2\frac{1}{2}}—w\ ^4D^o_{1\frac{1}{2}}$
2421. 232	15	41288. 75	
2420. 86	1	41295. 09	
2420. 180	45Z	41306. 69	$a\ ^4F_{1\frac{1}{2}}—y\ ^2D^o_{1\frac{1}{2}}$
2419. 84	3	41312. 49	$a\ ^4H_{5\frac{1}{2}}—x\ ^2G^o_{4\frac{1}{2}}$
2419. 530	2	41317. 79	
2419. 31	2	41321. 54	$a\ ^2F_{3\frac{1}{2}}—(3)^o_{3\frac{1}{2}}$
2419. 011	45Z	41326. 65	$b\ ^4D_{3\frac{1}{2}}—w\ ^4D^o_{2\frac{1}{2}}$ $a\ ^4F_{2\frac{1}{2}}—y\ ^2F^o_{3\frac{1}{2}}$
2418. 635	2	41333. 07	$b\ ^4G_{4\frac{1}{2}}—w\ ^2H^o_{5\frac{1}{2}}$
2418. 328	5	41338. 32	$a\ ^4F_{2\frac{1}{2}}—y\ ^2F^o_{2\frac{1}{2}}$
2417. 964	30Z	41344. 55	$a\ ^4D_{0\frac{1}{2}}—y\ ^4D^o_{1\frac{1}{2}}$
2417. 738	5	41348. 41	
2417. 485	10Z	41352. 74	$a\ ^4D_{1\frac{1}{2}}—z\ ^2S^o_{0\frac{1}{2}}$
2417. 367	20	41354. 76	$a\ ^2G_{3\frac{1}{2}}—x\ ^2G^o_{3\frac{1}{2}}$
2416. 182	20Z	41375. 04	$b\ ^4D_{3\frac{1}{2}}—w\ ^4D^o_{3\frac{1}{2}}$
2416. 13	3	41375. 93	
2415. 926	4	41379. 42	
2415. 038	2	41394. 63	
2414. 69	15	41400. 58	$a\ ^2P_{1\frac{1}{2}}—v\ ^2D^o_{2\frac{1}{2}}$
2414. 288	10	41407. 49	$a\ ^4F_{3\frac{1}{2}}—y\ ^2F^o_{3\frac{1}{2}}$
2413. 81	1	41415. 69	
2413. 61	1	41419. 12	$a\ ^4F_{3\frac{1}{2}}—y\ ^2F^o_{2\frac{1}{2}}$
2413. 41	3	41422. 56	$a\ ^2P_{0\frac{1}{2}}—w\ ^2P^o_{0\frac{1}{2}}$ $b\ ^4P_{1\frac{1}{2}}—x\ ^4P^o_{0\frac{1}{2}}$
2413. 017	50	41429. 30	$a\ ^4P_{0\frac{1}{2}}—y\ ^4D^o_{0\frac{1}{2}}$ $a\ ^4F_{3\frac{1}{2}}—y\ ^2H^o_{4\frac{1}{2}}$
2412. 837	40	41432. 39	$a\ ^2D_{2\frac{1}{2}}—z\ ^2F^o_{3\frac{1}{2}}$
2412. 06	1	41445. 74	$b\ ^2H_{4\frac{1}{2}}—u\ ^2F^o_{3\frac{1}{2}}$
2411. 836	40	41449. 59	$a\ ^4F_{4\frac{1}{2}}—y\ ^2H^o_{4\frac{1}{2}}$
2411. 272	40	41459. 28	$a\ ^2D_{2\frac{1}{2}}—x\ ^4F^o_{1\frac{1}{2}}$
2411. 04	3	41463. 27	
2409. 49	1	41489. 94	
2409. 230	8	41494. 42	$b\ ^4G_{2\frac{1}{2}}—w\ ^2G^o_{3\frac{1}{2}}$ $b\ ^2G_{4\frac{1}{2}}—t\ ^2F^o_{3\frac{1}{2}}$
2408. 908	20	41499. 96	
2408. 337	20	41509. 80	$a\ ^4F_{2\frac{1}{2}}—y\ ^2D^o_{1\frac{1}{2}}$
2408. 08	1	41514. 23	
2407. 151	50Z	41530. 25	$a\ ^2D_{1\frac{1}{2}}—z\ ^2F^o_{2\frac{1}{2}}$
2405. 33	1	41561. 69	$b\ ^2H_{4\frac{1}{2}}—v\ ^2G^o_{4\frac{1}{2}}$

TABLE 1. *Wavelengths and term combinations of* Mo II—Continued

Wavelength λ_{air}	Intensity	Wave No.	Term combination
2405. 202	8	41563. 90	$a\ ^4H_{4\frac{1}{2}}-x\ ^2G^\circ_{4\frac{1}{2}}$ $a\ ^2F_{2\frac{1}{2}}-w\ ^4D^\circ_{1\frac{1}{2}}$
2405. 05	1	41566. 53	
2404. 680	50Z	41572. 92	$a\ ^2F_{3\frac{1}{2}}-y\ ^2D^\circ_{2\frac{1}{2}}$
2404. 46	1	41576. 73	
2403. 60	50Z	41591. 60	$a\ ^4F_{4\frac{1}{2}}-y\ ^2H^\circ_{5\frac{1}{2}}$
2403. 428	40Z	41594. 58	$a\ ^4F_{1\frac{1}{2}}-x\ ^4G^\circ_{2\frac{1}{2}}$
2403. 026	2	41601. 54	
2402. 64	2	41608. 22	
2402. 52	2	41610. 30	$a\ ^2G_{3\frac{1}{2}}-w\ ^4F^\circ_{2\frac{1}{2}}$
2401. 940	40Z	41620. 35	$a\ ^4P_{1\frac{1}{2}}-y\ ^4D^\circ_{0\frac{1}{2}}$
2401. 650	2	41625. 37	
2401. 35	2	41630. 57	
240042	1	41646. 70	$a\ ^2G_{3\frac{1}{2}}-x\ ^2G^\circ_{4\frac{1}{2}}$
2400. 14	1	41651. 56	
2399. 753	2	41658. 28	
2399. 48	3	41663. 01	
2398. 981	10	41671. 68	$a\ ^4H_{3\frac{1}{2}}-x\ ^4P^\circ_{2\frac{1}{2}}$
2397. 846	30Z	41690. 73	$b\ ^4P_{2\frac{1}{2}}-x\ ^2D^\circ_{2\frac{1}{2}}$
2397. 492	2	41697. 56	
2397. 116	20Z	41704. 10	$b\ ^2H_{4\frac{1}{2}}-t\ ^2F^\circ_{3\frac{1}{2}}$
2396. 827	4	41709. 12	$a\ ^4D_{2\frac{1}{2}}-z\ ^4G^\circ_{2\frac{1}{2}}$
2396. 519	4	41714. 48	$b\ ^4D_{1\frac{1}{2}}-w\ ^4D^\circ_{0\frac{1}{2}}$
2396. 260	25	41718. 99	$a\ ^4H_{3\frac{1}{2}}-x\ ^2G^\circ_{3\frac{1}{2}}$
2396. 020	15	41723. 17	$a\ ^2D_{2\frac{1}{2}}-x\ ^4F^\circ_{2\frac{1}{2}}$
2395. 057	8	41739. 95	$b\ ^4D_{1\frac{1}{2}}-w\ ^4D^\circ_{1\frac{1}{2}}$
2394. 522	3	41749. 27	
2394. 293	2	41753. 26	
2393. 992	8	41758. 51	$a\ ^2D_{2\frac{1}{2}}-x\ ^4F^\circ_{3\frac{1}{2}}$
2393. 428	1	41768. 35	
2393. 29	2	41770. 76	
2393. 174	4	41772. 78	$b\ ^2D_{1\frac{1}{2}}-w\ ^4G^\circ_{2\frac{1}{2}}$
2392. 776	10	41779. 73	$b\ ^2G^\circ_{3\frac{1}{2}}-t\ ^2F^\circ_{2\frac{1}{2}}$
2392. 650	8	41781. 93	
2392. 327	40Z	41787. 57	$a\ ^2S_{0\frac{1}{2}}-x\ ^2D^\circ_{1\frac{1}{2}}$
2391. 743	45Z	41797. 77	$a\ ^4F_{2\frac{1}{2}}-x\ ^4G^\circ_{2\frac{1}{2}}$
2390. 95	1	41811. 64	
2390. 783	50Z	41814. 56	
2390. 102	20Z	41826. 47	$a\ ^2I_{6\frac{1}{2}}-z\ ^2H^\circ_{5\frac{1}{2}}$
2389. 797	15Z	41831. 81	$a\ ^2F_{2\frac{1}{2}}-w\ ^4D^\circ_{2\frac{1}{2}}$
2389. 686	3	41833. 75	
2389. 437	3	41838. 11	$b\ ^4P_{0\frac{1}{2}}-x\ ^4P^\circ_{1\frac{1}{2}}$
2389. 250	40Z	41841. 39	$a\ ^4F^\circ_{3\frac{1}{2}}-y\ ^2G^\circ_{4\frac{1}{2}}$
2388. 703	35Z	41850. 97	$b\ ^2F_{2\frac{1}{2}}-w\ ^2F^\circ_{3\frac{1}{2}}$
2388. 08	8	41861. 88	$a\ ^4F_{4\frac{1}{2}}-y\ ^2G^\circ_{4\frac{1}{2}}$
2387. 819	15	41866. 46	$a\ ^2I_{6\frac{1}{2}}-y\ ^4H^\circ_{6\frac{1}{2}}$
2387. 629	8	41869. 79	$b\ ^2D_{2\frac{1}{2}}-t\ ^2F^\circ_{3\frac{1}{2}}$
2386. 96	25Z	41881. 47	$a\ ^2F_{3\frac{1}{2}}-x\ ^4G^\circ_{4\frac{1}{2}}$
2386. 07	45Z	41897. 15	$a\ ^4F_{2\frac{1}{2}}-(3)^\circ_{3\frac{1}{2}}$
2385. 811	3	41901. 69	
2385. 500	2	41907. 16	
2385. 368	2	41909. 47	
2385. 117	3	41913. 88	
2383. 371	20Z	41944. 59	$a\ ^4F_{1\frac{1}{2}}-y\ ^2D^\circ_{2\frac{1}{2}}$
2383. 06	8	41950. 05	$a\ ^2D_{2\frac{1}{2}}-z\ ^2F^\circ_{2\frac{1}{2}}$
2382. 408	3	41961. 54	
2382. 23	3	41964. 64	$c\ ^4D_{2\frac{1}{2}}-w\ ^4G^\circ_{3\frac{1}{2}}$
2381. 65	1	41974. 90	$a\ ^4H_{3\frac{1}{2}}-w\ ^4F^\circ_{2\frac{1}{2}}$
2381. 480	40Z	41977. 89	$a\ ^4F_{3\frac{1}{2}}-(3)^\circ_{3\frac{1}{2}}$
2381. 14	40Z	41983. 94	$a\ ^2G_{4\frac{1}{2}}-x\ ^2G^\circ_{4\frac{1}{2}}$
2380. 15	3	42001. 35	$b\ ^4D_{0\frac{1}{2}}-w\ ^4D^\circ_{0\frac{1}{2}}$
2380. 008	25Z	42003. 85	$a\ ^4D_{2\frac{1}{2}}-y\ ^4D^\circ_{3\frac{1}{2}}$
2379. 726	2	42008. 83	$b\ ^4D_{1\frac{1}{2}}-w\ ^4D^\circ_{2\frac{1}{2}}$
2379. 59	1	42011. 23	$a\ ^4H_{3\frac{1}{2}}-x\ ^2G^\circ_{3\frac{1}{2}}$
2379. 128	2	42019. 38	
2378. 929	2	42022. 90	
2378. 677	5	42027. 35	$b\ ^4D_{0\frac{1}{2}}-w\ ^4D^\circ_{1\frac{1}{2}}$
2378. 28	1	42034. 37	
2378. 05	1	42038. 43	
2377. 852	8	42041. 93	$b\ ^4P_{0\frac{1}{2}}-y\ ^2P^\circ_{0\frac{1}{2}}$
2377. 589	2	42046. 58	$b\ ^2D_{2\frac{1}{2}}-t\ ^2F^\circ_{2\frac{1}{2}}$
2377. 13	10Z	42054. 68	
2375. 895	3	42076. 56	
2375. 56	1	42082. 49	
2375. 44	4	42084. 65	$b\ ^2H_{3\frac{1}{2}}-v\ ^2G^\circ_{3\frac{1}{2}}$
2374. 900	20	42094. 19	$a\ ^2I_{3\frac{1}{2}}-z\ ^2H^\circ_{3\frac{1}{2}}$
2374. 236	2	42105. 96	
2373. 946	5	42111. 10	$a\ ^2G_{4\frac{1}{2}}-w\ ^4F^\circ_{3\frac{1}{2}}$
2372. 979	15Z	42128. 26	
2372. 642	10	42134. 24	$a\ ^2I_{3\frac{1}{2}}-y\ ^4H^\circ_{5\frac{1}{2}}$ $a\ ^4D_{2\frac{1}{2}}-z\ ^4G^\circ_{3\frac{1}{2}}$
2372. 508	1	42136. 62	
2371. 88	5	42147. 78	$a\ ^4F_{2\frac{1}{2}}-y\ ^2D^\circ_{2\frac{1}{2}}$
2371. 82	10	42148. 85	
2371. 58	20Z	42153. 11	$a\ ^4F_{2\frac{1}{2}}-x\ ^4G^\circ_{3\frac{1}{2}}$
2371. 258	8Z	42158. 83	$a\ ^2F_{3\frac{1}{2}}-w\ ^4D^\circ_{2\frac{1}{2}}$ $b\ ^4F_{4\frac{1}{2}}-w\ ^2G^\circ_{3\frac{1}{2}}$
2370. 410	35Z	42173. 92	$a\ ^4D_{1\frac{1}{2}}-y\ ^4D^\circ_{2\frac{1}{2}}$
2370. 250	40Z	42176. 76	$a\ ^2I_{6\frac{1}{2}}-y\ ^2H^\circ_{5\frac{1}{2}}$
2370. 024	3	42180. 78	
2369. 88	1	42183. 34	
2369. 74	1	42185. 84	
2368. 661	4	42204. 95	$b\ ^4F_{3\frac{1}{2}}-w\ ^2G^\circ_{3\frac{1}{2}}$ $a\ ^6D_{1\frac{1}{2}}-z\ ^4D^\circ_{0\frac{1}{2}}$
2368. 07	1	42215. 58	
2367. 33	2	42228. 78	$a\ ^4F_{3\frac{1}{2}}-y\ ^2D^\circ_{2\frac{1}{2}}$
2367. 12	3	42232. 53	
2367. 028	10	42234. 17	$a\ ^4F_{3\frac{1}{2}}-x\ ^4G^\circ_{3\frac{1}{2}}$
2366. 931	8	42235. 90	$a\ ^4F_{1\frac{1}{2}}-w\ ^4D^\circ_{0\frac{1}{2}}$
2366. 371	10	42245. 89	$a\ ^6D_{4\frac{1}{2}}-z\ ^4D^\circ_{3\frac{1}{2}}$
2366. 286	8	42247. 44	
2366. 105	25Z	42250. 64	$a\ ^4P_{0\frac{1}{2}}-y\ ^4D^\circ_{1\frac{1}{2}}$
2365. 876	10	42254. 73	$a\ ^2G_{4\frac{1}{2}}-w\ ^4F^\circ_{3\frac{1}{2}}$ $a\ ^4F_{4\frac{1}{2}}-x\ ^4G^\circ_{3\frac{1}{2}}$
2365. 496	10	42261. 52	$a\ ^4F_{1\frac{1}{2}}-w\ ^4D^\circ_{1\frac{1}{2}}$
2365. 01	1	42270. 20	$a\ ^6D_{2\frac{1}{2}}-z\ ^4D^\circ_{1\frac{1}{2}}$
2364. 522	20Z	42278. 92	$a\ ^2H_{4\frac{1}{2}}-x\ ^2H^\circ_{4\frac{1}{2}}$ $b\ ^4D_{2\frac{1}{2}}-x\ ^2F^\circ_{3\frac{1}{2}}$
2364. 19	2	42284. 86	$c\ ^4D_{3\frac{1}{2}}-w\ ^4G^\circ_{3\frac{1}{2}}$
2363. 77	3	42292. 37	
2363. 69	5	42293. 80	
2363. 226	5	42302. 11	$a\ ^2I_{3\frac{1}{2}}-y\ ^2H^\circ_{4\frac{1}{2}}$
2363. 07	1	42304. 90	
2363. 00	10	42306. 15	$a\ ^2D_{2\frac{1}{2}}-z\ ^4S^\circ_{1\frac{1}{2}}$
2362. 57	2h	42313. 86	
2362. 47	3	42315. 05	$a\ ^6D_{3\frac{1}{2}}-z\ ^4D^\circ_{2\frac{1}{2}}$
2362. 42	5	42316. 54	$b\ ^4D_{3\frac{1}{2}}-x\ ^2F^\circ_{2\frac{1}{2}}$ $b\ ^4F_{2\frac{1}{2}}-w\ ^2G^\circ_{3\frac{1}{2}}$
2362. 258	5	42319. 44	$b\ ^2F_{3\frac{1}{2}}-w\ ^2F^\circ_{2\frac{1}{2}}$
2361. 59	1	42331. 41	
2361. 27	2	42337. 15	$c\ ^4D_{2\frac{1}{2}}-v\ ^4D^\circ_{2\frac{1}{2}}$
2360. 933	2	42343. 19	

Wavelength λ_{air}	Intensity	Wave No.	Term combination
2359.370	15Z	42371.24	$b\ ^4D_{3\frac{1}{2}}$—$x\ ^4P^o_{2\frac{1}{2}}$
2359.052	15	42376.95	$a\ ^2H_{4\frac{1}{2}}$—$w\ ^2F^o_{3\frac{1}{2}}$
2358.535	2	42386.24	$a\ ^2H_{3\frac{1}{2}}$—$x\ ^2H^o_{4\frac{1}{2}}$
2357.344	10Z	42407.65	$a\ ^2D_{1\frac{1}{2}}$—$y\ ^2F^o_{2\frac{1}{2}}$
2356.77	1	42417.98	$a\ ^2D_{2\frac{1}{2}}$—$y\ ^2G^o_{3\frac{1}{2}}$
2356.46	1	42423.56	
2356.06	5	42430.76	$b\ ^2G_{4\frac{1}{2}}$—$v\ ^2G^o_{4\frac{1}{2}}$
2355.460	30Z	42441.57	$a\ ^4P_{1\frac{1}{2}}$—$y\ ^4D^o_{1\frac{1}{2}}$
2355.309	15	42444.29	$a\ ^2I_{5\frac{1}{2}}$—$y\ ^2H^o_{5\frac{1}{2}}$
2355.022	15	42449.46	$a\ ^4P_{2\frac{1}{2}}$—$y\ ^4D^o_{1\frac{1}{2}}$
2354.702	15	42455.23	$a\ ^6D_{0\frac{1}{2}}$—$z\ ^4D^o_{0\frac{1}{2}}$
2354.186	20	42464.53	$a\ ^4G_{4\frac{1}{2}}$—$z\ ^4H^o_{3\frac{1}{2}}$
2351.547	1	42512.18	$a\ ^4F_{2\frac{1}{2}}$—$w\ ^4D^o_{1\frac{1}{2}}$
2351.132	1	42519.69	$b\ ^4F_{4\frac{1}{2}}$—$w\ ^2H^o_{5\frac{1}{2}}$
2350.550	5	42530.22	$a\ ^4F_{1\frac{1}{2}}$—$w\ ^4D^o_{2\frac{1}{2}}$
2350.120	25Z	42538.00	$a\ ^4F_{3\frac{1}{2}}$—$x\ ^4G^o_{4\frac{1}{2}}$
2349.005	10	42558.19	$a\ ^4F_{4\frac{1}{2}}$—$x\ ^4G^o_{4\frac{1}{2}}$
2348.832	20Z	42561.32	$a\ ^4G_{3\frac{1}{2}}$—$z\ ^4H^o_{3\frac{1}{2}}$
2347.802	30Z	42579.99	$a\ ^2D_{1\frac{1}{2}}$—$y\ ^2D^o_{1\frac{1}{2}}$
2347.07	5	42593.27	$b\ ^2G_{4\frac{1}{2}}$—$w\ ^4G^o_{3\frac{1}{2}}$
2346.673	10	42600.48	$b\ ^2F_{3\frac{1}{2}}$—$x\ ^2H^o_{4\frac{1}{2}}$
2345.80	1w	42616.33	$b\ ^4D_{2\frac{1}{2}}$—$x\ ^4P^o_{2\frac{1}{2}}$
2345.699	2	42618.16	
2345.54	1	42621.05	
2345.27	1	42625.96	
2344.676	10Z	42636.76	$a\ ^4P_{0\frac{1}{2}}$—$z\ ^2S^o_{0\frac{1}{2}}$
2344.33	3	42643.05	
2343.880	1	42651.23	
2343.752	10	42653.56	$a\ ^6D_{1\frac{1}{2}}$—$z\ ^4D^o_{1\frac{1}{2}}$
2343.54	3	42657.42	$c\ ^4D_{3\frac{1}{2}}$—$v\ ^4D^o_{2\frac{1}{2}}$
2343.04	4	42666.50	$a\ ^4D_{1\frac{1}{2}}$—$z\ ^2D^o_{1\frac{1}{2}}$
2342.616	10	42674.25	$b\ ^4D_{3\frac{1}{2}}$—$w\ ^4F^o_{2\frac{1}{2}}$
2342.292	8	42680.15	
2341.57	40Z	42693.31	$a\ ^4G_{2\frac{1}{2}}$—$z\ ^4H^o_{3\frac{1}{2}}$
2341.20	1	42700.05	
2340.88	1	42705.89	
2340.41	35Z	42714.47	$a\ ^2I_{5\frac{1}{2}}$—$y\ ^2G^o_{4\frac{1}{2}}$
2339.376	8	42733.34	$a\ ^4D_{3\frac{1}{2}}$—$z\ ^4I^o_{4\frac{1}{2}}$
2339.190	5	42736.74	$a\ ^4F_{2\frac{1}{2}}$—$w\ ^4D^o_{2\frac{1}{2}}$
2338.482	10	42749.68	$a\ ^4G_{5\frac{1}{2}}$—$z\ ^4H^o_{4\frac{1}{2}}$
2337.67	3	42764.53	
2337.432	15Z	42768.88	$a\ ^4G_{4\frac{1}{2}}$—$z\ ^4H^o_{4\frac{1}{2}}$
2337.053	5	42775.82	$c\ ^4D_{3\frac{1}{2}}$—$v\ ^4D^o_{3\frac{1}{2}}$
2336.68	1	42782.65	
2336.220	10	42791.07	$a\ ^4D_{2\frac{1}{2}}$—$z\ ^2G^o_{3\frac{1}{2}}$
2335.81	10	42798.58	$a\ ^6D_{2\frac{1}{2}}$—$z\ ^4D^o_{2\frac{1}{2}}$
2335.392	10	42806.24	$a\ ^6D_{3\frac{1}{2}}$—$z\ ^4D^o_{3\frac{1}{2}}$
2335.18	1	42810.12	$b\ ^4G_{3\frac{1}{2}}$—$w\ ^2D^o_{2\frac{1}{2}}$
2334.942	20Z	42814.49	$a\ ^4F_{3\frac{1}{2}}$—$w\ ^4D^o_{2\frac{1}{2}}$
2334.84	20Z	42816.36	$a\ ^2D_{2\frac{1}{2}}$—$y\ ^2F^o_{3\frac{1}{2}}$
2334.22	3	42827.73	$a\ ^4P_{1\frac{1}{2}}$—$z\ ^2S^o_{0\frac{1}{2}}$
2334.066	5	42830.55	
2333.870	3	42834.15	$b\ ^2F_{2\frac{1}{2}}$—$x\ ^2D^o_{2\frac{1}{2}}$
2333.650	5	42838.19	$b\ ^4D_{5\frac{1}{2}}$—$w\ ^4F^o_{5\frac{1}{2}}$
2332.67	3	42856.18	
2332.48	1	42859.68	
2332.307	3	42862.85	$a\ ^4F_{3\frac{1}{2}}$—$w\ ^4D^o_{3\frac{1}{2}}$
2332.131	40Z	42866.09	$a\ ^4G_{3\frac{1}{2}}$—$z\ ^4H^o_{4\frac{1}{2}}$
2331.192	10	42883.35	$a\ ^4F_{4\frac{1}{2}}$—$w\ ^4D^o_{3\frac{1}{2}}$
2330.05	25	42904.37	$a\ ^6D_{0\frac{1}{2}}$—$z\ ^4D^o_{1\frac{1}{2}}$
2330.03	5	42904.74	
2329.708	50Z	42910.67	$a\ ^4F_{4\frac{1}{2}}$—$x\ ^4G^o_{5\frac{1}{2}}$
2328.95	8	42924.63	$a\ ^2F_{2\frac{1}{2}}$—$x\ ^2G^o_{3\frac{1}{2}}$
2328.89	1	42925.74	
2328.367	2	42935.38	
2328.115	8Z	42940.03	$b\ ^2D_{2\frac{1}{2}}$—$v\ ^2D^o_{2\frac{1}{2}}$
2327.815	4	42945.56	$a\ ^2H_{4\frac{1}{2}}$—$x\ ^2H^o_{5\frac{1}{2}}$
2326.93	1	42961.89	
2325.86	8	42981.65	$b\ ^4D_{3\frac{1}{2}}$—$w\ ^4F^o_{4\frac{1}{2}}$
2324.876	50	42999.85	$a\ ^2D_{2\frac{1}{2}}$—$y\ ^2D^o_{1\frac{1}{2}}$
2324.29	1	43010.69	
2323.96	50	43016.79	$b\ ^4P_{2\frac{1}{2}}$—$w\ ^2D^o_{1\frac{1}{2}}$
2322.971	10	43035.10	$c\ ^4D_{3\frac{1}{2}}$—$w\ ^4G^o_{4\frac{1}{2}}$
2322.499	25Z	43043.85	$a\ ^2H_{5\frac{1}{2}}$—$x\ ^2H^o_{5\frac{1}{2}}$
2321.955	1	43053.93	$b\ ^4D_{1\frac{1}{2}}$—$x\ ^4P^o_{2\frac{1}{2}}$
2321.67	2	43059.22	
2321.23	2	43067.38	$b\ ^4D_{2\frac{1}{2}}$—$w\ ^4F^o_{3\frac{1}{2}}$
2321.06	3	43070.53	
2320.090	30	43088.54	$a\ ^2S_{0\frac{1}{2}}$—$w\ ^2D^o_{1\frac{1}{2}}$
2318.897	2	43110.71	$c\ ^4D_{3\frac{1}{2}}$—$v\ ^4F^o_{4\frac{1}{2}}$
2316.477	25Z	43155.74	$b\ ^4P_{1\frac{1}{2}}$—$x\ ^2D^o_{1\frac{1}{2}}$
2316.040	10	43163.88	
2315.632	25Z	43171.48	
2315.087	5	43181.65	$a\ ^6D_{1\frac{1}{2}}$—$z\ ^4D^o_{2\frac{1}{2}}$
2313.878	15	43204.21	$a\ ^2F_{3\frac{1}{2}}$—$x\ ^4P^o_{2\frac{1}{2}}$
2313.154	10	43217.73	$a\ ^2D_{1\frac{1}{2}}$—$y\ ^2D^o_{2\frac{1}{2}}$
2312.927	2	43221.97	
2312.233	10	43234.94	
2311.382	20	43250.86	$a\ ^2F_{3\frac{1}{2}}$—$x\ ^2G^o_{3\frac{1}{2}}$
2310.85	1	43260.82	
2310.66	1	43264.37	$a\ ^4H_{5\frac{1}{2}}$—$x\ ^2H^o_{4\frac{1}{2}}$
2309.485	20	43286.38	$a\ ^2H_{4\frac{1}{2}}$—$w\ ^2G^o_{4\frac{1}{2}}$
2309.40	1	43287.95	$a\ ^2D_{2\frac{1}{2}}$—$x\ ^4G^o_{2\frac{1}{2}}$
2309.33	1	43289.26	$a\ ^6D_{2\frac{1}{2}}$—$z\ ^4D^o_{3\frac{1}{2}}$
2308.897	2	43297.21	
2308.114	1	43312.07	
2307.994	30Z	43314.31	$b\ ^2F_{2\frac{1}{2}}$—$w\ ^2G^o_{3\frac{1}{2}}$
2307.178	1	43329.63	$a\ ^4G_{5\frac{1}{2}}$—$z\ ^4H^o_{5\frac{1}{2}}$
2306.990	50Z	43333.16	$b\ ^4D_{2\frac{1}{2}}$—$x\ ^4P^o_{1\frac{1}{2}}$
2305.874	8	43354.14	$a\ ^4G_{4\frac{1}{2}}$—$z\ ^4H^o_{5\frac{1}{2}}$
2305.673	30Z	43357.92	$a\ ^4P_{1\frac{1}{2}}$—$z\ ^4G^o_{2\frac{1}{2}}$
2305.453	5	43362.05	$a\ ^4D_{2\frac{1}{2}}$—$y\ ^4D^o_{3\frac{1}{2}}$
2305.276	8	43365.38	$a\ ^4P_{2\frac{1}{2}}$—$z\ ^4G^o_{3\frac{1}{2}}$
2304.261	80Z	43384.48	$a\ ^2H_{5\frac{1}{2}}$—$w\ ^2G^o_{4\frac{1}{2}}$
2302.995	8	43408.33	
2302.848	20	43411.13	$a\ ^2I_{5\frac{1}{2}}$—$x\ ^4G^o_{4\frac{1}{2}}$
2302.48	2	43418.06	
2302.143	8	43424.42	
2301.004	2	43445.91	
2300.697	1	43451.71	
2300.41	1	43457.13	$a\ ^4F_{2\frac{1}{2}}$—$x\ ^2F^o_{3\frac{1}{2}}$
2300.096	2	43463.06	
2299.876	10	43467.22	
2299.657	1	43471.36	
2298.888	3	43485.90	

TABLE 1. *Wavelengths and term combinations of* Mo II—Continued

Wavelength λ_{air}	Intensity	Wave No.	Term combination	Wavelength λ_{air}	Intensity	Wave No.	Term combination
2298. 386	8	43495. 40	$a\ ^2I_{6\frac{1}{2}}$—$x\ ^4G^\circ_{5\frac{1}{2}}$	2264. 746	10	44141. 41	$a\ ^4P_{1\frac{1}{2}}$—$z\ ^2D^\circ_{1\frac{1}{2}}$
2297. 650	5	43509. 33	$a\ ^2D_{1\frac{1}{2}}$—$w\ ^4D^\circ_{0\frac{1}{2}}$	2264. 461	2	44146. 96	
2297. 492	2	43512. 32		2264. 333	2	44149. 46	$a\ ^4P_{2\frac{1}{2}}$—$z\ ^2D^\circ_{1\frac{1}{2}}$
2297. 143	2	43518. 93		2264. 19	1	44152. 24	
2296. 98	5	43522. 02		2263. 793	5	44159. 99	$b\ ^2F_{2\frac{1}{2}}$—$w\ ^2D^\circ_{1\frac{1}{2}}$
2296. 28	1	43535. 28	$a\ ^2D_{1\frac{1}{2}}$—$w\ ^4D^\circ_{1\frac{1}{2}}$	2263. 664	5	44162. 50	$a\ ^4F_{3\frac{1}{2}}$—$w\ ^4F^\circ_{2\frac{1}{2}}$
2295. 86	1	43543. 25	$a\ ^2F_{3\frac{1}{2}}$—$x\ ^2G^\circ_{4\frac{1}{2}}$	2261. 981	30	44195. 36	$a\ ^2H_{4\frac{1}{2}}$—$w\ ^2H^\circ_{4\frac{1}{2}}$
2293. 74	1	43583. 49		2261. 79	1	44199. 09	$a\ ^4F_{3\frac{1}{2}}$—$x\ ^2G^\circ_{4\frac{1}{2}}$
2292. 968	3	43598. 16	$a\ ^2G_{3\frac{1}{2}}$—$x\ ^2H^\circ_{4\frac{1}{2}}$	2261. 51	1	44204. 56	
2292. 82	1	43600. 97	$b\ ^2F_{3\frac{1}{2}}$—$w\ ^2G^\circ_{4\frac{1}{2}}$	2260. 748	3	44219. 46	$a\ ^4F_{4\frac{1}{2}}$—$x\ ^2G^\circ_{4\frac{1}{2}}$
2292. 583	5	43605. 48	$a\ ^2F_{2\frac{1}{2}}$—$x\ ^4P^\circ_{1\frac{1}{2}}$	2260. 541	3	44223. 51	$a\ ^2D_{2\frac{1}{2}}$—$w\ ^4D^\circ_{2\frac{1}{2}}$
2292. 17	1	43613. 34	$a\ ^4H_{4\frac{1}{2}}$—$w\ ^2F^\circ_{3\frac{1}{2}}$	2260. 417	1	44225. 94	
2290. 870	40	43638. 08	$a\ ^2D_{2\frac{1}{2}}$—$y\ ^2D^\circ_{2\frac{1}{2}}$	2260. 07	20	44232. 73	$a\ ^4G_{5\frac{1}{2}}$—$z\ ^4I^\circ_{4\frac{1}{2}}$
2290. 311	50*Z*	43648. 73	$a\ ^4P_{1\frac{1}{2}}$—$y\ ^4D^\circ_{2\frac{1}{2}}$ $a\ ^4D_{2\frac{1}{2}}$—$z\ ^2D^\circ_{2\frac{1}{2}}$	2258. 87	1	44256. 22	
2289. 890	25*Z*	43656. 76	$a\ ^4P_{2\frac{1}{2}}$—$y\ ^4D^\circ_{2\frac{1}{2}}$	2258. 24	1	44268. 56	$a\ ^2S_{0\frac{1}{2}}$—$x\ ^2P^\circ_{1\frac{1}{2}}$
2289. 38	1	43666. 48		2258. 05	1	44272. 29	$a\ ^2D_{2\frac{1}{2}}$—$w\ ^4D^\circ_{3\frac{1}{2}}$
2289. 20	10	43669. 99	$a\ ^2F_{3\frac{1}{2}}$—$w\ ^4F^\circ_{3\frac{1}{2}}$	2257. 705	5	44279. 05	$a\ ^4G_{2\frac{1}{2}}$—$z\ ^4G^\circ_{3\frac{1}{2}}$
2288. 73	2	43678. 88	$c\ ^2F_{3\frac{1}{2}}$—$u\ ^2D^\circ_{2\frac{1}{2}}$	2257. 520	2	44282. 68	$a\ ^4D_{1\frac{1}{2}}$—$y\ ^4P^\circ_{1\frac{1}{2}}$
2287. 64	2	43699. 69		2256. 982	15	44293. 24	$a\ ^2H_{5\frac{1}{2}}$—$w\ ^2H^\circ_{5\frac{1}{2}}$
2287. 10	5	43710. 01		2256. 263	1	44307. 35	$a\ ^2G_{3\frac{1}{2}}$—$x\ ^2D^\circ_{2\frac{1}{2}}$
2286. 547	5	43720. 58		2255. 290	7	44326. 47	$a\ ^4F_{3\frac{1}{2}}$—$w\ ^4F^\circ_{3\frac{1}{2}}$
2286. 432	10	43722. 78	$a\ ^4G_{3\frac{1}{2}}$—$z\ ^4G^\circ_{2\frac{1}{2}}$	2254. 706	5	44337. 95	$a\ ^4D_{0\frac{1}{2}}$—$y\ ^4P^\circ_{0\frac{1}{2}}$
2284. 74	1	43755. 15	$a\ ^4D_{3\frac{1}{2}}$—$y\ ^4D^\circ_{3\frac{1}{2}}$	2254. 50	1	44342. 00	$b\ ^4F_{2\frac{1}{2}}$—$x\ ^2P^\circ_{1\frac{1}{2}}$
2283. 58	8	43777. 38		2254. 28	1	44346. 32	$a\ ^4F_{4\frac{1}{2}}$—$w\ ^4F^\circ_{3\frac{1}{2}}$
2283. 292	8	43782. 90	$b\ ^2F_{3\frac{1}{2}}$—$w\ ^2G^\circ_{3\frac{1}{2}}$ $b\ ^4D_{1\frac{1}{2}}$—$x\ ^4P^\circ_{1\frac{1}{2}}$	2254. 146	15	44348. 96	$a\ ^4G_{3\frac{1}{2}}$—$z\ ^4I^\circ_{4\frac{1}{2}}$
2282. 896	10	43790. 50	$b\ ^4D_{2\frac{1}{2}}$—$y\ ^2P^\circ_{1\frac{1}{2}}$	2253. 85	2	44354. 78	
2282. 218	3	43803. 50	$a\ ^2D_{1\frac{1}{2}}$—$w\ ^4D^\circ_{2\frac{1}{2}}$	2252. 13	1	44388. 66	$b\ ^4D_{3\frac{1}{2}}$—$w\ ^2F^\circ_{2\frac{1}{2}}$
2281. 45	2	43818. 25	$a\ ^4D_{1\frac{1}{2}}$—$z\ ^2D^\circ_{2\frac{1}{2}}$	2252. 05	3	44390. 23	$b\ ^4D_{1\frac{1}{2}}$—$x\ ^4P^\circ_{0\frac{1}{2}}$
2281. 39	1	43819. 40		2251. 423	3	44402. 59	$a\ ^4D_{2\frac{1}{2}}$—$z\ ^2P^\circ_{1\frac{1}{2}}$
2281. 34	2	43820. 36		2251. 316	3*5e*	44404. 70	
2281. 23	1	43822. 47		2251. 13	1	44408. 37	
2281. 05	1	43825. 93	$a\ ^4F_{2\frac{1}{2}}$—$x\ ^2G^\circ_{3\frac{1}{2}}$	2249. 315	20	44444. 20	$a\ ^4P_{2\frac{1}{2}}$—$z\ ^2G^\circ_{3\frac{1}{2}}$
2280. 29	1	43840. 54	$b\ ^4F_{3\frac{1}{2}}$—$w\ ^2D^\circ_{2\frac{1}{2}}$	2248. 75	15	44455. 37	
2280. 12	1	43843. 80		2247. 12	8	44487. 61	
2279. 586	8	43854. 07	$a\ ^4G_{2\frac{1}{2}}$—$z\ ^4G^\circ_{2\frac{1}{2}}$	2246. 980	40	44490. 38	$a\ ^4F_{4\frac{1}{2}}$—$w\ ^4F^\circ_{4\frac{1}{2}}$
2279. 30	1	43859. 58	$a\ ^4F_{3\frac{1}{2}}$—$x\ ^4P^\circ_{2\frac{1}{2}}$	2246. 34	20	44503. 06	$c\ ^2G_{4\frac{1}{2}}$—$u\ ^2G^\circ_{4\frac{1}{2}}$
2279. 13	1	43862. 85		2245. 28	1	44524. 07	$d\ ^2G_{3\frac{1}{2}}$—$t\ ^2D^\circ_{2\frac{1}{2}}$
2279. 04	1	43864. 58		2244. 64	1	44536. 76	
2278. 775	3	43869. 68		2242. 84	2	44572. 50	$a\ ^4D_{1\frac{1}{2}}$—$z\ ^2P^\circ_{1\frac{1}{2}}$
2278. 32	1	43878. 44	$a\ ^4F_{1\frac{1}{2}}$—$w\ ^4F^\circ_{2\frac{1}{2}}$	2242. 606	30	44577. 15	
2278. 074	3	43883. 18		2241. 63	3	44596. 56	$a\ ^2S^\circ_{0\frac{1}{2}}$—$w^2P_{0\frac{1}{2}}$
2276. 93	1	43905. 22		2241. 353	2	44602. 07	$a\ ^2G^\circ_{4\frac{1}{2}}$—$x\ ^2H^\circ_{5\frac{1}{2}}$
2276. 67	2	43910. 24		2241. 19	7	44605. 27	$a\ ^2G^\circ_{3\frac{1}{2}}$—$w^2G^\circ_{4\frac{1}{2}}$
2276. 198	40	43919. 34	$a\ ^2H_{5\frac{1}{2}}$—$w\ ^2H^\circ_{5\frac{1}{2}}$	2241. 045	1	44608. 20	
2274. 346	5	43955. 10	$a\ ^2D_{2\frac{1}{2}}$—$w\ ^4D^\circ_{1\frac{1}{2}}$	2240. 57	15	44617. 60	$b\ ^4D_{2\frac{1}{2}}$—$w^2F^\circ_{2\frac{1}{2}}$
2274. 07	1	43960. 44	$a\ ^4D_{1\frac{1}{2}}$—$y\ ^4P^\circ_{0\frac{1}{2}}$	2239. 77	6*w*	44633. 55	
2273. 961	5	43962. 54	$a\ ^4H_{3\frac{1}{2}}$—$x\ ^2H^\circ_{4\frac{1}{2}}$	2239. 42	50	44641. 32	$a\ ^2I^\circ_{5\frac{1}{2}}$—$z\ ^2K^\circ_{6\frac{1}{2}}$ $a\ ^4G_{2\frac{1}{2}}$—$z\ ^2D^\circ_{1\frac{1}{2}}$
2273. 240	40	43976. 49		2238. 88	5	44651. 29	
2271. 80	2*h*	44004. 36		2238. 42	18	44660. 46	$a\ ^4D_{0\frac{1}{2}}$—$y\ ^4P^\circ_{1\frac{1}{2}}$
2271. 14	1	44017. 14	$a\ ^4G_{3\frac{1}{2}}$—$y\ ^4D^\circ_{2\frac{1}{2}}$	2238. 02	7	44668. 44	
2270. 33	3	44032. 87	$a\ ^2G_{4\frac{1}{2}}$—$w\ ^2F^\circ_{3\frac{1}{2}}$	2237. 57	7	44677. 42	$b\ ^4D_{0\frac{1}{2}}$—$x\ ^4P^\circ_{0\frac{1}{2}}$
2270. 214	3	44035. 10		2236. 04	50	44707. 99	$a\ ^4G_{4\frac{1}{2}}$—$z\ ^2G^\circ_{3\frac{1}{2}}$
2269. 708	150*Z*	44044. 91	$a\ ^4G_{5\frac{1}{2}}$—$z\ ^4H^\circ_{6\frac{1}{2}}$	2235. 68	35	44715. 19	
2269. 407	8	44050. 75	$a\ ^4G_{4\frac{1}{2}}$—$z\ ^4G^\circ_{3\frac{1}{2}}$	2234. 97	4	44729. 39	
2268. 468	25	44068. 99	$b\ ^4D_{0\frac{1}{2}}$—$x\ ^4P^\circ_{1\frac{1}{2}}$	2234. 49	10	44739. 00	
2268. 05	1	44077. 11		2234. 15	2	44745. 81	
2267. 82	1	44081. 58	$a\ ^4F_{2\frac{1}{2}}$—$w\ ^4F^\circ_{2\frac{1}{2}}$	2233. 17	1	44765. 44	$a\ ^4F_{1\frac{1}{2}}$—$y\ ^2P^\circ_{1\frac{1}{2}}$
2267. 112	8	44095. 34	$c\ ^2G_{3\frac{1}{2}}$—$u\ ^2G^\circ_{3\frac{1}{2}}$	2232. 44	30	44780. 08	$a\ ^4G_{5\frac{1}{2}}$—$z\ ^4G^\circ_{4\frac{1}{2}}$
2266. 224	10	44112. 62	$a\ ^4D_{2\frac{1}{2}}$—$y\ ^4P^\circ_{1\frac{1}{2}}$	2232. 05	25	44787. 90	$a\ ^2G_{3\frac{1}{2}}$—$w^2G^\circ_{3\frac{1}{2}}$
2264. 956	3	44137. 31		2231. 49	18	44799. 14	$a\ ^4G_{4\frac{1}{2}}$—$z\ ^4G^\circ_{4\frac{1}{2}}$

TABLE 1. *Wavelengths and term combinations of* Mo II—Continued

Wavelength λ_{air}	Intensity	Wave No.	Term combination	Wavelength λ_{air}	Intensity	Wave No.	Term combination
2231. 23	7	44804. 36	$a\ ^4G_{3\frac{1}{2}}$—$z\ ^2G^\circ_{3\frac{1}{2}}$	2198. 52	1	45470. 90	
2231. 08	40	44807. 38	$a\ ^4H_{3\frac{1}{2}}$—$w\ ^2H^\circ_{3\frac{1}{2}}$	2198. 15	30*d*	45478. 56	$a\ ^2G_{4\frac{1}{2}}$—$w\ ^2H^\circ_{5\frac{1}{2}}$; $a\ ^4D_{3\frac{1}{2}}$—$y\ ^4P^\circ_{2\frac{1}{2}}$
2230. 07	35	44827. 67					
2229. 81	2	44832. 89					
2228. 24	4	44864. 48		2197. 48	100	45492. 41	$a\ ^2I_{5\frac{1}{2}}$—$y\ ^2I^\circ_{5\frac{1}{2}}$
				2197. 36	2	45494. 90	$a\ ^2F_{3\frac{1}{2}}$—$x\ ^2H^\circ_{4\frac{1}{2}}$
2226. 78	25	44893. 89	$a\ ^2F_{2\frac{1}{2}}$—$w\ ^2F^\circ_{2\frac{1}{2}}$	2197. 27	25	45496. 76	$a\ ^4G_{4\frac{1}{2}}$—$z\ ^4I^\circ_{5\frac{1}{2}}$
2226. 32	1	44903. 17		2196. 97	10	45502. 97	$a\ ^4G_{2\frac{1}{2}}$—$y\ ^4D^\circ_{3\frac{1}{2}}$
2226. 06	20	44908. 41	$a\ ^2I_{5\frac{1}{2}}$—$z\ ^2K^\circ_{6\frac{1}{2}}$	2196. 38	1	45515. 20	$a\ ^2G_{3\frac{1}{2}}$—$w\ ^2H^\circ_{4\frac{1}{2}}$
2225. 44	5	44920. 72					
2224. 64	35	44937. 07	$a\ ^4G_{2\frac{1}{2}}$—$z\ ^2G^\circ_{3\frac{1}{2}}$	2195. 95	1	45524. 11	
				2195. 83	3	45526. 60	$a\ ^4G_{3\frac{1}{2}}$—$z\ ^2G^\circ_{4\frac{1}{2}}$
2224. 37	3	44942. 53	$a\ ^2G_{4\frac{1}{2}}$—$w\ ^2G^\circ_{4\frac{1}{2}}$	2194. 94	12	45545. 06	$a\ ^4G_{4\frac{1}{2}}$—$z\ ^2G^\circ_{4\frac{1}{2}}$; $a\ ^4D_{3\frac{1}{2}}$—$x\ ^4D^\circ_{3\frac{1}{2}}$
2222. 95	2	44971. 23					
2222. 06	1	44989. 25	$b\ ^4D_{2\frac{1}{2}}$—$w\ ^2F^\circ_{3\frac{1}{2}}$	2193. 92	2	45566. 23	$a\ ^4P_{0\frac{1}{2}}$—$y\ ^4P^\circ_{1\frac{1}{2}}$
2221. 63	20	44997. 95	$a\ ^4D_{2\frac{1}{2}}$—$x\ ^4D^\circ_{3\frac{1}{2}}$	2193. 76	4	45569. 55	
2220. 99	65	45010. 92	$a\ ^4P_{2\frac{1}{2}}$—$y\ ^4D^\circ_{3\frac{1}{2}}$	2193. 65	5	45571. 84	$a\ ^2D_{2\frac{1}{2}}$—$w\ ^4F^\circ_{2\frac{1}{2}}$
				2193. 56	6	45573. 71	$a\ ^4D_{2\frac{1}{2}}$—$y\ ^4G^\circ_{3\frac{1}{2}}$
2219. 82	20	45034. 64		2192. 90	1	45587. 42	
2219. 22	1	45046. 81					
2218. 78	1	45055. 74		2192. 66	7	45592. 41	$a\ ^2F_{3\frac{1}{2}}$—$w\ ^2F^\circ_{3\frac{1}{2}}$; $a\ ^4F_{1\frac{1}{2}}$—$w\ ^2F^\circ_{2\frac{1}{2}}$
2217. 89	18	45073. 83	$b\ ^2F_{3\frac{1}{2}}$—$v\ ^2F^\circ_{2\frac{1}{2}}$	2191. 24	3	45621. 95	$b\ ^2F_{3\frac{1}{2}}$—$v\ ^2F^\circ_{3\frac{1}{2}}$
2217. 60	8	45079. 72					
				2191. 01	3	45626. 74	
2217. 52	10	45081. 34	$a\ ^4D_{2\frac{1}{2}}$—$y\ ^4P^\circ_{2\frac{1}{2}}$	2190. 26	10	45642. 35	$a\ ^4G_{3\frac{1}{2}}$—$z\ ^2G^\circ_{4\frac{1}{2}}$
2216. 60	40	45100. 05	$a\ ^2S_{0\frac{1}{2}}$—$w\ ^2P^\circ_{1\frac{1}{2}}$	2190. 00	20	45647. 78	$a\ ^4D_{3\frac{1}{2}}$—$(1)^\circ_{2\frac{1}{2}}$
2216. 48	5	45102. 49		2189. 40	50	45660. 29	$a\ ^2I_{6\frac{1}{2}}$—$y\ ^2I^\circ_{6\frac{1}{2}}$
2215. 05	1	45131. 61					
2214. 39	45	45145. 05	$d\ ^2D_{2\frac{1}{2}}$—$s\ ^2F^\circ_{3\frac{1}{2}}$	2188. 96	25	45669. 46	$b\ ^4D_{3\frac{1}{2}}$—$w\ ^2G^\circ_{4\frac{1}{2}}$; $a\ ^4G_{5\frac{1}{2}}$—$z\ ^4G^\circ_{5\frac{1}{2}}$
2214. 26	30	45147. 70	$a\ ^4D_{2\frac{1}{2}}$—$x\ ^4D^\circ_{3\frac{1}{2}}$	2188. 64	7	45676. 14	
2214. 02	10	45152. 60	$a\ ^4H_{3\frac{1}{2}}$—$w\ ^2G^\circ_{3\frac{1}{2}}$	2188. 27	2	45683. 86	
2213. 74	4	45158. 31		2188. 04	40	45688. 67	$a\ ^4G_{4\frac{1}{2}}$—$z\ ^4G^\circ_{5\frac{1}{2}}$
2213. 68	5	45159. 53	$b\ ^4G_{2\frac{1}{2}}$—$w\ ^4G^\circ_{2\frac{1}{2}}$	2187. 62	18	45697. 44	$a\ ^4D_{2\frac{1}{2}}$—$y\ ^4G^\circ_{2\frac{1}{2}}$
2213. 26	12	45168. 10	$a\ ^4D_{1\frac{1}{2}}$—$x\ ^4D^\circ_{2\frac{1}{2}}$	2187. 46	3	45700. 78	
2213. 00	1	45173. 41	$b\ ^4F_{2\frac{1}{2}}$—$w\ ^2P^\circ_{1\frac{1}{2}}$	2187. 10	1	45708. 30	
2212. 62	2	45181. 17	$a\ ^4H_{3\frac{1}{2}}$—$w\ ^2H^\circ_{4\frac{1}{2}}$	2186. 80	8	45714. 57	
2212. 16	7	45190. 56		2186. 38	8	45723. 38	$a\ ^6D_{2\frac{1}{2}}$—$y\ ^4D^\circ_{1\frac{1}{2}}$
2211. 39	10*w*	45206. 29	$a\ ^4D_{2\frac{1}{2}}$—$x\ ^4D^\circ_{1\frac{1}{2}}$	2185. 79	8	45735. 69	$a\ ^2D_{2\frac{1}{2}}$—$w\ ^4F^\circ_{3\frac{1}{2}}$
2210. 70	10	45220. 40	$a\ ^2F_{3\frac{1}{2}}$—$w\ ^2F^\circ_{2\frac{1}{2}}$	2185. 52	3	45741. 34	
2209. 83	18	45238. 20	$c\ ^2F_{2\frac{1}{2}}$—$u\ ^2G^\circ_{3\frac{1}{2}}$	2184. 89	25	45754. 53	$a\ ^4D_{0\frac{1}{2}}$—$x\ ^4D^\circ_{1\frac{1}{2}}$
2209. 56	25	45243. 73	$a\ ^4P_{0\frac{1}{2}}$—$y\ ^4P^\circ_{0\frac{1}{2}}$	2184. 73	12	45757. 88	$a\ ^4P_{1\frac{1}{2}}$—$y\ ^4P^\circ_{1\frac{1}{2}}$
2209. 21	3	45250. 89	$a\ ^4D_{1\frac{1}{2}}$—$y\ ^4P^\circ_{2\frac{1}{2}}$; $a\ ^4D_{2\frac{1}{2}}$—$(1)^\circ_{2\frac{1}{2}}$	2184. 59	10	45760. 81	$a\ ^4D_{2\frac{1}{2}}$—$y\ ^4F^\circ_{3\frac{1}{2}}$; $b\ ^4F_{3\frac{1}{2}}$—$t\ ^2F^\circ_{3\frac{1}{2}}$
2208. 72	2	45260. 93	$c\ ^2G_{4\frac{1}{2}}$—$t\ ^2G^\circ_{4\frac{1}{2}}$	2184. 46	20	45763. 53	$a\ ^4D_{1\frac{1}{2}}$—$x\ ^4D^\circ_{0\frac{1}{2}}$
2208. 18	40	45272. 00	$d\ ^2D_{2\frac{1}{2}}$—$t\ ^2D^\circ_{2\frac{1}{2}}$	2184. 36	100	45765. 64	$a\ ^4P_{2\frac{1}{2}}$—$y\ ^4P^\circ_{1\frac{1}{2}}$
				2183. 61	10	45781. 35	$a\ ^2D_{1\frac{1}{2}}$—$y\ ^2P^\circ_{0\frac{1}{2}}$
2207. 13	2	45293. 54	$a\ ^4P_{1\frac{1}{2}}$—$z\ ^2D^\circ_{2\frac{1}{2}}$	2183. 48	5	45784. 08	
2206. 84	30	45299. 49	$a\ ^4D_{0\frac{1}{2}}$—$z\ ^2P^\circ_{0\frac{1}{2}}$	2182. 76	10	45804. 00	$a\ ^2I_{6\frac{1}{2}}$—$z\ ^2K^\circ_{7\frac{1}{2}}$
2206. 44	25	45307. 70	$a\ ^2H_{4\frac{1}{2}}$—$v\ ^2F^\circ_{3\frac{1}{2}}$				
2206. 06	18	45315. 50	$a\ ^2D_{2\frac{1}{2}}$—$x\ ^2G^\circ_{3\frac{1}{2}}$	2181. 98	12*w*	45815. 54	$b\ ^4G_{3\frac{1}{2}}$—$w\ ^4G^\circ_{3\frac{1}{2}}$; $c\ ^2F_{3\frac{1}{2}}$—$u\ ^2G^\circ_{4\frac{1}{2}}$
2205. 40	2	45329. 06		2181. 36	22	45828. 56	$a\ ^4D_{1\frac{1}{2}}$—$y\ ^4F^\circ_{1\frac{1}{2}}$
2204. 86	22	45340. 16	$b\ ^2F_{2\frac{1}{2}}$—$x\ ^2P^\circ_{1\frac{1}{2}}$	2181. 01	2	45835. 92	
2204. 71	2	45343. 25	$a\ ^2I_{5\frac{1}{2}}$—$w\ ^4F^\circ_{4\frac{1}{2}}$				
2204. 59	2	45345. 72		2180. 26	15	45851. 68	$a\ ^2G_{4\frac{1}{2}}$—$w\ ^2H^\circ_{4\frac{1}{2}}$; $b\ ^4D_{3\frac{1}{2}}$—$w\ ^2G^\circ_{3\frac{1}{2}}$
2203. 33	3	45371. 64	$b\ ^4D_{3\frac{1}{2}}$—$x\ ^2D^\circ_{2\frac{1}{2}}$; $a\ ^4G_{3\frac{1}{2}}$—$y\ ^4D^\circ_{3\frac{1}{2}}$	2180. 02	8	45856. 73	$a\ ^4P_{0\frac{1}{2}}$—$z\ ^2P^\circ_{1\frac{1}{2}}$
2203. 14	4	45375. 56		2179. 02	2	45877. 77	
				2178. 32	2	45892. 51	
2202. 75	5	45383. 59		2177. 87	15	45901. 99	$a\ ^2F_{2\frac{1}{2}}$—$x\ ^2D^\circ_{1\frac{1}{2}}$
2202. 35	2	45391. 83		2177. 52	10	45909. 37	
2202. 11	4	45396. 78		2176. 65	3	45927. 72	$a\ ^2I_{5\frac{1}{2}}$—$y\ ^2I^\circ_{5\frac{1}{2}}$
2201. 89	3	45401. 31		2176. 40	2	45932. 99	
2201. 48	6	45409. 77		2176. 18	3	45937. 64	
2200. 99	40*d*	45419. 88	$b\ ^2F_{3\frac{1}{2}}$—$w\ ^2D^\circ_{2\frac{1}{2}}$; $a\ ^4D_{1\frac{1}{2}}$—$(1)^\circ_{2\frac{1}{2}}$	2175. 40	12	45954. 11	$a\ ^4D_{2\frac{1}{2}}$—$y\ ^4H^\circ_{3\frac{1}{2}}$
				2175. 06	1	45961. 29	
2200. 59	5	45428. 13		2174. 59	2	45971. 22	$a\ ^4D_{3\frac{1}{2}}$—$y\ ^4G^\circ_{3\frac{1}{2}}$
2200. 25	22	45435. 18	$b\ ^4P_{0\frac{1}{2}}$—$w\ ^2D^\circ_{1\frac{1}{2}}$; $a\ ^4P_{1\frac{1}{2}}$—$y\ ^4P^\circ_{0\frac{1}{2}}$	2174. 40	2	45975. 24	$b\ ^4F_{1\frac{1}{2}}$—$w\ ^4G^\circ_{2\frac{1}{2}}$
				2174. 08	15	45982. 00	$b\ ^4F_{2\frac{1}{2}}$—$w\ ^4G^\circ_{2\frac{1}{2}}$

TABLE 1. *Wavelengths and term combinations of* Mo II—Continued

Wavelength λ_{air}	Intensity	Wave No.	Term combination	Wavelength λ_{air}	Intensity	Wave No.	Term combination
2173. 70	3	45990. 04		2147. 12	6	46559. 30	$a\ ^4D_{2\frac{1}{2}}$—$x\ ^4F^\circ_{1\frac{1}{2}}$
2173. 54	1	45993. 42		2146. 85	10	46565. 16	$b\ ^4G_{3\frac{1}{2}}$—$w\ ^4G^\circ_{4\frac{1}{2}}$
2173. 14	12	46001. 89	$a\ ^2P_{1\frac{1}{2}}$—$u\ ^2D^\circ_{2\frac{1}{2}}$	2146. 46	10	46573. 62	$c\ ^2F_{3\frac{1}{2}}$—$t\ ^2G^\circ_{4\frac{1}{2}}$
2172. 90	15	46006. 97	$a\ ^4D_{3\frac{1}{2}}$—$y\ ^4G^\circ_{3\frac{1}{2}}$				
2170. 94	20	46048. 51	$a\ ^4D_{2\frac{1}{2}}$—$y\ ^4F^\circ_{2\frac{1}{2}}$	2146. 21	1	46579. 04	$b\ ^4D_{3\frac{1}{2}}$—$w\ ^2H^\circ_{4\frac{1}{2}}$
				2145. 24	7	46600. 10	$a\ ^4F_{1\frac{1}{2}}$—$x\ ^2D^\circ_{1\frac{1}{2}}$
2170. 15	10	46065. 27	$a\ ^4D_{3\frac{1}{2}}$—(2)$^\circ_{3\frac{1}{2}}$	2145. 09	6	46603. 36	
2169. 52	22	46078. 64	$a\ ^2G_{3\frac{1}{2}}$—$v\ ^2F^\circ_{2\frac{1}{2}}$ $b\ ^4D_{1\frac{1}{2}}$—$x\ ^2D^\circ_{1\frac{1}{2}}$	2144. 59	1	46614. 22	$a\ ^6S_{2\frac{1}{2}}$—$z\ ^6F^\circ_{2\frac{1}{2}}$
				2143. 25	40	46643. 36	$a\ ^4P_{1\frac{1}{2}}$—$x\ ^4D^\circ_{2\frac{1}{2}}$
2169. 39	5	46081. 40	$b\ ^4D_{2\frac{1}{2}}$—$w\ ^2G^\circ_{3\frac{1}{2}}$				
2168. 77	20	46094. 57	$a\ ^4D_{3\frac{1}{2}}$—$y\ ^4G^\circ_{3\frac{1}{2}}$	2142. 44	22	46661. 00	$a\ ^4P_{0\frac{1}{2}}$—$x\ ^4D^\circ_{1\frac{1}{2}}$
2167. 73	5	46116. 69		2141. 37	25	46684. 30	$a\ ^2F_{3\frac{1}{2}}$—$w\ ^2G^\circ_{3\frac{1}{2}}$
				2140. 50	1	46703. 28	
2166. 87	6	46134. 98	$b\ ^4G_{2\frac{1}{2}}$—$w\ ^4G^\circ_{3\frac{1}{2}}$	2140. 28	2	46708. 08	
2166. 58	18	46141. 16	$a\ ^4D_{0\frac{1}{2}}$—$x\ ^4D^\circ_{0\frac{1}{2}}$	2140. 05	5	46713. 10	
2166. 43	8	46144. 36					
2165. 80	22	46157. 78	$a\ ^4D_{3\frac{1}{2}}$—$y\ ^4F^\circ_{3\frac{1}{2}}$	2139. 45	25	46726. 20	$a\ ^4P_{1\frac{1}{2}}$—$y\ ^4P^\circ_{2\frac{1}{2}}$
2165. 19	75	46170. 78	$a\ ^4F_{4\frac{1}{2}}$—$x\ ^2H^\circ_{4\frac{1}{2}}$	2139. 29	10	46729. 70	$a\ ^4D_{1\frac{1}{2}}$—$x\ ^4F^\circ_{1\frac{1}{2}}$
				2139. 05	5	46734. 94	$a\ ^4P_{2\frac{1}{2}}$—$y\ ^4P^\circ_{2\frac{1}{2}}$
2164. 68	1	46181. 65		2138. 34	12	46750. 45	
2164. 43	2	46186. 99	$b\ ^4G_{3\frac{1}{2}}$—$v\ ^4D^\circ_{2\frac{1}{2}}$	2137. 58	10	46767. 07	$a\ ^2H_{4\frac{1}{2}}$—$u\ ^2F^\circ_{3\frac{1}{2}}$
2164. 12	5	46193. 60	$b\ ^4G_{3\frac{1}{2}}$—$w\ ^4G^\circ_{4\frac{1}{2}}$				
2163. 78	25	46200. 86	$a\ ^4G_{5\frac{1}{2}}$—$z\ ^4I^\circ_{6\frac{1}{2}}$	2136. 97	10	46780. 41	$c\ ^2D_{2\frac{1}{2}}$—$t\ ^2D^\circ_{2\frac{1}{2}}$
2163. 64	20	46203. 86	$a\ ^2F_{3\frac{1}{2}}$—$z\ ^2D^\circ_{2\frac{1}{2}}$	2136. 60	10	46788. 52	$a\ ^4H_{3\frac{1}{2}}$—$w\ ^2D^\circ_{2\frac{1}{2}}$
2163. 54	10	46205. 99	$a\ ^4P_{0\frac{1}{2}}$—$z\ ^2P^\circ_{0\frac{1}{2}}$ $a\ ^4D_{0\frac{1}{2}}$—$y\ ^4F^\circ_{1\frac{1}{2}}$	2136. 04	22	46800. 78	$a\ ^4P_{2\frac{1}{2}}$—$x\ ^4D^\circ_{3\frac{1}{2}}$ $b\ ^4F_{4\frac{1}{2}}$—$w\ ^4G^\circ_{3\frac{1}{2}}$
				2135. 96	5	46802. 54	
2162. 96	10	46218. 38	$a\ ^4D_{1\frac{1}{2}}$—$y\ ^4F^\circ_{2\frac{1}{2}}$	2135. 50	2	46812. 62	$b\ ^4P_{2\frac{1}{2}}$—$w\ ^4G^\circ_{3\frac{1}{2}}$
2162. 22	3	46234. 19					
2161. 67	25	46245. 95	$b\ ^4G_{3\frac{1}{2}}$—$v\ ^4F^\circ_{4\frac{1}{2}}$	2135. 13	2	46820. 73	
2160. 65	10	46267. 78	$b\ ^2F_{2\frac{1}{2}}$—$u\ ^2F^\circ_{2\frac{1}{2}}$	2135. 00	18	46821. 38	$b\ ^4F_{3\frac{1}{2}}$—$v\ ^4F^\circ_{2\frac{1}{2}}$
				2134. 43	8	46836. 08	$a\ ^4D_{3\frac{1}{2}}$—$y\ ^4F^\circ_{3\frac{1}{2}}$
2160. 14	1	46278. 71		2134. 01	10	46845. 30	$b\ ^4F_{3\frac{1}{2}}$—$w\ ^4G^\circ_{3\frac{1}{2}}$
2159. 79	2	46286. 20		2133. 71	7	46851. 88	$a\ ^4P_{1\frac{1}{2}}$—$x\ ^4D^\circ_{1\frac{1}{2}}$
2159. 36	1*w*	46295. 42					
2158. 90	2*w*	46305. 28	$b\ ^4G_{3\frac{1}{2}}$—$v\ ^4D^\circ_{3\frac{1}{2}}$	2133. 39	25	46858. 91	$a\ ^4D_{2\frac{1}{2}}$—$x\ ^4F^\circ_{3\frac{1}{2}}$
2158. 04	4	46323. 73		2133. 06	40	46866. 16	$a\ ^2D_{1\frac{1}{2}}$—$w\ ^2F^\circ_{2\frac{1}{2}}$
				2132. 94	3	46868. 79	
2157. 71	5	46330. 82		2131. 89	12	46891. 87	
2157. 33	12	46338. 98		2131. 69	1	46896. 27	
2157. 10	5	46343. 92					
2156. 74	30	46351. 65	$a\ ^4D_{3\frac{1}{2}}$—$y\ ^4H^\circ_{3\frac{1}{2}}$	2131. 39	7	46902. 87	$a\ ^4P_{2\frac{1}{2}}$— (1)$^\circ_{2\frac{1}{2}}$
2156. 47	8	46357. 45	$a\ ^2F_{2\frac{1}{2}}$—$w\ ^2G^\circ_{3\frac{1}{2}}$ $a\ ^6D_{0\frac{1}{2}}$—$y\ ^4D^\circ_{1\frac{1}{2}}$	2130. 86	7	46914. 54	
				2130. 29	4	46927. 09	$b\ ^4F_{1\frac{1}{2}}$—$v\ ^4F^\circ_{2\frac{1}{2}}$ $b\ ^4D_{2\frac{1}{2}}$—$w\ ^2D^\circ_{1\frac{1}{2}}$
2155. 84	12	46371. 00	$b\ ^4G_{4\frac{1}{2}}$—$w\ ^4G^\circ_{4\frac{1}{2}}$	2130. 15	10	46930. 18	$a\ ^4D_{3\frac{1}{2}}$—$z\ ^2F^\circ_{3\frac{1}{2}}$ $a\ ^6D_{2\frac{1}{2}}$—$y\ ^4D^\circ_{2\frac{1}{2}}$
2155. 54	4	46377. 45					
2155. 29	1	46382. 83		2129. 98	4	46933. 92	$b\ ^4F_{2\frac{1}{2}}$—$v\ ^4F^\circ_{2\frac{1}{2}}$
2155. 10	10	46386. 92					
2154. 63	10	46397. 04	$a\ ^4P_{1\frac{1}{2}}$—$z\ ^2P^\circ_{0\frac{1}{2}}$	2128. 92	5	46957. 29	$b\ ^4F_{2\frac{1}{2}}$—$w\ ^4G^\circ_{3\frac{1}{2}}$
				2128. 63	22	46963. 68	$a\ ^2G_{4\frac{1}{2}}$—$v\ ^2F^\circ_{3\frac{1}{2}}$
2154. 04	15	46409. 75		2127. 89	2	46980. 45	$b\ ^2F_{2\frac{1}{2}}$—$w\ ^4G^\circ_{2\frac{1}{2}}$
2153. 38	15	46423. 97	$a\ ^2G_{3\frac{1}{2}}$—$w\ ^2D^\circ_{2\frac{1}{2}}$ $b\ ^4G_{4\frac{1}{2}}$—$v\ ^4F^\circ_{4\frac{1}{2}}$	2127. 36	3	46991. 71	$a\ ^4H_{3\frac{1}{2}}$—$v\ ^2F^\circ_{3\frac{1}{2}}$
				2127. 27	18	46993. 70	$a\ ^4D_{1\frac{1}{2}}$—$x\ ^4F^\circ_{2\frac{1}{2}}$
2152. 77	3	46437. 12					
2152. 51	35	46442. 73	$c\ ^2G_{3\frac{1}{2}}$—$t\ ^2G^\circ_{3\frac{1}{2}}$ $c\ ^2G_{4\frac{1}{2}}$—$v\ ^2H^\circ_{5\frac{1}{2}}$ $a\ ^4H_{3\frac{1}{2}}$—$v\ ^2F^\circ_{2\frac{1}{2}}$	2127. 11	4	46997. 24	
				2126. 46	15	47011. 60	$a\ ^4G_{3\frac{1}{2}}$—$x\ ^4D^\circ_{2\frac{1}{2}}$
				2125. 92	75	47023. 54	$a\ ^2I_{5\frac{1}{2}}$—$x\ ^2H^\circ_{4\frac{1}{2}}$
2152. 01	1	46453. 52	$b\ ^4G_{4\frac{1}{2}}$—$v\ ^4F^\circ_{3\frac{1}{2}}$	2124. 84	18	47047. 44	$b\ ^2F_{2\frac{1}{2}}$—$t\ ^2F^\circ_{2\frac{1}{2}}$ $a\ ^4P_{0\frac{1}{2}}$—$x\ ^4D^\circ_{0\frac{1}{2}}$
2150. 70	4	46481. 81		2124. 37	2	47057. 85	
2150. 48	10	46486. 56					
2150. 23	4	46491. 97		2124. 18	4	47062. 05	
2149. 77	15	46501. 91	$a\ ^2F_{3\frac{1}{2}}$—$w\ ^2G^\circ_{4\frac{1}{2}}$	2124. 09	25	47064. 05	$a\ ^4G_{4\frac{1}{2}}$—$x\ ^4D^\circ_{3\frac{1}{2}}$
2149. 36	1	46510. 78		2123. 31	22	47081. 34	$b\ ^2F_{3\frac{1}{2}}$—$u\ ^2F^\circ_{3\frac{1}{2}}$
				2122. 13	20	47107. 51	$a\ ^4D_{0\frac{1}{2}}$—$x\ ^4F^\circ_{1\frac{1}{2}}$
2149. 12	6	46515. 98		2121. 88	15	47113. 06	$a\ ^4P_{0\frac{1}{2}}$—$y\ ^4F^\circ_{1\frac{1}{2}}$
2148. 94	2	46519. 87					
2148. 87	3	46521. 39		2121. 37	8	47124. 38	
2148. 31	8*d*?	46533. 51	$a\ ^4D_{2\frac{1}{2}}$—$z\ ^2F^\circ_{3\frac{1}{2}}$	2120. 53	15	47143. 05	$a\ ^4G_{2\frac{1}{2}}$—$x\ ^4D^\circ_{2\frac{1}{2}}$
2147. 82	10	46544. 13	$a\ ^4H_{4\frac{1}{2}}$—$v\ ^2F^\circ_{3\frac{1}{2}}$	2120. 17	10	47151. 05	$b\ ^2I_{5\frac{1}{2}}$—$u\ ^2G^\circ_{4\frac{1}{2}}$
2147. 67	12	46547. 38	$a\ ^4G_{2\frac{1}{2}}$—$z\ ^2P^\circ_{1\frac{1}{2}}$	2119. 71	25	47161. 29	$a\ ^4G_{3\frac{1}{2}}$—$x\ ^4D^\circ_{3\frac{1}{2}}$
2147. 52	10	46550. 63	$a\ ^4D_{3\frac{1}{2}}$—$y\ ^4H^\circ_{4\frac{1}{2}}$	2119. 11	1	47174. 64	

TABLE 1. *Wavelengths and term combinations of* Mo II—Continued

Wavelength λ_{air}	Intensity	Wave No.	Term combination
2118.89	2	47179.53	
2118.31	7	47192.45	
2118.23	8	47194.24	
2117.84	20	47202.93	$a\ ^2F_{2\frac{1}{2}}$—$w\ ^2D^\circ_{1\frac{1}{2}}$
2117.54	3	47209.61	
2117.18	10	47217.64	$b\ ^4F_{3\frac{1}{2}}$—$v\ ^4D^\circ_{2\frac{1}{2}}$
2116.98	12	47222.10	
2116.77	55	47226.78	$a\ ^4P_{2\frac{1}{2}}$—$y\ ^4G^\circ_{3\frac{1}{2}}$
2116.57	10	47231.24	$b\ ^4P_{1\frac{1}{2}}$—$w\ ^4G^\circ_{2\frac{1}{2}}$
2116.34	6	47236.37	
2115.98	1	47244.41	
2115.44	20	47256.47	$a\ ^4D_{3\frac{1}{2}}$—$x\ ^4F^\circ_{3\frac{1}{2}}$
2115.10	25	47264.06	$a\ ^4G_{3\frac{1}{2}}$— (1)$^\circ_{2\frac{1}{2}}$
2114.72	18	47272.55	$b\ ^4G_{3\frac{1}{2}}$—$w\ ^4G^\circ_{3\frac{1}{2}}$
2114.32	20	47281.50	$a\ ^4G_{3\frac{1}{2}}$—$z\ ^2I^\circ_{3\frac{1}{2}}$
2114.13	6	47285.75	$a\ ^2D_{2\frac{1}{2}}$—$w\ ^2F^\circ_{2\frac{1}{2}}$
2113.86	18	47291.79	
2113.36	18	47302.97	$b\ ^4P_{2\frac{1}{2}}$—$v\ ^4D^\circ_{3\frac{1}{2}}$ $a\ ^4P_{1\frac{1}{2}}$—$y\ ^4F^\circ_{1\frac{1}{2}}$
2112.98	8	47311.48	$a\ ^4P_{2\frac{1}{2}}$—$y\ ^4F^\circ_{1\frac{1}{2}}$
2112.31	1	47326.48	$a\ ^6D_{3\frac{1}{2}}$—$z\ ^4G^\circ_{4\frac{1}{2}}$
2111.97	8	47334.10	
2111.72	15	47339.71	$a\ ^4F_{3\frac{1}{2}}$—$w\ ^2G^\circ_{3\frac{1}{2}}$ $b\ ^2F_{3\frac{1}{2}}$—$t\ ^2F^\circ_{3\frac{1}{2}}$
2111.18	20*d*?	47351.81	$a\ ^4G_{2\frac{1}{2}}$—$x\ ^4D^\circ_{1\frac{1}{2}}$
2110.56	10	47365.72	
2110.25	2	47372.68	
2109.94	25	47379.64	$b\ ^4D_{1\frac{1}{2}}$—$w\ ^2D^\circ_{1\frac{1}{2}}$ $a\ ^4D_{3\frac{1}{2}}$—$x\ ^4F^\circ_{4\frac{1}{2}}$
2109.23	18	47395.59	$a\ ^4G_{2\frac{1}{2}}$— (1)$^\circ_{2\frac{1}{2}}$
2108.74	22	47406.60	$a\ ^4D_{2\frac{1}{2}}$—$z\ ^4S^\circ_{1\frac{1}{2}}$
2108.42	1	47413.79	$a\ ^4P_{2\frac{1}{2}}$—$y\ ^4F^\circ_{3\frac{1}{2}}$
2108.04	50	47422.33	$a\ ^2I_{6\frac{1}{2}}$—$x\ ^2H^\circ_{5\frac{1}{2}}$
2107.63	4	47431.56	
2106.99	2	47445.96	
2106.81	10	47450.02	$c\ ^2D_{1\frac{1}{2}}$—$t\ ^2D^\circ_{2\frac{1}{2}}$ $b\ ^4G_{4\frac{1}{2}}$—$w\ ^4G^\circ_{3\frac{1}{2}}$
2106.25	2	47462.63	
2105.94	1	47469.62	
2105.69	1	47475.25	
2105.40	2	47481.79	
2105.03	40	47490.14	$a\ ^4G_{4\frac{1}{2}}$—$y\ ^4G^\circ_{3\frac{1}{2}}$
2104.28	5	47507.06	$a\ ^4G_{5\frac{1}{2}}$—$y\ ^4G^\circ_{4\frac{1}{2}}$
2103.43	18	47526.26	$a\ ^4G_{4\frac{1}{2}}$—$y\ ^4G^\circ_{4\frac{1}{2}}$
2103.19	1	47527.16	
2102.77	7	47541.18	$b\ ^2D_{2\frac{1}{2}}$—$u\ ^2D^\circ_{2\frac{1}{2}}$
2102.65	2	47543.89	
2102.36	12	47550.44	$a\ ^2P_{1\frac{1}{2}}$—$v\ ^2P^\circ_{1\frac{1}{2}}$ $b\ ^4F_{4\frac{1}{2}}$—$w\ ^4G^\circ_{4\frac{1}{2}}$
2101.70	25	47565.37	
2101.21	15	47576.46	$a\ ^4D_{1\frac{1}{2}}$—$z\ ^4S^\circ_{1\frac{1}{2}}$
2100.83	50	47585.07	$c\ ^2F_{2\frac{1}{2}}$—$t\ ^2G^\circ_{3\frac{1}{2}}$ $a\ ^4G_{4\frac{1}{2}}$— (2)$^\circ_{3\frac{1}{2}}$
2100.70	30	47588.01	$a\ ^4G_{3\frac{1}{2}}$—$y\ ^4G^\circ_{3\frac{1}{2}}$
2100.36	10	47595.72	$b\ ^4F_{3\frac{1}{2}}$—$w\ ^4G^\circ_{4\frac{1}{2}}$
2100.04	15	47602.96	$b\ ^4F_{4\frac{1}{2}}$—$v\ ^4F^\circ_{4\frac{1}{2}}$
2099.71	3	47610.45	
2099.45	2	47616.34	
2099.34	1	47618.84	
2099.14	12	47623.37	$a\ ^4G_{3\frac{1}{2}}$—$y\ ^4G^\circ_{3\frac{1}{2}}$
2098.71	1	47633.13	$b\ ^4F_{4\frac{1}{2}}$—$v\ ^4F^\circ_{3\frac{1}{2}}$
2098.57	1	47636.32	
2098.04	12	47648.34	$a\ ^2F_{2\frac{1}{2}}$—$v\ ^2F^\circ_{2\frac{1}{2}}$ $b\ ^4F_{3\frac{1}{2}}$—$v\ ^4F^\circ_{4\frac{1}{2}}$
2097.62	1*w*	47657.88	$c\ ^4D_{2\frac{1}{2}}$—$u\ ^2G^\circ_{3\frac{1}{2}}$ $a\ ^2D_{2\frac{1}{2}}$—$w\ ^2F^\circ_{3\frac{1}{2}}$
2097.21	5*d*?	47667.19	$b\ ^4D_{0\frac{1}{2}}$—$w\ ^2D^\circ_{1\frac{1}{2}}$
2097.02	6	47671.51	
2096.73	12	47678.10	$b\ ^4F_{3\frac{1}{2}}$—$v\ ^4F^\circ_{3\frac{1}{2}}$
2096.55	12	47682.20	$a\ ^4G_{3\frac{1}{2}}$— (2)$^\circ_{3\frac{1}{2}}$
2096.16	12	47691.07	$b\ ^4D_{3\frac{1}{2}}$—$v\ ^2F^\circ_{3\frac{1}{2}}$
2096.04	5	47693.80	$a\ ^4P_{1\frac{1}{2}}$—$y\ ^4F^\circ_{2\frac{1}{2}}$
2095.67	4	47702.22	$a\ ^4P_{2\frac{1}{2}}$—$y\ ^4F^\circ_{2\frac{1}{2}}$
2095.29	35	47710.86	$a\ ^4G_{3\frac{1}{2}}$—$y\ ^4G^\circ_{2\frac{1}{2}}$
2094.94	2	47718.83	$a\ ^4G_{2\frac{1}{2}}$—$y\ ^4G^\circ_{3\frac{1}{2}}$
2094.54	1	47727.95	
2094.28	7*w*	47733.88	
2093.94	2	47741.62	$a\ ^2G_{3\frac{1}{2}}$—$u\ ^2F^\circ_{2\frac{1}{2}}$
2093.78	1	47745.27	
2093.58	1	47749.83	
2093.11	50	47760.55	$a\ ^4G_{5\frac{1}{2}}$—$y\ ^4G^\circ_{5\frac{1}{2}}$
2092.53	30	47773.78	$a\ ^4G_{5\frac{1}{2}}$—$y\ ^4F^\circ_{5\frac{1}{2}}$
2092.26	7	47779.95	$a\ ^4G_{4\frac{1}{2}}$—$y\ ^4G^\circ_{5\frac{1}{2}}$
2091.81	10	47790.23	$b\ ^4F_{2\frac{1}{2}}$—$v\ ^4F^\circ_{3\frac{1}{2}}$
2091.23	25	47803.48	$a\ ^4G_{2\frac{1}{2}}$—$y\ ^4F^\circ_{1\frac{1}{2}}$
2091.00	5	47808.74	
2090.64	1	47816.97	
2090.30	2	47824.75	$b\ ^4D_{1\frac{1}{2}}$—$v\ ^2F^\circ_{2\frac{1}{2}}$
2090.14	18	47828.41	$a\ ^4F_{1\frac{1}{2}}$—$x\ ^2P^\circ_{0\frac{1}{2}}$
2089.92	1	47833.44	
2089.53	40	47842.37	$a\ ^4G_{2\frac{1}{2}}$—$y\ ^4G^\circ_{2\frac{1}{2}}$
2089.22	2	47849.47	
2088.72	5	47860.92	
2088.30	30	47870.54	$a\ ^4G_{4\frac{1}{2}}$—$y\ ^4H^\circ_{3\frac{1}{2}}$
2088.16	10	47873.75	$a\ ^2D_{1\frac{1}{2}}$—$x\ ^2D^\circ_{1\frac{1}{2}}$
2087.65	1	47885.45	
2087.30	30	47893.47	
2086.77	20	47905.64	$a\ ^4D_{3\frac{1}{2}}$—$y\ ^2G^\circ_{3\frac{1}{2}}$ $a\ ^4G_{2\frac{1}{2}}$—$y\ ^4F^\circ_{3\frac{1}{2}}$
2086.19	2	47918.95	
2085.86	1	47926.53	
2085.57	1	47933.20	
2085.30	1	47939.40	
2085.08	10	47944.46	
2084.64	20	47954.58	$a\ ^4D_{0\frac{1}{2}}$—$z\ ^4S^\circ_{1\frac{1}{2}}$
2084.42	7	47959.64	
2084.12	3	47966.54	
2084.07	18	47967.69	$a\ ^4G_{3\frac{1}{2}}$—$y\ ^4H^\circ_{3\frac{1}{2}}$
2083.76	22	47974.83	$a\ ^2F_{3\frac{1}{2}}$—$v\ ^2F^\circ_{2\frac{1}{2}}$
2083.38	1	47983.58	
2082.52	6	48003.39	$a\ ^4H_{4\frac{1}{2}}$—$u\ ^2F^\circ_{3\frac{1}{2}}$
2081.67	25	48022.99	$a\ ^6S_{2\frac{1}{2}}$—$z\ ^4P^\circ_{1\frac{1}{2}}$
2081.46	7	48027.83	
2080.47	40	48050.68	$a\ ^4G_{5\frac{1}{2}}$—$y\ ^4H^\circ_{4\frac{1}{2}}$
2080.12	20	48058.77	$a\ ^2H_{5\frac{1}{2}}$—$v\ ^2G^\circ_{4\frac{1}{2}}$
2079.98	10	48062.00	$a\ ^4G_{3\frac{1}{2}}$—$y\ ^4F^\circ_{3\frac{1}{2}}$
2079.75	5	48067.32	$a\ ^4F_{3\frac{1}{2}}$—$w\ ^2H^\circ_{4\frac{1}{2}}$
2079.63	6	48070.09	$a\ ^4G_{4\frac{1}{2}}$—$y\ ^4H^\circ_{4\frac{1}{2}}$
2079.12	3	48081.88	
2078.85	3	48088.12	$a\ ^4F_{4\frac{1}{2}}$—$w\ ^2H^\circ_{4\frac{1}{2}}$
2078.36	6	48099.46	$a\ ^4G_{2\frac{1}{2}}$—$y\ ^4H^\circ_{3\frac{1}{2}}$
2078.15	7	48104.32	$a\ ^4F_{2\frac{1}{2}}$—$w\ ^2D^\circ_{2\frac{1}{2}}$
2077.73	10*w*	48114.05	
2077.57	2	48117.75	

TABLE 1. *Wavelengths and term combinations of* Mo II—Continued

Wavelength λ_{air}	Intensity	Wave No.	Term combination
2077. 22	5	48125. 86	
2076. 34	4	48146. 25	
2075. 43	10	48167. 36	$a\ ^4G_{3\frac{1}{2}}—y\ ^4H^o_{4\frac{1}{2}}$
2074. 65	20	48185. 46	$a\ ^4P_{2\frac{1}{2}}—z\ ^2F^o_{3\frac{1}{2}}$
2074. 46	10	48189. 88	
2074. 31	30	48193. 36	$a\ ^4G_{2\frac{1}{2}}—y\ ^4F^o_{2\frac{1}{2}}$
2073. 47	12	48212. 88	$a\ ^4P_{2\frac{1}{2}}—x\ ^4F^o_{1\frac{1}{2}}$
2073. 11	8	48221. 25	
2072. 80	3*w*	48228. 46	
2072. 05	7	48245. 92	
2071. 65	18	48255. 23	
2071. 37	4	48261. 75	$a\ ^4H_{4\frac{1}{2}}—t\ ^2F^o_{3\frac{1}{2}}$
2071. 07	18	48268. 75	$a\ ^2D_{2\frac{1}{2}}—x\ ^2D^o_{2\frac{1}{2}}$
2070. 90	10	48272. 71	$b\ ^2G_{4\frac{1}{2}}—u\ ^2G^o_{3\frac{1}{2}}$
2070. 37	2	48285. 06	$a\ ^6D_{2\frac{1}{2}}—y\ ^4D^o_{3\frac{1}{2}}$
2070. 00	18	48293. 69	$a\ ^2D_{2\frac{1}{2}}—x\ ^2D^o_{1\frac{1}{2}}$
2069. 80	20	48298. 36	$a\ ^2I_{6\frac{1}{2}}—w\ ^2H^o_{5\frac{1}{2}}$
2068. 95	2	48318. 20	
2068. 84	2	48320. 76	$a\ ^2F_{3\frac{1}{2}}—w\ ^2D^o_{2\frac{1}{2}}$
2068. 65	12	48325. 20	
2068. 25	4	48334. 55	
2068. 20	12	48335. 72	$a\ ^4D_{3\frac{1}{2}}—y\ ^2H^o_{4\frac{1}{2}}$; $a\ ^4G_{5\frac{1}{2}}—y\ ^4F^o_{4\frac{1}{2}}$
2067. 74	1	48346. 47	$a\ ^4F_{1\frac{1}{2}}—v\ ^2F^o_{2\frac{1}{2}}$
2067. 36	20	48355. 35	$a\ ^4G_{4\frac{1}{2}}—y\ ^4F^o_{4\frac{1}{2}}$
2066. 90	8	48366. 12	
2066. 50	3*w*	48375. 47	
2066. 18	10	48382. 96	$a\ ^2F_{2\frac{1}{2}}—x\ ^2P^o_{1\frac{1}{2}}$
2065. 71	2	48393. 97	
2065. 33	2	48402. 87	
2064. 96	1	48411. 55	
2064. 46	7	48423. 27	$a\ ^2G_{4\frac{1}{2}}—u\ ^2F^o_{3\frac{1}{2}}$
2064. 26	5	48427. 96	
2063. 34	5	48449. 55	$a\ ^4G_{4\frac{1}{2}}—y\ ^4F^o_{3\frac{1}{2}}$
2063. 26	18	48451. 43	
2063. 20	10	48452. 84	$a\ ^4G_{3\frac{1}{2}}—y\ ^4F^o_{4\frac{1}{2}}$; $a\ ^2G_{3\frac{1}{2}}—w\ ^4G^o_{2\frac{1}{2}}$
2062. 83	1	48461. 53	
2062. 50	4	48469. 28	$a\ ^4P_{1\frac{1}{2}}—x\ ^4F^o_{2\frac{1}{2}}$
2062. 18	1	48476. 80	$a\ ^4P_{2\frac{1}{2}}—x\ ^4F^o_{3\frac{1}{2}}$
2061. 98	8	48481. 50	$b\ ^2H_{4\frac{1}{2}}—u\ ^2G^o_{3\frac{1}{2}}$
2061. 72	8	48487. 62	$a\ ^4D_{2\frac{1}{2}}—(3)^5_{3\frac{1}{2}}$
2060. 65	4	48512. 79	$a\ ^4P_{2\frac{1}{2}}—x\ ^4F^o_{2\frac{1}{2}}$
2060. 33	40	48520. 32	$a\ ^2G_{3\frac{1}{2}}—t\ ^2F^o_{3\frac{1}{2}}$
2059. 54	6	48538. 93	
2059. 23	20	48546. 24	$a\ ^4G_{3\frac{1}{2}}—z\ ^4F^o_{3\frac{1}{2}}$
2058. 92	2	48553. 55	
2058. 82	3	48555. 91	
2058. 70	4	48558. 74	$a\ ^4D_{1\frac{1}{2}}—x\ ^4G^o_{2\frac{1}{2}}$; $b\ ^2I_{5\frac{1}{2}}—v\ ^2H^o_{4\frac{1}{2}}$
2058. 53	2	48562. 74	
2057. 85	3	48578. 79	$b\ ^4P_{1\frac{1}{2}}—v\ ^4D^o_{2\frac{1}{2}}$
2057. 46	25	48587. 99	
2056. 90	8	48601. 22	
2056. 22	1	48617. 29	
2055. 68	40	48630. 06	$b\ ^4F_{4\frac{1}{2}}—w\ ^4G^o_{5\frac{1}{2}}$
2054. 96	8	48647. 10	$b\ ^2D_{2\frac{1}{2}}—u\ ^2G^o_{3\frac{1}{2}}$
2054. 34	6	48661. 78	
2053. 53	2	48680. 97	$a\ ^2G_{4\frac{1}{2}}—t\ ^2F^o_{3\frac{1}{2}}$
2053. 00	3	48693. 54	$a\ ^4G_{5\frac{1}{2}}—y\ ^4H^o_{5\frac{1}{2}}$
2052. 91	3	48695. 67	$a\ ^4P_{1\frac{1}{2}}—z\ ^2F^o_{2\frac{1}{2}}$
2052. 55	6	48704. 21	$a\ ^4G_{2\frac{1}{2}}—x\ ^4F^o_{1\frac{1}{2}}$
2052. 52	12	48704. 92	
2052. 35	2	48708. 96	$a\ ^4H_{3\frac{1}{2}}—t\ ^2F^o_{3\frac{1}{2}}$
2052. 21	10	48712. 28	$a\ ^4G_{4\frac{1}{2}}—y\ ^4H^o_{5\frac{1}{2}}$
2051. 50	1	48729. 13	
2051. 09	2*w*	48738. 87	$a\ ^4D_{2\frac{1}{2}}—y\ ^2D^o_{2\frac{1}{2}}$
2050. 64	10	48749. 57	$a\ ^2D_{2\frac{1}{2}}—w\ ^2G^o_{3\frac{1}{2}}$
2050. 34	3*w*	48756. 70	
2050. 24	2*w*	48759. 08	
2049. 54	5	48775. 73	$a\ ^4G_{4\frac{1}{2}}—x\ ^4F^o_{3\frac{1}{2}}$
2048. 60	3	48798. 10	
2047. 97	1	48813. 11	
2047. 78	10	48817. 64	$a\ ^4H_{3\frac{1}{2}}—w\ ^4G^o_{2\frac{1}{2}}$
2046. 94	18	48837. 67	$a\ ^4G_{3\frac{1}{2}}—x\ ^4F^o_{2\frac{1}{2}}$
2045. 98	75	48860. 59	$a\ ^4P_{0\frac{1}{2}}—z\ ^4S^o_{1\frac{1}{2}}$; $a\ ^6S_{2\frac{1}{2}}—z\ ^4P^o_{2\frac{1}{2}}$
2045. 48	20	48872. 53	$a\ ^4G_{3\frac{1}{2}}—x\ ^4F^o_{3\frac{1}{2}}$
2045. 19	10	48879. 46	$a\ ^4G_{5\frac{1}{2}}—x\ ^4F^o_{4\frac{1}{2}}$
2044. 96	8	48885. 43	$a\ ^4H_{3\frac{1}{2}}—t\ ^2F^o_{3\frac{1}{2}}$
2044. 38	40	48898. 82	$a\ ^4G_{4\frac{1}{2}}—x\ ^4F^o_{4\frac{1}{2}}$
2042. 66	40	48939. 99	$a\ ^2I_{5\frac{1}{2}}—w\ ^2H^o_{4\frac{1}{2}}$
2042. 20	2	48951. 01	
2041. 99	10	48956. 05	$b\ ^2H_{5\frac{1}{2}}—u\ ^2G^o_{4\frac{1}{2}}$
2041. 45	20	48968. 99	$a\ ^4G_{2\frac{1}{2}}—x\ ^4F^o_{2\frac{1}{2}}$
2041. 14	2	48976. 43	$a\ ^4F_{3\frac{1}{2}}—w\ ^2D^o_{2\frac{1}{2}}$
2040. 85	2	48983. 39	
2040. 38	15	48994. 67	
2040. 34	10	48995. 63	$a\ ^4G_{3\frac{1}{2}}—x\ ^4F^o_{4\frac{1}{2}}$
2039. 98	3	49004. 27	$a\ ^4G_{2\frac{1}{2}}—x\ ^4F^o_{3\frac{1}{2}}$
2038. 46	75*r*	49040. 80	$a\ ^6S_{2\frac{1}{2}}—z\ ^6P^o_{1\frac{1}{2}}$
2038. 02	25	49051. 40	$a\ ^4P_{1\frac{1}{2}}—z\ ^4S^o_{1\frac{1}{2}}$
2037. 67	20	49059. 82	$a\ ^4P_{2\frac{1}{2}}—z\ ^4S^o_{1\frac{1}{2}}$
2037. 60	30	49061. 50	
2036. 77	6	49081. 50	$a\ ^4F_{1\frac{1}{2}}—x\ ^2P^o_{1\frac{1}{2}}$
2036. 41	7	49090. 17	$b\ ^2D_{2\frac{1}{2}}—v\ ^2P^o_{1\frac{1}{2}}$; $b\ ^2I_{5\frac{1}{2}}—v\ ^2H^o_{5\frac{1}{2}}$
2035. 90	15	49102. 46	$a\ ^2D_{1\frac{1}{2}}—x\ ^2P^o_{0\frac{1}{2}}$
2034. 90	2	49126. 59	
2034. 52	1	49135. 76	$a\ ^4D_{3\frac{1}{2}}—y\ ^2D^o_{2\frac{1}{2}}$
2034. 32	6	49140. 60	$a\ ^4D_{6\frac{1}{2}}—x\ ^4G^o_{5\frac{1}{2}}$
2033. 90	2	49150. 74	
2032. 91	10	49174. 68	$a\ ^2D_{1\frac{1}{2}}—w\ ^2D^o_{1\frac{1}{2}}$; $b\ ^4D_{0\frac{1}{2}}—w\ ^2P^o_{0\frac{1}{2}}$; $b\ ^2F_{3\frac{1}{2}}—w\ ^4G^o_{4\frac{1}{2}}$
2032. 71	1	49179. 51	$a\ ^4F_{3\frac{1}{2}}—v\ ^2F^o_{3\frac{1}{2}}$
2032. 61	10	49181. 93	
2032. 04	20	49195. 73	$a\ ^4G_{2\frac{1}{2}}—z\ ^2F^o_{2\frac{1}{2}}$
2031. 88	18	49199. 60	$a\ ^4F_{4\frac{1}{2}}—v\ ^2F^o_{3\frac{1}{2}}$; $a\ ^4D_{1\frac{1}{2}}—w\ ^4D^o_{0\frac{1}{2}}$
2031. 25	2	49214. 86	$a\ ^2F_{2\frac{1}{2}}—w\ ^2P^o_{1\frac{1}{2}}$
2031. 10	2*w*	49218. 49	
2030. 80	5	49225. 76	$a\ ^4D_{1\frac{1}{2}}—w\ ^4D^o_{1\frac{1}{2}}$
2030. 18	2	49240. 80	
2029. 62	5	49254. 37	
2028. 97	3	49270. 15	
2028. 29	25	49286. 67	
2028. 14	10	49290. 32	
2027. 69	3	49301. 25	
2027. 31	6	49310. 49	$a\ ^2F_{2\frac{1}{2}}—u\ ^2F^o_{2\frac{1}{2}}$
2026. 75	7	49324. 11	$a\ ^4D_{2\frac{1}{2}}—w\ ^4D^o_{2\frac{1}{2}}$
2025. 86	15	49345. 78	$a\ ^4H_{4\frac{1}{2}}—w\ ^4G^o_{3\frac{1}{2}}$
2025. 47	1	49355. 28	

TABLE 1. *Wavelengths and term combinations of* Mo II—Continued

Wavelength λ_{air}	Intensity	Wave No.	Term combination	Wavelength λ_{air}	Intensity	Wave No.	Term combination
2024.41	8	49381.12		2010.56	6	49721.24	$a\ ^4D_{3\frac{1}{2}}$—$w\ ^4D^o_{2\frac{1}{2}}$
2023.75	20	49397.22	$b\ ^2I_{6\frac{1}{2}}$—$v\ ^2H^o_{5\frac{1}{2}}$	2010.21	2	49729.89	
2023.28	3	49408.69	$a\ ^4F_{1\frac{1}{2}}$—$w\ ^2P^o_{0\frac{1}{2}}$	2009.52	5	49746.96	$a\ ^6D_{4\frac{1}{2}}$—$y\ ^4G^o_{3\frac{1}{2}}$; $b\ ^4D_{2\frac{1}{2}}$—$w\ ^4G^o_{2\frac{1}{2}}$
2023.22	2	49410.16	$b\ ^2G_{3\frac{1}{2}}$—$u\ ^2G^o_{4\frac{1}{2}}$	2009.29	1	49752.66	$a\ ^4P_{2\frac{1}{2}}$—$y\ ^2D^o_{1\frac{1}{2}}$
2022.64	6	49424.32	$a\ ^4G_{4\frac{1}{2}}$—$y\ ^2G^o_{3\frac{1}{2}}$	2009.06	1w	49758.36	
2021.79	6	49445.10	$a\ ^4D_{3\frac{1}{2}}$—$x\ ^4G^o_{4\frac{1}{2}}$				
2021.27	2	49457.82	$a\ ^6D_{4\frac{1}{2}}$—$y\ ^4G^o_{3\frac{1}{2}}$	2008.75	1	49766.03	$a\ ^2G_{4\frac{1}{2}}$—$w\ ^4G^o_{3\frac{1}{2}}$
2020.32	100r	49481.07	$a\ ^6S_{2\frac{1}{2}}$—$z\ ^6P^o_{3\frac{1}{2}}$	2008.60	4	49769.75	$a\ ^4D_{3\frac{1}{2}}$—$w\ ^4D^o_{3\frac{1}{2}}$
2019.32	2	49505.57		2008.33	1	49776.44	
2019.07	3	49511.70	$b\ ^2H_{4\frac{1}{2}}$—$u\ ^2G^o_{4\frac{1}{2}}$	2008.08	1	49782.64	
				2007.83	2	49888.83	
2018.89	1	49516.12					
2018.65	7	49522.00	$a\ ^4G_{3\frac{1}{2}}$—$y\ ^2G^o_{3\frac{1}{2}}$	2007.23	2	49803.71	
2018.49	8	49525.92	$a\ ^6D_{3\frac{1}{2}}$—$y\ ^4P^o_{2\frac{1}{2}}$	2006.98	3	49809.92	
2018.09	2	49535.74		2006.79	5	49814.63	
2018.00	1	49537.95		2006.36	25	49825.30	$c\ ^2F_{3\frac{1}{2}}$—$s\ ^2F^o_{3\frac{1}{2}}$
				2005.87	5	49837.47	$a\ ^6D_{4\frac{1}{2}}$—$y\ ^4H^o_{3\frac{1}{2}}$
2017.69	2	49545.56					
2017.44	1	49551.70	$a\ ^6D_{4\frac{1}{2}}$—(2)$^o_{3\frac{1}{2}}$; $a\ ^4G_{2\frac{1}{2}}$—$z\ ^4S^o_{1\frac{1}{2}}$	2005.70	3	49841.70	
2017.12	2	49559.56		2005.55	12	49845.43	$a\ ^2P_{0\frac{1}{2}}$—$v\ ^2P^o_{1\frac{1}{2}}$; $a\ ^4H_{5\frac{1}{2}}$—$w\ ^4G^o_{4\frac{1}{2}}$
2016.76	1	49568.41		2005.19	3	49854.37	$a\ ^4G_{4\frac{1}{2}}$—$y\ ^2H^o_{4\frac{1}{2}}$
2016.36	2	49578.23	$a\ ^4D_{0\frac{1}{2}}$—$w\ ^4D^o_{0\frac{1}{2}}$	2004.81	1	49863.82	
				2004.56	2	49870.04	
2016.24	1	49581.19	$a\ ^4P_{2\frac{1}{2}}$—$y\ ^2F^o_{2\frac{1}{2}}$				
2016.04	2	49586.10		2004.20	2	49879.00	
2015.67	6	49595.21	$a\ ^2D_{2\frac{1}{2}}$—$w\ ^2D^o_{1\frac{1}{2}}$	2004.12	2	49880.99	
2015.12	50	49608.74	$a\ ^6S_{2\frac{1}{2}}$—$z\ ^6P^o_{2\frac{1}{2}}$	2003.81	4w	49888.70	
2014.78	4	49617.11	$a\ ^2G_{4\frac{1}{2}}$—$v\ ^2G^o_{4\frac{1}{2}}$	2003.19	1	49904.14	
				2002.84	5	49912.86	$a\ ^4F_{1\frac{1}{2}}$—$w\ ^2P^o_{1\frac{1}{2}}$
2014.38	1	49626.96	$a\ ^4G_{5\frac{1}{2}}$—$z\ ^2H^o_{5\frac{1}{2}}$				
2014.14	6	49632.87		2002.12	18	49930.81	$a\ ^4G_{3\frac{1}{2}}$—$y\ ^2F^o_{3\frac{1}{2}}$
2013.98	4	49636.82	$a\ ^2F_{3\frac{1}{2}}$—$u\ ^2F^o_{2\frac{1}{2}}$	2001.65	3	49942.53	$a\ ^4G_{3\frac{1}{2}}$—$y\ ^2F^o_{2\frac{1}{2}}$
2013.67	1	49644.46	$a\ ^6D_{4\frac{1}{2}}$—$y\ ^4F^o_{3\frac{1}{2}}$	2001.26	1w	49952.26	$c\ ^2F_{3\frac{1}{2}}$—$t\ ^2D^o_{2\frac{1}{2}}$; $a\ ^4G_{3\frac{1}{2}}$—$y\ ^2H^o_{3\frac{1}{2}}$
2013.29	1	49653.83	$a\ ^4G_{2\frac{1}{2}}$—$y\ ^2G^o_{3\frac{1}{2}}$	2000.74	1	49965.24	$a\ ^2D_{1\frac{1}{2}}$—$w\ ^2D^o_{2\frac{1}{2}}$
				2000.66	2	49967.24	$a\ ^4P_{2\frac{1}{2}}$—$x\ ^2F^o_{2\frac{1}{2}}$
2013.04	1	49659.99					
2012.70	6	49668.38	$a\ ^4G_{5\frac{1}{2}}$—$y\ ^4H^o_{5\frac{1}{2}}$				
2012.52	6	49672.82		2000.24	20	49977.73	$a\ ^4G_{5\frac{1}{2}}$—$y\ ^2H^o_{5\frac{1}{2}}$
2011.05	4	49709.12		2000.05	10	49982.47	$a\ ^2F_{3\frac{1}{2}}$—$u\ ^2F^o_{3\frac{1}{2}}$
2010.86	25	49713.82	$b\ ^2H_{5\frac{1}{2}}$—$t\ ^2G^o_{4\frac{1}{2}}$	1999.47	8	49996.92	$a\ ^4G_{4\frac{1}{2}}$—$y\ ^2H^o_{5\frac{1}{2}}$

TABLE 2. *Wavelengths of* Mo II *in vacuum*

Wavelength computed	Intensity	Wave No.	Term combination	Wavelength computed	Intensity	Wave No.	Term combination
1998.41	12	50039.83	$a\ ^2D_{2\frac{1}{2}}$—$v\ ^2F^o_{2\frac{1}{2}}$	1985.94	4	50354.61	$a\ ^2D_{1\frac{1}{2}}$—$x\ ^2P^o_{1\frac{1}{2}}$
1997.54	10	50061.70	$a\ ^4G_{2\frac{1}{2}}$—$y\ ^2F^o_{3\frac{1}{2}}$; $a\ ^6D_{1\frac{1}{2}}$—$z\ ^2P^o_{0\frac{1}{2}}$	1985.53	5	50364.35	$b\ ^2H_{5\frac{1}{2}}$—$v\ ^2H^o_{4\frac{1}{2}}$; $a\ ^4G_{3\frac{1}{2}}$—$y\ ^2G^o_{4\frac{1}{2}}$
1997.02	5	50074.50	$a\ ^4G_{2\frac{1}{2}}$—$y\ ^2F^o_{2\frac{1}{2}}$; $a\ ^6D_{2\frac{1}{2}}$—$x\ ^4D^o_{3\frac{1}{2}}$	1985.35	4	50368.82	$a\ ^4D_{2\frac{1}{2}}$—$x\ ^4P^o_{2\frac{1}{2}}$
				1984.70	15	50385.42	$a\ ^2D_{2\frac{1}{2}}$—$w\ ^2D^o_{2\frac{1}{2}}$
1996.40	18	50090.08	$a\ ^2F_{2\frac{1}{2}}$—$t\ ^2F^o_{2\frac{1}{2}}$	1984.47	2	50391.25	$a\ ^4P_{2\frac{1}{2}}$—$y\ ^2D^o_{2\frac{1}{2}}$; $a\ ^6D_{1\frac{1}{2}}$—$y\ ^4P^o_{2\frac{1}{2}}$
1995.53	1	50111.91	$a\ ^6D_{3\frac{1}{2}}$—(2)$^o_{3\frac{1}{2}}$				
				1984.06	10	50401.67	$a\ ^4G_{3\frac{1}{2}}$—$x\ ^4G^o_{3\frac{1}{2}}$
1994.66	15	50133.76	$a\ ^6D_{2\frac{1}{2}}$—$x\ ^4D^o_{1\frac{1}{2}}$				$a\ ^4D_{2\frac{1}{2}}$—$x\ ^2G^o_{3\frac{1}{2}}$; $a\ ^6D_{4\frac{1}{2}}$—$z\ ^2F^o_{3\frac{1}{2}}$; $a\ ^2F_{3\frac{1}{2}}$—$t\ ^2F^o_{2\frac{1}{2}}$
1994.42	5	50139.87	$a\ ^4P_{2\frac{1}{2}}$—(3)$^o_{3\frac{1}{2}}$	1983.48	10	50416.41	
1992.89	3	50178.38	$a\ ^6D_{2\frac{1}{2}}$—(1)$^o_{3\frac{1}{2}}$; $a\ ^2G_{3\frac{1}{2}}$—$w\ ^4G^o_{4\frac{1}{2}}$	1981.08	1	50477.50	$a\ ^4D_{2\frac{1}{2}}$—$w\ ^4F^o_{3\frac{1}{2}}$
1992.35	10	50192.00	$a\ ^6S_{2\frac{1}{2}}$—$z\ ^6D^o_{1\frac{1}{2}}$	1980.49	7	50492.49	$b\ ^4D_{3\frac{1}{2}}$—$w\ ^4G^o_{3\frac{1}{2}}$; $a\ ^6D_{3\frac{1}{2}}$—$y\ ^4F^o_{3\frac{1}{2}}$
1992.07	2	50199.16	$b\ ^4D_{1\frac{1}{2}}$—$w\ ^4G^o_{2\frac{1}{2}}$	1979.83	2	50509.32	$a\ ^4P_{0\frac{1}{2}}$—$w\ ^4D^o_{1\frac{1}{2}}$
1990.44	15	50240.25	$a\ ^2F_{3\frac{1}{2}}$—$t\ ^2F^o_{3\frac{1}{2}}$				
1990.25	8	50245.05	$a\ ^4G_{2\frac{1}{2}}$—$y\ ^2D^o_{1\frac{1}{2}}$	1979.51	1	50516.49	$a\ ^2G_{4\frac{1}{2}}$—$w\ ^4C^o_{3\frac{1}{2}}$; $a\ ^6D_{1\frac{1}{2}}$—$x\ ^4D^o_{1\frac{1}{2}}$
1990.13	15	50247.94	$a\ ^4G_{3\frac{1}{2}}$—$y\ ^2G^o_{4\frac{1}{2}}$	1978.91	15	50532.98	$a\ ^4G_{2\frac{1}{2}}$—$x\ ^4G^o_{2\frac{1}{2}}$
1989.37	12	50267.07	$b\ ^4D_{1\frac{1}{2}}$—$t\ ^2F^o_{2\frac{1}{2}}$; $a\ ^4G_{4\frac{1}{2}}$—$y\ ^2G^o_{4\frac{1}{2}}$	1978.68	2	50538.82	$a\ ^4D_{1\frac{1}{2}}$—$x\ ^4P^o_{1\frac{1}{2}}$
				1978.24	18	50550.10	$a\ ^4H_{6\frac{1}{2}}$—$w\ ^4G^o_{5\frac{1}{2}}$
1987.97	20	50302.54	$a\ ^6S_{2\frac{1}{2}}$—$z\ ^6D^o_{3\frac{1}{2}}$	1977.17	20	50577.34	$a\ ^6S_{2\frac{1}{2}}$—$z\ ^6D^o_{2\frac{1}{2}}$

TABLE 2. *Wavelengths of* Mo II *in vacuum*—Continued

Wavelength computed	Intensity	Wave No.	Term combination	Wavelength computed	Intensity	Wave No.	Term combination
1976. 86	5	50585. 30	$a\ ^6D_{2½}—y\ ^4F°_{1½}$	1938. 16	2	51595. 32	$a\ ^2G_{4½}—w\ ^4G°_{5½}$
1975. 03	8	50632. 22	$a\ ^4G_{2½}—(3)\ ^3_{3½}$	1937. 76	5	51606. 01	$a\ ^2D_{2½}—w\ ^2P°_{1½}$
1973. 99	1	50658. 69	$a\ ^4F_{4½}—u\ ^2F°_{3½}$	1937. 46	4	51614. 01	$a\ ^6D_{4½}—z\ ^2H°_{3½}$
1973. 07	3	50682. 39	$a\ ^2D_{1½}—w\ ^2P°_{0½}$	1936. 28	2	51645. 52	$a\ ^4D_{0½}—x\ ^4P°_{1½}$
1972. 88	1	50687. 35	$a\ ^6D_{2½}—y\ ^4F°_{3½}$	1934. 16	15	51702. 14	$a\ ^2D_{2½}—u\ ^2F°_{2½}$
1972. 38	5	50700. 28	$a\ ^4P_{1½}—w\ ^4D°_{1½}$	1933. 16	8	51728. 70	$a\ ^4D_{1½}—y\ ^2P°_{1½}$
1971. 54	8	50721. 66	$a\ ^4F_{1½}—w\ ^4G°_{2½}$ $b\ ^4D_{2½}—w\ ^4G°_{3½}$	1931. 03	6	51785. 81	$a\ ^6D_{2½}—x\ ^4F°_{3½}$
1970. 74	4	50742. 33	$a\ ^6D_{4½}—x\ ^4F°_{3½}$	1930. 49	2	51800. 25	$a\ ^6D_{4½}—y\ ^2F°_{3½}$
1970. 17	8	50756. 99	$a\ ^4G_{3½}—x\ ^4G°_{3½}$	1928. 66	4	51849. 36	$a\ ^4D_{0½}—y\ ^2P°_{0½}$
1969. 79	20	50766. 71	$a\ ^4D_{3½}—x\ ^4P°_{2½}$ $a\ ^6D_{0½}—x\ ^4D°_{1½}$	1927. 69	25	51875. 65	$a\ ^4D_{1½}—x\ ^4P°_{0½}$
1969. 49	5	50774. 61	$a\ ^2D_{2½}—x\ ^2P°_{1½}$	1926. 79	18	51899. 81	$a\ ^4F_{2½}—w\ ^4G°_{3½}$
1966. 88	10	50841. 82	$a\ ^4D_{1½}—w\ ^4F°_{2½}$	1924. 42	1	51963. 69	$a\ ^4G_{4½}—x\ ^2F°_{3½}$
1965. 96	2	50865. 70	$a\ ^6D_{4½}—x\ ^4F°_{4½}$	1922. 57	12	52013. 76	$a\ ^4P_{1½}—x\ ^4P°_{2½}$
1965. 37	2	50880. 95	$a\ ^6D_{2½}—y\ ^4H°_{3½}$	1922. 27	18	52021. 70	$a\ ^4P_{2½}—x\ ^4P°_{2½}$
1965. 09	4	50888. 20	$a\ ^4G_{2½}—x\ ^4G°_{3½}$	1921. 33	2	52047. 18	$a\ ^2D_{2½}—u\ ^2F°_{3½}$
				1918. 56	2	52122. 44	$a\ ^4P_{1½}—w\ ^4F°_{1½}$
				1916. 00	4	52192. 18	$a\ ^4G_{2½}—x\ ^2F°_{3½}$
1964. 78	12	50896. 20	$b\ ^2H_{5½}—v\ ^2H°_{5½}$ $a\ ^4F_{3½}—t\ ^2F°_{3½}$	1913. 74	18	52253. 61	$a\ ^4D_{0½}—x\ ^4P°_{0½}$
1964. 00	3	50916. 37	$a\ ^4F_{4½}—t\ ^2F°_{3½}$	1911. 86	8	52305. 19	$a\ ^2D_{2½}—t\ ^2F°_{3½}$
1963. 69	8	50924. 50	$a\ ^4F_{2½}—w\ ^4G°_{3½}$ $a\ ^4H_{5½}—w\ ^4G°_{5½}$	1911. 43	7	52316. 76	$a\ ^4P_{1½}—w\ ^4F°_{2½}$
1962. 92	2	50944. 49	$a\ ^4G_{5½}—x\ ^4G°_{4½}$	1911. 09	12	52326. 12	$a\ ^4P_{2½}—w\ ^4F°_{2½}$ $a\ ^4G_{3½}—x\ ^2F°_{2½}$
1962. 18	15	50963. 72	$a\ ^4G_{4½}—x\ ^4G°_{3½}$	1910. 87	5	52332. 57	$a\ ^4G_{4½}—x\ ^2G°_{3½}$
1961. 99	6	50968. 67	$a\ ^4P_{1½}—w\ ^4D°_{2½}$ $a\ ^6D_{1½}—y\ ^4F°_{1½}$	1909. 83	10	52360. 62	$a\ ^6D_{1½}—z\ ^2F°_{2½}$ $a\ ^6D_{3½}—y\ ^2F°_{3½}$
1961. 70	10	50976. 12	$a\ ^6D_{2½}—y\ ^4F°_{2½}$ $a\ ^6D_{3½}—z\ ^2F°_{3½}$ $a\ ^4P_{2½}—w\ ^4D°_{2½}$	1909. 40	1	52372. 44	$a\ ^6D_{3½}—y\ ^2F°_{2½}$
				1909. 04	4	52382. 36	$a\ ^4G_{3½}—x\ ^4P°_{2½}$
				1907. 13	3	52434. 94	$a\ ^6D_{2½}—y\ ^2G°_{3½}$
1961. 42	10	50983. 42	$b\ ^4D_{3½}—v\ ^4D°_{3½}$	1905. 18	4	52488. 48	$a\ ^4P_{2½}—w\ ^4F°_{3½}$
1958. 45	10	51060. 90	$a\ ^4G_{3½}—x\ ^4G°_{4½}$	1905. 02	12	52492. 80	$b\ ^4F_{4½}—u\ ^2G°_{3½}$
1957. 17	4	51094. 30	$b\ ^4D_{2½}—v\ ^4D°_{2½}$	1903. 38	1	52538. 01	$b\ ^4F_{3½}—u\ ^2G°_{3½}$
1957. 04	30	51097. 56	$a\ ^4D_{2½}—x\ ^4P°_{1½}$	1902. 89	10	52551. 54	$a\ ^4P_{0½}—x\ ^4P°_{1½}$
1956. 73	4	51105. 69	$a\ ^4D_{3½}—x\ ^2G°_{4½}$	1902. 55	2	52561. 05	$a\ ^4G_{2½}—x\ ^2G°_{3½}$
1954. 07	6	51175. 30	$a\ ^2F_{3½}—w\ ^4G°_{4½}$	1900. 94	15	52605. 50	$a\ ^4G_{3½}—x\ ^2G°_{3½}$
1953. 66	6	51186. 01	$a\ ^2D_{1½}—w\ ^2P°_{1½}$	1898. 06	10	52685. 36	$a\ ^4G_{3½}—w\ ^4F°_{3½}$
1953. 12	5	51200. 19	$a\ ^4G_{2½}—w\ ^4D°_{1½}$	1896. 94	1	52716. 60	$a\ ^6D_{1½}—z\ ^4S°_{1½}$
1952. 62	7	51212. 73	$b\ ^4D_{2½}—v\ ^4D°_{3½}$	1896. 74	5	52721. 91	$a\ ^4G_{3½}—x\ ^2G°_{3½}$
1952. 39	10	51219. 22	$a\ ^6D_{0½}—y\ ^4F°_{1½}$	1896. 41	10	52731. 25	$a\ ^4F_{3½}—w\ ^4G°_{4½}$
1951. 87	2	51232. 92	$a\ ^4D_{3½}—w\ ^4F°_{3½}$	1896. 00	1	52742. 50	$a\ ^4P_{1½}—x\ ^4P°_{1½}$
1951. 49	7	51243. 02	$b\ ^4D_{3½}—w\ ^4G°_{4½}$	1895. 94	8	52744. 18	$a\ ^4P_{1½}—x\ ^4P°_{1½}$
1950. 55	15	51267. 54	$a\ ^4D_{1½}—x\ ^4P°_{1½}$ $a\ ^6D_{3½}—x\ ^4F°_{2½}$	1895. 72	10	52750. 44	$a\ ^4P_{2½}—x\ ^4P°_{1½}$
1950. 00	2	51282. 14	$a\ ^2D_{1½}—u\ ^2F°_{2½}$	1895. 65	18	52752. 38	$a\ ^4G_{4½}—w\ ^4F°_{3½}$ $a\ ^4F_{4½}—w\ ^4G°_{4½}$ $a\ ^4P_{0½}—y\ ^2P°_{0½}$
1949. 44	35	51296. 75	$a\ ^4G_{5½}—x\ ^4G°_{5½}$				
1949. 21	7	51302. 76	$a\ ^6D_{3½}—x\ ^4F°_{3½}$	1892. 80	7	52831. 90	$a\ ^6D_{3½}—x\ ^4G°_{2½}$
1948. 71	12	51315. 99	$a\ ^4G_{4½}—x\ ^4G°_{5½}$	1892. 18	15	52849. 14	$a\ ^4G_{3½}—w\ ^4F°_{3½}$
1948. 37	3	51325. 07	$a\ ^2F_{3½}—w\ ^4G°_{3½}$	1891. 20	10	52876. 53	$a\ ^4G_{5½}—w\ ^4F°_{4½}$
1947. 90	4	51337. 42	$a\ ^4G_{3½}—w\ ^4D°_{2½}$	1890. 51	3	52895. 77	$a\ ^4G_{4½}—w\ ^4F°_{4½}$
1947. 10	5	51358. 46	$a\ ^6D_{1½}—y\ ^4F°_{2½}$	1888. 70	8	52946. 34	$a\ ^4P_{1½}—y\ ^2P°_{0½}$
1946. 41	1	51376. 72	$a\ ^4D_{3½}—w\ ^4F°_{4½}$	1887. 96	3	52967. 30	$a\ ^6D_{0½}—z\ ^8S°_{1½}$
1946. 06	20	51385. 78	$a\ ^4G_{3½}—w\ ^4D°_{3½}$	1887. 04	5	52992. 94	$a\ ^4G_{3½}—w\ ^4F°_{3½}$
1944. 54	4	51426. 09	$a\ ^6D_{3½}—x\ ^4F°_{4½}$	1886. 34	20	53012. 68	$a\ ^4P_{0½}—y\ ^2P°_{1½}$
1943. 28	2	51459. 40	$a\ ^6D_{2½}—z\ ^2F°_{3½}$				
1942. 83	8	51471. 40	$a\ ^4G_{2½}—w\ ^4D°_{2½}$ $a\ ^4D_{1½}—y\ ^2P°_{0½}$	1881. 13	3	53159. 63	$a\ ^4P_{0½}—z\ ^4P°_{0½}$
				1879. 57	10	53203. 64	$a\ ^4P_{1½}—y\ ^2P°_{1½}$
1942. 25	1	51486. 62	$a\ ^6D_{2½}—x\ ^4F°_{1½}$	1879. 29	5	53211. 58	$a\ ^4P_{2½}—y\ ^2P°_{1½}$
1941. 10	8	51517. 09	$a\ ^4G_{2½}—w\ ^4D°_{3½}$	1876. 77	12	53283. 02	$a\ ^6D_{4½}—x\ ^4G°_{3½}$
1939. 54	25	51558. 70	$a\ ^4D_{2½}—y\ ^2P°_{1½}$	1874. 39	3	53350. 59	$a\ ^4P_{1½}—z\ ^4P°_{0½}$

TABLE 2. *Wavelengths of* Mo II *in vacuum*—Continued

Wavelength computed	Intensity	Wave No.	Term combination
1872. 30	3	53410. 24	$a\ ^6D_{1\frac{1}{2}}$—$y\ ^2D^\circ_{1\frac{1}{2}}$
1866. 79	1	53567. 94	$b\ ^4F_{3\frac{1}{2}}$—$u\ ^2G^\circ_{3\frac{1}{2}}$
1865. 53	10	53604. 12	$a\ ^2I_{5\frac{1}{2}}$—$w\ ^4G^\circ_{5\frac{1}{2}}$
1862. 26	1	53698. 17	$a\ ^6D_{1\frac{1}{2}}$—$x\ ^4G^\circ_{2\frac{1}{2}}$
1858. 66	18	53802. 28	$a\ ^2H_{4\frac{1}{2}}$—$u\ ^2G^\circ_{3\frac{1}{2}}$
1857. 66	20	53831. 06	$a\ ^4F_{4\frac{1}{2}}$—$w\ ^4G^\circ_{5\frac{1}{2}}$
1850. 80	3	54030. 74	$a\ ^4P_{1\frac{1}{2}}$—$w\ ^2F^\circ_{2\frac{1}{2}}$
1843. 29	4	54250. 70	$a\ ^6D_{2\frac{1}{2}}$—$w\ ^4D^\circ_{3\frac{1}{2}}$
1831. 83	7	54590. 29	$a\ ^6D_{0\frac{1}{2}}$—$w\ ^4D^\circ_{0\frac{1}{2}}$
1830. 96	6	54616. 08	$a\ ^6D_{1\frac{1}{2}}$—$w\ ^4D^\circ_{1\frac{1}{2}}$
1829. 04	5	54673. 55	$a\ ^4G_{3\frac{1}{2}}$—$x\ ^2H^\circ_{4\frac{1}{2}}$ $a\ ^4G_{4\frac{1}{2}}$—$w\ ^2F^\circ_{3\frac{1}{2}}$
1828. 71	4	54683. 44	$a\ ^2I_{5\frac{1}{2}}$—$w\ ^4G^\circ_{3\frac{1}{2}}$
1825. 08	5	54792. 20	$a\ ^4D_{1\frac{1}{2}}$—$x\ ^2P^\circ_{0\frac{1}{2}}$
1823. 75	7	54832. 21	$a\ ^2H_{4\frac{1}{2}}$—$u\ ^2G^\circ_{4\frac{1}{2}}$
1822. 66	4	54864. 90	$a\ ^4D_{1\frac{1}{2}}$—$w\ ^2D^\circ_{1\frac{1}{2}}$
1821. 42	8	54902. 30	$a\ ^4G_{2\frac{1}{2}}$—$w\ ^2F^\circ_{3\frac{1}{2}}$
1820. 50	12	54929. 90	$a\ ^2H_{5\frac{1}{2}}$—$u\ ^2G^\circ_{4\frac{1}{2}}$
1813. 56	2	55140. 09	$a\ ^4D_{2\frac{1}{2}}$—$v\ ^2F^\circ_{2\frac{1}{2}}$
1812. 57	20	55170. 16	$a\ ^4D_{0\frac{1}{2}}$—$x\ ^2P^\circ_{0\frac{1}{2}}$
1811. 07	6	55215. 85	$a\ ^6S_{2\frac{1}{2}}$—$z\ ^4D^\circ_{2\frac{1}{2}}$
1810. 82	10	55223. 60	$a\ ^4G_{5\frac{1}{2}}$—$x\ ^2H^\circ_{5\frac{1}{2}}$
1802. 27	5	55485. 52	$a\ ^4D_{2\frac{1}{2}}$—$w\ ^2D^\circ_{2\frac{1}{2}}$
1801. 73	4	55502. 31	$a\ ^4P_{2\frac{1}{2}}$—$w\ ^2G^\circ_{3\frac{1}{2}}$
1795. 12	6	55706. 57	$a\ ^6S_{2\frac{1}{2}}$—$z\ ^4D^\circ_{3\frac{1}{2}}$
1789. 71	6	55874. 87	$a\ ^4D_{2\frac{1}{2}}$—$x\ ^2P^\circ_{1\frac{1}{2}}$
1789. 09	15	55994. 28	$a\ ^4G_{2\frac{1}{2}}$—$w\ ^2G^\circ_{3\frac{1}{2}}$
1784. 94	4	56024. 38	$a\ ^6D_{2\frac{1}{2}}$—$x\ ^4P^\circ_{1\frac{1}{2}}$
1783. 29	2	56076. 18	$a\ ^4P_{0\frac{1}{2}}$—$x\ ^2P^\circ_{0\frac{1}{2}}$
1782. 99	18	56085. 50	$a\ ^4D_{3\frac{1}{2}}$—$v\ ^2F^\circ_{3\frac{1}{2}}$
1780. 98	25	56148. 88	$a\ ^4P_{0\frac{1}{2}}$—$w\ ^2D^\circ_{1\frac{1}{2}}$
1773. 91	2	56372. 65	$a\ ^4D_{1\frac{1}{2}}$—$w\ ^2P^\circ_{0\frac{1}{2}}$
1772. 81	3	56407. 60	$a\ ^6D_{1\frac{1}{2}}$—$x\ ^4P^\circ_{1\frac{1}{2}}$
1772. 59	3	56414. 70	$b\ ^4D_{2\frac{1}{2}}$—$u\ ^2G^\circ_{3\frac{1}{2}}$
1772. 33	3	56422. 83	$a\ ^4D_{0\frac{1}{2}}$—$x\ ^2P^\circ_{1\frac{1}{2}}$
1770. 37	8	56485. 52	$a\ ^6D_{2\frac{1}{2}}$—$y\ ^2P^\circ_{1\frac{1}{2}}$
1766. 43	2	56611. 44	$a\ ^6D_{1\frac{1}{2}}$—$y\ ^2P^\circ_{0\frac{1}{2}}$
1765. 51	1	56640. 85	$a\ ^6D_{4\frac{1}{2}}$—$w\ ^2F^\circ_{3\frac{1}{2}}$
1764. 97	8	56658. 30	$a\ ^6D_{0\frac{1}{2}}$—$x\ ^4P^\circ_{1\frac{1}{2}}$
1763. 47	5	56706. 27	$a\ ^4D_{2\frac{1}{2}}$—$w\ ^2P^\circ_{1\frac{1}{2}}$
1762. 10	3	56750. 61	$a\ ^4D_{0\frac{1}{2}}$—$w\ ^2P^\circ_{0\frac{1}{2}}$
1759. 33	15	56839. 75	$a\ ^4G_{2\frac{1}{2}}$—$w\ ^2D^\circ_{2\frac{1}{2}}$
1758. 64	15	56862. 14	$a\ ^6D_{0\frac{1}{2}}$—$y\ ^2P^\circ_{0\frac{1}{2}}$
1758. 43	12	56868. 74	$a\ ^6D_{1\frac{1}{2}}$—$y\ ^2P^\circ_{1\frac{1}{2}}$
1753. 90	15	57015. 69	$a\ ^6D_{1\frac{1}{2}}$—$x\ ^4P^\circ_{0\frac{1}{2}}$
1750. 72	4	57119. 44	$a\ ^6D_{0\frac{1}{2}}$—$y\ ^2P^\circ_{1\frac{1}{2}}$
1750. 14	10	57138. 40	$a\ ^4P_{2\frac{1}{2}}$—$w\ ^2D^\circ_{2\frac{1}{2}}$
1747. 78	1	57215. 32	$b\ ^4D_{3\frac{1}{2}}$—$u\ ^2G^\circ_{4\frac{1}{2}}$
1746. 22	22	57266. 39	$a\ ^6D_{0\frac{1}{2}}$—$x\ ^4P^\circ_{0\frac{1}{2}}$
1739. 16	6	57499. 06	$a\ ^4G_{3\frac{1}{2}}$—$w\ ^2D^\circ_{2\frac{1}{2}}$
1738. 53	1	57519. 81	$a\ ^4P_{1\frac{1}{2}}$—$x\ ^2P^\circ_{1\frac{1}{2}}$
1735. 20	4	57630. 37	$a\ ^4G_{2\frac{1}{2}}$—$w\ ^2D^\circ_{2\frac{1}{2}}$
1734. 41	3	57656. 63	$a\ ^4P_{0\frac{1}{2}}$—$w\ ^2P^\circ_{0\frac{1}{2}}$
1733. 90	1	57673. 62	$a\ ^4F_{3\frac{1}{2}}$—$u\ ^2G^\circ_{3\frac{1}{2}}$
1731. 54	50	57752. 07	$a\ ^4D_{1\frac{1}{2}}$—$t\ ^2F^\circ_{2\frac{1}{2}}$
1730. 02	2	57802. 77	$a\ ^4D_{3\frac{1}{2}}$—$t\ ^2F^\circ_{3\frac{1}{2}}$
1727. 35	5	57892. 05	$a\ ^6S_{2\frac{1}{2}}$—$z\ ^4H^\circ_{3\frac{1}{2}}$
1724. 75	3	57979. 39	$a\ ^4D_{3\frac{1}{2}}$—$t\ ^2F^\circ_{3\frac{1}{2}}$
1713. 76	1	58351. 21	$a\ ^4P_{1\frac{1}{2}}$—$w\ ^2P^\circ_{1\frac{1}{2}}$
1693. 39	3	59053. 32	$a\ ^6S_{2\frac{1}{2}}$—$z\ ^4G^\circ_{2\frac{1}{2}}$
1681. 29	2	59478. 34	$a\ ^6S_{2\frac{1}{2}}$—$z\ ^4G^\circ_{3\frac{1}{2}}$
1674. 29	1	59726. 92	$a\ ^4G_{2\frac{1}{2}}$—$t\ ^2F^\circ_{2\frac{1}{2}}$
1668. 63	3	59929. 29	$a\ ^6D_{3\frac{1}{2}}$—$w\ ^2D^\circ_{2\frac{1}{2}}$
1610. 97	12	62074. 26	$a\ ^6D_{2\frac{1}{2}}$—$u\ ^2F^\circ_{3\frac{1}{2}}$
1605. 99	5	62266. 77	$a\ ^6D_{0\frac{1}{2}}$—$w\ ^2P^\circ_{1\frac{1}{2}}$
1603. 24	4	62373. 67	$a\ ^6D_{4\frac{1}{2}}$—$w\ ^4G^\circ_{3\frac{1}{2}}$
1591. 73	2	62824. 80	$a\ ^6D_{1\frac{1}{2}}$—$w\ ^4G^\circ_{2\frac{1}{2}}$
1586. 99	5	63012. 24	$a\ ^6S_{2\frac{1}{2}}$—$(2)^4_{3\frac{1}{2}}$
1552. 90	3	64395. 44	$a\ ^6S_{2\frac{1}{2}}$—$z\ ^2F^\circ_{2\frac{1}{2}}$

TABLE 3. *Zeeman effect of* Mo II

Wavelengths	Magnetic patterns
5490. 78	(**0.091,** 0.269) **0.787,** 0.964, 1.138
5448. 80	(0.000W) 1.139A
5181. 54	(0.000W) 1.230A
4853. 63	(0.094) 0.837
4742. 61	(0.000) 1.200
4667. 40	(0.364) **1.459,** 2.186
4637. 95	(0.075) 1.597
4604. 20	(0.000) 1.07†
4565. 69	(0.00) 0.97†
4543. 40	(0.00) 1.10†
4553. 50	(0.00) 1.41†
4519. 60	(0.00*w*) 1.62*B*†
4452. 02	(0.00) 1.06†
4433. 49	(0.804) **0.396,** 1.993
4407. 38	(0.21) 1.01†
4403. 29	(0.28) 1.02†
4388. 26	(0.00) 1.06†
4377. 75	(1.374) 1.422
4363. 64	(**0.284,** 0.837) **0.420,** 0.992, 1.547, 2.093
4361. 91	(0.000) 1.111
4358. 27	(0.000*w*) 0.856A
4356. 10	(0.00) 1.50†
4328. 01	(**0.136,** 0.403) 0.955, 1.207, **1.465**
4315. 23	(**0.217,** 0.682, 1.137) **0.227,** 0.709, 1.144
4311. 65	(**0.388,** 1.145)—**0.080,** 0.689, 1.430, 2.180
4311. 64	(0.000) 1.038
4279. 02	(0.300, **0.943**) 0.877, **1.514,** 2.140
4274. 44	(0.000) 1.108
4250. 69	(**0.176,** 0.546, 0.905) **0.462,** 0.825, 1.198, 1.562, 1.928
4246. 58	(0.00) 4.61†
4244. 72	(0.000) 0.861
4227. 07	(0.883) 0.941, **2.689**
4209. 65	(0.269, 0.740, **1.229**) 0.535, 1.021, **1.512,** 2.004, 2.487
4192. 27	(**0.073,** 0.222, 0.359) 0.947, 1.089, 1.224, **1.367**
4191. 03	(?) 0.84†
4177. 94	(**0.550,** 1.595)—**0.319,** +0.737
4171. 79	(0.000*w*) 0.960*w*
4161. 25	(1.035, **1.731**) 0.000, 0.701, **1.400,** 2.113, 2.800
4150. 82	(0.000) 1.097
4146. 87	(0.239) **0.942,** 1.421

Wavelengths	Magnetic patterns
4141. 45	(0.757, **1.066**) 0.607, 0.916, 1.216, **1.507,** 1.810, 2.113, 2.416
4139. 78	(**0.105,** 0.333) 0.904, 1.119, **1.322**
4125. 63	(0.000) 1.170
4122. 35	(**0.054,** 0.174, 0.285) **0.780,** 0.902, 1.020, 1.136, 1.249
4119. 63	(**0.165,** 0.502, 0.828) **0.559,** 0.893, 1.222, 1.557, 1.892
4118. 53	(0.000*w*) 0.640*w*
4115. 76	(0.00) 1.21†
4100. 30	(1.702) 0.645, **1.752,** 2.854
4094. 96	(**0.219,** 0.661) 1.515, 1.965, **2.400**
4081. 07	(0.711, **1.147**) 0.583, 1.036, **1.488,** 1.945, 2.402
4077. 68	(0.333) **0.998,** 1.657
4058. 61	(?) 0.81†
4038. 81	(0.00) 1.10†
4029. 96	(0.283, **0.388**) 0.885, 0.981, 1.095, **1.201,** 1.313, 1.421, 1.530
4023. 54	(**0.138,** 0.460) 0.837, 1.130, 1.389, 1.670, **1.945**
4013. 20	(**0.072,** 0.198, 0.344) **0.574,** 0.716, 0.862, 1.007
4010. 31	(0.00) 1.32†
4005. 12	(0.254, 0.410, **0.564**) 0.996, 1.152, 1.328, **1.463,** 1.623, 1.779, 1.936
4002. 96	(?) 1.12*R*†
3999. 84	(**0.129,** 0.410, 0.653) **0.263,** 0.527, 0.786
3998. 56	(0.220) **1.012,** 1.442
3990. 79	(0.000) 1.229*R*
3986. 16	(**0.269,** 0.816) **0.459,** 0.995, 1.528, 2.066
3972. 95	(**0.234,** 0.468, 0.703) **0.291,** 0.525, 0.759
3968. 67	(**0.143,** 0.437) 1.433, 1.715, 1.982, **2.270**
3967. 80	(0.23) 0.40†
3961. 52	(**0.104,** 0.318, 0.532) **0.848,** 1.070, 1.284, 1.496, 1.708, 1.917
3952. 98	(0.975) **0.233,** 2.187
3942. 73	(**0.368,** 1.123) —**0.075,** 0.680, 1.425, 2.182
3941. 48	(**0.061,** 0.166, 0.287, 0.393) 1.110, 1.226, 1.449, 1.558, 1.665, 1.783, **1.909**
3930. 83	(**0.104,** 0.322, 0.533, 0.749) 1.260, 1.467, 1.675, 1.887, **2.103**
3929. 60	(0.383) **0.518,** 1.273
3925. 83	(0.519, **0.853**) 0.755, 1.099, **1.440,** 1.775, 2.113
3921. 53	(**0.111,** 0.345, 0.582) **0.371,** 0.610, 0.848
3919. 46	(0.000*w*) 1.360*R*
3917. 54	(0.37) 0.80†
3915. 43	(0.311, **0.911**) 0.892, **1.497,** 2.108
3908. 61	(1.547) 1.606
3906. 54	(0.000*w*) 0.943*w*
3904. 96	(0.000) 1.085
3882. 31	(0.67) 1.24*W*†
3871. 90	(0.873) 0.932, **2.674**
3871. 45	(0.000*w*) 1.020*wA*
3866. 88	(**0.043,** 0.129, 0.219) **0.848,** 0.931, 1.017
3861. 29	(**0.072,** 0.213, 0.364, 0.499, 0.647, 0.785) 1.131, 1.268, 1.419, 1.556, 1.705, 1.844, **1.987**
3858. 84	(0.00*w*) 1.27*w*†
3857. 20	(**0.203,** 0.614) 0.986, 1,393, 1.807, **2.211**
3848. 30	(**0.052,** 0.143, 0.249, 0.337) **0.993,** 1.088, 1.192, 1.285
3842. 59	(0.260) 0.938, **1.442**
3837. 20	(0.102, 0.307, **0.513**) 0.578, 0.761, **0.965,** 1.167, 1.374
3835. 33	(**0.069,** 0.186, 0.311, 0.431) 1.060, 1.209, 1.359, **1.494**
3833. 49	(0.000*W*) 1.185*wB*
3832. 36	(0.000*W*) 1.030*W*
3815. 27	(**0.216,** 0.642) 1.133, 1.498, 1.925, **2.355**
3813. 91	(**0.060,** 0.197, 0.344, 0.462) 1.280, 1.413, 1.561, **1.691**
3812. 21	(**0.055,** 0.181, 0.302, 0.410) 0.857, 0.985, 1.111, 1.223, 1.341, **1.463**
3811. 79	(**0.106,** 0.330, 0.552) **0.594,** 0.815, 1.029, 1.241
3786. 37	(0.491) 1.155
3783. 17	(0.091) 1.035*w*
3782. 06	(0.000*W*) 1.134*WB*
3767. 77	(**0.067,** 0.184, 0.309, 0.422) 0.965, 1.082, 1.206, 1.337, **1.462**
3762. 11	(0.000) 1.208
3755. 50	(0.113, 0.325, **0.542**) 0.728, 0.938, **1.156,** 1.368, 1.584
3754. 67	(**0.091,** 0.277, 0.465, 0.643, 0.827) 1.333, 1.514, 1.695, **1.880**
3753. 48	(0.180*wB*) 0.991*WD*
3748. 12	(**0.072,** 0.200, 0.344, 0.473) **0.809,** 0.943, 1.077, 1.216, 1.352
3746. 44	(**0.075,** 0.227, 0.380) **1.037,** 1.191, 1.341, 1.501, 1.655, 1.809
3744. 42	(0.000) 0.972*w*
3744. 37	(0.000*w*) 1.018
3742. 34	(0.376, **1.162**) 0.046, **0.809,** 1.585
3741. 78	(0.568, **0.793**) 0.808, 1.030, **1.249,** 1.473, 1.697
3738. 84	(**0.094,** 0.294, 0.484) 0.786, 0.995, 1.190, 1.382, **1.576**
3736. 40	(0.000*w*) 0.998*wA*
3730. 54	(0.000*WD*) 1.347*WB*
3728. 50	(**0.052,** 0.150, 0.243) **0.933,** 1.024, 1.124, 1.215, 1.312, 1.405
3720. 20	(0.069, 0.291, 0.522, **0.759**) 0.971, 1.177, **1.393,** 1.603, 1.826, 2.054
3719. 78	(0.174, 0.321, **0.460**) 0.935, 1.062, 1.192, **1.322,** 1.450, 1.581, 1.700
3719. 05	(0.000*w*) 1.152*wB*
3716. 92	(0.000) 1.050
3713. 92	(0.000) 1.080
3704. 15	(0.170, 0.274, **0.391**) 0.618, 0.730, 0.837, **0.950,** 1.058, 1.163, 1.278
3702. 55	(0 180) 0.235, **0.596**
3699. 84	(0.000*w*) 1.114*w*
3697. 02	(0.356, 0.613, **0.864**) 0.617, 0.875, 1.142, 1.381, 1.652, 1.888
3692. 65	(**0.074,** 0.217) **0.831,** 0.979, 1.121, 1.276
3690. 35	(0.000*w*) 0.898*wA*
3688. 31	(0.000) 1.257
3684. 18	(0.155*B*) 1.109*D*
3670. 67	(0.139) 0.366, **0.470,** 0.567
3658. 97	(0.104*B*) 0.957*WD*
3658. 29	(0.065) 1.178
3655. 79	(0.172*B*) 0.949*WD*
3652. 45	(0.000) 1.200*B*
3652. 32	(0.000*w*) 0.900*A*
3651. 10	(**0.106,** 0.302, 0.505) 0.749, 0.960, 1.159, 1.363, 1.567, **1.773**
3643. 47	(**0.297,** 0.904) 0.119, 0.716, 1.318, **1.914**
3639. 64	(0.000*w*) 1.164*w*
3637. 77	(**0.000,** 0.256) **0.793,** 1.044, 1.297, 1.554
3635. 14	(0.000) 1.305
3633. 31	(0.393, 0.533, 0.683, **0.834**) 0.393, 0.533, 0.683, 0.834, **0.984,** 1.134, 1.285, 1.435, 1.586
3627. 35	(0.000*WD*) 1.115*wB*
3625. 54	(**0.076,** 0.236, 0.387, 0.528, 0.669, 0.824) 1.433, 1.606, 1.773, **1.918**
3623. 68	(**0.186,** 0.507) **0.860,** 1.188, 1.538
3622. 84	(**0.260,** 0. 812) 0.217, 0.769, 1.318, **1.825**
3620. 18	(**0.169,** 0.510) 1.016, **1.365**
3618. 36	(**0.049,** 0.146, 0.229, 0.330, . . .) 1.357, 1.475, 1.545, **1.631**
3617. 56	(1.276) 1.276
3612. 12	(0.054) 1.128, **1.224**
3606. 90	(0.099) 0.765, **0.962**
3606. 64	(0.262*wB*) 1.052*WD*
3597. 68	(0.000) 0.979
3596. 75	(0.000*wD*) 1.175*wB*
3596. 35	(0.089) 1.028
3592. 61	(**0.118,** 0.305, 0.532, 0.738) 0.975, 1.200, 1.412, 1.622, **1.845**
3592. 27	(0.366, **0.457**) 0.766, 0.870, **0.982,** 1.085, 1.201, 1.300

Wavelengths	Magnetic patterns
3591. 64	(0.000) 0.922
3590. 13	(**0.150,** 0.444, 0.742) **0.159,** 0.450, 0.745, 1.048, 1.333
3589. 48	(0.000*WD*) 1.059, **1.198**
3585. 90	(**0.088,** 0.253, 0.412) 0.615, 0.782, 0.951, 1.115, 1.297, 1.458, **1.632**
3585. 67	(0.125) 1.082*w*
3582. 41	(. . . , 0.487) . . . , 1.318, **1.634**
3580. 54	(0.000) 1.014
3579. 06	(0.187, 0.306, **0.423**) 0.665, 0.781, 0.896, **1.019,** 1.129, 1.249, 1.363
3572. 56	(0.346, 0.561, 0.802, **1.024**) 0.192, 0.396, 0.623, 0.842, **1.070,** 1.308, 1.532, 1.751
3561. 38	(**0.120,** 0.355, 0.588, 0.814) 1.558, 1.794, 2.040, **2.267**
3559. 72	(0.670) **0.521,** 1.874
3556. 96	(0.137*B*) 0.836*WD*
3556. 32	(0.188*B*) 1.053*WD*
3553. 69	(0.228, **0.689**) 0.487, **0.948,** 1.407
3547. 94	(**0.052,** 0.142, 0.246, 0.353) **0.596,** 0.691, 0.801, 0.906, 0.998, 1.118, 1.210
3545. 98	(0.000*D*) 0.551*A*
3542. 39	(0.000) 1.219
3537. 12	(**0.085,** 0.276, 0.441, 0.610) 1.029, 1.197, 1.368, 1.540, **1.726**
3534. 70	(**0.125,** 0.363, 0.606) 0.650, 0.898, 1.136, 1.378, 1.612, **1.860**
3533. 00	(0.398, 0.669, **0.938**) 0.482, 0.744, 1.009, **1.285,** 1.552, 1.819, 2.089
3527. 88	(0.000) 1.093
3524. 70	(0.000) 1.183
3524. 50	(0.000) 1.145
3522. 06	(0.000*wD*) 1.409*B*
3520. 16	(0.060, 0.168, 0.275, **0.382**) 0.649, 0.776, 0.905, **1.025,** 1.131, 1.267, 1.367
3515. 68	(0.130) 0.327, **0.580**
3506. 70	(0.141, **0.406**) 0.286, **0.544,** 0.809
3502. 69	(0.000*WD*) 0.726*A*
3501. 94	(0.000*WD*) 0.758*A*
3499. 97	(**0.078,** 0.236, 0.399) 0.781, 0.934, 1.097, 1.258, **1.423**
3499. 08	(0.088) 1.148, **1.311**
3488. 15	(0.156, **0.483**) 0.729, **1.055,** 1.378
3485. 72	(0.000*W*, *D*) 0.844*A*
3484. 56	(**0.049,** 0.137, 0.236, 0.341, 0.447) 1.363, 1.459, 1.563, **1.645**
3482. 76	(**0.121,** 0.347) 1.039*w*
3463. 03	(**0.183,** 0.543) 0.875, 1.229, **1.595**
3462. 07	(**0.111,** 0.333, 0.543) . . . ?
3452. 82	(0.000*w*) 1.146*B*
3450. 59	(**0.082,** 0.265, 0.454) 0.582, 0.776, 0.955, 1.131, 1.313, **1.486**
3448. 53	(**0.072,** 0.235, 0.381) . . . ?
3446. 09	(0.205, 0.312) 1.546*w*
3435. 38	(0.283*wD*) 0.934*wA*
3432. 23	(0.182, 0.284, 0.324, 0.429, **0.534**) 0.543, 0.641, 0.731, 0.837, 0.926, **1.012,** 1.116, 1.219, 1.315, 1.416, 1.502
3428. 88	(**0.055,** 0.169) 0.578, 0.704, 0.821, 0.928, **1.037**
3427. 07	(**0.108,** 0.328) 0.879, 1.092, **1.333**
3422. 76	(**0.094,** 0.268, 0.451, 0.628) **0.320,** 0.497, 0.690, 0.872, 1.040, 1.223, 1.401, 1.565
3414. 43	(**0.147,** 0.439, 0.748) **0.147,** 0.439, 0.748, 1.033
3412. 96	(0.280, **0.463**) 0.712, 0.898, **1.070,** 1.266, 1.443
3412. 37	(**0.066,** 0.221, 0.385) 1.466, 1.612, 1.798, 1.970, **2.144**
3410. 62	(0.000*WD*) 0.961*A*
3408. 67	(**0.106,** 0.317, 0.520) **0.542,** 0.747, 0.955, . . .
3407. 63	(0.000*w*) 0.973
3407. 20	(0.000*WD*) 0.914*A*
3402. 81	(0.000) 1.215*B*
3400. 15	(0.000) 0.664, **0.821**
3395. 75	(0.000*W*) 1.186
3395. 36	(0.185, **0.314**) 0.551, 0.677, **0.811,** 0.923, 1.043
3394. 81	(**0.144,** 0.426, 0.679) **0.185,** 0.463, 0.741, 0.987
3391. 84	(0.000*WD*) 0.581*A*
3386. 98	(**0.194,** 0.560) . . . ?
3383. 98	(**0.086,** 0.267, 0.444) 0.985, 1.161, 1.337, **1.517**
3380. 22	(0.000*w*) 1.342*B*
3379. 75	(0.558) 0.660, **1.777**
3376. 71	(0.444, 0.646, 0.836, **1.023**) 0.225, 0.408, 0.592, 0.780, 0.957, **1.142,** 1.334, 1.524, 1.711, 1.883, 2.077
3374. 84	(0.268) 0.951, **1.491**
3373. 10	(**0.181,** 0.531, 0.895, 1.246) −**0.181,** +0.181, 0.531, 0.895, 1.246
3371. 69	(0.000) 1.127
3370. 54	(0.000*w*) 0.913*A*
3369. 93	(0.981, 1.518, **2.165**)−0.109, 0.494, **1.138,** 1.768, 2.327
3367. 96	(0.000) 0.938
3366. 93	(0.752) 0.959, **2.453**
3363. 01	(**0.085,** 0.257, 0.433, 0.619, 0.803) **0.306,** 0.495, 0.667, 0.849, 1.020, 1.186, 1.359
3360. 28	(0.000*w*) 0.814*wA*
3357. 07	(**0.086,** 0.262, 0.433) . . .?
3352. 83	(0.432, **0.742**) 0.424, 0.736, **1.035,** 1.340, 1.642
3348. 92	(**0.086,** 0.215) **0.827,** 0.979, 1.123, 1.269
3347. 25	(0.000) 0.000
3346. 39	(0.000) 1.438
3346. 12	(0.000) 0.838
3335. 50	(0.212) 0.879
3335. 11	(0.000*wD*) 0.914*A*
3332. 52	(0.173*B*) 1.106*D*
3331. 40	(0.239) 0.774
3329. 21	(0.000) 1.182
3328. 56	(0.372) 0.372
3325. 22	(**0.226,** 0.694, 1.159) 0.000, 0.436, 0.908, 1.383, 1.819 **2.282**
3322. 13	(0.663) 1.290
3321. 20	(0.245) **0.255,** 0.433
3320. 90	(0.235) 1.391
3309. 46	(**0.081,** 0.269, 0.466, 0.670) **0.226,** 0.414, 0.555, 0.787
3302. 69	(0.626, **0.809**) 0.450, 0.632, 0.822, 0.991, **1.183,** 1.360, 1.544, 1.722
3300. 57	(**0.081,** 0.236, 0.402, 0.566, 0.722) **0.214,** 0.375, 0.533, 0.690, 0.840
3299. 59	(0.781) 0.552, 0.857, **1.162,** 1.485, 1.806
3297. 68	(0.569) 0.628, **1.767**
3296. 57	(0.440, **0.761**) 0.845, 1.134, **1.414,** 1.689, 2.006, 2.299
3296. 24	(0.000) 0.932
3295. 76	(**0.078,** 0.209, 0.339) **0.818,** 0.982, 1.140 . . .
3292. 96	(**0.000,** 0.153, 0.311) **0.791,** 0.933, 1.064, 1.168, 1.320
3292. 31	(0.099) 1.388
3290. 70	(0.457, **0.763**) 0.592, 0.908, **1.207,** 1.514, 1.806
3287. 20	(1.014) 1.768
3284. 60	(**0.132,** 0.383, 0.639) 0.352, 0.613, 0.881, 1.133, 1.385, **1.643**
3282. 89	(0.315*b*) 1.017*wD*
3278. 86	(0.317, 0.519, **0.755**) 0.409, 0.593, 0.827, **1.034,** 1.248, 1.460, 1.634
3278. 05	(0.142, **0.495**) 0.544, **0.850,** 1.180
3276. 32	(0.253, **0.781**) 0.924, **1.437,** 1.963
3273. 57	(0.370*B*) 1.096*wD*
3272. 37	(0.348, **1.023**) **0.859,** 1.528
3271. 66	(0.102, **0.265**) 1.106, 1.269, 1.457, **1.635**
3268. 97	(**0.080,** 0.225, 0,366, 0.524, 0.680) 0.924, 1.061, 1.221, 1.377, 1.526, 1.672, 1.830, **1.992**
3267. 62	(**0.087,** 0.240, 0.393) 1.185, 1.323, 1.484, 1.653, **1.834**
3262. 16	(0.397, 0.657, 0.891, **1.168**) 0.114, 0.385, 0.635, 0.895, **1.148,** 1.406, 1.669, 1.929, 2.213
3258. 68	(**0.195,** 0.563) **0.871,** 1.256, 1.623, 2.004
3257. 37	(**0.055,** 0.169, 0.287, 0.387,) **0.615,** 0.729, 0.856, 0.971
3255. 24	(**0.072,** 0.252, 0.452, 0.639, 0.824) **0.172,** 0.374, 0.548, 0.731, 0.915, 1.092, 1.266, 1.453, 1.631

TABLE 3. *Zeeman effect of* Mo II—Continued

Wavelengths	Magnetic patterns
3254. 68	(1.165) 1.392
3253. 73	(0.284*B*) 1.245*wD*
3252. 34	(0.198*B*) 1.291*wD*
3250. 74	(0.090, **0.286**) **0.725,** 0.922, 1.116, 1.289
3243. 18	(**0.115,** 0.364) 0.811, 1.052, 1.326, **1.583**
3240. 72	(0.206, **0.632**) 1.180, **1.615,** 2.032
3238. 40	(**0.181,** 0.536) 0.819, 1.236, 1.607, 1.950, **2.301**
3237. 84	(0.000*WB*) 1.085*wD*
3235. 38	(0.000) 1.718
3235. 02	(0.000) 1.255
3230. 90	(**0.069,** 0.188) 0.843, 0.979, **1.114**
3229. 68	(0.000*D*) 1.255*B*
3226. 56	(0.000*w*) 1.156*B*
3225. 75	(0.000*wD*) 1.419*B*
3224. 56	(**0.284,** 0.832, 1.369) 0.493, 1.024, 1.563, 2.132, **2.677**
3222. 91	(0.213, 0.369, **0.524**) 0.573, 0.717, 0.860, **0.993,** 1.148, 1.279, 1.413
3219. 41	(0.000) 1.448
3218. 35	(0.431, **0.701**) 0.479, 0.753, **1.024,** 1.308, 1.584
3216. 06	(0.112) 0.981
3214. 39	(**0.138,** 0.413, 0.693, 0.967) 0.587, 0.866, 1.148, 1.423, 1.692, 1.972, **2.254**
3213. 13	(**0.278,** 0.845, 1.387)−**0.400,** +0.162, 0.723, 1.291, 1.852, 2.420
3211. 97	(0.000*WD*) 1.341*wB*
3210. 96	(0.177) 1.130
3209. 72	(0.341, **0.463**) 0.681, 0.805, 0.928, **1.060,** 1.199, 1.341, 1.458
3207. 19	(0. 00*d*?) 1.063
3206. 82	(0.339, **0.536**) 0. 579, **0.794,** 0.996, 1.218
3204. 93	(0.614, 1.039, 1.433, **1.832**) . . ., **1.108,** 1.510, 1.887, 2.297, 2.708
3201. 50	(0.538) 1.298, **2.357**
3200. 30	(**0.127,** 0.391, 0.658, 0.923) −**0.027,** +0.222, 0.486, 0.740, 1.002, 1.268
3199. 24	(0.000 *D*) 1.080 *B*
3198. 41	(**0.069,** 0.206, 0.340, 0.486, 0.634, 0.774) **0.344,** 0.474, 0.621, 0.769, 0.898, 1.036, 1.176, 1.318, 1.443
3195. 86	(0.527, **0.860**) 0.500, 0.856, **1.194,** 1.543
3195. 23	(0.196) 1.322, **1.709**
3193. 11	(0.000 *w*) 1.281 *w*
3192. 10	(0.447) 2.330
3189. 36	(0.488) **0.550,** 1.515
3188. 85	(0.000 *w*) 1.545 *w*
3187. 59	(**0.088,** 0.231, 0.387) **0.833,** 0.978, 1.149, 1.300, 1.444, 1.592
3186. 39	(0.336) 0.362, **1.019**
3185. 56	(**0.077,** 0.220, 0.347) 0.758, 0.886, 1.003, 1.125, 1.236, **1.355**
3183. 41	(**0.146,** 0.427, 0.713, 0.985) 0.846, 1.122, 1.401, 1.705, **1.972**
3181. 17	(**0.516,** 1.556) −**0.868,** +0.159, 1.192
3178. 00	(**0.085,** 0.248, 0.415, 0.588, 0.763) 0.356, 0.531, 0.705, 0.867, 1.043, 1.215, 1.387, 1.547, 1.727, **1.900**
3176. 33	(0.230 *B*) 1.059 *WD*
3175. 05	(0.329 *B*) 0.745 *WD*
3174. 23	(0.206) 0.733, **0.887,** 1.010
3173. 76	(0.301 *B*) 1.064 *WD*
3168. 73	(0.273) 0.408, **1.126**
3167. 73	(0.291, **0.482**) 0.618, 0.805, **1.000,** 1.207, 1.397
3167. 01	(0.000) 1.008
3163. 89	(0.000) 1.093
3161. 12	(0.000 *w*) 1.558 *w*
3160. 11	(0.000) 1.613
3159. 34	(**0.247,** 0.704, 1.171) 1.370, 1.872, **2.367**
3157. 33	(0.000) 1.169
3156. 85	(0.000) 1.265
3155. 66	(**0.123,** 0.390, 0.667) **0.638,** 0.917, 1.172, 1.434, 1.717, 1.971
3155. 01	(**0.183,** 0.536) 1.259, 1.557, 1.931, **2.278**
3152. 82	(0.105 *B*) 0.971 *w*
3151. 64	(**0.225,** 0.656) **0.613,** 1.054, 1.480, 1.912
3150. 35	(**0.213,** 0.658, 1.066, 1.486) . . . ?
3148. 30	(0.000 *w*) 1.059 *w*
3145. 74	(0.074) **0.449,** 0.603
3144. 62	(**0.083,** 0.247, 0.424, 0.588) 0.560, 0.705, 0.866, 1.036, 1.206, 1.381, **1.562**
3143. 31	(**0.122,** 0.350, 0.605, 0.816) **0.301,** 0.555, 0.786, 1.018
3143. 06	(0.000 *w*) 0.787 *A*
3141. 73	(0.000 *w*) 1.398 *B*
3141. 40	(0.313 *B*) 1.110 *D*
3139. 40	(0.000 *WD*) 0.823 *A*
3138. 73	(0.354 *B*) 0.738 *D*
3138. 48	(0.317, 0.537, **0.738**) 0.665, 0.862, 1.073, **1.290,** 1.486, 1.680, 1.917
3136. 47	(**0.063,** 0.217, 0.376) **0.868,** 0.999, 1.116, 1.233, 1.343, 1.468, 1.585
3130. 06	(0.266, 0.420, 0.617, **0.808**) 0.490, 0.662, 0.847, 1.018, **1.188,** 1.366, 1.541, 1.726, 1.915
3127. 82	(0.000) 0.907
3126. 78	(**0.102,** 0.308, 0.509) **0.508,** 0.713, 0.919, 1.099, 1.335, 1.530
3126. 32	(**0.071,** 0.232, 0.402) **1.035,** 1.198, . . .
3126. 02	(0.012) 1.024, **1.201,** 1.351
3124. 89	(**0.138,** 0.421, 0.686) . . . 1.052, **1.328**
3124. 21	(0.000) 1.066
3123. 99	(0.271 *B*) 1.285 *WD*
3123. 46	(0.000) 1.061
3122. 00	(0.101) 1.118
3121. 22	(**0.053,** 0.185, 0.336, 0.475, 0.565) 1.032, 1.190, 1.289, 1.435, 1.559, **1.699**
3119. 44	(0.000) 1.113
3118. 94	(0.000 *WD*) 1.315 *B*
3117. 46	(0.352, 0.564, **0.790**) 0.369, 0.594, 0.809, **1.044,** 1.259, 1.485, 1.704
3116. 10	(0.000 *WD*) 0.893 *A*
3114. 96	(0.000 *w*) 0.884 *A*
3113. 52	(**0.369,** 1.121) . . ., **1.954**
3111. 65	(0.284, 0.395, **0.500**) 1.032 *w D*
3111. 23	(0.000) 1.766
3108. 99	(**0.082,** 0.227, 0.390, 0.551) 0.565, 0.717, 0.878, 1.038, 1.205, 1.350, **1.513**
3107. 55	(0.000 *WD*) 1.465 *B*
3106. 94	(0.348) **0.943,** 1.631
3106. 25	(0.159) 2.140
3103. 47	(0.230, **0.395**) 0.939, 1.091, **1.247,** 1.411, 1.564
3101. 10	(0.000) 0.990
3100. 51	(0.000 *WD*) 0.902 *w A*
3100. 00	(**0.049,** 0.168) . . . 1.235, 1.344, **1.451**
3099. 25	(**0.070,** 0.191, 0.306) . . . 1.080, 1.205, **1.319**
3098. 47	(0 159, 0.424, **0.711**) 1.013, 1.296, **1.575,** 1.856, 2.138
3097. 69	(**0.044,** 0.168, 0.308, 0.454, 0.570) 0.675, 0.795, 0.924, 1.054, 1.182, 1.316, 1.443, 1.574, **1.689**
3092. 09	(**0.173,** 0.502) **0.969,** 1.302, 1.649, 1.985
3091. 54	(0.727, 1.002, 1.318, **1.602**) . . . 0.802, **1.049,** 1.365, 1.669, 1.965, 2.264
3089. 53	(0.209) 0.692, **0.816,** 0.972
3087. 63	(0.098) 1.202
3084. 52	(0.000*w*) 0.845*A*
3082. 22	(0.000*WD*) 1.433*A*
3081. 66	(0.236*B*) 1.050*D*
3078. 64	(0.350, 0.569, **0.804**) 0.492, 0.721, 0.957, **1.168,** 1.388, 1.611, 1.835
3078. 05	(0.000) 0.000
3077. 66	(0.000) 0.997
3075. 60	(0.535) 0.531, **1.721**
3074. 37	(**0.289,** 0.474) . . . **2.121**
3072. 89	(**0.127,** 0.388, 0.619) . . . 1.412, 1.657, **1.954**

Wave-lengths	Magnetic patterns
3070. 62	(0.000) 1.138
3069. 19	(0.000) 0.976
3068. 93	(**0.000,** 0.112, 0.227) 0.580*A*
3068. 78	(0.000) 1.051
3067. 64	(**0.078,** 0.241, 0.413, 0.575, 0.734, 0.903) **0.181,** 0.357, 0.515, 0.686, 0.841, 1.002, 1.168, 1.333, 1.502, 1.673, 1.839, 2.005
3062. 10	(**0.069,** 0.229, 0.365) 0.730, 0.850, 0.971, **1.096**
3060. 78	(**0.147,** 0.459, 0.760) **0.650,** 0.947, 1.275, 1.565, 1.863
3060. 03	(0.233, 0.371, **0.525**) 0.533, 0.697, 0.851, **1.002,** 1.132, 1.285, 1.442, 1.593
3058. 61	(0.232, 0.366, **0.499**) 0.427, 0.541, 0.700, 0.854, **0.981,** 1.111, 1.244, 1.387
3058. 37	(0.000) 0.979
3057. 86	(0.000) 1.165
3056. 82	(**0.096,** 0.284, 0.470, 0.663) 0.892, 1.086, 1.277, 1.471, 1.670, **1.880**
3054. 94	(**0.187,** 0.540) 1.417, 1.739, **2.091**
3054. 76	(0.664, **1.109**) . . . **0.968,** 1.421, 1.869
3053. 47	(0.102) 1.202
3052. 32	(0.000*WD*) 1.625*B*
3050. 37	(**0.123,** 0.375) 0.559, 0.799, 1.041, **1.288**
3048. 89	(0.254, 0.363, 0.514, 0.653, **0.765**) . . . 0.884, **0.993,** 1.124, 1.247, 1.363, 1.484, 1.596, 1.687
3048. 80	(0.000*w*) 0.902*wA*
3048. 31	(0.174, **0.438**) 0.681, **0.951,** 1.227
3048. 05	(0.116*w*) 1.294*w*
3046. 41	(0.000) 1.238
3045. 73	(**0.215,** 0.625) 1.087, 1.514, 1.925, **2.346**
3043. 44	(**0.181,** 0.559) **0.894,** 1.269, 1.618
3041. 01	(0.193) . . ., **1.148,** 1.311
3039. 06	(0.614, **1.036**) 0.125, 0.548, **0.971,** 1.380, 1.797
3037. 09	(0.130) 1.213
3035. 47	(**0.057,** 0.210, 0.345, 0.520) . . . 1.470, 1.594, **1.746**
3034. 92	(0.000*WD*) 1.657*B*
3034. 25	(0.073) 0.097
3033. 33	(0.156*w*) 1.114*w*
3033. 24	(**0.186,** 0.316) 1.508, 1.729, **1.838**
3030. 32	(0.000*WD*) 1.200*B*
3029. 99	(0.000*WD*) 1.481*B*
3029. 77	(**0.145,** 0.438) . . . 1.304, **1.581**
3028. 29	(**0.069,** 0.196, 0.317) 0.714, 0.850, 1.001, **1.118**
3027. 77	(0.207, **0.623**) 1.198, **1.601,** 2 003
3026. 80	(0 000*wD*) 1.404*B*
3025. 57	(0.000*WD*) 0.978*A*
3023. 30	(0.000) 0.942
3022. 75	(0.197, 0.346, **0.481**) 0.440, 0.600, . . ., . . ., 0.967, 1.122, 1.263
3021. 60	(**0.136,** 0.402, 0.671, 0.924) 0.660, 0.992, 1.287, **1.583**
3020. 68	(0.526, 0.870, 1.222, **1.565**) 0.193, 0.526, 0.907, **1.243,** 1.588, 1.925, 2.274, 2.622
3019. 72	(**0.114,** 0.299, 0.508, 0.720, 0.920) . . ., 1.573, 1.788, 2.003, **2.207**
3018. 56	(**0.163,** 0.297) 1.367, 1.490, 1.624, **1.751**
3018. 50	(0.000) 0.991*A*
3016. 87	(0.202*B*) 1.096*WD*
3015. 42	(1.202) 1.955
3014. 15	(0.172*B*) 1.392*D*
3011. 18	(0.000*w*) 1.158*B*
3010. 92	(0.107) 1.202*D*
3009. 79	(**0.171,** 0.482) . . ., 0.822, 1.156, **1.475**
3009. 46	(**0.130,** 0.371, 0.614) 0.677, 0.875, 1.125, 1.378, **1.604**
3008. 15	(0.234, **0.420**) 1.190, 1.362, **1.515,** 1.680, 1.855
3007. 47	(0.000*WD*) 0.857, **1.029**
3006. 77	(0.253, 0.432, **0.576**) 0.261, 0.425, 0.642, 0.826, **1.046,** 1.221, 1.372
3004. 45	(**0.110,** 0.348, 0.577, 0.810) 0.230, 0.452, 0.675, 0.911, 1.126, 1.359, 1.593, **1.830**
3003. 77	(0.000*w*) 0.811*A*
3000. 28	(0.000) 0.766
2999. 59	(**0.061,** 0.194, 0.327) **0.724,** 0.849, 1.007, 1.136, 1.236
2998. 37	P—B
2997. 96	(0.000*wD*) 0.991*A*
2997. 66	P—B
2997. 33	(0.000*w*) 1.276*B*
2997. 10	(0.196, 0.334, **0.459**) . . . **1.481,** 1.638, . . .
2996. 69	(0.000) 1.078
2996. 27	(**0.258,** 0.768) **0.424,** 0.929, 1.446, 1.902
2995. 53	(**0.065,** 0.180, 0.326, 0.459, 0.578) 1.291, 1.402, 1.521, 1.651, 1.803, **1.911**
2993. 50	(0.516) 1.272, **2.331**
2992. 25	(**0.078,** 0.216, 0.324, 0.479) 0.964, 1.117, 1.278, 1.399, **1.527**
2991. 51	(0.000*w*) 1.373*w*
2989. 86	(0.000*w*) 0.994*A*
2987. 96	(0.000) 1.273
2987. 35	(0.113) 0.927*A*
2986. 90	(**0.139,** 0.420, 0.701) **0.587,** 0.866, 1.149, 1.432, . . .
2986. 15	(0.000) 1.028
2984. 86	(**0.077,** 0.216, 0.368, 0.510, 0.646) 0.980, 1.156, 1.345, 1.496, 1.646, 1.824, **2.005**
2983. 59	(0.293) **1.410,** 2.010
2982. 77	(**0.078,** 0.229, 0.389, 0.555) 0.904, 1.071, 1.236, 1.397, 1.545, **1.690**
2982. 45	(0.000) 1.254
2979. 79	(**0.082,** 0 251, 0.402, 0.569, 0.729) 0.865, 1.019, 1.176, 1.362, 1.516, 1.670, 1.847, **2.027**
2978. 61	(0.000*w*) 0.991*A*
2977. 76	(0.204, 0.607, **1.003**) 0.583, 0.967, **1.399,** 1.763, 2.156
2976. 90	(0.000) 1.070
2975. 62	(0.000) 1.190
2975. 39	(**0.083,** 0.234, 0.411) 0.625, 0.821, 0.999, 1.170, **1.352**
2972. 61	(**0.098,** 0.288, 0.479) **0.921,** 1.116, 1.313, 1.497, 1.702, 1.880
2971. 90	(**0.105,** 0.332, 0.546, 0.774) 0.514, 0.730, 0.952, 1.149, 1.346, 1.565, **1.799**
2971. 14	(0.000) 0.953
2969. 36	P–B
2968. 78	P–B
2967. 08	(0.369, **0.654**) 0.406, 0.644, **0.891,** 1.143, 1.387
2965. 28	(**0.141,** 0.405, 0.670) 0.903, 1.174, 1.451, 1.671, 1.956, **2.258**
2963. 79	(**0.287,** 0.885) 0.775, 1.367, 1.942, **2.514**
2962. 21	(0.240, 0.396, 0.557, **0.727**) 0.495, 0.611, 0.721, 0.846, 0.970, **1.100,** 1.253, 1.390, 1.529, 1.671
2961. 33	(0.000*WD*) 1.846*B*
2960. 46	(0.064) 1.178
2960. 23	(**0.051,** 0.232, 0.398, 0.548) 1.269, 1.461, 1.639, 1.781, 1.945, **2.121**
2958. 73	(0.153*w*) 1.270*D*
2956. 92	(0.143*w*) 1.078*w*
2956. 79	(**0.085,** 0.298, 0.539, . . .) . . . , 1.731, 1.947, 2.185, **2.405**
2956. 06	(1.250) 3.105
2955. 83	(0.000*WD*) 1.274*B*
2955. 15	(0.000) 1.674
2954. 52	(**0.081,** 0.220, 0.384) . . . 1.669, **1.799**
2953. 94	(0.230*B*) 1.369*D*
2951. 82	(**0.174,** 0.481) **0.386,** 0.722, 1.057
2947. 29	(0.281) 1.258*W*, *D*
2946. 69	(0.247*w*) *B*
2945. 95	(0.000) 1.248
2944. 82	(0.000) 1.026
2943. 36	(0.000*WD*) 1.461*B*
2941. 21	(0.000) 1.164
2940. 09	(0.000) 1.243
2938. 51	(0.000*wD*) 1.300*wB*
2938. 29	(0.000*w*) 1.288*B*
2936. 77	(**0.131,** 0.388) 0.447, 0.624, 0.860, 1.109, **1.398**
2935. 70	(0.213) 0.236, **0.649**
2935. 20	(0.626) 2.517
2934. 30	(1.983) 1.329

Wavelengths	Magnetic patterns
2933.20	(**0.258,** 0.779, 1.304) −**0.260,** +0.260, 0.810, 1.347
2932.18	(0.306, 0.505, **0.726**) 0.082, 0.287, 0.495, 0.703, **0.903,** 1.098, 1.310, 1.531
2930.48	(0.391, **1.198**) 0.675, **1.452,** 2.254
2930.07	P–B
2929.49	(0.000) 0.762
2928.49	(0.000*WD*) 1.063*A*
2927.54	(0.000*w*) 1.133*B*
2926.74	P–B
2925.42	(0.173*w*) 0.994*wA*
2924.32	(0.218*w*) 1.216*B*
2923.39	(0.173, 0.515, **0.885**) 0.442, 0.796, 1.126, **1.471,** 1.819, 2.157
2922.73	(**0.092,** 0.317) 0.473, 0.656, 0.880, **1.110**
2921.92	(**0.166,** 0.475, 0.805, 1.125) −**0.147,** +0.147, 0.494, 0.825, 1.136
2920.25	(0.000) 1.176
2920.08	(0.000) 1.276
2918.84	(0.827) **0.699,** 2.334
2917.16	(0.000*wD*) 1.311*B*
2914.44	(0.000) 1.775
2914.31	(0.000*D*) 1.715*B*
2913.82	(0.333, 0.555, **0.785**) 0.362, 0.585, 0.807, **1.029,** 1.251, 1.473, 1.695
2913.74	(0.000*wD*) 1.059*A*
2911.92	(0.104, 0.282, 0.481, **0.672,** 0.906, 1.097, 4.292, **1.485,** 1.669, 1.853, 2.054
2910.93	(**0.124,** 0.385, 0.624, 0.832) **0.079,** 0.313, 0.580, 0.773, 1.025, 1.294
2909.11	(1.127) **0.000,** 2.171
2907.11	(0.238, 0.581, **0.973**) 0.464, 0.851, **1.248,** 1.624, 2.030
2905.83	(0.000*W*) 0.953*w*
2903.05	(0.000) 1.060
2901.79	(0.000*WD*) 0.698*A*
2900.78	(0.361, 0.560, 0.811, **1.045**) 0.261, 0.475, 0.723, 0.938, **1.159,** 1.395, 1.615, 1.844 2.094
2898.65	(0.000) 0.901
2898.48	(0.000) 1.126
2894.45	(0.173, 0.318, 0.441, **0.558**) 0.963, 1.103, 1.242, 1.356, **1.476,** 1.584, 1.719, 1.850 1.981
2892.82	(**0.167,** 0.514) **0.529,** 0.881, 1.223, 1.563
2892.04	(**0.157,** 0.469, 0.778, 1.122) . . .
2891.29	(0.160) . . ., 0.588
2890.99	(**0.275,** 0.828) **0.479,** 1.039, 1.583, 2.121
2888.70	(0.000*WD*) 1.188*B*
2888.17	(0.129) 0.872*A*
2886.98	(**0.122,** 0.341, 0.575, 0.811, 1.039) 0.400, 0.642, 0.865, 1.093, 1.326, 1.548, 1.771, 2.008, **2.245**
2885.76	(**0.040,** 0.186, 0.332) **0.572,** 0.700, 0.843, 0.985, 1.138, 1.249
2884.80	(0.000*w*) 1.056*A*
2883.97	(**0.075,** 0.234, 0.395) **1.028,** 1.211, 1.387
2883.32	(**0.084,** 0.248) 0.424, 0.597, 0.758, 0.925, **1.145**
2882.38	(0.209, 0.393, 0.536, 0.685, **0.833**) 0.453, 0.591, 0.741, 0.877, 1.030, **1.184,** 1.326, 1.486, 1.637, 1.786, 1.950
2882.04	(0.000) 1.246
2881.93	(0.000*w*) 1.353*B*
2881.39	(0.127) 0.776*wD*
2879.75	(0.420, **0.706**) 0.449, 0.727, **1.005,** 1.297, 1.599
2879.05	(0.000*w*) 0.921*A*
2876.83	(0.355) 0.396
2874.85	(**0.069,** 0.210, 0.351, 0.494) **0.743,** 0.910, 1.052, 1.189, 1.339, 1.474, 1.609, 1.749
2874.39	(**0.135,** 0.391, 0.655) **0.728,** 0.979, 1.243, 1.527
2872.90	(0.753) 0.436
2872.88	(0.449*B*) 1.109*D*
2871.51	(**0.150,** 0.384, 0.658) **0.715,** 0.979, 1.252, 1.512, 1.765, 2.042
2869.98	(0.316, **0.508**) 0.919, 1.121, **1.326,** 1.523, 1.728
2869.22	(**0.071,** 0.216, 0.366, 0.532) 0.838, 1.040, 1.183, 1.365, 1.513, 1.689, **1.834**
2868.33	(0.409) **1.234,** 2.102
2868.12	(0.000*w*) 0.780*A*
2866.70	(**0.086,** 0.269, 0.453) **0.802,** 0.992, 1.162, 1.360, 1.516, 1.676
2863.80	(0.000) 1.088
2863.20	(**0.092,** 0.251) 0.430, 0.590, 0.763, **0.923**
2859.00	(**0.250,** 0.771) **0.340,** 0.870, 1.395, 1.920
2858.08	(0.000*w*) 1.053
2856.90	(**0.590,** 1.814) −**1.219,** 0.000, +1.219
2856.01	(0.00) 0.960
2855.71	(0.435, 0.613, **0.809**) 0.399, 0.567, 0.736, 0.895, **1.065,** 1.213, 1.386, 1.552, 1.722
2853.22	(0.000*W*) 0.695*WA*
2850.68	(0.302, 0.495, 0.672, 0.849, **1.027**) 0.241, 0.464, 0.681, 0.904, 1.147, 1.385, 1.652, 1.867, 2.086
2848.24	(**0.206,** 0.376, 0.529) **0.861,** 1.013, 1.181, 1.332, 1.487, 1.653, 1.816, 1.968
2846.63	(0.524, **0.865**) 0.149, 0.504, **0.844,** 1.187, 1.528
2846.25	(0.000) 0.865
2845.67	(0.153) 1.241
2844.83	(**0.086,** 0.274, 0.471, 0.652, 0.836) **0.308,** 0.497, 0.679, 0.871, 1.058, 1.245
2843.73	(1.201) 1.201
2842.49	(0.000*WD*) 0.580*WA*
2842.15	(0.458) **1.384,** 2.325
2841.79	(0.000*WD*) 1.415*WB*
2840.08	(**0.268,** 0.797, 1.360) . . . 0.929, 1.480, 2.027, **2.544**
2839.25	(**0.368,** 1.130) 0.905, 1.652, **2.395**
2839.19	(0.000*wD*) 0.830*A*
2836.72	(0.000) 1.052
2836.31	(**0.305,** 0.933, 1.562) −**0.028,** +0.590
2835.34	(**0.122,** 0.355, 0.596, 0.830, 1.074) **0.191,** 0.423, 0.658, 0.904, 1.147, 1.466
2834.42	(0.244, 0.394, **0.551**) 0.860, 1.016, 1.175, **1.331,** 1.472, 1.632
2832.08	(0.000) 0.991
2832.00	(0.000) 1.037
2831.44	(0.000) 1.014
2829.04	(**0.057,** 0.177, 0.299, **0.406**) 1.206, 1.321, 1.476, 1.606. **1.666**
2827.75	(0.000) 1.126
2827.18	(0.286) 1.506*B*
2825.30	(0.000*WD*) 1.464*B*
2824.19	(**0.107,** 0.327) **0.411,** 0.616, 0.835, 1.034. 1.233
2822.94	(**0.419,** 1.270) — 0.419, +0.419, 1.270
2822.04	(0.257) 3.044
2821.84	(0.000*w*) 0.826*A*
2821.02	(0.000*w*) 1.105*wD*
2820.02	(**0.158,** 0.509) **1.069,** 1.418, 1.753
2819.59	(0.381, **0.534**) 1.014, 1.147, 1.293, **1.463,** 1.608, 1.763, 1.856
2817.54	(0.309*B*) 1.164*WD*
2817.44	(**0.000,** 0.738) — **0.313,** +1.158
2816.16	(0.000*w*) 0.814*A*
2815.00	(0.172, **0.324**) . . . **1.087,** 1.176
2814.68	(0.000*d*) 0.807
2814.12	(0.594) **0.652,** 1.820
2813.34	(0.000*WD*) 1.016*A*
2812.65	(0.000*W*) 1.394*WB*
2812.61	(0.000*w*) 0.709*A*
2811.39	(0.066) 0.855, **0.970**
2811.16	(**0.152,** 0.473) **0.751,** 1.068, 1.375
2810.45	(0.000) 1.046
2808.97	(0.000*wD*) 1.374*B*
2808.47	(0.000*w*) 0.966*w*
2807.75	(**0.093,** 0.260) **1.377,** 1.553, 1.734, 1.915
2807.02	(**0.124,** 0.389, 0.633, 0.913, 1.168, 1.405) . . . 1.571, 1.823, 2.094, 2.356, **2.612**
2806.19	(0.446, 0.728, **1.013**) 0.176, 0.447, 0.756, **1.049,** 1.349, 1.648, 1.941
2800.74	(0.315*B*) 1.125*WD*
2800.06	(0.199, **0.529**) 0.350, **0.688,** 1.025

TABLE 3. *Zeeman effect of* Mo II—Continued

Wavelengths	Magnetic patterns
2798. 91	(**0.125,** 0.366, 0.619, 0.847) **0.009,** 0.261, 0.538, . . .
2798. 07	(**0.182,** 0.552) **1.013,** 1.385, 1.750, 2.113
2796. 93	(0.000*W*) 1.045*WD*
2796. 78	(0.000) 0.758
2796. 34	(**0.116,** 0.344) **0.498,** 0.727, 0.955
2794. 60	(0.356*B*) 1.331*WD*
2791. 55	(0.067) 1.051
2790. 43	(**0.092,** 0.284, 0.488, 0.666) **0.339,** 0.543, 0.735, 0.929, 1.111, 1.310, 1.501, 1.711
2787. 32	(**0.129,** 0.370) 1.167, 1.426, 1.677, **1.918**
2786. 24	(0.163) 1.250*wD*
2785. 64	(0.377, 0.593, **0.827**) 0.323, 0.572, 0.819, **1.049,** 1.263, 1.501, 1.719
2784. 99	(0.000*w*) 1.224*A*
2784. 13	(**0.061,** 0.200, 0.354, 0.514) **0.557,** 0.690, 0.856, 1.012, 1.146
2781. 97	(?) **0.760,** 0.927, 1.122, 1.308, 1.465
2780. 02	(**0.087,** 0.266, 0.441) **1.124,** 1.304, 1.490, 1.663, 1.835, 2.026
2779. 24	(0.000*w*) 0.797*A*
2777. 86	(0.000*w*) 1.836
2776. 68	(**0.153,** 0.463, 0.776, 1.077) **—0.082,** 0.237, 0.523, 0.832, 1.138, 1.427
2775. 39	(**0.218,** 0.368, 0.516) **1.011,** 1.173, 1.318, 1.468, 1.601, 1.719, 1.904, 2.053
2774. 41	P—B
2773. 80	P—B
2771. 71	(0.150) 1.092 *WD*
2770. 60	(0.000*WD*) 0.803*WA*
2770. 18	(0.000*wD*) 0.981*A*
2769. 76	(0.000) 1.163
2763. 63	(**0.089,** 0.265) 0.285, 0.519, 0.683, **0.864**
2763. 30	(0.374*B*) 1.183*WD*
2762. 46	(0.000) 0.649
2760. 54	(0.000*WD*) 0.762*WA*
2760. 10	(0.000) 1.093
2759. 20	(**0.124,** 0.381, 0.626) **0.466,** 0.717, 0.968, 1.209, 1.457
2758. 63	(0.747) **1.081,** 2.561
2758. 51	(0.000*w*) 0.970*wA*
2756. 06	(0.000*W*) 1.001*WD*
2754. 49	(**0.083,** 0.283) **0.705,** 0.883, 1.079, 1.272
2753. 82	(**0.136,** 0.442, 0.730, 1.019) 0.133, 0.409, 0.702, 1.000, 1.265, 1.476, 1.729, 2.008, **2.291**
2750. 03	(0.281*B*) 1.220*wD*
2748. 44	(**0.169,** 0.507, 0.857, 1.186) **—0.332,** 0.000, 0.332, 0.705, 1.058, 1.399
2747. 16	(**0.077,** 0.245, 0.429) **0.378,** 0.539, 0.735, 0.875, 1.031
2746. 30	(0.086) 0.883*A*
2745. 29	(**0.081,** 0. 226, 0.393, 0.548, 0.691) 1.116, 1.273, 1.449, 1.615, **1.748**
2744. 19	(0.000) 0.956
2743. 18	(0.262*B*) 1.680
2742. 89	(**0.102,** 0.280, 0.458, 0.640, 0.801, 0.953) **0.099,** 0.261, 0.419, 0.567, 0.742
2741. 63	(0.000) 1.081
2741. 43	(0.000) 1.138
2741. 31	(0.609*WB*) 1.215*WD*
2740. 06	(**0.263,** 0.796) **1.016,** 1.555, 2.065
2738. 64	(**0.098,** 0.283, 0.467, 0.672, 0.855) **0.142,** 0.361, 0.586, 0.794, 0.979, 1.161, 1.366
2737. 87	(0.000) 1.021
2737. 11	(0.268, 0.464, 0.649, **0.868**) . . . ?
2736. 95	(**0.162,** 0.497) . . . , 0.802, 1.110, 1.398
2735. 32	(**0.201,** 0.629, 1.056, 1.496) 1.091, 1.506, 1.854, 2.264, **2.687**
2732. 89	(0.230*B*) 1.635*WD*
2732. 65	(0.000) 0.887
2730. 21	(0.000*w*) 0.766*A*
2729. 68	(**0.330,** 1.010) **0.636,** 1.309, 1.977
2728. 19	(0.000) 0.888
2727. 80	(**0.122,** 0.340, 0.570) **0.500,** 0.724, 0.937, 1.169
2726. 98	(0.000*WD*) 0.517*A*
2724. 02	(**0.094,** 0.264, 0.440, 0.620, 0.791) **0.271,** 0.455, 0.635, 0.803, 0.973, 1.154, 1.328
2723. 56	(0.000*w*) 1.014
2723. 37	(**0.070,** 0.217, 0.376) **1.198,** 1.318, 1.492, 1.629
2722. 57	(**0.137,** 0.388, 0.650, 0.916, 1.128) . . . 1.677, 1.912, 2.166, **2.404**
2721. 74	(0.136) 1.211
2719. 69	(0.000*WD*) 1.406*B*
2718. 97	(**0.134,** 0.411, 0.704) . . . 1.228, 1.458, 1.713, **1.980**
2717. 36	(0.000*W*) 0.860*A*
2713. 50	(0.000) 1.543
2712. 34	(0.000) 1.049*B*
2711. 48	(0.000) 1.276
2710. 93	(0.297, 0.495, **0.689**) 0.712, 0.912, **1.111,** 1.283, 1.479
2710. 21	(0.438, 0.706, **0.989**) 0.287, 0.570, 0.833, **1.128,** 1.392, 1.640, 1.961
2707. 01	(**0.091,** 0.252) **0.610,** 0.767, 0.931, 1.104
2705. 96	(0.000*WD*) 1.276*W*
2704. 93	(0.134) 0.958
2703. 86	(**0.061,** 0.215, 0.349) 0.964, 1.113, 1.273, **1.374**
2703. 62	(0.107, **0.261**) 0.598, **0.779,** 0.956
2703. 08	(**0.180,** 0.528, 0.849) . . ., 1.676, **2.014**
2702. 87	(**0.112,** 0.321, 0.533) **0.256,** 0.464, 0.679, 0.897
2701. 88	(0.000) 0.680
2701. 41	(0.234, **0.692**) 1.609, **2.074,** 2.535
2699. 99	(0.000*WD*) 1.728*B*
2699. 40	(**0.072,** 0.230) **0.509,** 0.649, 0.829, 0.993, 1.161
2697. 25	(0.000*W*) 1.782*B*
2696. 84	(0.094) 1.070
2695. 22	(**0.130,** 0.398, 0.647, 0.909) . . ., 0.664, 0.910, 1.175, 1.450, 1.706, **1.964**
2694. 72	(0.097) 1.133*w*
2693. 19	(0.000*WD*) 0.753*A*
2692. 94	(0.128, **0.354**) 1.579, **1.800,** 2.067
2692. 63	(0.000*w*) 0.791*A*
2691. 70	(0.450, 0.668, **0.861**) 0.427, 0.620, 0.824, 1.016, **1.203,** 1.410, 1.592, 1.768, 1.927
2690. 98	(0.034*B*) 1.341*WD*
2687. 99	(0.178) 1.679
2685. 78	(**0.072,** 0.206, 0.344) **0.707,** 0.834, 0.987, 1.144, 1.288
2684. 15	(0.176*B*) 1.557*w*
2683. 23	(0.472) **1.799,** 2.814
2682. 43	(0.000) 1.269
2681. 37	(0.407*WD*) 0.835*A*
2678. 47	(0.422, **0.683**) 0.624, 0.894, **1.174,** 1.470, 1.745
2677. 00	(**0.116,** 0.353) 1.326, 1.562, **1.818**
2676. 49	(**0.100,** 0.310, 0.514) **0.255,** 0.473, 0.689, 0.904, 1.100, 1.327
2673. 27	(0.477*WD*) 0.826*A*
2672. 84	(0.000) 1.553
2671. 86	(0.000) 1.164*B*
2670. 96	(0.000) 1.066
2670. 02	(0.308, 0.463) 0.463, 1.102
2669. 58	(0.129) 1.125*w*
2667. 94	(0.858, **1.173**) 0.136, 0.446, 0.797, **1.117,** 1.461, 1.801, 2.109
2664. 91	(0.101, **0.297**) 1.092, **1.288,** 1.494
2664. 29	(0.163) 1.154*w*
2663. 78	(**0.087,** 0.304, 0.500) **0.853,** 1.063, 1.287, 1.518
2660. 58	(0.000*w*) 1.557*A*
2659. 72	(0.338) 1.059*WD*
2657. 39	(0.000) 1.112
2657. 00	(0.000*WD*) 1.515*B*
2655. 82	(0.139) 0.974
2655. 14	(0.000) 0.906
2654. 85	(**0.125,** 0.363, 0.574) 1.144, 1.391, 1.630, **1.883**
2653. 80	(**0.093,** 0.319, 0.555, 0.765) **0.412,** 0.624, 0.837, 1.054, 1.288
2653. 35	(0.000) 1.551
2652. 37	(0.000*w*) 0.875*A*

Wavelengths	Magnetic patterns
2651. 73	(0.081, 0.231, 0.397, 0.559, 0.693) 1.069, 1.231, 1.394, 1.546, 1.688, **1.817**
2650. 01	(**0.074,** 0.231, 0.398, 0.544) . . ., 1.170, 1.320, **1.477**
2648. 22	(0.205) 0.930*w*
2647. 08	(0.000) 1.204
2646. 48	(**0.085,** 0.225) **1.396,** 1.552, 1.709, 1.867
2644. 88	(0.202) 1.164*w*
2644. 34	(0.000*WD*) 1.278*A*
2644. 14	(0.000*w*) 0.880
2642. 40	(0.000*w*) 1.226
2642. 40	(0.350, **0.588**) 0.641, 0.869, **1.098,** 1.311, 1.562
2641. 19	(0.345) 1.194*WD*
2640. 88	(0.000*WD*) 1.046*A*
2639. 68	(0.185) 1.382*w*
2638. 77	(0.155) 1.351*wA*
2636. 67	(0.641) **1.210,** 2.492
2635. 51	(0.000) 1.202
2635. 28	(0.000) 1.161
2634. 10	(**0.080,** 0.240, 0.367) 1.384*B*
2633. 67	(0.304) 0.231
2633. 52	(0.000*WD*) 1.835*B*
2633. 14	(0.000*WD*) 1.042*A*
2632. 86	(0.555, **0.641**) 0.920*WD*
2631. 56	(0.000) 0.770
2630. 74	(0.127) 1.214
2630. 23	(0.120) 1.055*w*
2627. 92	(0.000) 1.330
2626. 10	(0.000) 1.038
2625. 87	(0.000*WD*) 1.501*B*
2625. 15	(0.000*w*) 1.080*A*
2624. 64	(**0.076,** 0.241, 0.402, 0.540) 1.012, 1.156, 1.345, **1.473**
2623. 41	(**0.079,** 0.243) 0.977, 1.168, **1.305**
2620. 05	(**0.164,** 0.539, 0.871, 1.182) **0.164,** 0.539, 0.871, 1.182, 1.551, 1.880
2619. 34	(0.000) 3.206
2612. 29	(0.000) 1.053
2609. 22	(0.000 *w*) 0.999 *A*
2608. 88	(**0.073,** 0.237, 0.383, 0.532, . . .) . . ., 1.112, 1.267, 1.400, 1.566, **1.693**
2607. 78	(0.102) 1.117
2606. 60	(0.000) 1.406
2605. 95	(0.000) 1.369
2605. 83	(0.000) 0.957
2604. 60	(**0.172,** 0.496) **0.346,** 0.684, 1.006, 1.339
2602. 80	(0.747) **1.054,** 2.545
2601. 97	(0.269, **0.401**) 0.726, 0.825, 0.957, **1.067.** 1.187, 1.308, 1.422
2600. 10	(0.347, 0.571, **0.802**) 0.552, 0.793, **1.024,** 1.251, 1.486
2599. 19	(**0.083,** 0.235, 0.367) **0.544,** 0.735, 0.929
2597. 39	(**0.066,** 0.226, 0.357) 0.986, 1.157, 1.287, 1.462, **1.591,**
2596. 43	(0.000 *w*) 1.327 *w*
2593. 71	(**0.122,** 0.363) **1.210,** 1.477, 1.736, 1.955
2593. 38	(0.249 *B*) 1.133 *W D*
2592. 78	(**0.133,** 0.401, 0.672) 1.107, 1.392, 1.643, **1.890**
2591. 78	(0.000) 1.226
2588. 79	(**0.148,** 0.444) 0.550, 0.872, 1.164, **1.462**
2587. 85	(0.422) 0.489, **1.404**
2587. 05	(0.000 *W D*) 1.364 *B*
2585. 97	(0.000) 1.310
2585. 08	(0.000) 1.133
2584. 73	(0.149) 1.188
2584. 20	(0.000) 1.115
2583. 95	(0.000) 1.433
2583. 82	(. . . ?) 1.548 *W D*
2580. 98	(**0.097,** 0.281) **0.715,** 0.892, 1.097
2580. 48	(0.000 *w*) 1.069 *B*
2579. 44	(**0.151,** 0.429, 0.723, 0.988) 1.130, 1.389, 1.695, 1.971, 2.262, **2.540**
2578. 35	(0.000 *w*) 0.829 *A*
2576. 56	(0.239) 0.267, **0.759**
2575. 81	(0.365, **0.572**) 0.729, 0.924, **1.126,** 1.343, 1.556
2574. 43	(**0.262,** 0.797, 1.318) 0.294, 0.788, 1.310, 1,838, 2.366, **2.887**
2572. 24	(0.227, **0.594**) 0.313, **0.705,** 1.103
2571. 45	(**0.111,** 0.315, 0.499, 0.694) 0.897, 1.096, 1.306, 1.501, **1.715**
2571. 24	(0.118) 0.786, **1.017**
2567. 51	(0.000 *W D*) 1.717 *B*
2566. 26	(**0.603,** 1.845) 2.250, **3.469**
2566. 08	(0.000) 1.174
2564. 57	(0.000 *w*) 0.964 *A*
2564. 33	(**0.058,** 0.198, 0.334, 0.462) **0.781,** 0.894, 1.023, 1.168, 1.313, 1.453
2562. 08	(**0.119,** 0.340, 0.575, 0.799, 1.028) 0.622, 0.845, 1.098, 1.323, 1.529, 1.775, 2.005, **2.242**
2560. 67	(0.000 *w*) 1.251 *w*
2559. 69	(0.381, **0.631**) 0.653, 0.896, **1.149,** 1.418, 1.674
2557. 38	(0.000 *w D*) 1.104 *A*
2556. 76	(0.000) 1.213
2556. 31	(0.253, **0.412**) 0.596, 0.765, **0.930,** 1.101, 1.280
2555. 42	(0.329 *w*) 1.208 *w*
2552. 19	(0.000) 1.118
2550. 74	(0.000) 1.096
2549. 35	(0.286 *B*) 1.050 *w*
2548. 21	(0.197) **0.491,** 0.906
2547. 56	(**0.099,** 0.287, 0.478, 0.646) 1.067, 1.288, 1.480, **1.640**
2546. 92	(0.419, **0.623**) 0.589, 0.754, 0.914, **1.060,** 1.243, 1.446, 1.584
2544. 46	(0.000) 1.274
2544. 46	(**0.151,** 0.454, 0.776, 1.092) 0.803, 1.100, 1.416, 1.744, **2.045**
2543. 61	(**0.067,** 0.201) **0.940,** 1.085
2542. 67	(0.472, 0.781, **1.100**) 0.480, 0.808, 1.111, **1.439,** 1.737, 2.048, 2.362
2540. 58	(0.000) 0.948
2539. 44	(0.000) 1.139
2538. 44	(0.300, 0.474, 0.658, **0.830**) 0.718, 0.903, 1.090, 1.282, **1.456,** 1.638, 1.806, 1.977, 2.158
2537. 44	(0.000) 0.900
2534. 41	(0.765, **1.053**) 0.485, 0.784, **1.089,** 1.403, 1.588
2533. 58	(0.000) 1.011
2532. 62	(0.000*w*) 0.979*A*
2532. 30	(**0.190,** 0.575) 0.524, 0.890, 1.267, **1.643**
2531. 44	(0.221) **1.324,** 1.719
2530. 33	(**0.093,** 0.277) **0.793,** 0.992, 1.192
2528. 85	(0.233) 0.291, **0.764**
2528. 38	(**0.097,** 0.309) . . . 1.219, 1.448, **1.622**
2527. 14	(0.385, **0.631**) 0.439, 0.680, **0.925,** 1.175, 1.422
2523. 16	(**0.084,** 0.244, 0.427, 0.598) **0.355,** 0.532, 0.709, . . .
2522. 59	(0.000*w*) 1.302*B*
2521. 68	(**0.086,** 0.250, 0.416) **0.566,** 0.714, . . .
2521. 19	(0.000) 1.097
2521. 06	(**0.156,** 0.457, 0.763, 1.060) 0.955, 1.279, 1.564, 1.858, **2.155**
2519. 61	(**0.180,** 0.578, 0.977) **0.182,** 0.606, 1.001, 1.346, . . .
2518. 43	(0.612) 1.370
2516. 09	(0.120) 1.058*wD*
2515. 60	(**0.127,** 0.372, 0.614) **0.433,** . . .
2515. 10	(0.178) 0.945*WD*
2514. 16	(0.000) 1.109
2513. 95	(0.000) 0.512
2511. 80	(**0.175,** 0.578, 0.991) **0.232,** 0.645, 1.052, 1.477
2510. 34	(1.219) 0.772
2509. 15	(0.000) 0.664
2505. 64	(0.000) 1.073
2502. 83	(**0.107,** 0.315, 0.551, 0.765) **0.616,** 0.941, 1.152, 1.358, 1.561, 1.775
2502. 22	(0.291) **1.147,** 1.692
2500. 42	(0.260*B*) 1.143*WD*
2497. 37	(**0.247,** 0.756) 0.760, 1.269, **1.766**
2496. 28	(**0.109,** 0.307, 0.526) 1.165, 1.376, 1.605, **1.810**
2494. 68	(0.347) 0.343, **1.025**
2490. 64	(0.332) 0.574, **0.790,** 1.016
2484. 75	(0.000) 1.035
2484. 60	(0.000) 1.125

TABLE 3. *Zeeman effect of* Mo II—Continued

Wavelengths	Magnetic patterns
2482. 57	(**0.097,** 0.272, 0.447) 1 103, 1.302, 1.488, **1.669**
2479. 24	(0.143) 1.092*A*
2478. 67	(**0.271,** 0.749) 1.624, **2.025**
2478. 23	(**0.085,** 0.249) 1.269, 1.430, **1.616**
2478. 01	(0.335) 1.207
2477. 57	(0.000) 1.203
2474. 24	(0.000) 1.06*w*†
2470. 04	(0.000*w*) 1.340
2468. 79	(0.045) 1.315
2468. 76	(0.000) 1.285
2467. 35	(. . . ?) **0.332,** 0.463, 0.591, 0.752
2466. 97	(0.277) 0.477
2466. 67	(**0.157,** 0.467) 0.520, 0.834, 1.154, **1.480**
2462. 48	(0.571) 0.536, 0.745, **0.984,** 1.228, 1.461
2461. 80	(**0.149,** 0.465) 0.639, 0.919, 1.222, **1.509**
2459. 76	(0.000) 1.127
2458. 66	(0.000) 1.020
2457. 77	(**0.055,** 0.187, 0.322, 0.456, 0.583) 1.277, 1,407, 1.563, 1.680, **1.799**
2453. 36	(0.000) 0.874
2453. 14	(0.247) 1.004*WD*
2444. 74	(0.000) 0.818
2444. 48	(0.473, **0.790**) 0.257, 0.583, **0.895,** 1.217, 1.522
2443. 19	(0.000) 1.025
2440. 26	(0.315) 1.083, **1.285**, 1.490
2440. 05	(0.206) 1.234
2438. 57	(0.000) 1.018
2435. 94	(0.226) 0.468, **0.615,** 0.767
2433. 97	(0.354) **0.295,** 1.098
2430. 27	(**0.176,** 0.536) 0.700, 1.053, **1.374**
2429. 39	(0.000*w*) 0.675*A*
2428. 17	(0.000) 1.122*B*
2427. 29	(0.000) 1.076
2424. 26	(0.000*w*) 1.186*w*
2423. 99	(**0.106,** 0.319, 0.492, 0.709) **0.239,** 0.429, 0.629, 0.813, 1.003, . . .
2423. 72	(0.285) 1.064
2421. 65	(0.000) 0.943
2420. 18	(0.371) 0.388, **0.631,** 0.885
2419. 01	(0.000) 1.077
2417. 96	(0.206) 0.961, **1.399**
2417. 48	(0.110) **1.258,** 1.490
2416. 18	(0.000) 1.379
2407. 15	(0.000*wD*) 0.931*B*
2404. 68	(0.000) 1.064
2403. 60	(**0.105,** 0.296, 0.520, 0.661) **0.258,** 0.479, 0.681, 0.878, 1.046
2403. 43	(**0.133,** 0.352) 0.649, 0.846, **1.087**
2401. 94	(0.656) 0.854, **2.163**
2397. 85	(0.000*w*) 1.457*B*
2397. 12	(0.000) 0.825
2392. 33	(0.527) **0.405,** 1.483
2391. 74	(0.421, **0.694**) 0.349, 0.601, **0.889,** 1.136, 1.434
2390. 78	(0.102) 1.135
2390. 10	(0.000*w*) 0.951*A*
2389. 80	(0.387, **0.587**) . . ., 1.038, **1.243,** 1.490, 1.695
2389. 25	(0.000*WD*) 0.765*A*
2388. 70	(0.000) 0.891
2386. 96	(0.000) 1.054
2386. 07	(0.000) 1.057
2383. 37	(**0.332,** 0.985) 0.850, 1.496, **2.165**
2381. 48	(0.459, **0.615**) 0.700, 0.862, **0.998,** 1.205, 1.383
2381. 14	(0.315*B*) 1.046*w*
2380. 01	(0.416*B*) 1.321*WD*
2377. 13	(0.00) 1.07†
2372. 98	(0.00) 1.31†
2371. 58	(0.000*w*) 1.257*B*
2371. 26	(**0.084,** 0.258, 0.397) **0.697,** 0.845, 1.053, . . .
2370. 41	(0.000*w*) 1.142*A*
2370. 25	(0.000*w*) 0.857*A*
2366. 10	(0.366) **0.831,** 1.542
2364. 52	(0.000) 0.948
2359. 37	(0.000) 1.328
2357. 34	(0.000) 0.927
2355. 46	(0.159, **0.496**) 1.024, **1.355,** 1.693
2350. 12	(0.000*wD*) 0.764*A*
2348. 83	(0.688, **1.003**) ?
2347. 80	(0.083) 0.725
2344. 68	(0.142) 1.785
2341. 57	(0.000*w*) 0.923*B*
2340. 41	(0.000*WD*) **0.125,** 0.299, . . .
2337. 43	(0.88) 1.33†
2334. 94	(0.000) 1.088
2334. 84	(0.000) 0.999
2332. 13	(0.000) 0.933
2329. 71	(0.000*w*) 0.802*A*
2328. 12	(0.00) 1.63†
2322. 50	(0.000) 1.070
2316. 48	(0.000) 0.916
2315. 63	(0.000) 0.969
2307. 99	(0.403) 1.062*w*
2306. 99	(0.000*w*) 0.942*A*
2305. 67	(0.000*wD*) 1.011*A*
2304. 26	(0.000*w*) 0.907*A*
2290. 31	P–B
2289. 89	P–B
2269. 71	(0.000*w*) 0.949*A*

TABLE 4. *Even terms of* Mo II

Electron configuration	Term symbol	Level	$\Delta\nu$	Observed g
$4d^5$	$a\ ^6S_{2\frac{1}{2}}$	0. 00		
$4d^4\ (a\ ^5D)5s$	$a\ ^6D_{0\frac{1}{2}}$	11783. 36		3. 301
	$^6D_{1\frac{1}{2}}$	12034. 06	250. 70	1. 847
	$^6D_{2\frac{1}{2}}$	12417. 28	383. 22	1. 635
	$^6D_{3\frac{1}{2}}$	12900. 33	483. 05	1. 584
	$^6D_{4\frac{1}{2}}$	13460. 70	560. 37	1. 543
$4d^5$	$a\ ^4G_{2\frac{1}{2}}$	15199. 25		0. 61
	$^4G_{3\frac{1}{2}}$	15330. 56	131. 31	
	$^4G_{4\frac{1}{2}}$	15427. 73	97. 17	
	$^4G_{5\frac{1}{2}}$	15446. 97	19. 24	
$4d^5$	$a\ ^4P_{2\frac{1}{2}}$	15691. 22		1. 595
	$^4P_{1\frac{1}{2}}$	15699. 16	−7. 94	
	$^4P_{0\frac{1}{2}}$	15890. 12	−190. 96	
$4d^5$	$a\ ^4D_{0\frac{1}{2}}$	16796. 14		0. 758
	$^4D_{1\frac{1}{2}}$	17174. 10	377. 96	1. 391
	$^4D_{2\frac{1}{2}}$	17344. 10	170. 00	1. 433
	$^4D_{3\frac{1}{2}}$	16946. 78	−397. 32	1. 404
$4d^5$	$a\ ^2D_{2\frac{1}{2}}$	22444. 36		1. 082
	$^2D_{1\frac{1}{2}}$	22864. 36	−420. 00	0. 688
$4d^5$	$a\ ^2I_{5\frac{1}{2}}$	22980. 48		
	$^2I_{6\frac{1}{2}}$	23248. 19	267. 71	

TABLE 4. *Even terms of* Mo II—Continued

Electron configuration	Term symbol	Level	$\Delta\nu$	Observed g	Electron configuration	Term symbol	Level	$\Delta\nu$	Observed g
$4d^5$	$a\ ^4F_{4\frac{1}{2}}$	23832. 86		1. 300	$4d^4\ (a\ ^3P)5s$	$a\ ^2P_{0\frac{1}{2}}$	32124. 04	2295. 22	0. 672
	$^4F_{3\frac{1}{2}}$	23853. 35	−20. 49	1. 219		$^2P_{1\frac{1}{2}}$	34419. 26		1. 175
	$^4F_{2\frac{1}{2}}$	23934. 36	−81. 01	1. 018	$4d^5$	$b\ ^2D_{2\frac{1}{2}}$	32879. 55	−206. 73	1. 213
	$^4F_{1\frac{1}{2}}$	24137. 65	−203. 29	0. 514		$^2D_{1\frac{1}{2}}$	33086. 28		0. 889
$4d^4\ (a\ ^5D)5s$	$b\ ^4D_{0\frac{1}{2}}$	24372. 12		0. 058	$4d^4\ (a\ ^3H)5s$	$b\ ^2H_{4\frac{1}{2}}$	33045. 37	555. 70	0. 983
	$^4D_{1\frac{1}{2}}$	24659. 20	287. 08	1. 194		$^2H_{5\frac{1}{2}}$	33601. 07		1. 057
	$^4D_{2\frac{1}{2}}$	25112. 27	453. 07	1. 269	$4d^4\ (a\ ^1G)5s$	$b\ ^2G_{3\frac{1}{2}}$	33146. 30	108. 16	0. 904
	$^4D_{3\frac{1}{2}}$	25341. 58	229. 31	1. 387		$^2G_{4\frac{1}{2}}$	33254. 46		1. 043
$4d^5$	$a\ ^2F_{3\frac{1}{2}}$	24509. 30	−326. 79	1. 130	$4d^4\ (a\ ^3D)5s$	$c\ ^4D_{3\frac{1}{2}}$	33549. 28	−320. 44	1. 406
	$^2F_{2\frac{1}{2}}$	24836. 09		1. 054		$^4D_{2\frac{1}{2}}$	33869. 72	+344. 56	1. 323
$4d^4\ (a\ ^3H)5s$	$a\ ^4H_{3\frac{1}{2}}$	26041. 18	446. 97	0. 798		$^4D_{1\frac{1}{2}}$	33525. 16	−369. 90	1. 230
	$^4H_{4\frac{1}{2}}$	26488. 15	251. 32	0. 984		$^4D_{0\frac{1}{2}}$	33895. 06		0. 021
	$^4H_{5\frac{1}{2}}$	26739. 47	374. 36	1. 130	$4d^4\ (a\ ^1I)5s$	$b\ ^2I_{6\frac{1}{2}}$	35099. 46	−306. 56	1. 053
	$^4H_{6\frac{1}{2}}$	27113. 83		1. 193		$^2I_{5\frac{1}{2}}$	35406. 02		
$4d^5$	$a\ ^2G_{4\frac{1}{2}}$	26068. 60	−337. 01	1. 065	$4d^4\ (a\ ^3F)5s$	$c\ ^2F_{2\frac{1}{2}}$	36288. 80	452. 50	0. 913
	$^2G_{3\frac{1}{2}}$	26405. 61		0. 785		$^2F_{3\frac{1}{2}}$	36741. 30		1. 065
$4d^4\ (a\ ^3P)5s$	$b\ ^4P_{0\frac{1}{2}}$	26603. 55	1024. 00	2. 530	$4d^4\ (a\ ^3G)5s$	$c\ ^2G_{3\frac{1}{2}}$	37431. 45	622. 43	0. 927
	$^4P_{1\frac{1}{2}}$	27627. 55	1394. 57	1. 700		$^2G_{4\frac{1}{2}}$	38053. 88		1. 105
	$^4P_{2\frac{1}{2}}$	29022. 12		1. 574	$4d^4\ (a\ ^1D)5s$	$c\ ^2D_{1\frac{1}{2}}$	39243. 45	669. 50	0. 800
$4d^5$	$b\ ^2F_{3\frac{1}{2}}$	27410. 30	−468. 59	1. 148		$^2D_{2\frac{1}{2}}$	39912. 95		1. 203
	$^2F_{2\frac{1}{2}}$	27878. 89		0. 900	$4d^4\ (a\ ^3D)5s$	$d\ ^2D_{2\frac{1}{2}}$	41421. 34	−120. 66	
$4d^5$	$a\ ^2H_{5\frac{1}{2}}$	27627. 00	−97. 69	1. 086		$^2D_{1\frac{1}{2}}$	41542. 00		0. 761
	$^2H_{4\frac{1}{2}}$	27724. 69		0. 987	$4d^4\ (a\ ^1S)5s$	$b\ ^2S_{0\frac{1}{2}}$	41873. 66		1. 993
$4d^4\ (a\ ^3F)5s$	$b\ ^4F_{1\frac{1}{2}}$	28883. 69	−6. 87	0. 529	$4d^5$	$d\ ^2G_{3\frac{1}{2}}$	42169. 30	137. 32	
	$^4F_{2\frac{1}{2}}$	28876. 82	112. 14	1. 035		$^2G_{4\frac{1}{2}}$	42306. 62		
	$^4F_{3\frac{1}{2}}$	28988. 96	45. 21	1. 135	$4d^4\ (a\ ^1F)5s$	$d\ ^2F_{2\frac{1}{2}}$	42925. 34	66. 84	
	$^4F_{4\frac{1}{2}}$	29034. 17		1. 278		$^2F_{3\frac{1}{2}}$	42992. 18		1. 085
$4d^5$	$a\ ^2S_{0\frac{1}{2}}$	28950. 36		1. 968					
$4d^4\ (a\ ^3G)5s$	$b\ ^4G_{2\frac{1}{2}}$	29699. 32	320. 04	0. 758	$4d^4\ (b^3\ F)5s$	$c\ ^4F_{1\frac{1}{2}}$ $^4F_{2\frac{1}{2}}$ $^4F_{3\frac{1}{2}}$ $^4F_{4\frac{1}{2}}$	44212. 16		
	$^4G_{3\frac{1}{2}}$	30019. 36	194. 10	1. 059					
	$^4G_{4\frac{1}{2}}$	30213. 46	177. 82	1. 192					
	$^4G_{5\frac{1}{2}}$	30391. 28		1. 268					

TABLE 5. *Odd terms of* Mo II

Electron configuration	Term symbol	Level	Δν	Observed g
$4d^4\,(a\,^5D)5p$	$z\,^6F^\circ_{0½}$	45853. 08		−0. 650
	$^6F^\circ_{1½}$	46148. 12	295. 04	1. 072
	$^6F^\circ_{2½}$	46614. 14	466. 02	1. 305
	$^6F^\circ_{3½}$	47231. 98	617. 84	1. 375
	$^6F^\circ_{4½}$	47999. 47	767. 49	1. 415
	$^6F^\circ_{5½}$	48959. 68	960. 21	
$4d^4\,(a\,^5D)5p$	$z\,^4P^\circ_{0½}$	47208. 36		2. 779
	$^4P^\circ_{1½}$	48022. 45	814. 09	1. 818
	$^4P^\circ_{2½}$	48860. 57	838. 12	1. 742
$4d^4\,(a\,^5D)5p$	$z\,^6P^\circ_{1½}$	49040. 82		2. 305
	$^6P^\circ_{2½}$	49608. 74	567. 92	1. 718
	$^6P^\circ_{3½}$	49481. 04	−127. 70	1. 672
$4d^4\,(a^{\bar{}}{}^5D)5p$	$z\,^6D^\circ_{0½}$	49949. 45		3. 155
	$^6D^\circ_{1½}$	50192. 00	242. 55	1. 802
	$^6D^\circ_{2½}$	50577. 36	385. 36	1. 597
	$^6D^\circ_{3½}$	50302. 54	−274. 82	1. 552
	$^6D^\circ_{4½}$	50705. 52	402. 98	1. 502
$4d^4\,(a^{\bar{}}{}^5D)5p$	$z\,^4F^\circ_{1½}$	51372. 90		0. 412
	$^4F^\circ_{2½}$	51732. 39	359. 49	1. 045
	$^4F^\circ_{3½}$	52217. 30	484. 91	1. 262
	$^4F^\circ_{4½}$	52843. 10	625. 80	1. 362
$4d^4\,(a\,^5D)5p$	$z\,^4D^\circ_{0½}$	54238. 80		0. 042
	$^4D^\circ_{1½}$	54687. 61	448. 81	1. 197
	$^4D^\circ_{2½}$	55215. 85	528. 24	1. 376
	$^4D^\circ_{3½}$	55706. 57	490. 72	1. 413
$4d^4\,(a\,^3P)5p$	$y\,^4D^\circ_{0½}$	57319. 55		0. 200
	$^4D^\circ_{1½}$	58140. 75	821. 20	1. 183
	$^4D^\circ_{2½}$	59347. 94	1207. 19	1. 263
	$^4D^\circ_{3½}$	60702. 16	1354. 22	1. 305
$4d^4\,(a\,^3H)5p$	$z\,^4H^\circ_{3½}$	57892. 06		0. 710
	$^4H^\circ_{4½}$	58196. 68	304. 62	0. 960
	$^4H^\circ_{5½}$	58760. 95	564. 27	1. 110
	$^4H^\circ_{6½}$	59491. 83	730. 88	1. 206
$4d^4\,(a\,^3P)5p$	$z\,^2S^\circ_{0½}$	58527. 00		1. 651
$4d^4\,(a\,^3F)5p$	$z\,^4G^\circ_{2½}$	59053. 32		0. 672
	$^4G^\circ_{3½}$	59478. 34	425. 02	0. 923
	$^4G^\circ_{4½}$	60227. 00	748. 66	0. 884
	$^4G^\circ_{5½}$	61116. 18	889. 18	1. 210
$4d^4\,(a\,^3H)5p$	$z\,^4I^\circ_{4½}$	59679. 75		1. 027
	$^4I^\circ_{5½}$	60924. 53	1244. 78	0. 936
	$^4I^\circ_{6½}$	61647. 76	723. 23	1. 103
	$^4I^\circ_{7½}$	62151. 66	503. 90	
$4d^4\,(a\,^3F)5p$	$z\,^2D^\circ_{1½}$	59840. 70		0. 862
	$^2D^\circ_{2½}$	60992. 47	1151. 77	1. 205
$4d^4\,(a\,^3H)5p$	$z\,^2G^\circ_{3½}$	60135. 37		1. 011
	$^2G^\circ_{4½}$	60973. 14	837. 77	1. 101
$4d^4\,(a\,^3P)5p$	$y\,^4P^\circ_{0½}$	61134. 25		2. 299
	$^4P^\circ_{1½}$	61456. 77	322. 52	1. 656
	$^4P^\circ_{2½}$	62425. 47	968. 70	1. 185
$4d^4\,(a\,^3P)5p$	$z\,^2P^\circ_{1½}$	61746. 58		1. 220
	$^2P^\circ_{0½}$	62096. 05	−349. 47	1. 075
$4d^4\,(a\,^3F)5p$	$x\,^4D^\circ_{3½}$	62491. 78		1. 252
	$^4D^\circ_{2½}$	62342. 27	149. 51	1. 067
	$^4D^\circ_{1½}$	62551. 04	−208. 77	0. 707
	$^4D^\circ_{0½}$	62937. 45	−386. 41	0. 030
	$1^\circ_{2½}$	62594. 53		1. 14
$4d^4\,(a\,^3H)5p$	$z\,^2I^\circ_{5½}$	62728. 35		0. 902
	$^2I^\circ_{6½}$	62980. 24	251. 89	1. 091
$4d^4\,(a\,^3F)5p$	$y\,^4F^\circ_{1½}$	63002. 58		0. 899
	$^4F^\circ_{2½}$	63392. 52	389. 94	1. 002
	$^4F^\circ_{3½}$	63104. 63	−287. 89	1. 060
	$^4F^\circ_{4½}$	63783. 10	678. 47	
	$2^\circ_{3½}$	63012. 24		1. 186
$4d^4\,(a\,^3H)5p$	$y\,^4G^\circ_{2½}$	63041. 47		0. 851
	$^4G^\circ_{3½}$	62917. 94	−123. 53	1. 004
	$^4G^\circ_{4½}$	62953. 75	35. 81	1. 214
	$^4G^\circ_{5½}$	63207. 43	253. 68	1. 272

TABLE 5. *Odd terms of* Mo II—Continued

Electron configuration	Term symbol	Level	Δν	Observed g
$4d^4\,(a\,^3G)5p$	$y\,^4H^\circ_{3½}$	63298. 23		
			199. 31	0. 933
	$^4H^\circ_{4½}$	63497. 54		
			642. 44	1. 024
	$^4H^\circ_{5½}$	64139. 98		
			974. 85	1. 166
	$^4H^\circ_{6½}$	65114. 83		
$4d^4\,(a\,^3G)5p$	$z\,^2F^\circ_{3½}$	63876. 68		1. 105
			−517. 96	
	$^2F^\circ_{2½}$	64394. 64		0. 802
$4d^4\,(a\,^3G)5p$	$x\,^4F^\circ_{1½}$	63903. 90		0. 535
			263. 94	
	$^4F^\circ_{2½}$	64167. 84		1. 012
			35. 25	
	$^4F^\circ_{3½}$	64203. 09		1. 208
			123. 31	
	$^4F^\circ_{4½}$	64326. 40		1. 258
$4d^4\,(a\,^3H)5p$	$z\,^2H^\circ_{4½}$	64130. 22		0. 934
			944. 49	
	$^2H^\circ_{5½}$	65074. 71		1. 112
$4d^4\,(a\,^3P)5p$	$z\,^4S^\circ_{1½}$	64750. 66		1. 926
$4d^4\,(a\,^3F)5p$	$y\,^2G^\circ_{3½}$	64852. 22		1. 040
			842. 69	
	$^2G^\circ_{4½}$	65694. 91		1. 105
$4d^4\,(a\,^3F)5p$	$y\,^2F^\circ_{3½}$	65260. 95		
			−11. 82	0. 856
	$^2F^\circ_{2½}$	65272. 77		
$4d^4\,(a\,^3G)5p$	$y\,^2H^\circ_{4½}$	65282. 58		
			142. 07	1. 175
	$^2H^\circ_{5½}$	65424. 65		
$4d^4\,(a\,^3P)5p$	$y\,^2D^\circ_{1½}$	65444. 30		0. 769
			638. 01	
	$^2D^\circ_{2½}$	66082. 31		1. 166
$4d^4\,(a\,^3G)5p$	$x\,^4G^\circ_{2½}$	65732. 23		0. 751
			355. 32	
	$^4G^\circ_{3½}$	66087. 55		
			303. 91	
	$^4G^\circ_{4½}$	66391. 46		
			352. 26	
	$^4G^\circ_{5½}$	66743. 72		1. 209
	$3^\circ_{3½}$	65831. 24		1. 070
$4d^4\,(a\,^3D)5p$	$w\,^4D^\circ_{0½}$	66373. 65		
			25. 79	
	$^4D^\circ_{1½}$	66399. 44		1. 075
			268. 54	
	$^4D^\circ_{2½}$	66667. 98		1. 289
			48. 36	
	$^4D^\circ_{3½}$	66716. 34		1. 436
$4d^4\,(a\,^1G)5p$	$x\,^2F^\circ_{3½}$	67391. 42		1. 130
			−266. 71	
	$^2F^\circ_{2½}$	67658. 13		
$4d^4\,(a\,^3D)5p$	$x\,^4P^\circ_{2½}$	67712. 92		1. 426
			−728. 74	
	$^4P^\circ_{1½}$	68441. 66		1. 535
			−608. 09	
	$^4P^\circ_{0½}$	69049. 75		2. 410
$4d^4\,(a\,^3G)5p$	$x\,^2G^\circ_{3½}$	67760. 30		0. 921
			292. 17	
	$^2G^\circ_{4½}$	68052. 47		1. 150
$4d^4\,(a\,^3D)5p$	$w\,^4F^\circ_{1½}$	67821. 60		
			194. 32	
	$^4F^\circ_{2½}$	68015. 92		
			163. 78	
	$^4F^\circ_{3½}$	68179. 70		
			143. 80	
	$^4F^\circ_{4½}$	68323. 50		1. 250
$4d^4\,(a\,^1I)5p$	$z\,^2K^\circ_{6½}$	67888. 85		0. 933
			1158. 60	
	$^2K^\circ_{7½}$	69047. 45		
$4d^4\,(a\,^1I)5p$	$y\,^2I^\circ_{5½}$	68472. 84		
			435. 76	
	$^2I^\circ_{6½}$	68908. 60		
$4d^4\,(a\,^3D)5p$	$y\,^2P^\circ_{0½}$	68645. 50		0. 768
			257. 30	
	$^2P^\circ_{1½}$	68902. 80		1. 420
$4d^4\,(a\,^3D)5p$	$w\,^2F^\circ_{2½}$	69729. 90		0. 885
			371. 65	
	$^2F^\circ_{3½}$	70101. 55		1. 075
$4d^4\,(a\,^1G)5p$	$x\,^2H^\circ_{4½}$	70003. 84		
			666. 73	
	$^2H^\circ_{5½}$	70670. 57		
$4d^4\,(a\,^1D)5p$	$x\,^2D^\circ_{2½}$	70713. 10		
			−24. 90	
	$^2D^\circ_{1½}$	70738. 00		0. 946
$4d^4\,(a\,^1G)5p$	$w\,^2G^\circ_{4½}$	71011. 20		
			−182. 33	
	$^2G^\circ_{3½}$	71193. 53		
$4d^4\,(a\,^1I)5p$	$w\,^2H^\circ_{5½}$	71546. 56		
			−373. 66	
	$^2H^\circ_{4½}$	71920. 22		
$4d^4\,(a\,^1S)5p$	$x\,^2P^\circ_{0½}$	71966. 30		0. 670
			1252. 67	
	$^2P^\circ_{1½}$	73218. 97		1. 082
$4d^4\,(a\,^3D)5p$	$w\,^2D^\circ_{1½}$	72039. 00		1. 086
			790. 62	
	$^2D^\circ_{2½}$	72829. 62		1. 156
$4d^4\,(a\,^1D)5p$	$v\,^2F^\circ_{2½}$	72484. 19		
			548. 09	
	$^2F^\circ_{3½}$	73032. 28		
$4d^4\,(a\,^1D)5p$	$w\,^2P^\circ_{0½}$	73546. 75		
			503. 62	
	$^2P^\circ_{1½}$	74050. 37		1. 289
$4d^4\,(a\,^1F)5p$	$u\,^2F^\circ_{2½}$	74146. 50		
			345. 04	
	$^2F^\circ_{3½}$	74491. 54		
$4d^4\,(b\,^3F)5p$	$t\,^2F^\circ_{3½}$	74749. 55		
			−176. 62	
	$^2F^\circ_{2½}$	74926. 17		

TABLE 5. *Odd terms of* Mo II—Continued

Electron configuration	Term symbol	Level	$\Delta\nu$	Observed g
$4d^4\ (b\ ^3\mathrm{F})5p$	$w\ ^4\mathrm{G}^\circ_{2\frac{1}{2}}$	74858. 86		
	$^4\mathrm{G}^\circ_{3\frac{1}{2}}$	75834. 37	975. 51	
	$^4\mathrm{G}^\circ_{4\frac{1}{2}}$	76584. 60	750. 23	
	$^4\mathrm{G}^\circ_{5\frac{1}{2}}$	77663. 92	1079. 32	
$4d^4\ (b\ ^3\mathrm{P})5p$	$v\ ^2\mathrm{D}^\circ_{1\frac{1}{2}}$	--------		
	$^2\mathrm{D}^\circ_{2\frac{1}{2}}$	75819. 80		
$4d^4\ (b\ ^3\mathrm{P})5p$	$v\ ^4\mathrm{D}^\circ_{0\frac{1}{2}}$	--------		
	$^4\mathrm{D}^\circ_{1\frac{1}{2}}$	--------		
	$^4\mathrm{D}^\circ_{2\frac{1}{2}}$	76206. 57	118. 43	
	$^4\mathrm{D}^\circ_{3\frac{1}{2}}$	76325. 00		
$4d^4\ (a\ ^1\mathrm{F})5p$	$v\ ^2\mathrm{G}^\circ_{4\frac{1}{2}}$	75685. 65		1. 140
	$^2\mathrm{G}^\circ_{3\frac{1}{2}}$	--------		
$4d^4\ (b\ ^3\mathrm{F})5p$	$v\ ^4\mathrm{F}^\circ_{1\frac{1}{2}}$	--------		
	$^4\mathrm{F}^\circ_{2\frac{1}{2}}$	75810. 62?	856. 41	
	$^4\mathrm{F}^\circ_{3\frac{1}{2}}$	76667. 03	−29. 65	
	$^4\mathrm{F}^\circ_{4\frac{1}{2}}$	76637. 38		
$4d^4\ (a\ ^1\mathrm{F})5p$	$u\ ^2\mathrm{D}^\circ_{1\frac{1}{2}}$	--------		
	$^2\mathrm{D}^\circ_{2\frac{1}{2}}$	80420. 55		
$4d^4\ (b\ ^3\mathrm{F})5p$	$u\ ^2\mathrm{G}^\circ_{3\frac{1}{2}}$	81526. 97	1029. 93	
	$^2\mathrm{G}^\circ_{4\frac{1}{2}}$	82556. 90		
$4d^4\ (b\ ^1\mathrm{G})5p$	$t\ ^2\mathrm{G}^\circ_{4\frac{1}{2}}$	83314. 88	−559. 27	
	$^2\mathrm{G}^\circ_{3\frac{1}{2}}$	83874. 15		
$4d^4\ (b\ ^1\mathrm{G})5p$	$v\ ^2\mathrm{H}^\circ_{4\frac{1}{2}}$	83964. 88	531. 62	
	$^2\mathrm{H}^\circ_{5\frac{1}{2}}$	84496. 50		
$4d^4\ (b\ ^1\mathrm{G})5p$	$s\ ^2\mathrm{F}^\circ_{3\frac{1}{2}}$	86566. 24		
	$^2\mathrm{F}^\circ_{2\frac{1}{2}}$	--------		
$4d^4\ (b\ ^3\mathrm{F})5p$	$t\ ^2\mathrm{D}^\circ_{2\frac{1}{2}}$	86693. 42	−340. 18	
	$^2\mathrm{D}^\circ_{1\frac{1}{2}}$	87033. 60		

TABLE 6. *Theoretical terms of* Mo II

Electron configuration $1s^2\ 2s^2\ 2p^6\ 3s^2\ 3p^6\ 3d^{10}\ 4s^2\ 4p^6+$	Theoretical terms
$4d^5$	^{6}**S** ^{4}(**GD**) ^{4}(**FP**) ^{2}(**IGFDS**) ^{2}(**HGFDP**) ^{2}D
$4d^4\ 5s$	^{6,4}(**D**) ^{4,2}(**HGFDP**) ^{2}(**IGFDS**) ^{4,2}(**FP**) ^{2}(GDS)
$4d^3\ 5s^2$	^{4}(FP) ^{2}(HGFDP) ^{2}D
$4d^4\ 5p$	^{6,4}(**FDP**)° ^{4,2}(**IHG**)° ^{4,2}(**HGF**)° ^{4,2}(**GFD**)° ^{4,2}(**FDP**)° ^{4,2}(**DPS**)° ^{2}(**KIH**)° ^{2}(**HGF**)° ^{2}(**GFD**)° ^{2}(**FDP**)° ^{2}**P**° ^{4,2}(**GF**D)° ^{4,2}(**DPS**)° ^{2}(FDP)° ^{2}(**HGF**)° ^{2}P°

WASHINGTON, September 30, 1957.

U. S. GOVERNMENT PRINTING OFFICE: 1958

THE NATIONAL BUREAU OF STANDARDS

The scope of activities of the National Bureau of Standards at its headquarters in Washington, D. C., and its major laboratories in Boulder, Colo., is suggested in the following listing of the divisions and sections engaged in technical work. In general, each section carries out specialized research, development, and engineering in the field indicated by its title. A brief description of the activities, and of the resultant publications, appears on the inside front cover.

WASHINGTON, D. C.

Electricity and Electronics. Resistance and Reactance. Electron Devices. Electrical Instruments. Magnetic Measurements. Dielectrics. Engineering Electronics. Electronic Instrumentation. Electrochemistry.

Optics and Metrology. Photometry and Colorimetry. Optical Instruments. Photographic Technology. Length. Engineering Metrology.

Heat. Temperature Physics. Thermodynamics. Cryogenic Physics. Rheology. Engine Fuels. Free Radicals Research.

Atomic and Radiation Physics. Spectroscopy. Radiometry. Mass Spectrometry. Solid State Physics. Electron Physics. Atomic Physics. Neutron Physics. Nuclear Physics. Radioactivity. X-rays. Betatron. Nucleonic Instrumentation. Radiological Equipment.

Chemistry. Organic Coatings. Surface Chemistry. Organic Chemistry. Analytical Chemistry. Inorganic Chemistry. Electrodeposition. Molecular Structure and Properties of Gases. Physical Chemistry. Thermochemistry. Spectrochemistry. Pure Substances.

Mechanics. Sound. Mechanical Instruments. Fluid Mechanics. Engineering Mechanics. Mass and Scale. Capacity, Density, and Fluid Meters. Combustion Controls.

Organic and Fibrous Materials. Rubber. Textiles. Paper. Leather. Testing and Specifications. Polymer Structure. Plastics. Dental Research.

Metallurgy. Thermal Metallurgy. Chemical Metallurgy. Mechanical Metallurgy. Corrosion. Metal Physics.

Mineral Products. Engineering Ceramics. Glass. Refractories. Enameled Metals. Concreting Materials. Constitution and Microstructure.

Building Technology. Structural Engineering. Fire Protection. Air Conditioning, Heating, and Refrigeration. Floor, Roof, and Wall Coverings. Codes and Safety Standards. Heat Transfer.

Applied Mathematics. Numerical Analysis. Computation. Statistical Engineering. Mathematical Physics.

Data Processing Systems. SEAC Engineering Group. Components and Techniques. Digital Circuitry. Digital Systems. Analog Systems. Application Engineering.

Office of Basic Instrumentation.

• Office of Weights and Measures.

BOULDER, COLORADO

Cryogenic Engineering. Cryogenic Equipment. Cryogenic Processes. Properties of Materials. Gas Liquefaction.

Radio Propagation Physics. Upper Atmosphere Research. Ionospheric Research. Regular Propagation Services. Sun-Earth Relationships. VHF Research.

Radio Propagation Engineering. Data Reduction Instrumentation. Modulation Systems. Navigation Systems. Radio Noise. Tropospheric Measurements. Tropospheric Analysis. Radio Systems Application Engineering. Radio Meteorology.

Radio Standards. High Frequency Electrical Standards. Radio Broadcast Service. High Frequency Impedance Standards. Calibration Center. Microwave Physics. Microwave Circuit Standards.

Recent Publications of the National Bureau of Standards

Periodicals

Journal of Research of the National Bureau of Standards, Volume 60, No. 2, February 1958 (RP2824 to RP2832 incl.). 60 cents. Annual subscription $4.00, $1.25 additional for foreign mailing.

Technical News Bulletin, Volume 42, No. 2, February 1958. 10 cents. Annual subscription $1.00, 35 cents additional for foreign mailing.

Basic Radio Propagation Predictions for May 1958. Three months in advance. CRPL-D 162. Issued February 1958. 10 cents. Annual subscription $1.00, 25 cents additional for foreign mailing.

Circulars

C590. Methods of testing thermocouples and thermocouple materials. 20 cents.°

C591. Section 1. System design of digital computers at the National Bureau of Standards. 20 cents.°

C592. Nickel and its alloys. 60 cents.°

Miscellaneous Publications

M222. Report of the 42d National Conference on Weights and Measures. 55 cents.°

Available from the Superintendent of Documents, U. S. Government Printing Office, Washington 25, D. C. The three NBS periodicals are available on a 1-, 2-, or 3-year subscription basis, although no reduction in rates can be made.

°Foreign postage, one-fourth additional.

UNIVERSITY OF MICHIGAN
GENERAL LIBRARY
DOCUMENTS DIVISION
1276 ANN ARBOR MICH

UNITED S
GOVERNMENT PRINTING OFFICE
DIVISION OF PUBLIC DOCUMENTS
WASHINGTON 25, D. C.

OFFICIAL BUSINESS

PENALTY FOR PRIVATE USE TO AV
PAYMENT OF POSTAGE, $300
(GPO)

Journal of Research of the National Bureau of Standards Vol. 60, No. 4 April 19

Contents

		Page
Transient radio-frequency ground waves over the surface of a finitely conducting plane earth. J. R. Johler.	RP2844	281
Measurement of current with a Pellat-type electrodynamometer. R. L. Driscoll.	RP2845	287
Measurement of current with the National Bureau of Standards current balance. R. L. Driscoll and R. D. Cutkosky.	RP2846	297
Radial distribution of the center of gravity of random points on a unit circle. F. Scheid.	RP2847	307
An adiabatic calorimeter for the range 30° to 500° C. E. D. West and D. C. Ginnings.	RP2848	309
An evaluation of the luminous-transmittance requirements for railroad-signal glassware in terms of standard source A of the International Commission on Illumination. Francis C. Breckenridge.	RP2849	317
Random notes on matrices. K. Goldberg.	RP2850	321
Range finders using projected images. Robert E. Stephens.	RP2851	327
Effect of rib flexibility on the vibration modes of a delta-wing aircraft. Wilhelmina D. Kroll.	RP2852	335
Thermal degradation of cellulosic materials. S. L. Madorsky, V. E. Hart, and S. Straus.	RP2853	343
Role of vitrons in alkali silicate binary glasses. Leroy W. Tilton.	RP2854	351
Elastic problem for a ring of uniform force in an infinite body. William H. Pell.	RP2855	365
Description and analysis of the second spectrum of molybdenum, Mo II. C. C. Kiess.	RP2856	375

[A list of recent NBS publications is given on page 3 of the cover.]

For sale by the Superintendent of Documents, U. S. Government Printing Office, Washington 25, D. C. Price 60 cents (single co
Subscription price: $4.00 a year; $1.25 additional for foreign mailing.
UNITED STATES GOVERNMENT PRINTING OFFICE, WASHINGTON : 1958